Series on Advances in Statistical Mechanics – Volume 16

Non-Equilibrium Thermodynamics of Heterogeneous Systems

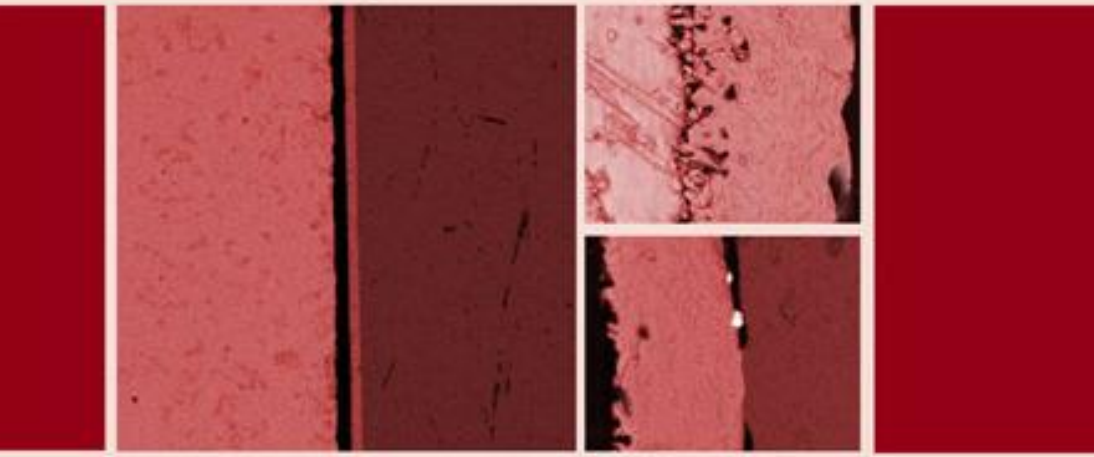

SIGNE KJELSTRUP DICK BEDEAUX

World Scientific

Non-Equilibrium Thermodynamics
of Heterogeneous Systems

SERIES ON ADVANCES IN STATISTICAL MECHANICS*

Editor-in-Chief: M. Rasetti *(Politecnico di Torino, Italy)*

Published

Vol. 6: New Problems, Methods and Techniques in Quantum Field Theory and Statistical Mechanics
edited by M. Rasetti

Vol. 7: The Hubbard Model – Recent Results
edited by M. Rasetti

Vol. 8: Statistical Thermodynamics and Stochastic Theory of Nonlinear Systems Far From Equilibrium
by W. Ebeling & L. Schimansky-Geier

Vol. 9: Disorder and Competition in Soluble Lattice Models
by W. F. Wreszinski & S. R. A. Salinas

Vol. 10: An Introduction to Stochastic Processes and Nonequilibrium Statistical Physics
by H. S. Wio

Vol. 12: Quantum Many-Body Systems in One Dimension
by Zachary N. C. Ha

Vol. 13: Exactly Soluble Models in Statistical Mechanics: Historical Perspectives and Current Status
edited by C. King & F. Y. Wu

Vol. 14: Statistical Physics on the Eve of the 21st Century: In Honour of J. B. McGuire on the Occasion of his 65th Birthday
edited by M. T. Batchelor & L. T. Wille

Vol. 15: Lattice Statistics and Mathematical Physics: Festschrift Dedicated to Professor Fa-Yueh Wu on the Occasion of his 70th Birthday
edited by J. H. H. Perk & M.-L. Ge

Vol. 16: Non-Equilibrium Thermodynamics of Heterogeneous Systems
by S. Kjelstrup & D. Bedeaux

*For the complete list of titles in this series, please go to
http://www.worldscibooks.com/series/sasm_series

Series on Advances in Statistical Mechanics – Volume 16

Non-Equilibrium Thermodynamics of Heterogeneous Systems

SIGNE KJELSTRUP DICK BEDEAUX

Norwegian University of Science and Technology

World Scientific

NEW JERSEY • LONDON • SINGAPORE • BEIJING • SHANGHAI • HONG KONG • TAIPEI • CHENNAI

Published by

World Scientific Publishing Co. Pte. Ltd.

5 Toh Tuck Link, Singapore 596224

USA office: 27 Warren Street, Suite 401-402, Hackensack, NJ 07601

UK office: 57 Shelton Street, Covent Garden, London WC2H 9HE

British Library Cataloguing-in-Publication Data
A catalogue record for this book is available from the British Library.

Series on Advances in Statistical Mechanics – Vol. 16
NON-EQUILIBRIUM THERMODYNAMICS OF HETEROGENEOUS SYSTEMS

ISBN-13 978-981-277-913-7
ISBN-10 981-277-913-2

Printed in Singapore.

We dedicate this book to our teacher and friend Peter Mazur

This page intentionally left blank

Preface

What the book is about

This book describes transport through complex, heterogeneous media. There are large coupling effects between transports of heat, mass, charge and chemical reactions in such media, and it is important to know how one should properly integrate across heterogeneous systems where different phases are in contact. Transports perpendicular to planar interfaces are treated.

How we were inspired to write it

Waldmann [1] was the first to point out that an analysis of boundary conditions should be incorporated in the framework of non-equilibrium thermodynamics. He did not include excess densities to describe the properties of the surface, however. In the 1970s and 1980s Bedeaux, Albano and Mazur [2–4] extended his work and laid the theoretical foundation for the description of non-equilibrium processes, including a full description of the thermodynamic properties of the surface. The work of Bedeaux, Albano and Mazur addressed not only transports into and through a surface, but also transports along surfaces as well as the motion of the surface itself. Their methods were inspired by concurrent work on the optical properties of surfaces by Bedeaux and Vlieger [5, 6], using generalized functions for the description of surface properties. The present work takes advantage of these methodologies.

Who it is meant for

The purpose of this book is to encourage the use of non-equilibrium thermodynamics to describe transport in complex, heterogeneous media. The book is written for a graduate level course for physicists, physical chemists, chemical or mechanical engineers. The book requires knowledge of basic thermodynamics corresponding to that given by Atkins, Physical

Chemistry (Oxford University Press), or Moran and Shapiro, Fundamentals of Engineering Thermodynamics (John Wiley & Sons).

Acknowledgments

A course on non-equilibrium thermodynamics has been taught at the Norwegian University of Science and Technology for many years. We are grateful to the graduate students who worked with us on related subjects and commented on preliminary versions of the text. In alphabetical order, we would like to mention Odne Stokke Burheim, Belinda Flem, Andreas Grimstvedt, Kirill Glavatskiy, Ellen Marie Hansen, Torleif Holt, Isabella Inzoli, Eivind Johannessen, Einar Eng Johnsen, Gelein de Koeijer, Lars Nummedal, Anne-Kristine Meland, Steffen Møller-Holst, Magnar Ottøy, Audun Røsjorde, Erik Sauar, Kristin Syverud, Preben Joakim Svela Vie, Jing Xu and Anita Zvolinschi. Discussions and collaborations with colleagues Bjørn Hafskjold, Jean-Marc Simon, Fernando Bresme and Edgar Blokhuis were appreciated.

During our peaceful and inspiring stay in Kyoto University in 2000, a large step forward was made. We are grateful to our host Prof. Yasuhiko Ito, and to coworkers, Profs. Yoichi Tomii, Yasuhiro Fukunaka, Drs. Toshiyuki Nohira and Koji Amezawa. The next large step was made in beautiful Barcelona in 2004, with our considerate host, Prof. Miguel Rubi of University of Barcelona.

We thank the Research Council of Norway for financial support over many years. Marian Palcut contributed the cover image, while Tharald Tharaldsen, Jaques van der Ploeg and Michel Uiterwijk contributed many figures.

Signe Kjelstrup* and Dick Bedeaux March 2008

Address for correspondence:

Department of Chemistry,
Norwegian University of Science and Technology,
NO-7491 Trondheim, Norway

*The author changed her name from Ratkje to Kjelstrup in 1996.

Contents

Preface vii

1 Scope **1**
1.1 What is non-equilibrium thermodynamics? 1
1.2 Non-equilibrium thermodynamics in the context of other theories 4
1.3 The purpose of this book 4

2 Why Non-Equilibrium Thermodynamics? **7**
2.1 Simple flux equations 8
2.2 Flux equations with coupling terms 9
2.3 Experimental designs and controls 11
2.4 Entropy production, work and lost work 12
2.5 Consistent thermodynamic models 14

3 Thermodynamic Relations for Heterogeneous Systems **17**
3.1 Two homogeneous phases separated by a surface in global equilibrium 18
3.2 The contact line in global equilibrium 22
3.3 Defining thermodynamic variables for the surface 23
3.4 Local thermodynamic identities 29
3.5 Defining local equilibrium 32
3.A Appendix: Partial molar properties 35
3.A.1 Homogeneous phases 36
3.A.2 The surface 38
3.A.3 The standard state 40

Part A: General Theory **45**

4 The Entropy Production for a Homogeneous Phase **47**
4.1 Balance equations 49
4.2 The entropy production 51

4.2.1 Why one should not use the dissipation function . 56
4.2.2 States with minimum entropy production 57
4.3 Examples 58
4.4 Frames of reference for fluxes in homogeneous systems . . 64
4.4.1 Definitions of frames of reference 64
4.4.2 Transformations between the frames of reference . 66
4.A Appendix: The first law and the heat flux 67

5 The Excess Entropy Production for the Surface 73
5.1 The discrete nature of the surface 74
5.2 The behavior of the electric fields and potential through the surface 75
5.3 Balance equations 77
5.4 The excess entropy production 79
5.4.1 Reversible processes at the interface and the Nernst equation 84
5.4.2 The surface potential jump at the hydrogen electrode 86
5.5 Examples 87

6 The Excess Entropy Production for a Three Phase Contact Line 91
6.1 The discrete nature of the contact line 92
6.2 Balance equations 94
6.3 The excess entropy production 95
6.4 Stationary states 96
6.5 Concluding comment 97

7 Flux Equations and Onsager Relations 99
7.1 Flux-force relations 99
7.2 Onsager's reciprocal relations 100
7.3 Relaxation to equilibrium. Consequences of violating Onsager relations 104
7.4 Force-flux relations 105
7.5 Coefficient bounds 106
7.6 The Curie principle applied to surfaces and contact lines . 108

8 Transport of Heat and Mass 111
8.1 The homogeneous phases 112
8.2 Coefficient values for homogeneous phases 114
8.3 The surface 117
8.3.1 Heats of transfer for the surface 119

8.4 Solution for the heterogeneous system 122
8.5 Scaling relations between surface and bulk resistivities . . 125

9 Transport of Heat and Charge 127
9.1 The homogeneous phases 128
9.2 The surface 130
9.3 Thermoelectric coolers 132
9.4 Thermoelectric generators 133
9.5 Solution for the heterogeneous system 135

10 Transport of Mass and Charge 139
10.1 The electrolyte 140
10.2 The electrode surfaces 143
10.3 Solution for the heterogeneous system 146
10.4 A salt power plant 147
10.5 Electric power from volume flow 148
10.6 Ionic mobility model for the electrolyte 150
10.7 Ionic and electronic model for the surface 154

Part B: Applications 155

11 Evaporation and Condensation 157
11.1 Evaporation and condensation in a pure fluid 158
11.1.1 The entropy production and the flux equations . . 158
11.1.2 Interface resistivities from kinetic theory 165
11.2 The sign of the heats of transfer of the surface 167
11.3 Coefficients from molecular dynamics simulations 169
11.4 Evaporation and condensation in a two-component fluid . 176
11.4.1 The entropy production and the flux equations . . 176
11.4.2 Interface resistivities from kinetic theory 179

12 Multi-Component Heat and Mass Diffusion 183
12.1 The homogeneous phases 184
12.2 The Maxwell–Stefan equations for multi-component diffusion 186
12.3 The Maxwell–Stefan equations for the surface 188
12.4 Multi-component diffusion 192
12.4.1 Prigogine's theorem 192
12.4.2 Diffusion in the solvent frame of reference 193
12.4.3 Other frames of reference 195
12.4.4 An example: Kinetic demixing of oxides 200

12.5 A relation between the heats of transfer and the enthalpy 202

13 A Nonisothermal Concentration Cell 205
13.1 The homogeneous phases 207
13.1.1 Entropy production and flux equations for the anode 207
13.1.2 Position dependent transport coefficients 210
13.1.3 The profiles of the homogeneous anode 211
13.1.4 Contributions from the cathode 212
13.1.5 The electrolyte contribution 213
13.2 Surface contributions 214
13.2.1 The anode surface 214
13.2.2 The cathode surface 217
13.3 The thermoelectric potential 218

14 The Transported Entropy 221
14.1 The Seebeck coefficient of cell a 222
14.2 The transported entropy of Pb^{2+} in cell a 226
14.3 The transported entropy of the cation in cell b 227
14.4 The transported entropy of the ions cell c 228
14.5 Transformation properties 230
14.6 Concluding comments 232

15 Adiabatic Electrode Reactions 235
15.1 The homogeneous phases 236
15.1.1 The silver phases 236
15.1.2 The silver chloride phases 236
15.1.3 The electrolyte 237
15.2 The interfaces 237
15.2.1 The silver-silver chloride interfaces 237
15.2.2 The silver chloride-electrolyte interfaces 239
15.3 Temperature and electric potential profiles 240

16 The Liquid Junction Potential 249
16.1 The flux equations for the electrolyte 250
16.2 The liquid junction potential 253
16.3 Liquid junction potential calculations compared 255
16.4 Concluding comments 258

17 The Formation Cell **261**
17.1 The isothermal cell 263
17.1.1 The electromotive force 263
17.1.2 The transference coefficient of the salt in the electrolyte 263
17.1.3 An electrolyte with a salt concentration gradient . 265
17.1.4 The Planck potential derived from ionic fluxes and forces 267
17.2 A non-isothermal cell with a non-uniform electrolyte . . . 268
17.2.1 The homogeneous anode phase 269
17.2.2 The electrolyte 270
17.2.3 The surface of the anode 272
17.2.4 The homogeneous phases and the surface of the cathode 273
17.2.5 The cell potential 275
17.3 Concluding comments 275

18 Power from Regular and Thermal Osmosis **277**
18.1 The potential work of a salt power plant 277
18.2 The membrane as a barrier to transport of heat and mass 279
18.3 Membrane transport of heat and mass 281
18.4 Osmosis 283
18.5 Thermal osmosis 285

19 Modeling the Polymer Electrolyte Fuel Cell **289**
19.1 The potential work of a fuel cell 290
19.2 The cell and its five subsystems 291
19.3 The electrode backing and the membrane 293
19.3.1 The entropy production in the homogeneous phases 293
19.3.2 The anode backing 295
19.3.3 The membrane 298
19.3.4 The cathode backing 300
19.4 The electrode surfaces 301
19.4.1 The anode catalyst surface 304
19.4.2 The cathode catalyst surface 306
19.5 A model in agreement with the second law 307
19.6 Concluding comments 310

20 Measuring Membrane Transport Properties 311
20.1 The membrane in equilibrium with electrolyte solutions . . 312
20.2 The membrane resistivity 312
20.3 Ionic transport numbers 316
20.4 The transference number of water and the water permeability 319
20.5 The Seebeck coefficient 322
20.6 Interdiffusion coefficients 323

21 The Impedance of an Electrode Surface 327
21.1 The hydrogen electrode. Mass balances 328
21.2 The oscillating field 331
21.3 Reaction Gibbs energies 332
21.4 The electrode surface impedance 332
21.4.1 The adsorption-diffusion layer in front of the catalyst 332
21.4.2 The charge transfer reaction 336
21.4.3 The impedance spectrum 337
21.5 A test of the model 338
21.6 The reaction overpotential 339

22 Non-Equilibrium Molecular Dynamics Simulations 341
22.1 The system 344
22.1.1 The interaction potential 346
22.2 Calculation techniques 347
22.3 Verifying the assumption of local equilibrium 351
22.3.1 Local equilibrium in a homogeneous binary mixture 351
22.3.2 Local equilibrium in a gas-liquid interface 353
22.4 Verifications of the Onsager relations 356
22.4.1 A homogeneous binary mixture 356
22.4.2 A gas-liquid interface 358
22.5 Linearity of the flux-force relations 359
22.6 Molecular mechanisms 359

23 The Non-Equilibrium Two-Phase van der Waals Model 361
23.1 Van der Waals equation of states 363
23.2 Van der Waals square gradient model for the interfacial region 366
23.3 Balance equations 369
23.4 The entropy production 371
23.5 Flux equations 372

23.6 A numerical solution method 373
23.7 Procedure for extrapolation of bulk densities and fluxes . . 376
23.8 Defining excess densities 378
23.9 Thermodynamic properties of Gibbs' surface 379
23.10 An autonomous surface 380
23.11 Excess densities depend on the choice of dividing surface . 384
23.11.1 Properties of dividing surfaces 384
23.11.2 Surface excess densities for two dividing surfaces 385
23.11.3 The surface temperature from excess density differences 386
23.12 The entropy balance and the excess entropy production . . 388
23.13 Resistivities to heat and mass transfer 390
23.14 Concluding comments 392

References **393**

Symbol Lists **415**

Index **423**

About the Authors **433**

This page intentionally left blank

Chapter 1

Scope

The aim of this book is to present a systematic theory of transport for heterogeneous systems. The theory is an extension of non-equilibrium thermodynamics for transport in homogeneous phases, a field that was established in 1931 and developed during the nineteen forties and fifties. The foundation to describe transports across surfaces in a systematic way was laid in the nineteen eighties. In this chapter, we put the theory in context and give perspectives on its application.

1.1 What is non-equilibrium thermodynamics?

Non-equilibrium thermodynamics describes transport processes in systems that are out of global equilibrium. The field resulted from the work of many scientists with the overriding aim to find a more useful formulation of the second law of thermodynamics in such systems. The effort started in 1856 with Thomson's studies of thermoelectricity [7]. Onsager however, is counted as the founder of the field with his papers from 1931 [8, 9], see also his collected works [10], because he put earlier research by Thomson, Boltzmann, Nernst, Duhem, Jauman and Einstein into the proper perspective. Onsager was given the Nobel prize in chemistry in 1968 for these works.

In non-equilibrium thermodynamics, the second law is reformulated in terms of the local entropy production in the system, σ, using the assumption of local equilibrium (see Sec. 3.5). The entropy production is given by the product sum of so-called conjugate fluxes, J_i, and forces, X_i, in the system. The second law becomes

$$\sigma = \sum_i J_i X_i \geq 0 \tag{1.1}$$

Each flux is a linear combination of all forces,

$$J_i = \sum_j L_{ij} X_j \tag{1.2}$$

The reciprocal relations

$$L_{ji} = L_{ij} \tag{1.3}$$

were proven for independent forces and fluxes, cf. Chapter 7 by Onsager [8, 9]. They now bear his name. All coefficients are essential, as explained in Chapter 2. In order to use non-equilibrium thermodynamics, one first has to identify the complete set of extensive, independent variables, A_i. We shall do that in Chapters 4–6 for homogeneous phases, surfaces and three phase contact lines respectively. The conjugate fluxes and forces are

$$J_i = dA_i/dt \qquad \text{and} \qquad X_i = \partial S/\partial A_i \tag{1.4}$$

Here t is the time and S is the entropy of the system. Some authors have erroneously stated that any set of fluxes and forces that fulfil (1.1) also obeys (1.3). This is not correct. We also need Eq. (1.4). Equations (1.1) to (1.4) contain all information on the non-equilibrium behavior of the system.

Following Onsager, a systematic theory of non-equilibrium processes was set up in the nineteen forties by Meixner [11–14] and Prigogine [15]. They found the rate of entropy production for a number of physical problems. Prigogine received the Nobel prize in 1977 for his work on the structure of systems that are not in equilibrium (dissipative structures), and Mitchell the year after for his application of the driving force concept to transport processes in biology [16].

Short and essential books were written early by Denbigh [17] and Prigogine [18]. The most general description of classical non-equilibrium thermodynamics is still the 1962 monograph of de Groot and Mazur [19], reprinted in 1985 [20]. Haase's book [21], also reprinted [22], contains many experimental results for systems in temperature gradients. Katchalsky and Curran developed the theory for biological systems [23]. Their analysis was carried further by Caplan and Essig [24], and Westerhoff and van Dam [25]. Førland and coworkers' book gave various applications in electrochemistry, in biology and geology [26]. This book, which presents the theory in a way suitable for chemists, has also been reprinted [27]. A simple introduction to non-equilibrium thermodynamics for engineers is given by Kjelstrup, Bedeaux and Johannessen [28, 29].

Non-equilibrium thermodynamics is all the time being applied in new directions. Fitts showed how to include viscous phenomena [30]. Kuiken [31] gave a general treatment of multicomponent diffusion and rheology of colloidal and other systems. Kinetic theory has been central for studies of evaporation [32–35], and we shall make a link between this theory and non-equilibrium thermodynamics [36–40] (see Chapter 11). A detailed discussion of the link between kinetic theory and non-equilibrium thermodynamics was made by Roldughin and Zhdanov [41]. The relation to the Maxwell–Stefan equations are given in Chapter 12, following Kuiken [31] and Krishna and Wesselingh [42]. Bedeaux and Mazur [43] extended non-equilibrium thermodynamics to quantum mechanical systems. All these efforts have together broadened the scope of non-equilibrium thermodynamics, so that it now appears as a versatile and strong tool for the general description of transport phenomena.

All the applications of non-equilibrium thermodynamics mentioned above use the linear relation between the fluxes and the forces given in Eq. (1.2). For chemical reactions the rate is given by the law of mass action, which is a nonlinear function of the driving force. This excludes a large class of important phenomena from a systematic treatment in terms of classical non-equilibrium thermodynamics. Much effort has therefore been devoted to solve this problem, see [44] for an overview. A promising effort seems to be to expand the variable set by including variables that are relevant for the mesoscopic level. The description on the mesoscopic level can afterwards be integrated to the macroscopic level. This was first done by Prigogine and Mazur, see the monograph by de Groot and Mazur [20], but Rubi and coworkers have pioneered the effort since then [45–47]. In this manner it has been possible to describe activated processes like nucleation [48]. Results compatible with results from kinetic theory [49] were derived [50], and a common thermodynamic basis was given to the Nernst and Butler–Volmer equations [51]. The systematic theory was also extended to active transport in biology [52, 53] and to describe single RNA unfolding experiments [54]. This theoretical branch, called *mesoscopic* non-equilibrium thermodynamics, is however outside the scope of the present book.

Newer books on equilibrium thermodynamics or statistical thermodynamics often include chapters on non-equilibrium thermodynamics, see e.g. [55]. In 1998 Kondepudi and Prigogine [56] presented an integrated approach to equilibrium and non-equilibrium thermodynamics. Öttinger addressed the non-linear regime in his book [57]. An excellent overview of the various extensions of non-equilibrium thermodynamic was given by Muschik *et al.* [44].

1.2 Non-equilibrium thermodynamics in the context of other theories

Non-equilibrium thermodynamics is a theory describing transport on a macroscopic level. Let us compare theories of transport on the particle level, the mesoscopic level, and the macroscopic level. Consider first equilibrium systems on all three levels, see Fig. 1.1. Classical mechanics and quantum mechanics describe the system on the particle level. Statistical mechanics provides the link from the particle level to both the mesoscopic level and the macroscopic level (indicated by arrows in the figure). The mesoscopic level describes the system on an intermediate time and length scale. Equilibrium correlation functions are calculated at this level. The macroscopic level is described by equilibrium thermodynamics, see Chapter 3 in this book. Many of these macroscopic properties can be calculated as integrals over equilibrium correlation functions. The same quantities can also be calculated using ensemble theory.

The description of non-equilibrium systems can be illustrated similarly, see Fig. 1.2. On the particle level, the time-dependence is again described by classical and quantum mechanics, while non-equilibrium statistical mechanics provides the link between this level and the mesoscopic and macroscopic levels. Theories for the particle- and mesoscopic level make it possible to calculate macroscopic transport coefficients. They use expressions for transport coefficients as integrals over equilibrium correlation functions of the fluxes, the Kubo relations. Transport coefficients can also be calculated using non-equilibrium statistical mechanics. The macroscopic level is now described by non-equilibrium thermodynamics. The present book is devoted to this description on the general level (Chapters 7–10) and in many applications (Chapters 11–23).

1.3 The purpose of this book

Most references mentioned above concern transport in homogeneous systems. It is known, however, that much entropy is produced at surfaces between homogeneous phases [41, 58], and the nature of the equations of transport for this region is also unexplored in many ways.

The aim of the present book is to further develop the theory of non-equilibrium thermodynamics to *transport in heterogeneous systems.* The foundation for the work was laid by Bedeaux, Albano and Mazur [2,3], see also Bertrand and Prud'homme [59, 60] and a review by Bedeaux [4]. We gave a short overview of the objectives and the methods used in [61].

Heterogeneous systems distinguish themselves from homogeneous systems by their inclusion of interfaces, or phase boundaries. The interface

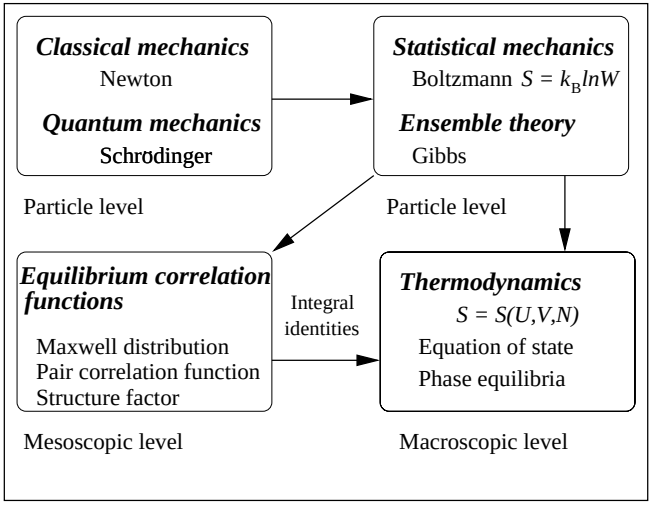

Figure 1.1 Theories for equilibrium systems on the particle-, mesoscopic- and macroscopic level.

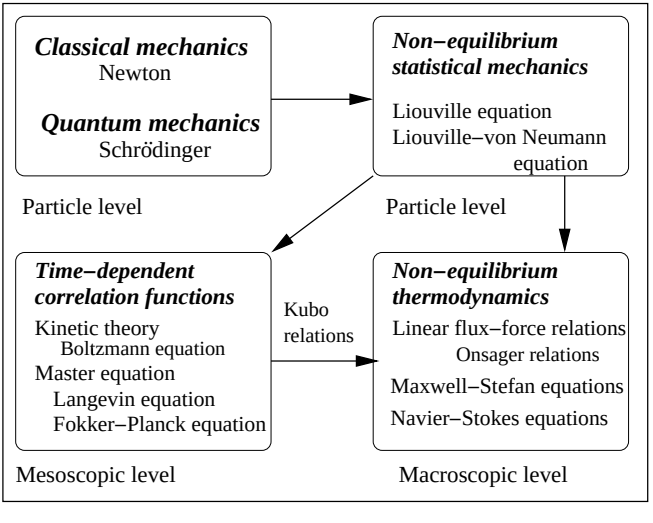

Figure 1.2 Theories for non-equilibrium systems on the particle-, mesoscopic- and macroscopic level.

can, according to Gibbs [62], be regarded as a separate two-dimensional thermodynamic system within the larger three-dimensional system. This implies the introduction of excess densities along the surface. *The purpose of this book is to extend the work of Gibbs to non-equilibrium systems.* This implies the introduction of not only time dependent excess densities for the surface but also of time dependent excess fluxes along the surface. In this manner we shall describe transport of heat, mass and charge and chemical reactions in heterogeneous systems.

Isotropic homogeneous systems have no coupling between vectorial phenomena (transport of heat, mass and charge) and scalar phenomena (chemical reactions). In these systems, the two classes can therefore be dealt with separately [20]. In a two-dimensional surface, all transport processes in the direction normal to the surface become scalar. This means that coupling can occur between transport of heat, mass and charge in that direction, and chemical reactions. The coupling is typical for electrode surfaces, phase transitions and membrane surfaces, and the coupling coefficients are often large. This coupling is special for heterogeneous systems, and is studied in many examples throughout the book. The flux equations at the surfaces give jumps in intensive variables, and define in this manner boundary conditions for integration through the surface. Such integrations can be found in several chapters. Electric potential changes shall be described by a change in the electromotive force, or in the electrochemical potential difference of the ion, which is reversible to the electrode pair [23, 27, 63].

With a short exception for the contact line (Chapter 6), we shall not consider transport along the surface. While this is an extremely important phenomenon, it would be too much new material to cover. We further neglect viscous phenomena. We shall not deal with systems where it is necessary to take fluxes along as variables [64]. We shall not introduce internal variables [45–47]. The transports considered in this book are almost all in the direction normal to the surface, and are therefore one-dimensional.

The book aims to make clear that non-equilibrium thermodynamics is a systematic theory that rests on sound assumptions. The assumption of local equilibrium is valid for systems in large gradients [65, 66], including surfaces [40, 67, 68], and does *not* depend on stationary state conditions, constant external forces, absence of electric polarization or isotropy, as has been claimed, see for instance [22].

Chapter 2

Why Non-Equilibrium Thermodynamics?

This chapter explains what the field of non-equilibrium thermodynamics adds to the analysis of common scientific and engineering problems. Accurate and reliable flux equations can be obtained. Experiments can be well defined. Knowledge of transport properties gives information on the system's ability to convert energy.

The most common industrial and living systems have transport of heat, mass and charge, alone or in combination with a chemical reaction. The process industry, the electrochemical industry, biological systems, as well as laboratory experiments, all concern heterogeneous systems, which are not in global equilibrium. There are four major reasons why non-equilibrium thermodynamics is important for such systems. In the first place, the theory gives an accurate description of coupled transport processes. In the second place, a framework is obtained for the definition of experiments. In the third place; the theory quantifies not only the entropy that is produced during transport, but also the work that is done and the lost work. Last but not least, this theory allows us to check that the thermodynamic equations we use to model our system are in agreement with the second law.

The aim of this book is to give a systematic description of transport in heterogeneous systems. Non-equilibrium thermodynamics has so far mostly been used in science [20,21,27]. Accurate expressions for the fluxes are now required also in engineering [29, 42, 69]. In order to see immediately what non-equilibrium thermodynamics can add to the description of real systems, we compare simple flux equations to flux equations given by non-equilibrium thermodynamics in the following four sections.

2.1 Simple flux equations

The simplest descriptions of heat, mass and charge transports are the equations of Fourier, Fick and Ohm. Fourier's law expresses the measurable heat flux in terms of the temperature gradient by:

$$J'_q = -\lambda \frac{dT}{dx} \tag{2.1}$$

where λ is the thermal conductivity, T is the absolute temperature, and the direction of transport is along the x-axis. Fick's law gives the flux of one of the components in terms of the gradient of its concentration c:

$$J = -D \frac{dc}{dx} \tag{2.2}$$

where D is the diffusion coefficient. Similarly, Ohm's law gives the electric current in terms of the gradient of the electric potential:

$$j = -\kappa \frac{d\phi}{dx} \tag{2.3}$$

where κ is the electrical conductivity, and ϕ is the electric potential.

In a stationary state, there is no accumulation of internal energy, mass or charge. This means that the heat, molar and electric fluxes are independent of position. The derivatives of the above equations with respect to x are then zero:

$$\frac{d}{dx} \lambda \frac{dT}{dx} = 0 \tag{2.4}$$

$$\frac{d}{dx} D \frac{dc}{dx} = 0 \tag{2.5}$$

$$\frac{d}{dx} \kappa \frac{d\phi}{dx} = 0 \tag{2.6}$$

These equations can be used to calculate the temperature, concentration and electric potential as a function of the position, when their values on the boundaries of the system and λ, D and κ are known. Such a calculation is illustrated by the following exercise.

Exercise 2.1.1. *Calculate the temperature as a function of position between two wall's at a distance of 10 cm which are kept at constant temperatures of 5 and 25 ^oC, assuming that the thermal conductivity is constant.*

- **Solution:** According to Eq. (2.4), $d^2T/dx^2 = 0$. The general solution of this equation is $T(x) = a + bx$. The constants a and b follow from the boundary condition. We have $T(0) = 5^oC$ and $T(10) = 25^oC$. It follows that $T(x) = (5 + 2x)^oC$.

Equations (2.1)–(2.3) describe a pure degradation of thermal, chemical and electrical energy. In reality there is also conversion between the energy forms. For an efficient exploitation of energy resources, such a conversion is essential. This is captured in non-equilibrium thermodynamics by the so-called coupling coefficients. Mass transport occurs, for instance, not only because $dc/dx \neq 0$, but also because $dT/dx \neq 0$ or $d\phi/dx \neq 0$.

Chemical and mechanical engineers need theories of transport for increasingly complex systems with gradients in pressure, concentration and temperature. Simple vectorial transport laws have long worked well in engineering, but there is now an increasing effort to be more precise. The books by Taylor and Krishna [69], Kuiken [31] and by Cussler [70], which use Maxwell–Stefan's formulation of the flux equations, are important books in this context. A need for more accurate flux equations in modeling [42, 69] makes non-equilibrium thermodynamics a necessary tool.

2.2 Flux equations with coupling terms

Many natural and man-made processes are not adequately described by the simple flux equations given above. There are, for instance, always large fluxes of mass and heat that accompany charge transport in batteries and electrolysis cells. The resulting local cooling in electrolysis cells may lead to unwanted freezing of the electrolyte. Electrical energy is frequently used to transport mass in biological systems. Large temperature gradients across space ships have been used to supply electric power to the ships. Salt concentration differences between river water and sea water can be used to generate electric power. Pure water can be generated from salt water by application of pressure gradients. In all these more or less randomly chosen examples, one needs transport equations that describe *coupling* between various fluxes. The flux equations given above become too simple.

Non-equilibrium thermodynamics introduces coupling among fluxes. Coupling means that transport of mass will take place in a system not only when the gradient in the chemical potential is different from zero, but also when there are gradients in temperature or electric potential. Coupling between fluxes can describe the phenomena mentioned above.

For example, in a bulk system with transport of heat, mass, and electric charge in the x-direction, we shall find that the linear relations (1.2) take

the form:

$$\begin{aligned} J'_q &= L_{qq}\left(\frac{d}{dx}\frac{1}{T}\right) + L_{q\mu}\left(-\frac{1}{T}\frac{d\mu_T}{dx}\right) + L_{q\phi}\left(-\frac{1}{T}\frac{d\phi}{dx}\right) \\ J &= L_{\mu q}\left(\frac{d}{dx}\frac{1}{T}\right) + L_{\mu\mu}\left(-\frac{1}{T}\frac{d\mu_T}{dx}\right) + L_{\mu\phi}\left(-\frac{1}{T}\frac{d\phi}{dx}\right) \\ j &= L_{\phi q}\left(\frac{d}{dx}\frac{1}{T}\right) + L_{\phi\mu}\left(-\frac{1}{T}\frac{d\mu_T}{dx}\right) + L_{\phi\phi}\left(-\frac{1}{T}\frac{d\phi}{dx}\right) \end{aligned} \tag{2.7}$$

where the forces of transport conjugate to the fluxes J'_q, J and j are the thermal force $d\,(1/T)\,/dx$, the chemical force $[-\,(1/T)\,(d\mu_T/dx)]$, and the electrical force $[-\,(1/T)\,(d\phi/dx)]$, respectively. The subscript T of the chemical potential, μ_T, indicates that the differential should be taken at constant temperature. The electric field is given in terms of the electric potential gradient by $E = -d\phi/dx$.

The L-coefficients are so-called phenomenological coefficients, or Onsager coefficients for conductivity, as we shall call them. The diagonal Onsager coefficients can be related to λ, D, and κ. They are called *main coefficients.* The off-diagonal L-coefficients describe the coupling between the fluxes. They are called *coupling coefficients.* Another common name is cross coefficients. According to Eq. (1.3), we have here three reciprocal relations or *Onsager relations* for these coupling coefficients

$$L_{\mu q} = L_{q\mu}, \qquad L_{q\phi} = L_{\phi q}, \qquad L_{\phi\mu} = L_{\mu\phi} \tag{2.8}$$

The Onsager relations simplify the system. Here, they reduce the number of independent coefficients from nine to six. Coupling coefficients are small in some cases, but large in others. We shall see in Chapter 7 that large coupling coefficients may lead to a low entropy production. This is why the coupling coefficients are so important in the design of industrial systems, see Sec. 2.4. The relation $L_{q\phi} = L_{\phi q}$ is Thomson's second relation, which dates from 1854, see Ref. [7]. Miller [71–74] and Spallek *et al.* [75] gave experimental evidence for the validity of the Onsager relations in electrolytes. Hafskjold and Kjelstrup Ratkje [65] and Xu and coworkers [67] proved their validity for heat and mass transfer, in homogeneous phases and at surfaces, using non-equilibrium molecular dynamics simulations, respectively. Annunziata *et al.* [76] took advantage of the Onsager relations to obtain thermodynamic data for an aqueous mixture of enzyme and salt near the solubility limit of the salt. Onsager's proof of the reciprocal relations shall be discussed in Chapter 7.

2.3 Experimental designs and controls

The importance of equilibrium thermodynamics for the design of experiments is well known. The definition of, say, a partial molar property, explains what shall be varied, and what shall be kept constant in the experimental determination of the quantity. Also, there are relations between thermodynamic variables that offer alternative measurements. For instance, the enthalpy of evaporation can be measured in a calorimeter, but it can also be determined by finding the vapor pressure of the evaporating gas as a function of temperature.

Non-equilibrium thermodynamics is in a similar way, instrumental for design of experiments that aim to find transport properties, cf. Chapter 20. To see this, consider the exercise below.

Exercise 2.3.1. *Find the electric current in terms of the electric field, $E = -d\phi/dx$, using Eq. (2.7), in a system where there is no transport of heat and mass, $J'_q = J = 0$.*

- **Solution:** It follows from Eqs. (2.7a) and (2.7b) that

$$\frac{L_{qq}}{T}\frac{d}{dx}T + L_{q\mu}\frac{d\mu_T}{dx} = L_{q\phi}E \quad \text{and} \quad \frac{L_{\mu q}}{T}\frac{d}{dx}T + L_{\mu\mu}\frac{d\mu_T}{dx} = L_{\mu\phi}E$$

Solving these equations, using the Onsager relations, one finds

$$\frac{1}{T}\frac{d}{dx}T = \frac{L_{q\phi}L_{\mu\mu} - L_{\mu\phi}L_{q\mu}}{L_{qq}L_{\mu\mu} - L_{q\mu}^2}E \quad \text{and} \quad \frac{d\mu_T}{dx} = \frac{L_{qq}L_{\mu\phi} - L_{\mu q}L_{q\phi}}{L_{qq}L_{\mu\mu} - L_{q\mu}^2}E$$

Substitution into Eq. (2.7c) then gives

$$j = \frac{E}{T}\left[L_{\phi\phi} - L_{\phi q}\frac{L_{q\phi}L_{\mu\mu} - L_{\mu\phi}L_{q\mu}}{L_{qq}L_{\mu\mu} - L_{q\mu}^2} - L_{\phi\mu}\frac{L_{qq}L_{\mu\phi} - L_{\mu q}L_{q\phi}}{L_{qq}L_{\mu\mu} - L_{q\mu}^2}\right]$$

This exercise shows that the electric conductivity, that one measures as the ratio of measured values of j and E, is not necessarily given by $L_{\phi\phi}/T$ as one might have thought, considering Eq. (2.7c). In the stationary state, the coupling coefficients lead to temperature and chemical potential gradients, which again affect the electric current. Mathematically speaking, the electric conductivity then becomes a combination of the conductivity of a homogeneous conductor, found if one could measure with zero chemical potential and temperature gradients, and additional terms. The combination of coefficients divided by the temperature, is the stationary state conductivity. The stationary state electric conductivity, measured with $J'_q = J = 0$, is experimentally distinguishable from the Ohmic electric conductivity of

the homogeneous conductor, measured with $dT/dx = d\mu_T/dx = 0$. Non-equilibrium thermodynamics helps define conditions that give well defined experiments.

One important practical consequence of the Onsager relations is to offer alternative measurements for the same property. For instance, if it is difficult to measure the coefficient $L_{q\phi}$, one may rather measure $L_{\phi q}$ [77–80]. A valuable consistency check for measurements is provided if one measures both coupling coefficients in the relation. So, similar to the situation in equilibrium, also the non-equilibrium systems have possibilities for control of internal consistency.

2.4 Entropy production, work and lost work

Non-equilibrium thermodynamics is probably the only method that can be used to assess how energy resources are exploited within a system. This is because the theory deals with energy conversion on the local level in a system, i.e. at the electrode surface [81] or in a biological membrane [52]. By integration to the system level, we obtain a link to exergy analysis [82]. To see the relation between non-equilibrium thermodynamics and exergy analysis, consider again the thermodynamic fluxes and forces, derived from the local entropy production

$$\sigma = \sum_i J_i X_i \geq 0 \tag{2.9}$$

The total entropy production is the integral of σ over the volume V of the system

$$\frac{dS_{\text{irr}}}{dt} = \int \sigma dV \tag{2.10}$$

The quantity dS_{irr}/dt makes it possible to calculate the energy dissipated as heat or the lost work in a system (see below).

In an industrial plant, the materials undergo certain transformations in a time interval dt. Materials are taken in and are leaving the plant at the conditions of the environment. The environment is a natural choice as frame of reference for the analysis. It has constant pressure, p_0 (1 bar), and constant temperature, T_0 (for instance 298 K) and some average composition that needs to be defined. The first law of thermodynamics gives the energy change of the process per unit of time:

$$\frac{dU}{dt} = \frac{dQ}{dt} - p_0 \frac{dV}{dt} + \frac{dW}{dt} \tag{2.11}$$

Here dQ/dt is the rate that heat is delivered to the materials, $p_0 dV/dt$ is the work that the system does per unit of time by volume expansion against the

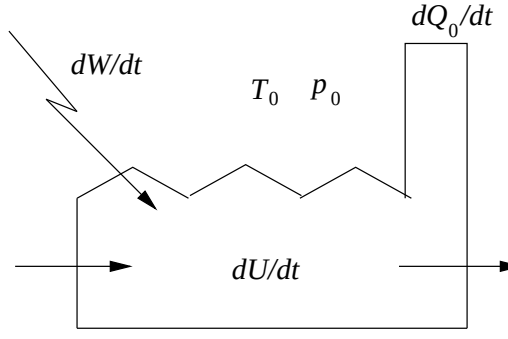

Figure 2.1 A schematic illustration of thermodynamic variables that are essential for the lost work in an industrial plant.

pressure of the environment, and dW/dt is the work done on the materials per unit of time.

The minimum work needed to perform a process, is the least amount of energy that must be supplied, when at the conclusion of the process, the only systems which have undergone any change are the process materials [83]. To see this, we replace dQ/dt by minus the heat delivered to the environment per unit of time, $dQ/dt = -dQ_0/dt$:

$$\frac{dU}{dt} = -\frac{dQ_0}{dt} - p_0\frac{dV}{dt} + \frac{dW}{dt} \tag{2.12}$$

The second law gives

$$\frac{dS}{dt} + \frac{dS_0}{dt} \geq 0 \tag{2.13}$$

where dS/dt is the rate of entropy change of the process materials and dS_0/dt is the rate of entropy change in the environment. For a completely reversible process the sum of these entropy rate changes is zero. For a non-equilibrium process, the sum is *the total entropy production,* dS_{irr}/dt,

$$\frac{dS_{\text{irr}}}{dt} \equiv \frac{dS}{dt} + \frac{dS_0}{dt} \geq 0 \tag{2.14}$$

The entropy change in the surroundings is $dS_0/dt = (dQ_0/dt)/T_0$. By introducing dQ_0/dt into the expression for the entropy production, and combining the result with the first law, we obtain after some rearrangement:

$$\frac{dW}{dt} = T_0\frac{dS_{\text{irr}}}{dt} + \frac{dU}{dt} + p_0\frac{dV}{dt} - T_0\frac{dS}{dt} \tag{2.15}$$

The left hand side of this equation is the work that is needed to accomplish the process with a particular value of the entropy production, $dS_{\rm irr}/dt$. Since $dS_{\rm irr}/dt \geq 0$, the ideal (reversible) work requirement of this process is:

$$\frac{dW_{\rm ideal}}{dt} = \frac{dU}{dt} + p_0\frac{dV}{dt} - T_0\frac{dS}{dt} \tag{2.16}$$

We see that dS/dt changes the ideal work. By comparing Eqs. (2.15) and (2.16), we see that $T_0(dS_{\rm irr}/dt)$ is the additional quantity of work per unit of time that must be used in the actual process, compared to the work in an ideal (reversible) process. Thus, $T_0(dS_{\rm irr}/dt)$ is the wasted or lost work per unit of time:

$$\frac{dW_{\rm lost}}{dt} = T_0\frac{dS_{\rm irr}}{dt} \tag{2.17}$$

The lost work is the energy dissipated as heat in the surroundings. The relation is called the Gouy–Stodola theorem [84, 85]. The right hand side of Eq. (2.16) is also called the time rate of change of the availability or the exergy [62, 82]. We shall learn how to derive σ in subsequent chapters. One aim of the process operator or designer should be to minimize $dW_{\rm lost}/dt$ [86], which is equivalent to entropy production minimization, see Ref. [85] page 227 and Ref. [29] Chapter 6. Knowledge about the sources of entropy production is central for work to improve the energy efficiency of processes. In a recent book "Elements of irreversible thermodynamics for engineers" [28, 29], we discussed how irreversible thermodynamics can be used to map the lost work in an industrial process. The aluminium electrolysis was used as an example to illustrate the importance of such a mapping. Furthermore the first steps in a systematic method for the minimization of entropy production was described, with its basis in non-equilibrium thermodynamics. Second law optimization [85, 87–92] in mechanical and chemical engineering may become increasingly important in the design of systems that waste less work. Non-equilibrium thermodynamics will play a unique role in this context. For details on how to map the second law efficiency of an industrial system or how to systematically improve this efficiency, we refer to Bejan [84, 85] and to the book "Elements of irreversible thermodynamics for engineers" [28, 29].

2.5 Consistent thermodynamic models

The entropy balance of the system and the expression for the entropy production can be used for control of the internal consistency of the thermodynamic description. The change of the entropy in a volume element in a homogeneous phase is given by the flow of entropy in and out of the volume

element and by the entropy production inside the element:

$$\frac{\partial s}{\partial t} = -\frac{\partial}{\partial x} J_s + \sigma \tag{2.18}$$

where we take the entropy flux in the x-direction. In the stationary state, there is no change in the system's entropy and

$$\sigma = \frac{\partial}{\partial x} J_s \tag{2.19}$$

By integrating over the system's extension, keeping its cross-sectional area Ω constant, we obtain

$$\frac{dS_{\mathrm{irr}}}{dt} = \Omega(J_s^{\mathrm{o}} - J_s^{\mathrm{i}}) \tag{2.20}$$

The left hand side is obtained from σ, which is a function of transport coefficients, fluxes and forces, Eqs. (1.1)–(1.3). The right hand side of this equation, the difference in the entropy flows, $J_s^{\mathrm{o}} - J_s^{\mathrm{i}}$, can be calculated from knowledge of the heat flux, and of the entropy carried by components into the surroundings. These quantities do not depend on the system's transport properties. The two calculations must give the same result. Chapter 19 gives an example of such a comparison. Other examples were given by Kjelstrup *et al.* [29], see also Zvolinschi *et al.* [92].

This page intentionally left blank

Chapter 3

Thermodynamic Relations for Heterogeneous Systems

This chapter gives thermodynamic relations for heterogeneous systems that are in global equilibrium, and discusses the meaning of local equilibrium in homogeneous phases, at surfaces and along three phase contact lines.

The heterogeneous systems that are treated in this book exchange heat, mass and charge with their surroundings. The systems have homogeneous phases separated by an interfacial region. They are electroneutral, but polarizable. The words surface and interface will be used interchangeably to indicate the interfacial region. Gibbs [62] calls the interfacial region "the surface of discontinuity". Thermodynamic relations for homogeneous phases, as well as for surfaces, are mandatory for the chapters to follow. Such equations are therefore presented here [62,93]. Equations for the three phase contact line are also given, but are less central. The equations are given first for systems that are in global equilibrium, and next for non-equilibrium systems where only local equilibrium applies.

A thermodynamic description of equilibrium surfaces in terms of excess densities was constructed by Gibbs [62]. This description treats the surface as an autonomous thermodynamic system. We use this description in terms of excess densities as our basis also in non-equilibrium systems. This implies for instance that the surface has its own temperature. All excess densities of a surface depend on this temperature alone and not on the temperatures in the adjacent phases*. We present evidence for this assumption using non-equilibrium molecular dynamics simulations (Chapter 22) and the square gradient model of van der Waals (Chapter 23).

*This property of the surface has been defended by some authors [94,95], but rejected by others [96].

We extend Gibbs' formulation for the surface to the contact line. Equilibrium relations for the three phase contact lines can be formulated for excess *line densities*. The line, described in this manner, is also an autonomous thermodynamic system.

3.1 Two homogeneous phases separated by a surface in global equilibrium

Consider two phases of a multi-component system in equilibrium with each other. The system is polarizable in an electric field. The last property is relevant for electrochemical systems. In systems that transport heat and mass only, this property is not relevant. The homogeneous phases, i and o, have their internal energies, U^{i} and U^{o}, entropies, S^{i} and S^{o}, mole numbers, N_j^{i} and N_j^{o} of the components j (see for instance [97]), and their polarizations in the direction normal to the surface, P^{i} and P^{o}. For the total system, we have:

$$U = U^{\mathrm{i}} + U^{\mathrm{s}} + U^{\mathrm{o}} \tag{3.1}$$

The internal energy for the total system, U, minus the sum of the two bulk values gives the internal energy of the interfacial region U^{s} [62,93]. For the entropy, the mole numbers and the polarization, we similarly have:

$$\begin{aligned} S &= S^{\mathrm{i}} + S^{\mathrm{s}} + S^{\mathrm{o}} \\ N_j &= N_j^{\mathrm{i}} + N_j^{\mathrm{s}} + N_j^{\mathrm{o}} \\ \mathsf{P} &= \mathsf{P}^{\mathrm{i}} + \mathsf{P}^{\mathrm{s}} + \mathsf{P}^{\mathrm{o}} \end{aligned} \tag{3.2}$$

The surface consists of layer(s) of molecules or atoms, with negligible volume, so

$$V = V^{\mathrm{i}} + V^{\mathrm{o}} \tag{3.3}$$

The surface area, Ω, is an extensive variable of the surface, comparable to the volume as a variable of a homogeneous phase. The surface tension, γ, plays a similar role for the surface as the pressures, p^{i} and p^{o}, do for the homogeneous phases.

The polarizations of the homogeneous phases can be expressed in terms of the polarization densities (polarization per unit of volume), P^{i} and P^{o}, by

$$\mathsf{P}^{\mathrm{i}} = P^{\mathrm{i}} V^{\mathrm{i}} \quad \text{and} \quad \mathsf{P}^{\mathrm{o}} = P^{\mathrm{o}} V^{\mathrm{o}} \tag{3.4}$$

The polarization of the surface can similarly be expressed as the polarization per unit of surface area, P^{s}:

$$\mathsf{P}^{\mathrm{s}} = P^{\mathrm{s}} \Omega \tag{3.5}$$

The polarization density is particular for both homogeneous phases and the surface. The system may contain polarizable molecules (apolar), polar molecules and free charges. An electric field leads to polarization of the apolar molecules and to orientation of the polar molecules. Furthermore, it leads to a redistribution of free charges. In all cases, polarization occurs in a manner that keeps homogeneous phases and surfaces electroneutral. For a double layer, we define a surface polarization. For a conductor, we define a polarization density. The divergence of the polarization of a conductor equals the charge distribution, but the induced charge distribution in an electric field integrates to zero net charge.

In this book, we restrict ourselves to surfaces that are planar and contact lines that are straight. From the second Maxwell equation, and the condition of electroneutrality, we have

$$\frac{d}{dx}D = 0 \tag{3.6}$$

where D is the displacement field normal to the surface. The normal component of the displacement field across an electroneutral surface is continuous, and has accordingly no contribution for the surface; $D^{\mathrm{s}} = 0$. The normal component of the displacement field is therefore constant throughout a heterogeneous system. Its value can be controlled from the outside by putting the system between a parallel plate capacitor. In this book, we do not consider electric potential gradients along the surface. Assuming the system furthermore to be invariant for translations along the surface, rotations around a normal on the surface and reflection in planes normal to the surface, it follows that electric fields, displacement fields and polarizations are normal to the surface. The displacement field is related to the electric fields in the two phases by

$$D = \varepsilon_0 E^{\mathrm{i}} + P^{\mathrm{i}} = \varepsilon_{\mathrm{i}} E^{\mathrm{i}} \quad \text{and} \quad D = \varepsilon_0 E^{\mathrm{o}} + P^{\mathrm{o}} = \varepsilon_{\mathrm{o}} E^{\mathrm{o}} \tag{3.7}$$

where ε_{i} and ε_{o} are the dielectric constants of the phases i and o respectively. Furthermore, ε_0 is the dielectric constant of vacuum. A similar relation can be written for the electric field of the surface

$$D^{\mathrm{s}} = 0 = \varepsilon_0 E^{\mathrm{s}} + P^{\mathrm{s}} \rightarrow P^{\mathrm{s}} = -\varepsilon_0 E^{\mathrm{s}} \tag{3.8}$$

For more precise definitions of the interfacial densities we refer to the next section and to Sec. 5.2. For an in-depth discussion of the excess polarization and electric field, we refer to the book by Bedeaux and Vlieger, *Optical Properties of Surfaces* [5, 6].

Remark 3.1. *The surface polarization is equal to minus ε_0 times the excess electric field of the surface. This follows from the following argument:*

The displacement field is the sum of ε_0 times the electric field plus the polarization density. The displacement field is continuous through the surface. The sum of the electric field times ε_0 plus the surface polarization density must therefore be zero.

For heterogeneous, polarizable systems, we can then write the internal energy as a total differential of the extensive variables S, N_j, V, Ω, P^{i}, P^{o} and P^{s}:

$$dU = TdS - pdV + \gamma d\Omega + \sum_{j=1}^{n} \mu_j dN_j + D_{\mathrm{eq}} d\left(\frac{\mathsf{P}^{\mathrm{i}}}{\varepsilon_{\mathrm{i}}} + \frac{\mathsf{P}^{\mathrm{s}}}{\varepsilon_0} + \frac{\mathsf{P}^{\mathrm{o}}}{\varepsilon_{\mathrm{o}}}\right) \tag{3.9}$$

where D_{eq} is the displacement field that derives from a reversible transformation. This is the *Gibbs equation* [62], extended with terms due to polarization. By integrating with constant intensive variables, the energy of the system becomes

$$U = TS - pV + \gamma\Omega + \sum_{j=1}^{n} \mu_j N_j + D_{\mathrm{eq}} \left(\frac{\mathsf{P}^{\mathrm{i}}}{\varepsilon_{\mathrm{i}}} + \frac{\mathsf{P}^{\mathrm{s}}}{\varepsilon_0} + \frac{\mathsf{P}^{\mathrm{o}}}{\varepsilon_{\mathrm{o}}}\right) \tag{3.10}$$

Since we are dealing with state functions, this result is generally valid. The contributions to the internal energy from the polarization are $D_{\mathrm{eq}}\mathsf{P}^{\mathrm{i}}/\varepsilon_{\mathrm{i}}$ and $D_{\mathrm{eq}}\mathsf{P}^{\mathrm{o}}/\varepsilon_{\mathrm{o}}$ in the homogeneous phases and $D_{\mathrm{eq}}\mathsf{P}^{\mathrm{s}}/\varepsilon_0$ [3] for the surface.

Remark 3.2. *The contributions to the total polarization, i.e. from polarizable molecules, from polar molecules and from free charges, have very different relaxation times. They should therefore be counted as separate contributions $\mathsf{P}^{\alpha} = \sum_k \mathsf{P}^{\alpha}_k$, where α equals i, o or s. The corresponding equilibrium displacement fields, $D_{eq,k}$, found from a reversible transformation, are also different for the different contributions to the polarization. We shall not make the formulae more cumbersome by distinguishing these different contributions.*

The surface tension is, like the pressure, a function of T, μ_j, and D_{eq}. The most directly observable effect of the surface tension is found when the interface between two phases is curved. Consider for instance a spherical bubble in a liquid. The pressure inside the bubble is higher than the pressure outside. The same is true for a liquid droplet in air. The pressure difference, called the capillary pressure, is given in terms of the surface tension by $2\gamma/\mathrm{R}$, where R is the radius of the droplet. The capillary pressure is the reason why water rises in a capillary. The following exercise demonstrates that the energy represented by a surface can be compared to the energy of a homogeneous phase.

Exercise 3.1.1. *Use the expression for the capillary pressure to derive a formula for the rise of liquid in a capillary as function of the diameter d of the capillary. The liquid wets the surface. Calculate the capillary rise of water in a capillary with a diameter of a micron. The surface tension of water is* $\gamma_w = 75 \times 10^{-3}$ *N/m.*

- **Solution:** If the diameter of the capillary is not too large, and when the liquid wets the surface, the interface between the water and the air is a half sphere with radius $d/2$. This gives a capillary pressure of $4\gamma/d$. This would cause an under-pressure in the liquid below the surface. In order to have a normal atmospheric pressure at the bottom of the capillary, the water rises until the weight of the column gives the capillary pressure. This implies that $\pi(d/2)^2 hg\rho/\pi(d/2)^2 = hg\rho = 4\gamma/d$ where h is the height of the column, ρ is the density in kg/m^3 of water and g is the acceleration of gravity. The capillary rise is therefore $h = 4\gamma/dg\rho$. In a capillary with a diameter of a micron, the capillary rise of water is 30 m.

In this book we restrict ourselves to surfaces that are flat. The equilibrium pressure is therefore always constant throughout the system, $p^{\mathrm{i}} = p^{\mathrm{o}} = p$.

The Gibbs equation (3.9) gives the energy of both homogeneous phases plus the surface. We need also equations for the separate homogeneous phases and for the surface alone. With Eqs. (3.1)–(3.3), we have for phase i:

$$dU^{\mathrm{i}} = TdS^{\mathrm{i}} - pdV^{\mathrm{i}} + \sum_{j=1}^{n} \mu_j dN_j^{\mathrm{i}} + D_{\mathrm{eq}} d\frac{\mathsf{P}^{\mathrm{i}}}{\varepsilon_{\mathrm{i}}} \tag{3.11}$$

This is the Gibbs equation for phase i. We integrate the equation for constant composition, temperature, pressure and displacement field. This gives:

$$U^{\mathrm{i}} = TS^{\mathrm{i}} - pV^{\mathrm{i}} + \sum_{j=1}^{n} \mu_j N_j^{\mathrm{i}} + D_{\mathrm{eq}} \frac{\mathsf{P}^{\mathrm{i}}}{\varepsilon_{\mathrm{i}}} \tag{3.12}$$

The energy is a state function, so the result is generally valid (compare Eq. (3.10)). By differentiating this expression and subtracting Eq. (3.11), we obtain Gibbs–Duhem's equation:

$$0 = S^{\mathrm{i}} dT - V^{\mathrm{i}} dp + \sum_{j=1}^{n} N_j^{\mathrm{i}} d\mu_j + \frac{\mathsf{P}^{\mathrm{i}}}{\varepsilon_{\mathrm{i}}} dD_{\mathrm{eq}} \tag{3.13}$$

Similar equations can be written for phase o.

The Gibbs equation for the surface is likewise:

$$dU^{\mathrm{s}} = TdS^{\mathrm{s}} + \gamma d\Omega + \sum_{j=1}^{n} \mu_j dN_j^{\mathrm{s}} + \left(\frac{D_{\mathrm{eq}}}{\varepsilon_0}\right) d\mathsf{P}^{\mathrm{s}} \tag{3.14}$$

By integration for constant surface tension, temperature, composition and displacement field, we obtain

$$U^{\mathrm{s}} = TS^{\mathrm{s}} + \gamma\Omega + \sum_{j=1}^{n} \mu_j N_j^{\mathrm{s}} + \left(\frac{D_{\mathrm{eq}}}{\varepsilon_0}\right) \mathsf{P}^{\mathrm{s}} \tag{3.15}$$

Gibbs–Duhem's equation for the surface follows by differentiating this equation and subtracting Eq. (3.14):

$$0 = S^{\mathrm{s}}dT + \Omega d\gamma + \sum_{j=1}^{n} N_j^{\mathrm{s}} d\mu_j + \mathsf{P}^{\mathrm{s}} d\left(\frac{D_{\mathrm{eq}}}{\varepsilon_0}\right) \tag{3.16}$$

The thermodynamic relations for the autonomous surface, Eqs. (3.14)-(3.16), are identical in form to the thermodynamic relations for the homogeneous phases, compare Eqs. (3.11)–(3.13).

Global equilibrium in a heterogeneous, polarizable system in a displacement field can now be defined. The chemical potentials and the temperature are constant throughout the system

$$\begin{aligned} \mu_j^{\mathrm{i}} &= \mu_j^{\mathrm{s}} = \mu_j^{\mathrm{o}} = \mu_j \\ T^{\mathrm{i}} &= T^{\mathrm{s}} = T^{\mathrm{o}} = T \end{aligned} \tag{3.17}$$

Furthermore, the normal component of the pressure and of the displacement field are the same in the adjacent homogeneous phases:

$$p^{\mathrm{i}} = p^{\mathrm{o}} = p \quad \text{and} \quad D_{\mathrm{eq}} \text{ constant} \tag{3.18}$$

For curved surfaces the normal component of the pressure is not constant and we refer to Blokhuis, Bedeaux and Groenewold [98–103].

The surface energy, and therefore also the surface entropy and surface mole numbers, have so far been defined from the total values minus the bulk values. We shall see in Sec. 3.3, how more direct definitions can be formulated.

3.2 The contact line in global equilibrium

Consider three phases of a multi-component system in equilibrium with each other. The three surfaces separating these phases come together in a contact

line. For simplicity, we assume that the contact line is not polarizable. In the previous section we have seen that the thermodynamic relations for an autonomous surface has the same form as for homogeneous phases. The same is true for the autonomous three-phase contact line. The Gibbs equation for the contact line is:

$$dU^{\mathrm{c}} = TdS^{\mathrm{c}} + \gamma^{\mathrm{c}} dL + \sum_{j=1}^{n} \mu_j dN_j^{\mathrm{c}} \tag{3.19}$$

Superscript c indicates a contribution of the contact line, γ^{c} is the line tension and L is the length of the line. The curvature of the line is assumed to be negligible, so that there are no contributions to dU^{c} from changes in the curvature. By integration for constant line tension, temperature and composition, we obtain

$$U^{\mathrm{c}} = TS^{\mathrm{c}} + \gamma^{\mathrm{c}} L + \sum_{j=1}^{n} \mu_j N_j^{\mathrm{c}} \tag{3.20}$$

The line energy, and therefore also the line entropy and the line mole numbers, have here been defined as the total values minus the bulk and the surface values.

Gibbs–Duhem's equation for the line follows by differentiating this equation and subtracting Eq. (3.19):

$$0 = S^{\mathrm{c}} dT + Ld\gamma^{\mathrm{c}} + \sum_{j=1}^{n} N_j^{\mathrm{c}} d\mu_j \tag{3.21}$$

When the contact line is part of a heterogeneous system in global equilibrium, the chemical potentials and the temperature are constant throughout the system. For the contact line, we therefore also have

$$\mu_j^{\mathrm{c}} = \mu_j \quad \text{and} \quad T^{\mathrm{c}} = T \tag{3.22}$$

More direct definitions of thermodynamic properties of the line, can be obtained, following the procedure for the surface in the next section.

3.3 Defining thermodynamic variables for the surface

The relations for global equilibrium cannot be used to describe systems with gradients in μ, p, T or the electric field. We must therefore also formulate relations for local equilibrium. We need local forms of the Gibbs and Gibbs–Duhem equations. These will be given after we have first defined the surface variables.

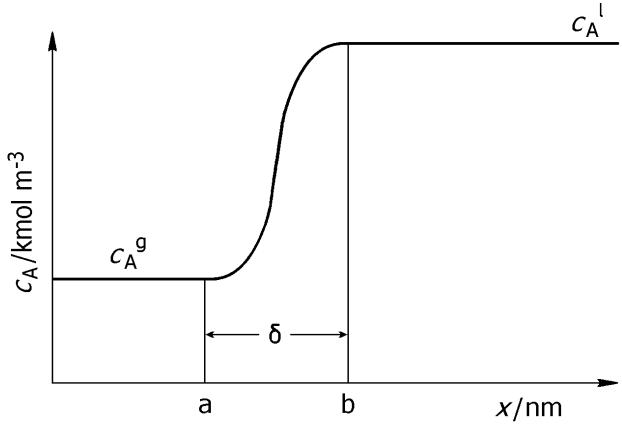

Figure 3.1 Variation in the molar density of a fluid if we go from the gas to the liquid state. The vertical lines indicate the extension of the surface. The scale of the x-axis is measured in nanometer.

An *interface* is the thin layer between two homogeneous phases. We restrict ourselves to flat surfaces, that are perpendicular to the x-axis. The thermodynamic properties of the interface shall now be given by the values of the excess densities of the interface. The value of these densities and the location of the interface will be defined through the example of a gas-liquid interface. We shall correspondingly indicate these phases with the superscripts g and l.

Figure 3.1 shows the variation in concentration of A, in a mixture of several components, as we go from the gas to the liquid phase. The surface thickness is usually a fraction of a nm. The x-axis of Fig. 3.1 has coordinates in nm, it has a molecular scale. A continuous variation in the concentration is seen. Gibbs [62] defined the *surface of discontinuity* as a transition region with a finite thickness bounded by planes of similarly chosen points. In the figure two such planes are indicated by vertical lines. The position a is the point in the gas left of the closed surface where $c_A(x)$ starts to *differ* from the concentration of the gas, c_A^g, and the position b is the point in the liquid right of the closed surface, where $c_A(x)$ starts to *differ* from the concentration of the liquid, c_A^l. The surface thickness is then $\delta = b - a$. It refers to component A. Other components may yield somewhat different planes.

Gibbs defined the *dividing surface* as "a geometrical plane, going through points in the interfacial region, similarly situated with respect to

conditions of adjacent matter". Many different planes of this type can be chosen. While the position of the dividing surface depends on this choice; it is normally somewhere between the vertical lines in Fig. 3.1. The planes that separate the closed surface from the homogeneous phases are parallel to the dividing surface. The continuous density, integrated over δ, gives the *excess* surface concentration of the component A as a function of the position, (y, z), along the surface:

$$\Gamma_{\mathrm{A}}(y,z) = \int_a^b \left[c_{\mathrm{A}}(x,y,z) - c_{\mathrm{A}}^{\mathrm{g}}(a,y,z)\theta(d-x) - c_{\mathrm{A}}^{\mathrm{l}}(b,y,z)\theta(x-d)\right] dx \tag{3.23}$$

where d is the position of the dividing surface. The surface concentration is often called the *adsorption* (in $\mathrm{mol/m^2}$). The Heaviside function, θ, is by definition unity when the argument is positive and zero when the argument is negative. It is common to choose d between a and b. Other excess variables than Γ_{A} are defined similarly. All excess properties of a surface can be given by integrals like Eq. (3.23). The excess variables are the extensive variables of the surface. They describe how the surface *differs* from adjacent homogeneous phases.

Remark 3.3. *It is clear from Fig. 3.1 that one may shift the position a to the left and b to the right without changing the adsorption. This shows why the precise location of a and b is not important for the value of the adsorption.*

Gibbs defined the excess concentrations for global equilibrium. Equation (3.23) will be used in this book also for systems which are not in global equilibrium. In fact, Γ_{A}, c_{A}, $c_{\mathrm{A}}^{\mathrm{g}}$ and $c_{\mathrm{A}}^{\mathrm{l}}$ as well as a, b and d, may all depend on the time. For ease of notation this was not explicitly indicated.

The *equimolar surface* of component A is a special dividing surface. The location is such that the surplus of moles of the component on one side of the surface is equal to the deficiency of moles of the component on the other side of the surface, see Fig. 3.2. The position, d, of the equimolar surface obeys:

$$\int_a^d \left[c_{\mathrm{A}}(x,y,z) - c_{\mathrm{A}}^{\mathrm{g}}(a,y,z)\right] dx = -\int_d^b \left[c_{\mathrm{A}}(x,y,z) - c_{\mathrm{A}}^{\mathrm{l}}(b,y,z)\right] dx \tag{3.24}$$

According to Eqs. (3.23) and (3.24), $\Gamma_A = 0$, when the surface has this position, see Fig. 3.2. The shaded areas in the figure are equal. In a multi-component systems, each component has its "equimolar" surface, but we have to make one choice for the position of the dividing surface. We usually choose the position of the surface as the equimolar surface of the

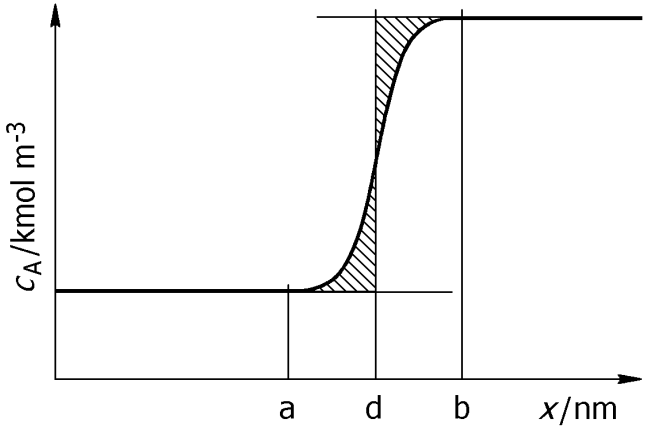

Figure 3.2 Determination of the position of the equimolar surface of component A. The vertical line is drawn so that the areas between the curve and the bulk densities are the same.

reference component. This component has then no excess concentration, while another component B, like the one sketched in Fig. 3.3, has an excess concentration.

Remark 3.4. *In homogeneous phases it is common to use densities per mole or per unit of mass. For the surface this is possible, but not practical. The reason for this is that this would imply dividing the extensive properties of the surface by the excess molar density of the reference component. As we have just explained it is common to use the equimolar surface defined by this reference component. In that case the excess molar density of the reference component is zero and we cannot divide by it. To avoid confusion we will always use excess densities per unit of surface area.*

Thermodynamic properties of homogeneous systems are usually plotted on scales with greater dimension than nm. In Fig. 3.4, $c_A(x)$ is plotted on a μm scale. The fine details of Fig. 3.1 disappear, and the surface appears as a discontinuity. When plotted on a macroscopic scale, a non-zero excess surface density, like that of component B, appears as a singularity at the position of the dividing surface. On this scale the possible choices of the dividing surface can no longer be distinguished, and the surface can be regarded as a two-dimensional thermodynamic system. The system has properties that are integrated out in the x-direction and are given per surface area. Dependence on the coordinates y and z remains. When excess

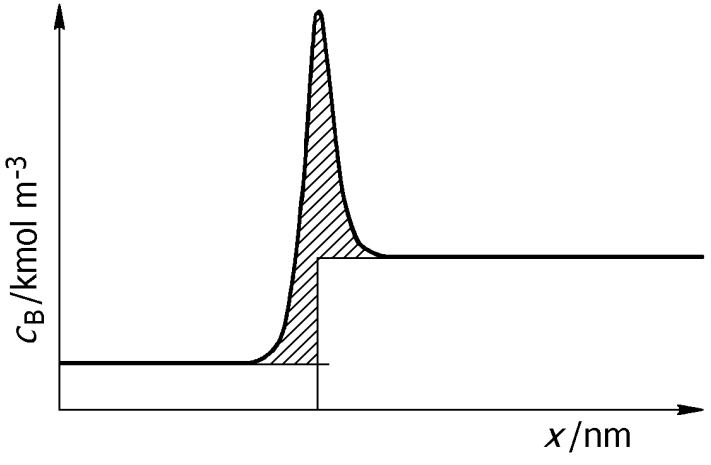

Figure 3.3 Variation in the density of component B across the surface. The excess surface concentration of component B is the integral under the curve in the figure.

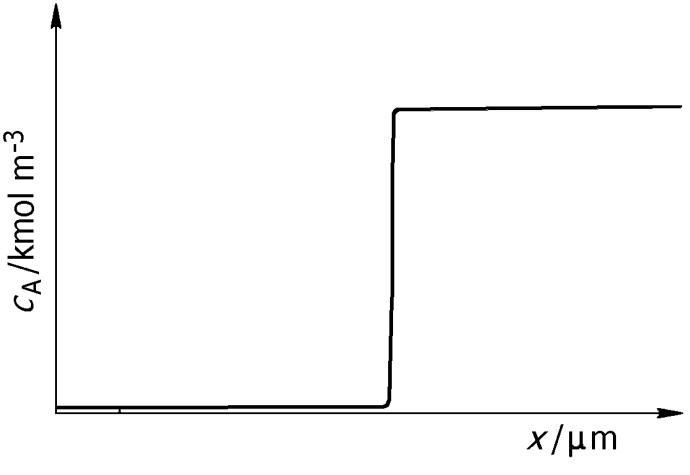

Figure 3.4 The equimolar surface plotted on a micrometer scale appears as a jump between bulk densities.

surface densities are defined in this manner, the normal thermodynamic relations, like the first and second laws are valid [62].

Remark 3.5. *Excess densities for the surface can be much larger than the typical value of the integrated quantity times the thickness of the surface of discontinuity. The surface tension of a liquid-vapor is for instance a factor between 10^3 to 10^4 larger than the typical pressure of 1 bar times 3 Angstroms. This implies that contributions from the surface play a much more important role than what the volume of the surface of discontinuity would suggest.*

Van der Waals constructed a continuous model for the liquid-vapor interface at equilibrium, around the end of the 19th century [104]. In this model one adds to the Helmholtz energy density per unit of volume a contribution proportional to the square of the gradient of the density. It is therefore often called the square gradient model. The model was reinvented by Cahn and Hilliard in 1958 [105]. It has become an important model for studies of the equilibrium structure of the interface [93,102]. The model gives a density profile through the closed surface and enables one to calculate, for instance, the surface tension. An extension of his model to non-equilibrium systems [106–108] is discussed in Chapter 23. It is found in the context of this model [107] that the surface, as described by excess densities, is in local equilibrium.

Exercise 3.3.1. *The variation in density of A across a vapor-liquid interface between $a = 0$ and $b = 5$ nm is given by $c_A(x) = Cx^3 + 50$ mol/m^3. The vapor density is $c_A^g = 50$ mol/m^3 and the liquid density is $c_A^l = 50000$ mol/m^3. Determine the value of C and the position of the equimolar surface.*

- **Solution:** The density function at b gives

$$C(5 \times 10^{-9})^3 + 50 = 5 \times 10^4 \Rightarrow C = 4 \times 10^{29} \text{mol/m}^6$$

For the equimolar surface, we have:

$$\int_0^d Cx^3 dx = -\int_d^b (Cx^3 - 49950)dx$$

$$\Rightarrow \frac{1}{4}Cd^4 = -\frac{1}{4}C(b^4 - d^4) + 49950(b - d)$$

This results in the position $d = 3.75$ nm. The equimolar surface is close to the liquid side.

3.4 Local thermodynamic identities

In the first section of this chapter, we considered a heterogeneous system in global equilibrium. The temperature, the chemical potentials, the pressure and the displacement field were constant throughout the system, Eqs. (3.17) and (3.18). In the previous section, we defined excess densities using expressions that can also be used in non-equilibrium systems. In order to use the thermodynamic identities from the first section for the excess densities, we need to cast the Gibbs equation and its equivalent forms into a local form.

For the homogeneous phases we introduce the extensive variables per unit of volume. In the i-phase we then have $u^{\mathrm{i}} = U^{\mathrm{i}}/V^{\mathrm{i}}$, $s^{\mathrm{i}} = S^{\mathrm{i}}/V^{\mathrm{i}}$, $c_j^{\mathrm{i}} = N_j^{\mathrm{i}}/V^{\mathrm{i}}$ and the polarization density P^{i}. By dividing Eq. (3.12) by V^{i} the internal energy density becomes

$$u^{\mathrm{i}} = Ts^{\mathrm{i}} - p + \sum_{j=1}^{n} \mu_j c_j^{\mathrm{i}} + D_{\mathrm{eq}} \frac{P^{\mathrm{i}}}{\varepsilon_{\mathrm{i}}} \tag{3.25}$$

By replacing U^{i} by $u^{\mathrm{i}}V^{\mathrm{i}}$ etc. in Eq. (3.11), differentiating and using Eq. (3.25), we obtain:

$$du^{\mathrm{i}} = Tds^{\mathrm{i}} + \sum_{j=1}^{n} \mu_j dc_j^{\mathrm{i}} + D_{\mathrm{eq}} d\frac{P^{\mathrm{i}}}{\varepsilon_{\mathrm{i}}} \tag{3.26}$$

Gibbs–Duhem's equation becomes

$$0 = s^{\mathrm{i}} dT - dp + \sum_{j=1}^{n} c_j^{\mathrm{i}} d\mu_j + \frac{P^{\mathrm{i}}}{\varepsilon_{\mathrm{i}}} dD_{\mathrm{eq}} \tag{3.27}$$

All quantities in these equations refer now to a local position in space.

All expressions for phase i, are also true for phase o. (Replace all the super- and subscripts i by o). Other thermodynamic relations can also be defined. We give below the i-phase internal energy, Gibbs energy, Helmholtz energy, internal energy density, Gibbs energy density and the Helmholtz

energy density:

$$
\begin{aligned}
U^{\mathrm{i}} &= TS^{\mathrm{i}} - pV^{\mathrm{i}} + \sum_{j=1}^{n} \mu_j N_j^{\mathrm{i}} + D_{\mathrm{eq}} \left(\mathsf{P}^{\mathrm{i}} / \varepsilon_{\mathrm{i}} \right) \\
G^{\mathrm{i}} &\equiv U^{\mathrm{i}} - TS^{\mathrm{i}} + pV^{\mathrm{i}} = \sum_{j=1}^{n} \mu_j N_j^{\mathrm{i}} + D_{\mathrm{eq}} \left(\mathsf{P}^{\mathrm{i}} / \varepsilon_{\mathrm{i}} \right) \\
F^{\mathrm{i}} &\equiv U^{\mathrm{i}} - TS^{\mathrm{i}} = -pV^{\mathrm{i}} + \sum_{j=1}^{n} \mu_j N_j^{\mathrm{i}} + D_{\mathrm{eq}} \left(\mathsf{P}^{\mathrm{i}} / \varepsilon_{\mathrm{i}} \right) \\
u^{\mathrm{i}} &= Ts^{\mathrm{i}} - p + \sum_{j=1}^{n} \mu_j c_j^{\mathrm{i}} + D_{\mathrm{eq}} \left(P^{\mathrm{i}} / \varepsilon_{\mathrm{i}} \right) \\
g^{\mathrm{i}} &= u^{\mathrm{i}} - Ts^{\mathrm{i}} + p = \sum_{j=1}^{n} \mu_j c_j^{\mathrm{i}} + D_{\mathrm{eq}} \left(P^{\mathrm{i}} / \varepsilon_{\mathrm{i}} \right) \\
f^{\mathrm{i}} &= u^{\mathrm{i}} - Ts^{\mathrm{i}} = -p + \sum_{j=1}^{n} \mu_j c_j^{\mathrm{i}} + D_{\mathrm{eq}} \left(P^{\mathrm{i}} / \varepsilon_{\mathrm{i}} \right)
\end{aligned}
\tag{3.28}
$$

For the surface, the local variables are given per unit of surface area. These are the excess internal energy density $u^{\mathrm{s}} = U^{\mathrm{s}}/\Omega$, the adsorptions $\Gamma_j = N_j^{\mathrm{s}}/\Omega$, the excess entropy density, $s^{\mathrm{s}} = S^{\mathrm{s}}/\Omega$, and the surface polarization, P^{s}. When we introduce these variables into Eq. (3.14), and use Eq. (3.15), we obtain the Gibbs equation for the surface:

$$
du^{\mathrm{s}} = Tds^{\mathrm{s}} + \sum_{j=1}^{n} \mu_j d\Gamma_j + D_{\mathrm{eq}} d\frac{P^{\mathrm{s}}}{\varepsilon_0} \tag{3.29}
$$

The surface excess internal energy density is

$$
u^{\mathrm{s}} = Ts^{\mathrm{s}} + \gamma + \sum_{j=1}^{n} \mu_j \Gamma_j + D_{\mathrm{eq}} \frac{P^{\mathrm{s}}}{\varepsilon_0} \tag{3.30}
$$

and Gibbs–Duhem's equation becomes

$$
0 = s^{\mathrm{s}} dT + d\gamma + \sum_{j=1}^{n} \Gamma_j d\mu_j + \frac{P^{\mathrm{s}}}{\varepsilon_0} dD_{\mathrm{eq}} \tag{3.31}
$$

We give below the surface internal energy, surface internal energy density, Gibbs equation, Gibbs–Duhem's equation, surface Gibbs energy density

and the surface Helmholtz energy density:

$$\begin{aligned}
U^{\mathrm{s}} &= TS^{\mathrm{s}} + \gamma\Omega + \sum_{j=1}^{n} \mu_j N_j^{\mathrm{s}} + D_{\mathrm{eq}} \left(\mathsf{P}^{\mathrm{s}}/\varepsilon_0\right) \\
u^{\mathrm{s}} &= Ts^{\mathrm{s}} + \gamma + \sum_{j=1}^{n} \mu_j \Gamma_j + D_{\mathrm{eq}} \left(P^{\mathrm{s}}/\varepsilon_0\right) \\
du^{\mathrm{s}} &= Tds^{\mathrm{s}} + \sum_{j=1}^{n} \mu_j d\Gamma_j + D_{\mathrm{eq}} d\left(P^{\mathrm{s}}/\varepsilon_0\right) \\
0 &= s^{\mathrm{s}} dT + d\gamma + \sum_{j=1}^{n} \Gamma_j d\mu_j + \left(P^{\mathrm{s}}/\varepsilon_0\right) dD_{\mathrm{eq}} \\
g^{\mathrm{s}} &= u^{\mathrm{s}} - Ts^{\mathrm{s}} - \gamma = \sum_{j=1}^{n} \mu_j \Gamma_j + D_{\mathrm{eq}} \left(P^{\mathrm{s}}/\varepsilon_0\right) \\
f^{\mathrm{s}} &= u^{\mathrm{s}} - Ts^{\mathrm{s}} = \gamma + \sum_{j=1}^{n} \mu_j \Gamma_j + D_{\mathrm{eq}} \left(P^{\mathrm{s}}/\varepsilon_0\right)
\end{aligned} \tag{3.32}$$

For the contact line, local variables are given per unit of length. These are the excess internal energy density $u^{\mathrm{c}} = U^{\mathrm{c}}/L$, the adsorptions $\Gamma_j^{\mathrm{c}} = N_j^{\mathrm{c}}/L$ and the excess entropy density, $s^{\mathrm{c}} = S^{\mathrm{c}}/L$. When we introduce these variables into Eq. (3.19), and use Eq. (3.20), we obtain the Gibbs equation for the line:

$$du^{\mathrm{c}} = Tds^{\mathrm{c}} + \sum_{j=1}^{n} \mu_j d\Gamma_j^{\mathrm{c}} \tag{3.33}$$

The contact line excess internal energy density is

$$u^{\mathrm{c}} = Ts^{\mathrm{c}} + \gamma^{\mathrm{c}} + \sum_{j=1}^{n} \mu_j \Gamma_j^{\mathrm{c}} \tag{3.34}$$

and Gibbs-Duhem's equation becomes

$$0 = s^{\mathrm{c}} dT + d\gamma^{\mathrm{c}} + \sum_{j=1}^{n} \Gamma_j^{\mathrm{c}} d\mu_j \tag{3.35}$$

Thermodynamic relations for the contact line are given below. We give the line internal energy, line internal energy density, Gibbs equation, Gibbs–Duhem's equation, contact line Gibbs energy density and the contact line

Helmholtz energy density:

$$\begin{aligned} U^{\mathrm{c}} &= TS^{\mathrm{c}} + \gamma^{\mathrm{c}} L + \sum_{j=1}^{n} \mu_j N_j^{\mathrm{c}} \\ u^{\mathrm{c}} &= Ts^{\mathrm{c}} + \gamma^{\mathrm{c}} + \sum_{j=1}^{n} \mu_j \Gamma_j^{\mathrm{c}} \\ du^{\mathrm{c}} &= Tds^{\mathrm{c}} + \sum_{j=1}^{n} \mu_j d\Gamma_j^{\mathrm{c}} \\ 0 &= s^{\mathrm{c}} dT + d\gamma^{\mathrm{c}} + \sum_{j=1}^{n} \Gamma_j^{\mathrm{c}} d\mu_j \\ g^{\mathrm{c}} &= u^{\mathrm{c}} - Ts^{\mathrm{c}} - \gamma^{\mathrm{c}} = \sum_{j=1}^{n} \mu_j \Gamma_j^{\mathrm{c}} \\ f^{\mathrm{c}} &= u^{\mathrm{c}} - Ts^{\mathrm{c}} = \gamma^{\mathrm{c}} + \sum_{j=1}^{n} \mu_j \Gamma_j^{\mathrm{c}} \end{aligned} \tag{3.36}$$

3.5 Defining local equilibrium

We have so far considered global and local thermodynamic relations for heterogeneous systems that are in *global equilibrium*. We shall now move one step further and introduce the assumption of local equilibrium. For a volume element in the homogeneous phase i, we say, following Fitts [30], Bedeaux and Kjelstrup [61] and Ortiz and Sengers [109], that there is *local equilibrium* when the thermodynamic relations (3.25)–(3.27) are valid:

$$\begin{aligned} u^{\mathrm{i}}(x,t) &= T^{\mathrm{i}}(x,t) s^{\mathrm{i}}(x,t) - p^{\mathrm{i}}(x,t) + \sum_{j=1}^{n} \mu_j^{\mathrm{i}}(x,t) c_j^{\mathrm{i}}(x,t) + D_{\mathrm{eq}}(t) \frac{P^{\mathrm{i}}(x,t)}{\varepsilon_{\mathrm{i}}} \\ du^{\mathrm{i}}(x,t) &= T^{\mathrm{i}}(x,t) ds^{\mathrm{i}}(x,t) + \sum_{j=1}^{n} \mu_j^{\mathrm{i}}(x,t) dc_j^{\mathrm{i}}(x,t) + D_{\mathrm{eq}}(t) d\frac{P^{\mathrm{i}}(x,t)}{\varepsilon_{\mathrm{i}}} \\ 0 &= s^{\mathrm{i}}(x,t) dT^{\mathrm{i}}(x,t) - dp^{\mathrm{i}}(x,t) + \sum_{j=1}^{n} c_j^{\mathrm{i}}(x,t) d\mu_j^{\mathrm{i}}(x,t) + \frac{P^{\mathrm{i}}(x,t)}{\varepsilon_{\mathrm{i}}} dD_{\mathrm{eq}}(t) \end{aligned} \tag{3.37}$$

The position and time dependence of all the quantities are now explicitly indicated. We used that D_{eq} is independent of the position in electroneutral systems. The subscript "eq" of the electric field indicates that this

is the value of the electric field when the system is in global equilibrium, with entropy density, concentrations and polarization density constant and equal to the values of the volume element. The actual displacement field in the volume element is not equal to $D_{\mathrm{eq}}(t)$ when the system is not in global equilibrium. Local equilibrium is defined in the same manner for the o-phase.

The use of the word local in this context means that the quantities are averages over sensibly chosen volume elements and time intervals. By a sensibly chosen volume element, we mean a volume element that is large compared to microscopic distances, and small compared to the distance over which the averaged quantities vary. A sensibly chosen time interval is long compared to microscopic times, but small compared to the time rate of variation of the averaged quantities. The choices of the size of the volume element and the time interval are not independent. With a slowly varying process, the volume element may be chosen small, and the time interval large. These statements can be made precise by non-equilibrium molecular dynamics simulations, see Chapter 22.

For a surface element, we say that there is *local equilibrium* when the thermodynamic relations (3.29)–(3.31) are valid:

$$u^{\mathrm{s}}(t) = T^{\mathrm{s}}(t)s^{\mathrm{s}}(t) + \gamma(t) + \sum_{j=1}^{n} \mu_j^{\mathrm{s}}(t)\Gamma_j(t) + D_{\mathrm{eq}}(t)\frac{P^{\mathrm{s}}(t)}{\varepsilon_0}$$

$$du^{\mathrm{s}}(t) = T^{\mathrm{s}}(t)ds^{\mathrm{s}}(t) + \sum_{j=1}^{n} \mu_j^{\mathrm{s}}(t)d\Gamma_j(t) + D_{\mathrm{eq}}(t)d\frac{P^{\mathrm{s}}(t)}{\varepsilon_0}$$

$$0 = s^{\mathrm{s}}(t)dT^{\mathrm{s}}(t) + d\gamma(t) + \sum_{j=1}^{n} \Gamma_j(t)d\mu_j^{\mathrm{s}}(t) + \frac{P^{\mathrm{s}}(t)}{\varepsilon_0}dD_{\mathrm{eq}}(t) \tag{3.38}$$

The intensive thermodynamic variables for the surface, indicated by superscript s, are derivatives:

$$T^{\mathrm{s}} = \left(\frac{du^{\mathrm{s}}}{ds^{\mathrm{s}}}\right)_{\Gamma_j, P^{\mathrm{s}}} \quad \text{and} \quad \mu_j^{\mathrm{s}} = \left(\frac{du^{\mathrm{s}}}{d\Gamma_j}\right)_{s^{\mathrm{s}}, \Gamma_k, P^{\mathrm{s}}} \tag{3.39}$$

The temperature and chemical potentials, defined in this manner, depend only on the surface excess variables, not on bulk variables. By introducing these definitions, we therefore allow for the possibility that the surface has a different temperature and/or chemical potentials than the adjacent homogeneous systems have. The equilibrium displacement field for the surface is defined by

$$D_{\mathrm{eq}} = \varepsilon_0 \left(\frac{du^{\mathrm{s}}}{dP^{\mathrm{s}}}\right)_{s^{\mathrm{s}}, \Gamma_j} \tag{3.40}$$

The actual displacement field, $D(t)$, which is externally controlled, and which is also independent of x, is not equal to $D_{\mathrm{eq}}(t)$. In the surface, a suitable surface element and time interval must be chosen for the averaging procedure, when thermodynamic quantities are determined.

For a contact line element, we say that there is *local equilibrium* when the thermodynamic relations (3.33)–(3.35) are valid:

$$u^{\mathrm{c}}(t) = T^{\mathrm{c}}(t)s^{\mathrm{c}}(t) + \gamma^{\mathrm{c}}(t) + \sum_{j=1}^{n} \mu_j^{\mathrm{c}}(t)\Gamma_j^{\mathrm{c}}(t)$$

$$du^{\mathrm{c}}(t) = T^{\mathrm{c}}(t)ds^{\mathrm{c}}(t) + \sum_{j=1}^{n} \mu_j^{\mathrm{c}}(t)d\Gamma_j^{\mathrm{c}}(t)$$

$$0 = s^{\mathrm{c}}(t)dT^{\mathrm{c}}(t) + d\gamma^{\mathrm{c}}(t) + \sum_{j=1}^{n} \Gamma_j^{\mathrm{c}}(t)d\mu_j^{\mathrm{c}}(t) \tag{3.41}$$

The intensive thermodynamic variables for the contact line, indicated by superscript c, are derivatives:

$$T^{\mathrm{c}} = \left(\frac{du^{\mathrm{c}}}{ds^{\mathrm{c}}}\right)_{\Gamma_j^{\mathrm{c}}} \quad \text{and} \quad \mu_j^{\mathrm{c}} = \left(\frac{du^{\mathrm{c}}}{d\Gamma_j^{\mathrm{c}}}\right)_{s^{\mathrm{c}},\Gamma_k^{\mathrm{c}}} \tag{3.42}$$

The temperature and chemical potentials, defined in this manner, depend only on the excess variables for the contact line, not on bulk or surface variables. By introducing these definitions, we therefore allow for the possibility that the contact line has a different temperature and/or chemical potentials than the adjacent homogeneous phases and surfaces. Along the contact line, suitable line elements and time intervals must be chosen for the averaging procedure, when the thermodynamic quantities are determined.

The assumption of local equilibrium, as formulated above, does not imply that there is local chemical equilibrium [20, 68]. According to the original formulation of Prigogine [110], the Gibbs equation remains valid for a large class of irreversible processes, provided that the Maxwell distribution of molecular velocities are perturbed only slightly. The class includes also chemical reactions slow enough not to disturb the equilibrium form of the distribution to an appreciable extent.

The thermodynamic variables are, with the above relations, position dependent. In particular, the thermodynamic variables for the surface depend on the position along the surface. Most excess densities depend on the choice of the dividing surface. The surface tension of a flat surface, however, does not depend on the position of the surface when the system is in mechanical equilibrium.

An essential and surprising aspect of the local equilibrium assumption for the surface and the adjacent homogeneous phases is that the temperature and chemical potentials on both sides of the surface may differ, not only from each other, but also from the values found for the surface.

The surface temperature represents the thermodynamic state of the surface. This temperature depends in principle on the choice of the dividing surface, but we have found that this dependence, both in molecular dynamics simulations [39] and in the dynamic van der Waals square gradient model [107], is negligible. The surface temperature can be calculated in molecular dynamics simulations, assuming the validity of the equipartition principle. We can then find the surface temperature from the kinetic energy. This is discussed in Chapter 22. It is difficult to imagine a direct measurement of the surface temperature. A direct measurement is hampered by the thickness of the thermocouple leads, and the positioning of the thermocouple. The description of the liquid-vapor interface, using a dynamic extension of the van der Waals model, is discussed in Chapter 23.

Whether the non-equilibrium surface as described by excess densities is an autonomous or self-contained thermodynamic system or not is an important question. Our results [39,107] support the validity of this property, see Chapters 22 and 23. Its validity is crucial for the treatment given in this book. It has been defended by some authors [94, 95] and rejected by others [96]. Molecular dynamics simulations support the validity of the assumption of local equilibrium [65–67,111,112]. This is discussed in Chapter 22 for homogeneous phases as well as for surfaces.

Given that there is very often local equilibrium in systems with large gradients, one may ask: Can we distinguish between volume elements that belong to a system in global equilibrium and those that belong to a system out of global equilibrium? The answer is yes — they differ in the nature of their fluctuations, as shown convincingly in the book by Ortiz and Sengers [109]. Equal time correlations around stationary states become long-range. In equilibrium, these correlations are short-range. Zielinska *et al.* [4, 113] have discussed the description of fluctuations for an interface.

3.A Appendix: Partial molar properties

We give the fundamental thermodynamic relations that define partial molar quantities, among them the chemical potential. The various contributions to the chemical potential are given and standard states are defined. Symbols are defined in the symbol list.

3.A.1 *Homogeneous phases*

The starting point for our derivations is the Gibbs equation

$$dU = TdS - pdV + \sum_{j=1}^{n} \mu_j dN_j + E_{\mathrm{eq}} d\mathsf{P} \tag{3.43}$$

By integrating the Gibbs equation with constant composition, temperature, pressure and displacement field, we obtain:

$$U = TS - pV + \sum_{j=1}^{n} \mu_j N_j + E_{\mathrm{eq}} \mathsf{P} \tag{3.44}$$

The *Gibbs energy* can then be defined:

$$G \equiv U - TS + pV - E_{\mathrm{eq}} \mathsf{P} = \sum_{j=1}^{n} \mu_j N_j \tag{3.45}$$

By using again the Gibbs equation, we have

$$dG \equiv -SdT + Vdp - \mathsf{P} dE_{\mathrm{eq}} + \sum_{j=1}^{n} \mu_j dN_j \tag{3.46}$$

Two equivalent definitions are obtained from these equations for the chemical potential, the partial energy change that follows when we add a particular component to a system:

$$\mu_j \equiv \left(\frac{\partial U}{\partial N_j} \right)_{S,V,N_k,\mathsf{P}}, \qquad \mu_j \equiv \left(\frac{\partial G}{\partial N_j} \right)_{p,T,N_k,E_{\mathrm{eq}}} \tag{3.47}$$

We note that $\mu_j = G_j$. By using Maxwell relations for Eq. (3.46), we find the following expressions for the partial molar volume, entropy and polarization:

$$V_j \equiv \left(\frac{\partial \mu_j}{\partial p} \right)_{T,N_k,E_{\mathrm{eq}}}, \quad S_j \equiv -\left(\frac{\partial \mu_j}{\partial T} \right)_{p,N_k,E_{\mathrm{eq}}}, \quad P_j \equiv -\left(\frac{\partial \mu_j}{\partial E_{\mathrm{eq}}} \right)_{p,T,N_k} \tag{3.48}$$

This results in the following expression for a change in the chemical potential

$$\begin{aligned} d\mu_j &= -S_j dT + V_j dp - P_j dE_{\text{eq}} + \sum_{k=1}^{n} \left(\frac{\partial \mu_j}{\partial N_k} \right)_{T,p,N_l,E_{\text{eq}}} dN_k \\ &= -S_j dT + V_j dp - P_j dE_{\text{eq}} + \sum_{k=1}^{n} \left(\frac{\partial \mu_j}{\partial c_k} \right)_{T,p,c_l,E_{\text{eq}}} dc_k \\ &\equiv -S_j dT + V_j dp - P_j dE_{\text{eq}} + d\mu_j^c \end{aligned} \tag{3.49}$$

A frequently used combination of terms is

$$d\mu_{j,T} = d\mu_j + S_j dT \tag{3.50}$$

where we used the partial molar entropy. In order to find $d\mu_{j,T}$ we differentiate $d\mu_j$ at constant temperature. Equivalent expressions for unpolarized systems are

$$\begin{aligned} d\mu_{j,T} &= d\mu_j^{\text{c}} + V_j dp \\ &= dH_j - T dS_j \end{aligned} \tag{3.51}$$

The partial molar volume, the partial molar entropy and the partial molar polarization for the i-phase are, respectively:

$$V_j \equiv \left(\frac{\partial V}{\partial N_j} \right)_{p,T,N_k,E_{\text{eq}}}, \quad S_j \equiv \left(\frac{\partial S}{\partial N_j} \right)_{p,T,N_k,E_{\text{eq}}}, \quad P_j \equiv \left(\frac{\partial \mathsf{P}}{\partial N_j} \right)_{p,T,N_k,E_{\text{eq}}} \tag{3.52}$$

Furthermore we have

$$\sum_j c_j V_j = 1, \qquad \sum_j c_j S_j = s, \qquad \sum_j c_j P_j = P \tag{3.53}$$

With these partial molar quantities, we can define the partial molar internal energy and enthalpy

$$\begin{aligned} U_j &= TS_j - pV_j + \mu_j + E_{\text{eq}} P_j \\ H_j &= -pV_j + \mu_j + E_{\text{eq}} P_j \end{aligned} \tag{3.54}$$

The U_j and H_j are functions of p, T, c_k and E_{eq}.

3.A.2 *The surface*

The Gibbs equation for the surface is:

$$dU^{\mathrm{s}} = T^{\mathrm{s}} dS^{\mathrm{s}} + \gamma d\Omega + \sum_{i=1}^{n} \mu_i^{\mathrm{s}} dN_i^{\mathrm{s}} + \left(\frac{D_{\mathrm{eq}}^{\mathrm{s}}}{\varepsilon_0} \right) d\mathsf{P}^{\mathrm{s}} \tag{3.55}$$

In this expression $U^{\mathrm{s}}, S^{\mathrm{s}}, N_i^{\mathrm{s}}, \mathsf{P}^{\mathrm{s}}$ are extensive quantities which are proportional to the surface area. These extensive quantities were obtained as excesses of the corresponding three-dimensional densities. The variables $T^{\mathrm{s}}, \gamma, \mu_i^{\mathrm{s}}, D_{\mathrm{eq}}^{\mathrm{s}}$ are intensive variables of the surface, indicated by superscript s. The temperature, surface tension, chemical potentials and the displacement field are intensive variables and have no excesses.

By integration with constant surface tension, temperature, composition and displacement field, we obtain

$$U^{\mathrm{s}} = T^{\mathrm{s}} S^{\mathrm{s}} + \gamma \Omega + \sum_{i=1}^{n} \mu_i^{\mathrm{s}} N_i^{\mathrm{s}} + \left(\frac{D_{\mathrm{eq}}^{\mathrm{s}}}{\varepsilon_0} \right) \mathsf{P}^{\mathrm{s}} \tag{3.56}$$

The Gibbs energy can now be defined by:

$$G^{\mathrm{s}} \equiv U^{\mathrm{s}} - T^{\mathrm{s}} S^{\mathrm{s}} - \gamma \Omega - \left(\frac{D_{\mathrm{eq}}^{\mathrm{s}}}{\varepsilon_0} \right) \mathsf{P}^{\mathrm{s}} = \sum_{j=1}^{n} \mu_j^{\mathrm{s}} N_j^{\mathrm{s}} \tag{3.57}$$

By using Gibbs equation again, we have

$$dG^{\mathrm{s}} \equiv -S^{\mathrm{s}} dT^{\mathrm{s}} - \Omega d\gamma - \mathsf{P}^{\mathrm{s}} d\left(\frac{D_{\mathrm{eq}}^{\mathrm{s}}}{\varepsilon_0} \right) + \sum_{j=1}^{n} \mu_j^{\mathrm{s}} dN_j^{\mathrm{s}} \tag{3.58}$$

The chemical potential obtains two equivalent definitions from these relations:

$$\mu_j^{\mathrm{s}} \equiv \left(\frac{\partial U^{\mathrm{s}}}{\partial N_j^{\mathrm{s}}} \right)_{S,\Omega,N_k,\mathsf{P}^{\mathrm{s}}}, \qquad \mu_j^{\mathrm{s}} \equiv \left(\frac{\partial G^{\mathrm{s}}}{\partial N_j^{\mathrm{s}}} \right)_{p,T,N_k,E_{\mathrm{eq}}} \tag{3.59}$$

where $\mu_j^{\mathrm{s}} = G_j^{\mathrm{s}}$. The superscript indicating the surface has been dropped in the subscripts of the differentiation. By using Maxwell relations for the definition of G^{s}, we find the following expressions for the partial molar quantities:

$$\begin{gathered} \Omega_j \equiv -\left(\frac{\partial \mu_j^{\mathrm{s}}}{\partial \gamma} \right)_{T,N_k,E_{\mathrm{eq}}}, \quad S_j^{\mathrm{s}} \equiv -\left(\frac{\partial \mu_j^{\mathrm{s}}}{\partial T^{\mathrm{s}}} \right)_{\gamma,N_k,E_{\mathrm{eq}}}, \\ P_j^{\mathrm{s}} \equiv -\left(\frac{\partial \mu_j^{\mathrm{s}}}{\partial \left(D_{\mathrm{eq}}^{\mathrm{s}} / \varepsilon_0 \right)} \right)_{\gamma,T,N_k} \end{gathered} \tag{3.60}$$

This results in the following expression for a change in the chemical potential

$$\begin{aligned} d\mu_j^{\mathrm{s}} &= -S_j^{\mathrm{s}} dT^{\mathrm{s}} - \Omega_j d\gamma - P_j^{\mathrm{s}} d\left(\frac{D_{\mathrm{eq}}^{\mathrm{s}}}{\varepsilon_0}\right) + \sum_{k=1}^{n} \left(\frac{\partial \mu_j^{\mathrm{s}}}{\partial N_k^{\mathrm{s}}}\right)_{T,p,N_l,E_{\mathrm{eq}}} dN_k^{\mathrm{s}} \\ &= -S_j^{\mathrm{s}} dT^{\mathrm{s}} - \Omega_j d\gamma - P_j^{\mathrm{s}} d\left(\frac{D_{\mathrm{eq}}^{\mathrm{s}}}{\varepsilon_0}\right) + \sum_{k=1}^{n} \left(\frac{\partial \mu_j^{\mathrm{s}}}{\partial \Gamma_k}\right)_{T,p,\Gamma_l,E_{\mathrm{eq}}} d\Gamma_k \\ &\equiv -S_j^{\mathrm{s}} dT^{\mathrm{s}} - \Omega_j d\gamma - P_j^{\mathrm{s}} d\left(\frac{D_{\mathrm{eq}}^{\mathrm{s}}}{\varepsilon_0}\right) + d\mu_j^{\mathrm{s},c} \end{aligned} \tag{3.61}$$

The following combination is used in expression (4.15) for the entropy production and flux equations that derive from this:

$$d\mu_{j,T}^{\mathrm{s}} = d\mu_j^{\mathrm{s}} + S_j^{\mathrm{s}} dT^{\mathrm{s}} \tag{3.62}$$

Alternative expressions are:

$$\begin{aligned} d\mu_{j,T}^{\mathrm{s}} &= d\mu_j^{\mathrm{s,c}} - \Omega_j d\gamma \\ &= dH_j^{\mathrm{s}} - T dS_j^{\mathrm{s}} \end{aligned} \tag{3.63}$$

The partial molar surface area, the partial molar entropy and the partial molar polarization for the surface are, respectively:

$$\begin{gathered} \Omega_j \equiv \left(\frac{\partial \Omega}{\partial N_j^{\mathrm{s}}}\right)_{\gamma,T,N_k,E_{\mathrm{eq}}}, \qquad S_j^{\mathrm{s}} \equiv \left(\frac{\partial S^{\mathrm{s}}}{\partial N_j^{\mathrm{s}}}\right)_{\gamma,T,N_k,E_{\mathrm{eq}}}, \\ P_j^{\mathrm{s}} \equiv \left(\frac{\partial \mathsf{P}^{\mathrm{s}}}{\partial N_j^{\mathrm{s}}}\right)_{\gamma,T,N_k,E_{\mathrm{eq}}} \end{gathered} \tag{3.64}$$

Furthermore, we have

$$\sum_j \Gamma_j \Omega_j = 1, \qquad \sum_j \Gamma_j S_j^{\mathrm{s}} = s^{\mathrm{s}}, \qquad \sum_j \Gamma_j P_j^{\mathrm{s}} = P^{\mathrm{s}} \tag{3.65}$$

By using the partial molar quantities defined above, one may also define the partial molar internal energy and enthalpy

$$\begin{aligned} U_j^{\mathrm{s}} &= T^{\mathrm{s}} S_j^{\mathrm{s}} + \gamma \Omega_j + \mu_j^{\mathrm{s}} + \left(D_{\mathrm{eq}}^{\mathrm{s}}/\varepsilon_0\right) P_j^{\mathrm{s}} \\ H_j^{\mathrm{s}} &= \gamma \Omega_j + \mu_j^{\mathrm{s}} + \left(D_{\mathrm{eq}}^{\mathrm{s}}/\varepsilon_0\right) P_j^{\mathrm{s}} \end{aligned} \tag{3.66}$$

where these functions, according to the above construction, are functions of $\gamma, T^{\mathrm{s}}, \Gamma_k$ and $\left(D_{\mathrm{eq}}^{\mathrm{s}}/\varepsilon_0\right)$.

Exercise 3.A.1. *Find a form of Gibbs–Duhem's equation for the surface that contains $d\mu^{\mathrm{s}}_{j,T}$ instead of $d\mu^{\mathrm{s}}_{j}$.*

- **Solution:** If we substitute Eq. (3.62) into Eq. (3.32d), we have

$$0 = s^{\mathrm{s}} dT^{\mathrm{s}} + d\gamma + \sum_{j=1}^{n} \Gamma_j d\mu^{\mathrm{s}}_{j,T} - \sum_{j=1}^{n} \Gamma_j S^{\mathrm{s}}_j dT^{\mathrm{s}} + P^{\mathrm{s}} d\left(D^{\mathrm{s}}_{\mathrm{eq}}/\varepsilon_0\right)$$

  By using $\sum_{j=1}^{n} \Gamma_j S^{\mathrm{s}}_j = s^{\mathrm{s}}$, Gibbs–Duhem's equation for the surface is reduced to

$$d\gamma = -\sum_{j=1}^{n} \Gamma_j d\mu^{\mathrm{s}}_{j,T} - P^{\mathrm{s}} d\left(D^{\mathrm{s}}_{\mathrm{eq}}/\varepsilon_0\right)$$

3.A.3 *Standard states*

The internal energy or the various derivatives of this energy, including the partial molar energies cannot be measured, only energy differences are measurable. In order to establish a measuring scale, we introduce the *standard state* as a point of reference. The standard state may be chosen freely, and different conventions have been made. Common to all choices is that they can be derived from each other by well-defined measurements.

The standard state for gases used in the SI system is *the state of an ideal gas at 1 bar and constant temperature*. The temperature is not specified in the definition of the standard state. Standard state values are often tabulated at 298 K, however. The definition of the chemical potential then relates any state to the standard state via

$$\int_{\mu^0}^{\mu} d\mu = \int_{p^0}^{p} V_m dp \tag{3.67}$$

where V_m is the molar volume. For an ideal gas, we obtain:

$$\mu_{\mathrm{id}} = \mu^0 + RT \ln \frac{p}{p^0} \tag{3.68}$$

where μ^0 is the standard chemical potential and $p^0 = 1$ bar. The energy of a real gas is measured with respect to this standard state, with the fugacity f replacing the pressure p of the gas. The chemical potential is:

$$\mu = \mu^0 + RT \ln \frac{f}{p^0} = \mu^0 + RT \ln \frac{\phi p}{p^0} = \mu_{\mathrm{id}} + RT \ln \phi \tag{3.69}$$

where the fugacity coefficient, defined by the ratio $\phi = f/p$, measures the deviation of the real gas from the ideal state, see Fig. 3.5 and exercise 3.A.2.

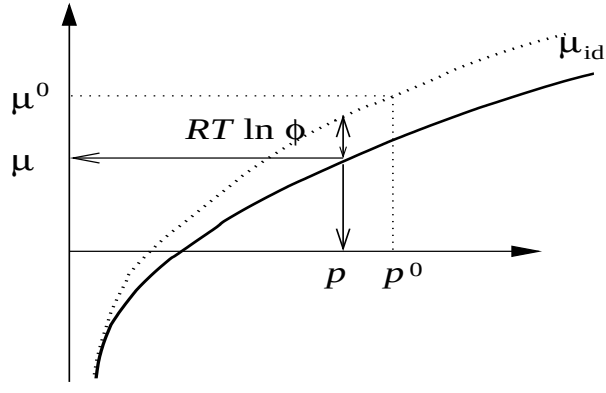

Figure 3.5 The chemical potential of an ideal gas (stippled line) and a real gas (whole line). The standard state, μ^0, at $p^0 = 1$ bar is shown for the ideal gas. The deviation of the chemical potential of the real gas from the corresponding ideal gas value at p is measured by the term $RT \ln \phi$.

The chemical potential of ideal and real gases are illustrated in this figure. When $\mu - \mu_{\mathrm{id}} < 0$ and $\phi < 1$, attractive forces are important.

For a liquid solution, we use a liquid state as the standard state. The numbers to be compared then become closer to each other. Two choices are common; the Raoultian standard state (used for solvents) and the Henrian standard state (used for solutes). The Raoultian standard state is the state of a solution which obeys Raoult's law. In this law, the vapor pressure above the solution is proportional to the mole fraction of the solvent (component 1):

$$p_1 = x_1 p_1^* \tag{3.70}$$

where p_1^* is the vapor pressure above the pure solvent. We assume that the vapor above the solution is an ideal gas. Equation (3.68) then gives:

$$\mu_1 = \mu^0 + RT \ln \frac{p_1^*}{p^0} + RT \ln \frac{p_1}{p_1^*} \tag{3.71}$$

which can be rearranged into

$$\mu_1 = \mu^* + RT \ln x_1 \tag{3.72}$$

The Raoultian standard state for the solvent is defined by

$$\mu^* \equiv \mu^0 + RT \ln \frac{p_1^*}{p^0} \tag{3.73}$$

The Raoultian standard state is thus determined from the standard state of the ideal gas plus a term that contains the vapor pressure of the solvent. A deviation from the Raoultian state is expressed by

$$\mu_1 = \mu^* + RT \ln a_1 = \mu^* + RT \ln y_1 x_1 \tag{3.74}$$

where y_1 is the activity coefficient that measures deviation from ideal behavior, and a_1 is the activity, $a_1 = p_1/p_1^*$. The situation with $y_1 > 0$ is illustrated in Fig. 3.6. Such a value means that there are repulsive forces in the liquid that enhance the vapor pressure above the liquid more than in the case of a solvent that follows Raoult's law. This standard state is used in Chapter 11 on evaporation and condensation.

The Henrian standard state is defined by a solution with a solute (component 2) of concentration $m_2^0 = 1$ molal, that obeys Henry's law:

$$p_2 = K_2 m_2^0 \tag{3.75}$$

Here, K_2 is Henry's law's constant. The standard state is hypothetical as no solution is known to obey Henry's law at this concentration. The constant K_2 is determined by measuring the vapor pressure above dilute solutions. The state is determined by extrapolation of this line to $m_2^0 = 1$ molal (see Fig. 3.6). By following the same procedure as above, we obtain for the chemical potential of an ideal solution:

$$\mu_2 = \mu^+ + RT \ln m_2/m_2^0 \tag{3.76}$$

Henry's law standard state is:

$$\mu^+ = \mu^0 + RT \ln \frac{K_2}{p^0} \tag{3.77}$$

This standard state is commonly used also for electrolyte solutions. There are two particles formed in a dilute solution per formula weight of salt dissolved, leading in the ideal case to

$$\mu_2 = \mu^+ + RT \ln m_{2,+} m_{2,-} / \left(m_2^0\right)^2 \tag{3.78}$$

or in the non-ideal case to:

$$\mu_2 = \mu^+ + RT \ln \gamma_{\pm,m}^2 m_{2,+} m_{2,-} / \left(m_2^0\right)^2 \tag{3.79}$$

where $\gamma_\pm^2$ is the mean square activity coefficient of the cation and anion. This standard state, or the state based on molar concentrations, μ^0, in

$$\mu_2 = \mu^0 + RT \ln \gamma_\pm^2 c_{2,+} c_{2,-} / \left(c_2^0\right)^2 \tag{3.80}$$

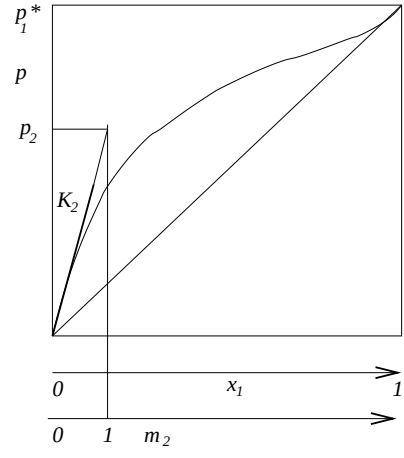

Figure 3.6 The phase diagram for a solution that follows Raoult's law ($p_1 = p_1^* x_1$) when $x_1 \to 1$ and Henry's law ($p_2 = K_2 m_2$) when $m_2 \to 1$.

are used with chemical potentials of electrolytes, cf. Chapter 10. The value of μ^0 is found from μ^+ by converting molalities into concentrations at the standard state. The mean square activity coefficient is given by Debije–Hückel's formula, when the solution is dilute.

The chemical potential of a surface-adsorbed component can be referred to a standard state with (a hypothetical) one molar surface excess concentration of the component, or a standard state referred to unit coverage, θ, of the surface:

$$\begin{aligned} \mu_j^{\mathrm{s}} &= \mu^{0,\mathrm{s}} + RT \ln \Gamma_j / \Gamma^0 \\ &= \mu^{0,\mathrm{s}} + RT \ln \theta_j \end{aligned} \tag{3.81}$$

The standard state must be connected to properties of the adjacent phase, in a similar way as the ideal gas standard state is connected to the Raoultian standard state. The symbol $\theta_j = \Gamma_j / \Gamma^0$ denotes fractional coverage. Activity coefficients corrections to the ideal formula can be substantial if the surface is polarized:

$$\mu_j^{\mathrm{s}} = \mu^{0,\mathrm{s}} + RT \ln \theta_j y_j^s \tag{3.82}$$

where y^s is the surface activity coefficient of component j.

We did not specify the temperature in these definitions. In fact, any temperature can be chosen. When one wants to compare standard states

at different temperatures, one will have to use the general relation which applies to any state, including the standard state:

$$\left(\frac{d\mu}{dT}\right)_p = -S \tag{3.83}$$

Expressions for activity coefficients in gases and liquids can be found in Perry and Green [114].

Exercise 3.A.2. *Express the fugacity coefficient ϕ of a gas in terms of its molar volume. The fugacity coefficient is defined as $\phi = f/p$, the ratio of the gas fugacity over the pressure of an ideal gas at corresponding conditions.*

- **Solution:** Equation (3.49) reduces to

$$d\mu \equiv V_m dp$$

for a pure isothermal gas. V_m is its molar volume. This equation is true for all gases whether they are ideal or not. The fugacity of a gas is defined by (see e.g. [97])

$$d\mu = RT d\ln f$$

For densities that are low enough, the gas follows the ideal gas law, $pV_{\text{ideal}} = RT$. This will always happen at some pressure p' when $p \to 0$

$$\int_{\mu'}^{\mu} d\mu = \int_{p'}^{p} V_m dp = RT \ln \frac{f}{p'}$$

For an ideal gas, the corresponding expression is

$$\int_{p'}^{p} V_{\text{ideal}} dp = RT \ln \frac{p}{p'}$$

Subtraction and introduction of $p' = 0$ gives

$$\ln \frac{f}{p} = \ln \phi = \frac{1}{RT} \int_0^p (V_m - V_{\text{ideal}})\, dp$$

The fugacity coefficient is expressed by measurable quantities in this formula.

Part A: General Theory

This page intentionally left blank

Chapter 4

The Entropy Production for a Homogeneous Phase

We derive the entropy production in a volume element in a homogeneous phase for transport of heat, mass, charge and chemical reactions. The entropy production determines the conjugate fluxes and forces in the phase. Equivalent forms of the entropy production are given.

The second law of thermodynamics, Eq. (2.14), says that the entropy change of the system plus its surroundings is positive for irreversible processes and zero for reversible processes. The law gives the direction of a process; it does not give its rate. Non-equilibrium thermodynamics assumes that the second law remains valid locally, cf. Eq. (1.1). In this chapter, we shall derive the entropy production for a volume element in a homogeneous phase. In the next chapters, we shall find the corresponding expressions for a surface area element and a three phase contact line element. In total, we will then be able to describe the rate of changes in heterogeneous systems.

The change of the entropy in a volume element in a homogeneous phase is given by the flow of entropy in and out of the volume element and by the entropy production inside the volume element:

$$\frac{\partial s(x,t)}{\partial t} = -\frac{\partial}{\partial x} J_s(x,t) + \sigma(x,t) \tag{4.1}$$

Here, $s(x,t)$ is the entropy density, $J_s(x,t)$ is the entropy flux in the laboratory frame of reference and $\sigma(x,t)$ is the entropy production. As the entropy density and flux depend on both position and time, we use partial derivatives. We consider only one-dimensional transport problems.

Below a more explicit expression for σ will be found by combining

- mass balances

- the first law of thermodynamics
- the local form of the Gibbs equation.

We shall do this and compare the resulting expression for the time rate of change of the entropy density with Eq. (4.1). This will make it possible to identify the entropy flux as well as the entropy production. We shall find that σ can be written as the product sum of the conjugate fluxes and forces in the system, see Sec. 1.1. In the derivation, we follow references [20] and [27]. Electroneutral-, polarizable-, non-equilibrium systems with and without chemical reactions are of interest. These are the systems that we encounter most often in nature, and also in industry. We shall model transport of heat, mass and charge in systems where reactions occur. We recommend using the symbol list for checking of dimensions in the equations. An introduction to non-equilibrium thermodynamics for homogeneous systems was given by Kjelstrup, Bedeaux and Johannessen [28, 29].

Consider a volume element, V, which is in local equilibrium in a polarizable, electroneutral bulk phase. The volume element does not move with respect to the walls (the laboratory frame of reference), see Fig. 4.1. All fluxes are with respect to the laboratory frame of reference.

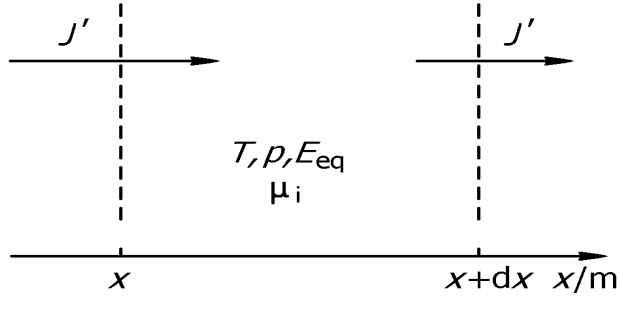

Figure 4.1 A volume element in a bulk phase with transport where j' indicates one of the fluxes.

The volume element has a sufficient number of particles to give a statistical basis for thermodynamic calculations. Its state is given by the temperature $T(x,t)$, chemical potentials $\mu_j(x,t)$ for all the n neutral components, pressure $p(x,t)$ and the equilibrium electric field $E_{eq}(x,t) = D_{eq}(t)/\varepsilon(x,t)$. We shall take ε constant in the homogeneous phases. Both equilibrium

electric fields are then independent of the position:

$$E^{\mathrm{i}}_{eq}(t) = D_{eq}(t)/\varepsilon_{\mathrm{i}} \quad \text{and} \quad E^{\mathrm{o}}_{eq}(t) = D_{eq}(t)/\varepsilon_{\mathrm{o}} \tag{4.2}$$

The number of positive particles equals the number of negative particles, but their distribution within the volume element can lead to a polarization density.

4.1 Balance equations

The balance equation for component j is

$$\frac{\partial c_j(x,t)}{\partial t} = -\frac{\partial}{\partial x} J_j(x,t) + \nu_j r(x,t) \quad \text{for} \quad j = 1, ..., n \tag{4.3}$$

where $J_j(x,t)$ are the component fluxes in the laboratory frame of reference, all directed along the x-axis. Furthermore, ν_j is the stoichiometric constant of component j in a chemical reaction, which is positive if j is a product and negative if j is a reactant, and $r(x,t)$ is the reaction rate in the volume element. For simplicity, we consider only one reaction. It is easy to add more reactions [20]. The reaction Gibbs energy is

$$\Delta_r G(x,t) = \sum_{j=1}^{n} \nu_j \mu_j(x,t) \tag{4.4}$$

In our description of reactions at surfaces, we shall also need the contribution to the reaction Gibbs energy due to the neutral species

$$\Delta_n G(x,t) \equiv \sum_{j \,\in\, neutral} \nu_j \mu_j(x,t) \tag{4.5}$$

where the sum in Eq. (4.5) is only over the neutral components. The difference between $\Delta_n G$ and the usual expression $\Delta_r G$, is due to the chemical potentials of ions and electrons. We explain why we need $\Delta_n G$ in Secs. 10.6–10.7.

Exercise 4.1.1. *Derive Eq. (4.3) for $r = 0$ by considering changes in a volume element that is fixed with respect to the walls.*

- **Solution:** The change in the number of moles of a component, $N_j(x,t)$, in a small volume V, is due to the flux of the component in and out of the volume. We have:

$$\frac{dN_j(x,t)}{dt} = -\Omega[J_j(x+dx,t) - J_j(x,t)]$$

where Ω is the cross sectional area of the volume orthogonal to the flux direction (the fluxes are flows per unit of area). The area is equal to the volume divided by dx. In the limit of small dx, we have

$$\frac{dN_j(x,t)}{dt} = -V\frac{[J_j(x+dx,t) - J_j(x,t)]}{dx} = -V\frac{\partial J_j(x,t)}{\partial x}$$

By dividing this equation left and right by the (constant) volume, one obtains Eq. (4.3).

The conservation equation for charge is

$$\frac{\partial z(x,t)}{\partial t} = -\frac{\partial}{\partial x} j(x,t) \tag{4.6}$$

where $z(x,t)$ is the charge density. The systems that we consider, can all be described as electroneutral. It follows that $\partial j/\partial x = 0$, so that the electric current density, j, is constant. The electric current is due to the relative motion of the charge carriers in the system, like for instance of electrons relative to the metal ion lattice. This relative motion is such that it preserves charge neutrality.

According to the first law of thermodynamics, the change in internal energy density per unit of time is equal to:

$$\frac{\partial u(x,t)}{\partial t} = -\frac{\partial}{\partial x} J_q(x,t) - \frac{\partial \phi(x,t)}{\partial x} j + E(x,t)\frac{\partial P(x,t)}{\partial t} \tag{4.7}$$

where $J_q(x,t)$ is the total heat flux in the laboratory frame of reference. The product $-[\partial\phi(x,t)/\partial x]\, j$ is the electrical work done to the volume element. The time derivative of the polarization density is the displacement current, $j_{\mathrm{displ}}(x,t) \equiv \partial P(x,t)/\partial t$. The product $E(x,t) j_{\mathrm{displ}}(x,t)$ gives the work per unit of volume by the displacement current. This is a capacitive contribution which, for instance, is important when there is an oscillatory electric field (see Chapter 21). In the appendix at the end of this chapter a discussion is given of the relation between Eq. (4.7), the first law, the definition of the total heat flux, and the relation between $\partial\phi(x,t)/\partial x$ and $E(x,t)$. An important assumption in the derivation of Eq. (4.7) is that the system is in mechanical equilibrium, a condition we shall use throughout this book. Contrary to the situation in vacuum, the electric field in a medium is not a conservative field.

The total heat flux across the volume element is given by

$$J_q(x,t) = J'_q(x,t) + \sum_{j=1}^{n} H_j(x,t) J_j(x,t) \tag{4.8}$$

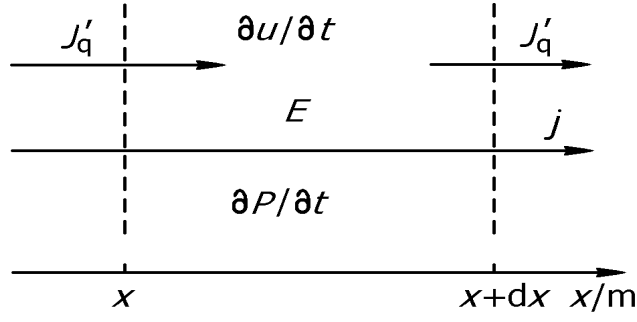

Figure 4.2 The energy change of a volume element with fluxes of heat and charge across the boundaries.

It consists of the measurable heat flux, $J'_q(x,t)$, and the partial molar enthalpies, $H_j(x,t)$, carried by the neutral component fluxes, $J_j(x,t)$. The measurable heat flux is independent of the frame of reference. This is not the case for the total heat flux. We discuss the frame of reference further in Secs. 4.2, 4.4, Appendix 4.A, and also in Chapter 12, which deals with multi-component diffusion. The first law is illustrated in Fig. 4.2. De Groot and Mazur [20] used charged and uncharged components, which is appropriate for systems that are not electroneutral, and defined a reduced heat flux in analogy with Eq. (4.8). In the electroneutral systems, which we consider, it is more appropriate to use the smaller number of uncharged components. The measurable heat flux differs from the reduced heat flux by a contribution proportional to the electric current density, see Appendix 4.A for a discussion.

4.2 The entropy production

The Gibbs equation in its local form, Eq. (3.26) together with Eq. (3.7),

$$du = Tds + \sum_{j=1}^{n} \mu_j dc_j + E_{\text{eq}} dP \tag{4.9}$$

is needed to calculate the entropy production. The time derivative of the entropy density becomes, using Eq. (4.9):

$$\frac{\partial s(x,t)}{\partial t} = \frac{1}{T(x,t)} \frac{\partial u(x,t)}{\partial t} - \sum_{j=1}^{n} \frac{\mu_j(x,t)}{T(x,t)} \frac{\partial c_j(x,t)}{\partial t} - \frac{E_{\text{eq}}(t)}{T(x,t)} \frac{\partial P(x,t)}{\partial t} \tag{4.10}$$

Partial derivatives are used since the variables are position and time dependent.

Exercise 4.2.1. *Derive Eq. (4.1) by considering changes in a volume element fixed with respect to the walls.*

- **Solution:** The change of entropy is due to the flux in and out of the volume element plus an increase due to the entropy production:

$$\frac{dS(x,t)}{dt} = -\Omega[J_s(x+dx,t) - J_s(x,t)] + V\sigma(x,t)$$

where $\sigma(x,t)$ is the entropy production per unit of volume. The cross section is equal to the volume divided by dx. We obtain in the limit of small dx

$$\begin{aligned}\frac{dS(x,t)}{dt} &= -V\frac{[J_s(x+dx,t) - J_s(x,t)]}{dx} + V\sigma(x,t)\\ &= -V\frac{dJ_s(x,t)}{dx} + V\sigma(x,t)\end{aligned}$$

By dividing this equation left and right by the volume, one obtains Eq. (4.1).

By introducing Eqs. (4.3) and (4.7) into (4.10), using the rule for derivation of products, and solving for $\partial s(x,t)/\partial t$, we obtain as balance equation for the entropy density:

$$\begin{aligned}\frac{\partial s(x,t)}{\partial t} = &-\frac{\partial}{\partial x}\left[\frac{1}{T(x,t)}\left(J_q(x,t) - \sum_{j=1}^{n}\mu_j(x,t)J_j(x,t)\right)\right]\\ &+ J_q(x,t)\left(\frac{\partial}{\partial x}\frac{1}{T(x,t)}\right) + \sum_{j=1}^{n}J_j(x,t)\left(-\frac{\partial}{\partial x}\frac{\mu_j(x,t)}{T(x,t)}\right)\\ &+ j\left(-\frac{1}{T(x,t)}\frac{\partial\phi(x,t)}{\partial x}\right)\\ &+ \frac{\partial P(x,t)}{\partial t}\left[\frac{E(x,t) - E_{\mathrm{eq}}(x,t)}{T(x,t)}\right] + r(x,t)\left(-\frac{\Delta_r G(x,t)}{T(x,t)}\right)\end{aligned} \tag{4.11}$$

To simplify notation, we usually suppress the (x,t) for all variables. By comparing the above equation with Eq. (4.1), we identify the entropy flux

$$J_s = \frac{1}{T}\left(J_q - \sum_{j=1}^{n}\mu_j J_j\right) = \frac{1}{T}J'_q + \sum_{j=1}^{n} S_j J_j \tag{4.12}$$

and the entropy production in the system

$$\sigma = J_q\left(\frac{\partial}{\partial x}\frac{1}{T}\right) + \sum_{j=1}^{n} J_j\left(-\frac{\partial}{\partial x}\frac{\mu_j}{T}\right) + j\left(-\frac{1}{T}\frac{\partial\phi}{\partial x}\right) + \frac{\partial P}{\partial t}\left(\frac{E-E_{\rm eq}}{T}\right) + r\left(-\frac{\Delta_r G}{T}\right) \tag{4.13}$$

Here, S_j is the partial molar entropy of component j. By replacing the total heat flux, J_q, by the entropy flux, J_s, we obtain an alternative expression

$$\sigma = J_s\left(-\frac{1}{T}\frac{\partial T}{\partial x}\right) + \sum_{j=1}^{n} J_j\left(-\frac{1}{T}\frac{\partial\mu_j}{\partial x}\right) + j\left(-\frac{1}{T}\frac{\partial\phi}{\partial x}\right) + \frac{\partial P}{\partial t}\left(\frac{E-E_{\rm eq}}{T}\right) + r\left(-\frac{\Delta_r G}{T}\right) \tag{4.14}$$

We furthermore replace the total heat flux, J_q, by the often more practical measurable heat flux, J'_q, using Eq. (4.12). The result is

$$\sigma = J'_q\left(\frac{\partial}{\partial x}\frac{1}{T}\right) + \sum_{j=1}^{n} J_j\left(-\frac{1}{T}\frac{\partial\mu_{j,T}}{\partial x}\right) + j\left(-\frac{1}{T}\frac{\partial\phi}{\partial x}\right) + \frac{\partial P}{\partial t}\left(\frac{E-E_{\rm eq}}{T}\right) + r\left(-\frac{\Delta_r G}{T}\right) \tag{4.15}$$

where $\partial\mu_{j,T}/\partial x = \partial\mu_j/\partial x + S_j\partial T/\partial x$ is the derivative of the chemical potential keeping the temperature constant, see Appendix 3.A. Finally, when one describes heat and charge transport, it is sometimes convenient to replace the total heat flux by the energy flux J_u, which is defined by (see Chapters 9, 15 and 19)

$$J_u \equiv J_q + \phi j = J'_q + \sum_{j=1}^{n} H_j J_j + \phi j \tag{4.16}$$

This gives for the entropy production

$$\sigma = J_u \left(\frac{\partial}{\partial x} \frac{1}{T} \right) + \sum_{j=1}^{n} J_j \left(-\frac{\partial}{\partial x} \frac{\mu_j}{T} \right) + j \left(-\frac{\partial}{\partial x} \frac{\phi}{T} \right) + \frac{\partial P}{\partial t} \left(\frac{E - E_{\text{eq}}}{T} \right) + r \left(-\frac{\Delta_r G}{T} \right) \tag{4.17}$$

The results for σ were derived using only the assumption of local equilibrium, see Sec. 3.5. Local equilibrium does not imply local *chemical* equilibrium. Local chemical equilibrium is a special case of local equilibrium [20, 68].

The entropy production contains pairs of fluxes and forces. These are the *conjugate fluxes and forces* defined in Chapter 1. The conjugate flux-force pairs in Eqs. (4.13), (4.14), (4.15) and (4.17) are different. The different sets of pairs are, however, equivalent and describe the same physical situation. The problem one wants to describe, dictates the form that is most convenient. Convenient is a form that describes the system in the most direct way. If, for instance, the system is such that the chemical potentials of all components are constant, Eq. (4.14) is convenient because all terms containing their gradients are zero. The four alternative expressions have been given, as a help to find the appropriate final form. All forces and fluxes have a direction, except the last pair, and are thus vectors. The chemical reaction has a scalar flux and force. We shall discuss the consequences of this for isotropic systems in Sec. 7.6.

Remark 4.1. *De Groot and Mazur [20] use fluxes in the barycentric frame of reference. We always use fluxes in the laboratory frame of reference. The entropy production is invariant for this transformation. This can be verified for instance in Eq. (4.15). In this expression the only fluxes that depend on the frame of reference are the component fluxes. Subtracting from these component fluxes, the molar densities times the barycentric velocity, gives a total change which is zero according to Gibbs–Duhem's equation. It follows that one may replace the component fluxes in the laboratory frame of reference by those in the barycentric frame of reference. See also Sec. 4.4.2.*

The separate products do not only give pure losses of work (compare Secs. 2.4 and 7.5). Their sum does. For instance, the electric power per unit of volume, $-(j\partial\phi/\partial x)$, does not necessarily give only an ohmic contribution to the entropy production, there may also be electric work terms included in the product, as we shall see in detail in Chapters 9 and 10. Each product contains normally work terms as well as energy storage terms. It is *their combination* which gives the entropy production rate, and the work that is

lost per unit of time, $dW_{lost}/dt = T_0 \int \sigma dV$ (see Sec. 2.4). The expressions (4.13)–(4.15) and (4.17) can thus be used to find the second law efficiency of a process [29].

De Groot and Mazur [20] used the affinity, A, of the chemical reaction, rather than the reaction Gibbs energy, in Eq. (4.15). According to Kondepudi and Prigogine [56] (page 111), the reaction Gibbs energy is primarily used in connection with equilibrium states and reversible processes, while de Donder's affinity concept is more general, it relates chemical reactions to entropy. We dispute that there is a principle difference between the two concepts. The affinity is simply equal to minus of the reaction Gibbs energy. We use the reaction Gibbs energy, because chemists are more familiar with this concept.

Ross and Mazur [115] showed that the contribution to σ from the chemical reaction was equal to the product of r and the driving force, $-\Delta_r G/T$, also when the reaction rate is a non-linear function of the driving force, provided that the ensemble of particles is nearly Maxwellian. Prigogine showed that the Gibbs relation was valid for such conditions [110].

Haase [21] defined and used the dissipation function in his monograph on "Thermodynamics of Irreversible Processes". The dissipation function is still in focus in many books, see e.g. Demirel [116]. In homogeneous systems, Haase defined $\Psi = T dS_{irr}/dt$, where dS_{irr}/dt is the rate of increase of the entropy due to processes which occur inside the system. For a continuous system, in which the temperature can vary from point to point, he used the definition $\Psi = T\sigma$, [22] page 83. This last definition is analogous to Raleigh's dissipation function for hydrodynamic flow. For heterogeneous systems, which are discussed in this book, neither of the above definitions can be used. On pages 161-164, Haase considered the case of two phases in thermal contact with each other. After calculating the entropy production, he multiplied it with the temperature of one of the phases. In the resulting expression, he then needed to linearize in the temperature difference of the phases, in order to obtain an expression for Ψ which is linear in the temperature difference. He contributed thereby to the erroneous idea that a non-equilibrium thermodynamic description should be fully linearized. The entropy production he first derived was perfectly linear in the difference of the inverse temperature. When one uses the entropy production rather than Ψ, as is systematically done in this book, there is no need to further linearize. Instead of multiplying with the temperature of one of the phases, it is appropriate to multiply with the temperature of the environment as is done in exergy analysis to find the lost work. We discussed in Sec. 2.4 that this gives the lost work. We strongly advise against using Ψ in heterogeneous systems, see Sec. 4.2.1 for further arguments.

Changing the frame of reference does not change the value or the physical interpretation of σ. The entropy production is an absolute quantity. It is *invariant* for transformations to other frames of reference, i.e. it is "Galilean invariant". Possible choices for the frame of reference will be discussed in Sec. 4.4.

As mentioned above, we are dealing only with one-dimensional transport problems in this book. That is, we consider only transport normal to the surface. All densities and fluxes are assumed to be independent of the coordinates along the surface and the vectorial fluxes are assumed to be directed normal to the surface. These assumptions can be made because the systems we consider are isotropic along the surface. A system is isotropic if it is invariant for translation along the surface, for rotation around a normal on the surface, and for reflection with respect to planes normal to the surface.

Compression is a scalar phenomenon that couples to the reactions in the bulk phases. This coupling is small, however, since density variations relax on a time scale of the size of the system divided by the velocity of sound. The assumption of mechanical equilibrium, grad $p = 0$, used to derive Eq. (4.7), is therefore often valid, see [20] for a discussion of the more general case. In the absence of compression, the compressional (bulk) viscosity does not play a role.

Convection and shear flow will disturb chemical reactions and transport of heat and mass, but do not couple to them directly. Convection and/or shear flow can be described by non-equilibrium thermodynamics, see e.g. [30, 31], but will not be considered in this book.

4.2.1 *Why one should not use the dissipation function*

Consider three thermal reservoirs with internal energies U_a, U_b, U_c and temperatures T_a, T_b, T_c. The reservoirs are in thermal contact and the rates of change of these internal energies are

$$\frac{dU_a}{dt} = -J_q^{ab} - J_q^{ac}, \quad \frac{dU_b}{dt} = -J_q^{ba} - J_q^{bc}, \quad \frac{dU_c}{dt} = -J_q^{ca} - J_q^{cb}$$

where $J_q^{ij} = -J_q^{ji}$ is the heat flux from reservoir i to reservoir j. The total internal energy $U = U_a + U_b + U_c$ is conserved

$$\frac{dU}{dt} = \frac{dU_a}{dt} + \frac{dU_b}{dt} + \frac{dU_c}{dt} = 0$$

The rate of change of the entropy of the reservoirs is given by the Gibbs relation

$$\frac{dS_i}{dt} = \frac{1}{T_i}\frac{dU_i}{dt} \quad \text{for} \quad i = a, b, c$$

The total entropy production is

$$\frac{dS_{\text{irr}}}{dt} = \frac{dS_a}{dt} + \frac{dS_b}{dt} + \frac{dS_c}{dt} = \frac{1}{T_a}\frac{dU_a}{dt} + \frac{1}{T_b}\frac{dU_b}{dt} + \frac{1}{T_c}\frac{dU_c}{dt}$$
$$= J_q^{ab}\left(\frac{1}{T_b} - \frac{1}{T_a}\right) + J_q^{ac}\left(\frac{1}{T_c} - \frac{1}{T_a}\right) + J_q^{bc}\left(\frac{1}{T_c} - \frac{1}{T_b}\right)$$

For the total dissipation function we obtain

$$\Psi = T_a\frac{dS_a}{dt} + T_b\frac{dS_b}{dt} + T_c\frac{dS_c}{dt} = \frac{dU_a}{dt} + \frac{dU_b}{dt} + \frac{dU_c}{dt} = 0$$

Linear force-flux relations follow in a straight forward manner from dS_{irr}/dt. The total dissipation function is zero, however, and does not give any force-flux pairs. Haase tried to save himself from this dilemma by multiplying the entropy productions of all reservoirs with the same temperature. Haase [22] (pages 161-164) chose the temperature of one of the reservoirs in a case with two reservoirs. This procedure is unsystematic as the answer depends on the reservoir chosen.

Also, exergy analysis (cf. Sec. 2.4) tells that the proper temperature for multiplication with the entropy production is the temperature of the environment. Correct linear force-flux relations are therefore obtained from the entropy production, or equivalently from the lost exergy, but not from the dissipation function.

4.2.2 *States with minimum entropy production*

When a system is close to global equilibrium, one may linearize the equations that describe the time evolution of the system. All the transport coefficients in Eq. (1.2) are then constant. Prigogine showed that stationary states of discontinuous systems, maintained for instance by a temperature difference, have a minimum entropy production [15]. This is sometimes called the Prigogine principle. For stationary states far from global equilibrium, the transport coefficients are no longer constant across the whole system, and the stationary state has no longer a minimum entropy production compared to non-stationary states [117, 118].

In the design of industrial systems, it is fruitful to ask a different question. We can ask for the path that a system must follow to obtain minimum entropy production [119]. This question leads to an optimization problem that is constrained by the performance, for instance by the composition of the chemicals that are produced. The transport coefficients of the system are then considered as given. The nature of systems with minimum total entropy production dS_{irr}/dt has been studied extensively since 1982

by Bejan and coworkers, see [84, 85] (mostly mechanical systems) and by Kjelstrup and coworkers since 1995, see [29] (mostly chemical systems).

Johannessen and Kjelstrup [91] found that much of the path of an optimal chemical reactor was characterised by constant local entropy production, provided that the system had enough degrees of freedom to find this path. This was called the *highway hypothesis*. In all cases, the entropy production and not the dissipation function, was used as proper objective function. Bejan [85] (page 227) showed that the state of minimum entropy production was equal to the state of maximum power, contrary to other claims [120], see also [29].

4.3 Examples

The exercises below illustrate how single contributions arise in the entropy production. Some exercises are meant to illustrate the theory. The remaining give numerical and physical insight. Transport of heat at low temperatures and chemical reactions give relatively large losses of work.

Exercise 4.3.1. *Consider the special case that only component number j is transported. The densities of the other components, the internal energy, the molar volume and the polarization densities are all constant. Show that the entropy production is given by*

$$\sigma = -J_j \frac{\partial}{\partial x}\left(\frac{\mu_j}{T}\right)$$

- **Solution:** In this case Eq. (4.10) reduces to

$$T\frac{\partial s}{\partial t} + \mu_j \frac{\partial c_j}{\partial t} = 0$$

The rate of change of the entropy is therefore given by

$$\frac{\partial s}{\partial t} = -\frac{\mu_j}{T}\frac{\partial c_j}{\partial t}$$

Now we use Eq. (4.3) for component j and obtain

$$\frac{\partial s}{\partial t} = \frac{\mu_j}{T}\frac{\partial}{\partial x}J_j = \frac{\partial}{\partial x}\left(\frac{\mu_i}{T}J_j\right) - J_j\frac{\partial}{\partial x}\frac{\mu_j}{T}$$

Comparing this equation with Eq. (4.1) we may identify the entropy flux and the entropy production as

$$J_s = -\frac{\mu_j}{T}J_j \quad \text{and} \quad \sigma = -J_j\frac{\partial}{\partial x}\left(\frac{\mu_j}{T}\right)$$

Exercise 4.3.2. *Consider the case that only heat is transported. The molar densities, the molar volume and the polarization densities are all constant. Show that the entropy production is given by*

$$\sigma = J'_q \frac{\partial}{\partial x}\left(\frac{1}{T}\right)$$

- **Solution:** In this case Eq. (4.10) reduces to

$$\frac{\partial u}{\partial t} = T\frac{\partial s}{\partial t}$$

The rate of change of the entropy is therefore given by

$$\frac{\partial s}{\partial t} = \frac{1}{T}\frac{\partial u}{\partial t}$$

Eq. (4.7) reduces to

$$\frac{\partial u}{\partial t} = -\frac{\partial}{\partial x}J'_q$$

By substituting this into the equation above, we obtain

$$\frac{\partial s}{\partial t} = -\frac{1}{T}\frac{\partial}{\partial x}J'_q = -\frac{\partial}{\partial x}\frac{1}{T}J'_q + J'_q\frac{\partial}{\partial x}\frac{1}{T}$$

By comparing this equation with Eq. (4.1), we can identify the entropy flux and the entropy production as

$$J_s = \frac{1}{T}J'_q \quad \text{and} \quad \sigma = J'_q\frac{\partial}{\partial x}\left(\frac{1}{T}\right)$$

Exercise 4.3.3. *Find the entropy production due to the heat flux through a sidewalk pavement by a hot plate placed $d = 8$ cm under the top of the pavement. The plate has a temperature of 343 K, and the surface is in contact with melting ice (273 K). The Fourier type thermal conductivity of the pavement is 0.7 W/m K.*

- **Solution:** Fourier's law for heat conduction is $J'_q = -\lambda(dT/dx)$. The entropy production per m^2 is rather large:

$$\frac{1}{d}\int_0^d \sigma dx = \frac{1}{d}\int_0^d J'_q\frac{\partial}{\partial x}\left(\frac{1}{T}\right)dx = -\lambda\frac{\Delta T}{d^2}\left(\frac{1}{T_2} - \frac{1}{T_1}\right)$$

$$= -0.7\frac{(-70)}{(0.08)^2}\left(\frac{1}{273} - \frac{1}{343}\right) = 5.7 \text{ W/K m}^3$$

It is typical for heat conduction around room temperature that losses are large.

Exercise 4.3.4. *Consider a system with two components ($n = 2$), having $dT = 0$, $dp = 0$, and $dE_{eq} = 0$. Show, using Gibbs–Duhem's equation, that one may reduce the description in terms of two components to one with only one component.*

- **Solution:** Gibbs–Duhem, Eq. (3.27), gives:

$$c_1 d\mu_1 + c_2 d\mu_2 = 0$$

The entropy production of Eq. (4.13) reduces for these conditions to:

$$\sigma = \left(\frac{J_1}{c_1} - \frac{J_2}{c_2} \right) \left[-\frac{c_1}{T} \frac{\partial \mu_1}{\partial x} \right]$$

The equation contains only one independent force. Energy is lost by *interdiffusion* of the two components. We can also write this entropy production by

$$\sigma = \mathrm{v}_{12} \left[-\frac{c_1}{T} \frac{\partial \mu_1}{\partial x} \right]$$

with $\mathrm{v}_{12} \equiv J_1/c_1 - J_2/c_2$. This is the velocity of component 1 relative to the velocity of component 2. Note that v_{12} is independent of the frame of reference.

Exercise 4.3.5. *We are interested in the filtering of water (w) across a sandy layer of 1 m at 293 K. Evaluate the entropy production for a water flux of 10^{-6} kg/m^{2}s. The density of the sand at 293 K is ρ =1940 kg/m^3 [121]. The volume of water per unit of mass is $V_w = 10^3$ m^3/kg.*

- **Solution:** The only contribution to the chemical potential gradient is from the pressure ($d\mu_{\mathrm{w}}^c = 0$), so $d\mu_{\mathrm{w},T} = V_{\mathrm{w}} dp$. The pressure on water at a distance x from the surface is given by the weight of the sand, $p = \rho g x$. This gives $d\mu_{\mathrm{w},T}/dx = V_{\mathrm{w}} \rho g$, and

$$\sigma = -J_{\mathrm{w}} \frac{1}{T} V_{\mathrm{w}} \rho g = 6.5 \times 10^{-8} \text{ W/ K m}^3$$

This value is considerably smaller than the value for transport of heat across a pavement (see exercise 4.3.3).

Exercise 4.3.6. *Give the details of the derivation of Eq. (4.15) from Eq. (4.13).*

- **Solution:** We first rewrite the negative force as

$$\begin{aligned}\frac{\partial}{\partial x}\left(\frac{\mu_j}{T}\right) &= \frac{\partial}{\partial x}\left(\frac{\mu_j}{T}\right)_T + \frac{\partial}{\partial T}\left(\frac{\mu_j}{T}\right)\frac{\partial T}{\partial x} \\ &= \frac{1}{T}\frac{\partial}{\partial x}\mu_{j,T} + \left(\frac{1}{T}\frac{\partial \mu_j}{\partial T} - \frac{\mu_j}{T^2}\right)\frac{\partial T}{\partial x} \\ &= \frac{1}{T}\frac{\partial}{\partial x}\mu_{j,T} - \frac{1}{T^2}\left(TS_j + \mu_j\right)\frac{\partial T}{\partial x} = \frac{1}{T}\frac{\partial}{\partial x}\mu_{j,T} + H_j\frac{\partial}{\partial x}\frac{1}{T}\end{aligned}$$

  By substituting this result into Eq. (4.13), we obtain

$$\begin{aligned}\sigma = &\left(J_q - \sum_{j=1}^{n} H_j J_j\right)\frac{\partial}{\partial x}\left(\frac{1}{T}\right) + \sum_{j=1}^{n} J_j\left(-\frac{1}{T}\frac{\partial}{\partial x}\mu_{j,T}\right) \\ &+ j\left(-\frac{1}{T}\frac{\partial \phi}{\partial x}\right) + \frac{\partial P}{\partial t}\left[-\frac{1}{T}\frac{\partial(\phi - \phi_{\mathrm{eq}})}{\partial x}\right]\end{aligned}$$

  By using $J_q = J_q' + \sum_{j=1}^{n} H_j J_j$, Eq. (4.15) follows.

Exercise 4.3.7. *Derive the entropy production for an isothermal two-component system that does not transport charge. The solvent is the frame of reference for the fluxes.*

- **Solution:** In an isothermal system, $\partial(1/T)/\partial x = 0$. Furthermore, there is no charge transport so that $j = 0$. Finally, the solvent is the frame of reference, so $J_{solvent} = 0$. There remains only one force-flux pair, namely for transport of solute. Using Eq. (4.15), we then find

$$\sigma = -\frac{J}{T}\frac{\partial \mu_T}{\partial x}$$

  for the entropy production. Using that $\sigma \geq 0$ it follows that the solute will move from a higher to a lower value of its chemical potential.

Exercise 4.3.8. *What is the entropy production for systems that are described by Eqs. (2.1), (2.2) and (2.3)?*

- **Solution:** Substitution of these equations into Eq. (4.15), setting the reaction rate and the displacement current zero, yields

$$\begin{aligned}\sigma &= \frac{\lambda}{T^2}\left(\frac{\partial T}{\partial x}\right)^2 + \frac{D}{T}\frac{\partial \mu_T}{\partial x}\frac{\partial c}{\partial x} + \frac{\kappa}{T}\left(\frac{\partial \phi}{\partial x}\right)^2 \\ &= \frac{\lambda}{T^2}\left(\frac{\partial T}{\partial x}\right)^2 + \frac{D}{T}\frac{\partial \mu_T}{\partial c}\left(\frac{\partial c}{\partial x}\right)^2 + \frac{\kappa}{T}\left(\frac{\partial \phi}{\partial x}\right)^2 \\ &\equiv \sigma_T + \sigma_\mu + \sigma_\phi\end{aligned}$$

Typical values in an electrolyte are: $\lambda = 2$ J/msK, $T = 300$ K, $dT/dx = 100$ K/m, $D = 10^{-9}$ m^2/s, $\partial\mu_T/\partial c = RT/c$, $c = 100$ kmol/m^3, $dc/dx = 10^{-5}$ mol/m^4, $\kappa = 400$ Si/m, $d\phi/dx = 10^{-2}$ V/m. The resulting entropy productions are: $\sigma_T = 0.2$ J/Ksm^3, $\sigma_\mu = 10^{-13}$ J/Ksm^3 and $\sigma_\phi = 10^{-4}$ J/Ksm^3. Heat conduction therefore clearly gives the largest contribution to the entropy production in electrolytes.

Exercise 4.3.9. *What is the first law efficiency η_I for a Carnot machine? Compare this efficiency with the expression for the entropy production of a system that transports heat from a hot reservoir to the surroundings.*

- **Solution:** The Carnot machine transforms heat into work in a reversible way. The efficiency is defined as the work output divided by the heat input [97,122]. This efficiency is $(T_h - T_c)/T_h$, where T_h and T_c are the temperatures of the hot and the cold reservoir, respectively. If we do not use the heat to produce work, but simply bring the hot and cold reservoirs in thermal contact with one another, one gets a heat flow from the hot to the cold reservoir. The entropy production for the whole (one-dimensional) path, with a cross section Ω is:

$$\frac{dS_{\rm irr}}{dt} = \Omega \int \sigma(x) dx = \Omega \int J'_q(x) \frac{\partial}{\partial x} \left(\frac{1}{T(x)} \right) dx$$

As there is no other transport of thermal energy, the heat flux is constant and equal to dQ/dt for a unit area. This results in

$$\frac{dS_{\rm irr}}{dt} = J'_q \Omega \int \frac{\partial}{\partial x} \left(\frac{1}{T(x)} \right) dx = J'_q \Omega \int_{T_h}^{T_c} \frac{\partial}{\partial T} \left(\frac{1}{T} \right) dT$$

$$= \Omega \frac{dQ}{dt} \left(\frac{1}{T_c} - \frac{1}{T_h} \right) = \Omega \frac{dQ}{dt} \left(\frac{T_h - T_c}{T_h T_c} \right) = \Omega \frac{\eta_I}{T_c} \frac{dQ}{dt}$$

The work lost per unit of time, $T_c dS_{\rm irr}/dt$, is identical to the work that can be obtained by a Carnot cycle, $\Omega\eta_I(dQ/dt)$, per unit of time. This can be used as a derivation of the first law efficiency of the Carnot machine. This machine is reversible and has as a consequence no lost work. This implies that the work done by the Carnot machine must be equal to $\Omega\eta_I(dQ/dt)$.

Exercise 4.3.10. *Consider the reaction:*

$$B + C \rightleftarrows D$$

The driving force of the reaction is the reaction Gibbs energy:

$$\Delta_r G = \mu_D - \mu_C - \mu_B$$

In the absence of chemical equilibrium, there are three independent chemical potentials. The contribution to σ is:

$$\sigma_{chem} = r\left(-\frac{\Delta_r G}{T}\right)$$

Derive this expression for σ_{chem}, assuming that the reaction takes place in a reactor in which the internal energy is independent of the time.

- **Solution:** The n components of Eq. (4.3) are B, C and D. The balance equations for mass have a source term from the reaction rate:

$$\frac{\partial c_{\mathrm{B}}}{\partial t} = -\frac{\partial}{\partial x} J_{\mathrm{B}} - r$$

$$\frac{\partial c_{\mathrm{C}}}{\partial t} = -\frac{\partial}{\partial x} J_{\mathrm{C}} - r$$

$$\frac{\partial c_{\mathrm{D}}}{\partial t} = -\frac{\partial}{\partial x} J_{\mathrm{D}} + r$$

Using that the internal energy is independent of the time Eq. (4.10) reduces to

$$T\frac{\partial s}{\partial t} + \sum_{j=1}^{3} \mu_j \frac{\partial c_j}{\partial t} = 0$$

The rate of change of entropy is therefore given by

$$\frac{\partial s}{\partial t} = -\sum_{j=1}^{3} \frac{\mu_j}{T} \frac{\partial c_j}{\partial t}$$

We substitute the balance equations in this expression, and obtain

$$\begin{aligned}\frac{\partial s}{\partial t} &= \frac{\mu_{\mathrm{B}}}{T}\left(\frac{\partial}{\partial x} J_{\mathrm{B}} + r\right) + \frac{\mu_{\mathrm{C}}}{T}\left(\frac{\partial}{\partial x} J_{\mathrm{C}} + r\right) + \frac{\mu_{\mathrm{D}}}{T}\left(\frac{\partial}{\partial x} J_{\mathrm{D}} - r\right) \\ &= \frac{\partial}{\partial x}\left(\frac{\mu_{\mathrm{B}}}{T} J_{\mathrm{B}} + \frac{\mu_{\mathrm{C}}}{T} J_{\mathrm{C}} + \frac{\mu_D}{T} J_{\mathrm{D}}\right) - J_{\mathrm{B}} \frac{\partial}{\partial x}\left(\frac{\mu_{\mathrm{B}}}{T}\right) \\ &\quad - J_{\mathrm{C}} \frac{\partial}{\partial x}\left(\frac{\mu_{\mathrm{C}}}{T}\right) - J_{\mathrm{D}} \frac{\partial}{\partial x}\left(\frac{\mu_{\mathrm{D}}}{T}\right) + \left(\frac{\mu_{\mathrm{B}}}{T} + \frac{\mu_{\mathrm{C}}}{T} - \frac{\mu_{\mathrm{D}}}{T}\right) r\end{aligned}$$

By comparing this equation with Eq. (4.1), we may identify the entropy flux as

$$J_s = -\frac{\mu_{\rm B}}{T} J_{\rm B} - \frac{\mu_{\rm C}}{T} J_{\rm C} - \frac{\mu_{\rm D}}{T} J_{\rm D}$$

and the entropy production as

$$\sigma = -J_{\rm B} \frac{\partial}{\partial x}\left(\frac{\mu_{\rm B}}{T}\right) - J_{\rm C} \frac{\partial}{\partial x}\left(\frac{\mu_{\rm C}}{T}\right) - J_{\rm D} \frac{\partial}{\partial x}\left(\frac{\mu_{\rm D}}{T}\right) + \left(\frac{\mu_{\rm B}}{T} + \frac{\mu_{\rm C}}{T} - \frac{\mu_{\rm D}}{T}\right) r$$

By writing this entropy production as a sum of a scalar and a vectorial part, $\sigma = \sigma_{vect} + \sigma_{scal}$, we find

$$\sigma_{vect} = -J_{\rm B} \frac{\partial}{\partial x}\left(\frac{\mu_{\rm B}}{T}\right) - J_{\rm C} \frac{\partial}{\partial x}\left(\frac{\mu_{\rm C}}{T}\right) - J_{\rm D} \frac{\partial}{\partial x}\left(\frac{\mu_{\rm D}}{T}\right)$$

$$\sigma_{scal} = \left(\frac{\mu_{\rm B}}{T} + \frac{\mu_{\rm C}}{T} - \frac{\mu_{\rm D}}{T}\right) r = -\frac{r \Delta_r G}{T} = \sigma_{chem}$$

In this way, we find the vectorial contributions due to diffusion and the scalar contribution due to the reaction.

4.4 Frames of reference for fluxes in homogeneous systems

In this section, we define the various frames of reference that are used in homogeneous systems. We consider first the transformations between different frames of reference for molar fluxes. We subsequently give the definition of the heat fluxes in the different frames of reference.

4.4.1 *Definitions of frames of reference*

The laboratory frame of reference or the wall frame of reference. The experimental apparatus is at rest in this frame of reference. We define the velocities of the various components in this frame of reference by:

$$J_{\rm A} \equiv c_{\rm A} {\rm v}_{\rm A} \tag{4.18}$$

where $c_{\rm A}$ is the concentration of A in mol/m^3.

The flux of A (in mol/m^2 s) in a frame of reference which is moving with a velocity $\mathrm{v}_{\rm ref}$ relative to the laboratory is given by

$$J_{\rm A,ref} = c_{\rm A}({\rm v}_{\rm A} - {\rm v}_{\rm ref}) \tag{4.19}$$

The solvent frame of reference. This frame of the reference is typical when there is an excess of one component, the solvent. For transport of A relative to the solvent one has:

$$J_{\mathrm{A,solv}} = c_{\mathrm{A}} \left(\mathrm{v}_{\mathrm{A}} - \mathrm{v}_{\mathrm{solv}} \right) \quad \text{and} \quad \mathrm{v}_{\mathrm{ref}} = \mathrm{v}_{\mathrm{solv}} \tag{4.20}$$

The frame of reference moves with the velocity of the solvent, $\mathrm{v}_{\mathrm{solv}}$.

The average molar frame of reference. In a multicomponent mixture, there is no excess of one component, and we use the average molar velocity:

$$\mathrm{v}_{\mathrm{molar}} \equiv \frac{1}{c} \sum_j c_j \mathrm{v}_j = \sum_j x_j \mathrm{v}_j \tag{4.21}$$

Here, $x_j = c_j/c$ is the mole fraction of component j. This gives as flux of A:

$$J_{\mathrm{A,molar}} \equiv c_{\mathrm{A}} \left(\mathrm{v}_{\mathrm{A}} - \mathrm{v}_{\mathrm{molar}} \right) \tag{4.22}$$

The average volume frame of reference is used when transport occurs in a closed volume. The average volume velocity is

$$\mathrm{v}_{\mathrm{vol}} \equiv \sum_j c_j V_j \mathrm{v}_j \tag{4.23}$$

where V_j is the molar volume of component j. The flux of A becomes

$$J_{\mathrm{A,vol}} \equiv c_{\mathrm{A}} \left(\mathrm{v}_{\mathrm{A}} - \mathrm{v}_{\mathrm{vol}} \right) \tag{4.24}$$

The barycentric (average center of mass) frame of reference. This frame of reference is used in the Navier–Stokes equation. The average mass velocity is

$$\mathrm{v}_{\mathrm{bar}} \equiv \frac{1}{\rho} \sum_j \rho_j \mathrm{v}_j \tag{4.25}$$

where ρ is the mass density of the fluid, and ρ_j are the partial mass densities. The flux of A in $\mathrm{mol/m^2 s}$ in the barycentric frame of reference is therefore

$$J_{\mathrm{A,bar}} \equiv c_{\mathrm{A}} \left(\mathrm{v}_{\mathrm{A}} - \mathrm{v}_{\mathrm{bar}} \right) \tag{4.26}$$

In the barycentric frame of reference, the dimension of the component fluxes used is normally $\mathrm{kg/m^2 s}$ [20]. The flux in $\mathrm{kg/m^2 s}$ is found by multiplication with M_{A}, the molar mass, $M_{\mathrm{A}} J_{\mathrm{A,bar}} \equiv \rho_{\mathrm{A}} \left(\mathrm{v}_{\mathrm{A}} - \mathrm{v} \right)$. This is the diffusion flux of component A. The sum of these diffusion fluxes (in $\mathrm{kg/m^2 s}$) over all neutral components is equal to zero.

Remark 4.2. *In our analysis we only consider electroneutral systems. The sum in Eq. (4.25) is therefore over neutral components. In charged systems, like those considered by de Groot and Mazur [20], the sum is over charged and uncharged components. For electroneutral systems, this results in an average mass velocity which differs from the one that we use by a term proportional to the electric current density. We refer to the Appendix at the end of this chapter for an example.*

In this book, we consider heterogeneous systems. As will be explained in the next two sections, the excess entropy production of a surface and a three phase contact line should be calculated in a frame of reference which moves along with the surface or the contact line. We refer to these as *the surface frame of reference* and *the contact line frame of reference*. For practical reasons, the same frame of reference is usually taken for fluxes in the adjacent homogeneous phases. As will be explained in Chapter 12, for multi-component diffusion, one can use Gibbs–Duhem's equation to obtain flux-force relations, which are independent of the frame of reference. For each example considered in this book, we shall indicate which frame of reference is used and why.

4.4.2 *Transformations between the frames of reference*

In an electroneutral system, the electric current density j is independent of the frame of reference. The measurable heat flux, J'_q, is also independent of the frame of reference. The total heat flux, the mass fluxes and the entropy flux depend on the frame of reference. In the laboratory or the wall frame of reference, we denote these fluxes by J_q, J_k and J_s. In any other frame of reference they become:

$$\begin{aligned} J_{q,\mathrm{ref}} &= J_q + \mathrm{v}_{\mathrm{ref}} \sum_{j=1}^{n} c_j H_j = J_q + \mathrm{v}_{\mathrm{ref}} H \\ J_{k,\mathrm{ref}} &= J_k + \mathrm{v}_{\mathrm{ref}} c_k \\ J_{s,\mathrm{ref}} &= J_s + \mathrm{v}_{\mathrm{ref}} \sum_{j=1}^{n} c_j S_j = J_q + \mathrm{v}_{\mathrm{ref}} S \end{aligned} \tag{4.27}$$

All frames of reference defined above can be used for $\mathrm{v}_{\mathrm{ref}}$.

We consider in this book systems that are in mechanical equilibrium. The hydrostatic pressure is then constant and there are no shear forces.

The Gibbs–Duhem's equation for constant pressure is:

$$sdT + \sum_{j=1}^{n} c_j d\mu_j = 0 \tag{4.28}$$

By substituting $J_{q,\mathrm{ref}}$, $J_{j,\mathrm{ref}}$ and $J_{s,\mathrm{ref}}$ into Eqs. (4.13)–(4.15), we find, using Gibbs-Duhem's equation, that the term proportional to $\mathrm{v}_{\mathrm{ref}}$ gives a zero contribution to the entropy production. This result is Prigogine's theorem [20].

Gibbs–Duhem's equation gives a possibility to eliminate a thermodynamic force. Galilean invariance gives a possibility to eliminate a mass flux. One property is a consequence of the other, as we have seen above. De Groot and Mazur [20] used systematically the barycentric frame of reference, because they also treated hydrodynamic phenomena. In this frame of reference, the sum of the mass (diffusion) fluxes is zero (see above). The total heat flux $J_{q,\mathrm{bar}}$ equals the heat flux J_q used by de Groot and Mazur.

4.A Appendix: The first law and the heat flux

The purpose of this appendix is to show how the description of de Groot and Mazur is compatible with the one used in this book. The analysis uses as starting point Chapter XIV in de Groot and Mazur [20]. We restrict ourselves to the case that the magnetic field and the magnetization are zero. The system is also electroneutral. As a final simplification we shall assume the system to be in mechanical equilibrium. The last simplification leads to a form of the first law appropriate for the systems described in this book, Eq. (4.7). Vectors shall be indicated by bold letters in this appendix, meaning that they have an arbitrary direction, rather than being restricted to the x-direction as in most of the book.

For a system in which there are no magnetic field or magnetization, the Maxwell equations (in SI units) can be written as

$$\begin{aligned} \varepsilon_0 \operatorname{div} \mathbf{E} &= -\operatorname{div} \mathbf{P} \\ \operatorname{rot} \mathbf{E} &= 0 \\ \varepsilon_0 \frac{\partial}{\partial t}\mathbf{E} &= \mathbf{j} - \frac{\partial}{\partial t}\mathbf{P} \end{aligned} \tag{4.29}$$

where ε_0 is the dielectric constant of vacuum, $\mathbf{E}$ the electric field, $\mathbf{j}$ the electric current density and $\mathbf{P}$ the polarization density (in $\mathrm{C/m^2}$).

For the molar density of component j, we have the following conservation equation

$$\frac{\partial c_j}{\partial t} = -\operatorname{div}(c_j \mathbf{v}_j) = -\operatorname{div}\mathbf{J}_j \tag{4.30}$$

where $\mathbf{v}_j$ and $\mathbf{J}_j$ are the velocity and the molar flux of component j. The potential energy density satisfies

$$\frac{\partial}{\partial t}\sum_j c_j\psi_j = -\operatorname{div}\left(\sum_j \psi_j \mathbf{J}_j\right) + \sum_j \mathbf{J}_j \cdot \mathbf{F}_j \tag{4.31}$$

where ψ_j is the potential energy per mole of component j, and $\mathbf{F}_j = -\operatorname{grad}\psi_j$ is the external force acting on component j, due to this potential. For the energy of the electric field, we have

$$\frac{\partial}{\partial t}\left(\frac{1}{2}\varepsilon_0 E^2\right) = \varepsilon_0 \mathbf{E}\cdot\frac{\partial}{\partial t}\mathbf{E} = -\mathbf{E}\cdot\left(\mathbf{j}+\frac{\partial}{\partial t}\mathbf{P}\right) \tag{4.32}$$

where we used the third Maxwell equation, Eq. (4.29c). Adding the last two equations results in

$$\begin{aligned}\frac{\partial}{\partial t}\left(\sum_j c_j\psi_j + \frac{1}{2}\varepsilon_0 E^2\right) &= -\operatorname{div}\sum_j \psi_j \mathbf{J}_j \\ &\quad - \mathbf{E}\cdot\left(\mathbf{j}+\frac{\partial}{\partial t}\mathbf{P}\right) - \sum_j \mathbf{F}_j\cdot\mathbf{J}_j\end{aligned} \tag{4.33}$$

Integrating this relation over a time independent volume V, gives

$$\begin{aligned}\frac{d}{dt}\int_V \left(\sum_j c_j\psi_j + \frac{1}{2}\varepsilon_0 E^2\right) d\mathbf{r} &= -\int_O \sum_j \psi_j J_{j,n}\, dO \\ &\quad - \int_V \left[\mathbf{E}\cdot\left(\mathbf{j}+\frac{\partial}{\partial t}\mathbf{P}\right) + \sum_j \mathbf{F}_j\cdot\mathbf{J}_j\right] d\mathbf{r}\end{aligned} \tag{4.34}$$

where O is the surface of the volume, $d\mathbf{r} \equiv dxdydz$ is the volume element, and subscript n indicates the component of a vector normal to the surface. This expression shows that the sum of the potential and electromagnetic energies changes due to two terms. The first gives the potential energy losses from mass flow through the surface. The second term describes the

energy conversion inside the volume. The above expression for the time rate of change of the sum of the potential and electric field energy follows from conservation of mass and the Maxwell equations. No energy conservation has yet been used.

The total energy density per unit of volume, e, also contains the internal energy density per unit of volume u. We therefore have

$$e = u + \sum_j c_j \psi_j + \frac{1}{2}\varepsilon_0 E^2 \tag{4.35}$$

In the description in this book we use fluxes in the laboratory frame of reference. We do not use fluxes in the barycentric frame of reference. Therefore, we do not subtract kinetic energy from e in order to get u. As the total energy is conserved, one has

$$\frac{\partial e}{\partial t} = -\operatorname{div} \mathbf{J}_e \tag{4.36}$$

where $\mathbf{J}_e$ is the total energy flux. In order to proceed, we need an expression for the total heat flux.

Consider the example of an electrolyte solution of NaCl. The salt is completely dissociated into ions and due to the reactions at the electrode surfaces, the chloride ion carries the charge. The system is electroneutral and as a consequence

$$c_{\mathrm{Cl}^-}(\mathbf{r}, t) = c_{\mathrm{Na}^+}(\mathbf{r}, t) = c_{\mathrm{NaCl}}(\mathbf{r}, t) \tag{4.37}$$

The time rate of change of these concentrations is given by

$$\frac{\partial c_{\mathrm{NaCl}}}{\partial t} = -\operatorname{div} \mathbf{J}_{\mathrm{Cl}^-} = -\operatorname{div} \mathbf{J}_{\mathrm{Na}^+} \tag{4.38}$$

The electric current density is

$$\mathbf{j} = F\,(\mathbf{J}_{\mathrm{Na}^+} - \mathbf{J}_{\mathrm{Cl}^-}) \tag{4.39}$$

where F is faraday's constant. Together with Eq. (4.38) it follows that

$$\operatorname{div} \mathbf{j} = 0 \tag{4.40}$$

This also follows from the electroneutrality condition. Given that the sodium ions only move as part of the salt, it follows that the ion fluxes are given by

$$\mathbf{J}_{\mathrm{Na}^+} = \mathbf{J}_{\mathrm{NaCl}} \quad \text{and} \quad \mathbf{J}_{\mathrm{Cl}^-} = \mathbf{J}_{\mathrm{NaCl}} - \frac{\mathbf{j}}{F} \tag{4.41}$$

in terms of the salt flux and the electric current density.

The energy flux in the laboratory frame of reference consists of potential energy which flows along with the molar fluxes, energy of the charge carrier which is carried by the electric current density and of the total heat flux in the laboratory frame of reference

$$\mathbf{J}_e = \sum_j \psi_j \mathbf{J}_j - \mu_{\mathrm{Cl}^-} \frac{\mathbf{j}}{F} + \mathbf{J}_q \tag{4.42}$$

In order to see how the first law of thermodynamics reads for the internal energy, we subtract Eq. (4.33) from Eq. (4.36) and use Eqs. (4.35) and (4.42). This results in

$$\frac{\partial u}{\partial t} = -\operatorname{div} \mathbf{J}_q + \left(\mathbf{E} + \operatorname{grad} \frac{\mu_{\mathrm{Cl}^-}}{F}\right) \cdot \mathbf{j} + \mathbf{E} \cdot \frac{\partial}{\partial t} \mathbf{P} + \sum_j \mathbf{F}_j \cdot \mathbf{J}_j \tag{4.43}$$

The electric field is equal to minus the gradient of the Maxwell potential

$$\mathbf{E}(\mathbf{r}, \mathbf{t}) = -\operatorname{grad} \psi(\mathbf{r}, t) \tag{4.44}$$

The ϕ-potential we use in Eq. (4.7) is equal to

$$\phi(\mathbf{r}, t) \equiv \psi(\mathbf{r}, t) - \frac{\mu_{\mathrm{Cl}^-}(\mathbf{r}, t)}{F} \tag{4.45}$$

This is equal to minus the electrochemical potential of chloride ions divided by the charge of a mole of chloride ions. Electrochemical potentials were first defined by Guggenheim [63, 95]. Using this potential, Eq. (4.43) can be written as

$$\frac{\partial u}{\partial t} = -\operatorname{div} \mathbf{J}_q - \operatorname{grad} \phi \cdot \mathbf{j} + \mathbf{E} \cdot \frac{\partial}{\partial t} \mathbf{P} + \sum_j \mathbf{F}_j \cdot \mathbf{J}_j \tag{4.46}$$

Integrating this relation over a time independent volume V gives

$$\begin{aligned} \frac{d}{dt} \int_V u d\mathbf{r} = &- \int_O J_{q,n} dO \\ &+ \int_V \left[- \operatorname{grad} \phi \cdot \mathbf{j} + \mathbf{E} \cdot \frac{\partial}{\partial t} \mathbf{P} + \sum_j \mathbf{F}_j \cdot \mathbf{J}_j \right] d\mathbf{r} \end{aligned} \tag{4.47}$$

This is a more familiar form of the first law. The internal energy changes due to a total heat flux through the surface. The volume integral contains work added to the system. The first term is the electric work added, and

the second is the work done by the displacement current. In the absence of external forces, and with one-dimensional flow conditions, Eq. (4.46) reduces to Eq. (4.7). Though we restricted the analysis to an example, the result is generally valid. We also refer to Sec.10.6 in this context.

To further compare our analysis with that of de Groot and Mazur, we verify that the barycentric velocity in a description using charged components differs from that in a description using uncharged components, i.e. when the system is electroneutral. We do this for the example above, NaCl in water. The barycentric velocity in the description using charged components is

$$\begin{aligned}
\mathbf{v}^{\text{charged}} &= \frac{M_{\text{Na}^+}\mathbf{J}_{\text{Na}^+} + M_{\text{Cl}^-}\mathbf{J}_{\text{Cl}^-} + M_{\text{H}_2\text{O}}\mathbf{J}_{\text{H}_2\text{O}}}{M_{\text{Na}^+}c_{\text{Na}^+} + M_{\text{Cl}^-}c_{\text{Cl}^-} + M_{\text{H}_2\text{O}}c_{\text{H}_2\text{O}}} \\
&= \frac{M_{\text{Na}^+}\mathbf{J}_{\text{NaCl}} + M_{\text{Cl}^-}\left(\mathbf{J}_{\text{NaCl}} - \frac{\mathbf{j}}{F}\right) + M_{\text{H}_2\text{O}}\mathbf{J}_{\text{H}_2\text{O}}}{M_{\text{Na}^+}c_{\text{Na}^+} + M_{\text{Cl}^-}c_{\text{Cl}^-} + M_{\text{H}_2\text{O}}c_{\text{H}_2\text{O}}} \\
&= \frac{M_{\text{NaCl}}\mathbf{J}_{\text{NaCl}} - M_{\text{Cl}^-}\frac{\mathbf{j}}{F} + M_{\text{H}_2\text{O}}\mathbf{J}_{\text{H}_2\text{O}}}{M_{\text{NaCl}}c_{\text{NaCl}} + M_{\text{H}_2\text{O}}c_{\text{H}_2\text{O}}} \\
&= \frac{M_{\text{NaCl}}\mathbf{J}_{\text{NaCl}} + M_{\text{H}_2\text{O}}\mathbf{J}_{\text{H}_2\text{O}}}{M_{\text{NaCl}}c_{\text{NaCl}} + M_{\text{H}_2\text{O}}c_{\text{H}_2\text{O}}} - \frac{M_{\text{Cl}^-}}{M_{\text{NaCl}}c_{\text{NaCl}} + M_{\text{H}_2\text{O}}c_{\text{H}_2\text{O}}}\frac{\mathbf{j}}{F} \\
&= \mathbf{v}^{\text{uncharged}} - \frac{M_{\text{Cl}^-}}{M_{\text{NaCl}}c_{\text{NaCl}} + M_{\text{H}_2\text{O}}c_{\text{H}_2\text{O}}}\frac{\mathbf{j}}{F}
\end{aligned} \tag{4.48}$$

The electric current does not only carry charge, but also mass. This gives a difference between the barycentric velocities calculated using only neutral components and the one calculated using charged components. *As we do not use fluxes in the barycentric frame of reference in this book, this does not lead to any complications in our analysis.*

Also the measurable heat flux is different in the two descriptions. We have

$$\begin{aligned}
\mathbf{J}_q'^{\text{charged}} &= \mathbf{J}_q - h_{\text{Na}^+}\mathbf{J}_{\text{Na}^+} - h_{\text{Cl}^-}\mathbf{J}_{\text{Cl}^-} - h_{\text{H}_2\text{O}}\mathbf{J}_{\text{H}_2\text{O}} \\
&= \mathbf{J}_q - h_{\text{NaCl}}\mathbf{J}_{\text{NaCl}} - h_{\text{H}_2\text{O}}\mathbf{J}_{\text{H}_2\text{O}} + h_{\text{Cl}^-}\frac{\mathbf{j}}{F} \\
&= \mathbf{J}_q'^{\text{uncharged}} + h_{\text{Cl}^-}\frac{\mathbf{j}}{F}
\end{aligned} \tag{4.49}$$

The difference is the enthalpy of the charge carrier carried along by the electric current. We note that $\mathbf{J}_q$ and $\mathbf{J}_s$, both in the laboratory frame of

reference, are the same whether one uses charged or uncharged components. In view of the fact that h_{Cl^-} is not measurable it is appropriate to call $\mathbf{J}_q'^{\text{uncharged}}$ as measurable. De Groot and Mazur named $\mathbf{J}_q'^{\text{charged}}$ the reduced heat flux.

Finally, we show, again for the same example, that both descriptions give the same entropy production. To simplify the system further we neglect the contribution due to the displacement current. This is the case considered by de Groot and Mazur [20] in Chapter XIII. On page 344 in Eq. (40) they give the entropy production in a system with no magnetic field,

$$\begin{aligned} T\sigma = &-\mathbf{J}_s \cdot \operatorname{grad} T - \mathbf{J}_{\mathrm{Na}^+} \cdot (\operatorname{grad} \mu_{\mathrm{Na}^+} - F\mathbf{E}) - \mathbf{J}_{\mathrm{Cl}^-} \cdot (\operatorname{grad} \mu_{\mathrm{Cl}^-} + F\mathbf{E}) \\ &- \mathbf{J}_{\mathrm{H_2O}} \cdot \operatorname{grad} \mu_{\mathrm{H_2O}} \end{aligned} \tag{4.50}$$

In the analysis of de Groot and Mazur all fluxes are in the barycentric frame of reference. For a system in mechanical equilibrium, one may replace all of them by their value in the laboratory frame of reference. The difference is a term which is zero, according to Gibbs–Duhem's equation. The fact that the expression is correct in an arbitrary frame of reference if the system is in mechanical equilibrium, is called Prigogine's theorem [15]. Using Eq. (4.41) for the ion fluxes, we obtain

$$\begin{aligned} T\sigma &= -\mathbf{J}_s \cdot \operatorname{grad} T - \mathbf{J}_{\mathrm{NaCl}} \cdot \operatorname{grad} \mu_{\mathrm{Na}^+}\mu_{\mathrm{Cl}^-} \\ &\quad - \mathbf{J}_{\mathrm{H_2O}} \cdot \operatorname{grad} \mu_{\mathrm{H_2O}} + \frac{\mathbf{j}}{F} \cdot (\operatorname{grad} \mu_{\mathrm{Cl}^-} + F\mathbf{E}) \\ &= -\mathbf{J}_s \cdot \operatorname{grad} T - \mathbf{J}_{\mathrm{NaCl}} \cdot \operatorname{grad} \mu_{\mathrm{NaCl}} - \mathbf{J}_{\mathrm{H_2O}} \cdot \operatorname{grad} \mu_{\mathrm{H_2O}} - \mathbf{j} \cdot \operatorname{grad} \phi \end{aligned} \tag{4.51}$$

This is the expression we gave in Eq. (4.14) for the case that there is no polarization and no chemical reaction.

Chapter 5

The Excess Entropy Production for the Surface

We derive the entropy production for a surface area element. The entropy production determines the conjugate fluxes and forces. Equivalent forms of the entropy production are given. The forms contain finite differences of intensive variables into, out of and across the surface as driving forces.

We are interested in the energy conversion that takes place at surfaces. The surface has a thickness that is small compared to the thickness of the adjacent homogeneous phases. The thermodynamic properties of the surface can then be defined using Gibbs method, as *surface excess densities* of mass, entropy, energy and polarization, see Chapter 3. Following Bedeaux, Albano and Mazur [2,3] and Bertrand and Prud'homme [59,60], we shall now make the crucial assumption that surface excess densities can be defined, and thermodynamic relations remain valid, also when the system is out of equilibrium. That is, we assume local equilibrium in the surface, cf. Sec. 3.5.

We are seeking a systematic way to set up equations of transport for heat, mass and charge into, out of and across such autonomous surfaces. Such equations will allow us to model, for instance, electrochemical reactions or phase transitions, phenomena that need a surface to occur. In the homogeneous phases, the variables are continuous. In contrast, at the surface, we have a discrete situation with fluxes directed into and out of the surface. The surface may act as a source of heat or energy, and fluxes may be discontinuous. The situation is typical for phase transitions, distillation, heterogeneous catalysis, electrochemical reactions to name a few [38, 61, 123–125]. We shall not consider transport along the surface. For this we refer to [2,3].

We stated in Chapter 4 that the second law must apply to any volume element of a homogeneous phase. This statement is now extended to the surface area element, with the entropy balance

$$\frac{d}{dt}s^{\mathrm{s}}(t) - J_s^{\mathrm{i,o}}(t) + J_s^{\mathrm{o,i}}(t) = \sigma^{\mathrm{s}}(t) \geq 0 \tag{5.1}$$

Here, $ds^{\mathrm{s}}(t)/dt$ is the rate of change of the excess entropy density per unit of surface area. This is equal to the entropy flux into the surface, minus the entropy flux out of the surface, plus the excess entropy production, $\sigma^{\mathrm{s}}(t)$. The asymptotic value of the entropy flux in phase i, $J_s^{\mathrm{i,o}}(t)$, is directed into the surface, while the entropy flux in phase o, $J_s^{\mathrm{o,i}}(t)$, is directed out of the surface, see Fig. 5.1. According to the second law, this excess entropy production is positive for the surface.

We use straight derivatives, because the excess surface entropy depends only on the time, not on the position. The first roman superscript gives the phase; i, s or o in this case. The second superscript, o or i, indicates the phase across the surface. The combination i,o means therefore the value in phase i as close as possible to the o-phase at the interface. The notation is also illustrated in Fig. 5.5. Balance equations of the form (5.1) can be derived from a continuous description, as was done by Albano *et al.* [106,126], or using non-equilibrium statistical mechanics as was done by Ronis *et al.* [127,128].

A short overview of the objectives and the methods used was given by Bedeaux and Kjelstrup [61].

5.1 The discrete nature of the surface

On a macroscopic scale the surface is two-dimensional. In Fig. 5.1, we give an enlarged picture of the surface using a nanometer scale. On this scale the surface area element appears as a volume element with thickness δ. On the nanometer scale the fluxes in the homogeneous phases are in very good approximation constant, and we may therefore define the asymptotic values of these fluxes by:

$$J_s^{\mathrm{i,o}}(t) \equiv J_s^{\mathrm{i}}(a,t) \quad \text{and} \quad J_s^{\mathrm{o,i}}(t) \equiv J_s^{\mathrm{o}}(b,t) \tag{5.2}$$

where a refers to the start, and b refers to the end of the surface, see Fig. 3.2.

We shall find explicit expressions for $\sigma^{\mathrm{s}}(t)$, along the same lines as for $\sigma(x,t)$ of the homogeneous phase in Chapter 4 by combining:

- mass balances
- the first law of thermodynamics

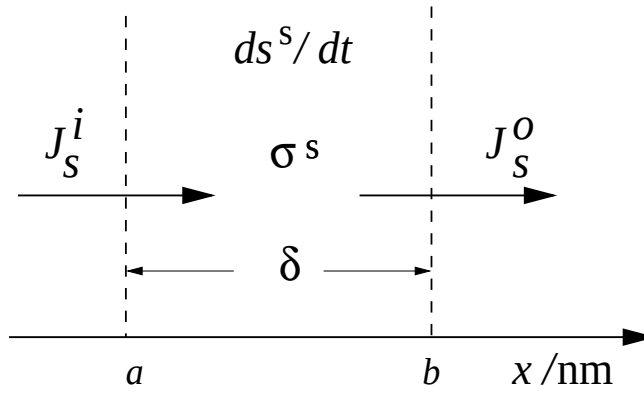

Figure 5.1 The change of the excess surface entropy density due to entropy fluxes in and out of the surface and entropy production in the surface. The surface thickness, $\delta = b - a$, is small compared to the thickness of the adjacent phases.

- the local form of the Gibbs equation.

We shall see that also $\sigma^{\mathrm{s}}(t)$ can be written as the product sum of thermodynamic fluxes and forces in the system. These are the *conjugate* fluxes and forces for the surface. The fluxes and forces will be used in subsequent chapters to describe transports across and into the surface in various heterogeneous systems. Again, we choose *the positive direction of transport from left to right.* The fluxes in this chapter are always in the surface frame of reference, which is the frame of reference in which the surface is at rest. In other frames of reference, see Sec. 4.4, the balance equations for the excess densities, like Eq. (5.1) for the excess entropy density, have to be modified with terms linear in the velocity of the surface [2–4]. We recommend to use the symbol list for a check of the dimensions in the equations.

5.2 The behavior of the electric fields and potential through the surface

The excess entropy production of the surface can contain electric driving forces. We define here the excess electric field E^{s} and excess polarization P^{s}. The normal component of the homogeneous displacement field, D, is continuous through the surface in an electroneutral system. The displacement field therefore has no excess, $D^{\mathrm{s}} = 0$. The normal components of E

and P both have a peak in the interfacial region. From $D^{\mathrm{s}} = \varepsilon_0 E^{\mathrm{s}} + P^{\mathrm{s}} = 0$, it follows that $\varepsilon_0 E^{\mathrm{s}} = -P^{\mathrm{s}}$, where ε_0 is the dielectric constant of vacuum. One must use the constant displacement field, rather than the strongly varying electric field, in the driving force for polarization changes of the surface (see Refs. [3, 5, 6, 126] for more fundamental reasons). The fields and the polarization density are perpendicular to the interface. Components of these vectors parallel to the surface are not the topic of this book.

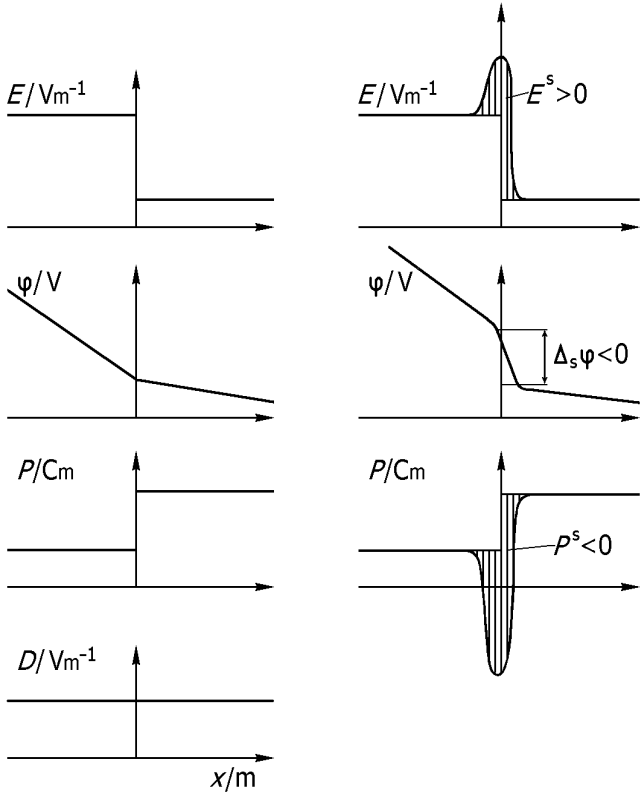

Figure 5.2 The various electric fields, polarizations and electric potential at an unpolarized (left) and a polarized (right) electrode surface.

The various electromagnetic fields and potentials through a surface are illustrated in Fig. 5.2. To the left in the figure is shown the electric field, the electric potential, the polarization and the displacement field

in the absence of excess surface polarization. The right part of the figure shows the modifications due to excess surface polarization and electric field. The excess electric field, or equivalently the excess surface polarization, results in a *jump* in the electric potential. The displacement field is not modified.

Bedeaux and Vlieger wrote a book entitled *Optical Properties of Surfaces* [5, 6] using a description of the surface in terms of E^{s} and P^{s}. This book contains an in-depth discussion of the behavior of electromagnetic fields near surfaces.

5.3 Balance equations

The adsorption Γ_j of component j increases when the influx of j is larger than the outflux or when a chemical reaction produces the component:

$$\frac{d}{dt}\Gamma_j(t) = J_j^{\mathrm{i,o}}(t) - J_j^{\mathrm{o,i}}(t) + \nu_j r^{\mathrm{s}}(t) \tag{5.3}$$

The asymptotic value of the flux of j from phase i into the surface is $J_j^{\mathrm{i,o}}(t)$, while the asymptotic value of the flux out of the surface into phase o is $J_j^{\mathrm{o,i}}(t)$, cf. Fig. 5.3. The excess chemical reaction rate in the surface element is $r^{\mathrm{s}}(t)$, and ν_j is a stoichiometric constant. The surface is again the frame of reference for the fluxes.

At electrode surfaces, there is always a discontinuity of charge carrier from electron to ion. The electrode reaction describes this change. The reaction Gibbs energy is

$$\Delta_r G^{\mathrm{s}}(t) \equiv \sum_j \nu_j \mu_j^{\mathrm{s}} \tag{5.4}$$

where the sum in Eq. (5.4) is over all species involved in the reaction. In our description of the surface we shall also need the contribution to the reaction Gibbs energy due to the neutral species

$$\Delta_n G^{\mathrm{s}}(t) \equiv \sum_{j \,\in\, neutral} \nu_j \mu_j^{\mathrm{s}} \tag{5.5}$$

where the sum in Eq. (5.5) is only over the neutral components. The difference between $\Delta_n G^{\mathrm{s}}$ and the usual expression $\Delta_r G^{\mathrm{s}}$, is due to the chemical potentials of ions and electrons. We explain why we need $\Delta_n G^{\mathrm{s}}(t)$ in Secs. 10.6–10.7.

The surface may be polarized and include a double layer. Including the double layer, the surface is still electroneutral. The thermodynamic state of the surface is determined using absorptions of neutral components only.

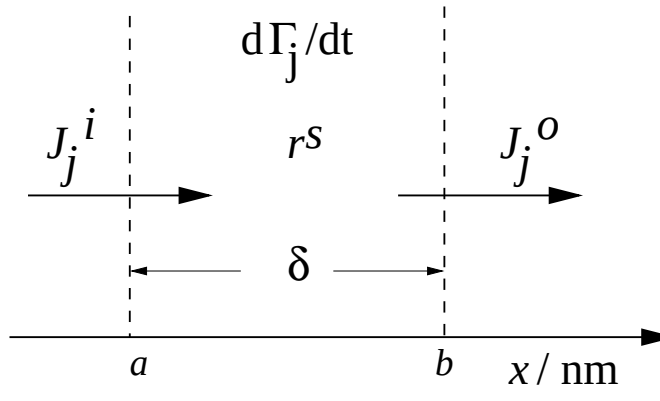

Figure 5.3 The mass balance for a surface with a chemical reaction r^s, according to Eq. (5.3). The surface has a thickness $\delta = b - a$.

The balance equation for the excess charge, $z^{\mathrm{s}}(t)$, in the surface is

$$\frac{d}{dt} z^{\mathrm{s}}(t) = j^{\mathrm{i,o}}(t) - j^{\mathrm{o,i}}(t) \tag{5.6}$$

where $j^{\mathrm{i,o}}(t)$ is the asymptotic value of the homogeneous electric current from the adjacent phase i into the surface and $j^{\mathrm{o,i}}(t)$ is the asymptotic value of the homogeneous electric current from the surface into the adjacent phase o. We can and will always choose the surface so that it has no *excess* charge density. The surface thus includes, for instance, the polarization due to the electric double layer in an electrolyte. This polarization can be calculated for instance using the Debije–Hückel theory. When $z^{\mathrm{s}}(t) = 0$, the electric current density is constant through the surface, $j^{\mathrm{i,o}}(t) = j^{\mathrm{o,i}}(t)$. Electroneutrality in the homogeneous phases means that the electric current densities are independent of the position. We obtain $j^{\mathrm{i,o}}(t) = j^{\mathrm{i}}(t)$ and $j^{\mathrm{o,i}}(t) = j^{\mathrm{o}}(t)$, and conclude that the electric current density is independent of the position throughout the system

$$j^{\mathrm{i}}(t) = j^{\mathrm{o}}(t) = j(t) \tag{5.7}$$

Exercise 5.3.1. *Derive Eq. (5.3) using Fig. 5.3.*

- **Solution:** In Fig. 5.3 we see that the change in the number of moles of a component is due to the flux in of this component at position a and out at position b of the surface area element. One has therefore

$$\frac{d}{dt} N_j^{\mathrm{s}}(t) = -\Omega[J_j^{\mathrm{o}}(b,t) - J_j^{\mathrm{i}}(a,t)] \pm \Omega(b-a)\nu_j r(t)$$

where Ω is the surface area orthogonal to the flow direction (the fluxes are per unit of surface area) and r is the reaction rate per unit of volume between a and b. By dividing this equation left and right by the (time independent) surface area, defining $r^{\mathrm{s}}(t) = (b-a)r(t)$ and identifying $J_j^{\mathrm{i}}(a,t) = J_j^{\mathrm{i,o}}(t)$ and $J_j^{\mathrm{o}}(b,t) = J_j^{\mathrm{o,i}}(t)$, we obtain Eq. (5.3).

Remark 5.1. *The surface does not have to be microscopically thin to qualify as a surface in the Gibbs sense. The only important condition is that the homogeneous regions adjacent to the surface are much thicker than the surface and that the variation in parameters like the temperature or the potentials over a distance comparable to the surface thickness in the homogeneous regions is comparatively small.*

The first law of thermodynamics for the electroneutral, polarizable surface is:

$$\frac{du^{\mathrm{s}}(t)}{dt} = J_q^{\mathrm{i,o}}(t) - J_q^{\mathrm{o,i}}(t) - j(t)[\phi^{\mathrm{o,i}}(t) - \phi^{\mathrm{i,o}}(t)] + \frac{D(t)}{\varepsilon_0}\frac{dP^{\mathrm{s}}(t)}{dt} \tag{5.8}$$

The time rate of change in the excess energy density of the surface, u^{s}, is given in this equation by the asymptotic value of the total heat flux from the adjacent phase i into the surface from the left, $J_q^{\mathrm{i,o}}$, minus the asymptotic value of the total heat flux out of the surface into the adjacent phase o, $J_q^{\mathrm{o,i}}$, the electric work per area done to the surface, $-j(\phi^{\mathrm{o,i}} - \phi^{\mathrm{i,o}})$, and the polarization work done per area, $(D/\varepsilon_o)(dP^{\mathrm{s}}/dt)$. In this last term, dP^{s}/dt gives a non-faradaic contribution to the current due to the changing dipole moment of the surface. The electric current density through the adjacent homogeneous materials and the surface is j, and $\phi^{\mathrm{o,i}}$ and $\phi^{\mathrm{i,o}}$ are the electric potentials in the homogeneous phases close to the surface.

The energy change in the surface is illustrated in Fig. 5.4. The work per unit of time due to a change in the polarization, for instance of an electric double layer, leads to measurable changes in the electric potential difference across the system.

5.4 The excess entropy production

The Gibbs equation in its local form, (3.29), is

$$du^{\mathrm{s}} = T^{\mathrm{s}}ds^{\mathrm{s}} + \sum_{j=1}^{n} \mu_j^{\mathrm{s}} d\Gamma_j + \frac{D_{\mathrm{eq}}}{\varepsilon_0} dP^{\mathrm{s}} \tag{5.9}$$

The energy change due to polarization changes for surfaces can be large. An example is the polarization of an electrode due to the double layer of

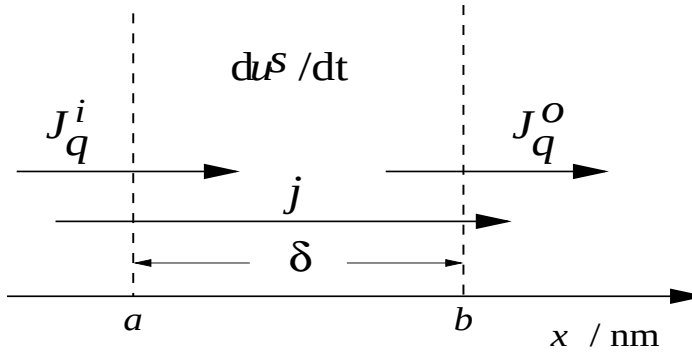

Figure 5.4 The energy change in the surface with fluxes of energy, cf. Eq. (5.8), and of electric current.

an electrolyte. The polarization is in general a sum of a number of contributions. All these contributions should be taken into account as separate contributions in the above expressions, with their own equilibrium displacement fields. For ease of notation we restrict ourselves to only one such contribution. From here on, the time dependence shall not be explicitly indicated. The time derivative of the entropy density is:

$$\frac{ds^{\mathrm{s}}}{dt} = \frac{1}{T^{\mathrm{s}}}\frac{du^{\mathrm{s}}}{dt} - \frac{1}{T^{\mathrm{s}}}\sum_{j=1}^{n}\mu_j^{\mathrm{s}}\frac{d\Gamma_j}{dt} - \frac{1}{T^{\mathrm{s}}}\frac{D_{\mathrm{eq}}}{\varepsilon_0}\frac{dP^{\mathrm{s}}}{dt} \tag{5.10}$$

By introducing Eqs. (5.8) and (5.3) into Eq. (5.10), and comparing the result to the entropy balance Eq. (5.1), we find the excess entropy production:

$$\begin{aligned}\sigma^{\mathrm{s}} = {} & J_q^{\mathrm{i,o}}\left(\frac{1}{T^{\mathrm{s}}} - \frac{1}{T^{\mathrm{i,o}}}\right) + J_q^{\mathrm{o,i}}\left(\frac{1}{T^{\mathrm{o,i}}} - \frac{1}{T^{\mathrm{s}}}\right) + \sum_{j=1}^{n} J_j^{\mathrm{i,o}}\left[-\left(\frac{\mu_j^{\mathrm{s}}}{T^{\mathrm{s}}} - \frac{\mu_j^{\mathrm{i,o}}}{T^{\mathrm{i,o}}}\right)\right] \\ & + \sum_{j=1}^{n} J_j^{\mathrm{o,i}}\left[-\left(\frac{\mu_j^{\mathrm{o,i}}}{T^{\mathrm{o,i}}} - \frac{\mu_j^{\mathrm{s}}}{T^{\mathrm{s}}}\right)\right] + j\left[-\frac{1}{T^{\mathrm{s}}}(\phi^{\mathrm{o,i}} - \phi^{\mathrm{i,o}})\right] \\ & + \frac{dP^{\mathrm{s}}}{dt}\left[\frac{1}{T^{\mathrm{s}}}\left(\frac{D - D_{eq}}{\varepsilon_0}\right)\right] + r^{\mathrm{s}}\left(-\frac{1}{T^{\mathrm{s}}}\Delta_n G^{\mathrm{s}}\right)\end{aligned} \tag{5.11}$$

All the fluxes in this equation are in the surface reference frame. We may alternatively write this expression using the entropy fluxes. From Eqs. (4.8)

and (4.12), we have

$$J_q(x,t) = T(x,t)J_s(x,t) + \sum_{j=1}^{n} \mu_j(x,t)J_j(x,t)$$
$$= J'_q(x,t) + \sum_{j=1}^{n} H_j(x,t)J_j(x,t) \tag{5.12}$$

Using this equation on both sides of the surface gives

$$\sigma^{\mathrm{s}} = J_s^{\mathrm{i,o}} \left(-\frac{\Delta_{\mathrm{i,s}} T}{T^{\mathrm{s}}} \right) + J_s^{\mathrm{o,i}} \left(-\frac{\Delta_{\mathrm{s,o}} T}{T^{\mathrm{s}}} \right) + \sum_{j=1}^{n} J_j^{\mathrm{i,o}} \left(-\frac{\Delta_{\mathrm{i,s}} \mu_j}{T^{\mathrm{s}}} \right)$$
$$+ \sum_{j=1}^{n} J_j^{\mathrm{o,i}} \left(-\frac{\Delta_{\mathrm{s,o}} \mu_j}{T^{\mathrm{s}}} \right) + j \left[-\frac{1}{T^{\mathrm{s}}} \Delta_{\mathrm{i,o}} \phi \right]$$
$$+ \frac{dP^{\mathrm{s}}}{dt} \left[\frac{1}{T^{\mathrm{s}}} \left(\frac{D - D_{eq}}{\varepsilon_0} \right) \right] + r^{\mathrm{s}} \left(-\frac{1}{T^{\mathrm{s}}} \Delta_n G^{\mathrm{s}} \right) \tag{5.13}$$

where the entropy flux in the nearby phases is given by

$$J_s(x,t) = \frac{1}{T(x,t)} \left[J_q(x,t) - \sum_{j=1}^{n} \mu_j(x,t) J_j(x,t) \right]$$
$$= \frac{J'_q(x,t)}{T(x,t)} + \sum_{j=1}^{n} s_j(x,t) J_j(x,t) \tag{5.14}$$

Furthermore, we give the form of σ^{s} which we are going to use most often. It is obtained by replacing the total heat fluxes by the measurable heat fluxes, using Eq. (5.12):

$$\sigma^{\mathrm{s}} = J_q'^{\mathrm{i,o}} \Delta_{\mathrm{i,s}} \frac{1}{T} + J_q'^{\mathrm{o,i}} \Delta_{\mathrm{s,o}} \frac{1}{T} + \sum_{j=1}^{n} J_j^{\mathrm{i,o}} \left[-\frac{1}{T^{\mathrm{s}}} \Delta_{\mathrm{i,s}} \mu_{j,T}(T^{\mathrm{s}}) \right]$$
$$+ \sum_{j=1}^{n} J_j^{\mathrm{o,i}} \left[-\frac{1}{T^{\mathrm{s}}} \Delta_{\mathrm{s,o}} \mu_{j,T}(T^{\mathrm{s}}) \right] + j \left(-\frac{1}{T^{\mathrm{s}}} \Delta_{\mathrm{i,o}} \phi \right)$$
$$+ \frac{dP^{\mathrm{s}}}{dt} \left[\frac{1}{T^{\mathrm{s}}} \left(\frac{D - D_{eq}}{\varepsilon_0} \right) \right] + r^{\mathrm{s}} \left(-\frac{1}{T^{\mathrm{s}}} \Delta_n G^{\mathrm{s}} \right) \tag{5.15}$$

When we describe heat, mass and charge transport it is sometimes convenient to use the energy flux J_u (see e.g. Chapter 19) which is defined by

$$J_u(x,t) = J_q(x,t) + \phi(x,t)j = J'_q(x,t) + \sum_{j=1}^{n} H_j(x,t)J_j(x,t) + \phi(x,t)j \tag{5.16}$$

The excess entropy production then becomes

$$\begin{aligned}\sigma^{\mathrm{s}} = {} & J_u^{\mathrm{i,o}}\left(\Delta_{\mathrm{i,s}}\frac{1}{T}\right) + J_u^{\mathrm{o,i}}\left(\Delta_{\mathrm{s,o}}\frac{1}{T}\right) + \sum_{j=1}^{n} J_j^{\mathrm{i,o}}\left(-\Delta_{\mathrm{i,s}}\frac{\mu_j}{T}\right) \\ & + \sum_{j=1}^{n} J_j^{\mathrm{o,i}}\left(-\Delta_{\mathrm{s,o}}\frac{\mu_j}{T}\right) + j\left(-\Delta_{\mathrm{i,o}}\frac{\phi}{T}\right) \\ & + \frac{dP^{\mathrm{s}}}{dt}\left[\frac{1}{T^{\mathrm{s}}}\left(\frac{D - D_{eq}}{\varepsilon_0}\right)\right] + r^{\mathrm{s}}\left(-\frac{1}{T^{\mathrm{s}}}\Delta_n G^{\mathrm{s}}\right)\end{aligned} \tag{5.17}$$

All fluxes in the equations for the excess entropy production are in the surface frame of reference.

Remark 5.2. *The excess entropy production is independent of the frame of reference. We can derive expressions for other frames of reference, but the resulting expressions are complicated and not needed for applications in this book. Expressions valid in an arbitrary frame of reference can be found in references [2–4, 60, 129].*

Remark 5.3. *In this chapter we use $J^{i,o}$ and $T^{o,i}$, and not J^i and T^o, when we mean the value of this quantity next to the interface. In subsequent chapters we shall, when this is not confusing, drop the second index in order to simplify notation.*

Remark 5.4. *In a given situation, we choose a form of the excess entropy production that is practical. Integration through the surface is simplest with constant fluxes, so a form with constant fluxes can be convenient in some cases. When the aim is to describe calorimetric measurements, one has to use the measurable heat flux.*

Equations (5.13) and (5.15) introduced the notation for jumps in a variable at the surface. Using the temperature as an example:

$$\begin{aligned}\Delta_{\mathrm{i,o}}T &\equiv T^{\mathrm{o,i}} - T^{\mathrm{i,o}} \\ \Delta_{\mathrm{i,s}}T &\equiv T^{\mathrm{s}} - T^{\mathrm{i,o}} \\ \Delta_{\mathrm{s,o}}T &\equiv T^{\mathrm{o,i}} - T^{\mathrm{s}}\end{aligned} \tag{5.18}$$

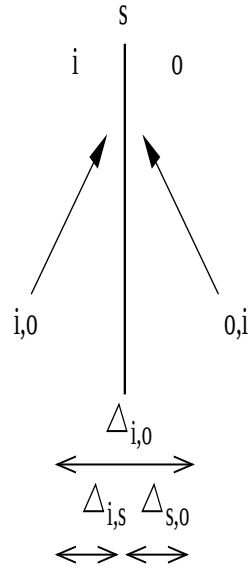

Figure 5.5 Standard notation for transport across surfaces.

The differences of the surface chemical potentials at constant temperature are given in terms of the values in the homogeneous phases close to the surface, in the points a and b, at the temperature of the surface:

$$\begin{aligned} \Delta_{\mathrm{i,s}}\mu_{j,T}(T^{\mathrm{s}}) &= \mu_j^{\mathrm{s}}(T^{\mathrm{s}}) - \mu_j^{\mathrm{i,o}}(T^{\mathrm{s}}) \\ \Delta_{\mathrm{s,o}}\mu_{j,T}(T^{\mathrm{s}}) &= \mu_j^{\mathrm{o,i}}(T^{\mathrm{s}}) - \mu_j^{\mathrm{s}}(T^{\mathrm{s}}) \end{aligned} \tag{5.19}$$

A subscript T indicates a chemical potential difference at a constant surface temperature. Each jump is written as the value to the right minus the value to the left. This choice gives the jumps the same sign as the gradients in the homogeneous phases for increasing or decreasing variables. The subscripts of Δ refer to the two locations between which the difference is taken. The notation is further illustrated in Fig. 5.5.

It is interesting to compare Eqs. (5.11), (5.13), (5.15) and (5.17) with Eqs. (4.13)–(4.15) and (4.17), that we use for the homogeneous phase. The gradients of the temperature and the chemical potentials have been replaced by jumps of these variables into and out of the surface, the fluxes are the same. The gradient of the electric potential has been replaced by a jump across the surface. These replacements represent the discrete nature of the surface and are typical for transport between different homogeneous parts of a system [130].

Most of the contributions to the excess entropy production of a planar, isotropic surface given above are due to fluxes of heat, mass and charge in the homogeneous phases outside the surface. The contribution from the chemical reaction is, however, a specific *surface* contribution. For further details, we refer to Sec. 7.5 [3, 4, 60, 129]. At the surface, the system is no longer isotropic in the normal direction, so that all the normal fluxes, unlike in a homogeneous phase, are scalar under rotations and reflections in the plane of the surface. We therefore have coupling between chemical reactions and such fluxes of heat, mass and charge at a surface. Mass transport fueled by energy from a chemical reaction is called active transport in biology [24,52]. The coupling that takes place between scalar fluxes at the surface makes transports in heterogeneous systems different from transports in homogeneous system.

We need a *common* frame of reference for the fluxes when we want to describe transport in heterogeneous materials. In electroneutral systems, the electric current density, j, is constant throughout the system and independent of the frame of reference. Mass fluxes, on the other hand, depend on the frame of reference. The frame of reference that gives a simple realistic description of the surface is the surface itself. In this frame of reference, the observer moves along with the surface. If the surface is at rest, so is the observer. This is then also the laboratory frame of reference. It is difficult to describe the surface processes, without using the surface as a frame of reference. The natural choice of the frame of reference for a heterogeneous system is therefore the *surface frame of reference*. All expressions for the entropy production of the surface, contain fluxes relative to this frame of reference. We shall proceed to use this frame of reference *also for the adjacent homogeneous phases*, when nothing else is stated. For a definition of the various frames of reference, and transformations between them, we refer to Sec. 4.4.

The excess entropy production is independent of the frame of reference, and so are the notions, reversible and irreversible. They are in other words invariant under a coordinate transformation. We may therefore convert all fluxes and conjugate forces from any frame of reference to the surface frame of reference and back without changing the entropy productions, σ^{i}, σ^{s} and σ^{o}.

5.4.1 *Reversible processes at the interface and the Nernst equation*

The expression for the excess entropy production contains information about the interface at equilibrium. Take as an example an electrode surface. At equilibrium, the excess entropy production is zero. Using Eq. (5.15)

as a starting point, we see that the equilibrium conditions are constant temperature

$$T^{\mathrm{o,i}} = T^{\mathrm{s}} = T^{\mathrm{i,o}} \tag{5.20}$$

equilibrium for adsorbed components;

$$\mu_j^{\mathrm{i,o}}(T^{\mathrm{s}}) = \mu_j^{\mathrm{s}}(T^{\mathrm{s}}) = \mu_j^{\mathrm{o,i}}(T^{\mathrm{s}}) \tag{5.21}$$

and constant polarization

$$\frac{dP^{\mathrm{s}}}{dt} = 0 \tag{5.22}$$

During an emf measurement, very small electric currents are passing the electrode. The constant current means that the electrode reaction is also constant, and $r^{\mathrm{s}} = j/F$. By introducing these conditions into Eq. (5.15) the remaining terms combine to

$$-\left[\Delta_{\mathrm{i,o}}\phi + \Delta_n G^{\mathrm{s}}/F\right](j/T^{\mathrm{s}}) = 0 \tag{5.23}$$

meaning that

$$\Delta_{\mathrm{i,o}}\phi = -\Delta_n G^{\mathrm{s}}/F \tag{5.24}$$

The reversible process is characterized by a balance of forces. The electrical force is balanced by the chemical driving force. The equation is the Nernst equation. It is written for the surface alone. The choice of variables in the excess entropy production, means that we can calculate the surface potential drop, since all contributions to $\Delta_n G^{\mathrm{s}}$ are well-defined and often accessible in thermochemical tables.

Remark 5.5. *The value of $\Delta_{i,o}\phi$ depends on the standard state that is chosen for the chemical potential of the neutral components. It is thus not an absolute quantity. When the potential difference is calculated between two electrodes, this arbitrariness disappears, if care is taken to use the same standard states, see Appendix 3.A.*

Remark 5.6. *The description using absorptions of neutral components only is equivalent to a description using both charged and uncharged components. This can be seen from the contribution $\left[j(-\Delta_{i,o}\phi) + r^s(-\Delta_n G^s)\right]/T^s$ when $j/F = r^s$. The difference ϕ^o-ϕ^i is equal to the Maxwell potential difference ψ^o- ψ^i plus the sum of the chemical potentials of the charge carriers divided by Faraday's constant. This gives $\Delta_{i,o}\phi + \Delta_n G^s/F = \Delta_{i,o}\psi + \Delta_r G^s/F$ where $\Delta_r G^s$ is the total reaction Gibbs energy, cf. Eq. (5.4). The Nernst equation for the Maxwell potential difference obtains thereby its more usual form. This shall be shown in Sec. 10.7. See also Appendix 4.A.*

Away from equilibrium also other forces in the expression for σ^{s} contribute to $\Delta_{\mathrm{i,o}}\phi$. In addition to a concentration overpotential ($\mu_j^{\mathrm{i,o}}(T^{\mathrm{s}}) \neq \mu_j^{\mathrm{s}}(T^{\mathrm{s}})$), there can be a thermal overpotential ($T^{\mathrm{o,i}} \neq T^{\mathrm{s}}$). The important reaction overpotential, the resistance of the chemical reaction to charge transfer, can only be described in its linear regime with the theory of this book. In order to describe the activated process with a thermodynamic basis, we need to introduce so-called internal variables and extend non-equilibrium thermodynamics to the mesoscopic level, cf. Sec. 1.1 [51].

5.4.2 *The surface potential jump at the hydrogen electrode*

The hydrogen electrode is used to build standard electrochemical tables. The electrode reaction is

$$\frac{1}{2}\mathrm{H_2}(g) \rightleftharpoons \mathrm{H^+} + e^- \tag{5.25}$$

The standard reduction potential of the hydrogen electrode is set to zero, and other electrode reactions are measured with reference to this value. At standard conditions the hydrogen pressure is 1 bar. According to Eq. (5.24), the surface potential jump is given by the standard chemical potential of hydrogen gas, which is zero by definition

$$\Delta_{\mathrm{a,e}}\phi(\mathrm{H_2}) = -\frac{1}{2F}\mu^0_{\mathrm{H_2}} \equiv 0 \tag{5.26}$$

At any other pressure, the surface potential drop from the anode (a) to the electrolyte (e) becomes

$$\Delta_{\mathrm{a,e}}\phi(\mathrm{H_2}) = -\frac{1}{2F}\mu_{\mathrm{H_2}} = -\frac{1}{2F}(\mu^0_{\mathrm{H_2}} + RT\ln p_{\mathrm{H_2}}/p^0) \tag{5.27}$$

This expression shall be used in Chapter 19 to calculate the surface potential drop at the anode of the fuel cell. The value of $\Delta_{\mathrm{a,e}}\phi(\mathrm{H_2})$ for the anode in the polymer electrolyte fuel cell, where the electrolyte is an acid membrane is 0.23 V at 340 K and a hydrogen pressure of 0.76 bar, see Figs. 19.3 and 19.4.

Out of equilibrium, when the electric current density may become sizeable, temperature differences may arise, and the other terms in the entropy production may become important. All forces and fluxes in Eq. (5.15) are coupled. The coupling of these phenomena is further described in the applied part of the book.

Remark 5.7. *The advantage of using $\Delta_{i,o}\phi$ is its relation to measurable quantities, as discussed by Guggenheim [63, 95]. The alternative form of*

the Nernst equation includes chemical potentials of ions, which cannot be measured. The meaning of the term $-j\Delta_{i,o}\phi$ comes from Eq. (5.8). The product is the electric work done to the interface when the current j is passing the cell. In the absence of an external circuit and an electric current, the term disappears from the entropy production.

Remark 5.8. *When the standard reduction potential for hydrogen is expressed in terms of the Maxwell potential jump, the convention $\mu^0_{H^+} + \mu^0_{e^-} - \frac{1}{2}\mu^0_{H_2} = 0$ is used to construct standard tables of reduction potentials.*

5.5 Examples

The details of the derivation of the excess entropy production is illustrated by the following exercises.

Exercise 5.5.1. *Consider the special case that one component k is transported through an isothermal surface. The densities of the other components, the internal energy, the molar surface area and the polarization densities are all independent of the time. Show that the excess entropy production is given by*

$$\sigma^s = J_k^{i,o}\left[-\frac{1}{T^s}\left(\mu_k^s - \mu_k^{i,o}\right)\right] + J_k^{o,i}\left[-\frac{1}{T^s}\left(\mu_k^{o,i} - \mu_k^s\right)\right]$$

- **Solution:** In this case, Eq. (5.10) reduces to

$$T^{\mathrm{s}}\frac{ds^{\mathrm{s}}}{dt} + \mu_k^{\mathrm{s}}\frac{d\Gamma_k}{dt} = 0$$

The rate of change of the entropy is therefore given by

$$\frac{ds^{\mathrm{s}}}{dt} = -\frac{\mu_k^{\mathrm{s}}}{T^{\mathrm{s}}}\frac{d\Gamma_k}{dt} = -\frac{\mu_k^{\mathrm{s}}}{T^{\mathrm{s}}}\left(J_k^{\mathrm{i,o}} - J_k^{\mathrm{o,i}} + r_k^{\mathrm{s}}\right)$$

where we substituted Eq. (5.3). Setting $r_k^{\mathrm{s}} = 0$ one obtains

$$\begin{aligned}\frac{ds^{\mathrm{s}}}{dt} &= -\frac{\mu_k^{\mathrm{s}}}{T^{\mathrm{s}}}\left(J_k^{\mathrm{i,o}} - J_k^{\mathrm{o,i}}\right)\\ &= -\frac{\mu_k^{\mathrm{i,o}}}{T^{\mathrm{s}}}J_k^{\mathrm{i,o}} + \frac{\mu_k^{\mathrm{o,i}}}{T^{\mathrm{s}}}J_k^{\mathrm{o,i}} - J_k^{\mathrm{i,o}}\left(\frac{\mu_k^{\mathrm{s}}}{T^{\mathrm{s}}} - \frac{\mu_k^{\mathrm{i,o}}}{T^{\mathrm{s}}}\right) - J_k^{\mathrm{o,i}}\left(\frac{\mu_k^{\mathrm{o,i}}}{T^{\mathrm{s}}} - \frac{\mu_k^{\mathrm{s}}}{T^{\mathrm{s}}}\right)\\ &= J_s^{\mathrm{i,o}} - J_s^{\mathrm{o,i}} + J_k^{\mathrm{i,o}}\left[-\frac{1}{T^{\mathrm{s}}}\left(\mu_k^{\mathrm{s}} - \mu_k^{\mathrm{i,o}}\right)\right] + J_k^{\mathrm{o,i}}\left[-\frac{1}{T^{\mathrm{s}}}\left(\mu_k^{\mathrm{o,i}} - \mu_k^{\mathrm{s}}\right)\right]\end{aligned}$$

By comparing this equation with Eq. (5.1), we can identify the wanted excess entropy production.

Exercise 5.5.2. *Consider the special case that only heat is transported. Show that the excess entropy production is given by*

$$\sigma^s = J_q'^{i,o}\left(\frac{1}{T^s} - \frac{1}{T^{i,o}}\right) + J_q'^{o,i}\left(\frac{1}{T^{o,i}} - \frac{1}{T^s}\right)$$

- **Solution:** In this case Eq. (5.10) reduces to

$$\frac{du^{\mathrm{s}}}{dt} = T^{\mathrm{s}}\frac{ds^{\mathrm{s}}}{dt}.$$

The rate of change of the entropy is therefore given by

$$\frac{ds^{\mathrm{s}}}{dt} = \frac{1}{T^{\mathrm{s}}}\frac{du^{\mathrm{s}}}{dt}.$$

Eq. (5.8) reduces to

$$\frac{du^{\mathrm{s}}}{dt} = J_q'^{\mathrm{i,o}} - J_q'^{\mathrm{o,i}}$$

By combining the three equations, we obtain

$$\begin{aligned}\frac{ds^{\mathrm{s}}}{dt} &= \frac{1}{T^{\mathrm{s}}}\left(J_q'^{\mathrm{i,o}} - J_q'^{\mathrm{o,i}}\right)\\ &= \frac{1}{T^{\mathrm{i,o}}}J_q'^{\mathrm{i,o}} - \frac{1}{T^{\mathrm{o,i}}}J_q'^{\mathrm{o,i}} + J_q'^{\mathrm{i,o}}\left(\frac{1}{T^{\mathrm{s}}} - \frac{1}{T^{\mathrm{i,o}}}\right) + J_q'^{\mathrm{o,i}}\left(\frac{1}{T^{\mathrm{o,i}}} - \frac{1}{T^{\mathrm{s}}}\right)\\ &= J_s^{\mathrm{i,o}} - J_s^{\mathrm{o,i}} + J_q'^{\mathrm{i,o}}\left(\frac{1}{T^{\mathrm{s}}} - \frac{1}{T^{\mathrm{i,o}}}\right) + J_q'^{\mathrm{o,i}}\left(\frac{1}{T^{\mathrm{o,i}}} - \frac{1}{T^{\mathrm{s}}}\right)\end{aligned}$$

By comparing this equation with Eq. (5.1), we can identify the excess entropy production.

Exercise 5.5.3. *Consider stationary state evaporation of A from a solution. The flux is 1.6 10^{-6} mol/m^{2}s. The other component does not evaporate. The concentrations close to the surface are $c_A^i = 0.05$ kmol/m^{-3} on the liquid side, and $c_A^o = 0.01$ kmol/m^{-3} on the gas side. What is the excess entropy production in the surface?*

- **Solution:** At stationary state, there is no accumulation of A in the surface and $J_{\mathrm{A}}^{\mathrm{i,o}} = J_{\mathrm{A}}^{\mathrm{o,i}}$. When the temperature is constant, the excess entropy production is

$$\begin{aligned}\sigma^{\mathrm{s}} &= J_{\mathrm{A}}^{\mathrm{i,o}}\left[-\frac{1}{T^{\mathrm{s}}}(\mu_{\mathrm{A}}^{\mathrm{s}} - \mu_{\mathrm{A}}^{\mathrm{i,o}})\right] + J_{\mathrm{A}}^{\mathrm{o,i}}\left[-\frac{1}{T^{\mathrm{s}}}(\mu_{\mathrm{A}}^{\mathrm{o,i}} - \mu_{\mathrm{A}}^{\mathrm{s}})\right]\\ &= J_{\mathrm{A}}\left[-\frac{1}{T^{\mathrm{s}}}\left(\mu_{\mathrm{A}}^{\mathrm{o,i}} - \mu_{\mathrm{A}}^{\mathrm{i,o}}\right)\right] = J_{\mathrm{A}}R\ln\frac{c_{\mathrm{A}}^i}{c_{\mathrm{A}}^o} = 2.1\times10^{-5}\ \mathrm{W/Km^2}\end{aligned}$$

The excess entropy production is no direct function of the temperature. In order to compare the surface excess entropy production to the one in homogeneous phases, we divide this value with the thickness of the surface, which is order of magnitude 10^{-9} m. The result is very large compared to i.e. the one we calculated in Exercise 4.3.3. This shows that the interface is relatively speaking the source of much entropy production.

Exercise 5.5.4. *Derive Eq. (5.15) from Eq. (5.11).*

- **Solution:** We have

$$\begin{aligned}
\Delta_{\mathrm{i,s}}\left(\frac{\mu_j}{T}\right) &= \frac{\mu_j^{\mathrm{s}}(T^{\mathrm{s}})}{T^{\mathrm{s}}} - \frac{\mu_j^{\mathrm{i,o}}(T^{\mathrm{i,o}})}{T^{\mathrm{i,o}}} \\
&= \frac{\mu_j^{\mathrm{s}}(T^{\mathrm{s}})}{T^{\mathrm{s}}} - \frac{\mu_j^{\mathrm{i,o}}(T^{\mathrm{s}})}{T^{\mathrm{s}}} + \frac{\mu_j^{\mathrm{i,o}}(T^{\mathrm{s}})}{T^{\mathrm{s}}} - \frac{\mu_j^{\mathrm{i,o}}(T^{\mathrm{i,o}})}{T^{\mathrm{i,o}}} \\
&= \frac{1}{T^s}\Delta_{\mathrm{i,s}}\mu_{j,T} + \left(\frac{\partial}{\partial T}\frac{\mu_j^{\mathrm{i,o}}}{T}\right)_{T=T^{\mathrm{i,o}}} (T^{\mathrm{s}} - T^{\mathrm{i,o}}) \\
&= \frac{1}{T^s}\Delta_{\mathrm{i,s}}\mu_{j,T} - \left(\frac{1}{T^{\mathrm{i,o}}}S_j^{\mathrm{i,o}} + \frac{\mu_j^{\mathrm{i,o}}}{(T^{\mathrm{i,o}})^2}\right)(T^{\mathrm{s}} - T^{\mathrm{i,o}}) \\
&= \frac{1}{T^{\mathrm{s}}}\Delta_{\mathrm{i,s}}\mu_{j,T} + \left(S_j^{\mathrm{i}} + \frac{\mu_j^{\mathrm{i,o}}}{T^{\mathrm{i;o}}}\right) T^{\mathrm{s}}\Delta_{\mathrm{i,s}}\left(\frac{1}{T}\right) \\
&= \frac{1}{T^{\mathrm{s}}}\Delta_{\mathrm{i,s}}\mu_{j,T} + H_j^{\mathrm{i,o}}\left(\frac{T^{\mathrm{s}}}{T^{\mathrm{i,o}}}\right)\Delta_{\mathrm{i,s}}\left(\frac{1}{T}\right)
\end{aligned}$$

We can assume that, $T^{\mathrm{s}} \approx T^{\mathrm{i}}$, so that

$$\Delta_{\mathrm{i,s}}\left(\frac{\mu_j}{T}\right) = \frac{1}{T^{\mathrm{s}}}\Delta_{\mathrm{i,s}}\mu_{j,T} + H_j^{\mathrm{i,o}}\Delta_{\mathrm{i,s}}\left(\frac{1}{T}\right)$$

By substituting this result, and the analogous result for the other side of the surface, for all components into Eq. (5.11), using the definition of the measurable heat fluxes on both sides, we obtain Eq. (5.15).

This page intentionally left blank

Chapter 6

The Excess Entropy Production for a Three Phase Contact Line

We derive the excess entropy production for exchange of heat and mass with a straight three phase contact line. The entropy production determines the conjugate thermodynamic forces and fluxes. We formulate an extension of Young's law for surfaces that are not in equilibrium with each other.

In a three phase system, we distinguish three homogeneous bulk phases, three interfaces, which separate the homogeneous phases, and a contact line, where the three interfaces come together, see Fig. 6.1. The equilibrium contact line was defined as an autonomous thermodynamic system in Sec. 3.2. Using this property also for non-equilibrium systems, we shall derive the excess entropy production for the three phase contact line, denoted by c in this figure, following the procedure established in Chapters 4 and 5.

The three phase contact line is important for transport from one interface to another. The path of transport goes then via the contact line on to the next interface. Mass transport along this path is important for the understanding of the motion of the contact line. Components can react on the surfaces or at the contact line. In a polymer fuel cell, for instance, the chemical reaction takes place at a platinum surface. Gas diffuses to the active site via pore surfaces, via the contact line and onto the surface of the catalyst [81], see also Chapter 19. This example is too complicated for analysis here, however. We shall limit ourselves to transport of heat and mass in the situation pictured in Fig. 6.1.

Already without reactions, mass transports play an important role in the description of the motion of the contact line. One reason to include this chapter, is that many problems have not yet been resolved for the contact line. Shikhmurzaev [131] gave the first satisfactory description of the motion of the contact line for a liquid- and a vapor-phase along a

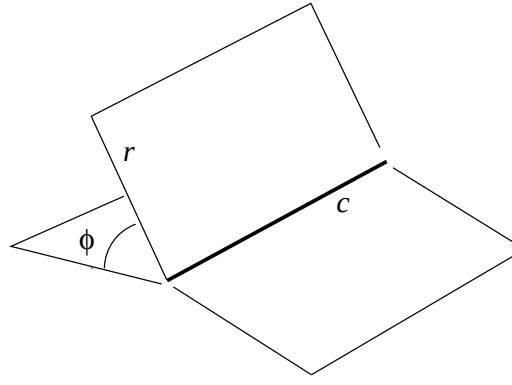

Figure 6.1 The geometry around the contact line, *c*. The distance to the line is *r*, and ϕ is the angle around the line.

flat solid wall. He used non-equilibrium thermodynamics for the surfaces following, and extending, the method of Bedeaux *et al.* [2]. He described the contact line, choosing boundary conditions for the surfaces at the contact line. We shall generalize Shikhmurzaev's analysis by treating the contact line as a thermodynamic system. The excess entropy production along the line gives a proper basis for the boundary conditions to be chosen. We refer to Bedeaux [132] for a more detailed presentation.

6.1 The discrete nature of the contact line

The excess densities of the contact line were described in Sec. 3.2. These apply to a point on the contact line. In order to write balance equations for the line, we need to consider its surroundings. We introduce a coordinate c along the line, a distance r to the contact line and an angle φ around the contact line, see Fig. 6.1. Close to the contact line these are cylindrical coordinates*. We assume that the contact line is straight and that the interfaces are flat. Furthermore, we restrict ourselves to the case that all densities and fluxes are independent of c, and that there are no fluxes parallel to the contact line, neither in the homogeneous phases, nor along the surfaces. This is appropriate for exchange of heat and mass with the contact line. We recommend to use the symbol list for a check of the dimensions in the equations.

*Farther away from and along the contact line, one should in the general case use orthonormal curvilinear coordinates, see Refs. [2–4].

The balance equation for the excess entropy density s^{c} of the contact line is:

$$\frac{d}{dt}s^{\mathrm{c}} + \sum_{\nu=1}^{3} \mathbf{J}_s^{\mathrm{s},\nu}.\widehat{\mathbf{n}}_\nu = \frac{d}{dt}s^{\mathrm{c}} + \sum_{\nu=1}^{3} J_{s,r}^{\mathrm{s},\nu} = \sigma^{\mathrm{c}} \tag{6.1}$$

The indices $\nu = 1, 2$ and 3 label the homogeneous phases, counted clockwise around the contact line, and the surfaces, counted clockwise around the contact line, respectively. The first surface comes after the first bulk phase, etc. $\mathbf{J}_s^{\mathrm{s},\nu}$ are the excess entropy fluxes along the dividing surfaces. The normal to the contact line, that is directed away from the contact line in the ν-th interface, is denoted $\widehat{\mathbf{n}}_\nu$. We use a subscript r to label the component of the flux along the interface normal to the contact line.

Remark 6.1. *In Chapter 5, we did not consider excess fluxes along the surface. In this chapter only these fluxes give exchange of heat and mass with the contact line. Excess fluxes along the surfaces are defined in the same way as the excess densities for the surfaces in Sec. 3.2.*

The excess entropy fluxes are given in terms of the total excess heat fluxes, the excess measurable heat fluxes and the excess mass fluxes along the surfaces by

$$\mathbf{J}_s^{\mathrm{s},\nu} = \frac{1}{T^{\mathrm{s},\nu}}\left(\mathbf{J}_q^{\mathrm{s},\nu} - \sum_{j=1}^{n} \mu_j^{\mathrm{s},\nu}\mathbf{J}_j^{\mathrm{s},\nu}\right) = \frac{1}{T^{\mathrm{s},\nu}}\mathbf{J}_q^{\prime,\mathrm{s},\nu} + \sum_{j=1}^{n} S_j^{\mathrm{s},\nu}\mathbf{J}_j^{\mathrm{s},\nu} \tag{6.2}$$

All fluxes are given in the *contact line frame of reference* (the contact line is not moving):

$$\mathbf{v}_j^{\mathrm{c}} = \mathrm{v}_{j,r}^{\mathrm{c}} = \mathbf{v}^{\mathrm{c}} = \mathrm{v}_r^{\mathrm{c}} = 0 \tag{6.3}$$

The time derivative d/dt in Eq. (6.1), is in this frame of reference. It is appropriate to use d/dt because the excess entropy density depends only on the time. The definition of excess densities for the contact line was discussed in Sec. 3.2.

The second law gives for the contact line $\sigma^{\mathrm{c}}(t) \geq 0$. We shall find more explicit expressions for $\sigma^{\mathrm{c}}(t)$ by combining:

- mass balances
- the first law of thermodynamics
- the local form of the Gibbs equation

The same procedure was used in Chapters 4 and 5. We shall see that also $\sigma^{\mathrm{c}}(t)$ can be written as the product sum of *conjugate* fluxes and forces for the contact line. The fluxes and forces describe exchange of heat and mass between the contact line and the surfaces.

6.2 Balance equations

Conservation of component j along a contact line gives

$$\frac{\mathrm{d}}{\mathrm{d}t}\Gamma_j^{\mathrm{c}} = -\sum_{\nu=1}^{3} \mathbf{J}_j^{\mathrm{s},\nu}.\widehat{\mathbf{n}}_\nu = -\sum_{\nu=1}^{3} J_{j,r}^{\mathrm{s},\nu} \tag{6.4}$$

where Γ_j^{c} are the excess line concentrations (adsorptions per unit of length). Furthermore $J_{j,r}^{\mathrm{s},\nu}$ is the excess flux of component j along the surface ν away from the contact line, see Fig. 6.1. The adsorptions depend only on the time.

With the chosen frame of reference, the velocity of the line is zero, but the line can be accelerated in the plane normal to the line. For such a comoving acceleration, we have

$$\frac{\mathrm{d}}{\mathrm{d}t}\left(m^{\mathrm{c}}\Gamma^{\mathrm{c}}\mathbf{v}_\perp^{\mathrm{c}}\right) = \sum_{\nu=1}^{3}\left(\gamma^\nu - m^\nu\Gamma^\nu \mathrm{v}_r^{\mathrm{s},\nu}\mathrm{v}_r^{\mathrm{s},\nu}\right)\widehat{\mathbf{n}}_\nu \tag{6.5}$$

where $m^{\mathrm{c}}\Gamma^{\mathrm{c}}$ and $m^\nu\Gamma^\nu$ are the average excess mass densities per unit of length along the contact line and along the dividing surfaces, respectively. They are defined by

$$m^{\mathrm{c}}\Gamma^{\mathrm{c}} \equiv \sum_{j=1}^{n} m_j\Gamma_j^{\mathrm{c}} \quad \text{and} \quad m^\nu\Gamma^\nu \equiv \sum_{j=1}^{n} m_j\Gamma_j^\nu \tag{6.6}$$

The barycentric velocities along the *dividing surfaces*, $\mathbf{v}^{\mathrm{s},\nu}$ are:

$$m^\nu\Gamma^\nu\mathbf{v}^{\mathrm{s},\nu} \equiv \sum_{j=1}^{n} m_j\mathbf{J}_j^{\mathrm{s},\nu} \equiv \sum_{j=1}^{n} m_j\Gamma_j^\nu\mathbf{v}_j^{\mathrm{s},\nu} \tag{6.7}$$

The first term on the right hand side of Eq. (6.5), gives the terms that appear in Young's law for a contact line. The second term gives a convective correction to this law, needed in the non-equilibrium case.

Conservation of excess internal energy density, u^{c}, per unit of length means that:

$$\frac{\mathrm{d}}{\mathrm{d}t}u^{\mathrm{c}} = -\sum_{\nu=1}^{3} \mathbf{J}_q^{\mathrm{s},\nu}.\widehat{\mathbf{n}}_\nu = -\sum_{\nu=1}^{3} J_{q,r}^{\mathrm{s},\nu} \tag{6.8}$$

The excess total heat fluxes are given in terms of the excess measurable heat fluxes along the interfaces:

$$\mathbf{J}_q^{\mathrm{s},\nu} = \mathbf{J}_q'^{,\mathrm{s},\nu} + \sum_{j=1}^{n} H_j^{\mathrm{s},\nu}\mathbf{J}_j^{\mathrm{s},\nu} \tag{6.9}$$

where $H_j^{\mathrm{s},\nu}$ are the partial molar excess enthalpies along the dividing surfaces.

Remark 6.2. *In Eqs. (6.1), (6.4) and (6.8) there are no direct fluxes from the homogeneous phases to the contact line. The geometry around the contact line is such that such fluxes would diverge inversely proportional to the distance to the contact line. As a consequence such fluxes are impossible.*

This property has a bearing on the gas transport to the three phase contact line that we discuss in Chapter 21. Transport occurs via the planes.

6.3 The excess entropy production

We assume that there is local equilibrium everywhere along the contact line. The Gibbs equation (3.33) for the line gives:

$$T^{\mathrm{c}}\frac{\mathrm{d}s^{\mathrm{c}}}{\mathrm{d}t} = \frac{\mathrm{d}u^{\mathrm{c}}}{\mathrm{d}t} - \sum_{j=1}^{n}\mu_j^{\mathrm{c}}\frac{\mathrm{d}\Gamma_j^{\mathrm{c}}}{\mathrm{d}t} \tag{6.10}$$

We substitute Eqs. (6.4) and (6.8) into this equation. By using Eq. (6.2) and comparing the result with Eq. (6.1), we can identify the entropy production:

$$\sigma^{\mathrm{c}} = \sum_{\nu=1}^{3} J_{q,r}^{\mathrm{s},\nu}\left(\frac{1}{T^{\mathrm{s},\nu}} - \frac{1}{T^{\mathrm{c}}}\right) - \sum_{\nu=1}^{3}\sum_{j=1}^{n} J_{j,r}^{\mathrm{s},\nu}\left(\frac{\mu_j^{\mathrm{s},\nu}}{T^{\mathrm{s},\nu}} - \frac{\mu_j^{\mathrm{c}}}{T^{\mathrm{c}}}\right) \tag{6.11}$$

This is caused by transport of heat and mass into and out of the contact line. The force-flux pairs have a similar form as for the surface. By using Eq. (6.2), we can eliminate the total heat fluxes in terms of the entropy fluxes

$$\sigma^{\mathrm{c}} = \sum_{\nu=1}^{3} T^{\mathrm{s},\nu} J_{s,r}^{\mathrm{s},\nu}\left(\frac{1}{T^{\mathrm{s},\nu}} - \frac{1}{T^{\mathrm{c}}}\right) - \frac{1}{T^{\mathrm{c}}}\sum_{\nu=1}^{3}\sum_{j=1}^{n} J_{j,r}^{\mathrm{s},\nu}\left(\mu_j^{\mathrm{s},\nu} - \mu_j^{\mathrm{c}}\right) \tag{6.12}$$

By using Eq. (6.9), we can eliminate the total heat fluxes in terms of the measurable heat fluxes

$$\begin{aligned}\sigma^{\mathrm{c}} &= \sum_{\nu=1}^{3} J_{q,r}^{\prime,\mathrm{s},\nu}\left(\frac{1}{T^{\mathrm{s},\nu}} - \frac{1}{T^{\mathrm{c}}}\right)\\ &\quad - \sum_{\nu=1}^{3}\sum_{j=1}^{n} J_{j,r}^{\mathrm{s},\nu}\left[\left(\frac{\mu_j^{\mathrm{s},\nu}}{T^{\mathrm{s},\nu}} - \frac{\mu_j^{\mathrm{c}}}{T^{\mathrm{c}}}\right) - H_j^{\mathrm{s},\nu}\left(\frac{1}{T^{\mathrm{s},\nu}} - \frac{1}{T^{\mathrm{c}}}\right)\right]\\ &= \sum_{\nu=1}^{3} J_{q,r}^{\prime,\mathrm{s},\nu}\left(\frac{1}{T^{\mathrm{s},\nu}} - \frac{1}{T^{\mathrm{c}}}\right) - \frac{1}{T^{\mathrm{c}}}\sum_{\nu=1}^{3}\sum_{j=1}^{n} J_{j,r}^{\mathrm{s},\nu}\left(\mu_j^{\mathrm{s},\nu}\left(T^{\mathrm{c}}\right) - \mu_j^{\mathrm{c}}\right)\end{aligned} \tag{6.13}$$

All contributions are scalar. When there are fluxes along the contact line [132], additional terms appear in Eq. (6.13). Gradients in temperature and absorption along the line, which were not considered in the analysis above, result in a so-called Marangoni effect. The so-called tears of wine are an example of the Marangoni effect for a surface. Take a glass of strong port wine. When one wets a part of the surface with the port, tears will appear along the contact line between the dry and the wet surface. This is due to evaporation of alcohol, which increases the surface tension close to the line. The tears grow until they become so heavy that they fall down along the surface of the glass.

6.4 Stationary states

Stationary state conditions reduce the number of independent flux-force pairs significantly, from $3(n+1)$ to $2(n+1)$. In a stationary state, the conservation equation for component j in the contact line, Eq. (6.4), reduces to

$$\sum_{\nu=1}^{3} J_{j,r}^{\mathrm{s},\nu} = 0 \tag{6.14}$$

There is mechanical equilibrium in the direction normal to the contact line. This gives, from Eq. (6.5)

$$\sum_{\nu=1}^{3} \gamma^{\nu} \widehat{\mathbf{n}}_{\nu} = 0 \tag{6.15}$$

for sufficiently low velocities along the surfaces. This is Young's law for surfaces which are not in equilibrium with each other. The contact angles in the formula deviate from their equilibrium values. The balance of internal energy, Eq. (6.8), reduces to

$$\sum_{\nu=1}^{3} J_{q,r}^{\mathrm{s},\nu} = 0 \tag{6.16}$$

Using Eqs. (6.14) and (6.16), the excess entropy production along the contact line can be written as

$$\sigma^{\mathrm{c}} = \sum_{\nu=1}^{2} J_{q,r}^{\mathrm{s},\nu} \left(\frac{1}{T^{\mathrm{s},\nu}} - \frac{1}{T^{\mathrm{s},3}} \right) - \sum_{\nu=1}^{2} \sum_{j=1}^{n} J_{j,r}^{\mathrm{s},\nu} \left(\frac{\mu_j^{\mathrm{s},\nu}}{T^{\mathrm{s},\nu}} - \frac{\mu_j^{\mathrm{s},3}}{T^{\mathrm{s},3}} \right) \tag{6.17}$$

This reduces the number of independent force-flux pairs from $3(n+1)$ to $2\,(n+1)$. A simplification is also that the thermodynamic forces no longer depend on the temperature and the chemical potentials along the contact

line. We eliminate the total excess heat fluxes in terms of the excess entropy fluxes or the excess measurable heat fluxes, using Eqs. (6.2) and (6.9). This results in

$$\sigma^{\mathrm{c}} = \sum_{\nu=1}^{2} T^{\mathrm{s},\nu} J_{s,r}^{\mathrm{s},\nu} \left(\frac{1}{T^{\mathrm{s},\nu}} - \frac{1}{T^{\mathrm{s},3}} \right) - \frac{1}{T^{\mathrm{s},3}} \sum_{\nu=1}^{2} \sum_{j=1}^{n} J_{j,r}^{\mathrm{s},\nu} \left(\mu_j^{\mathrm{s},\nu} - \mu_j^{\mathrm{s},3} \right) \quad (6.18)$$

and

$$\sigma^{\mathrm{c}} = \sum_{\nu=1}^{2} J_{q,r}^{\prime,\mathrm{s},\nu} \left(\frac{1}{T^{\mathrm{s},\nu}} - \frac{1}{T^{\mathrm{s},3}} \right) - \frac{1}{T^{\mathrm{s},3}} \sum_{\nu=1}^{2} \sum_{j=1}^{n} J_{j,r}^{\mathrm{s},\nu} \left(\mu_j^{\mathrm{s},\nu} \left(T^{\mathrm{s},3} \right) - \mu_j^{\mathrm{s},3} \right) \quad (6.19)$$

For isothermal conditions, the three equations are the same. The entropy production gives the basis for the force-flux relations, which can be used to study the motion of the contact line during heat and mass transport. In the many papers about the contact line, its motion is one of the problems typically considered. We refer to Bedeaux [132] and Shikmurzaev [131, 133] for these expressions.

6.5 Concluding comment

The description of the contact line gives a perspective on the other transport processes in this book. We only deal with transport perpendicular to the surface. The remark 6.2 shows, however, that transport along the surface has important consequences.

This page intentionally left blank

Chapter 7

Flux Equations and Onsager Relations

We present the flux equations that follow from the entropy production on a general form. Onsager's proof for the reciprocal relations is discussed. The validity of the Onsager relations assures that, in the absence of constraints, the system relaxes to equilibrium. The second law leads to restrictions on the transport coefficients. In the stationary state, it is an advantage to write the forces as functions of fluxes. The meaning of the Curie principle is discussed for surfaces and contact lines.

This chapter gives the general properties of the flux-force equations in non-equilibrium thermodynamics. The properties are not only applicable to the phenomena treated in this book, they are also valid for phenomena that we omit, like for instance viscous flow. Explicit expressions for transport of heat, mass and charge in two flux-two force systems follow in Chapters 8–10. After that we go to more complicated applications.

7.1 Flux-force relations

As explained in Chapter 1, non-equilibrium thermodynamics has as basis the entropy production, which has the general form

$$\sigma = \sum_{i=1}^{n} J_i X_i \tag{7.1}$$

where J_i and X_i are the so-called conjugate thermodynamic fluxes and forces, cf. Eq. (1.4). There are n independent flux-force pairs. The conjugate pairs were derived in Chapters 4–6. The meaning of being conjugate shall be further discussed in the next section. A basic assumption in

non-equilibrium thermodynamics is that each flux is a linear function of all forces:

$$J_i = \sum_{j=1}^{n} L_{ij} X_j \tag{7.2}$$

The relationship is linear in the sense that the Onsager conductivity matrix L_{ij} *does not depend* on X_j. The coefficients are functions of the state variables, for instance, like the local pressure and temperature, but not of the forces. The theory therefore prescribes that coefficients, like the thermal conductivity, can depend on the temperature, but not on the gradient of the temperature.

7.2 Onsager's reciprocal relations

Onsager [8, 9] showed that the matrix of coefficients for Eq. (7.2) is symmetric, using the microscopic time reversibility of the system. Consider, as Onsager did, a system described by thermodynamic variables A_i which are symmetric (even) with respect to reversal of the time. Examples of A_i are the internal energy density and the molar densities of volume elements in the homogeneous phases, of area elements along the dividing surfaces, and of length elements along the contact line. The fluctuations α_i of the thermodynamic variables A_i are defined by:

$$\alpha_i \equiv A_i - < A_i > \tag{7.3}$$

Microscopic reversibility means that the probability to observe, on the average, that a fluctuation α_i in some property at time t, is followed by another fluctuation α_j after a time lag τ, is equal to the probability to observe the reverse situation — that the fluctuation α_j at time t, is followed by α_i after a time lag τ. Mathematically this implies that:

$$< \alpha_i(t)\alpha_j(t+\tau) > = < \alpha_j(t)\alpha_i(t+\tau) > \tag{7.4}$$

where the brackets $< ... >$ mean that averages have been calculated over the equilibrium distribution given in Eq. (7.7), see Eq. (7.11) for an explicit definition of such an average. Microscopic time reversibility is a characteristic property of Newton's equations. The motion of a particle in a fluid according to Newton's equations is illustrated in Sec. 22.1, Fig. 22.1.

The entropy of the system, S, has a maximum, S_{eq}, at equilibrium. Away from equilibrium it is:

$$S = S_{eq} + \Delta S(\alpha_1, ..., \alpha_n) = S_{eq} - \frac{1}{2} \sum_{j,i=1}^{n} g_{ji} \alpha_j \alpha_i + ... \tag{7.5}$$

where ΔS describes the deviation* from the equilibrium value. The tensor $\{g_{ji}\}$ is defined by the elements

$$g_{ji} \equiv - \left. \frac{\partial^2 \Delta S}{\partial \alpha_j \partial \alpha_i} \right|_{\alpha_1 = ... = \alpha_n = 0} \tag{7.6}$$

As S_{eq} is a maximum, there is no linear term in the expansion. Furthermore, $\{g_{ji}\}$ is a positive definite and real symmetric matrix. It follows that the eigenvalues are all real and positive. We can choose the amplitudes of the eigenvectors divided by the square root of their eigenvalues as a new set of variables $\{\alpha_i'\}$. The resulting $\{g_{ji}'\}$ is then equal to the unit tensor.

From Boltzmann we have the normalized probability density for the fluctuations:

$$f(\alpha_1, ..., \alpha_n) = \exp(\Delta S / k_B) \, / \int_{-\infty}^{\infty} d\alpha_1 ... d\alpha_n \exp(\Delta S / k_B) \tag{7.7}$$

where k_B is the Boltzmann constant. The integral is taken over all n fluctuation variables. The thermodynamic forces X_i in the system were defined by Onsager:

$$X_i \equiv \frac{\partial S}{\partial A_i} = \frac{\partial \Delta S}{\partial \alpha_i} = - \sum_{j=1}^{n} g_{ij} \alpha_j + ... \tag{7.8}$$

Here we used ΔS as given in Eq. (7.5). The conjugate fluxes were defined by:

$$J_i(t) = \frac{dA_i(t)}{dt} = \frac{d\alpha_i(t)}{dt} \tag{7.9}$$

From Eqs. (7.7) and (7.8) we have:

$$X_i = k_B \frac{\partial \ln f}{\partial \alpha_i} = \frac{k_B}{f} \frac{\partial f}{\partial \alpha_i} \tag{7.10}$$

Using the definition of X_i and partial integration, it follows that the expectation value of the product $\alpha_i X_j$ is

$$< \alpha_i X_j > \equiv \int_{-\infty}^{\infty} d\alpha_1 ... d\alpha_n \; \alpha_i X_j \; f(\alpha_1, ..., \alpha_n) = -k_B \delta_{ij} \tag{7.11}$$

where δ_{ij} is the Kronecker delta, $\delta_{ij} \equiv 1$ if $i = j$ and $\delta_{ij} \equiv 0$ if $i \neq j$.

On a microscopic time scale one observes collisions between particles. Figure 22.1 shows the path of one particle in a fluid. A discontinuity in

*The deviation ΔS is not necessarily a quadratic form of the fluctuations, see [20] p. 91, as is frequently assumed.

the path means that a collision takes place. A collision leads to a rapid change in the variables α_i. In order to find the macroscopic behavior, one must integrate over a sufficiently long time to no longer see these rapid changes. The rapid fluctuations have then re-established the equilibrium distribution. The time needed depends on the system under consideration. It can be vastly different for a chemical reaction, for a diffusing polymer or for a diffusing argon fluid such as the one in Fig. 22.1. Onsager assumed that the *microscopic* fluctuation in α_i and the flux J_i obeyed the linear *macroscopic* relation given in Eq. (7.2):

$$J_i(t) = \sum_{j=1}^{n} L_{ij} X_j(t) \tag{7.12}$$

This is called the *regression hypothesis*. By integrating Eq. (7.9) from t to $t + \tau$, using Eq. (7.12), he then found that:

$$\alpha_i(t + \tau) = \alpha_i(t) + \tau \sum_{j=1}^{n} L_{ij} X_j(t) \tag{7.13}$$

to linear order in τ. By introducing Eq. (7.13) on both sides of Eq. (7.4) using Eq. (7.11), the reciprocal relations followed.

$$L_{ij} = L_{ji} \tag{7.14}$$

These are the Onsager relations for conductivity coefficients. They make the matrix of the coefficients in the flux equations symmetric[†]. The Onsager relations simplify the transport problem greatly, because they reduce the number of independent conductivity coefficients from n^2 to $\frac{1}{2}n(n+1)$. When the Onsager coefficients L_{ij} are known, we know how the different processes are coupled to one another. We can even take advantage of the situation to find thermodynamic data which are otherwise difficult to measure, see Ref. [76]. The coefficients must be determined from experiments. The Onsager relations have been verified experimentally for many systems [71–74]. They have also been verified by non-equilibrium molecular dynamics simulations [65, 67].

Let us summarize the conditions for validity of Onsager's reciprocal relations, Eq. (7.14):

- The state variables $A_i(t)$ are independent.

[†]When odd variables are used in combination with even variables, the corresponding coupling coefficents become antisymmetric [20].

- The fluxes and forces are conjugate; i.e. for each variable $A_i(t)$, a flux is defined as $d\alpha_i(t)/dt$ and the conjugate force is defined as $d\Delta S/d\alpha_i$.

- The fluxes are linear functions of the conjugate thermodynamic forces. The coefficients L_{ij} may therefore depend on the state variables, but not on the forces.

Freedom exists, as is normal in thermodynamics, to choose alternative sets of variables. Choosing different variables changes the α_i's and accordingly modifies the fluxes and the conjugate forces. Onsager's prescription makes clear how to find the conjugate flux-force pairs. Regretfully enough, Onsager's analysis and the consequences thereof have been presented in a misleading manner, for instance by Coleman and Truesdell [134] and Wei [135], questioning their validity and/or usefulness. For a discussion of the points raised by these authors, see de Groot and Mazur [20] Sec. VI.5.

When the set of variables $A_i(t)$ is overcomplete, it can be shown that a symmetric coefficient matrix can be *chosen*, see [20] Sec. VI.3. The set of independent $A_i(t)$ leads to the smallest number of independent phenomenological coefficients and is usually most efficient. The Maxwell–Stefan formulation is an important exception to this, see Sec. 12.2.

The equations that describe the dynamics of the system are *non-linear*. To refer to non-equilibrium thermodynamics as a linear theory, as is often done [64], is therefore misleading. De Groot and Mazur pointed out in the preface to the Dover edition of their monograph [20], that these equations are "non-linear for a variety of reasons, such as (i) the presence of convection terms and of (ii) quadratic source terms in, e.g. the energy equation, (iii) the non-linear character of the equation of state and (iv) the dependence of the phenomenological transport coefficients on the state variables".

To illustrate the non-linearity of the equations by an example, consider the dynamics of an isothermal fluid. The dynamics is described by the continuity equation and the Navier–Stokes equation, classical examples of non-linear equations. The phenomenological coefficients, giving the linear dissipative contributions to the fluxes, are the shear viscosity and the bulk viscosity. For large Reynolds numbers the viscous contributions can be neglected and the equations reduce to the Euler equation. These equations describe classic non-linear reversible flow phenomena, like turbulence, and have $L_{ij} = 0$. The transition to turbulence in a fluid is therefore not due to the appearance of contributions in the fluxes which are non-linear in the thermodynamic forces. On the contrary, the dissipative contributions to the fluxes in the Euler equations are in fact negligible.

Exercise 7.2.1. *Derive Eq. (7.11) from Eqs. (7.3) to (7.8).*

- **Solution:** Using Eq. (7.8) we have

$$< \alpha_i X_j > \equiv \int_{-\infty}^{\infty} d\alpha_1 ... d\alpha_n \; \alpha_i X_j \; f(\alpha_1, ..., \alpha_n)$$

$$= k_B \int_{-\infty}^{\infty} d\alpha_1 ... d\alpha_n \; \alpha_i \frac{\partial ln f}{\partial \alpha_j} \; f(\alpha_1, ..., \alpha_n)$$

$$= k_B \int_{-\infty}^{\infty} d\alpha_1 ... d\alpha_n \; \alpha_i \frac{\partial}{\partial \alpha_j} \; f(\alpha_1, ..., \alpha_n)$$

We use

$$\frac{\partial}{\partial \alpha_j} \; \alpha_i f = \alpha_i \frac{\partial f}{\partial \alpha_j} + f \frac{\partial \alpha_i}{\partial \alpha_j} = \alpha_i \frac{\partial f}{\partial \alpha_j} + f \delta_{ij}$$

to find an expression for $\alpha_i \, (\partial f / \partial \alpha_j)$. The integral contains two parts that can be integrated separately. We use the normalization condition for f and the fact that f goes to zero for large values of the fluctuations and obtain:

$$< \alpha_i X_j > \equiv k_B \int_{-\infty}^{\infty} d\alpha_1 ... d\alpha_n \; \left[\frac{\partial}{\partial \alpha_j} \; \alpha_i f - f \delta_{ij} \right] = -k_B \delta_{ij}$$

Exercise 7.2.2. *Onsager chose the time a particle needs to diffuse over its own diameter as a measure of the time the system takes to come to local equilibrium (and for Eq. (7.12) to apply). Suggest a way to estimate this time to about* $10^{-6} s$.

- **Solution:** The time is given by the diameter squared divided by the diffusion constant (see Sec. 8.2). A diameter of 0.5 nm and a diffusion constant of $2.5 \times 10^5 (\text{nm})^2/\text{s}$ gives the time 10^{-6} s.

7.3 Relaxation to equilibrium. Consequences of violating Onsager relations

Thermodynamic systems will always go to equilibrium, when the system is closed. The reason for this is that Onsager relations are valid. We illustrate below in an exercise, that a violation of the Onsager relations may lead to oscillatory behavior around the equilibrium state. Equilibrium is then never reached.

We show first why an isolated system always approaches equilibrium. Consider variables that make $\{g_{ji}\}$ equal to the unit tensor. Below Eq. (7.6)

we explained why the system can be described in terms of such variables. It then follows from Eq. (7.8) that $X_i = -\alpha_i$. Close to equilibrium we may neglect possible higher order contributions. Equation (7.2) then gives, using Eq. (7.9) for the time derivative of α_i,

$$\frac{d\alpha_i}{dt} = -\sum_{j=1}^{n} L_{ij}\alpha_j \tag{7.15}$$

When one diagonalizes the matrix of conductivities, it follows from the Onsager reciprocal relations that all the eigenvalues are real and non-negative. As a consequence the system will go to equilibrium.

The following exercise illustrates what goes wrong when the phenomenological coefficient are chosen such that they neither satisfy the Onsager relations nor the inequalities which follow from the second law (see Sec. 7.5).

Exercise 7.3.1. *Consider a system described by Eq. (7.15) with two forces and fluxes. Use* $L_{11} = L_{22} = 0$ *and* $L_{12} = -L_{21}$. *Calculate* $\alpha_1(t)$ *using the initial value* $\alpha_1(0) = A$ *and* $(d\alpha_1/dt)(t = 0) = 0$.

- **Solution**: Equation (7.15) gives $d\alpha_1/dt = -L_{12}\alpha_2$ and $d\alpha_2/dt = L_{12}\alpha_1$. The second derivative of α_1 becomes $d^2\alpha_1/dt^2 = -L_{12}d\alpha_2/dt = -L_{12}^2\alpha_1$. The solution of this equation for the given initial conditions is $\alpha_1(t) = A\cos(L_{12}t)$.

The system in the exercise has an oscillating solution, which does not go to equilibrium.

Remark 7.1. *Onsager's relations provide the general reason why oscillating behavior around equilibrium does not exist in systems described by non-equilibrium thermodynamics.*

When there are external forces which bring the system far away from equilibrium, for instance by keeping one of the variables constant, the properties of the system change, see Prigogine and coworkers [136]. Multiple stationary states may then exist and oscillatory and more complex behavior can develop. But that is not the subject of this book.

7.4 Force-flux relations

In the inverted form of Eq. (7.2), the forces are linear functions of the fluxes:

$$X_i = \sum_{j=1}^{n} R_{ij}J_j \tag{7.16}$$

The resistivity matrix, R_{ij}, is the inverse of the conductivity matrix:

$$\sum_{j=1}^{n} R_{ij} L_{ji} = \delta_{ij} \tag{7.17}$$

In stationary states the fluxes are often constant in space. The force-flux relations are then particularly convenient. We use Kramer's rule to find the matrix elements. An element R_{ij} in the resistivity matrix is equal to the subdeterminant of the conductivity matrix (the determinant of the matrix in which the i$^{\text{th}}$ row and the j$^{\text{th}}$ column have been crossed out, times $(-1)^{i+j}$, divided by the determinant of the conductivity matrix). For $n = 2$, we find

$$\begin{gathered} R_{11} = \frac{L_{22}}{L_{11}L_{22} - L_{12}^2}, \quad R_{12} = R_{21} = -\frac{L_{12}}{L_{11}L_{22} - L_{12}^2}, \\ R_{22} = \frac{L_{11}}{L_{11}L_{22} - L_{12}^2} \end{gathered} \tag{7.18}$$

The matrix of resistivity coefficients satisfies the Onsager reciprocal relations, just like the matrix of conductivity coefficients:

$$R_{ij} = R_{ji} \tag{7.19}$$

7.5 Coefficient bounds

The second law imposes certain bounds on the Onsager coefficients. By substituting the linear laws into σ, we have:

$$\sigma = \sum_i X_i \sum_j L_{ij} X_j = \sum_{i,j} X_i L_{ij} X_j \geq 0 \tag{7.20}$$

The second law gives the inequality. By taking all forces, except one, equal to zero, it follows that main coefficients are always positive

$$L_{ii} \geq 0 \tag{7.21}$$

A consequence of the second law of thermodynamics is also that all pairs of coefficients obey:

$$L_{ii} L_{jj} - L_{ij} L_{ji} \geq 0 \tag{7.22}$$

This can be found by taking all except two forces equal to zero, and subsequently eliminating one of the two forces in terms of the corresponding flux. We have

$$\begin{aligned} J_1 &= L_{11}X_1 + L_{12}X_2 \\ J_2 &= L_{21}X_1 + L_{22}X_2 \end{aligned} \tag{7.23}$$

By eliminating X_2 in the first equation by means of the second, we obtain

$$J_1 = \left(L_{11} - \frac{L_{12}L_{21}}{L_{22}}\right) X_1 + \frac{L_{12}}{L_{22}} J_2 \tag{7.24}$$

When this is introduced into the entropy production, we find:

$$\begin{aligned} \sigma &= \left(L_{11} - \frac{L_{12}L_{21}}{L_{22}}\right) X_1^2 + \frac{L_{12}}{L_{22}} J_2 X_1 - \frac{L_{21}}{L_{22}} J_2 X_1 + \frac{J_2^2}{L_{22}} \\ &= \left(L_{11} - \frac{L_{12}L_{21}}{L_{22}}\right) X_1^2 + \frac{J_2^2}{L_{22}} \end{aligned} \tag{7.25}$$

Two of the terms cancel because of the Onsager relation, Eq. (7.14). We must have $\sigma \geq 0$, also for the special case that $J_2 = 0$. Equations (7.22) follow from this. It is interesting to note that by keeping the flux J_2 rather than the force X_2 equal to zero, the entropy production is reduced from $L_{11}X_1^2$ to $(L_{11} - L_{12}L_{21}/L_{22})X_1^2$.

Remark 7.2. *When $X_1 = 0$, a finite flux J_2 gives rise to a flux $J_1 = (L_{12}/L_{22})J_2$, see Eq. (7.24). The expression for the entropy production, Eq. (7.25), shows, however, that this contribution to J_1 does not contribute to the entropy production. This transport along with J_2 is therefore reversible. The coupling coefficients therefore describe reversible contributions to σ. This is why they are important for a proper description of energy conversion, cf. Secs. 2.1, 9.3, 9.4, 10.1 and 10.6.*

An equality sign in Eq. (7.22) implies that two fluxes are proportional to one another. In our example, $J_1 = (L_{12}/L_{22})J_2$. This is called complete coupling. A consequence is that the number of fluxes, and therefore the number of variables, can be reduced.

For the force-flux relations we find, by substituting Eq. (7.16) into Eq. (1.1):

$$\sigma = \sum_i J_i \sum_j R_{ij} J_j = \sum_{i,j} J_i R_{ij} J_j \geq 0 \tag{7.26}$$

The second law gives now:

$$R_{ii} \geq 0 \tag{7.27}$$

and

$$R_{ii}R_{jj} - R_{ij}R_{ji} \geq 0 \tag{7.28}$$

The resistivity coefficients have similar properties as the conductivity coefficients.

7.6 The Curie principle applied to surfaces and contact lines

As we go from a three-, to a two-, and a one-dimensional phase, the symmetry properties of the phases are gradually reduced. Symmetry properties restrict the possibilities for coupling between transport phenomena. This was first recognized by Pierre Curie [137], and has been referred to as the *Curie principle*.

Transport phenomena are scalar, vectorial or tensorial. Chemical reactions are scalar, and are classified with a tensorial rank 0. Vectorial heat-, mass-, and charge transport have rank 1. Momentum transport is a tensorial phenomenon of rank 2. Curie saw that components of different rank tensors have different transformation properties under rotations and reflections of the system. The entropy production (4.13)–(4.15) for the *homogeneous phase* used in this book, contains phenomena of two tensorial ranks, scalar chemical reactions and vectorial transports of heat, mass and charge. There is no coupling between chemical reactions and the vectorial phenomena in the homogeneous phase. De Groot and Mazur [20] discussed coupling in homogeneous phases from this perspective, see Sec. VI, 2; page 57.

The symmetries change when we consider the surface. *The surface* can be symmetric for two-dimensional transformations along the surface, but it has no symmetries in the direction normal to the surface. A surface is called isotropic when it is invariant for rotations around, and reflections with respect to any normal. Scalar phenomena in the homogeneous regions have their scalar counterpart at the surface, the typical example being chemical reactions. Vectorial phenomena in the homogeneous region must be split into the projection along the surface, and the component normal to the surface. In the excess entropy production of the surface, see Eqs. (5.11), (5.13) and (5.15), the 2-dimensional projection of the 3-dimensional vectorial flux or force, has the same symmetry as vectorial fluxes and forces along the surface. The normal component of the 3-dimensional vector has the symmetry of a scalar along the surface. Similarly, a 3×3 tensor in the homogeneous phase, gives a 2×2 tensor, two 2-dimensional vectors and one scalar along the surface.

We are dealing in this book with one-dimensional transport processes with a direction normal to the surface. All contributions to the excess entropy production of the surface are therefore scalar, they are chemical reactions or normal components of 3-dimensional vectors. *The important consequence is that coupling is possible between the chemical forces and electrical, thermal and diffusional forces into or across the surface.* This possibility was pointed out by Bertrand and Prud'homme [59, 60] and Bedeaux and coworkers [2, 4]. We shall elaborate on this in the following chapters. The coupling between the chemical reaction and the electric potential jump at the surface is a large effect, leading for instance to the Nernst equation for the surface, see Secs. 5.4 and 10.7. It is known from biology, that chemical reaction energy can be transformed to give directed transport across a membrane (so-called active transport, see [23, 24, 52]). This type of coupling is possible only at the membrane surface, according to the Curie principle.

The three phase contact line has only scalar contributions to its excess entropy production, Eqs. (6.11)–(6.13). All these scalar fluxes may couple. The normal component of an excess vectorial flux along the two-phase surfaces at the contact line, will for instance, couple to a chemical reaction along the line. This may have a bearing on electrochemical reactions, which often take place between reactants and products that are distributed in different phases, see Chapters 10, and 13–17.

This page intentionally left blank

Chapter 8

Transport of Heat and Mass

We present flux equations for transport of heat and mass in a simple heterogeneous system. Transport coefficients for homogeneous phases have been measured or modeled. We give the Onsager coefficients in terms of such coefficients.

Heat and mass transport is central in mechanical as well as in chemical engineering. Several books have been written on such transports, e.g. [69, 84, 138]. Also, in nature there are frequently temperature and density gradients, and as a consequence, transport of heat and mass. Our presentation aims to add to these descriptions, by giving complete sets of transport coefficients for heterogeneous systems. Onsager coefficients for heat and mass transfer shall be specified, both for the homogeneous regions and for the surfaces between them. They shall also be related to measured coefficients, like the thermal conductivity, the diffusion coefficient and the Soret coefficient.

We consider the simplest heterogeneous system to bring out the physical phenomena; a series of two homogeneous phases and a flat surface between them. We are concerned with transport of heat and one component in the direction normal to the surface. The other component is not moving and is used as the frame of reference. The dividing surface is defined as the equimolar surface of this component and is also not moving. The description in terms of the measurable heat flux, J'_q, and the molar flux of the moving component, J_m, brings out the importance of the enthalpy. At the surface, the molar enthalpy, H_m, of the moving component usually changes abruptly. This leads to substantial heat effects at the surface and a corresponding discontinuity in the temperature profile, and the measurable heat flux.

8.1 The homogeneous phases

We are seeking a set of flux equations that can be related to experiments. The entropy production for transport of heat and one component is, see Eq. (4.15):

$$\sigma = J'_q \frac{\partial}{\partial x}\left(\frac{1}{T}\right) + J_m\left(-\frac{1}{T}\frac{\partial \mu_{m,T}}{\partial x}\right) \tag{8.1}$$

where μ_m and J_m are the chemical potential and flux of the moving component, respectively. A second component is at rest with respect to the surface*. The linear relations for the forces are:

$$\begin{aligned} \frac{\partial}{\partial x}\frac{1}{T} &= r_{qq}J'_q + r_{qm}J_m \\ -\frac{1}{T}\frac{\partial \mu_{m,T}}{\partial x} &= r_{mq}J'_q + r_{mm}J_m \end{aligned} \tag{8.2}$$

The Onsager relation is $r_{qm} = r_{mq}$. These equations give the gradients in temperature and concentration c_m of the moving component:

$$\begin{aligned} \frac{\partial T}{\partial x} &= -T^2 r_{qq}\left(J'_q + \frac{r_{qm}}{r_{qq}}J_m\right) \\ \frac{\partial c_m}{\partial x} &= \frac{1}{T}\left(\frac{\partial \mu_{m,T}}{\partial c_m}\right)^{-1}\frac{r_{mq}}{r_{qq}}\frac{\partial T}{\partial x} - T\left(\frac{\partial \mu_{m,T}}{\partial c_m}\right)^{-1}\left(r_{mm} - \frac{r_{mq}r_{qm}}{r_{qq}}\right)J_m \end{aligned} \tag{8.3}$$

Temperature and concentration differences across the system lead to simultaneous heat and mass fluxes.

We determine from experiments the *thermal conductivity at zero mass flux*, λ, and the *measurable heat of transfer*†, q^*_m, *at constant temperature*.

$$\lambda = -\left[\frac{J'_q}{dT/dx}\right]_{J_m=0} = \frac{1}{T^2 r_{qq}} \quad \text{and} \quad q^*_m = \left(\frac{J'_q}{J_m}\right)_{dT=0} = -\frac{r_{qm}}{r_{qq}} \tag{8.4}$$

*$\partial\mu_{2,T}/\partial x$ for the non-moving component can be found using Gibbs–Duhem's equation, see Appendix 3.A. It does not play any role in the further analysis.

†De Groot and Mazur [20] use the "reduced heat of transfer," and the reduced heat flux, see Appendix 4.A.

The measured *interdiffusion coefficient* and *thermal diffusion coefficient* are defined by:

$$\begin{aligned} D_m &= -\left[\frac{J_m}{\partial c_m/\partial x}\right]_{dT=0} = \frac{1}{T}\frac{\partial \mu_{m,T}}{\partial c_m}\left(r_{mm} - \frac{r_{mq}r_{qm}}{r_{qq}}\right)^{-1} \\ &= \frac{1}{T}\frac{\partial \mu_{m,T}}{\partial c_m}\left(r_{mm} - r_{qq}\left(q_m^*\right)^2\right)^{-1} \\ D_T &= -\left[\frac{J_m}{c_m \partial T/\partial x}\right]_{dc_m=0} = -\frac{r_{mq}/r_{qq}}{c_m T^2}\left(r_{mm} - \frac{r_{mq}r_{qm}}{r_{qq}}\right)^{-1} \\ &= \frac{q_m^*}{c_m T^2}\left(r_{mm} - r_{qq}\left(q_m^*\right)^2\right)^{-1} \end{aligned} \tag{8.5}$$

With these coefficients, the gradients of the temperature and the concentration of the moving component become:

$$\begin{aligned} \frac{\partial T}{\partial x} &= -\frac{1}{\lambda}\left(J_q' - q_m^* J_m\right) \\ \frac{\partial c_m}{\partial x} &= -c_m \frac{D_T}{D_m}\frac{\partial T}{\partial x} - \frac{1}{D_m} J_m \end{aligned} \tag{8.6}$$

The relations Eq. (8.6), which are equivalent to the linear relations Eq. (8.2), contain transport coefficients which are known for many systems. The Onsager resistivity matrix can be found from such tabulated transport coefficients using the following formulae:

$$r_{qq} = \frac{1}{\lambda T^2}, \quad r_{qm} = r_{mq} = -\frac{q_m^*}{\lambda T^2} \quad \text{and} \quad r_{mm} = \frac{\left(q_m^*\right)^2}{\lambda T^2} + \frac{1}{T D_m}\frac{\partial \mu_{m,T}}{\partial c_m} \tag{8.7}$$

The *Soret effect* is mass transport that takes place due to a temperature gradient. The ratio of the thermal diffusion coefficient and the interdiffusion coefficient is called the *Soret coefficient*, s_T. In a stationary state $J_m = 0$, and the Soret coefficient can be determined from the ratio of the concentration gradient and the temperature gradient:

$$s_T = -\left(\frac{\partial c_m/\partial x}{c_m \partial T/\partial x}\right)_{J_m=0} = \frac{D_T}{D_m} = \frac{q_m^*}{c_m T}\left(\frac{\partial \mu_{m,T}}{\partial c_m}\right)^{-1} \tag{8.8}$$

We can alternatively measure the ratio of the heat flux and the molar flux at constant temperature to find the heat of transfer q_m^*, and then calculate the Soret coefficient. Heat transport due to a concentration gradient is

called the *Dufour effect*. This effect is the *reciprocal* effect to the Soret effect. The Dufour coefficient is

$$D_D = -\left(\frac{J'_q}{\partial c_m/\partial x}\right)_{dT=0} = q^*_m D_m = c_m T \frac{\partial \mu_{m,T}}{\partial c_m} D_T \tag{8.9}$$

From the positive nature of the entropy production, it follows that the diffusion coefficient and the thermal conductivity are positive, cf. Eq. (7.21). The thermal diffusion coefficient, the measurable heat of transfer and the Soret coefficient can be positive or negative. From the inequality (7.22), using Eq. (8.7), we obtain

$$(r_{mq})^2 \leq r_{mm} r_{qq} \rightarrow \left(\frac{q^*_m}{\lambda T^2}\right)^2 \leq \left(\frac{(q^*_m)^2}{\lambda T^2} + \frac{1}{T D_m}\frac{\partial \mu_{m,T}}{\partial c_m}\right)\frac{1}{\lambda T^2}$$

$$\rightarrow 0 \leq \frac{\partial \mu_{m,T}}{\partial c_m} \tag{8.10}$$

The chemical potential will always increase when the concentration increases.

8.2 Coefficient values for homogeneous phases

Diffusion coefficients vary by orders of magnitude when one compares gases, liquids and solid phases, see Table 8.1. Within one phase, the variation is not so large for similar species. Diffusion coefficients are measured by spectroscopic and analytical techniques [70, 139, 140].

Table 8.1 Examples of diffusion coefficients in binary mixtures D_m

Component m	Reference component	$D/\mathrm{m^2 s^{-1}}$
CH_4	nitrogen gas	5×10^{-5}
NaCl	water	1.3×10^{-9}
Sucrose	water	4.5×10^{-10}
C	steel	1×10^{-20}

One can obtain an estimate for D from the *self-diffusion coefficient*, D_s, which is measured with NMR. The self-diffusion coefficient describes the Brownian motion of a single particle at equilibrium, and can therefore also be defined for pure components. The self-diffusion coefficient of water (in water) is 2.3×10^{-9} $\mathrm{m^2 s^{-1}}$ at 298 K [141].

For gases, the kinetic theory gives $D_s = \ell \mathrm{v}/3$, where ℓ is the mean free path of the molecule and v is the mean thermal velocity. In a one-component gas $\ell = \left(\pi a^2 c_m N\right)^{-1}$, where a is the diameter of the particles, and $\mathrm{v} = \sqrt{3RT/M}$. With values $\ell = 30$ nm and $\mathrm{v} = 300$ ms^{-1} typical for air one finds $D_s = 3\times\ 10^{-6}$ m^{2}s^{-1}. This estimate can be compared to the diffusion coefficients for methane in nitrogen in Table 8.1. For low density gas mixtures the diffusion and the self-diffusion coefficient are the same. For liquid mixtures they are not.

The Soret coefficient in gases is usually small. Nevertheless, the Soret effect has been used to separate isotopes, a difficult separation. Isotopes differ by their masses only (m_2 and m_1). As a first approximation, Furry and Onsager [142] used

$$s_T = \frac{0.35(m_2 - m_1)}{T(m_2 + m_1)} \tag{8.11}$$

to describe a mass effect. This expression was used to design separation columns for radioactive isotopes. Isotope separation in salt mixtures was measured by Lundén [143].

The interaction energy or the enthalpy is also important for the magnitude and sign of s_T [144]. A formula for the *thermal diffusion factor*, $\alpha \equiv T s_T$, which has proven accurate for mixtures of two hydrocarbons, was proposed by Kempers [145].

$$\alpha_T \equiv -\frac{T}{x_1 x_2}\frac{\partial x_1}{\partial T} = -\left(\frac{V_1 V_2}{x_1 V_1 + x_2 V_2}\right)\frac{H_1/V_1 - H_2/V_2}{x_1(\partial \mu_1/\partial x_1)_{p,T}} \tag{8.12}$$

Here x_i is the mole fraction, while V_i and H_i are the partial molar volume and enthalpy, respectively. We return to this model in Sec. 12.5.

The Soret coefficient is often positive for the lighter component (negative for the heavier component) as predicted from Eq. (8.11). Intermolecular interactions may alter this. The Soret effect is larger in liquids than in gases, and the magnitude increases, the closer one comes to the critical point [21]. A similar formula to Eq. (8.12) [21, 146] was used to predict composition variations with depth in oil reservoirs [147]. The variation was equally large as the separation due to gravity for methane in decane [147]. Some Soret coefficients for non-electrolytes are given in Table 8.2 [138]. More data for electrolytes are given by Agar [148] and Fitts [30].

The effect of temperature gradients on mass transport can not only be determined by experiments, but also by molecular dynamics simulations, see Chapter 22, and Fig. 22.7 [149]. In these simulations a temperature difference is maintained over a box with two kinds of particles, by thermostatting the velocity of the molecules at the boundaries. The heavy

Table 8.2 Soret coefficient for some binary mixtures. The mole fraction $x_m = c_m/c$ applies to component m.

Component m	Reference component	x_m	T/K	p/bar	s_T/K^{-1}
Methane	propane	0.34	346	60800	0.042
Methane	cyclopentane	0.0026	293	1	−0.016
i-butane	methylcyclopentane	0.5	293	1	−0.0096
Cyclohexane	benzene	0.5	293	1	−0.0063
Carbon dioxide	hydrogen	0.51	223	15	0.00046

component concentrated on the cold side, and the light component on the warm side. The consequence of the temperature difference was thus first a mass flux, and eventually a concentration gradient. At stationary state, there were no longer mass fluxes relative to the walls.

Remark 8.1. *In an experiment to measure the thermal conductivity, one starts in an equilibrium state. This implies that the concentrations are constant. After switching on a temperature gradient, one first measures* $\lambda_m = -J'_q/(\partial T/\partial x) = \lambda + q^*_m c_m D_T$. *The temperature gradient proceeds to give a mass flux, which results after a while in a non-equilibrium distribution of the concentration, such that the mass flux again becomes zero. In this stationary state one measures* λ. *This is why we will refer to* λ_m *as the initial thermal conductivity and to* λ *as the stationary state thermal conductivity. The initial thermal conductivity is larger than the stationary state thermal conductivity, because* $q^*_m D_T > 0$.

Exercise 8.2.1. *Express* J'_q *and* J_m *in terms of* $-T^{-2}\,(\partial T/\partial x)$ *and* $-T^{-1}\partial\mu_{m,T}/\partial x$.

- **Solution:** By inverting Eqs. (8.2) we have:

$$J'_q = l_{qq}\left(-\frac{1}{T^2}\frac{\partial T}{\partial x}\right) + l_{qm}\left(-\frac{1}{T}\frac{\partial \mu_{m,T}}{\partial x}\right)$$

and

$$J_m = l_{mq}\left(-\frac{1}{T^2}\frac{\partial T}{\partial x}\right) + l_{mm}\left(-\frac{1}{T}\frac{\partial \mu_{m,T}}{\partial x}\right)$$

with

$$l_{qq} = \frac{r_{mm}}{r_{qq}r_{mm} - r_{mq}r_{qm}}, \quad l_{mq} = l_{qm} = \frac{-r_{qm}}{r_{qq}r_{mm} - r_{mq}r_{qm}},$$

$$l_{mm} = \frac{r_{qq}}{r_{qq}r_{mm} - r_{mq}r_{qm}}$$

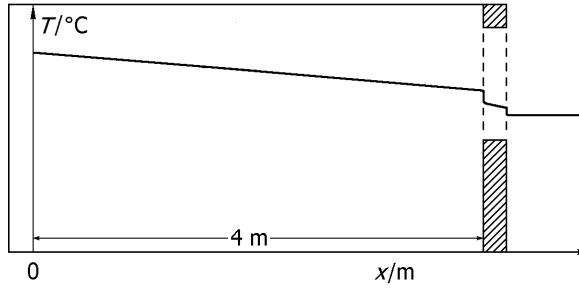

Figure 8.1 The stationary state temperature profile across a room and a double window in the absence of convection.

Exercise 8.2.2. *Consider a room with air and a trace (10 ppm) of perfume, see Fig. 8.1. Near the wall, the temperature is 20 °C ($x = 0$). Near the window at a distance of 4 m, the temperature is 10 °C. One may use ideal solution conditions. The measurable heat of transfer of perfume in air is $q_m^* = 700$ J/mol. The thermal conductivity is constant. Calculate the concentration difference of perfume between the window and the wall in the stationary state. The room has heat leakage to one side only, as illustrated in the figure.*

- **Solution:** In the stationary state there is no perfume flux. This implies that, cf. Eq. (8.8),

$$\frac{dc_m}{dx} = -c_m s_T \frac{dT}{dx} = -\frac{q_m^*}{T\partial\mu_{m,T}/\partial c_m}\frac{dT}{dx} = -\frac{c_m q_m^*}{RT^2}\frac{dT}{dx}$$

The heat flux is constant so that $T(x) = 20 - 2.5x$ and a similar expression for the molar density profile. This gives a temperature gradient of -2.5 K/m. The concentration gradient is therefore approximately $dc_m/dx = 7000\,(8.31)^{-1}\,(300)^{-2}\,2.5 \simeq 0.025$ ppm/m. This gives a concentration of 0.1 ppm higher at the window than close to the wall. Perfume concentrates at the cold side, it is heavier than air.

8.3 The surface

Consider next two homogeneous phases like the one described above, separated by an interface. The phase at $x < 0$ is labeled with superscript i, and the phase at $x > 0$ is labeled with superscript o. The excess entropy production for the transport of heat and mass across the surface is, according to Eq. (5.15):

$$\sigma^{\mathrm{s}} = J_q'^{\mathrm{i}} \Delta_{\mathrm{i,s}} \frac{1}{T} + J_q'^{\mathrm{o}} \Delta_{\mathrm{s,o}} \frac{1}{T} + J_m^{\mathrm{i}} \left(-\frac{1}{T^{\mathrm{s}}} \Delta_{\mathrm{i,s}} \mu_{m,T} \left(T^{\mathrm{s}} \right) \right)$$

$$+ J_m^{\mathrm{o}} \left(-\frac{1}{T^{\mathrm{s}}} \Delta_{\mathrm{s,o}} \mu_{m,T} \left(T^{\mathrm{s}} \right) \right) \tag{8.13}$$

The notation of the forces was illustrated in Fig. 5.5. The force-flux pairs in the excess entropy production may be divided into two groups. The first group contains coupling of fluxes and forces on the incoming side of the surface and the second group contains coupling of fluxes and forces on the outgoing side. Because the processes on the two sides of the surface occur in series, it is expected that they are weakly coupled. We shall therefore neglect coupling *across* the surface. In that case, the force-flux relations become

$$\begin{aligned} \Delta_{\mathrm{i,s}} \frac{1}{T} &= r_{qq}^{\mathrm{s,i}} J_q'^{\mathrm{i}} + r_{qm}^{\mathrm{s,i}} J_m^{\mathrm{i}} \\ -\frac{1}{T^{\mathrm{s}}} \Delta_{\mathrm{i,s}} \mu_{m,T} \left(T^{\mathrm{s}} \right) &= r_{mq}^{\mathrm{s,i}} J_q'^{\mathrm{i}} + r_{mm}^{\mathrm{s,i}} J_m^{\mathrm{i}} \end{aligned} \tag{8.14}$$

for side i of the surface and

$$\begin{aligned} \Delta_{\mathrm{s,o}} \frac{1}{T} &= r_{qq}^{\mathrm{s,o}} J_q'^{\mathrm{o}} + r_{qm}^{\mathrm{s,o}} J_m^{\mathrm{o}} \\ -\frac{1}{T^{\mathrm{s}}} \Delta_{\mathrm{s,o}} \mu_{m,T} \left(T^{\mathrm{s}} \right) &= r_{mq}^{\mathrm{s,o}} J_q'^{\mathrm{o}} + r_{mm}^{\mathrm{s,o}} J_m^{\mathrm{o}} \end{aligned} \tag{8.15}$$

for side o. All coefficients have the dimensionality of the resistivity coefficients for the homogeneous phase, see Eqs. (8.2), times a length (the surface thickness). All resistivity coefficients have superscript s to indicate the surface. The next superscript gives the side of the surface for which the force is evaluated. The number of independent resistivities is six.

Remark 8.2. *The force-flux relations for the surface serve as boundary conditions for integrations of temperature and chemical potential across adjacent bulk phases.*

The *measurable heats of transfer* can be defined in a similar manner as for the homogeneous system:

$$q_m^{*\mathrm{i}} \left(T^{\mathrm{s}} \right) = \left(\frac{J_q'^{\mathrm{i}}}{J_m^{\mathrm{i}}} \right)_{\Delta_{\mathrm{i,s}} T = 0} = -\frac{r_{qm}^{\mathrm{s,i}} \left(T^{\mathrm{s}} \right)}{r_{qq}^{\mathrm{s,i}} \left(T^{\mathrm{s}} \right)}$$

and

$$q_m^{*\mathrm{o}} \left(T^{\mathrm{s}} \right) = \left(\frac{J_q'^{\mathrm{o}}}{J_m^{\mathrm{o}}} \right)_{\Delta_{\mathrm{s,o}} T = 0} = -\frac{r_{qm}^{\mathrm{s,o}} \left(T^{\mathrm{s}} \right)}{r_{qq}^{\mathrm{s,o}} \left(T^{\mathrm{s}} \right)} \tag{8.16}$$

With these definitions, Eqs. (8.14) and (8.15) can be written as

$$\begin{aligned}\Delta_{\mathrm{i,s}}\frac{1}{T} &= r^{\mathrm{s,i}}_{qq}\left(J'^{\mathrm{i}}_q - q^{*\mathrm{i}}_m J^{\mathrm{i}}_m\right)\\ \frac{1}{T^{\mathrm{s}}}\Delta_{\mathrm{i,s}}\mu_{m,T}\left(T^{\mathrm{s}}\right) &= r^{\mathrm{s,i}}_{qq}q^{*\mathrm{i}}_m J'^{\mathrm{i}}_q - r^{\mathrm{s,i}}_{mm}J^{\mathrm{i}}_m\end{aligned} \tag{8.17}$$

for side i of the surface and

$$\begin{aligned}\Delta_{\mathrm{s,o}}\frac{1}{T} &= r^{\mathrm{s,o}}_{qq}\left(J'^{\mathrm{o}}_q - q^{*\mathrm{o}}_m J^{\mathrm{o}}_m\right)\\ \frac{1}{T^{\mathrm{s}}}\Delta_{\mathrm{s,o}}\mu_{m,T}\left(T^{\mathrm{s}}\right) &= r^{\mathrm{s,o}}_{qq}q^{*\mathrm{o}}_m J'^{\mathrm{o}}_q - r^{\mathrm{s,o}}_{mm}J^{\mathrm{o}}_m\end{aligned} \tag{8.18}$$

for side o. *The measurable heats of transfer are ratios of fluxes in the homogeneous phases, so their values at the surface are equal to the values in the homogeneous phases next to the surface.* The only new coefficients, that are needed to describe transport through the surface, are then the four diagonal coefficients in Eqs. (8.14) and (8.15).

8.3.1 *Heats of transfer for the surface*

The description in the beginning of the section uses the temperature of the surface as a variable. We can eliminate T^{s} for stationary state conditions, when the total heat flux $J_q = J'^{\mathrm{i}}_q + H^{\mathrm{i}}_m J^{\mathrm{i}}_m = J'^{\mathrm{o}}_q + H^{\mathrm{o}}_m J^{\mathrm{o}}_m$, and the molar flux $J_m = J^{\mathrm{i}}_m = J^{\mathrm{o}}_m$ are constant. The jumps across the surface of the inverse temperature and the chemical potential, become with the addition of Eqs. (8.17) and (8.18):

$$\begin{aligned}\Delta_{\mathrm{i,o}}\frac{1}{T} &= r^{\mathrm{s,i}}_{qq}\left(J'^{\mathrm{i}}_q - q^{*\mathrm{i}}_m J_m\right) + r^{\mathrm{s,o}}_{qq}\left(J'^{\mathrm{o}}_q - q^{*\mathrm{o}}_m J_m\right)\\ &= \left(r^{\mathrm{s,i}}_{qq} + r^{\mathrm{s,o}}_{qq}\right)J'^{\mathrm{i}}_q - \left[r^{\mathrm{s,i}}_{qq}q^{*\mathrm{i}}_m + r^{\mathrm{s,o}}_{qq}\left(q^{*\mathrm{o}}_m + \Delta_{\mathrm{i,o}}H_m\right)\right]J_m\\ \frac{1}{T^{\mathrm{s}}}\Delta_{\mathrm{i,o}}\mu_{m,T}\left(T^{\mathrm{s}}\right) &= r^{\mathrm{s,i}}_{qq}q^{*\mathrm{i}}_m J'^{\mathrm{i}}_q - r^{\mathrm{s,i}}_{mm}J_m + r^{\mathrm{s,o}}_{qq}q^{*\mathrm{o}}_m J'^{\mathrm{o}}_q - r^{\mathrm{s,o}}_{mm}J_m\\ &= \left(r^{\mathrm{s,i}}_{qq}q^{*\mathrm{i}}_m + r^{\mathrm{s,o}}_{qq}q^{*\mathrm{o}}_m\right)J'^{\mathrm{i}}_q - \left(r^{\mathrm{s,i}}_{mm} + r^{\mathrm{s,o}}_{mm} + r^{\mathrm{s,o}}_{qq}q^{*\mathrm{o}}_m\Delta_{\mathrm{i,o}}H_m\right)J_m\end{aligned} \tag{8.19}$$

The matrix of coefficients is no longer symmetric. The reason for this is that we have eliminated J'^{o}_q without making a corresponding change in the forces. This can be done by using $\Delta_{\mathrm{i,o}}\mu_{m,T}\left(T^{\mathrm{o}}\right)/T^{\mathrm{o}}$ instead of $\Delta_{\mathrm{i,o}}\mu_{m,T}\left(T^{\mathrm{s}}\right)/T^{\mathrm{s}}$. To simplify, we now replace superscript o,i of T by o only. The difference is

$$\frac{1}{T^{\mathrm{s}}}\Delta_{\mathrm{i,o}}\mu_{m,T}\left(T^{\mathrm{s}}\right) = \frac{1}{T^{\mathrm{o}}}\Delta_{\mathrm{i,o}}\mu_{m,T}\left(T^{\mathrm{o}}\right) - \Delta_{\mathrm{i,o}}H_m\Delta_{\mathrm{s,o}}\frac{1}{T} \tag{8.20}$$

By introducing this into Eq. (8.19), we find:

$$\begin{aligned} \Delta_{\mathrm{i,o}}\frac{1}{T} &= r^{\mathrm{s}}_{qq}J'^{\mathrm{i}}_{q} + r^{\mathrm{s,l}}_{qm}J_m \\ -\frac{1}{T^{\mathrm{o}}}\Delta_{\mathrm{i,o}}\mu_{m,T}\left(T^{\mathrm{o}}\right) &= r^{\mathrm{s,l}}_{mq}J'^{\mathrm{i}}_{q} + r^{\mathrm{s,l}}_{mm}J_m \end{aligned} \tag{8.21}$$

where

$$\begin{aligned} r^{\mathrm{s}}_{qq} \equiv r^{\mathrm{s,i}}_{qq} + r^{\mathrm{s,o}}_{qq}, \quad r^{\mathrm{s,l}}_{qm} = r^{\mathrm{s,l}}_{mq} \equiv -r^{\mathrm{s,i}}_{qq}q^{*\mathrm{i}} - r^{\mathrm{s,o}}_{qq}\left(q^{*\mathrm{o}}_{m} + \Delta_{\mathrm{i,o}}H_m\right) \\ r^{\mathrm{s,l}}_{mm} \equiv r^{\mathrm{s,i}}_{mm} + r^{\mathrm{s,o}}_{mm} + r^{\mathrm{s,o}}_{qq}\Delta_{\mathrm{i,o}}H_m\left(2q^{*\mathrm{o}}_{m} + \Delta_{\mathrm{i,o}}H_m\right) \end{aligned} \tag{8.22}$$

The *heat of transfer for the whole surface, derived from the measurable heat flux at the left hand side of the surface* can then be defined as

$$q^{*\mathrm{s,i}}_{m} = \left(\frac{J'^{\mathrm{i}}_{q}}{J_m}\right)_{\Delta_{\mathrm{i,o}}T=0} = -\frac{r^{\mathrm{s,l}}_{qm}}{r^{\mathrm{s}}_{qq}} = \frac{r^{\mathrm{s,i}}_{qq}q^{*\mathrm{i}}_{m} + r^{\mathrm{s,o}}_{qq}\left(q^{*\mathrm{o}}_{m} + \Delta_{\mathrm{i,o}}H_m\right)}{r^{\mathrm{s,i}}_{qq} + r^{\mathrm{s,o}}_{qq}} \tag{8.23}$$

As is clear from this relation $q^{*\mathrm{s,i}}_{m}$ is unequal to $q^{*\mathrm{i}}_{m}$. In this context, $\Delta_{\mathrm{i,o}}T = 0$ does not mean that $\Delta_{\mathrm{i,s}}T = 0$. Using the measurable heat of transfer, Eq. (8.21) becomes

$$\begin{aligned} \Delta_{\mathrm{i,o}}T &= T^{\mathrm{i}}T^{\mathrm{o}}r^{\mathrm{s}}_{qq}\left(J'^{\mathrm{i}}_{q} - q^{*\mathrm{s,i}}_{m}J_m\right) \\ -\frac{1}{T^{\mathrm{o}}}\Delta_{\mathrm{i,o}}\mu_{m,T}\left(T^{\mathrm{o}}\right) &= -\frac{q^{*\mathrm{s,i}}_{m}}{T^{\mathrm{i}}T^{\mathrm{o}}}\Delta_{\mathrm{i,o}}T + \left(r^{\mathrm{s,l}}_{mm} - r^{\mathrm{s}}_{qq}q^{*\mathrm{s,i}}_{m}q^{*\mathrm{s,i}}_{m}\right)J_m \end{aligned} \tag{8.24}$$

It is also possible to eliminate the measurable heat flux on the left hand side of the surface in Eq. (8.19). Instead of Eq. (8.21) we then obtain

$$\begin{aligned} \Delta_{\mathrm{i,o}}\frac{1}{T} &= r^{\mathrm{s}}_{qq}J'^{\mathrm{o}}_{q} + r^{\mathrm{s,r}}_{qm}J_m \\ -\frac{1}{T^{\mathrm{i}}}\Delta_{\mathrm{i,o}}\mu_{m,T}\left(T^{\mathrm{i}}\right) &= r^{\mathrm{s,r}}_{mq}J'^{\mathrm{o}}_{q} + r^{\mathrm{s,r}}_{mm}J_m \end{aligned} \tag{8.25}$$

where

$$\begin{aligned} r^{\mathrm{s}}_{qq} \equiv r^{\mathrm{s,i}}_{qq} + r^{\mathrm{s,o}}_{qq}, \quad r^{\mathrm{s,r}}_{qm} = r^{\mathrm{s,r}}_{mq} \equiv -r^{\mathrm{s,i}}_{qq}\left(q^{*\mathrm{i}}_{m} - \Delta_{\mathrm{i,o}}H_m\right) - r^{\mathrm{s,o}}_{qq}q^{*\mathrm{o}}_{m} \\ r^{\mathrm{s,r}}_{mm} \equiv r^{\mathrm{s,i}}_{mm} + r^{\mathrm{s,o}}_{mm} - r^{\mathrm{s,i}}_{qq}\Delta_{\mathrm{i,o}}H_m\left(2q^{*\mathrm{i}}_{m} - \Delta_{\mathrm{i,o}}H_m\right) \end{aligned} \tag{8.26}$$

For *the heat of transfer for the whole surface, derived from the measurable heat flux at the right hand side of the surface* we find

$$q^{*\mathrm{s,o}}_{m} = \left(\frac{J'^{\mathrm{o}}_{q}}{J_m}\right)_{\Delta_{\mathrm{i,o}}T=0} = -\frac{r^{\mathrm{s,r}}_{qm}}{r^{\mathrm{s}}_{qq}} = \frac{r^{\mathrm{s,i}}_{qq}\left(q^{*\mathrm{i}}_{m} - \Delta_{\mathrm{i,o}}H_m\right) + r^{\mathrm{s,o}}_{qq}q^{*\mathrm{o}}_{m}}{r^{\mathrm{s,i}}_{qq} + r^{\mathrm{s,o}}_{qq}} \tag{8.27}$$

Equation (8.25) in terms of the measurable heat of transfer, becomes

$$\begin{aligned} \Delta_{\mathrm{i,o}} T &= T^{\mathrm{i}} T^{\mathrm{o}} r^{\mathrm{s}}_{qq} \left(J'^{\mathrm{o}}_q - q^{*\mathrm{s,o}}_m J_m \right) \\ -\frac{1}{T^{\mathrm{i}}} \Delta_{\mathrm{i,o}} \mu_{m,T} \left(T^{\mathrm{i}} \right) &= -\frac{q^{*\mathrm{s,o}}_m}{T^{\mathrm{i}} T^{\mathrm{o}}} \Delta_{\mathrm{i,o}} T + \left(r^{\mathrm{s,r}}_{mm} - r^{\mathrm{s}}_{qq} q^{*\mathrm{s,o}}_m q^{*\mathrm{s,o}}_m \right) J_m \end{aligned} \tag{8.28}$$

An interesting identity which follows from Eqs. (8.23) and (8.27) is

$$q^{*\mathrm{s,o}}_m - q^{*\mathrm{s,i}}_m = -\Delta_{\mathrm{i,o}} H_m \tag{8.29}$$

This shows that the difference of the measurable heats of transfer that can be defined for the whole surface, is equal to the enthalpy difference across the surface. The rather common practice to take the coupling coefficient equal to zero, suggested by the small $q^{*\mathrm{i}}_m$ and $q^{*\mathrm{o}}_m$, *is therefore in violation with this identity [61].* Given the fact that the enthalpy difference across a phase boundary is normally substantial, this can give a serious error.

Remark 8.3. *In a practical situation, only one of the equation sets, Eq. (8.21) or (8.25), is needed to describe the transports at the surface. We shall see in Sec. 11.3 that one set has larger coefficients than the other, and may therefore be easier to determine.*

Remark 8.4. *In Sec. 12.2, we derive an equivalent relation, cf. Eq. (12.64), for the difference of the measurable heats of transfer across a finite film in a homogeneous phase. In that case, the enthalpy differences are, however, much smaller. An interesting consequence of the validity of both these relations is that one may combine them and obtain the same relation for transport between two arbitrary planes between which there is a sequence of homogeneous films with surfaces in between.*

Exercise 8.3.1. *Consider again the room with a trace of perfume from the previous exercise. We want to take into account that perfume adsorbs to the window. The perfume does not cross the window to disappear in the air outside. The temperature of the air just outside the window is* $-10\ ^\circ C$ *while the temperature in the room 4m away from the window,* T^{il}*, is again* $20\ ^\circ C$*. How do the linear laws (8.17) and (8.18), which neglect the coupling resistances across the surface, simplify in a stationary state? The mass fluxes are again zero. The thermal conductivity of air* λ *with perfume is 0.01 W/Km, and the thermal resistivities for both sides of the window* $r^{s,i}_{qq}$ *and* $r^{s,o}_{qq}$ *are 0.002* m^2/WK*. What is the resulting temperature profile and how does this affect the perfume concentration difference?*

- **Solution:** Since there is no perfume flux in the stationary state, $J^{\mathrm{i}} = J^{\mathrm{o}} = 0$, the total heat flux is equal to the measurable heat

flux. We know furthermore that the total heat flux and therefore the measurable heat flux is constant throughout the system, $J_q'^{\mathrm{i}} = J_q'^{\mathrm{o}} = J_q'$. The force-flux equations become

$$\Delta_{\mathrm{i,s}} \frac{1}{T} = r_{qq}^{\mathrm{s,i}} J_q' \quad \text{and} \quad \Delta_{\mathrm{s,o}} \frac{1}{T} = r_{qq}^{\mathrm{s,o}} J_q'$$

$$\Delta_{\mathrm{i,s}} \frac{\mu}{T} = r_{qq}^{\mathrm{s,i}} q^{*\mathrm{i}} J_q' \quad \text{and} \quad \Delta_{\mathrm{s,o}} \frac{\mu}{T} = r_{qq}^{\mathrm{s,o}} q^{*\mathrm{o}} J_q'$$

By adding the first two equations, we find $1/T^{\mathrm{o}} - 1/T^{\mathrm{i}} = \left(r_{qq}^{\mathrm{s,i}} + r_{qq}^{\mathrm{s,o}}\right) J_q'$. As a consequence, $T^{\mathrm{o}} - T^{\mathrm{i}} = -T^{\mathrm{o}} T^{\mathrm{i}} \left(r_{qq}^{\mathrm{s,i}} + r_{qq}^{\mathrm{s,o}}\right) J_q' = -360 J_q'$. Furthermore, we know that in the room $T^{\mathrm{i}} - T^{\mathrm{il}} = -(4/\lambda) J_q' = -400 J_q'$. The sum gives $30 = T^{\mathrm{il}} - T^{\mathrm{o}} = 760 J_q'$ or $J_q' = 0.04$ W/m^2. The temperature difference across the room is therefore $T^{\mathrm{il}} - T^{\mathrm{i}} = 400 \times 0.04 = 16$°C. In the previous exercise, the temperature difference was 10 degrees across the room, which made the concentration 0.10 ppm higher at the window. Now the perfume concentration is 0.16 ppm (60%) higher at the window. This example shows that the surface can play a significant role.

Remark 8.5. *The example is, of course, artificial in the sense that we do not allow the air to circulate. This would homogenize both the temperature and the concentration. The surface above has a thickness of mm rather than nm. A surface does not have to be microscopically thick to qualify as a surface in the Gibbs sense. The only important condition is that the bulk region adjacent to the surface is much thicker than the surface, and that the change of the temperature in the bulk over a distance comparable to the thickness of the surface is small, just as in the above exercise.*

8.4 Solution for the heterogeneous system

For an analysis of the heterogeneous system, we write Eq. (8.2) after some algebra in the following form

$$\begin{aligned} \frac{\partial}{\partial x} \frac{1}{T} &= r_{qq} \left(J_q - Q_m^* J_m\right) \\ \frac{\partial}{\partial x} \frac{\mu_m}{T} &= r_{qq} Q_m^* J_q - \left[r_{mm} + H_m r_{qq} \left(2q_m^* + H_m\right)\right] J_m \\ &\equiv r_{qq} Q_m^* J_q - r_{\mu\mu} J_m \end{aligned} \tag{8.30}$$

where we used $J'_q = J_q - H_m J_m$ and the thermodynamic identity

$$\frac{\partial \mu_m/T}{\partial 1/T} = \mu_m - T\frac{\partial \mu_m}{\partial T} = \mu_m + TS_m = H_m \tag{8.31}$$

Furthermore, we defined the *total heat of transfer* by:

$$Q^*_m = \left(\frac{J_q}{J_m}\right)_{dT=0} = \left(\frac{J'_q + H_m J_m}{J_m}\right)_{dT=0} = q^*_m + H_m = -\frac{r_{qm}}{r_{qq}} + H_m \tag{8.32}$$

and defined the resistivity $r_{\mu\mu}$ in the last equality in Eq. (8.30).

In the stationary state, energy and molar densities are independent of time. As a consequence the total heat flux, J_q, and the component flux, J_m, are constant, both as a function of time and position. This makes Eq. (8.30) suitable for integration. The measurable heat flux is not constant as a function of position due to the variation of the enthalpy density as a function of the local temperature and the concentrations.

For the surface, we obtain in a similar manner from Eqs. (8.14) and (8.15)

$$\begin{aligned}
\Delta_{\mathrm{i,s}}\frac{1}{T} &= r^{\mathrm{s,i}}_{qq}\left[J_q - \left(q^{*\mathrm{i}}_m + H^{\mathrm{i}}_m\right) J_m\right] = r^{\mathrm{s,i}}_{qq}\left(J_q - Q^{*\mathrm{i}}_m J_m\right) \\
\Delta_{\mathrm{i,s}}\frac{\mu_m}{T} &= r^{\mathrm{s,i}}_{qq}\left(q^{*\mathrm{i}}_m + H^{\mathrm{i}}_m\right) J_q - \left[r^{\mathrm{s,i}}_{mm} + r^{\mathrm{s,i}}_{qq} H^{\mathrm{i}}_m \left(2q^{*\mathrm{i}}_m + H^{\mathrm{i}}_m\right)\right] J_m \\
&= r^{\mathrm{s,i}}_{qq} Q^{*\mathrm{i}} J_q - r^{\mathrm{s,i}}_{\mu\mu} J_m
\end{aligned} \tag{8.33}$$

for side i of the surface and

$$\begin{aligned}
\Delta_{\mathrm{s,o}}\frac{1}{T} &= r^{\mathrm{s,o}}_{qq}\left[J_q - \left(q^{*\mathrm{o}}_m + H^{\mathrm{o}}_m\right) J_m\right] = r^{\mathrm{s,o}}_{qq}\left(J_q - Q^{*\mathrm{o}}_m J_m\right) \\
\Delta_{\mathrm{s,o}}\frac{\mu_m}{T} &= r^{\mathrm{s,o}}_{qq}\left(q^{*\mathrm{o}}_m + H^{\mathrm{o}}_m\right) J_q - \left[r^{\mathrm{s,o}}_{mm} + r^{\mathrm{s,o}}_{qq} H^{\mathrm{o}}_m \left(2q^{*\mathrm{o}}_m + H^{\mathrm{o}}_m\right)\right] J_m \\
&= r^{\mathrm{s,o}}_{qq} Q^{*\mathrm{o}} J_q - r^{\mathrm{s,o}}_{\mu\mu} J_m
\end{aligned} \tag{8.34}$$

for side o. The coefficients $r^{\mathrm{s,i}}_{\mu\mu}$ and $r^{\mathrm{s,o}}_{\mu\mu}$ are defined in the last identities.

We are now set to solve the temperature and concentration profiles across a heterogeneous system. Consider therefore two homogeneous phases with an interface between them. The zero along the x-axis is chosen to coincide with the position of the dividing surface. The left homogeneous phase is between $-d_{in}$ and 0 and the right homogeneous phase is between 0 and d_{out}. The system is in a stationary state, so that the total heat

flux, J_q, and the mass flux, J_m, are constant throughout the system. The temperatures at the ends are $T_{in} = T(-d_{in})$ and $T_{out} = T(d_{out})$, and the chemical potentials are $\mu_{in} = \mu_m(-d_{in})$ and $\mu_{out} = \mu_m(d_{out})$. In order to simplify the calculation, we assume that the resistivities and the enthalpies (and as a consequence the heats of transfer) are constant. It then follows from Eq. (8.30) that the gradients of $1/T$ and μ/T in the two homogeneous phases are constant. By integrating these equations over the homogeneous phases, we find:

$$\begin{aligned}
\frac{1}{T_{out}} - \frac{1}{T_{in}} &= \left(\frac{1}{T_{out}} - \frac{1}{T^{\mathrm{o}}}\right) + \left(\frac{1}{T^{\mathrm{o}}} - \frac{1}{T^{\mathrm{s}}}\right) \\
&\quad + \left(\frac{1}{T^{\mathrm{s}}} - \frac{1}{T^{\mathrm{i}}}\right) + \left(\frac{1}{T^{\mathrm{i}}} - \frac{1}{T_{in}}\right) \\
&= \left(d_{out} r^{\mathrm{o}}_{qq} + r^{\mathrm{s,o}}_{qq} + r^{\mathrm{s,i}}_{qq} + d_{in} r^{\mathrm{i}}_{qq}\right) J_q \\
&\quad - \left[\left(d_{out} r^{\mathrm{o}}_{qq} + r^{\mathrm{s,o}}_{qq}\right) Q^{*\mathrm{o}}_m + \left(r^{\mathrm{s,i}}_{qq} + d_{in} r^{\mathrm{i}}_{qq}\right) Q^{*\mathrm{i}}_m\right] J_m
\end{aligned}$$

$$\begin{aligned}
\frac{\mu_{out}}{T_{out}} - \frac{\mu_{in}}{T_{in}} &= \left(\frac{\mu_{out}}{T_{out}} - \frac{\mu^{\mathrm{o}}_m}{T^{\mathrm{o}}}\right) + \left(\frac{\mu^{\mathrm{o}}_m}{T^{\mathrm{o}}} - \frac{\mu^{\mathrm{s}}_m}{T^{\mathrm{s}}}\right) \\
&\quad + \left(\frac{\mu^{\mathrm{s}}_m}{T^{\mathrm{s}}} - \frac{\mu^{\mathrm{i}}_m}{T^{\mathrm{i}}}\right) + \left(\frac{\mu^{\mathrm{i}}_m}{T^{\mathrm{i}}} - \frac{\mu_{in}}{T_{in}}\right) \\
&= \left[\left(d_{out} r^{\mathrm{o}}_{qq} + r^{\mathrm{s,o}}_{qq}\right) Q^{*\mathrm{o}}_m + \left(r^{\mathrm{s,i}}_{qq} + d_{in} r^{\mathrm{i}}_{qq}\right) Q^{*\mathrm{i}}_m\right] J_q \\
&\quad - \left(d_{out} r^{\mathrm{o}}_{\mu\mu} + r^{\mathrm{s,o}}_{\mu\mu} + r^{\mathrm{s,i}}_{\mu\mu} + d_{in} r^{\mathrm{i}}_{\mu\mu}\right) J_m
\end{aligned} \tag{8.35}$$

These equations make it possible to calculate T_{out} and μ_{out} given T_{in}, μ_{in}, J_q and J_m, or alternatively J_q and J_m given T_{in}, μ_{in}, T_{out} and μ_{out}. In general, four of these quantities make it possible to calculate the two others. Once the six quantities are known, it follows for the inverse temperature that

$$\begin{aligned}
\frac{1}{T(x)} &= \frac{1}{T_{in}} + (x + d_{in})\, r^{\mathrm{i}}_{qq} \left(J_q - Q^{*\mathrm{i}}_m J_m\right) \quad \text{for} \quad -d_{in} < x < 0 \\
\frac{1}{T^{\mathrm{s}}} &= \frac{1}{T_{in}} + \left(d_{in} r^{\mathrm{i}}_{qq} + r^{\mathrm{s,i}}_{qq}\right) \left(J_q - Q^{*\mathrm{i}}_m J_m\right) \\
\frac{1}{T(x)} &= \frac{1}{T_{out}} + (x - d_{out})\, r^{\mathrm{o}}_{qq} \left(J_q - Q^{*\mathrm{o}}_m J_m\right) \quad \text{for} \quad 0 < x < d_{out}
\end{aligned} \tag{8.36}$$

For μ_m/T we find similarly that

$$\begin{aligned}
\frac{\mu_m(x)}{T(x)} &= \frac{\mu_{in}}{T_{in}} + (x + d_{in})\left(r^{\mathrm{i}}_{qq} Q^{*\mathrm{i}}_m J_q - r^{\mathrm{i}}_{\mu\mu} J_m\right) \quad \text{for} \quad -d_{in} < x < 0 \\
\frac{\mu^{\mathrm{s}}_m}{T^{\mathrm{s}}} &= \frac{\mu_{in}}{T_{in}} + \left(d_{in} r^{\mathrm{i}}_{qq} + r^{\mathrm{s,i}}_{qq}\right) Q^{*\mathrm{i}}_m J_q - \left(d_{in} r^{\mathrm{i}}_{\mu\mu} + r^{\mathrm{s,i}}_{\mu\mu}\right) J_m \\
\frac{\mu_m(x)}{T(x)} &= \frac{\mu_{out}}{T_{out}} + (x - d_{out})\left(r^{\mathrm{o}}_{qq} Q^{*\mathrm{o}}_m J_q - r^{\mathrm{o}}_{\mu\mu} J_m\right) \quad \text{for} \quad 0 < x < d_{out}
\end{aligned} \tag{8.37}$$

Equations (8.36) and (8.37) give the temperature and the chemical potential profiles through the system.

The above calculation, taking some quantities constant, should be seen as an illustration. For temperature dependent coefficients Eq. (8.30) must be integrated numerically to obtain the temperature and the chemical potential profiles in the homogeneous phases.

The Soret (or Dufour) effect is not a big effect in gases or liquids. It can therefore often be neglected in descriptions of transport in homogeneous systems. When it comes to heterogeneous systems this picture changes dramatically. The coupling coefficients for interface transports, here represented by $r^{\mathrm{s,i}}_{qq} Q^{*\mathrm{i}}_m$ and $r^{\mathrm{s,o}}_{qq} Q^{*\mathrm{o}}_m$, are large, as follows from Eq. (8.29). These terms are the origin of the power that can be created in a thermal osmosis plant, see Chapter 18.

It has been verified that the temperature of a catalytic surface can be different from that of the adjacent homogeneous phases [125, 150, 151].

8.5 Scaling relations between surface and bulk resistivities

In order to compare surface and bulk main resistivities, we divide their ratio by the thickness of the surface, δ. A dimensionless scaling coefficient is obtained[‡]. For the left hand side of the surface, this gives:

$$k^{\mathrm{i}} = \frac{r^{\mathrm{s,i}}}{r^{\mathrm{i}}\delta} \tag{8.38}$$

Such a ratio can be defined for the surface main resistivities. The Onsager coefficient that describes the thermal resistivity for side i of the surface can, using such a scaling coefficient, be written as

$$r^{\mathrm{s,i}}_{qq} = k^{\mathrm{i}}_q \delta r^{\mathrm{i}}_{qq} = \frac{k^{\mathrm{i}}_q \delta}{\lambda^{\mathrm{i}} \left(T^{\mathrm{i}}\right)^2} \tag{8.39}$$

[‡]Hansen [152] does this for the conductivities rather than for the resistivities. It is better to do this for the resistivities, as the resistivities are in series.

where λ^{i} is the thermal conductivity and T^{i} is the temperature of the bulk material on side i. The mass transfer coefficient for side i, is similarly (for systems with constant activity):

$$r^{\mathrm{s,i}}_{\mu\mu} = k^{\mathrm{i}}_{\mu}\delta r^{\mathrm{i}}_{\mu\mu} = k^{\mathrm{i}}_{\mu}\delta\frac{D^{\mathrm{i}}c^{\mathrm{i}}}{RT^{\mathrm{i}}} \tag{8.40}$$

Similar expressions may be written down for the other side of the surface. The scaling coefficients measure how surface resistivities differ from bulk resistivities. *The surface is only interesting as a separate system if it has a substantial resistivity to transport*, that is, when k^{i} is substantially larger than unity. When k^{i} is of the order unity or smaller, one may ignore the surface resistivity. In the above formulae, it is the product $k^{\mathrm{i}}\delta$ rather than the scaling coefficient that has a physical significance. There is some freedom in the choice for the thickness of the surface δ but not in the product. For many heterogeneous systems, the transition from one homogeneous phase to the other is very abrupt. For the interface between them, a thickness of 1.5 times the diameter of the molecules is commonly used [93]. In Chapter 22 we will discuss how to define a thickness for a vapor-liquid interface appropriate for the interpretation of the results of molecular dynamics simulations [39].

Chapter 9

Transport of Heat and Charge

We present flux equations for transport of heat and charge, with the aim to be able to integrate across heterogeneous systems. We give the Onsager coefficients in terms of the measured coefficients and discuss some coefficient models. We show how thermal energy can be used to produce electric power.

This chapter concerns transports of heat and charge. Coupling occurs between such transports in many solid state electrochemical systems, e.g. batteries and fuel cells. The coupling is important because it is the origin of work in these systems. It is the only way in which one can produce work from low temperature heat reservoirs; in thermoelectric power generators. Thermoelectric effects have been known since the 19^{th} century. Seebeck found in 1821 that heating of one junction of a bimetalic couple and cooling another gave rise to an electromotive force in the circuit. Thirteen years later Peltier found that passage of an electric current through a bimetalic circuit caused adsorption of heat. The coupling between transport of heat and charge explains the function of the common thermocouple and thermoelectric heat pumps [153]. Such devices consist of two or more conductors or semiconductors.

We give the basic equations for such transports across two homogeneous conductors, joined together by a surface. More complicated examples are given in Chapters 13–21. The electric current density is constant through the system, and we have no mass flux.

The aim is to give equations that can be integrated through the heterogeneous system, to obtain the performance of the total system. The surface is always the frame of reference for the transport processes. Experimental or other conditions determine the entropy production of the surface and of the homogeneous phases.

9.1 The homogeneous phases

Consider an electric conductor. The temperature changes as a function of position and so does the electric potential. By convention, the electric current from left to right is positive. The entropy production for the homogeneous phase is obtained from Eq. (4.15), which here reduces to:

$$\sigma = J'_q \left(\frac{d}{dx} \frac{1}{T} \right) + j \left(-\frac{1}{T} \frac{d\phi}{dx} \right) \tag{9.1}$$

The resulting equations for the forces are

$$\begin{aligned} \frac{d}{dx} \frac{1}{T} &= r_{qq} J'_q + r_{q\phi} j \\ -\frac{1}{T} \frac{d\phi}{dx} &= r_{\phi q} J'_q + r_{\phi\phi} j \end{aligned} \tag{9.2}$$

These coefficients can be identified with coefficients that are obtained from measurements. Measurements define the stationary state thermal conductivity (Fourier's law):

$$\lambda \equiv -\left(\frac{J'_q}{dT/dx} \right)_{j=0} = \frac{1}{T^2 r_{qq}} \tag{9.3}$$

and the Ohm's law resistivity

$$r \equiv -\left(\frac{d\phi/dx}{j} \right)_{dT=0} = T \left(r_{\phi\phi} - \frac{r_{q\phi} r_{\phi q}}{r_{qq}} \right) \tag{9.4}$$

The Peltier coefficient, π, is the heat transferred *reversibly* with the electric current (cf. remark under Eq. 7.25)

$$\pi \equiv \left(\frac{J'_q}{j/F} \right)_{dT=0} = -F \frac{r_{q\phi}}{r_{qq}} \tag{9.5}$$

Neither J'_q nor j depend on the frame of reference, so π is absolute. Because the Peltier coefficient concerns reversible heat transport, it has been associated with an entropy, the *transported entropy of the charge carrier*:

$$\pi \equiv T S^* \tag{9.6}$$

Here S^* is the transported entropy of the charge carrier. We can express the resistivities in terms of the transport coefficients found from experiment as

$$r_{qq} = \frac{1}{T^2 \lambda}, \quad r_{q\phi} = r_{\phi q} = -\frac{\pi}{F T^2 \lambda}, \quad r_{\phi\phi} = \frac{1}{T} \left(r + \frac{\pi^2}{F^2 T \lambda} \right) \tag{9.7}$$

By introducing these expressions into Eq. (9.2), the gradients in T and ϕ become

$$\begin{aligned} \frac{dT}{dx} &= -\frac{J'_q}{\lambda} + \frac{\pi}{\lambda}\frac{j}{F} \\ \frac{d\phi}{dx} &= -\frac{S^*}{F}\frac{dT}{dx} - rj \end{aligned} \tag{9.8}$$

The Onsager relation $r_{q\phi} = r_{\phi q}$ was used. By convention, the transported entropy is positive when entropy is transported in the direction of the positive electric current. Transported entropies are kinetic, not thermodynamic properties. Electronic conductors have transported entropies between -1 and -20 J/K mol [154]. Some transition metals like Mo, Cr and W have *positive* transported entropies, even if the charge carrier is an electron. The maximum value in molybdenum is $S^*_{\mathrm{e}^-,\mathrm{Mo}} = 17$ J/K mol at 900 K [154]. For the same temperature, $S^*_{\mathrm{e}^-,\mathrm{Pb}} = -5$ J/K mol. The transported entropy of electrons in lead is a commonly used reference value. The variation in the transported entropy was to some extent explained by the number of electrons available for transport above the Fermi energy level (ε_F) at a given temperature. Mott and Wilson, see Cahn [155], proposed that

$$S^* = \frac{\pi}{3}\frac{k_B^2 T}{e\kappa}\left[\frac{d\kappa}{d\varepsilon_\mathrm{F}}\right]_{\varepsilon_\mathrm{F}} \tag{9.9}$$

Here κ is the specific electric conductivity, e is the absolute charge of the electron, k_B is Boltzmann's constant and π is the mathematical constant. The derivative is taken at the value of the Fermi energy level, ε_F.

The transported entropy is a function of the temperature. This is described by the *Thomson* coefficient:

$$\tau \equiv T\frac{d}{dT}\left(\frac{\pi}{T}\right) = T\frac{dS^*}{dT} \tag{9.10}$$

If the transported entropy is zero at 0 K, we can find the transported entropy at any temperature by integrating τ from 0 K to T.

$$S^* = \int_0^T \frac{\tau}{T} dT = \frac{\pi(T)}{T} \tag{9.11}$$

The result gives an absolute value for $\pi(T)/T$ for a material. The *Thomson heat* [7] is the heat added to a conductor to keep its temperature constant per faraday of positive charges passing the conductor from left to right.

Exercise 9.1.1. *Consider an electric current of $10A/m^2$ through a piece of lead. Entropy will be transported, and if the system is thermally isolated,*

a temperature gradient will build up. Calculate the maximum temperature gradient that arise in the metal. Use a thermal conductivity of 5 W/Km and an average temperature of 300 K. The transported entropy is -5 *J/K mol.*

- **Solution:** Eq. (9.8) gives the heat flux in terms of the temperature gradient and the electric current

$$J'_q = -\lambda_{\rm Pb}\frac{dT}{dx} + \pi_{\rm Pb}\frac{j}{F}$$

With a constant electric current, the heat flux through the system will vary (the variation is given by the energy balance for the isolated metal). The smallest value of the heat flux is zero. In that case all thermal energy is converted to work (electric energy). It follows then that $dT/dx = \pi_{\rm Pb} j/F\lambda_{\rm Pb}$. By substituting the values of all coefficients we obtain $dT/dx = -3 \times 10^{-2}$ K/m.

9.2 The surface

Consider next the surface between the two phases, i and o. The excess entropy production of Eq. (5.15) reduces to

$$\sigma^{\rm s} = J'^{\rm i}_q \Delta_{\rm i,s}\frac{1}{T} + J'^{\rm o}_q \Delta_{\rm s,o}\frac{1}{T} + j\left(-\frac{\Delta_{\rm i,o}\phi}{T^{\rm s}}\right) \tag{9.12}$$

There is one heat flux into the surface, $J'^{\rm i}_q$, and one heat flux out of the surface, $J'^{\rm o}_q$, but $j = j^{\rm i} = j^{\rm o}$. We use the assumption that there is no coupling between fluxes on different sides of the surface, cf. Sec. 8.4. The forces become:

$$\begin{aligned}
\Delta_{\rm i,s}\frac{1}{T} &= r^{\rm s,i}_{qq} J'^{\rm i}_q + r^{\rm s}_{{\rm i}\phi} j \\
\Delta_{\rm s,o}\frac{1}{T} &= r^{\rm s,o}_{qq} J'^{\rm o}_q + r^{\rm s}_{{\rm o}\phi} j \\
-\frac{1}{T^{\rm s}}\Delta_{\rm i,o}\phi &= r^{\rm s}_{\phi{\rm i}} J'^{\rm i}_q + r^{\rm s}_{\phi{\rm o}} J'^{\rm o}_q + r^{\rm s}_{\phi\phi} j
\end{aligned} \tag{9.13}$$

These expressions are analogous to Eqs. (8.14) and (8.15) with a constant mass flux. The Onsager relations are: $r^{\rm s}_{{\rm i}\phi} = r^{\rm s}_{\phi{\rm i}}$ and $r^{\rm s}_{{\rm o}\phi} = r^{\rm s}_{\phi{\rm o}}$. Notation is further illustrated in Fig. 9.1. Each resistivity is a function of the temperature of the surface. The definitions of the Fourier type thermal conductivities for the two sides are:

$$\lambda^{\rm s,i} \equiv -\left(\frac{J'^{\rm i}_q}{\Delta_{\rm i,s}T}\right)_{j=0} = \frac{1}{T^{\rm i}T^{\rm s}r^{\rm s,i}_{qq}} \quad \text{and} \quad \lambda^{\rm s,o} \equiv -\left(\frac{J'^{\rm o}_q}{\Delta_{\rm s,o}T}\right)_{j=0} = \frac{1}{T^{\rm s}T^{\rm o}r^{\rm s,o}_{qq}} \tag{9.14}$$

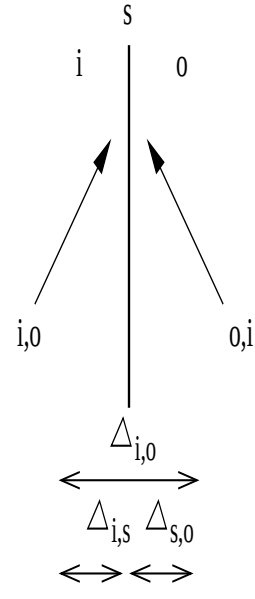

Figure 9.1 Standard notation used for transport across surfaces.

The Peltier coefficients are defined in the same manner as for the homogeneous phases:

$$\pi^{\mathrm{i}}(T^{\mathrm{s}}) \equiv \left(\frac{J_q'^{\mathrm{i}}}{j/F}\right)_{\Delta_{\mathrm{i,s}}T=0} = -F\frac{r^{\mathrm{s}}_{\mathrm{i}\phi}(T^{\mathrm{s}})}{r^{\mathrm{s,i}}_{qq}(T^{\mathrm{s}})}$$

and

$$\pi^{\mathrm{o}}(T^{\mathrm{s}}) \equiv \left(\frac{J_q'^{\mathrm{o}}}{j/F}\right)_{\Delta_{\mathrm{s,o}}T=0} = -F\frac{r^{\mathrm{s}}_{\mathrm{o}\phi}(T^{\mathrm{s}})}{r^{\mathrm{s,o}}_{qq}(T^{\mathrm{s}})} \tag{9.15}$$

These coefficients are ratios of fluxes in the homogeneous phases and are therefore equal to the corresponding values in these homogeneous phases at the temperature of the surface. The ohmic resistivity of the surface is:

$$r^{\mathrm{s}} \equiv -\left(\frac{\Delta_{\mathrm{i,o}}\phi}{j}\right)_{T^{\mathrm{i}}=T^{\mathrm{s}}=T^{\mathrm{o}}} = T^{\mathrm{s}}\left(r^{\mathrm{s}}_{\phi\phi} - \frac{r^{\mathrm{s}}_{\phi\mathrm{i}}r^{\mathrm{s}}_{\mathrm{i}\phi}}{r^{\mathrm{s,i}}_{qq}} - \frac{r^{\mathrm{s}}_{\phi\mathrm{o}}r^{\mathrm{s}}_{\mathrm{o}\phi}}{r^{\mathrm{s,o}}_{qq}}\right) \tag{9.16}$$

The resistivities can be expressed in the transport coefficients just defined as:

$$r_{qq}^{\mathrm{s,i}} = \frac{1}{T^{\mathrm{i}}T^{\mathrm{s}}\lambda^{\mathrm{s,i}}} \quad \text{and} \quad r_{qq}^{\mathrm{s,o}} = \frac{1}{T^{\mathrm{s}}T^{\mathrm{o}}\lambda^{\mathrm{s,o}}}$$

$$r_{\mathrm{i}\phi}^{\mathrm{s}} = r_{\phi\mathrm{i}}^{\mathrm{s}} = -\frac{\pi^{\mathrm{i}}}{FT^{\mathrm{i}}T^{\mathrm{s}}\lambda^{\mathrm{s,i}}} \quad \text{and} \quad r_{\mathrm{o}\phi}^{\mathrm{s}} = r_{\phi\mathrm{o}}^{\mathrm{s}} = -\frac{\pi^{\mathrm{o}}}{T^{\mathrm{s}}T^{\mathrm{o}}\lambda^{\mathrm{s,o}}}$$

$$r_{\phi\phi}^{\mathrm{s}} = \frac{1}{T^{\mathrm{s}}}\left[r^{\mathrm{s}} + \left(\frac{\pi^{\mathrm{i}}}{F}\right)^2 \frac{1}{T^{\mathrm{i}}\lambda^{\mathrm{s,i}}} + \left(\frac{\pi^{\mathrm{o}}}{F}\right)^2 \frac{1}{T^{\mathrm{o}}\lambda^{\mathrm{s,o}}}\right] \tag{9.17}$$

The jumps in the intensive variables into and across the surface are:

$$\begin{aligned}
\Delta_{\mathrm{i,s}}T &= T^{\mathrm{s}} - T^{\mathrm{i}} = -\frac{1}{\lambda^{\mathrm{s,i}}}\left(J_q'^{\mathrm{i}} - \pi^{\mathrm{i}}\frac{j}{F}\right) \\
\Delta_{\mathrm{s,o}}T &= T^{\mathrm{o}} - T^{\mathrm{s}} = -\frac{1}{\lambda^{\mathrm{s,o}}}\left(J_q'^{\mathrm{o}} - \pi^{\mathrm{o}}\frac{j}{F}\right) \\
\Delta_{\mathrm{i,o}}\phi &= \phi^{\mathrm{o}} - \phi^{\mathrm{i}} = -\frac{1}{F}S_{\mathrm{i}}^{*}\Delta_{\mathrm{i,s}}T - \frac{1}{F}S_{\mathrm{o}}^{*}\Delta_{\mathrm{s,o}}T - r^{\mathrm{s}}j
\end{aligned} \tag{9.18}$$

When the surface temperature differs from the temperatures in the adjacent phases, finite contributions to the cell potential result.

9.3 Thermoelectric coolers

The *Peltier heat* is defined for junctions [27]. The Peltier heat of a surface (the junction) is defined by the heat needed to keep the surface at constant temperature when one faraday of positive charges is passing it from left to right:

$$\pi^{\mathrm{s}}\left(T^{\mathrm{s}}\right) \equiv -\left(\frac{J_q'^{\mathrm{i}} - J_q'^{\mathrm{o}}}{j/F}\right)_{T^{\mathrm{i}}=T^{\mathrm{s}}=T^{\mathrm{o}}} = \pi^{\mathrm{o}}\left(T^{\mathrm{s}}\right) - \pi^{\mathrm{i}}\left(T^{\mathrm{s}}\right) \tag{9.19}$$

The Peltier heat of a surface is the difference between the Peltier coefficients in the two conductors, $\pi^{\mathrm{o}} - \pi^{\mathrm{i}}$. The Peltier effect is used to make coolers, like for instance wine coolers. In a thermoelectric cooler, an electric current is used to transport heat from a low temperature reservoir to a high temperature reservoir.

Let us calculate the electricity needed to cool a glass of wine (25 cm^3) at 300 K by 5 K, using a Mo–Pb element with the values for S^* given in Sec. 9.1. The heat capacity of wine (water) is 72 J/K mol. The Peltier heat of the device is $\pi^{\mathrm{o}} - \pi^{\mathrm{i}} = [17 - (-5)]\ 300\ \mathrm{J/mol} = 6.6\ \mathrm{kJ/mol}$. There

are $25 \cdot 10^{-3} \cdot 55.5 = 0.14$ mol water in the glass. The number of joules needed for cooling is taken from the junction of the element $0.14 \cdot 72 \cdot 5 = 6.6$ kJ/mol $\cdot\, Q/F$, where Q is the number of coulombs and F is Faraday's constant. The relation demands 760 C, or 0.84 A in 900 s.

The reciprocal effect of the Peltier effect, the Seebeck effect, can be used to generate electric power from geothermal and other heat sources. In that case a temperature difference exists (see below). It is easier to measure an electric potential with high precision than a heat effect at zero temperature rise. The Seebeck coefficient can therefore be more accurately determined, and can be used to determine the Peltier coefficient via Onsager's reciprocal relations, see for instance Flem and coworkers [78, 80].

9.4 Thermoelectric generators

A thermoelectric generator takes advantage of the heat flux between a high and a low temperature reservoir to generate electric power. The generator consists of a p- and an n-semiconductor in series. Their junction is kept at the low temperature T_L, while the other ends (the terminals) have temperature T_H. The system is illustrated in Fig. 9.2. An electric current is produced, and a potential can be measured between the terminals. The distance between the thermal reservoirs through both the p- and an n-semiconductor, l, is small, usually only a few mm. The geometry of the system is such that $x = 0$ at the terminal and $x = l$ at the cold end in the p-semiconductor (phase i). The n-semiconductor (phase o) bends back and goes from $x = l$ at the cold end to $x = 0$ at the terminal, parallel to the p-semiconductor.

The electric potential of the generator is obtained by integrating from terminal to terminal:

$$\Delta\phi = \int_0^l \left(-\frac{S_\mathrm{i}^*}{F}\frac{dT}{dx} - r^\mathrm{i} j \right) dx + \Delta_{\mathrm{i,o}}\phi + \int_l^0 \left(-\frac{S_\mathrm{o}^*}{F}\frac{dT}{dx} - r^\mathrm{o} j \right) dx \quad (9.20)$$

Combining the integrals, taking $T^\mathrm{i} = T^\mathrm{s} = T^\mathrm{o}$, we obtain:

$$\Delta\phi = \int_0^l \left[-\eta_S \frac{dT}{dx} - \left(r^\mathrm{i} + r^\mathrm{o} \right) j \right] dx - r^\mathrm{s} j \quad (9.21)$$

where η_S is the Seebeck coefficient of *the device*:

$$\eta_S = \left. \frac{\Delta\phi}{(T_H - T_L)} \right|_{j=0} = \frac{1}{F}(S_\mathrm{i}^* - S_\mathrm{o}^*) \quad (9.22)$$

where we took the transported entropies independent of the temperature to obtain the last identity. The electric potential difference is generated between the terminals, because there is a difference in the transported entropy

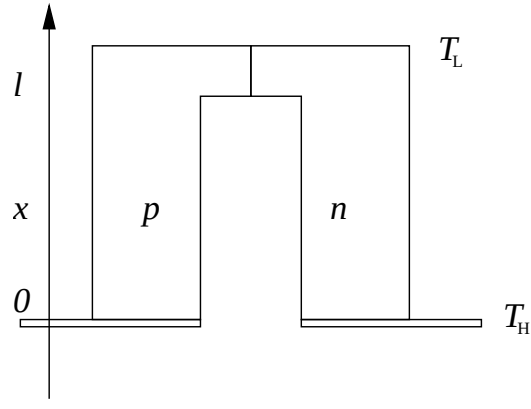

Figure 9.2 The thermo-electric generator composed of a p- and n-semiconductor, between thermal reservoirs with temperatures T_H and T_L.

of the charge carriers in the conductors. The maximum electric potential is obtained when $j = 0$. The electric potential for $j = 0$ (the reversible potential) is given by the *net* heat added to the system from the surroundings divided by F (i.e. the first law applies for the total system). For a finite j the potential becomes, using temperature independent electric resistivities,

$$\Delta\phi = \eta_S(T_H - T_L) - \left(lr^{\mathrm{i}} + r^{\mathrm{s}} + lr^{\mathrm{o}}\right) j \equiv \eta_S(T_H - T_L) - r_{\mathrm{total}} j \quad (9.23)$$

The thermoelectric power

$$P \equiv j\Delta\phi = \eta_S(T_H - T_L)j - r_{\mathrm{total}} j^2 \quad (9.24)$$

has a maximum $P_{\max} = \eta_S^2(T_H - T_L)^2/4r_{\mathrm{total}}$ as a function of the current density. The current density delivered is determined by the resistance of the external circuit. Harman and Honig [153] gave the general expressions for temperature dependent transport coefficients.

Exercise 9.4.1. *Calculate the Seebeck coefficient at 900 K for Mo Pb Mo and find the maximum potential generated by a geothermal source of 90 $^o C$ lying next to a glacier.*

- **Solution:** By introducing the transported entropies given below Eq. (9.8), we find $\eta_S = 21\ \mu\mathrm{V/K}$. With $\Delta T = 90K, E = 180\mu\mathrm{V}$ for a single cell. By stacking many cells, one can generate a potential difference that supplies electric light to a nearby greenhouse.

Exercise 9.4.2. *Find the entropy production in a thermoelectric generator.*

- **Solution:** The entropy production for one semiconductor (arm), say the i-phase is:

$$\sigma = -\left(\lambda^{\mathrm{i}}\frac{dT}{dx} + S_{\mathrm{i}}^{*}T\frac{j}{F}\right)\frac{dT}{T^2dx} - \left(-\frac{S_{\mathrm{i}}^{*}}{F}\frac{dT}{dx} - r^{\mathrm{i}}j\right)\frac{1}{T}j$$

$$= \frac{\lambda^{\mathrm{i}}}{T^2}\left(\frac{dT}{dx}\right)^2 + \frac{1}{T}r^{\mathrm{i}}j^2$$

The reversible contributions to the entropy production containing S_{i}^{*} cancel. The entropy production for the whole device is

$$\frac{dS_{irr}}{dt} = \Omega\int_0^l \left(\frac{\lambda}{T^2}(\frac{dT}{dx})^2 + \frac{1}{T}rj^2\right)dx$$

where λ is the sum of the thermal conductivities of the homogeneous phases (the surface is isothermal) and Ω is the cross-sectional area. The terms in the entropy production are proportional to the square of the gradient in temperature and the square of the current density. The entropy production times the temperature of the surroundings gives the lost work per unit of time. The power is, on the other hand, a linear function of the temperature gradient. We therefore expect a maximum energy efficiency for a given temperature gradient.

We have seen that the examples in this chapter give relatively small effects. Still, the effect may be useful for dedicated purposes. The electric potential created by a temperature difference is order of magnitude 1 mV, and relatively much electricity is needed to provide cooling. The efficiency of these devices can be considerably improved if S^{*} is raised. This gives a motivation to study thermogalvanic cells, see Chapters 13 and 14.

We have found that the main reason for energy conversion is the difference in the transported entropies in the two phases. This is exploited in devices like coolers and generators. The larger the difference is, the larger is the efficiency of the device in its conversion of energy from one form to another.

9.5 Solution for the heterogeneous system

In order to solve the heterogeneous system, it is convenient to use the fluxes that are constant through the surface. These are the electric current j, and the energy current $J_u \equiv J_q + j\phi = J_q' + j\phi$. The entropy production in the homogeneous phases in terms of these fluxes becomes (cf. Eq. (4.17)),

$$\sigma = J_u\left(\frac{d}{dx}\frac{1}{T}\right) + j\left(-\frac{d}{dx}\frac{\phi}{T}\right) \tag{9.25}$$

The resulting equations for the forces are

$$\begin{aligned} \frac{d}{dx}\frac{1}{T} &= r_{ee}J_u + r_{e\phi}j \\ -\frac{d}{dx}\frac{\phi}{T} &= r_{\phi e}J_u + r^e_{\phi\phi}j \end{aligned} \tag{9.26}$$

By comparing with Eq. (9.2), we can identify

$$r_{qq} = r_{ee}, \quad r_{q\phi} = r_{\phi q} = r_{e\phi} + \phi r_{ee}, \quad r_{\phi\phi} = r^e_{\phi\phi} + 2\phi r_{e\phi} + \phi^2 r_{ee} \tag{9.27}$$

Inverting these relations, we have

$$r_{ee} = r_{qq}, \quad r_{e\phi} = r_{\phi e} = r_{q\phi} - \phi r_{qq}, \quad r^e_{\phi\phi} = r_{\phi\phi} - 2\phi r_{q\phi} + \phi^2 r_{qq} \tag{9.28}$$

where we used that both matrices, used in Eqs. (9.2) and (9.26), satisfy the Onsager symmetry relations.

The excess entropy production of the surface, Eq. (5.17), becomes

$$\sigma^{\mathrm{s}} = J_u \left(\Delta_{\mathrm{i,o}}\frac{1}{T}\right) + j\left(-\Delta_{\mathrm{i,o}}\frac{\phi}{T}\right) \tag{9.29}$$

where we used that $J_u^{\mathrm{i}} = J_u^{\mathrm{o}} = J_u$. The continuity of both fluxes through the surface results in the elimination of a force-flux pair of the surface. As a consequence, the excess entropy production no longer depends on the temperature differences with the surface. The forces become:

$$\begin{aligned} \Delta_{\mathrm{i,o}}\frac{1}{T} &= r^{\mathrm{s}}_{ee}J_u + r^{\mathrm{s}}_{e\phi}j \\ -\Delta_{\mathrm{i,o}}\frac{\phi}{T} &= r^{\mathrm{s}}_{\phi e}J_u + r^{\mathrm{s},e}_{\phi\phi}j \end{aligned} \tag{9.30}$$

By calculating the same jumps, using the expressions for the forces (9.13), one can identify

$$\begin{aligned} r^{\mathrm{s}}_{ee} &= r^{\mathrm{s,i}}_{qq} + r^{\mathrm{s,o}}_{qq}, \quad r^{\mathrm{s}}_{e\phi} = r^{\mathrm{s}}_{\phi e} = r^{\mathrm{s}}_{\mathrm{i}\phi} + r^{\mathrm{s}}_{\mathrm{o}\phi} - \phi^{\mathrm{i}} r^{\mathrm{s,i}}_{qq} - \phi^{\mathrm{o}} r^{\mathrm{s,o}}_{qq} \\ r^{\mathrm{s},e}_{\phi\phi} &= r^{\mathrm{s}}_{\phi\phi} - 2\phi^{\mathrm{i}} r^{\mathrm{s}}_{\mathrm{i}\phi} - 2\phi^{\mathrm{o}} r^{\mathrm{s}}_{\mathrm{o}\phi} + \left(\phi^{\mathrm{i}}\right)^2 r^{\mathrm{s,i}}_{qq} + \left(\phi^{\mathrm{o}}\right)^2 r^{\mathrm{s,o}}_{qq} \end{aligned} \tag{9.31}$$

These equations give the three coefficients used in Eq. (9.30) in terms of the five coefficients used in Eq. (9.13). It is therefore not possible to invert this identification.

We are now set to solve the temperature and electric potential profiles across the heterogeneous system. Consider therefore two homogeneous phases with an interface between them. The zero along the x-axis is chosen to coincide with the position of the dividing surface. The left homogeneous phase is between $-d_{in}$ and 0 and the right homogeneous phase is between 0 and d_{out}. The temperatures at the ends are $T_{in} = T(-d_{in})$ and $T_{out} = T(d_{out})$, and the electric potentials are $\phi_{in} = \phi(-d_{in})$ and $\phi_{out} = \phi(d_{out})$. In order to simplify the calculation, we assume that the resistivities in both phases are independent of the position. It then follows from Eq. (9.26) that the gradients of $1/T$ and ϕ/T in the two homogeneous phases are constant. By integrating these equations over the homogeneous phases, using Eq. (9.30) for the surface, we find:

$$\begin{aligned}
\frac{1}{T_{out}} - \frac{1}{T_{in}} &= \left(\frac{1}{T_{out}} - \frac{1}{T^{\mathrm{o}}}\right) + \left(\frac{1}{T^{\mathrm{o}}} - \frac{1}{T^{\mathrm{i}}}\right) + \left(\frac{1}{T^{\mathrm{i}}} - \frac{1}{T_{in}}\right) \\
&= \left(d_{out} r^{\mathrm{o}}_{ee} + r^{\mathrm{s}}_{ee} + d_{in} r^{\mathrm{i}}_{ee}\right) J_u + \left(d_{out} r^{\mathrm{o}}_{e\phi} + r^{\mathrm{s}}_{e\phi} + d_{in} r^{\mathrm{i}}_{e\phi}\right) j \\
\frac{\phi_{out}}{T_{out}} - \frac{\phi_{in}}{T_{in}} &= \left(\frac{\phi_{out}}{T_{out}} - \frac{\phi^{\mathrm{o}}}{T^{\mathrm{o}}}\right) + \left(\frac{\phi^{\mathrm{o}}}{T^{\mathrm{o}}} - \frac{\phi^{\mathrm{i}}}{T^{\mathrm{i}}}\right) + \left(\frac{\phi^{\mathrm{i}}}{T^{\mathrm{i}}} - \frac{\phi_{in}}{T_{in}}\right) \\
&= -\left(d_{out} r^{\mathrm{o}}_{e\phi} + r^{\mathrm{s}}_{e\phi} + d_{in} r^{\mathrm{i}}_{e\phi}\right) J_u - \left(d_{out} r^{\mathrm{o}}_{\phi\phi} + r^{\mathrm{s}}_{\phi\phi} + d_{in} r^{\mathrm{i}}_{\phi\phi}\right) j
\end{aligned} \tag{9.32}$$

These equations make it possible to calculate T_{out} and ϕ_{out} given T_{in}, ϕ_{in}, J_u and j, or alternatively J_u and j given T_{in}, ϕ_{in}, T_{out} and ϕ_{out}. In general, four of these quantities make it possible to calculate the two others. Once the six quantities are known, it follows for the inverse temperature profile that

$$\begin{aligned}
\frac{1}{T(x)} &= \frac{1}{T_{in}} + (x + d_{in})\left(r^{\mathrm{i}}_{ee} J_u + r^{\mathrm{i}}_{e\phi} j\right) \quad \text{for} \quad -d_{in} < x < 0 \\
\frac{1}{T^{\mathrm{o}}} &= \frac{1}{T_{in}} + d_{in}\left(r^{\mathrm{i}}_{ee} J_u + r^{\mathrm{i}}_{e\phi} j\right) \\
\frac{1}{T^{\mathrm{i}}} &= \frac{1}{T^{\mathrm{o}}} + r^{\mathrm{s}}_{ee} J_u + r^{\mathrm{s}}_{e\phi} j \\
\frac{1}{T(x)} &= \frac{1}{T^{\mathrm{i}}} + x\ \left(r^{\mathrm{o}}_{ee} J_u + r^{\mathrm{o}}_{e\phi} j\right) \\
&= \frac{1}{T_{out}} + (x - d_{out})\left(r^{\mathrm{o}}_{ee} J_u + r^{\mathrm{o}}_{e\phi} j\right) \quad \text{for} \quad 0 < x < d_{out}
\end{aligned} \tag{9.33}$$

For $\phi(x)/T(x)$, we similarly find

$$\begin{aligned}
\frac{\phi(x)}{T(x)} &= \frac{\phi_{in}}{T_{in}} - (x + d_{in})\left(r^{\mathrm{i}}_{\phi e} J_u + r^{\mathrm{i}}_{\phi\phi} j\right) \quad \text{for} \quad -d_{in} < x < 0 \\
\frac{\phi^{\mathrm{o}}}{T^{\mathrm{o}}} &= \frac{\phi_{in}}{T_{in}} - d_{in}\left(r^{\mathrm{i}}_{\phi e} J_u + r^{\mathrm{i}}_{\phi\phi} j\right) \\
\frac{\phi^{\mathrm{i}}}{T^{\mathrm{i}}} &= \frac{\phi^{\mathrm{s}}}{T^{\mathrm{s}}} - r^{\mathrm{s}}_{\phi e} J_u - r^{\mathrm{s}}_{\phi\phi} j \\
\frac{\phi(x)}{T(x)} &= \frac{\phi^{\mathrm{i}}}{T^{\mathrm{i}}} - x\left(r^{\mathrm{o}}_{\phi e} J_u + r^{\mathrm{o}}_{\phi\phi} j\right) \\
&= \frac{\phi_{out}}{T_{out}} - (x - d_{out})\left(r^{\mathrm{o}}_{\phi e} J_u + r^{\mathrm{o}}_{\phi\phi} j\right) \quad \text{for} \quad 0 < x < d_{out} \qquad (9.34)
\end{aligned}$$

Equations (9.33) and (9.34) give the temperature and electric potential profiles through the system. Given these profiles one can calculate the heat flux $J'_q(x) \equiv J_u - j\phi(x)$ everywhere in the system. Equation (9.18) makes it then possible to calculate the temperature of the surface. When r^{i}_{ee}, $r^{\mathrm{i}}_{e\phi} = r^{\mathrm{i}}_{\phi e}$, $r^{\mathrm{i}}_{\phi\phi}$, r^{o}_{ee}, $r^{\mathrm{o}}_{e\phi} = r^{\mathrm{o}}_{\phi e}$, $r^{\mathrm{o}}_{\phi\phi}$ depend on the temperature and/or the electric potential, numerical integration is necessary to obtain the temperature and electric potential profiles in the homogeneous phases.

By comparing Secs. 9.5 and 8.4, we see that J_q and J_u play comparable roles in the solution for the heterogeneous system. The two constant fluxes are practical for the integration procedure. After integration, we need to reintroduce J'_q to be able to describe experiments or device performances. In order to find the terminal potential of a thermoelectric generator under operation, and internal gradients of $T(x)$ and $\phi(x)$, we replace J_u in the equations above by $J'_q + j\phi$.

Chapter 10

Transport of Mass and Charge

We give flux equations for transport of mass and charge in an electrochemical cell. We give the Onsager coefficients in terms of measured coefficients, and present expressions for electrode potential jumps. We show how power production is related to the coupling coefficients.

This chapter concerns mass and charge transports. Such transport occurs in electrochemical systems, e.g. electrolysis cells, batteries and fuel cells, but also in biological systems. The coupling between mass and charge transport is frequently large, meaning that simple transport laws are inadequate. In order to bring out the meaning of coupling, we consider again only coupling of two fluxes with two forces. The aim is to give equations that can be integrated through the heterogeneous system, to obtain the performance of the total system. We lay here a basis for the description of such transports, building on Guggenheim, Førland *et al.* and Katchalsky and Curran [23, 27, 63]. The concentration overpotential, but not the activation overpotential, is described. More complicated examples are given in Chapters 13–21.

The cell used to illustrate the principles is the isothermal concentration cell,

$$\mathrm{Ag\,(s)\,|AgNO_3\,(aq)|\,Ag\,(s)} \tag{10.1}$$

The electrodes are made of pure solid silver, which is a good electric conductor. The electric potential in both electrodes can therefore be taken constant. On the left hand surface, we have oxidation of silver:

$$\mathrm{Ag} \rightarrow \mathrm{Ag^+} + e^- \tag{10.2}$$

The electrolyte is $\mathrm{AgNO_3}$ in water, and there is a varying concentration of the salt across the cell. Silver ions go into solution from the anode surface and are deposited on the cathode surface as silver after the reverse reaction,

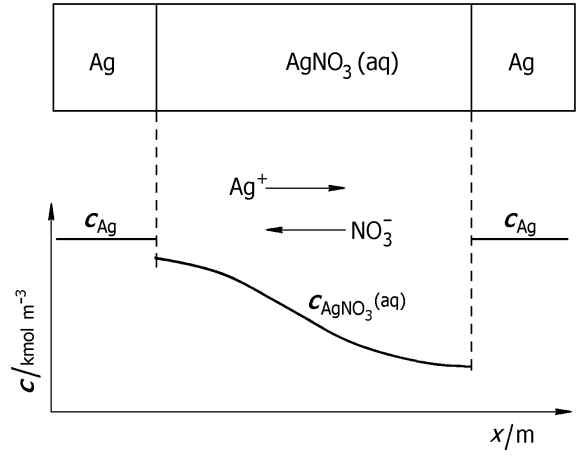

Figure 10.1 An isothermal electrochemical cell with a concentration gradient.

$Ag^+ + e^- \rightarrow Ag$. Electric current is passing the cell from left to right. In the stationary state, both surfaces have the same velocity. All fluxes are calculated with the surfaces as frame of reference. The velocity of the silver both in the anode and the cathode relative to these surfaces is j/Fc_{Ag}. We continue to deal with one-dimensional transports through a heterogeneous system, in the direction normal to a flat surface, in the same manner as described in Chapters 8 and 9. The fluxes at the surface not only have a bearing on the form we choose for the entropy production at the surface, but also on the form chosen in the homogeneous phases.

In order to demonstrate the importance of coupling we consider two examples of coupled mass and charge transport, a salt power plant and electric power from volume flow.

10.1 The electrolyte

Consider first the aqueous solution of $AgNO_3$, see Fig. 10.1. The solution is electroneutral, so the concentration of salt is equal to that of the cation and of the anion:

$$c_{AgNO_3} = c_{Ag^+} = c_{NO_3^-} \tag{10.3}$$

The mass balance for the salt is:

$$\frac{\partial}{\partial t} c_{AgNO_3}(x,t) = -\frac{\partial}{\partial x} J_{AgNO_3}(x,t) \tag{10.4}$$

so the two ions diffuse together.

The entropy production, cf. Eq. (4.15) is:

$$\sigma = J_{\mathrm{AgNO_3}} \left(-\frac{1}{T} \frac{\partial \mu_{\mathrm{AgNO_3}}}{\partial x} \right) + j \left(-\frac{1}{T} \frac{\partial \phi}{\partial x} \right) \tag{10.5}$$

The temperature is constant, so we drop subscript T for $\mu_{\mathrm{AgNO_3}}$. Chemical potentials for strong electrolytes were defined in Appendix 3.A.3. As will be explained in Sec. 10.3, the electric potential ϕ is equal to $\psi + \mu_{\mathrm{Ag^+}}/F$, where ψ is the electric potential referred to vacuum (the Maxwell potential). We shall use the ϕ-potential, because of its closer relation to measurable quantities. The force-flux relations are:

$$\begin{aligned} -\frac{1}{T} \frac{\partial}{\partial x} \mu_{\mathrm{AgNO_3}} &= r_{\mu\mu} J_{\mathrm{AgNO_3}} + r_{\mu\phi} j \\ -\frac{1}{T} \frac{\partial \phi}{\partial x} &= r_{\phi\mu} J_{\mathrm{AgNO_3}} + r_{\phi\phi} j \end{aligned} \tag{10.6}$$

In the surface frame of reference, water is at rest. We define the experimental coefficients first. The diffusion coefficient, $D_{\mathrm{AgNO_3}}$, in Fick's law is defined when $j = 0$:

$$D_{\mathrm{AgNO_3}} \equiv -\left(\frac{J_{\mathrm{AgNO_3}}}{\partial c_{\mathrm{AgNO_3}}/\partial x} \right)_{j=0} = \frac{1}{T r_{\mu\mu}} \frac{\partial \mu_{\mathrm{AgNO_3}}}{\partial c_{\mathrm{AgNO_3}}} \tag{10.7}$$

The ohmic resistivity of the homogeneous solution is

$$r^{\mathrm{e}} = -\left(\frac{\partial \phi/\partial x}{j} \right)_{d\mu_{\mathrm{AgNO_3}}=0} = T \left(r_{\phi\phi} - \frac{r_{\phi\mu} r_{\mu\phi}}{r_{\mu\mu}} \right) \tag{10.8}$$

and the *transference coefficient* of $AgNO_3$ is the flux of salt divided by the electric current density over F:

$$t_{\mathrm{AgNO_3}} = \left(\frac{J_{\mathrm{AgNO_3}}}{j/F} \right)_{d\mu_{\mathrm{AgNO_3}}=0} = -F \frac{r_{\mu\phi}}{r_{\mu\mu}} \tag{10.9}$$

With these definitions, we can identify the resistivities in the force-flux matrix in terms of the measured transport coefficients by:

$$\begin{gathered} r_{\mu\mu} = \frac{1}{T D_{\mathrm{AgNO_3}}} \frac{\partial \mu_{\mathrm{AgNO_3}}}{\partial c_{\mathrm{AgNO_3}}}, \quad r_{\mu\phi} = r_{\phi\mu} = -\frac{t_{\mathrm{AgNO_3}}}{F T D_{\mathrm{AgNO_3}}} \frac{\partial \mu_{\mathrm{AgNO_3}}}{\partial c_{\mathrm{AgNO_3}}} \\ r_{\phi\phi} = \frac{r^{\mathrm{e}}}{T} + \left(\frac{t_{\mathrm{AgNO_3}}}{F} \right)^2 \frac{\partial \mu_{\mathrm{AgNO_3}}/\partial c_{\mathrm{AgNO_3}}}{T D_{\mathrm{AgNO_3}}} \end{gathered} \tag{10.10}$$

The concentration gradient and the electric force become, using the measured transport coefficients:

$$\begin{aligned} \frac{\partial c_{\mathrm{AgNO_3}}}{\partial x} &= -\frac{J_{\mathrm{AgNO_3}}}{D_{\mathrm{AgNO_3}}} + \frac{t_{\mathrm{AgNO_3}}}{D_{\mathrm{AgNO_3}}}\frac{j}{F} \\ \frac{\partial \phi}{\partial x} &= -\frac{t_{\mathrm{AgNO_3}}}{F}\frac{\partial \mu_{\mathrm{AgNO_3}}}{\partial x} - r^{\mathrm{e}} j \end{aligned} \tag{10.11}$$

The first term on the right hand side in Eq. (10.11b) gives the reversible chemical work done by the system on expense of its internal energy. This can be seen by introducing Eq. (10.6) into Eq. (10.5) and comparing compensating terms, see also Eq. (7.25). The transference coefficient can be determined by a *Hittorf* experiment [97]. In this experiment, an electric current is passing a cell of a uniform composition. A differential amount of salt will accumulate on one of the sides, and can be taken for analysis to determine the number of moles transported per moles of electric charge that is passing. The anode produces one mole of silver ion, and the cathode consumes one mole per faraday of electrons passing the outer circuit. These changes plus the transport in the electrolyte lead to a change in composition on both sides. The total flux of silver nitrate is found from Eq. (10.11a). The equation says that, in order to find $t_{\mathrm{AgNO_3}}$, one must correct for diffusion. This can be done by measuring the concentration gradient for small values of j for a decreasing period of time and extrapolating to a zero period of time.

Equation (10.11b) can be used to find $t_{\mathrm{AgNO_3}}$ in the limit $j \to 0$, when the chemical potential is known at the two electrodes. The electric potential difference can be measured with high accuracy. This value may be more accurate than that obtained from Hittorf experiments.

The transport number *of an ion* is the fraction of the electric current carried by the ion:

$$t_{\mathrm{Ag^+}} = F\left(\frac{J_{\mathrm{Ag^+}}}{j}\right)_{d\mu_{\mathrm{AgNO_3}}=0} \quad \text{and} \quad t_{\mathrm{NO_3^-}} = -F\left(\frac{J_{\mathrm{NO_3^-}}}{j}\right)_{d\mu_{\mathrm{AgNO_3}}=0} \tag{10.12}$$

The two ions move in opposite directions, but together they are responsible for the total electric current, therefore

$$t_{\mathrm{Ag^+}} + t_{\mathrm{NO_3^-}} = 1 \tag{10.13}$$

The electrode surface reactions are here reversible to $\mathrm{Ag^+}$ ions on both sides. The $\mathrm{NO_3^-}$ ions do not leave the electrolyte. The flux of the $\mathrm{Ag^+}$ ions

is therefore equal to j/F plus the salt flux, while the flux of NO_3^- ions is equal to the salt flux alone:

$$J_{Ag^+} = j/F + J_{AgNO_3} \quad \text{and} \quad J_{NO_3^-} = J_{AgNO_3} \tag{10.14}$$

We obtain as a consequence

$$t_{AgNO_3} = -t_{NO_3^-} \tag{10.15}$$

The transference coefficient for salt can thus be expressed in two alternative ways:

$$t_{AgNO_3} = -t_{NO_3^-} = -1 + t_{Ag^+} \tag{10.16}$$

A model for transport numbers in terms of mobilities is discussed in Sec. 10.6.

Remark 10.1. *The transference coefficient for a salt in the electrolyte is determined by the transport number of the ion for which the reaction at the electrode surfaces is reversible [27]. Transference coefficients are therefore not a material property of the electrolyte alone. The transport numbers, however, are properties of the electrolyte.*

10.2 The electrode surfaces

Consider again the electrode reaction

$$Ag \rightarrow Ag^+ + e^- \tag{10.17}$$

The surface dissolves as the reaction proceeds. This particular reaction is normally in equilibrium, but for the example, we include its reaction Gibbs energy. The excess entropy production of the isothermal anode surface becomes:

$$\sigma^{s,a} = J^{e,a}_{AgNO_3}\left(-\frac{\Delta_{s,e}\mu_{AgNO_3}}{T}\right) + j\left(-\frac{\Delta_{a,e}\phi + \Delta_n G^{s,a}/F}{T}\right) \tag{10.18}$$

cf. Eq. (5.15). The Gibbs energy change of the neutral components is

$$\Delta_n G^{s,a} = -\mu^a_{Ag} \tag{10.19}$$

The silver phase on the left end is denoted a (from anode), the electrolyte phase is denoted e. The terminology was further explained in Fig. 5.5. The frame of reference, moving relative to the laboratory frame, is the equimolar surface of silver. The electric current density is constant. The reaction rate is given by $r^{s,a} = j/F$.

The electric potential in the anode ϕ^{a} is equal to the Maxwell potential minus the chemical potential of the electron divided by F, $\phi^{\mathrm{a}} = \psi^{\mathrm{a}} - \mu^{\mathrm{a}}_{e^-}/F$, see also the Appendix 4.A and Sec. 10.7 [23, 27, 63]. In the electrolyte one similarly has $\phi^{\mathrm{e}} = \psi^{\mathrm{e}} + \mu^{\mathrm{e}}_{\mathrm{Ag}^+}/F$. A reversible electrode has $\sigma^{\mathrm{s,a}} = 0$, meaning that $\Delta_{\mathrm{s,e}}\mu_{\mathrm{AgNO_3}} = 0$, and

$$\Delta_{\mathrm{a,e}}\phi = \phi^{\mathrm{e}} - \phi^{\mathrm{a}} = -\frac{\Delta_n G^{\mathrm{s,a}}}{F} \rightarrow \Delta_{\mathrm{a,e}}\psi = \psi^{\mathrm{e}} - \psi^{\mathrm{a}} = -\frac{\Delta_r G^{\mathrm{s,a}}}{F} \tag{10.20}$$

where

$$\Delta_r G^{\mathrm{s,a}} = \mu^{\mathrm{e}}_{\mathrm{Ag}^+} + \mu^{\mathrm{a}}_{e^-} - \mu^{\mathrm{a}}_{\mathrm{Ag}} \tag{10.21}$$

Equation (10.20) is the Nernst equation. The thermodynamic force is minus $\Delta_{\mathrm{a,e}}\phi + \Delta_n G^{\mathrm{s,a}}/F = \Delta_{\mathrm{a,e}}\psi + \Delta_r G^{\mathrm{s,a}}/F$ divided by the temperature, see Sec. 10.7.

There are thus only two independent fluxes and forces:

$$\begin{aligned} -\frac{\Delta_{\mathrm{s,e}}\mu_{\mathrm{AgNO_3}}}{T} &= r^{\mathrm{s,a}}_{\mu\mu} J^{\mathrm{e,a}}_{\mathrm{AgNO_3}} + r^{\mathrm{s,a}}_{\mu\phi} j \\ -\frac{1}{T}\left(\Delta_{\mathrm{a,e}}\phi + \frac{\Delta_n G^{\mathrm{s,a}}}{F}\right) &= r^{\mathrm{s,a}}_{\phi\mu} J^{\mathrm{e,a}}_{\mathrm{AgNO_3}} + r^{\mathrm{s,a}}_{\phi\phi} j \end{aligned} \tag{10.22}$$

The adsorption coefficient for the motion of $\mathrm{AgNO_3}$ from the electrolyte to or from the surface is:

$$\ell^{\mathrm{s,a}}_{\mathrm{AgNO_3}} \equiv -\left(\frac{J^{\mathrm{e,a}}_{\mathrm{AgNO_3}}}{\Delta_{\mathrm{s,e}}\mu_{\mathrm{AgNO_3}}}\right)_{j=0} = \frac{1}{r^{\mathrm{s,a}}_{\mu\mu} T} \tag{10.23}$$

The stationary state ohmic resistivity of the surface becomes

$$r^{\mathrm{s,a}} \equiv -\left(\frac{\Delta_{\mathrm{a,e}}\phi + \Delta_n G^{\mathrm{s,a}}/F}{j}\right)_{\Delta_{\mathrm{s,e}}\mu_{\mathrm{AgNO_3}}=0} = T\left(r^{\mathrm{s,a}}_{\phi\phi} - \frac{r^{\mathrm{s,a}}_{\phi\mu} r^{\mathrm{s,a}}_{\mu\phi}}{r^{\mathrm{s,a}}_{\mu\mu}}\right) \tag{10.24}$$

The *transference coefficient* is the ratio of two bulk fluxes and is therefore equal to the value in the electrolyte

$$t^{\mathrm{e}}_{\mathrm{AgNO_3}} \equiv \left(\frac{J^{\mathrm{e,a}}_{\mathrm{AgNO_3}}}{j/F}\right)_{\Delta_{s,o}\mu_{AgNO_3}=0} = -F\frac{r^{\mathrm{s,a}}_{\mu\phi}}{r^{\mathrm{s,a}}_{\mu\mu}} = -t^{\mathrm{e}}_{\mathrm{NO_3^-}} \tag{10.25}$$

With these definitions, we can identify the resistivities in the force-flux

matrix in terms of the measured transport coefficients by:

$$\begin{aligned} r^{\mathrm{s,a}}_{\mu\mu} &= \frac{1}{T\ell^{\mathrm{s,a}}_{\mathrm{AgNO_3}}}\,, \quad r^{\mathrm{s,a}}_{\mu\phi} = r^{\mathrm{s,a}}_{\phi\mu} = -\frac{t^{\mathrm{e}}_{\mathrm{AgNO_3}}}{FT\ell^{\mathrm{s,a}}_{\mathrm{AgNO_3}}}\,, \\ r^{\mathrm{s,a}}_{\phi\phi} &= \frac{r^{\mathrm{s,a}}}{T} + \left(\frac{t^{\mathrm{e}}_{\mathrm{AgNO_3}}}{F}\right)^2 \frac{1}{T\ell^{\mathrm{s,a}}_{\mathrm{AgNO_3}}} \end{aligned} \tag{10.26}$$

The chemical potential difference of $AgNO_3$ out of the surface and the surface potential drop become:

$$\begin{aligned} \Delta_{\mathrm{s,e}}\mu_{\mathrm{AgNO_3}} &= -\frac{1}{\ell^{\mathrm{s,a}}_{\mathrm{AgNO_3}}} J^{\mathrm{e,a}}_{\mathrm{AgNO_3}} + \frac{t^{\mathrm{e}}_{\mathrm{AgNO_3}}}{\ell^{\mathrm{s,a}}_{\mathrm{AgNO_3}}}\frac{j}{F} \\ \Delta_{\mathrm{a,e}}\phi + \frac{\Delta_n G^{\mathrm{s,a}}}{F} &= -\frac{t^{\mathrm{e}}_{\mathrm{AgNO_3}}}{F}\Delta_{\mathrm{s,e}}\mu_{\mathrm{AgNO_3}} - r^{\mathrm{s,a}} j \end{aligned} \tag{10.27}$$

According to the last term of Eq. (10.27a) and Eq. (10.25), the electric current transports salt in direction of the anode surface. This leads to an increase in the salt concentration near the surface. The concentration can increase until $J^{\mathrm{e,a}}_{\mathrm{AgNO_3}} = 0$. The chemical potential drop has then increased to its maximum value. The driving force for desorption is then balanced by the migration of ions with the electric current.

The above analysis can be used in an analogous manner for the isothermal cathode surface.

Exercise 10.2.1. *Calculate the stationary state ($J^{e,a}_{AgNO_3} = 0$) chemical potential jump from the silver surface to the silver nitrate solution, for an electric current density of 10 A/m^2. The mobility coefficient of $AgNO_3$ in and out of the surface is $\ell^{s,a}_{AgNO_3} = 7.5 \times 10^{-8}\ mol^2/sJm^2$. The transport number for nitrate is $t^e_{NO_3^-} = 0.6$.*

- **Solution:** Using Eq. (10.27a), one finds the chemical potential difference equal to $-jt^{\mathrm{e}}_{\mathrm{NO_3^-}}/F\ell^{\mathrm{s,a}}_{\mathrm{AgNO_3}}$. That gives a chemical potential jump from the surface to the solution of -800 J/mol.

The jump in chemical potential gives a change in electric potential at the surface, which is called the concentration overpotential, i.e. the change in the surface potential drop caused by lack of equilibrium between the surface and the nearby electrolyte solution [156]. In order to describe the activation overpotential [156], we need to consider the activated process on a mesoscopic level [51]. It is then possible to find the Butler–Volmer equation from σ^{s}. This is however outside the scope of this book.

10.3 Solution for the heterogeneous system

The electrodes are good conductors and we can therefore take the electric potentials ϕ^{a} and ϕ^{c} as constant. The chemical potential of the pure silver in both electrodes is the same on both sides at constant T and p, $\mu^{\mathrm{a}}_{\mathrm{Ag}} = \mu^{\mathrm{c}}_{\mathrm{Ag}}$. The origin of the x-axis is set at the silver-electrolyte interface. The thickness of the electrolyte layer is d_{e}. The electric potential difference across the cell is

$$\begin{aligned}\phi^{\mathrm{c}} - \phi^{\mathrm{a}} &= \phi^{\mathrm{c}} - \phi^{\mathrm{e,c}} + \phi^{\mathrm{e,c}} - \phi^{\mathrm{e,a}} + \phi^{\mathrm{e,a}} - \phi^{\mathrm{a}} \\ &= \Delta_{\mathrm{a,e}}\phi + \Delta_{\mathrm{e}}\phi + \Delta_{\mathrm{e,c}}\phi \\ &= -\frac{1}{F} t_{\mathrm{AgNO_3}} \left(\mu^{\mathrm{s,c}}_{\mathrm{AgNO_3}} - \mu^{\mathrm{s,a}}_{\mathrm{AgNO_3}} \right) - \left(r^{\mathrm{s,a}} + r^{\mathrm{e}} d_{\mathrm{e}} + r^{\mathrm{s,c}} \right) j \end{aligned} \tag{10.28}$$

For the last identity we integrated Eq. (10.11b), assuming that the transference number as well as the resistivity of the electrolyte are constant (taken at the average salt concentration). Furthermore we used Eq. (10.27) for the anode surface and the analogous equation for the cathode surface. Finally, we used $\mu^{\mathrm{a}}_{\mathrm{Ag}} = \mu^{\mathrm{c}}_{\mathrm{Ag}}$ so that $\Delta_n G^{\mathrm{s,a}} + \Delta_n G^{\mathrm{s,c}} = 0$, and $\Delta_{\mathrm{a,e}}\phi + \Delta_{\mathrm{e,c}}\phi = 0$.

Assume next that $r_{\phi\phi}$ and $r_{\mu\phi}$ in the electrolyte are constant (depend only on the average salt concentration). In the stationary state, the salt flux is zero. From Eqs. (10.6) and (10.22), we obtain the electric potential difference

$$\phi^{\mathrm{c}} - \phi^{\mathrm{a}} = -T \left(r^{\mathrm{s,a}}_{\phi\phi} + d_{\mathrm{e}} r^{\mathrm{e}}_{\phi\phi} + r^{\mathrm{s,c}}_{\phi\phi} \right) j \tag{10.29}$$

and the chemical potential difference

$$\begin{aligned}\mu^{\mathrm{s,c}}_{\mathrm{AgNO_3}} - \mu^{\mathrm{s,a}}_{\mathrm{AgNO_3}} &= \mu^{\mathrm{s,c}}_{\mathrm{AgNO_3}} - \mu^{\mathrm{e,c}}_{\mathrm{AgNO_3}} + \mu^{\mathrm{e,c}}_{\mathrm{AgNO_3}} - \mu^{\mathrm{e,a}}_{\mathrm{AgNO_3}} \\ &\quad + \mu^{\mathrm{e,a}}_{\mathrm{AgNO_3}} - \mu^{\mathrm{s,a}}_{\mathrm{AgNO_3}} \\ &= \Delta_{\mathrm{s,e}}\mu_{\mathrm{AgNO_3}} + \Delta_{\mathrm{e}}\mu_{\mathrm{AgNO_3}} + \Delta_{\mathrm{e,s}}\mu_{\mathrm{AgNO_3}} \\ &= -T \left(r^{\mathrm{s,a}}_{\mu\phi} + d_{\mathrm{e}} r^{\mathrm{e}}_{\mu\phi} + r^{\mathrm{s,c}}_{\mu\phi} \right) j \end{aligned} \tag{10.30}$$

In this approximation, the chemical potential difference is linear in x and given by

$$\mu^{\mathrm{e}}_{\mathrm{AgNO_3}}(x) = 2\mu^{\mathrm{e}}_{\mathrm{Ag^+}}(x) = 2\mu^{\mathrm{e}}_{\mathrm{NO_3^-}}(x) = \mu^{\mathrm{e}}_{\mathrm{AgNO_3}}(0) - xTr^{\mathrm{e}}_{\mu\phi} \tag{10.31}$$

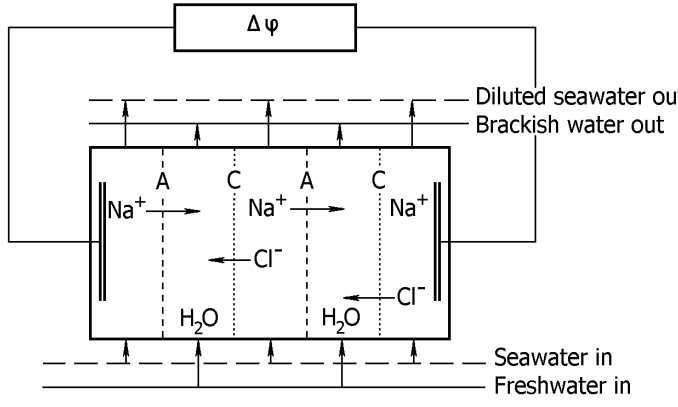

Figure 10.2 The principle of a salt power plant that uses reverse electrodialysis. The concentration difference of sodium chloride, between the sea water and the fresh water, drives an electric current and creates an electric power. Sodium ion is transported through cation exchange membranes, and chloride ions through anion exhange membranes.

10.4 A salt power plant

In order to see the importance of coupling coefficients for work production, consider first a salt power plant. This plant uses an electrolyte concentration difference to give electric current. The plant that uses reverse electrodialysis is illustrated in Fig. 10.2. Salt power plants can also use reverse osmosis, see Chapter 18. The plant operates at the sea level. Sea water and fresh water are fed into alternating compartments that are separated by ion-exchange membranes. The membranes alternate between cation exchange membranes (A) and anion exchange membranes (C). One cell unit consists of a salt water compartment, an anion exchange membrane, a fresh water compartment, a cation exchange membrane and a salt water compartment. Several units in series add to the cell potential. The figure shows two units. The gradient in chemical potential of salt drives chloride ions through the anion-exchange membrane and sodium ions through the cation-exchange membrane. The electric field that arises causes the electric current between the electrodes. The chloride electrode, on the left hand side, may be of titanium oxide. On the right hand side, hydrogen rather than Na will be produced, typically on a nickel electrode. We assume equilibrium at the electrodes.

For each membrane, the electric potential difference is given by an expression like Eq. (10.28). For the first membrane A in Fig. 10.2,

$t_{\mathrm{NaCl}} = t_{\mathrm{Na^+}} = 1$.

$$\Delta\phi = -\frac{t_{\mathrm{Na^+}}}{F}\left[\mu_{\mathrm{NaCl}}\left(fresh\right) - \mu_{\mathrm{NaCl}}\left(sea\right)\right] - r^{\mathrm{m}} d_{\mathrm{m}} j \tag{10.32}$$

where we took the electric resistance of the membrane, $r^{\mathrm{m}} d_{\mathrm{m}}$, to be large compared to other resistances. The absolute value of the coupling coefficient, $|r_{\mu\phi}| = r_{\mu\mu} t_{\mathrm{Na^+}}/F$, has its maximum when $t_{\mathrm{Na^+}} = 1$, see Eq. (10.9). Diffusion of salt reduces the electric power. Such a loss of power is prevented with this type of membrane arrangement. Eventually, there will be some salt in the fresh water compartment to lower the chemical potential difference. But some salt is also required to give an acceptable ohmic resistance in this compartment.

10.5 Electric power from volume flow

Work can also be obtained from volume transport between two pressure levels. This transport can lead to charge transport in an outer circuit. Consider the transport of water across a cation exchange membrane in the cell

$$(\mathrm{Pt})\,\mathrm{H_2}, \mathrm{H_2O}(l)|\mathrm{HM}|\mathrm{H_2}, \mathrm{H_2O}(l)\,(\mathrm{Pt}) \tag{10.33}$$

A platinum catalyst is located on the electrode-membrane interfaces. The membrane HM is a proton conductor, for instance a Nafion membrane that is used in fuel cells (see Chapter 19). The membrane needs water to conduct well. Hydrogen gas disproportionates on the left hand side giving protons in the membrane and electrons in the metal. The protons react on the right hand side to form hydrogen gas. We assume now equilibrium at both electrodes. The entropy production of the membrane is, cf. Eq. (4.14):

$$\sigma = J_{\mathrm{w}}\left(-\frac{1}{T}\frac{\partial\mu_{\mathrm{w}}}{\partial x}\right) + j\left(-\frac{1}{T}\frac{\partial\phi}{\partial x}\right) \tag{10.34}$$

The proton concentration in the membrane is everywhere fixed by the cation sites of the membrane, so the flux of protons is identical to the electric current j. The temperature is assumed to be constant so we drop the subscript T in μ_{w}. The flux equations are:

$$\begin{aligned} J_{\mathrm{w}} &= -L_{\mu\mu}\frac{1}{T}\frac{\partial}{\partial x}\mu_{\mathrm{w}} - L_{\mu\phi}\frac{1}{T}\frac{\partial\phi}{\partial x} \\ j &= -L_{\phi\mu}\tfrac{1}{T}\frac{\partial}{\partial x}\mu_{\mathrm{w}} - L_{\phi\phi}\frac{1}{T}\frac{\partial\phi}{\partial x} \end{aligned} \tag{10.35}$$

The frame of reference for transport are the membrane surfaces. In this frame of reference, water can move due to a pressure difference between the two sides.

The electric conductivity of the membrane is

$$\kappa^{\mathrm{e}} \equiv \frac{L_{\phi\phi}}{T} \tag{10.36}$$

Following the same procedure as in Secs. 10.1–10.3, we arrive at an expression for the water flux

$$J_{\mathrm{w}} = -D_{\mathrm{w}} \frac{\partial}{\partial x} c_{\mathrm{w}} + \frac{t_{\mathrm{w}}}{F} j \tag{10.37}$$

where D_{w} is the diffusion coefficient of water in the membrane

$$D_{\mathrm{w}} = \left(L_{\mu\mu} - \frac{L_{\mu\phi} L_{\phi\mu}}{L_{\phi\phi}} \right) \frac{\partial \mu_{\mathrm{w}}}{\partial c_{\mathrm{w}}} \tag{10.38}$$

while the *transference coefficient of water* is defined as:

$$t_{\mathrm{w}} = F \left(\frac{J_{\mathrm{w}}}{j} \right)_{d\mu_{\mathrm{w}}=0} = F \frac{L_{\mu\phi}}{L_{\phi\phi}} \tag{10.39}$$

When the water concentration is the same on the two sides, and a hydrostatic pressure difference exists, $d\mu_{\mathrm{w}} = V_{\mathrm{w}} dp$, where V_{w} is the partial molar volume of water. We solve Eq. (10.35) using $L_{\phi\mu} = L_{\mu\phi}$ and obtain:

$$\Delta\phi = -\int_0^{d^{\mathrm{e}}} \left(\frac{L_{\phi\mu}}{L_{\phi\phi}} \frac{d\mu_{\mathrm{w}}}{dx} - \frac{j}{\kappa^{\mathrm{e}}} \right) dx = -\frac{t_{\mathrm{w}}}{F} \int_0^{d^{\mathrm{e}}} d\mu_{\mathrm{w}} - \frac{j}{\kappa^{\mathrm{e}}} d^{\mathrm{e}} = -\frac{t_{\mathrm{w}}}{F} V_{\mathrm{w}} \Delta_{\mathrm{e}} p - \frac{j}{\kappa^{\mathrm{e}}} d^{\mathrm{e}} \tag{10.40}$$

The pressure driven flow is able to generate an electric potential, however, this is small. This phenomenon is also called friction electricity. The magnitude of the work is proportional to t_{w} or in other words, to the coupling coefficient $L_{\phi\mu}$.

The transference coefficient can be found by measuring the water flux or the volume flow caused by electric current through the membrane, or by measuring the electric potential difference with different water pressures on the two sides [157]. The relation between the two experiments is given by the Onsager relation:

$$\left(\frac{\Delta_{\mathrm{e}} \phi}{\Delta_{\mathrm{e}} p} \right)_{j=0} = -\left(\frac{J_{\mathrm{w}}}{j} \right)_{d\mu_{\mathrm{w}}=0} = -\frac{t_{\mathrm{w}}}{F} \tag{10.41}$$

This is known as the Saxén relation. Volume flow by electric current is called electro-osmosis, while an electric potential generated by pressure difference is called a streaming potential [27].

10.6 Ionic mobility model for the electrolyte

In an electroneutral system, the independent composition variables are the salt concentrations. The electrolyte can be regarded as electroneutral. Jackson [158] calculated that electroneutrality was obtained in a liquid junction within 10^{-9} s, the time an ion takes to diffuse over a typical Debije length. We are normally dealing with much larger time scales, compare Exercise 7.2.2. It is still more common to use ions as basic variables for fluxes and forces. We shall therefore explain how to go from one description to the other. This is useful for comparison with data in the literature.

The electrochemical potential for an ion was defined by Guggenheim [63, 95].

$$\begin{aligned} \tilde{\mu}_+ &= \mu_+ + z_+ F\psi \\ \tilde{\mu}_- &= \mu_- - z_- F\psi \end{aligned} \tag{10.42}$$

where μ_+ and μ_- are the chemical potentials for the cation and anion respectively, ψ is the electrostatic potential referred to vacuum (the Maxwell potential), and z_+ and z_- are ion valences (1 for both Ag^+ and NO_3^-).

In the ionic formulation the entropy production is given by:

$$\sigma = J_{Ag^+}\left[-\frac{1}{T}\frac{\partial}{\partial x}\left(\mu_{Ag^+} + F\psi\right)\right] + J_{NO_3^-}\left[-\frac{1}{T}\frac{\partial}{\partial x}\left(\mu_{NO_3^-} - F\psi\right)\right] \tag{10.43}$$

By substituting $J_{Ag^+} = j/F + J_{AgNO_3}$, $J_{AgNO_3} = J_{NO_3^-}$ and $\mu_{NO_3^-} + \mu_{Ag^+} = \mu_{AgNO_3}$, we see that this equation is equivalent to (10.5), given that

$$\phi = \psi + \frac{\mu_{Ag^+}}{F} \tag{10.44}$$

The difference $\Delta\phi$ is therefore equal to the electrochemical potential difference divided by F of the ion that enters the electrode reaction, or the (measured) electromotive at reversible conditions [23, 27, 63]. The ionic fluxes, that follow from the entropy production (10.43), are:

$$\begin{aligned} J_{Ag^+} &= -L^{++}\frac{1}{T}\frac{\partial}{\partial x}\left(\mu_{Ag^+} + F\psi\right) - L^{+-}\frac{1}{T}\frac{\partial}{\partial x}\left(\mu_{NO_3^-} - F\psi\right) \\ J_{NO_3^-} &= -L^{-+}\frac{1}{T}\frac{\partial}{\partial x}\left(\mu_{Ag^+} + F\psi\right) - L^{--}\frac{1}{T}\frac{\partial}{\partial x}\left(\mu_{NO_3^-} - F\psi\right) \end{aligned} \tag{10.45}$$

In this formulation, Nernst–Einstein assumption *holds* for each ion. By

introducing measurable forces, we obtain:

$$\begin{aligned} J_{\mathrm{Ag^+}} &= -L^{+-}\frac{1}{T}\frac{\partial}{\partial x}\mu_{\mathrm{AgNO_3}} - (L^{++}-L^{+-})\frac{F}{T}\frac{\partial\phi}{\partial x} \\ J_{\mathrm{NO_3^-}} &= -L^{--}\frac{1}{T}\frac{\partial}{\partial x}\mu_{\mathrm{AgNO_3}} - (L^{-+}-L^{--})\frac{F}{T}\frac{\partial\phi}{\partial x} \end{aligned} \tag{10.46}$$

By expressing the salt flux and the electric current in terms of the ionic coefficients, we obtain:

$$\begin{aligned} J_{\mathrm{AgNO_3}} &= -L^{--}\frac{1}{T}\frac{\partial}{\partial x}\mu_{\mathrm{AgNO_3}} - (L^{+-}-L^{--})\frac{F}{T}\frac{\partial\phi}{\partial x} \\ &= -L_{\mu\mu}\frac{1}{T}\frac{\partial}{\partial x}\mu_{\mathrm{AgNO_3}} - L_{\mu\phi}\frac{1}{T}\frac{\partial\phi}{\partial x} \\ j &= -(L^{+-}-L^{--})\frac{F}{T}\frac{\partial}{\partial x}\mu_{\mathrm{AgNO_3}} - (L^{++}-2L^{+-}+L^{--})\frac{F^2}{T}\frac{\partial\phi}{\partial x} \\ &= -L_{\phi\mu}\frac{1}{T}\frac{\partial}{\partial x}\mu_{\mathrm{AgNO_3}} - L_{\phi\phi}\frac{1}{T}\frac{\partial\phi}{\partial x} \end{aligned} \tag{10.47}$$

which gives as relations for the conductivities in the salt representation:

$$L_{\mu\mu} = L^{--},\quad L_{\mu\phi} = L_{\phi\mu} = (L^{+-}-L^{--})F,\quad L_{\phi\phi} = (L^{++}-2L^{+-}+L^{--})F^2 \tag{10.48}$$

The conductivity matrix ($L_{\mu\mu}$, $L_{\mu\phi}$, $L_{\phi\mu}$, $L_{\phi\phi}$) is the inverse of the resistivity matrix ($r_{\mu\mu}$, $r_{\mu\phi}$, $r_{\phi\mu}$, $r_{\phi\phi}$) in Eq. (10.6). In the ionic mobility model *one neglects* $L^{+-} = L^{-+}$, which is of the second order in the salt concentration, see below.

Remark 10.2. *The relations between the ion fluxes, the salt fluxes and the electric current depend on the reversibility of the electrode surface reactions for the ions. Formulae, which follow by writing the entropy production with salt fluxes and the electric current, therefore depend on the electrode surface reaction.*

A common model for the Onsager coefficients of an electrolytic solution uses mobilities of ions, here $u^{\mathrm{e}}_{\mathrm{Ag^+}}$ and $u^{\mathrm{e}}_{\mathrm{NO_3^-}}$. The mobility of an ion is the ratio between the stationary velocity of the ion in a constant electric field, divided by the electric field. This model is useful for calculation of liquid junctions, cf. Chapter 16. It neglects coupling between the ion fluxes. Up to linear order in the salt concentration, the resulting ionic conductivities are

$$L^{--} = \frac{T}{F}c_{\mathrm{NO_3^-}}u_{\mathrm{NO_3^-}},\quad L^{-+} = L^{+-} = 0,\quad L^{++} = FTc_{\mathrm{Ag^+}}u_{\mathrm{Ag^+}} \tag{10.49}$$

The ion concentrations are equal to the salt concentration, cf. Eq. (10.1). This gives for the conductivities in the salt representation [97]

$$L_{\mu\mu} = \frac{T}{F} c_{\mathrm{AgNO_3}} u_{\mathrm{NO_3^-}}, \quad L_{\phi\mu} = L_{\mu\phi} = -T c_{\mathrm{AgNO_3}} u_{\mathrm{NO_3^-}}$$
$$L_{\phi\phi} = FT c_{\mathrm{AgNO_3}} \left(u_{\mathrm{NO_3^-}} + u_{\mathrm{Ag^+}} \right) \tag{10.50}$$

The transference number of an ion becomes

$$t_{\mathrm{ion}} = \frac{z_{\mathrm{ion}} c_{\mathrm{ion}} u_{\mathrm{ion}}}{\sum_j z_j c_j u_j} \tag{10.51}$$

where the summation is carried out for all ions. Using $z_- = z_+ = 1$ and given that the ion concentrations are the same, this gives

$$t_{\mathrm{NO_3^-}} = \frac{u_{\mathrm{NO_3^-}}}{u_{\mathrm{NO_3^-}} + u_{\mathrm{Ag^+}}}, \quad t_{\mathrm{Ag^+}} = \frac{u_{\mathrm{Ag^+}}}{u_{\mathrm{NO_3^-}} + u_{\mathrm{Ag^+}}} \tag{10.52}$$

The resulting electric conductivity is, cf. Eq. (10.22),

$$\kappa^{\mathrm{e}} = \frac{1}{r^{\mathrm{e}}} = \frac{L_{\phi\phi}}{T} = F c_{\mathrm{AgNO_3}} \left(u_{\mathrm{NO_3^-}} + u_{\mathrm{Ag^+}} \right) \tag{10.53}$$

The transference coefficient for $AgNO_3$ is, cf. Eq. (10.16),

$$t_{\mathrm{AgNO_3}} = -t_{\mathrm{NO_3^-}} = -\frac{u_{\mathrm{NO_3^-}}}{u_{\mathrm{NO_3^-}} + u_{\mathrm{Ag^+}}} \tag{10.54}$$

In an ideal electrolyte solution the diffusion coefficient for the salt becomes, cf. Eq. (10.7),

$$D_{\mathrm{AgNO_3}} = \frac{1}{T r_{\mu\mu}} \frac{\partial \mu_{\mathrm{AgNO_3}}}{\partial c_{\mathrm{AgNO_3}}} = \frac{R \left(L_{\phi\phi} L_{\mu\mu} - L_{\phi\mu} L_{\mu\phi} \right)}{c_{\mathrm{AgNO_3}} L_{\phi\phi}} = \frac{2RT u_{\mathrm{Ag^+}} u_{\mathrm{NO_3^-}}}{F(u_{\mathrm{Ag^+}} + u_{\mathrm{NO_3^-}})} \tag{10.55}$$

where we used $\mu_{\mathrm{AgNO_3}} = \mu^0_{\mathrm{AgNO_3}} + 2RT \ln c_{\mathrm{AgNO_3}}/c^0$, cf. Appendix 3.A.3. This estimate of the diffusion coefficient has been used widely in electrolytes [114]. Measurements show that $D_{\mathrm{AgNO_3}}$ and $t_{\mathrm{NO_3^-}}$ are weakly dependent on the concentration. Mobilities depend on the concentration, but the ratio of mobilities is only weakly dependent on the concentration. Transport numbers and mobilities at infinite dilution [159] are given in Table 10.1. More data can be found in the literature [159].

Table 10.1 Transport numbers and ionic mobilities at infinitely dilute solution for some selected ions.

Salt, MX	t_{M^+}	κ_{MX}/c_{MX}	u_{M^+}
		$/10^2 \mathrm{ohm}^{-1}\mathrm{mol}^{-1}\mathrm{m}^2$	$/10^{-8}\mathrm{m}^2\mathrm{s}^{-1}\mathrm{V}^{-1}$
HCl	0.8209	426.16	36.23
LiCl	0.3360	114.99	73.52
NaCl	0.3870	126.50	5.19
KCl	0.4905	149.85	7.62
KBr	0.4846	151.67	

By introducing the mobilities in the expression for the electric potential drop across the electrolyte, we obtain using Eq. (10.11):

$$\Delta_e\phi = \frac{2RT}{F}\frac{u_{NO_3^-}}{u_{Ag^+}+u_{NO_3^-}}\ln\frac{c_{AgNO_3}(d_e)}{c_{AgNO_3}(0)} - \frac{j}{\kappa^e}d_e \tag{10.56}$$

for an ideal solution. The mobility model is further discussed in the chapter on liquid junctions, Chapter 16.

Exercise 10.6.1. *For a low density of ions the coupling coefficients, that are proportional to the salt density squared, can be neglected. Motivate the relation between L^{--}, L^{++} and the mobilities on this background.*

- **Solution:** The mobility of an ion times the electric field on the ion, gives by definition the ion velocity. The electric field on e.g. the Ag^+ ion is $-\partial\phi/\partial x = -\partial(\psi + \mu_{Ag^+}/F)/\partial x$. This ion therefore gets as velocity $-u_{Ag^+}\partial\phi/\partial x$. If we then multiply this with the molar concentration one finds the positive ion flux. The resulting expression for the Onsager coefficient is $L^{++} = Tc_{Ag^+}u_{Ag^+}/F = Tc_{AgNO_3}u_{Ag^+}/F$. We also obtain $L^{--} = Tc_{NO_3^-}u_{NO_3^-}/F = Tc_{AgNO_3}u_{NO_3^-}/F$ for the flux of nitrate ion.

Exercise 10.6.2. *Calculate the stationary state chemical potential gradient of $AgNO_3$ in a solution of concentration 100 mol/m^3. The electric current density is 10 A/m^2. Use as diffusion coefficient $10^{-9}\,m^2/s$, transference coefficient 0.6 and temperature 300 K.*

- **Solution:** By using Eq. (10.5) one finds for the chemical potential gradient $2RTt_{AgNO_3}j/D_{AgNO_3}c_{AgNO_3}$, which gives the large value 2.9×10^3 kJ/mol m.

10.7 Ionic and electronic model for the surface

Using the chemical potential for the ions in the electrolyte and for the electrons in the conduction band in the silver, the excess entropy production rate of the surface becomes

$$\sigma^{\mathrm{s,a}} = J_{e^-}^{\mathrm{a,e}} \left(-\frac{\Delta_{\mathrm{a,s}} \left(\mu_{e^-} - F\psi \right)}{T} \right) + J_{\mathrm{Ag^+}}^{\mathrm{e,a}} \left(-\frac{\Delta_{\mathrm{s,e}} \left(\mu_{\mathrm{Ag^+}} + F\psi \right)}{T} \right)$$

$$+ J_{\mathrm{NO_3^-}}^{\mathrm{e,a}} \left(-\frac{\Delta_{\mathrm{s,e}} \left(\mu_{\mathrm{NO_3^-}} - F\psi \right)}{T} \right) + \frac{j}{F} \left(-\frac{\Delta_r G^{\mathrm{s,a}}}{T} \right) \tag{10.57}$$

in the last contribution on the right hand side, we used the reaction rate that is equal to j/F. After substituting $J_{\mathrm{Ag^+}}^{\mathrm{e,a}} = j/F + J_{\mathrm{AgNO_3}}^{\mathrm{e,a}}$, $J_{e^-}^{\mathrm{a,e}} = -j/F$ and $J_{\mathrm{NO_3^-}}^{\mathrm{e,a}} = J_{\mathrm{AgNO_3}}^{\mathrm{e,a}}$ this equation becomes

$$\sigma^{\mathrm{s,a}} = j \left[-\frac{\left(\mu_{e^-}^{\mathrm{a,e}} - F\psi^{\mathrm{a,e}} \right) + \left(\mu_{\mathrm{Ag^+}}^{\mathrm{e,a}} + F\psi^{\mathrm{e,a}} \right) - \mu_{e^-}^{\mathrm{s,a}} - \mu_{\mathrm{Ag^+}}^{\mathrm{s,a}} + \Delta_r G^{\mathrm{s,a}}}{FT} \right]$$

$$+ J_{\mathrm{AgNO_3}}^{\mathrm{e,a}} \left[\left(-\frac{\Delta_{\mathrm{s,e}} \left(\mu_{\mathrm{NO_3^-}} + \mu_{\mathrm{Ag^+}} \right)}{T} \right) \right] \tag{10.58}$$

Next, we substitute $\phi^{\mathrm{e,a}} = \psi^{\mathrm{e,a}} + \mu_{\mathrm{Ag^+}}^{\mathrm{e,a}}/F$, $\phi^{\mathrm{a,e}} = \psi^{\mathrm{a,e}} - \mu_{e^-}^{\mathrm{a,e}}/F$, $\mu_{\mathrm{AgNO_3}} = \mu_{\mathrm{NO_3^-}} + \mu_{\mathrm{Ag^+}}$, and $\Delta_r G^{\mathrm{s,a}} = \mu_{e^-}^{\mathrm{s,a}} + \mu_{\mathrm{Ag^+}}^{\mathrm{s,a}} + \Delta_n G^{\mathrm{s,a}}$, which results in

$$\sigma^{\mathrm{s,a}} = J_{\mathrm{AgNO_3}}^{\mathrm{e,a}} \left(-\frac{\Delta_{\mathrm{s,e}} \mu_{\mathrm{AgNO_3}}}{T} \right) + j \left(-\frac{\Delta_{\mathrm{a,e}} \phi + \Delta_n G^{\mathrm{s,a}}/F}{T} \right) \tag{10.59}$$

This is Eq. (10.18), which we used. This further clarifies the relation between $\phi^{\mathrm{e,a}}, \phi^{\mathrm{a,e}}$ and $\psi^{\mathrm{e,a}}, \psi^{\mathrm{a,e}}$ in the homogeneous phases and the relation between $\Delta_n G^{\mathrm{s,a}}$ and $\Delta_r G^{\mathrm{s,a}}$ at the surface. Equation (10.59) uses the independent fluxes and forces for the surface. It follows from Eq. (10.59) that the surface potential drop under reversible conditions is

$$\Delta_{\mathrm{a,e}} \phi = -\frac{\Delta_n G^{\mathrm{s,a}}}{F} = \frac{\mu_{\mathrm{Ag}}^{\mathrm{s,a}}}{F} \tag{10.60}$$

The corresponding Maxwell potential is

$$\Delta_{\mathrm{a,e}} \psi = -\frac{\mu_{\mathrm{Ag^+}}^{\mathrm{e,a}} + \mu_{e^-}^{\mathrm{a,e}} - \mu_{\mathrm{Ag}}^{\mathrm{s,a}}}{F} \tag{10.61}$$

Part B: Applications

This page intentionally left blank

Chapter 11

Evaporation and Condensation

We study the conditions at the liquid-vapor interface during stationary evaporation or condensation. A pure fluid is described first. The equations that determine the temperature profile and the variation in the chemical potential, are given. The description of evaporation and condensation of a mixture follows. We present resistivity coefficients for the surface obtained using non-equilibrium molecular dynamics and compare them with values found using kinetic theory.

Evaporation or condensation occur when there is a temperature difference across a liquid-vapor interface, or when the pressure in the vapor differs from the vapor pressure of the liquid. Distillation is a process where mixtures are separated by differences in such variables. Evaporation of seawater by the sun is driven by a temperature difference. Significant temperature jumps have been measured across the surface during evaporation of water, octane, methyl-cyclohexane [160–162], aniline [163] and water-glycerol [164] around room temperatures, but also during crystallization of He-3 from the superfluid phase [165]. A reduction in the pressure above an oil-gas mixture, leads to evaporation of volatile components. Due to such a pressure driven evaporation process, temperature differences of several tens of degrees can arise in the system. This may cause damage to the pipe or block it by gas clathrate formation. Knowledge about the detailed conditions at the surface of the evaporating or condensing liquid, and the coupling between temperature and pressure driven processes is important for handling technical problems in a proper way. In this chapter we shall give governing equations for such phenomena. Bond and Struchtrup [166] have reviewed the literature on evaporation.

Consider first a liquid in equilibrium with its vapor. The thermodynamic equilibrium conditions for the surface are:

$$\mu_{\rm i}^{\rm g} = \mu_{\rm i}^{\rm l} \quad \text{and} \quad T^{\rm g} = T^{\rm l} \tag{11.1}$$

where $\mu_{\rm i}$ is the chemical potential of component i, and T is the temperature. Superscripts g and l denote the gas (vapor) and the liquid phase, respectively. These conditions are, according to observations of Fang and Ward [160–162], not fulfilled when rates of evaporation or condensation are large. We shall see how stationary evaporation and condensation can then be described by non-equilibrium thermodynamics. A detailed analysis in this context was given earlier for a one-component system [36] and for a dilute mixture [37]. Bedeaux and Kjelstrup [38] verified that the results of Fang and Ward could be described using this approach. We are interested in expressions for the variation in the temperature and the chemical potentials close to and at the interface. We divide the system into three subsystems; the liquid phase, l, the interface, s, and the gas phase, g, where the liquid is on the left, $x < 0$, and the vapor on the right, $x > 0$, of the origin. We describe a pure fluid and a two-component mixture. Values for the various transport coefficients are given, using results of non-equilibrium molecular dynamics simulations [40, 67] and of kinetic theory [32–34].

We have shown elsewhere [50], using mesoscopic non-equilibrium thermodynamics, that evaporation and condensation can be described as an activated process. This approach is able to reproduce interesting results by Tsuruta and Nagayama [49] which they obtained using non-equilibrium molecular dynamics simulations. This is an interesting direction for further work.

11.1 Evaporation and condensation in a pure fluid

11.1.1 *The entropy production and the flux equations*

Take the evaporation of a one component fluid like pure water. The evaporation takes place from a funnel that is partially filled, see Fig. 11.1. Fluid is supplied at a constant rate at the bottom of the funnel, while gas is withdrawn at the top at the same rate. We do not consider viscous effects, and the pressure is constant throughout the system. The flux of fluid through the interface is J. The entropy production for the homogeneous phases is given by Eq. (4.15), which reduces for the one-component liquid to:

$$\sigma^{\rm l} = J_q'^{\rm l} \frac{\partial}{\partial x}\left(\frac{1}{T^{\rm l}}\right) = J_q'^{\rm l}\left[-\frac{1}{(T^{\rm l})^2}\frac{\partial T^{\rm l}}{\partial x}\right] \tag{11.2}$$

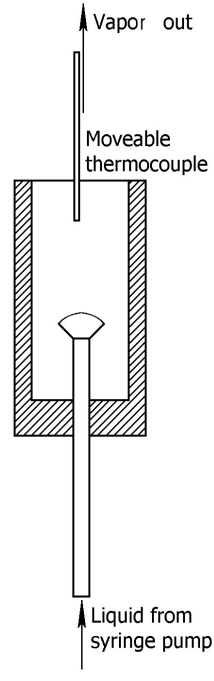

Figure 11.1 Sketch of experimental setup to measure temperature profiles during evaporation. Vapor is withdrawn from the cell at the same rate as liquid is supplied. The thermocouple can be lowered to measure temperatures near the surface of the evaporating liquid. There is a curvature of the meniscus in the funnel container for the liquid, but the surface can be regarded as flat on a molecular scale.

The resulting flux equation is:

$$J_q'^{\mathrm{l}} = -\lambda_{\mathrm{l}} \frac{\partial T^{\mathrm{l}}}{\partial x} \tag{11.3}$$

where λ_{l} is the thermal conductivity. These equations are also valid in the vapor phase with the sub- and superscripts l replaced by g. The thermal conductivity of the liquid is usually considerably higher than that of the vapor.

The flux of, say water, J, is constant in stationary evaporation or condensation. The flux is the same in the liquid, across the surface and in the gas. The measurable heat flux from the liquid into the surface, $J_q'^{\mathrm{l}}$, is however, not the same as the measurable heat flux out of the surface into the gas, $J_q'^{\mathrm{g}}$, because heat is not conserved. The total heat flux through

the surface, J_q, is on the other hand, constant. The total heat flux is the measurable heat flux plus the enthalpy carried by the water flux:

$$J_q = J_q'^{\mathrm{g}} + H^{\mathrm{g}} J = J_q'^{\mathrm{l}} + H^{\mathrm{l}} J \tag{11.4}$$

As frame of reference for the mass flux we have the equimolar surface of water [62].

The entropy production for heat and mass transport into and out of the liquid-vapor interface in a one-component system is, according to Eq. (5.15):

$$\begin{aligned}\sigma^{\mathrm{s}} = {} & J_q'^{\mathrm{l}} \left[\frac{1}{T^{\mathrm{s}}} - \frac{1}{T^{\mathrm{l}}}\right] + J_q'^{\mathrm{g}} \left[\frac{1}{T^{\mathrm{g}}} - \frac{1}{T^{\mathrm{s}}}\right] - J^{\mathrm{l}} \left[\frac{\mu^{\mathrm{s}}(T^{\mathrm{s}}) - \mu^{\mathrm{l}}(T^{\mathrm{s}})}{T^{\mathrm{s}}}\right] \\ & - J^{\mathrm{g}} \left[\frac{\mu^{\mathrm{g}}(T^{\mathrm{s}}) - \mu^{\mathrm{s}}(T^{\mathrm{s}})}{T^{\mathrm{s}}}\right]\end{aligned} \tag{11.5}$$

For a stationary state $J^{\mathrm{l}} = J^{\mathrm{g}} = J$. We can eliminate the heat flux in the liquid phase from the entropy production, using Eq. (11.4). Using Gibbs–Helmholtz' equation

$$\frac{\partial\,(\mu/T)}{\partial\,(1/T)} = H \tag{11.6}$$

for the liquid as well as the vapor, we obtain to linear order in the forces

$$\begin{aligned}\frac{1}{T^{\mathrm{s}}}\left[\mu^{\mathrm{g}}(T^{\mathrm{s}}) - \mu^{\mathrm{l}}(T^{\mathrm{s}})\right] &= \frac{1}{T^{\mathrm{l}}}\left[\mu^{\mathrm{g}}(T^{\mathrm{l}}) - \mu^{\mathrm{l}}(T^{\mathrm{l}})\right] \\ &\quad + \left\{\frac{\partial}{\partial\,(1/T)}\left[\frac{\mu^{\mathrm{g}}(T) - \mu^{\mathrm{l}}(T)}{T}\right]\right\}_{T=T^{\mathrm{l}}} \left(\frac{1}{T^{\mathrm{s}}} - \frac{1}{T^{\mathrm{l}}}\right) \\ &= \left[\frac{\mu^{\mathrm{g}}(T^{\mathrm{l}}) - \mu^{\mathrm{l}}(T^{\mathrm{l}})}{T^{\mathrm{l}}}\right] + \left(H^{\mathrm{g}} - H^{\mathrm{l}}\right)\left(\frac{1}{T^{\mathrm{s}}} - \frac{1}{T^{\mathrm{l}}}\right)\end{aligned} \tag{11.7}$$

The resulting entropy production in the surface becomes the sum of two independent terms:

$$\begin{aligned}\sigma^{\mathrm{s}} &= J_q'^{\mathrm{g}} \left[\frac{1}{T^{\mathrm{g}}} - \frac{1}{T^{\mathrm{l}}}\right] + J\left[-\frac{\mu^{\mathrm{g}}(T^{\mathrm{l}}) - \mu^{\mathrm{l}}(T^{\mathrm{l}})}{T^{\mathrm{l}}}\right] \\ &\equiv J_q'^{\mathrm{g}} \Delta_{\mathrm{l,g}}\left(\frac{1}{T}\right) + J\left[-\frac{\Delta_{\mathrm{l,g}}\mu(T^{\mathrm{l}})}{T^{\mathrm{l}}}\right]\end{aligned} \tag{11.8}$$

There are thus only two independent driving forces for transport of heat and mass across the surface, a thermal force and a chemical force. The chemical

potential difference across the interface is evaluated at the temperature of the adjacent liquid. In the stationary state, the Helmholtz energy of the surface, which is equal to the surface tension for a one-component system, is independent of time and there is no exchange of surface energy with the liquid or the vapor. As a consequence, the surface temperature is not needed in the description of stationary evaporation and condensation. Alternatively, we may eliminate the heat flux in the vapor. Along the same lines we then find for the entropy production

$$\begin{aligned}\sigma^{\mathrm{s}} &= J_q^{\prime\mathrm{l}}\left[\frac{1}{T^{\mathrm{g}}}-\frac{1}{T^{\mathrm{l}}}\right]+J\left[-\frac{\mu^{\mathrm{g}}(T^{\mathrm{g}})-\mu^{\mathrm{l}}(T^{\mathrm{g}})}{T^{\mathrm{g}}}\right]\\ &\equiv J_q^{\prime\mathrm{l}}\Delta_{\mathrm{l,g}}\left(\frac{1}{T}\right)+J\left[-\frac{\Delta_{\mathrm{l,g}}\mu(T^{\mathrm{g}})}{T^{\mathrm{g}}}\right]\end{aligned} \tag{11.9}$$

The standard state for the liquid is the pure liquid at p_0 (1 bar) (see Appendix 3.A). The chemical potential of the pure liquid in equilibrium with and ideal vapor at the liquid temperature is

$$\mu^{\mathrm{l}}(T)=\mu^{\mathrm{g},0}(T)+RT\ln\frac{p^*(T)}{p_0} \tag{11.10}$$

where $p^*(T)$ is the pressure of the vapor in equilibrium with the liquid at the temperature T. This pressure is referred to as the vapor pressure of the liquid or the saturation pressure. The chemical potential of an ideal vapor at the temperature T and at the real pressure, p, is:

$$\mu^{\mathrm{g}}(T)=\mu^{\mathrm{g},0}(T)+RT\ln\frac{p}{p_0} \tag{11.11}$$

By subtracting Eq. (11.10) from Eq. (11.11), we find:

$$-\frac{\Delta_{\mathrm{l,g}}\mu(T)}{T}=-R\ln\frac{p}{p^*(T)} \tag{11.12}$$

This expression assumes the gas to be ideal. For a non-ideal gas one must replace the pressure by the fugacity (see Appendix 3.A). The curvature of the meniscus in Fig. 11.1 is too large to have an impact on the chemical potential. By substituting this relation into the entropy production, Eqs. (11.8) and (11.9), we obtain

$$\sigma^{\mathrm{s}}=J_q^{\prime\mathrm{g}}\Delta_{\mathrm{l,g}}(\frac{1}{T})+J\left[-R\ln\frac{p}{p^*(T^{\mathrm{l}})}\right]=J_q^{\prime\mathrm{l}}\Delta_{\mathrm{l,g}}\left(\frac{1}{T}\right)+J\left[-R\ln\frac{p}{p^*(T^{\mathrm{g}})}\right] \tag{11.13}$$

If the temperature is continuous and the vapor pressure of the liquid is larger than the pressure in the vapor, there will be evaporation. When it is lower, there is condensation. A temperature difference may also give rise to evaporation or condensation. Some temperature conditions may give rise to a vapor which is supersaturated with respect to the liquid [36].

Exercise 11.1.1. *Derive that* $\Delta_{l,g}\mu(T^l) = (p - p^*(T^l))/c^g$ *for any gas, using Gibbs–Duhem's equation. Show that this is equivalent to Eq. (11.12) for an ideal gas.*

- **Solution:** According to Gibbs–Duhem's equation for the liquid and the vapor, $d\mu = c^{-1}dp - sdT$. In global equilibrium with both phases present, the chemical potentials are uniquely determined by the temperature. Thus, for the temperature of the liquid, T^{l}, the corresponding saturation pressure, $p^*(T^{\mathrm{l}})$, and chemical potential, $\mu^*(T^{\mathrm{l}})$, are known. We write

$$\Delta_{\mathrm{l,g}}\mu(T^{\mathrm{l}}) = \mu^{\mathrm{g}}(T^{\mathrm{l}}) - \mu^{\mathrm{l}}(T^{\mathrm{l}}) = \mu^{\mathrm{g}}(T^{\mathrm{l}}) - \mu^*(T^{\mathrm{l}}) + \mu^*(T^{\mathrm{l}}) - \mu^{\mathrm{l}}(T^{\mathrm{l}})$$

  By using Gibbs–Duhem's equation, it follows that

$$\Delta_{\mathrm{l,g}}\mu(T^{\mathrm{l}}) = (p - p^*(T^{\mathrm{l}}))/c^{\mathrm{g}} + (p^*(T^{\mathrm{l}}) - p)/c^{\mathrm{l}}$$

  Because $c^{\mathrm{l}} \gg c^{\mathrm{g}}$ it follows that $\Delta_{\mathrm{l,g}}\mu(T^{\mathrm{l}}) = (p - p^*(T^{\mathrm{l}}))/c^{\mathrm{g}}$, which is what we set out to derive. By using the small difference between the gas pressure and the vapor pressure of the liquid, we also have

$$\ln\left[p/p^*(T^{\mathrm{l}})\right] = \ln[1 - (p^*(T^{\mathrm{l}}) - p)/p^*(T^{\mathrm{l}})] = -(p^*(T^{\mathrm{l}}) - p)/p^*(T^{\mathrm{l}})$$

  The ideal gas law then gives

$$R\ln\left[p/p^*(T^{\mathrm{l}})\right] = (p - p^*(T^{\mathrm{l}}))/c^{\mathrm{g}}T^{\mathrm{l}}$$

  which shows the equivalence.

Exercise 11.1.2. *Derive the thermodynamic identity (11.6).*

- **Solution:** We have

$$\left[\frac{\partial\,(\mu/T)}{\partial\,(1/T)}\right]_p = \frac{1}{T}\left[\frac{\partial\mu}{\partial\,(1/T)}\right]_p + \mu = \frac{1}{T}\left(\frac{\partial\mu}{\partial T}\right)_p \frac{dT}{d(1/T)} + \mu$$
$$= -T\left(\frac{\partial\mu}{\partial T}\right)_p + \mu$$

where we used the chain rule in the second equality. The chemical potential satisfies

$$d\mu = Vdp - SdT$$

The derivative is, accordingly,

$$\left[\frac{\partial\left(\mu/T\right)}{\partial\left(1/T\right)}\right]_p = TS + \mu = H$$

which proves the thermodynamic identity.

The flux equations that follow from Eq. (11.13), are either

$$\begin{aligned}\Delta_{\mathrm{l,g}}\left(\frac{1}{T}\right) &= r^{\mathrm{s,g}}_{qq}J'^{\mathrm{g}}_{q} + r^{\mathrm{s,g}}_{q\mu}J\\ -R\ln\frac{p}{p^*(T^{\mathrm{l}})} &= r^{\mathrm{s,g}}_{\mu q}J'^{\mathrm{g}}_{q} + r^{\mathrm{s,g}}_{\mu\mu}J\end{aligned} \tag{11.14}$$

or

$$\begin{aligned}\Delta_{\mathrm{l,g}}\left(\frac{1}{T}\right) &= r^{\mathrm{s,l}}_{qq}J'^{\mathrm{l}}_{q} + r^{\mathrm{s,l}}_{q\mu}J\\ -R\ln\frac{p}{p^*(T^{\mathrm{g}})} &= r^{\mathrm{s,l}}_{\mu q}J'^{\mathrm{l}}_{q} + r^{\mathrm{s,l}}_{\mu\mu}J\end{aligned} \tag{11.15}$$

Onsager relations apply, so $r^{\mathrm{s,g}}_{q\mu} = r^{\mathrm{s,g}}_{\mu q}$ and $r^{\mathrm{s,l}}_{q\mu} = r^{\mathrm{s,l}}_{\mu q}$. Using the relation between the heat fluxes in the vapor and the liquid given in Eq. (11.4) and Eq. (11.6) one may derive the following relation between the interface resistivities for both sides of the surface:

$$\begin{aligned}r^{\mathrm{s,l}}_{qq} &= r^{\mathrm{s,g}}_{qq} \equiv r^{\mathrm{s}}_{qq}\\ r^{\mathrm{s,l}}_{q\mu} &= r^{\mathrm{s,l}}_{\mu q} = r^{\mathrm{s,g}}_{q\mu} - \Delta_{vap}Hr^{\mathrm{s}}_{qq} = r^{\mathrm{s,g}}_{\mu q} - \Delta_{vap}Hr^{\mathrm{s}}_{qq}\\ r^{\mathrm{s,l}}_{\mu\mu} &= r^{\mathrm{s,g}}_{\mu\mu} - 2\Delta_{vap}Hr^{\mathrm{s,g}}_{\mu q} + \left(\Delta_{vap}H\right)^2 r^{\mathrm{s}}_{qq}\end{aligned} \tag{11.16}$$

where we used the Onsager symmetry relations and where $\Delta_{vap}H \equiv H^{\mathrm{g}} - H^{\mathrm{l}}$ is the enthalpy of evaporation. Because of the Onsager relations there are only three independent coefficients that describe the transport of heat and mass *across* the surface in stationary evaporation and condensation. We shall use the name *interface resistivities* or *interface transfer coefficients* for the surface coefficients*. When the heat and the mass transfer coefficients are negligible, the temperatures on both sides of the surface become identical, while the pressure becomes equal to the vapor pressure. The liquid and the vapor close to the surface are then in equilibrium with

*In Refs. [36–38] we absorbed a common factor T^{l} in these interface resistivities.

one another. The temperature and pressure are then related by Clausius–Clapeyron's equation. For larger interface resistivities, the pressure will deviate from the vapor pressure of the liquid, and the temperatures of the liquid and the vapor close to the surface will differ from each other.

The temperature, the pressure and the mass flux can be measured. It is then convenient to write, using the Onsager relations, the flux-force relations in the following form

$$\begin{aligned} \Delta_{\mathrm{l,g}}T &= -\frac{1}{\lambda^{\mathrm{s,g}}}\left(J_q'^{\mathrm{g}} - q^{*,\mathrm{s,g}}J\right) \\ -R\ln\frac{p}{p^*(T^{\mathrm{l}})} &= q^{*,\mathrm{s,g}}\frac{\Delta_{\mathrm{l,g}}T}{T^{\mathrm{l}}T^{\mathrm{g}}} + \left(r_{\mu\mu}^{\mathrm{s,g}} - r_{qq}^{\mathrm{s,g}}\left(q^{*,\mathrm{s,g}}\right)^2\right)J \end{aligned} \tag{11.17}$$

where the thermal conductivity at zero mass flux and the heat of transfer at the vapor side of the surface are defined by

$$\lambda^{\mathrm{s,g}} \equiv -\left[\frac{J_q'^{\mathrm{g}}}{\Delta_{\mathrm{l,g}}T}\right]_{J=0} = \frac{1}{T^{\mathrm{l}}T^{\mathrm{g}}r_{qq}^{\mathrm{s,g}}} \quad \text{and} \quad q^{*,\mathrm{s,g}} = \left(\frac{J_q'^{\mathrm{g}}}{J}\right)_{\Delta_{\mathrm{l,g}}T=0} = -\frac{r_{q\mu}^{\mathrm{s,g}}}{r_{qq}^{\mathrm{s,g}}} \tag{11.18}$$

In the absence of a mass flux, the heat of transfer can also be found from the known temperatures and pressures:

$$q^{*,\mathrm{s,g}} = -\left[\frac{RT^{\mathrm{l}}T^{\mathrm{g}}\ln\left(p/p^*(T^{\mathrm{l}})\right)}{\Delta_{\mathrm{l,g}}T}\right]_{J=0} \tag{11.19}$$

where we used the Onsager relation.

Using the measurable heat flux, one may alternatively write the flux-force relations in the following form

$$\begin{aligned} \Delta_{\mathrm{l,g}}T &= -\frac{1}{\lambda^{\mathrm{s,l}}}\left(J_q'^{\mathrm{l}} - q^{*,\mathrm{s,l}}J\right) \\ -R\ln\frac{p}{p^*(T^{\mathrm{g}})} &= q^{*,\mathrm{s,l}}\frac{\Delta_{\mathrm{l,g}}T}{T^{\mathrm{l}}T^{\mathrm{g}}} + \left(r_{\mu\mu}^{\mathrm{s,l}} - r_{qq}^{\mathrm{s,l}}\left(q^{*,\mathrm{s,l}}\right)^2\right)J \end{aligned} \tag{11.20}$$

where the thermal conductivity at zero mass flux and the heat of transfer at the liquid side of the surface are defined by

$$\lambda^{\mathrm{s,l}} \equiv -\left[\frac{J_q'^{\mathrm{l}}}{\Delta_{\mathrm{l,g}}T}\right]_{J=0} = \frac{1}{T^{\mathrm{l}}T^{\mathrm{g}}r_{qq}^{\mathrm{s,l}}} \quad \text{and} \quad q^{*,\mathrm{s,l}} = \left(\frac{J_q'^{\mathrm{l}}}{J}\right)_{\Delta T=0} = -\frac{r_{q\mu}^{\mathrm{s,l}}}{r_{qq}^{\mathrm{s,l}}} \tag{11.21}$$

In the absence of a mass flux, the heat of transfer can also be found from the known temperatures and pressures:

$$q^{*,\mathrm{s,l}} = -\left[\frac{RT^{\mathrm{l}}T^{\mathrm{g}}\ln\left(p/p^*(T^{\mathrm{g}})\right)}{\Delta_{\mathrm{l,g}}T}\right]_{J=0} \tag{11.22}$$

where we used the Onsager relation.

Bedeaux *et al.* [36, 37] and Kjelstrup *et al.* [167] used these equations to discuss the possibility of an inverted temperature profile in front of the surface of an evaporating fluid.

11.1.2 *Interface resistivities from kinetic theory*

Considerable work has been done on evaporation and condensation, using the kinetic theory of gases, cf. [36,37] and references therein. The resistivity transfer coefficients of Eqs. (11.14) according to kinetic theory are [34, 36, 168]:

$$\begin{aligned} r_{qq}^{\mathrm{s,g}} &= \frac{\sqrt{\pi}}{4c_{eq}^{\mathrm{g}}(T^{\mathrm{s}})R(T^{\mathrm{s}})^2\mathrm{v}_{mp}(T^{\mathrm{s}})}\left(1+\frac{104}{25\pi}\right) \\ r_{q\mu}^{\mathrm{s,g}} &= r_{\mu q}^{\mathrm{s,g}} = \frac{\sqrt{\pi}}{8T^{\mathrm{s}}c_{eq}^{\mathrm{g}}(T^{\mathrm{s}})\mathrm{v}_{mp}(T^{\mathrm{s}})}\left(1+\frac{16}{5\pi}\right) \\ r_{\mu\mu}^{\mathrm{s,g}} &= \frac{2R\sqrt{\pi}}{c_{eq}^{\mathrm{g}}(T^{\mathrm{s}})\mathrm{v}_{mp}(T^{\mathrm{s}})}\left(\sigma^{-1}+\frac{1}{\pi}-\frac{23}{32}\right) \end{aligned} \tag{11.23}$$

Here $\mathrm{v}_{mp}\ (T^{\mathrm{s}}) \equiv \sqrt{2\mathrm{R}T^{\mathrm{s}}/M}$ is the most probable thermal velocity and M is the molar mass. The condensation coefficient, σ, is defined as the fraction of incident particles which, after collision with the liquid surface, are absorbed by the liquid. Compared to the expressions we gave in [36] we replaced all the temperatures by the temperature of the surface and took the equilibrium coexistence density of the gas. In view of the fact that the interface resistivities are properties of the surface they should only depend on variables characteristic for the surface. The surface temperature is such a variable. In molecular dynamics simulations with a relatively short-range Lennard-Jones spline potential [67] we found this choice to give better agreement with kinetic theory.

The expressions are most appropriate for hard spheres near the triple point. The number of moles of particles that collide with the liquid surface is proportional to the mean thermal velocity, v_{mp}, times the molar density in the gas, c^{g}. The prefactor is characteristic for the quantity transported,

and follows from a comparison with the flux-force relation. Experimental values of σ between 0.1 and 1 have been reported [169]. The actual value is somewhat controversial. In an ideal gas, the most probable thermal velocity is equal to $\sqrt{6/5}$ times the velocity of sound. Only one resistivity depends on the condensation coefficient. The set of resistivities is thus most suitable for comparison with kinetic theory. Once $r^{\mathrm{s,g}}_{\mu\mu}$ is known, it gives a unique way to fit the condensation coefficient. Polyatomic gases have also been described by kinetic theory [35], but similarly convenient expressions are not available.

The heat of transfer of the surface becomes

$$q^{*,\mathrm{s,g}} = -\frac{5}{2}\left(\frac{5\pi+16}{25\pi+104}\right) RT^{\mathrm{s}} \tag{11.24}$$

and the thermal conductivity at zero mass flux is

$$\lambda^{\mathrm{s,g}} = \frac{100\sqrt{\pi}c^{\mathrm{g}}_{eq}(T^{\mathrm{s}})R\mathrm{v}_{mp}(T^{\mathrm{s}})}{(25\pi+104)} \tag{11.25}$$

Neither of these coefficients depend on the condensation coefficient. An important property of the heat of transfer $q^{*,\mathrm{s,g}}$ found by kinetic theory is that it is negative.

The scaling coefficients k_q and k_μ (see Sec. 8.5) can be found with kinetic theory as basis. The thermal conductivity and the self-diffusion coefficient in a low density gas are given by

$$\lambda_{\mathrm{g}} = \frac{1}{2}c^{\mathrm{g}}_{eq}(T^{\mathrm{s}})\mathrm{v}_{mp}(T^{\mathrm{s}})\ell(T^{\mathrm{s}})R\sqrt{3/2} \quad \text{and} \quad D_{s,\mathrm{g}} = \ell(T^{\mathrm{s}})\mathrm{v}_{mp}(T^{\mathrm{s}})/\sqrt{6} \tag{11.26}$$

where $\ell(T^{\mathrm{s}}) = (\pi a^2 c^{\mathrm{g}}_{eq}(T^{\mathrm{s}})\mathrm{N})^{-1}$ is the mean free path, or the Knudsen length in equilibrium at the temperature of the surface. The scaling coefficients for heat and mass transport of the surface are therefore

$$\begin{aligned} k_q &= \frac{r^{\mathrm{s,g}}_{qq}}{r^{\mathrm{g}}_{qq}\delta} \simeq \frac{\lambda_{\mathrm{g}}}{\lambda_{\mathrm{s}}\delta} = 0.63905\left(\frac{\ell(T^{\mathrm{s}})}{\delta}\right) \\ k_\mu &= \frac{r^{\mathrm{s}}_{\mu\mu}c^{\mathrm{g}}_{eq}(T^{\mathrm{s}})D_{s,\mathrm{g}}}{R\delta} = 1.44720\left(\sigma^{-1}-0.39856\right)\left(\frac{\ell(T^{\mathrm{s}})}{\delta}\right) \end{aligned} \tag{11.27}$$

The order of magnitude of both scaling coefficients is determined by $\ell(T^{\mathrm{s}})/\delta$. When the thickness of the surface is of the same order as 1.5 times the diameter of the particles the ratio $\ell(T^{\mathrm{s}})/\delta$ is roughly equal to

the volume of the particles divided by the available volume per particle ($\simeq c^{\mathrm{l}}/c^{\mathrm{g}} \simeq 1000$ for water). The scaling coefficients show how effective the surface is as a barrier for transport: A surface with a thickness of about a nanometer insulates just as well as a vapor layer of about a micrometer thick. The scaling coefficient for heat transfer is independent of the condensation coefficient, while the scaling coefficient for mass transfer depends on this parameter.

11.2 The sign of the heats of transfer of the surface

In the analysis above, we used the stationary nature of the problem to reduce the number of independent flux-force pairs to two. Alternatively, one can use all four force flux-pairs in Eq. (11.5). Neglecting the coupling of forces and fluxes from different sides of the surface it follows, analogous to the derivation of Eqs. (8.14) and (8.15), that

$$\begin{aligned}
\frac{1}{T^{\mathrm{s}}} - \frac{1}{T^{\mathrm{l}}} &= R^{\mathrm{s,l}}_{qq} J'^{\mathrm{l}}_q + R^{\mathrm{s,l}}_{q\mu} J \\
-\frac{\mu^{\mathrm{s}}(T^{\mathrm{s}}) - \mu^{\mathrm{l}}(T^{\mathrm{s}})}{T^{\mathrm{s}}} &= R^{\mathrm{s,l}}_{\mu q} J'^{\mathrm{l}}_q + R^{\mathrm{s,l}}_{\mu\mu} J \\
\frac{1}{T^{\mathrm{g}}} - \frac{1}{T^{\mathrm{s}}} &= R^{\mathrm{s,g}}_{qq} J'^{\mathrm{g}}_q + R^{\mathrm{s,g}}_{q\mu} J \\
-\frac{\mu^{\mathrm{g}}(T^{\mathrm{s}}) - \mu^{\mathrm{s}}(T^{\mathrm{s}})}{T^{\mathrm{s}}} &= R^{\mathrm{s,g}}_{\mu q} J'^{\mathrm{g}}_q + R^{\mathrm{s,g}}_{\mu\mu} J
\end{aligned} \tag{11.28}$$

where we used $J^{\mathrm{l}} = J^{\mathrm{g}} = J$. The heats of transfer in the pure fluids are zero. This gives

$$R^{\mathrm{s,l}}_{q\mu} = R^{\mathrm{s,l}}_{\mu q} = -R^{\mathrm{s,l}}_{qq} q^{*,\mathrm{l}} = 0 \quad \text{and} \quad R^{\mathrm{s,g}}_{q\mu} = R^{\mathrm{s,g}}_{\mu q} = -R^{\mathrm{s,g}}_{qq} q^{*,\mathrm{g}} = 0 \tag{11.29}$$

Eq. (11.28) therefore reduces to

$$\begin{aligned}
\frac{1}{T^{\mathrm{s}}} - \frac{1}{T^{\mathrm{l}}} &= R^{\mathrm{s,l}}_{qq} J'^{\mathrm{l}}_q, \quad & -\frac{\mu^{\mathrm{s}}(T^{\mathrm{s}}) - \mu^{\mathrm{l}}(T^{\mathrm{s}})}{T^{\mathrm{s}}} &= R^{\mathrm{s,l}}_{\mu\mu} J \\
\frac{1}{T^{\mathrm{g}}} - \frac{1}{T^{\mathrm{s}}} &= R^{\mathrm{s,g}}_{qq} J'^{\mathrm{g}}_q, \quad & -\frac{\mu^{\mathrm{g}}(T^{\mathrm{s}}) - \mu^{\mathrm{s}}(T^{\mathrm{s}})}{T^{\mathrm{s}}} &= R^{\mathrm{s,g}}_{\mu\mu} J
\end{aligned} \tag{11.30}$$

Addition of the inverse temperature differences gives

$$\frac{1}{T^{\mathrm{g}}} - \frac{1}{T^{\mathrm{l}}} = R^{\mathrm{s,l}}_{qq} J'^{\mathrm{l}}_q + R^{\mathrm{s,g}}_{qq} J'^{\mathrm{g}}_q = \left(R^{\mathrm{s,l}}_{qq} + R^{\mathrm{s,g}}_{qq}\right) J'^{\mathrm{g}}_q + R^{\mathrm{s,l}}_{qq} \Delta_{vap} H J \tag{11.31}$$

Addition of the chemical potential differences gives

$$\begin{aligned}
-\frac{\mu^{\mathrm{g}}(T^{\mathrm{s}})-\mu^{\mathrm{l}}(T^{\mathrm{s}})}{T^{\mathrm{s}}} &= -\frac{\mu^{\mathrm{g}}(T^{\mathrm{l}})-\mu^{\mathrm{l}}(T^{\mathrm{l}})}{T^{\mathrm{l}}} \\
&\quad - \left[\frac{\partial}{\partial(1/T)}\left(\frac{\mu^{\mathrm{g}}}{T}-\frac{\mu^{\mathrm{l}}}{T}\right)_{T=T^{\mathrm{l}}}\right]\left(\frac{1}{T^{\mathrm{s}}}-\frac{1}{T^{\mathrm{l}}}\right) \\
&= -\frac{\mu^{\mathrm{g}}(T^{\mathrm{l}})-\mu^{\mathrm{l}}(T^{\mathrm{l}})}{T^{\mathrm{l}}} - R^{\mathrm{s,l}}_{qq}\Delta_{vap}H J^{\prime\mathrm{l}}_{q} \\
&= -\frac{\mu^{\mathrm{g}}(T^{\mathrm{l}})-\mu^{\mathrm{l}}(T^{\mathrm{l}})}{T^{\mathrm{l}}} - R^{\mathrm{s,l}}_{qq}\Delta_{vap}H J^{\prime\mathrm{g}}_{q} - R^{\mathrm{s,l}}_{qq}\left(\Delta_{vap}H\right)^2 J \\
&= \left(R^{\mathrm{s,l}}_{\mu\mu}+R^{\mathrm{s,g}}_{\mu\mu}\right) J
\end{aligned} \tag{11.32}$$

It follows that

$$-\frac{\mu^{\mathrm{g}}(T^{\mathrm{l}})-\mu^{\mathrm{l}}(T^{\mathrm{l}})}{T^{\mathrm{l}}} = R^{\mathrm{s,l}}_{qq}\Delta_{vap}H J^{\prime\mathrm{g}}_{q} + \left(R^{\mathrm{s,l}}_{\mu\mu}+R^{\mathrm{s,g}}_{\mu\mu}+R^{\mathrm{s,l}}_{qq}\left(\Delta_{vap}H\right)^2\right) J \tag{11.33}$$

By comparing Eqs. (11.31) and (11.33) with Eq. (11.14) and Eq. (11.12), we conclude that

$$\begin{gathered}
r^{\mathrm{s,g}}_{qq} = R^{\mathrm{s,l}}_{qq} + R^{\mathrm{s,g}}_{qq}, \quad r^{\mathrm{s,g}}_{q\mu} = r^{\mathrm{s,g}}_{\mu q} = R^{\mathrm{s,l}}_{qq}\Delta_{vap}H \\
r^{\mathrm{s,g}}_{\mu\mu} = R^{\mathrm{s,l}}_{\mu\mu} + R^{\mathrm{s,g}}_{\mu\mu} + R^{\mathrm{s,l}}_{qq}\left(\Delta_{vap}H\right)^2
\end{gathered} \tag{11.34}$$

Since $R^{\mathrm{s,l}}_{qq}$, $R^{\mathrm{s,g}}_{qq}$ and $\Delta_{vap}H$ are positive, $q^{*,\mathrm{s,g}}$ is negative. This is an independent confirmation of the result found in kinetic theory. Its absolute size is given by the fraction of the thermal resistivity located on the liquid side of the surface times the latent heat, $\Delta_{vap}H$. It is clear that $q^{*,\mathrm{s,g}}$ has no relation to the transported heats in the liquid and the vapor, which are both zero. Using Eq. (11.16b) it follows that

$$\begin{gathered}
r^{\mathrm{s,l}}_{qq} = r^{\mathrm{s,g}}_{qq} = R^{\mathrm{s,l}}_{qq} + R^{\mathrm{s,g}}_{qq}, \quad r^{\mathrm{s,l}}_{q\mu} = r^{\mathrm{s,l}}_{\mu q} = -R^{\mathrm{s,g}}_{qq}\Delta_{vap}H \\
r^{\mathrm{s,l}}_{\mu\mu} = R^{\mathrm{s,l}}_{\mu\mu} + R^{\mathrm{s,g}}_{\mu\mu} + R^{\mathrm{s,g}}_{qq}\left(\Delta_{vap}H\right)^2
\end{gathered} \tag{11.35}$$

This implies that $q^{*,\mathrm{s,l}}$ is positive. An important property that follows from Eqs. (11.34), (11.35) and the definition of the heat transfer coefficients is

$$q^{*,\mathrm{s,g}} - q^{*,\mathrm{s,l}} = -\Delta_{vap}H \tag{11.36}$$

Compare with Eq. (8.29).

Using the ideal gas value of the enthalpy in the vapor, $H^{\mathrm{g}} = 2.5RT^{\mathrm{s}}$, and the estimate $H^{\mathrm{l}} = -1.5RT^{\mathrm{s}}$ for the liquid, the latent heat becomes $\Delta_{vap}H \simeq 4RT^{\mathrm{s}}$. Together with the expressions (11.23) from kinetic theory, one obtains

$$\begin{aligned} R_{qq}^{\mathrm{s,l}} &= \frac{r_{q\mu}^{\mathrm{s,g}}}{\Delta_{vap}H} = \frac{\sqrt{\pi}}{40R(T^{\mathrm{s}})^2 c_{eq}^{\mathrm{g}}(T^{\mathrm{s}})\mathrm{v}_{mp}(T^{\mathrm{s}})}\left(1+\frac{16}{5\pi}\right) \\ R_{qq}^{\mathrm{s,g}} &= r_{qq}^{\mathrm{s,g}} - \frac{r_{q\mu}^{\mathrm{s,g}}}{\Delta_{vap}H} = \frac{\sqrt{\pi}}{4R(T^{\mathrm{s}})^2 c_{eq}^{\mathrm{g}}(T^{\mathrm{s}})\mathrm{v}_{mp}(T^{\mathrm{s}})}\left(\frac{7}{8}+\frac{94}{25\pi}\right) \\ R_{\mu\mu}^{\mathrm{s,l}} + R_{\mu\mu}^{\mathrm{s,g}} &= r_{\mu\mu}^{\mathrm{s}} - r_{q\mu}^{\mathrm{s}}\Delta_{vap}H = \frac{2R\sqrt{\pi}}{c_{eq}^{\mathrm{g}}(T^{\mathrm{s}})\mathrm{v}_{mp}(T^{\mathrm{s}})}\left(\sigma^{-1}+\frac{1}{5\pi}-\frac{31}{32}\right) \end{aligned} \tag{11.37}$$

The thermal resistivity on the vapor side is thus about 10 times the thermal resistivity on the liquid side. This depends on the choice of H^{l}. If we reduce H^{l} to zero this ratio decreases to 5. When we choose $H^{\mathrm{l}} = -2.5RT^{\mathrm{s}}$ it follows that $R_{\mu\mu}^{\mathrm{s,l}} + R_{\mu\mu}^{\mathrm{s,g}}$ is negative for $\sigma = 1$. This is why we used the not unreasonable estimate $H^{\mathrm{l}} = -1.5RT^{\mathrm{s}}$. Because $J^{\mathrm{l}} = J^{\mathrm{g}} = J$, it is not possible to give expressions for $R_{\mu\mu}^{\mathrm{s,l}}$ and $R_{\mu\mu}^{\mathrm{s,g}}$ separately.

Remark 11.1. *One might think that kinetic theory gives only the resistivities on the vapor side of the surface. This is not correct. Kinetic theory uses boundary conditions, which model the whole surface. The above analysis shows this very clearly.*

11.3 Coefficients from molecular dynamics simulations

In non-equilibrium molecular dynamics simulations (NEMD), the computer is used to solve Newton's equations for a many particle system. The particles interact with a Lennard-Jones type potential. The way such simulations are done is described in Chapter 22.

It was verified by Røsjorde *et al.* [39] and by Simon *et al.* [112] that the surface temperature was the same function of the surface tension in stationary state simulations as in equilibrium simulations. This implies that the surface is in local equilibrium (see also Chapters 22 and 23).

NEMD was also used to determine the interface transfer coefficients of a pure fluid [40,67,170] and of a two-component fluid [171]. The Lennard-Jones spline potential was used to describe the interparticle interaction in these simulations. The potential minimum and the diameter were chosen identical to those of argon in the one-component fluid.

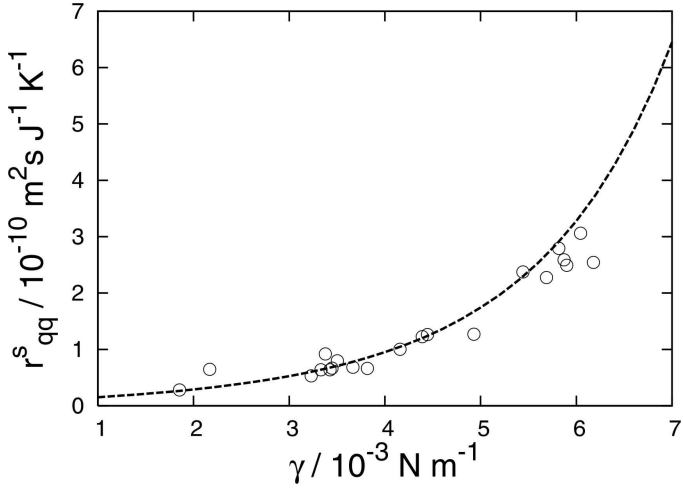

Figure 11.2 The main coefficients for heat transfer, $r^s_{qq} = r^{s,g}_{qq} = r^{s,l}_{qq}$, from NEMD simulations in $m^2 s\ J^{-1} K^{-1}$, as a function of the surface tension. The dashed line is the value predicted by kinetic theory. Reproduced from J. Colloid Interface Sci. 299 (2006) 452–463 with permission from Elsevier.

Figures 11.2–11.4 show the results of the simulations for the interface resistivities in the pure fluid [67]. The resistivities are plotted as functions of the surface tension. The surface tension increases as we move from the critical point ($\gamma = 0$) to the triple point in the phase diagram.

In Figs. 11.2 and 11.4 the values predicted by kinetic theory are plotted as dashed, dotted or dash-dotted lines. All interface resistivities go to zero towards the critical point, when $\gamma = 0$. As the liquid and the vapor become indistinguishable in that limit, this is to be expected. The variation observed in the figures as a function of the surface tension is therefore physically reasonable. The surface tension is a unique function of the surface temperature. A high surface tension corresponds to a low temperature. At the triple point, the vapor is closest to being ideal. The surface has its maximum resistance to transfer of both heat and mass close to the triple point.

Figure 11.4 shows that the coupling coefficients, $r^{s,g}_{q\mu}$, $r^{s,g}_{\mu q}$ on the vapor side and $r^{s,l}_{q\mu}$, $r^{s,l}_{\mu q}$ on the liquid side, satisfy the Onsager symmetry relations within the accuracy of the simulation. These simulations [67] were the first simulations which verified the validity of the Onsager relations for the surface. In Fig. 11.5, the resulting heats of transfer are plotted. These are labelled $q^{*,s,g}_{q\mu}$, $q^{*,s,g}_{\mu q}$ and $q^{*,s,l}_{q\mu}$, $q^{*,s,l}_{\mu q}$ to indicate the cross coefficient from

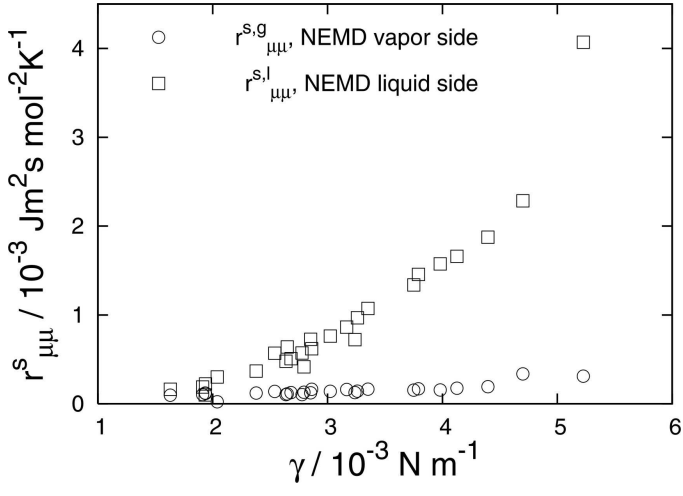

Figure 11.3 The main coefficients for mass transfer, $r^{s,g}_{\mu\mu}$ and $r^{s,l}_{\mu\mu}$, from NEMD simulations in J m^{2}s mol^{-2}K^{-1}, as a function of surface tension. Reproduced from J. Colloid Interface Sci. 299 (2006) 452–463 with permission from Elsevier.

which they were calculated. A special feature of $q^{*,s,g}$ is its negative sign. The origin of this negative sign was explained in the previous section. One similarly finds that $q^{*,s,l}$ is positive. For condensation, this means that there is transport of heat by mass transport both through the vapor and through the liquid away from the surface. During evaporation, it means that there is heat transport by mass transport to the surface both through the vapor and through the liquid.

In the simulations the coefficients were derived for a condensing system, but they are equally valid for an evaporating system. They describe evaporation and condensation of a Lennard-Jones spline, one-component fluid for most conditions encountered in practice. We have found that the flux-force relations are linear, in spite of the very large temperature gradient across the system used in the simulations (10^8 K/m). It is therefore likely that the flux-force relations will be linear for the considerably smaller gradients that are encountered in practice.

The simulation results for the interface resistivity for heat transfer, $r^{s,g}_{qq} = r^{s,l}_{qq}$, and the coupling interface resistivity, $r^{s,g}_{q\mu} = r^{s,g}_{\mu q}$ and $r^{s,l}_{q\mu} = r^{s,l}_{\mu q}$, agree very well with the values predicted by kinetic theory, see Figs. 11.2 and 11.4. The agreement is better close to the triple point. In the just mentioned figures this is not so visible because the resistivities are small

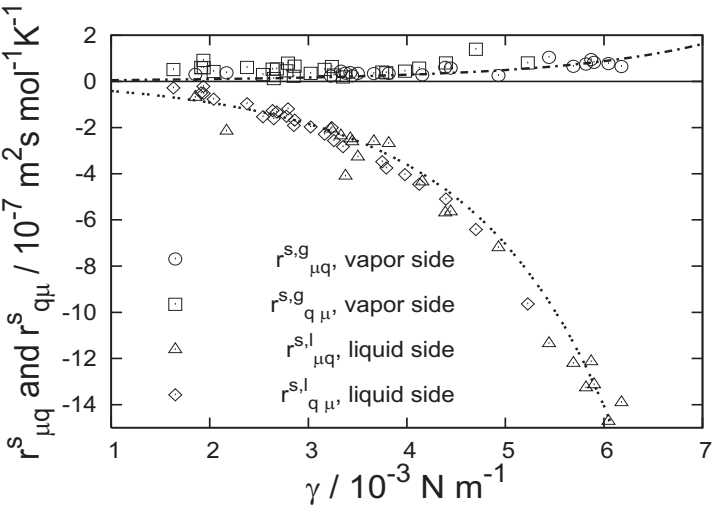

Figure 11.4 The coupling coefficients for heat and mass transfer, $r^{s,g}_{q\mu}$, $r^{s,g}_{\mu q}$ and $r^{s,l}_{q\mu}$, $r^{s,l}_{\mu q}$ from NEMD simulations (in m^2s $mol^{-1}K^{-1}$), as a function of the surface tension. The dotted and the dash-dotted lines are the predictions from kinetic theory. Reproduced from J. Colloid Interface Sci. 299 (2006) 452–463 with permission from Elsevier.

close to the critical point. In Fig. 11.5 for the heats of transfer, which are the ratios of two interface resistivities, this lack of agreement close to the critical point is more clearly visible. This agreement of the simulation data with kinetic theory is special for the Lennard-Jones spline potential. There is no such agreement for the simulations for octane [112] or for a cut-off Lennard-Jones potential [167]. In recent simulations using a longer range Lennard-Jones spline potential, we found that in particular the size of the coupling coefficient increases substantially above the kinetic theory value.

The value predicted by kinetic theory for the interface resistivity to mass transfer on the vapor side, $r^{s,g}_{\mu\mu}$, contains the condensation coefficient. It was possible to fit this coefficient using the values obtained for the interface resistivity in the NEMD simulations using a Lennard-Jones spline potential, see Fig. 11.6. The accuracy of the resulting values is about 20%. The value increases from a value near 0.1 near the critical point to a value of about 0.8 near the triple point. The value is reasonable, and agrees with molecular dynamics simulations by Tsuruta and Nagayama [172].

Kinetic theory and NEMD are helpful in the sense that they give a mechanistic picture of the collision of particles in the vapor phase with

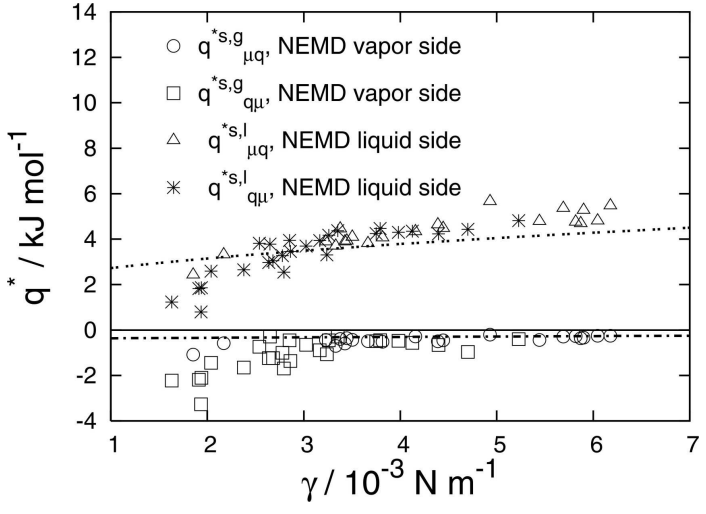

Figure 11.5 The heats of transfer, $q^{*,s,g}_{q\mu}$, $q^{*,s,g}_{\mu q}$ and $q^{*,s,l}_{q\mu}$, $q^{*,s,l}_{\mu q}$ from NEMD simulations (in kJ mol^{-1}), as a function of the surface tension. Reproduced from J. Colloid Interface Sci. 299 (2006) 452–463 with permission from Elsevier.

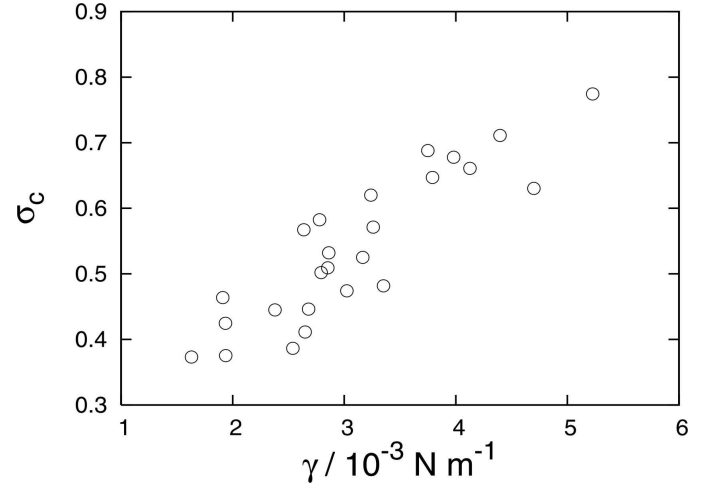

Figure 11.6 The condensation coefficient for molecular dynamics simulations of a fluid using a Lennard-Jones spline potential as a function of the surface tension. Reproduced from J. Colloid Interface Sci. 299 (2006) 452–463 with permission from Elsevier.

the liquid surface. The NEMD simulations for the relatively short-range Lennard-Jones spline fluid reproduced the interface resistivities from kinetic theory along the coexistence curve from the triple point until about halfway to the critical point. The density of the vapor is lowest close to the triple point. It is therefore not unexpected that the agreement between simulated and computed results is best near the triple point. As the Lennard-Jones spline vapor is still far from ideal in the triple point, the agreement is better than what one might have expected.

The values of the interface resistivities found from both NEMD simulations and from kinetic theory lead to discontinuities in the temperature at the surface of a few tenths of a degree rather than a few degrees. As shown by Bedeaux and Kjelstrup [38] it is necessary to use much larger interface resistivities to explain the temperature differences of several degrees found by Fang and Ward [160–162] or Phillips and coworkers [163, 164, 173]. The non-equilibrium van der Waals square gradient model contains a free parameter related to the behavior of the thermal resistivity in the interfacial region. This makes it possible to model larger interfacial resistivities [108]. It is interesting to study their relative size, but it does not resolve the question of why they are possibly so large.

Exercise 11.3.1. *Consider stationary evaporation of water. The liquid enters the evaporation chamber at $x = -2$ cm with room temperature (300 K), and is evacuated by an under-pressure of 2 Pa at $x = 2$ cm with room temperature. The liquid-vapor interface is at $x = 0$. The temperature at the liquid side of the surface is 0.9°C. At the vapor side of the surface, the temperature is $-2.8\,^{\circ}$C.*

Calculate the temperature profile, the heat fluxes and the mass flux, using a saturation pressure of 600 Pa and a heat of evaporation of 45 kJ/mol [174]. Find the transfer coefficients for transport across the surface. Use $r^{s,g}_{\mu q} = r^{s,g}_{q\mu} = 0.01\Delta_{vap}H\ r^{s,g}_{qq}$ for the coupling coefficients. The thermal conductivity of liquid water and water-vapor are 0.61 and 0.018 J/Kms [114], respectively.

- **Solution:** In the liquid as well as in the vapor we have

$$\partial J_q/\partial x = \partial J'_q/\partial x + \partial(hJ)/\partial x = -\partial\left(\lambda \partial T/\partial x\right)\partial x + \partial(hJ)/\partial x = 0$$

cf. Eqs. (11.3) and (11.4). As λ, h and J are all constant it follows that $\partial T/\partial x$ is constant, so that T is a linear function of position. Therefore, we have

$$T^{\mathrm{l}}(x) = T^{\mathrm{l}}(0) + (x/0.02)(T^{\mathrm{l}}(0) - 300) = T^{\mathrm{l,g}} + (x/0.02)(T^{\mathrm{l,g}} - 300)$$
$$T^{\mathrm{g}}(x) = T^{\mathrm{g}}(0) - (x/0.02)(T^{\mathrm{g}}(0) - 300) = T^{\mathrm{g,l}} - (x/0.02)(T^{\mathrm{g,l}} - 300)$$

The resulting heat fluxes in the liquid and the vapor are constant, cf. Eq. (11.3), and given by:

$$J_q'^{\mathrm{l}} = -30.5(T^{\mathrm{l,g}} - 300) = 793 \quad \text{and} \quad J_q'^{\mathrm{g}} = 0.9(T^{\mathrm{g,l}} - 300) = -26.7$$

in J/m^{2}s. Heat needed to provide the enthalpy of evaporation is conducted to the surface from the gas as well as from the liquid.

The constant mass flux is obtained from the energy balance

$$J = \frac{J_q'^{\mathrm{l}} - J_q'^{\mathrm{g}}}{\Delta_{vap}H} = 0.017 \text{ mol/m}^2\text{s}$$

The driving forces are

$$\frac{\Delta_{\mathrm{l,g}}T}{T^{\mathrm{l,g}}T^{\mathrm{g,l}}} = -\frac{274.05 - 270.35}{270.35 \times 274.05} = -0.5 \times 10^{-4} \text{ /K}$$

$$R\ln\frac{p}{p^*} = 8.314 \times \ln\left(\frac{598}{600}\right) = -2.8 \times 10^{-2} \text{ J/mol K}$$

With knowledge of the fluxes and forces, there are three unknown coefficients in the flux equations for the surface. Substituting also the relation given for the coupling resistivities, we find

$$\begin{aligned}
\frac{\Delta_{\mathrm{l,g}}T}{T^{\mathrm{l,g}}T^{\mathrm{g,l}}} &= -26.7r_{qq}^{\mathrm{s,g}} + 0.017r_{q\mu}^{\mathrm{s,g}} = -\left(26.7 - 0.00017\Delta_{vap}H\right)r_{qq}^{\mathrm{s,g}} \\
&= -19.0r_{qq}^{\mathrm{s,g}} = -0.5 \times 10^{-4} \text{ /K} \\
-R\ln\frac{p}{p^*} &= -26.7r_{\mu q}^{\mathrm{s,g}} + 0.017r_{\mu\mu}^{\mathrm{s,g}} = -0.267\Delta_{vap}Hr_{qq}^{\mathrm{s,g}} + 0.017r_{\mu\mu}^{\mathrm{s,g}} \\
&= -12000r_{qq}^{\mathrm{s,g}} + 0.017r_{\mu\mu}^{\mathrm{s,g}} = 2.8 \times 10^{-2}\text{J/mol K}
\end{aligned}$$

By solving the two unknowns from these equations, and obtaining the coupling resistivity using the expression given above, we find

$$r_{qq}^{\mathrm{s,g}} = 2.63 \times 10^{-5} \text{ m}^2\text{s/JK}, \quad r_{\mu q}^{\mathrm{s,g}} = r_{q\mu}^{\mathrm{s,g}} = 1.18 \times 10^{-2} \text{ m}^2\text{s/mol K}$$

$$r_{\mu\mu}^{\mathrm{s,g}} = 20.2 \text{ J m}^2\text{s/mol}^2\text{K}$$

These values are about 3 orders of magnitude larger than the values one would obtain from kinetic theory. The temperature and pressure differences predicted by kinetic theory for this case are too small to measure.

The exercise above used tabulated thermodynamic and transport data for water, but the temperature jump and pressure difference were chosen as an example. The calculated transfer coefficients are therefore not realistic. Water has a very large heat of evaporation. In such a case, one must use a heat of transfer that is substantially smaller than the enthalpy of evaporation in order to obtain a measurable temperature difference. The ratio of $q^{*,\mathrm{s,g}}$ and $\Delta_{vap}H$ of 0.18 predicted by the kinetic theory for the monatomic fluid, is then much too large. In the exercise, the value 0.01 was used. Larger values would lead to negative values of $r^{\mathrm{s,g}}_{\mu\mu}$ for the given temperature difference, which is not allowed.

11.4 Evaporation and condensation in a two-component fluid

11.4.1 *The entropy production and the flux equations*

Consider again the liquid funnel in Fig. 11.1, but now with a solute in the solvent. The solvent can be for instance, water. The solute can be an electrolyte, like NaCl, an organic compound with a low vapor pressure, like glycerol, or an organic compound with high vapor pressure, like ethanol. The liquid is on the left, $x < 0$, and the vapor on the right, $x > 0$. The entropy production for the liquid phase is given by Eq. (4.15):

$$\sigma^{\mathrm{l}} = J'^{\mathrm{l}}_q \frac{\partial}{\partial x}\left(\frac{1}{T^{\mathrm{l}}}\right) + J_{\mathrm{sol}}\left[-\frac{1}{T^{\mathrm{l}}}\frac{\partial \mu^{\mathrm{l}}_{\mathrm{sol},T}}{\partial x}\right] \tag{11.38}$$

The subscript "sol" indicates solute, and $J^{\mathrm{l}}_{\mathrm{sol}}$ is the (molar) flux of the solute. The flux equations are

$$\begin{aligned} \frac{\partial}{\partial x}\left(\frac{1}{T^{\mathrm{l}}}\right) &= r^{\mathrm{l}}_{qq} J'^{\mathrm{l}}_q + r^{\mathrm{l}}_{qs} J^{\mathrm{l}}_{\mathrm{sol}} \\ -\frac{1}{T^{\mathrm{l}}}\frac{\partial \mu^{\mathrm{l}}_{\mathrm{sol},T}}{\partial x} &= r^{\mathrm{l}}_{sq} J'^{\mathrm{l}}_q + r^{\mathrm{l}}_{ss} J^{\mathrm{l}}_{\mathrm{sol}} \end{aligned} \tag{11.39}$$

The chemical potential of a non-electrolyte solute is:

$$\mu^{\mathrm{l}}_{\mathrm{sol}} = \mu^{0,\mathrm{l}}_{\mathrm{sol}} + RT\ln(c^{\mathrm{l}}_{\mathrm{sol}} y^{\mathrm{l}}_{\mathrm{sol}}) \tag{11.40}$$

where $c^{\mathrm{l}}_{\mathrm{sol}}$ is the molar concentration of the solute, $y^{\mathrm{l}}_{\mathrm{sol}}$ the activity coefficient (equal to unity for Henrian solutions), and $\mu^{0,\mathrm{l}}_{\mathrm{sol}}$ is the chemical potential in the standard state (of 1 molal), see Appendix 3.A. We assume ideal solution, $y^{\mathrm{l}}_{\mathrm{sol}} = 1$, and neglect the Soret effect, $r^{\mathrm{l}}_{qs} = r^{\mathrm{l}}_{sq} = 0$. This

reduces the above equations to:

$$\begin{aligned} J_q'^{\mathrm{l}} &= -\frac{1}{(T^{\mathrm{l}})^2 r^{\mathrm{l}}_{qq}} \frac{\partial T^{\mathrm{l}}}{\partial x} = -\lambda^{\mathrm{l}}_{\mathrm{sol}} \frac{\partial T^{\mathrm{l}}}{\partial x} \\ J^{\mathrm{l}}_{\mathrm{sol}} &= -\frac{1}{T^{\mathrm{l}} r^{\mathrm{l}}_{ss}} \frac{\partial \mu^{\mathrm{l}}_{\mathrm{sol},T}}{\partial x} = -\frac{R}{c^{\mathrm{l}}_{\mathrm{sol}} r^{\mathrm{l}}_{ss}} \frac{\partial c^{\mathrm{l}}_{\mathrm{sol}}}{\partial x} = -D^{\mathrm{l}}_{\mathrm{sol}} \frac{\partial c^{\mathrm{l}}_{\mathrm{sol}}}{\partial x} \end{aligned} \tag{11.41}$$

The last equation is new compared to Sec. 11.2. It gives the flux of the solute in the liquid phase. In the vapor phase all the above equations are the same with the super- or subscript l replaced by g.

In the description of the surface we use the equimolar surface of the solvent as the frame of reference for the fluxes. The solvent flux, J_{w}, is then constant through the surface, but the solute flux is not necessarily constant through the surface. Usually, there is adsorption of solute at the surface:

$$\frac{d\Gamma_{\mathrm{sol}}}{dt} = J^{\mathrm{l}}_{\mathrm{sol}} - J^{\mathrm{g}}_{\mathrm{sol}} \tag{11.42}$$

Adsorption of solute at the surface reduces the surface tension. In a stationary system, the concentration of solute and its absorption at the surface are constant everywhere, so that not only J_{w}, but also J_{sol} is constant throughout the system. The analysis in this chapter is restricted to this case.

The measurable heat flux from the liquid into the surface, $J_q'^{\mathrm{l}}$, is not the same as the measurable heat flux out of the surface into the gas, $J_q'^{\mathrm{g}}$, because the enthalpies differ in the two phases. The total heat flux in the system, J_q, is the conserved flux. The total heat flux is the measurable heat flux plus the enthalpy carried by the solvent and the solute fluxes. In a stationary state J_q is constant throughout the system and one has:

$$J_q = J_q'^{\mathrm{g}} + H^{\mathrm{g}}_{\mathrm{w}} J_{\mathrm{w}} + H^{\mathrm{g}}_{\mathrm{sol}} J_{\mathrm{sol}} = J_q'^{\mathrm{l}} + H^{\mathrm{l}}_{\mathrm{w}} J_{\mathrm{w}} + H^{\mathrm{l}}_{\mathrm{sol}} J_{\mathrm{sol}} \tag{11.43}$$

The entropy production for the liquid-vapor interface in the two-component system is analogous to Eq. (8.13):

$$\begin{aligned} \sigma^{\mathrm{s}} = {} & J_q'^{\mathrm{l}} \Delta_{\mathrm{l,s}} \left(\frac{1}{T}\right) + J_q'^{\mathrm{g}} \Delta_{\mathrm{s,g}} \left(\frac{1}{T}\right) + J_{\mathrm{sol}} \left[-\frac{1}{T^{\mathrm{s}}} \Delta_{\mathrm{l,g}} \mu_{\mathrm{sol},T}(T^{\mathrm{s}})\right] \\ & + J_{\mathrm{w}} \left[-\frac{1}{T^{\mathrm{s}}} \Delta_{\mathrm{l,g}} \mu_{\mathrm{w},T}(T^{\mathrm{s}})\right] \end{aligned} \tag{11.44}$$

The chemical potential differences are evaluated at temperature T^{s}, cf. Eq. (5.19). The heat flux in the liquid may be eliminated using Eq. (11.43).

Following the procedure outlined in Sec. 11.1.1, this results in

$$\sigma^{\mathrm{s}} = J_q'^{\mathrm{g}}\Delta_{\mathrm{l,g}}\left(\frac{1}{T}\right) + J_{\mathrm{sol}}\left[-\frac{1}{T^{\mathrm{l}}}\Delta_{\mathrm{l,g}}\mu_{\mathrm{sol},T}(T^{\mathrm{l}})\right] + J_{\mathrm{w}}\left[-\frac{1}{T^{\mathrm{l}}}\Delta_{\mathrm{l,g}}\mu_{\mathrm{w},T}(T^{\mathrm{l}})\right] \tag{11.45}$$

where the chemical potential differences are now evaluated at the temperature of the liquid, T^{l}. For the solvent and the solute we will again use Eqs. (11.10)–(11.13) to express the chemical potential differences in the partial pressures. The force conjugate to J_{w} is therefore:

$$-\frac{1}{T^{\mathrm{l}}}\Delta_{\mathrm{l,g}}\mu_{\mathrm{w},T}(T^{\mathrm{l}}) = -R\ln\frac{p_{\mathrm{w}}^{\mathrm{g}}}{p_{\mathrm{w}}^{\mathrm{g}*}(T^{\mathrm{l}})} \tag{11.46}$$

and the force conjugate to J_{sol} is:

$$-\frac{1}{T^{\mathrm{l}}}\Delta_{\mathrm{l,g}}\mu_{\mathrm{sol},T}(T^{\mathrm{l}}) = -R\ln\frac{p_{\mathrm{sol}}^{\mathrm{g}}}{p_{\mathrm{sol}}^{\mathrm{g}*}(T^{\mathrm{l}})} \tag{11.47}$$

The partial pressures are divided by the partial pressures for saturated vapor at the temperature of the liquid, T^{l}. When the vapor is not ideal, we must use the fugacities instead of the pressures, see Appendix 3.A. Expressions for activity coefficients in non-ideal gas and in liquid mixtures can be found in Perry [114].

The flux equations derived from Eq. (11.45), together with Eqs. (11.46) and (11.47), are:

$$\begin{aligned}
J_q'^{\mathrm{g}} &= l_{qq}^{\mathrm{s,g}}\Delta_{\mathrm{l,g}}\left(\frac{1}{T}\right) + l_{qs}^{\mathrm{s,g}}\left(-R\ln\frac{p_{\mathrm{sol}}^{\mathrm{g}}}{p_{\mathrm{sol}}^{\mathrm{g}*}(T^{\mathrm{l}})}\right) + l_{qw}^{\mathrm{s,g}}\left(-R\ln\frac{p_{\mathrm{w}}^{\mathrm{g}}}{p_{\mathrm{w}}^{\mathrm{g}*}(T^{\mathrm{l}})}\right)\\
J_{\mathrm{sol}} &= l_{sq}^{\mathrm{s,g}}\Delta_{\mathrm{l,g}}\left(\frac{1}{T}\right) + l_{ss}^{\mathrm{s,g}}\left(-R\ln\frac{p_{\mathrm{sol}}^{\mathrm{g}}}{p_{\mathrm{sol}}^{\mathrm{g}*}(T^{\mathrm{l}})}\right) + l_{sw}^{\mathrm{s,g}}\left(-R\ln\frac{p_{\mathrm{w}}^{\mathrm{g}}}{p_{\mathrm{w}}^{\mathrm{g}*}(T^{\mathrm{l}})}\right)\\
J_{\mathrm{w}} &= l_{wq}^{\mathrm{s,g}}\Delta_{\mathrm{l,g}}\left(\frac{1}{T}\right) + l_{ws}^{\mathrm{s,g}}\left(-R\ln\frac{p_{\mathrm{sol}}^{\mathrm{g}}}{p_{\mathrm{sol}}^{\mathrm{g}*}(T^{\mathrm{l}})}\right) + l_{ww}^{\mathrm{s,g}}\left(-R\ln\frac{p_{\mathrm{w}}^{\mathrm{g}}}{p_{\mathrm{w}}^{\mathrm{g}*}(T^{\mathrm{l}})}\right)
\end{aligned} \tag{11.48}$$

The reason to use conductivities in this case is that this simplifies the definition of the heats of transfer and of the co-transfer coefficient. In the following subsection, we will also give the linear laws using resistivities. In addition to the heat of transfer for the solvent, we define the heat of transfer for the solute:

$$\begin{aligned}
q_{\mathrm{w}}^{*\mathrm{s,g}} &\equiv \left(\frac{J_q'^{\mathrm{g}}}{J_{\mathrm{w}}}\right)_{\Delta T=\Delta\mu_{\mathrm{sol}}=0} = \frac{l_{qw}^{\mathrm{s,g}}}{l_{ww}^{\mathrm{s.g}}}\\
q_{\mathrm{sol}}^{*\mathrm{s,g}} &\equiv \left(\frac{J_q'^{\mathrm{g}}}{J_{\mathrm{sol}}}\right)_{\Delta T=\Delta\mu_{\mathrm{w}}=0} = \frac{l_{qs}^{\mathrm{s,g}}}{l_{ss}^{\mathrm{s.g}}}
\end{aligned} \tag{11.49}$$

We also define the *co-transfer coefficient*:

$$\tau^{\mathrm{s,g}}_{\mathrm{sol}} \equiv \left(\frac{J_{\mathrm{sol}}}{J_{\mathrm{w}}}\right)_{\Delta T=\Delta\mu_{\mathrm{sol}}=0} = \frac{l^{\mathrm{s,g}}_{sw}}{l^{\mathrm{s,g}}_{ww}} \tag{11.50}$$

By introducing the heats of transfer and the co-transfer coefficient, the linear relations become:

$$\begin{aligned}
J'^{\mathrm{g}}_q &= l^{\mathrm{s,g}}_{qq}\Delta_{\mathrm{l,g}}\left(\frac{1}{T}\right) - q^{*\mathrm{s,g}}_{\mathrm{sol}} l^{\mathrm{s,g}}_{ss} R\ln\frac{p^{\mathrm{g}}_{\mathrm{sol}}}{p^{\mathrm{g}*}_{\mathrm{sol}}} - q^{*\mathrm{s,g}}_{\mathrm{w}} l^{\mathrm{s,g}}_{ww} R\ln\frac{p^{\mathrm{g}}_{\mathrm{w}}}{p^{\mathrm{g}*}_{\mathrm{w}}} \\
J_{\mathrm{sol}} &= q^{*\mathrm{s,g}}_{\mathrm{sol}} l^{\mathrm{s,g}}_{ss}\Delta_{\mathrm{l,g}}\left(\frac{1}{T}\right) - l^{\mathrm{s,g}}_{ss} R\ln\frac{p^{\mathrm{g}}_{\mathrm{sol}}}{p^{\mathrm{g}*}_{\mathrm{sol}}} - \tau^{\mathrm{s,g}}_{\mathrm{sol}} l^{\mathrm{s,g}}_{ww} R\ln\frac{p^{\mathrm{g}}_{\mathrm{w}}}{p^{\mathrm{g}*}_{\mathrm{w}}} \\
J_{\mathrm{w}} &= q^{*\mathrm{s,g}}_{\mathrm{w}} l^{\mathrm{s,g}}_{ww}\Delta_{\mathrm{l,g}}\left(\frac{1}{T}\right) - \tau^{\mathrm{s,g}}_{\mathrm{sol}} l^{\mathrm{s,g}}_{ww} R\ln\frac{p^{\mathrm{g}}_{\mathrm{sol}}}{p^{\mathrm{g}*}_{\mathrm{sol}}} - l^{\mathrm{s,g}}_{ww} R\ln\frac{p^{\mathrm{g}}_{\mathrm{w}}}{p^{\mathrm{g}*}_{\mathrm{w}}}
\end{aligned} \tag{11.51}$$

These equations govern evaporation and condensation of a binary ideal mixture.

11.4.2 *Interface resistivities from kinetic theory*

Kinetic theory gives equations of transport also for more components [34]. Take the case of a solvent with one solute. Kinetic theory uses two condensation coefficients, σ_{sol} and σ_{w}, for the solute and the solvent particles respectively. The condensation coefficients give the fractions of particles absorbed by the liquid surface. The rest is reflected with a Boltzmann distribution of velocities at the temperature of the liquid [37].

The resistivity coefficients are the inverse of the conductivity coefficients, given by

$$\begin{pmatrix} l^{\mathrm{s,g}}_{qq} & l^{\mathrm{s,g}}_{qs,g} & l^{\mathrm{s,g}}_{qw} \\ l^{\mathrm{s,g}}_{s,gq} & l^{\mathrm{s,g}}_{ss} & l^{\mathrm{s,g}}_{sw} \\ l^{\mathrm{s,g}}_{wq} & l^{\mathrm{s,g}}_{ws} & l^{\mathrm{s,g}}_{ww} \end{pmatrix} \times \begin{pmatrix} r^{\mathrm{s,g}}_{qq} & r^{\mathrm{s,g}}_{qs} & r^{\mathrm{s,g}}_{qw} \\ r^{\mathrm{s,g}}_{sq} & r^{\mathrm{s,g}}_{ss} & r^{\mathrm{s,g}}_{sw} \\ r^{\mathrm{s,g}}_{wq} & r^{\mathrm{s,g}}_{ws} & r^{\mathrm{s,g}}_{ww} \end{pmatrix} = \begin{pmatrix} 1 & 0 & 0 \\ 0 & 1 & 0 \\ 0 & 0 & 1 \end{pmatrix} \tag{11.52}$$

With these resistivities, the linear relations become

$$\begin{aligned}
\Delta_{\mathrm{l,g}}\left(\frac{1}{T}\right) &= r^{\mathrm{s,g}}_{qq} J'^{\mathrm{g}}_q + r^{\mathrm{s,g}}_{qs} J_{\mathrm{sol}} + r^{\mathrm{s,g}}_{qw} J_{\mathrm{w}} \\
-R\ln\frac{p^{\mathrm{g}}_{\mathrm{sol}}}{p^{\mathrm{g}*}_{\mathrm{sol}}(T^{\mathrm{l}})} &= r^{\mathrm{s,g}}_{sq} J'^{\mathrm{g}}_q + r^{\mathrm{s,g}}_{ss} J_{\mathrm{sol}} + r^{\mathrm{s,g}}_{sw} J_{\mathrm{w}} \\
-R\ln\frac{p^{\mathrm{g}}_{\mathrm{w}}}{p^{\mathrm{g}*}_{\mathrm{w}}(T^{\mathrm{l}})} &= r^{\mathrm{s,g}}_{wq} J'^{\mathrm{g}}_q + r^{\mathrm{s,g}}_{ws} J_{\mathrm{sol}} + r^{\mathrm{s,g}}_{ww} J_{\mathrm{w}}
\end{aligned} \tag{11.53}$$

Kinetic theory now gives [37, 168]†:

$$
\begin{aligned}
r_{qq}^{\mathrm{s,g}} &= \frac{\sqrt{\pi}}{4R(T^{\mathrm{s}})^2 c_{eq}^{\mathrm{g}}(T^{\mathrm{s}})\mathrm{v}_{mp}(T^{\mathrm{s}})} \\
&\quad \times \left\{ 1 + \frac{104}{25\pi} \left\{ \left(\frac{\lambda_{\mathrm{sol}}^{\mathrm{g}}}{\lambda^{\mathrm{g}}} \right)^2 \left[1 + \frac{c_{\mathrm{w}}^{\mathrm{g}}}{c_{\mathrm{sol}}^{\mathrm{g}}} \sqrt[4]{\frac{M_{\mathrm{sol}}}{M_{\mathrm{w}}}} \right] \right. \right. \\
&\quad \left. \left. + \left(\frac{\lambda_{\mathrm{w}}^{\mathrm{g}}}{\lambda^{\mathrm{g}}} \right)^2 \left[1 + \frac{c_{\mathrm{sol}}^{\mathrm{g}}}{c_{\mathrm{w}}^{\mathrm{g}}} \sqrt[4]{\frac{M_{\mathrm{w}}}{M_{\mathrm{sol}}}} \right] \right\} \right\} \\
r_{ss}^{\mathrm{s,g}} &= \frac{R\sqrt{\pi}}{16 c_{eq}^{\mathrm{g}}(T^{\mathrm{s}})\mathrm{v}_{mp}(T^{\mathrm{s}})} \left\{ 1 + 32 \left[\sigma_{\mathrm{sol}}^{-1} + \frac{1}{\pi} - \frac{3}{4} \right] \left[1 + \frac{c_{\mathrm{w}}^{\mathrm{g}}}{c_{\mathrm{sol}}^{\mathrm{g}}} \sqrt[4]{\frac{M_{\mathrm{sol}}}{M_{\mathrm{w}}}} \right] \right\} \\
r_{ww}^{\mathrm{s,g}} &= \frac{R\sqrt{\pi}}{16 c_{eq}^{\mathrm{g}}(T^{\mathrm{s}})\mathrm{v}_{mp}(T^{\mathrm{s}})} \left\{ 1 + 32 \left[\sigma_{\mathrm{w}}^{-1} + \frac{1}{\pi} - \frac{3}{4} \right] \left[1 + \frac{c_{\mathrm{sol}}^{\mathrm{g}}}{c_{\mathrm{w}}^{\mathrm{g}}} \sqrt[4]{\frac{M_{\mathrm{w}}}{M_{\mathrm{sol}}}} \right] \right\} \\
r_{qs}^{\mathrm{s,g}} &= r_{sq}^{\mathrm{s,g}} = \frac{\sqrt{\pi}}{8T^{\mathrm{s}} c_{eq}^{\mathrm{g}}(T^{\mathrm{s}})\mathrm{v}_{mp}(T^{\mathrm{s}})} \left\{ 1 + \frac{16\lambda_{\mathrm{sol}}^{\mathrm{g}}}{5\pi\lambda^{\mathrm{g}}} \left[1 + \frac{c_{\mathrm{w}}^{\mathrm{g}}}{c_{\mathrm{sol}}^{\mathrm{g}}} \sqrt[4]{\frac{M_{\mathrm{sol}}}{M_{\mathrm{w}}}} \right] \right\} \\
r_{qw}^{\mathrm{s,g}} &= r_{wq}^{\mathrm{s,g}} = \frac{\sqrt{\pi}}{8T^{\mathrm{s}} c_{eq}^{\mathrm{g}}(T^{\mathrm{s}})\mathrm{v}_{mp}(T^{\mathrm{s}})} \left\{ 1 + \frac{16\lambda_{\mathrm{w}}^{\mathrm{g}}}{5\pi\lambda^{\mathrm{g}}} \left[1 + \frac{c_{\mathrm{sol}}^{\mathrm{g}}}{c_{\mathrm{w}}^{\mathrm{g}}} \sqrt[4]{\frac{M_{\mathrm{w}}}{M_{\mathrm{sol}}}} \right] \right\} \\
r_{sw}^{\mathrm{s,g}} &= r_{ws}^{\mathrm{s,g}} = \frac{R\sqrt{\pi}}{16 c_{eq}^{\mathrm{g}}(T^{\mathrm{s}})\mathrm{v}_{mp}(T^{\mathrm{s}})}
\end{aligned}
\tag{11.54}
$$

In these expressions $\mathrm{v}_{mp}(T^{\mathrm{s}})$ is the average of the most probable velocities of the two components at temperature T^{s}:

$$
\mathrm{v}_{mp} = (c_{\mathrm{sol}}^{\mathrm{g}} \mathrm{v}_{\mathrm{sol},mp} + c_{\mathrm{w}}^{\mathrm{g}} \mathrm{v}_{\mathrm{w},mp})/c^{\mathrm{g}} \tag{11.55}
$$

with

$$
\mathrm{v}_{\mathrm{sol},mp} = \sqrt{2RT^{\mathrm{s}}/M_{\mathrm{sol}}} \quad \text{and} \quad \mathrm{v}_{\mathrm{w},mp} = \sqrt{2RT^{\mathrm{s}}/M_{\mathrm{w}}} \tag{11.56}
$$

Expressions Eq. (11.23) for the one-component system gave the interface resistivities as function of variables characteristic for the surface. In the equations (11.54) we therefore again used the surface temperature and the

†The formulae given in [37] contained errors which are corrected in the expressions given below, see [175].

densities at equilibrium at this temperature, rather than the temperature and densities of the gas as used before [37,175].

The thermal conductivity is the sum of the contributions due to both components,

$$\lambda^{\mathrm{g}} = \lambda^{\mathrm{g}}_{\mathrm{sol}} + \lambda^{\mathrm{g}}_{\mathrm{w}} \tag{11.57}$$

where

$$\lambda^{\mathrm{g}}_{\mathrm{sol}} = \frac{1}{3}\ell_{\mathrm{sol}}\mathrm{v}_{\mathrm{sol},mp}c^{\mathrm{g}}_{\mathrm{sol}}C^{\mathrm{g}}_{\mathrm{sol},V} \quad \text{and} \quad \lambda^{\mathrm{g}}_{\mathrm{w}} = \frac{1}{3}\ell_{\mathrm{w}}\mathrm{v}_{\mathrm{w},mp}c^{\mathrm{g}}_{\mathrm{w}}C^{\mathrm{g}}_{\mathrm{w},V} \tag{11.58}$$

Here ℓ_i and $C^{\mathrm{g}}_{i,V}$ are the mean free path and the partial specific heat at constant volume of component i. The molar density in the gas is

$$c^{\mathrm{g}} = c^{\mathrm{g}}_{\mathrm{sol}} + c^{\mathrm{g}}_{\mathrm{w}} \tag{11.59}$$

Even though this is not explicitly indicated everywhere, the equilibrium value is used for all quantities in Eqs. (11.54)–(11.59) at the temperature of the surface, T^{s}. This is an improvement compared to the expressions given in [37,175].

A special case of interest is the dilute solution, when only a small amount of solute is present. In that case

$$c^{\mathrm{g}}_{\mathrm{sol}} \ll c^{\mathrm{g}}_{\mathrm{w}} \simeq c^{\mathrm{g}}, \quad \lambda^{\mathrm{g}}_{\mathrm{sol}} \ll \lambda^{\mathrm{g}}_{\mathrm{w}} \simeq \lambda^{\mathrm{g}}, \quad c^{\mathrm{g}}_{\mathrm{sol},V} \ll c^{\mathrm{g}}_{\mathrm{w},V} \simeq c^{\mathrm{g}}_{V} \tag{11.60}$$

The resistivity coefficients then simplify to

$$\begin{aligned}
r^{\mathrm{s,g}}_{qq} &= \frac{\sqrt{\pi}}{4R(T^{\mathrm{s}})^2 c^{\mathrm{g}}_{eq}(T^{\mathrm{s}})\mathrm{v}_{mp}(T^{\mathrm{s}})}\left(1+\frac{104}{25\pi}\right)\\
r^{\mathrm{s,g}}_{ss} &= \frac{2R\sqrt{\pi}}{c^{\mathrm{g}}_{\mathrm{sol}}\mathrm{v}_{mp}(T^{\mathrm{s}})}\left(\sigma^{-1}_{\mathrm{sol}}+\frac{1}{\pi}-\frac{3}{4}\right)\sqrt[4]{\frac{M_{\mathrm{sol}}}{M_{\mathrm{w}}}}\\
r^{\mathrm{s,g}}_{ww} &= \frac{2R\sqrt{\pi}}{c^{\mathrm{g}}_{eq}(T^{\mathrm{s}})\mathrm{v}_{mp}(T^{\mathrm{s}})}\left(\sigma^{-1}_{\mathrm{w}}+\frac{1}{\pi}-\frac{23}{32}\right)\\
r^{\mathrm{s,g}}_{qs} &= r^{\mathrm{s,g}}_{sq} = \frac{\sqrt{\pi}}{8T^{\mathrm{s}}c^{\mathrm{g}}_{eq}(T^{\mathrm{s}})\mathrm{v}_{mp}(T^{\mathrm{s}})}\left(1+\frac{16\lambda^{\mathrm{g}}_{\mathrm{sol}}c^{\mathrm{g}}_{eq}}{5\pi\lambda^{\mathrm{g}}c^{\mathrm{g}}_{\mathrm{sol}}}\sqrt[4]{\frac{M_{\mathrm{sol}}}{M_{\mathrm{w}}}}\right)\\
r^{\mathrm{s,g}}_{qw} &= r^{\mathrm{s,g}}_{wq} = \frac{\sqrt{\pi}}{8T^{\mathrm{s}}c^{\mathrm{g}}_{eq}(T^{\mathrm{s}})\mathrm{v}_{mp}(T^{\mathrm{s}})}\left(1+\frac{16}{5\pi}\right)\\
r^{\mathrm{s,g}}_{sw} &= r^{\mathrm{s,g}}_{ws} = \frac{R\sqrt{\pi}}{16c^{\mathrm{g}}_{eq}(T^{\mathrm{s}})\mathrm{v}_{mp}(T^{\mathrm{s}})}
\end{aligned} \tag{11.61}$$

Even though this is not explicitly indicated everywhere, the equilibrium value is used for all quantities in Eqs. (11.60) and (11.61) at the temperature

of the surface, T^{s}. The resistivities $r^{\mathrm{s,g}}_{qq}$, $r^{\mathrm{s,g}}_{qw} = r^{\mathrm{s,g}}_{wq}$ and $r^{\mathrm{s,g}}_{ww}$ are identical to those given in Sec. 11.1.2 for the one-component case. A small concentration of solute does thus not change these coefficients. In the linear relations for the forces and fluxes, Eq. (11.53), one may use the fact that $J^{\mathrm{g}}_{\mathrm{sol}}$ is small, like $c^{\mathrm{g}}_{\mathrm{sol}}$. This implies, given the value of the coupling coefficients, that

$$\begin{aligned} \Delta_{\mathrm{l,g}} \left(\frac{1}{T} \right) &= r^{\mathrm{s,g}}_{qq} J'^{\mathrm{g}}_{q} + r^{\mathrm{s,g}}_{qw} J_{\mathrm{w}} \\ -R \ln \frac{p^{\mathrm{g}}_{\mathrm{w}}}{p^{\mathrm{g*}}_{\mathrm{w}}(T^{\mathrm{l}})} &= r^{\mathrm{s,g}}_{wq} J'^{\mathrm{g}}_{q} + r^{\mathrm{s,g}}_{ww} J_{\mathrm{w}} \end{aligned} \tag{11.62}$$

The heat and solvent fluxes are consequently not affected by the solute if it is sufficiently dilute. The analysis in Sec. 11.1 is adequate for that case. For the solute one has

$$-R \ln \frac{p^{\mathrm{g}}_{\mathrm{sol}}}{p^{\mathrm{g*}}_{\mathrm{sol}}(T^{\mathrm{l}})} = r^{\mathrm{s,g}}_{sq} J'^{\mathrm{g}}_{q} + r^{\mathrm{s,g}}_{ss} J_{\mathrm{sol}} + r^{\mathrm{s,g}}_{sw} J_{\mathrm{w}} \tag{11.63}$$

In this expression, it is important that $r^{\mathrm{s,g}}_{ss}$ is inversely proportional to $c^{\mathrm{g}}_{\mathrm{sol}}$ so that the term $r^{\mathrm{s,g}}_{ss} J^{\mathrm{g}}_{\mathrm{sol}}$ is of the same order of magnitude as the other two terms. Therefore, if the overall concentration of solute is small, one may have a *backup of solute in front of the surface*. This may lead locally to considerable concentration gradients, in which case the coupling to $J^{\mathrm{g}}_{\mathrm{sol}}$ will become important. It was shown that the solute concentration is negligible, as long as the equilibrium temperature and concentrations in the vapor satisfy

$$\frac{c^{\mathrm{g}}_{\mathrm{sol}}}{c^{\mathrm{g}}_{eq}(T^{\mathrm{s}})} \ll \frac{\Delta H_{\mathrm{w,vap}}}{RT} \frac{\ell}{d_{\mathrm{g}}} \tag{11.64}$$

where d_{g} is the thickness of the vapor phase [37]. This is a rather small upper bound on the concentration of the solute in most cases. It is often difficult in practice to purify fluids sufficiently to avoid solute trace elements [176]. Non-equilibrium molecular dynamics simulations avoid this difficulty [171].

Chapter 12

Multi-Component Heat and Mass Diffusion

In this chapter we describe multi-component mass and heat transport in a heterogeneous system. After a general introduction about the homogeneous phases, we discuss the Maxwell–Stefan equations for multi-component diffusion in the presence of a temperature gradient. We then discuss the transport of mass and heat through the surface and combine the description of the two homogeneous phases with the one for the surface. We also discuss multi-component diffusion in the homogeneous phase using various frames of reference.

Diffusion takes place in all chemical mixtures and is often the rate limiting process. The simplest equation that describes diffusion of one component in another is Fick's law, Eq. (1.2). The diffusion of one component is often influenced by concentration gradients of other components, however. In other words, there is coupling of diffusion fluxes. Such coupling is efficiently described using the Maxwell–Stefan equations [42, 69]. Also heat is transported along with components, so diffusion couples to heat transport.

In the following section, we explain how we can obtain Maxwell–Stefan equations including coupling of heat and mass transport, within the context of non-equilibrium thermodynamics. We also show how these equations are related to other descriptions of multi-component diffusion, and how they can be combined to deal with interface transport.

12.1 The homogeneous phases

Consider an isobaric, nonisothermal system with three components in a homogeneous phase*. There are then three independent driving forces in the system, one thermal and two component driving forces. In order to deal with the components on the same footing, however, we write the entropy production using *four* forces:

$$\begin{aligned}\sigma &= J_q \frac{\partial}{\partial x}\frac{1}{T} - J_{\mathrm{A}}\frac{\partial}{\partial x}\frac{\mu_{\mathrm{A}}}{T} - J_{\mathrm{B}}\frac{\partial}{\partial x}\frac{\mu_{\mathrm{B}}}{T} - J_{\mathrm{C}}\frac{\partial}{\partial x}\frac{\mu_{\mathrm{C}}}{T} \\ &= J'_q \frac{\partial}{\partial x}\frac{1}{T} - \mathrm{v}_{\mathrm{A}}\frac{c_{\mathrm{A}}}{T}\frac{\partial \mu_{\mathrm{A},T}}{\partial x} - \mathrm{v}_{\mathrm{B}}\frac{c_{\mathrm{B}}}{T}\frac{\partial \mu_{\mathrm{B},T}}{\partial x} - \mathrm{v}_{\mathrm{C}}\frac{c_{\mathrm{C}}}{T}\frac{\partial \mu_{\mathrm{C},T}}{\partial x}\end{aligned} \tag{12.1}$$

where the velocity of component i (i = A, B or C) is defined by $\mathrm{v}_i \equiv J_i/c_i$. We have suppressed the superscript i or o, indicating the phase, as the expressions are the same in both phases. For stationary states, the total heat flux, $J_q = J'_q + H_{\mathrm{A}}J_{\mathrm{A}} + H_{\mathrm{B}}J_{\mathrm{B}} + H_{\mathrm{C}}J_{\mathrm{C}}$, and the molar fluxes, J_j, are constant throughout the system. The component forces are related by Gibbs–Duhem's equation

$$c_{\mathrm{A}}\frac{\partial \mu_{\mathrm{A},T}}{\partial x} + c_{\mathrm{B}}\frac{\partial \mu_{\mathrm{B},T}}{\partial x} + c_{\mathrm{C}}\frac{\partial \mu_{\mathrm{C},T}}{\partial x} = 0 \tag{12.2}$$

Only two of these forces are therefore independent.

Following Eq. (12.1), the equations for the thermodynamic forces can be written as

$$\begin{aligned}\frac{\partial}{\partial x}\frac{1}{T} &= r_{qq}J'_q + r_{q\mathrm{A}}\mathrm{v}_{\mathrm{A}} + r_{q\mathrm{B}}\mathrm{v}_{\mathrm{B}} + r_{q\mathrm{C}}\mathrm{v}_{\mathrm{C}} \\ -\frac{c_{\mathrm{A}}}{T}\frac{\partial \mu_{\mathrm{A},T}}{\partial x} &= r_{\mathrm{A}q}J'_q + r_{\mathrm{AA}}\mathrm{v}_{\mathrm{A}} + r_{\mathrm{AB}}\mathrm{v}_{\mathrm{B}} + r_{\mathrm{AC}}\mathrm{v}_{\mathrm{C}} \\ -\frac{c_{\mathrm{B}}}{T}\frac{\partial \mu_{\mathrm{B},T}}{\partial x} &= r_{\mathrm{B}q}J'_q + r_{\mathrm{BA}}\mathrm{v}_{\mathrm{A}} + r_{\mathrm{BB}}\mathrm{v}_{\mathrm{B}} + r_{\mathrm{BC}}\mathrm{v}_{\mathrm{C}} \\ -\frac{c_{\mathrm{C}}}{T}\frac{\partial \mu_{\mathrm{C},T}}{\partial x} &= r_{\mathrm{C}q}J'_q + r_{\mathrm{CA}}\mathrm{v}_{\mathrm{A}} + r_{\mathrm{CB}}\mathrm{v}_{\mathrm{B}} + r_{\mathrm{CC}}\mathrm{v}_{\mathrm{C}}\end{aligned} \tag{12.3}$$

The sum of three terms on the left hand side of Eq. (12.3) is zero according to Gibbs–Duhem's equation. Onsager relations were shown to apply in Eq. (12.3), when the forces depend via Gibbs–Duhem's equation, see

*For a discussion of the nonisobaric system with an arbitrary number of components, see Kuiken [31], and Krishna and coworkers [42, 69].

de Groot and Mazur [20], page 67. This gives:

$$\begin{aligned} r_{\mathrm{A}q} = r_{q\mathrm{A}}, \quad r_{\mathrm{B}q} = r_{q\mathrm{B}}, \quad r_{\mathrm{C}q} = r_{q\mathrm{C}} \\ r_{\mathrm{AB}} = r_{\mathrm{BA}}, \quad r_{\mathrm{AC}} = r_{\mathrm{CA}}, \quad r_{\mathrm{BC}} = r_{\mathrm{CB}} \end{aligned} \tag{12.4}$$

As Eqs. (12.3) hold for any arbitrary measurable heat flux and arbitrary velocities of the components, it follows that the resistivities in the matrix are dependent, and satisfy

$$\begin{aligned} r_{\mathrm{A}q} + r_{\mathrm{B}q} + r_{\mathrm{C}q} &= 0 \\ r_{\mathrm{AA}} + r_{\mathrm{BA}} + r_{\mathrm{CA}} &= 0 \\ r_{\mathrm{AB}} + r_{\mathrm{BB}} + r_{\mathrm{CB}} &= 0 \\ r_{\mathrm{AC}} + r_{\mathrm{BC}} + r_{\mathrm{CC}} &= 0 \end{aligned} \tag{12.5}$$

From the Onsager relations, it follows that also

$$\begin{aligned} r_{q\mathrm{A}} + r_{q\mathrm{B}} + r_{q\mathrm{C}} &= 0 \\ r_{\mathrm{AA}} + r_{\mathrm{AB}} + r_{\mathrm{AC}} &= 0 \\ r_{\mathrm{BA}} + r_{\mathrm{BB}} + r_{\mathrm{BC}} &= 0 \\ r_{\mathrm{CA}} + r_{\mathrm{CB}} + r_{\mathrm{CC}} &= 0 \end{aligned} \tag{12.6}$$

There are thus only six independent resistivities. Once these have been obtained from experiments, the others can be calculated using the above relations. The resistivity matrix has an eigenvalue equal to zero, and thus a zero determinant. *It cannot therefore be inverted into a conductivity matrix!*

For our further analysis, it is convenient to write Eq. (12.3) in the following form

$$\begin{aligned} \frac{\partial T}{\partial x} &= -\frac{1}{\lambda}\left(J'_q - c_{\mathrm{A}} q^*_{\mathrm{A}} \mathrm{v}_{\mathrm{A}} - c_{\mathrm{B}} q^*_{\mathrm{B}} \mathrm{v}_{\mathrm{B}} - c_{\mathrm{C}} q^*_{\mathrm{C}} \mathrm{v}_{\mathrm{C}}\right) \\ \frac{c_{\mathrm{A}}}{T}\frac{\partial \mu_{\mathrm{A},T}}{\partial x} &= -\frac{c_{\mathrm{A}} q^*_{\mathrm{A}}}{T^2}\frac{\partial T}{\partial x} - R_{\mathrm{AA}}\mathrm{v}_{\mathrm{A}} - R_{\mathrm{AB}}\mathrm{v}_{\mathrm{B}} - R_{\mathrm{AC}}\mathrm{v}_{\mathrm{C}} \\ \frac{c_{\mathrm{B}}}{T}\frac{\partial \mu_{\mathrm{B},T}}{\partial x} &= -\frac{c_{\mathrm{B}} q^*_{\mathrm{B}}}{T^2}\frac{\partial T}{\partial x} - R_{\mathrm{BA}}\mathrm{v}_{\mathrm{A}} - R_{\mathrm{BB}}\mathrm{v}_{\mathrm{B}} - R_{\mathrm{BC}}\mathrm{v}_{\mathrm{C}} \\ \frac{c_{\mathrm{C}}}{T}\frac{\partial \mu_{\mathrm{C},T}}{\partial x} &= -\frac{c_{\mathrm{C}} q^*_{\mathrm{C}}}{T^2}\frac{\partial T}{\partial x} - R_{\mathrm{CA}}\mathrm{v}_{\mathrm{A}} - R_{\mathrm{CB}}\mathrm{v}_{\mathrm{B}} - R_{\mathrm{CC}}\mathrm{v}_{\mathrm{C}} \end{aligned} \tag{12.7}$$

where the thermal conductivity, the measurable heats of transfer and the resistivities for component fluxes at constant temperature are defined by:

$$\lambda \equiv \frac{1}{T^2 r_{qq}}, \quad c_j q_j^* \equiv -\frac{r_{qj}}{r_{qq}}$$

and
$$R_{jk} \equiv r_{jk} - \frac{r_{jq} r_{qk}}{r_{qq}} \quad \text{for} \quad j,k = \text{ A, B or C} \tag{12.8}$$

The measurable heats of transfer satisfy, see Eq. (12.5a),

$$c_{\mathrm{A}} q_{\mathrm{A}}^* + c_{\mathrm{B}} q_{\mathrm{B}}^* + c_{\mathrm{C}} q_{\mathrm{C}}^* = 0 \tag{12.9}$$

The resistivities for mass flow at constant temperature satisfy, see Eq. (12.5),

$$\begin{aligned} R_{\mathrm{AA}} + R_{\mathrm{BA}} + R_{\mathrm{CA}} &= 0 \\ R_{\mathrm{AB}} + R_{\mathrm{BB}} + R_{\mathrm{CB}} &= 0 \\ R_{\mathrm{AC}} + R_{\mathrm{BC}} + R_{\mathrm{CC}} &= 0 \end{aligned} \tag{12.10}$$

From the Onsager relations, cf. Eq. (12.6), it follows that also

$$\begin{aligned} R_{\mathrm{AA}} + R_{\mathrm{AB}} + R_{\mathrm{AC}} &= 0 \\ R_{\mathrm{BA}} + R_{\mathrm{BB}} + R_{\mathrm{BC}} &= 0 \\ R_{\mathrm{CA}} + R_{\mathrm{CB}} + R_{\mathrm{CC}} &= 0 \end{aligned} \tag{12.11}$$

Using Eqs. (12.9) and (12.11) in Eq. (12.7), one may verify that the right (and therefore the left) hand sides are independent of the choice of the frame of reference. Possible choices of the velocity $\mathrm{v}_{\mathrm{ref}}$ of the frame of reference, see Section 4.4 [20], are the center of mass, the average volume, the average molar velocity and the solvent velocity. We discuss these choices in Sec. 12.4.

12.2 The Maxwell–Stefan equations for multi-component diffusion

The Maxwell–Stefan equations give a convenient way to describe multi-component diffusion [31, 42] because the description is independent of the frame of reference, and the diffusion coefficients contain binary interdiffusion coefficients. Such coefficients are easily available from experiments [139].

The Maxwell–Stefan diffusion coefficients, $Đ_{jk}$, are defined from[†]

$$R_{AB} \equiv -cR\frac{x_A x_B}{Đ_{AB}}, \quad R_{AC} \equiv -cR\frac{x_A x_C}{Đ_{AC}}, \quad R_{BC} \equiv -cR\frac{x_B x_C}{Đ_{BC}} \tag{12.12}$$

where $x_i \equiv c_i/c$ is the mole fraction of component i, and the diagonal coefficients, R_{AA}, R_{BB} and R_{CC}, are found from Eq. (12.11). The Maxwell–Stefan diffusion coefficients are symmetric, $Đ_{jk}$=$Đ_{kj}$. The heats of transfer can be written in terms of the thermal diffusion coefficients, $D_{T,j}$, such that they satisfy Eq. (12.9), as

$$q_j^* \equiv \sum_{k\neq j}^{n} \frac{RTx_k}{Đ_{jk}}\left(\frac{D_{T,j}}{\rho_j} - \frac{D_{T,k}}{\rho_k}\right) \tag{12.13}$$

Here $\rho_j \equiv c_j M_j$ is the mass density in kg/m^3 and M_j the molar weight in kg/mol of component j. Using Eqs. (12.9) and (12.12) we can write the linear laws (12.7) in the following form

$$\begin{aligned}
\frac{\partial T}{\partial x} &= -\frac{1}{\lambda}\left[J_q' - c_B q_B^*\left(v_B - v_A\right) - c_C q_C^*\left(v_C - v_A\right)\right] \\
\frac{x_B}{RT}\frac{\partial \mu_{B,T}}{\partial x} &= -\frac{x_B q_B^*}{RT^2}\frac{\partial T}{\partial x} + \frac{x_A x_B}{Đ_{AB}}\left(v_A - v_B\right) + \frac{x_B x_C}{Đ_{BC}}\left(v_C - v_B\right) \\
\frac{x_C}{RT}\frac{\partial \mu_{C,T}}{\partial x} &= -\frac{x_C q_C^*}{RT^2}\frac{\partial T}{\partial x} + \frac{x_A x_C}{Đ_{AC}}\left(v_A - v_C\right) + \frac{x_B x_C}{Đ_{BC}}\left(v_B - v_C\right)
\end{aligned} \tag{12.14}$$

We left the equation for $\partial \mu_{A,T}/\partial x$ out as it is redundant. It follows from the last two equations using Gibbs–Duhem's equation. To keep the expression a bit more elegant we did not substitute the expressions for the measurable heats of transfer in terms of the thermal diffusion coefficients. Only velocity differences enter. The description is thus independent of the frame of reference.

Binary diffusion coefficients are reasonably well known [31,69,139,177]. Heats of transfer are not so well known. Approximate expressions have been given by Kempers [145,178] and by Haase [22] for binary mixtures, see Sec. 8.2. Given the Maxwell–Stefan diffusion coefficients, one can calculate the resistivities R_{AB}, R_{AC} and R_{BC}, using Eq. (12.12) and then the diagonal coefficients, R_{AA}, R_{BB} and R_{CC}, using Eq. (12.11). Using also the thermal conductivity and the heats of transfer, the resistivities r_{qq}, $r_{qk} = r_{jq}$ and $r_{jk} = r_{kj}$ follow from Eq. (12.8).

[†]We follow Krishna and Wesselingh [42] in this definition rather than Kuiken [31] who uses the pressure p instead of cRT.

The chemical potentials of the components;

$$\mu_i = \mu_i^0(T) + RT \ln x_i \gamma_i \tag{12.15}$$

where $\mu_i^0(T)$ is the standard chemical potential, x_i is the mole fraction and γ_i is the activity coefficient, give relations between the chemical potential at constant temperature and the gradient in mole fraction:

$$\frac{x_i}{RT}\frac{\partial \mu_{i,T}}{\partial x} = \frac{\partial x_i}{\partial x}\left(1 + \frac{\partial \ln \gamma_i}{\partial \ln x_i}\right) \tag{12.16}$$

Remark 12.1. *The use of the Maxwell–Stefan formalism for diffusion has a number of important advantages: In the first place, the diffusion coefficients are symmetric for the interchange of components, this is contrary to all other descriptions of multi-component diffusion. In the second place, the formalism is valid in an arbitrary frame of reference, also contrary to other descriptions. A third property, found experimentally and which is very useful, is that the Maxwell–Stefan diffusion coefficients are rather independent of the concentrations [31, 42]. Finally, it is also found that the coefficient for two given components remains more or less the same if the third component is changed. This makes it possible to model diffusion in multi-component mixtures with data from binary mixtures.*

12.3 The Maxwell–Stefan equations for the surface

Maxwell–Stefan equations for the surface have their basis in the entropy production of the surface. Equation (5.15) is used to give a formulation in terms of velocities:

$$\begin{aligned}
\sigma^{\mathrm{s}} &= J_q'^{\mathrm{i}} \Delta_{\mathrm{i,s}}\left(\frac{1}{T}\right) + J_q'^{\mathrm{o}} \Delta_{\mathrm{s,o}}\left(\frac{1}{T}\right) + \sum_{j=\mathrm{A,B,C}} J_j^{\mathrm{i}}\left(-\frac{\Delta_{\mathrm{i,s}}\mu_{j,T}}{T^{\mathrm{s}}}\right) \\
&\quad + \sum_{j=\mathrm{A,B,C}} J_j^{\mathrm{o}}\left(-\frac{\Delta_{\mathrm{s,o}}\mu_{j,T}}{T^{\mathrm{s}}}\right) \\
&= J_q'^{\mathrm{i}} \Delta_{\mathrm{i,s}}\left(\frac{1}{T}\right) + J_q'^{\mathrm{o}} \Delta_{\mathrm{s,o}}\left(\frac{1}{T}\right) + \sum_{j=\mathrm{A,B,C}} \mathrm{v}_j^{\mathrm{i}}\left(-\frac{c_j^{\mathrm{i}}}{T^{\mathrm{s}}}\Delta_{\mathrm{i,s}}\mu_{j,T}\right) \\
&\quad + \sum_{j=\mathrm{A,B,C}} \mathrm{v}_j^{\mathrm{o}}\left(-\frac{c_j^{\mathrm{o}}}{T^{\mathrm{s}}}\Delta_{\mathrm{s,o}}\mu_{j,T}\right)
\end{aligned} \tag{12.17}$$

All velocities in the equations for the excess entropy production have the surface as their frame of reference. Assuming that there are no coupling

coefficients from one side of the surface to the other, the equations for the thermodynamic forces can be written as

$$\begin{aligned}
\Delta_{\mathrm{i,s}}\left(\frac{1}{T}\right) &= r^{\mathrm{s,i}}_{qq}J'^{\mathrm{i}}_q + r^{\mathrm{s,i}}_{q\mathrm{A}}\mathrm{v}^{\mathrm{i}}_{\mathrm{A}} + r^{\mathrm{s,i}}_{q\mathrm{B}}\mathrm{v}^{\mathrm{i}}_{\mathrm{B}} + r^{\mathrm{s,i}}_{q\mathrm{C}}\mathrm{v}^{\mathrm{i}}_{\mathrm{C}} \\
-\frac{c^{\mathrm{i}}_{\mathrm{A}}}{T^{\mathrm{s}}}\Delta_{\mathrm{i,s}}\mu_{\mathrm{A},T} &= r^{\mathrm{s,i}}_{\mathrm{A}q}J'^{\mathrm{i}}_q + r^{\mathrm{s,i}}_{\mathrm{AA}}\mathrm{v}^{\mathrm{i}}_{\mathrm{A}} + r^{\mathrm{s,i}}_{\mathrm{AB}}\mathrm{v}^{\mathrm{i}}_{\mathrm{B}} + r^{\mathrm{s,i}}_{\mathrm{AC}}\mathrm{v}^{\mathrm{i}}_{\mathrm{C}} \\
-\frac{c^{\mathrm{i}}_{\mathrm{B}}}{T^{\mathrm{s}}}\Delta_{\mathrm{i,s}}\mu_{\mathrm{B},T} &= r^{\mathrm{s,i}}_{\mathrm{B}q}J'^{\mathrm{i}}_q + r^{\mathrm{s,i}}_{\mathrm{BA}}\mathrm{v}^{\mathrm{i}}_{\mathrm{A}} + r^{\mathrm{s,i}}_{\mathrm{BB}}\mathrm{v}^{\mathrm{i}}_{\mathrm{B}} + r^{\mathrm{s,i}}_{\mathrm{BC}}\mathrm{v}^{\mathrm{i}}_{\mathrm{C}} \\
-\frac{c^{\mathrm{i}}_{\mathrm{C}}}{T^{\mathrm{s}}}\Delta_{\mathrm{i,s}}\mu_{\mathrm{C},T} &= r^{\mathrm{s,i}}_{\mathrm{C}q}J'^{\mathrm{i}}_q + r^{\mathrm{s,i}}_{\mathrm{CA}}\mathrm{v}^{\mathrm{i}}_{\mathrm{A}} + r^{\mathrm{s,i}}_{\mathrm{CB}}\mathrm{v}^{\mathrm{i}}_{\mathrm{B}} + r^{\mathrm{s,i}}_{\mathrm{CC}}\mathrm{v}^{\mathrm{i}}_{\mathrm{C}}
\end{aligned} \tag{12.18}$$

and

$$\begin{aligned}
\Delta_{\mathrm{s,o}}\left(\frac{1}{T}\right) &= r^{\mathrm{s,o}}_{qq}J'^{\mathrm{o}}_q + r^{\mathrm{s,o}}_{q\mathrm{A}}\mathrm{v}^{\mathrm{o}}_{\mathrm{A}} + r^{\mathrm{s,o}}_{q\mathrm{B}}\mathrm{v}^{\mathrm{o}}_{\mathrm{B}} + r^{\mathrm{s,o}}_{q\mathrm{C}}\mathrm{v}^{\mathrm{o}}_{\mathrm{C}} \\
-\frac{c^{\mathrm{o}}_{\mathrm{A}}}{T^{\mathrm{s}}}\Delta_{\mathrm{s,o}}\mu_{\mathrm{A},T} &= r^{\mathrm{s,o}}_{\mathrm{A}q}J'^{\mathrm{o}}_q + r^{\mathrm{s,o}}_{\mathrm{AA}}\mathrm{v}^{\mathrm{o}}_{\mathrm{A}} + r^{\mathrm{s,o}}_{\mathrm{AB}}\mathrm{v}^{\mathrm{o}}_{\mathrm{B}} + r^{\mathrm{s,o}}_{\mathrm{AC}}\mathrm{v}^{\mathrm{o}}_{\mathrm{C}} \\
-\frac{c^{\mathrm{o}}_{\mathrm{B}}}{T^{\mathrm{s}}}\Delta_{\mathrm{s,o}}\mu_{\mathrm{B},T} &= r^{\mathrm{s,o}}_{\mathrm{B}q}J'^{\mathrm{o}}_q + r^{\mathrm{s,o}}_{\mathrm{BA}}\mathrm{v}^{\mathrm{o}}_{\mathrm{A}} + r^{\mathrm{s,o}}_{\mathrm{BB}}\mathrm{v}^{\mathrm{o}}_{\mathrm{B}} + r^{\mathrm{s,o}}_{\mathrm{BC}}\mathrm{v}^{\mathrm{o}}_{\mathrm{C}} \\
-\frac{c^{\mathrm{o}}_{\mathrm{C}}}{T^{\mathrm{s}}}\Delta_{\mathrm{s,o}}\mu_{\mathrm{C},T} &= r^{\mathrm{s,o}}_{\mathrm{C}q}J'^{\mathrm{o}}_q + r^{\mathrm{s,o}}_{\mathrm{CA}}\mathrm{v}^{\mathrm{o}}_{\mathrm{A}} + r^{\mathrm{s,o}}_{\mathrm{CB}}\mathrm{v}^{\mathrm{o}}_{\mathrm{B}} + r^{\mathrm{s,o}}_{\mathrm{CC}}\mathrm{v}^{\mathrm{o}}_{\mathrm{C}}
\end{aligned} \tag{12.19}$$

where the Onsager relations apply for the same reason as for the homogeneous phase.

We will now first consider the i-side of the surface. Equation (12.18) is used to find the surface equivalent form to Eq. (12.7):

$$\begin{aligned}
\Delta_{\mathrm{i,s}}T &= -\frac{1}{\lambda^{\mathrm{s,i}}}\left(J'^{\mathrm{i}}_q - c^{\mathrm{i}}_{\mathrm{A}}q^{*,\mathrm{i}}_{\mathrm{A}}\mathrm{v}^{\mathrm{i}}_{\mathrm{A}} - c^{\mathrm{i}}_{\mathrm{B}}q^{*,\mathrm{i}}_{\mathrm{B}}\mathrm{v}^{\mathrm{i}}_{\mathrm{B}} - c^{\mathrm{i}}_{\mathrm{C}}q^{*,\mathrm{i}}_{\mathrm{C}}\mathrm{v}^{\mathrm{i}}_{\mathrm{C}}\right) \\
\frac{c^{\mathrm{i}}_{\mathrm{A}}}{T^{\mathrm{s}}}\Delta_{\mathrm{i,s}}\mu_{\mathrm{A},T} &= -\frac{c^{\mathrm{i}}_{\mathrm{A}}q^{*,\mathrm{i}}_{\mathrm{A}}}{T^{\mathrm{i}}T^{\mathrm{s}}}\Delta_{\mathrm{i,s}}T - R^{\mathrm{s,i}}_{\mathrm{AA}}\mathrm{v}^{\mathrm{i}}_{\mathrm{A}} - R^{\mathrm{s,i}}_{\mathrm{AB}}\mathrm{v}^{\mathrm{i}}_{\mathrm{B}} - R^{\mathrm{s,i}}_{\mathrm{AC}}\mathrm{v}^{\mathrm{i}}_{\mathrm{C}} \\
\frac{c^{\mathrm{i}}_{\mathrm{B}}}{T^{\mathrm{s}}}\Delta_{\mathrm{i,s}}\mu_{\mathrm{B},T} &= -\frac{c^{\mathrm{i}}_{\mathrm{B}}q^{*,\mathrm{i}}_{\mathrm{B}}}{T^{\mathrm{i}}T^{\mathrm{s}}}\Delta_{\mathrm{i,s}}T - R^{\mathrm{s,i}}_{\mathrm{BA}}\mathrm{v}^{\mathrm{i}}_{\mathrm{A}} - R^{\mathrm{s,i}}_{\mathrm{BB}}\mathrm{v}^{\mathrm{i}}_{\mathrm{B}} - R^{\mathrm{s,i}}_{\mathrm{BC}}\mathrm{v}^{\mathrm{i}}_{\mathrm{C}} \\
\frac{c^{\mathrm{i}}_{\mathrm{C}}}{T^{\mathrm{s}}}\Delta_{\mathrm{i,s}}\mu_{\mathrm{C},T} &= -\frac{c^{\mathrm{i}}_{\mathrm{C}}q^{*,\mathrm{i}}_{\mathrm{C}}}{T^{\mathrm{i}}T^{\mathrm{s}}}\Delta_{\mathrm{i,s}}T - R^{\mathrm{s,i}}_{\mathrm{CA}}\mathrm{v}^{\mathrm{i}}_{\mathrm{A}} - R^{\mathrm{s,i}}_{\mathrm{CB}}\mathrm{v}^{\mathrm{i}}_{\mathrm{B}} - R^{\mathrm{s,i}}_{\mathrm{CC}}\mathrm{v}^{\mathrm{i}}_{\mathrm{C}}
\end{aligned} \tag{12.20}$$

where thermal conductivity, the heats of transfer and the resistivities for component fluxes at constant temperature are defined by:

$$\lambda^{\mathrm{s,i}} \equiv \frac{1}{T^{\mathrm{i}} T^{\mathrm{s}} r^{\mathrm{s,i}}_{qq}}, \quad c^{\mathrm{i}}_j q^{*,\mathrm{i}}_j \equiv -\frac{r^{\mathrm{s,i}}_{qj}}{r^{\mathrm{s,i}}_{qq}}$$

and
$$R^{\mathrm{s,i}}_{jk} \equiv r^{\mathrm{s,i}}_{jk} - \frac{r^{\mathrm{s,i}}_{jq} r^{\mathrm{s,i}}_{qk}}{r^{\mathrm{s,i}}_{qq}} \quad \text{for} \quad j,k = \text{ A, B or C} \tag{12.21}$$

The $R^{\mathrm{s,i}}_{jk}$ matrix is again a symmetric matrix, and the coefficients can be determined via Maxwell–Stefan diffusion coefficients for the surface, as was done in Eq. (12.12), except that they must be multiplied with a surface characteristic length, to account for the different dimensionality. The heats of transfer are ratios of bulk fluxes at a constant temperature and have in this model the same value as in the adjacent bulk phase i. They satisfy the relation given in Eq. (12.9)

$$c^{\mathrm{i}}_{\mathrm{A}} q^{*,\mathrm{i}}_{\mathrm{A}} + c^{\mathrm{i}}_{\mathrm{B}} q^{*,\mathrm{i}}_{\mathrm{B}} + c^{\mathrm{i}}_{\mathrm{C}} q^{*,\mathrm{i}}_{\mathrm{C}} = 0 \tag{12.22}$$

It can similarly be argued that a ratio of $R^{\mathrm{s,i}}_{jk}$ coefficients is equal to the ratio of the resistivities in the bulk phase i. This implies that also Eqs. (12.10) and (12.11) are valid for these coefficients

$$\begin{aligned}
R^{\mathrm{s,i}}_{\mathrm{AA}} + R^{\mathrm{s,i}}_{\mathrm{BA}} + R^{\mathrm{s,i}}_{\mathrm{CA}} &= R^{\mathrm{s,i}}_{\mathrm{AA}} + R^{\mathrm{s,i}}_{\mathrm{AB}} + R^{\mathrm{s,i}}_{\mathrm{AC}} = 0 \\
R^{\mathrm{s,i}}_{\mathrm{AB}} + R^{\mathrm{s,i}}_{\mathrm{BB}} + R^{\mathrm{s,i}}_{\mathrm{CB}} &= R^{\mathrm{s,i}}_{\mathrm{BA}} + R^{\mathrm{s,i}}_{\mathrm{BB}} + R^{\mathrm{s,i}}_{\mathrm{BC}} = 0 \\
R^{\mathrm{s,i}}_{\mathrm{AC}} + R^{\mathrm{s,i}}_{\mathrm{BC}} + R^{\mathrm{s,i}}_{\mathrm{CC}} &= R^{\mathrm{s,i}}_{\mathrm{CA}} + R^{\mathrm{s,i}}_{\mathrm{CB}} + R^{\mathrm{s,i}}_{\mathrm{CC}} = 0
\end{aligned} \tag{12.23}$$

While we have for their ratios

$$\frac{R^{\mathrm{s,i}}_{jk}}{R^{\mathrm{s,i}}_{lm}} = \frac{R^{\mathrm{i}}_{jk}}{R^{\mathrm{i}}_{lm}} \quad \text{for} \quad j,k,l,m = \text{ A, B or C} \tag{12.24}$$

It follows that a relation *similar to Gibbs–Duhem's equation* in the homogeneous i-phase is valid for the chemical forces:

$$c^{\mathrm{i}}_{\mathrm{A}} \Delta_{\mathrm{i,s}} \mu_{\mathrm{A},T} + c^{\mathrm{i}}_{\mathrm{B}} \Delta_{\mathrm{i,s}} \mu_{\mathrm{B},T} + c^{\mathrm{i}}_{\mathrm{C}} \Delta_{\mathrm{i,s}} \mu_{\mathrm{C},T} = 0 \tag{12.25}$$

This may be shown by adding Eqs. (12.20b)–(12.20d) and using Eqs. (12.22) and (12.23). A relation like Eq. (12.25) can also be derived for the other side. These relations must not be confused with Gibbs–Duhem's equation for the surface, cf. Eq. (3.32).

Remark 12.2. *The reason that we find a relation analogous to Gibbs–Duhem's equation is the assumption that the ratios of the interface resistivities are the same as they are in the homogeneous regions next to the surface. This assumption may not be correct or only approximately correct. It is made because it may serve as a first order approximation that helps reduce the number of new independent resistivities introduced by the surface.*

Using Eq. (12.23) we can now write Eq. (12.20) in a form that is equivalent to Eq. (12.14):

$$\begin{aligned}
\Delta_{\mathrm{i,s}}T &= -\frac{1}{\lambda^{\mathrm{s,i}}}\left[J_q'^{\mathrm{i}} - c_{\mathrm{B}}^{\mathrm{i}} q_{\mathrm{B}}^{*,\mathrm{i}}\left(\mathrm{v}_{\mathrm{B}}^{\mathrm{i}} - \mathrm{v}_{\mathrm{A}}^{\mathrm{i}}\right) - c_{\mathrm{C}}^{\mathrm{i}} q_{\mathrm{C}}^{*,\mathrm{i}}\left(\mathrm{v}_{\mathrm{C}}^{\mathrm{i}} - \mathrm{v}_{\mathrm{A}}^{\mathrm{i}}\right)\right] \\
\frac{c_{\mathrm{B}}^{\mathrm{i}}}{T^{\mathrm{s}}}\Delta_{\mathrm{i,s}}\mu_{\mathrm{B},T} &= -\frac{c_{\mathrm{B}}^{\mathrm{i}} q_{\mathrm{B}}^{*,\mathrm{i}}}{T^{\mathrm{i}}T^{\mathrm{s}}}\Delta_{\mathrm{i,s}}T - R_{\mathrm{BA}}^{\mathrm{s,i}}\left(\mathrm{v}_{\mathrm{A}}^{\mathrm{i}} - \mathrm{v}_{\mathrm{B}}^{\mathrm{i}}\right) - R_{\mathrm{BC}}^{\mathrm{s,i}}\left(\mathrm{v}_{\mathrm{C}}^{\mathrm{i}} - \mathrm{v}_{\mathrm{B}}^{\mathrm{i}}\right) \\
\frac{c_{\mathrm{C}}^{\mathrm{i}}}{T^{\mathrm{s}}}\Delta_{\mathrm{i,s}}\mu_{\mathrm{C},T} &= -\frac{c_{\mathrm{C}}^{\mathrm{i}} q_{\mathrm{C}}^{*,\mathrm{i}}}{T^{\mathrm{i}}T^{\mathrm{s}}}\Delta_{\mathrm{i,s}}T - R_{\mathrm{CA}}^{\mathrm{s,i}}\left(\mathrm{v}_{\mathrm{A}}^{\mathrm{i}} - \mathrm{v}_{\mathrm{C}}^{\mathrm{i}}\right) - R_{\mathrm{CB}}^{\mathrm{s,i}}\left(\mathrm{v}_{\mathrm{B}}^{\mathrm{i}} - \mathrm{v}_{\mathrm{C}}^{\mathrm{i}}\right)
\end{aligned} \tag{12.26}$$

We left the equation for $\Delta_{\mathrm{i,s}}\mu_{\mathrm{A},T}$ out because it is redundant in view of Eq. (12.25). These are now the Maxwell–Stefan equations for the surface. The surface coefficients are equal to some characteristic length times the corresponding coefficient in the homogeneous phase.

For the o-side, the analysis is identical to the one given above for the i-side. The corresponding formulae are obtained from Eqs. (12.20) to (12.26) by replacing i by o in the superscripts and $\Delta_{\mathrm{i,s}}$ by $\Delta_{\mathrm{s,o}}$. The formulae equivalent to Eqs. (12.14) and (12.26) become, for instance,

$$\begin{aligned}
\Delta_{\mathrm{s,o}}T &= -\frac{1}{\lambda^{\mathrm{s,o}}}\left[J_q'^{\mathrm{o}} - c_{\mathrm{B}}^{\mathrm{o}} q_{\mathrm{B}}^{*,\mathrm{o}}\left(\mathrm{v}_{\mathrm{B}}^{\mathrm{o}} - \mathrm{v}_{\mathrm{A}}^{\mathrm{o}}\right) - c_{\mathrm{C}}^{\mathrm{o}} q_{\mathrm{C}}^{*,\mathrm{o}}\left(\mathrm{v}_{\mathrm{C}}^{\mathrm{o}} - \mathrm{v}_{\mathrm{A}}^{\mathrm{o}}\right)\right] \\
\frac{c_{\mathrm{B}}^{\mathrm{o}}}{T^{\mathrm{s}}}\Delta_{\mathrm{s,o}}\mu_{\mathrm{B},T} &= -\frac{c_{\mathrm{B}}^{\mathrm{o}} q_{\mathrm{B}}^{*,\mathrm{o}}}{T^{\mathrm{o}}T^{\mathrm{s}}}\Delta_{\mathrm{s,o}}T - R_{\mathrm{BA}}^{\mathrm{s,o}}\left(\mathrm{v}_{\mathrm{A}}^{\mathrm{o}} - \mathrm{v}_{\mathrm{B}}^{\mathrm{o}}\right) - R_{\mathrm{BC}}^{\mathrm{s,o}}\left(\mathrm{v}_{\mathrm{C}}^{\mathrm{o}} - \mathrm{v}_{\mathrm{B}}^{\mathrm{o}}\right) \\
\frac{c_{\mathrm{C}}^{\mathrm{o}}}{T^{\mathrm{s}}}\Delta_{\mathrm{s,o}}\mu_{\mathrm{C},T} &= -\frac{c_{\mathrm{C}}^{\mathrm{o}} q_{\mathrm{C}}^{*,\mathrm{o}}}{T^{\mathrm{o}}T^{\mathrm{s}}}\Delta_{\mathrm{s,o}}T - R_{\mathrm{CA}}^{\mathrm{s,o}}\left(\mathrm{v}_{\mathrm{A}}^{\mathrm{o}} - \mathrm{v}_{\mathrm{C}}^{\mathrm{o}}\right) - R_{\mathrm{CB}}^{\mathrm{s,o}}\left(\mathrm{v}_{\mathrm{B}}^{\mathrm{o}} - \mathrm{v}_{\mathrm{C}}^{\mathrm{o}}\right)
\end{aligned} \tag{12.27}$$

We note that the ratios of the resistivities in Eq. (12.26) and also in Eq. (12.27) are equal to the ratios of the corresponding resistivities in the adjacent homogeneous phases, as can be seen in Eq. (12.24). This implies that on each side of the surface only two new coefficients are needed when the coefficients in the homogeneous phases are known. On the i-side $\lambda^{\mathrm{s,i}}$

and $R^{\mathrm{s,i}}_{\mathrm{BA}}$ would for instance be enough. In an analysis of heat and mass diffusion through a surface one should combine Eq. (12.14) for the homogeneous phases with Eqs. (12.26) and (12.27) for the surface.

12.4 Multi-component diffusion

We continue to show how the Maxwell–Stefan equations are related to other ways of describing multi-component diffusion.

12.4.1 *Prigogine's theorem*

Prigogine showed in 1947 that an arbitrary frame of reference can be chosen for systems in mechanical equilibrium [15], see Sec. 4.4. This property is known as Prigogine's theorem. Using Eq. (12.5), we can write Eq. (12.3) in the form

$$\begin{aligned}
\frac{\partial}{\partial x}\frac{1}{T} &= r_{qq}J'_q + r_{q\mathrm{A}}\left(\mathrm{v_A}-\mathrm{v_{ref}}\right) + r_{q\mathrm{B}}\left(\mathrm{v_B}-\mathrm{v_{ref}}\right) + r_{q\mathrm{C}}\left(\mathrm{v_C}-\mathrm{v_{ref}}\right)\\
-\frac{c_{\mathrm{A}}}{T}\frac{\partial \mu_{\mathrm{A},T}}{\partial x} &= r_{\mathrm{A}q}J'_q + r_{\mathrm{AA}}\left(\mathrm{v_A}-\mathrm{v_{ref}}\right) + r_{\mathrm{AB}}\left(\mathrm{v_B}-\mathrm{v_{ref}}\right) + r_{\mathrm{AC}}\left(\mathrm{v_C}-\mathrm{v_{ref}}\right)\\
-\frac{c_{\mathrm{B}}}{T}\frac{\partial \mu_{\mathrm{B},T}}{\partial x} &= r_{\mathrm{B}q}J'_q + r_{\mathrm{BA}}\left(\mathrm{v_A}-\mathrm{v_{ref}}\right) + r_{\mathrm{BB}}\left(\mathrm{v_B}-\mathrm{v_{ref}}\right) + r_{\mathrm{BC}}\left(\mathrm{v_C}-\mathrm{v_{ref}}\right)\\
-\frac{c_{\mathrm{C}}}{T}\frac{\partial \mu_{\mathrm{C},T}}{\partial x} &= r_{\mathrm{C}q}J'_q + r_{\mathrm{CA}}\left(\mathrm{v_A}-\mathrm{v_{ref}}\right) + r_{\mathrm{CB}}\left(\mathrm{v_B}-\mathrm{v_{ref}}\right) + r_{\mathrm{CC}}\left(\mathrm{v_C}-\mathrm{v_{ref}}\right)
\end{aligned} \tag{12.28}$$

where $\mathrm{v_{ref}}$ is an arbitrary reference velocity. This shows that we can use an arbitrary frame of reference for the transports, see also [20] Sec. V.2. A system in mechanical equilibrium becomes isobaric when the external forces vanish and the viscous forces are negligible.

By introducing molar fluxes relative to the arbitrary frame of reference, $J_{j,\mathrm{ref}} \equiv c_j\left(\mathrm{v}_j - \mathrm{v_{ref}}\right)$, the above equations can be written as:

$$\begin{aligned}
\frac{\partial T}{\partial x} &= -\frac{1}{\lambda}\left(J'_q - q^*_{\mathrm{A}}J_{\mathrm{A,ref}} - q^*_{\mathrm{B}}J_{\mathrm{B,ref}} - q^*_{\mathrm{C}}J_{\mathrm{C,ref}}\right)\\
\frac{c_{\mathrm{A}}}{T}\frac{\partial \mu_{\mathrm{A},T}}{\partial x} &= -\frac{c_{\mathrm{A}}q^*_{\mathrm{A}}}{T^2}\frac{\partial T}{\partial x} - \frac{R_{\mathrm{AA}}}{c_{\mathrm{A}}}J_{\mathrm{A,ref}} - \frac{R_{\mathrm{AB}}}{c_{\mathrm{B}}}J_{\mathrm{B,ref}} - \frac{R_{\mathrm{AC}}}{c_{\mathrm{C}}}J_{\mathrm{C,ref}}\\
\frac{c_{\mathrm{B}}}{T}\frac{\partial \mu_{\mathrm{B},T}}{\partial x} &= -\frac{c_{\mathrm{B}}q^*_{\mathrm{B}}}{T^2}\frac{\partial T}{\partial x} - \frac{R_{\mathrm{BA}}}{c_{\mathrm{A}}}J_{\mathrm{A,ref}} - \frac{R_{\mathrm{BB}}}{c_{\mathrm{B}}}J_{\mathrm{B,ref}} - \frac{R_{\mathrm{BC}}}{c_{\mathrm{C}}}J_{\mathrm{C,ref}}\\
\frac{c_{\mathrm{C}}}{T}\frac{\partial \mu_{\mathrm{C},T}}{\partial x} &= -\frac{c_{\mathrm{C}}q^*_{\mathrm{C}}}{T^2}\frac{\partial T}{\partial x} - \frac{R_{\mathrm{CA}}}{c_{\mathrm{A}}}J_{\mathrm{A,ref}} - \frac{R_{\mathrm{CB}}}{c_{\mathrm{B}}}J_{\mathrm{B,ref}} - \frac{R_{\mathrm{CC}}}{c_{\mathrm{C}}}J_{\mathrm{C,ref}}
\end{aligned} \tag{12.29}$$

where thermal conductivity, the heats of transfer and the resistivities for component fluxes at constant temperature are defined in Eq. (12.8). The heats of transfer and the resistivities for component fluxes at constant temperature satisfy Eqs. (12.9)–(12.11).

The result is that we can measure six independent coefficients in any frame of reference, and calculate the other coefficients using Eqs. (12.9)–(12.11). Subsequently we can use the coefficients in all other frames of reference with Eqs. (12.29). In order to clarify this procedure, we consider the solvent frame of reference specifically.

12.4.2 *Diffusion in the solvent frame of reference*

When there is an excess of one component, say component C, it is convenient to use the velocity of that component as a frame of reference, $\mathrm{v_{ref}} = \mathrm{v_{solv}} = \mathrm{v_C}$. In this solvent frame of reference $J_{\mathrm{C,ref}} = J_{\mathrm{C,solv}} = 0$. One term in the entropy production disappears. The remaining set of linear laws reduces to

$$\begin{aligned}
\frac{\partial T}{\partial x} &= -\frac{1}{\lambda}\left(J'_q - q^*_{\mathrm{A}} J_{\mathrm{A,solv}} - q^*_{\mathrm{B}} J_{\mathrm{B,solv}}\right) \\
\frac{c_{\mathrm{A}}}{T}\frac{\partial \mu_{\mathrm{A},T}}{\partial x} &= -\frac{c_{\mathrm{A}} q^*_{\mathrm{A}}}{T^2}\frac{\partial T}{\partial x} - \frac{R_{\mathrm{AA}}}{c_{\mathrm{A}}} J_{\mathrm{A,solv}} - \frac{R_{\mathrm{AB}}}{c_{\mathrm{B}}} J_{\mathrm{B,solv}} \\
\frac{c_{\mathrm{B}}}{T}\frac{\partial \mu_{\mathrm{B},T}}{\partial x} &= -\frac{c_{\mathrm{B}} q^*_{\mathrm{B}}}{T^2}\frac{\partial T}{\partial x} - \frac{R_{\mathrm{BA}}}{c_{\mathrm{A}}} J_{\mathrm{A,solv}} - \frac{R_{\mathrm{BB}}}{c_{\mathrm{B}}} J_{\mathrm{B,solv}}
\end{aligned} \tag{12.30}$$

Using Onsager symmetry, these expressions contain the six independent transport coefficients. Solving Eqs. (12.30b, c) for the molar fluxes relative to the solvent velocity gives

$$\begin{aligned}
J_{\mathrm{A,solv}} &= -L_{\mathrm{AA}}\frac{c_{\mathrm{A}}^2}{T}\left(\frac{\partial \mu_{\mathrm{A},T}}{\partial x} + \frac{q^*_{\mathrm{A}}}{T}\frac{\partial T}{\partial x}\right) - L_{\mathrm{AB}}\frac{c_{\mathrm{A}} c_{\mathrm{B}}}{T}\left(\frac{\partial \mu_{\mathrm{B},T}}{\partial x} + \frac{q^*_{\mathrm{B}}}{T}\frac{\partial T}{\partial x}\right) \\
J_{\mathrm{B,solv}} &= -L_{\mathrm{BA}}\frac{c_{\mathrm{B}} c_{\mathrm{A}}}{T}\left(\frac{\partial \mu_{\mathrm{A},T}}{\partial x} + \frac{q^*_{\mathrm{A}}}{T}\frac{\partial T}{\partial x}\right) - L_{\mathrm{BB}}\frac{c_{\mathrm{B}}^2}{T}\left(\frac{\partial \mu_{\mathrm{B},T}}{\partial x} + \frac{q^*_{\mathrm{B}}}{T}\frac{\partial T}{\partial x}\right)
\end{aligned} \tag{12.31}$$

where

$$\begin{aligned}
L_{\mathrm{AA}} &= \frac{R_{\mathrm{BB}}}{R_{\mathrm{AA}}R_{\mathrm{BB}} - R_{\mathrm{BA}}R_{\mathrm{AB}}}, \quad L_{\mathrm{AB}} = L_{\mathrm{BA}} = \frac{-R_{\mathrm{AB}}}{R_{\mathrm{AA}}R_{\mathrm{BB}} - R_{\mathrm{BA}}R_{\mathrm{AB}}} \\
L_{\mathrm{BB}} &= \frac{R_{\mathrm{AA}}}{R_{\mathrm{AA}}R_{\mathrm{BB}} - R_{\mathrm{BA}}R_{\mathrm{AB}}}
\end{aligned} \tag{12.32}$$

and vice versa

$$R_{\mathrm{AA}} = \frac{L_{\mathrm{BB}}}{L_{\mathrm{AA}}L_{\mathrm{BB}} - L_{\mathrm{BA}}L_{\mathrm{AB}}}, \quad R_{\mathrm{AB}} = R_{\mathrm{BA}} = \frac{-L_{\mathrm{AB}}}{L_{\mathrm{AA}}L_{\mathrm{BB}} - L_{\mathrm{BA}}L_{\mathrm{AB}}}$$

$$R_{\mathrm{BB}} = \frac{L_{\mathrm{AA}}}{L_{\mathrm{AA}}L_{\mathrm{BB}} - L_{\mathrm{BA}}L_{\mathrm{AB}}} \tag{12.33}$$

The heat and molar fluxes may also be expressed in terms of the temperature and chemical potential gradients

$$\begin{aligned}
J'_q = &- \left[\lambda + L_{\mathrm{AA}}\left(\frac{c_{\mathrm{A}}q^*_{\mathrm{A}}}{T}\right)^2 + 2L_{\mathrm{AB}}\frac{c_{\mathrm{A}}q^*_{\mathrm{A}}c_{\mathrm{B}}q^*_{\mathrm{B}}}{T^2} + L_{\mathrm{BB}}\left(\frac{c_{\mathrm{B}}q^*_{\mathrm{B}}}{T}\right)^2\right]\frac{\partial T}{\partial x} \\
&- \left(c_{\mathrm{A}}q^*_{\mathrm{A}}L_{\mathrm{AA}} + c_{\mathrm{B}}q^*_{\mathrm{B}}L_{\mathrm{BA}}\right)\frac{c_{\mathrm{A}}}{T}\frac{\partial \mu_{\mathrm{A},T}}{\partial x} \\
&- \left(c_{\mathrm{A}}q^*_{\mathrm{A}}L_{\mathrm{AB}} + c_{\mathrm{B}}q^*_{\mathrm{B}}L_{\mathrm{BB}}\right)\frac{c_{\mathrm{B}}}{T}\frac{\partial \mu_{\mathrm{B},T}}{\partial x} \\
J_{\mathrm{A,solv}} = &- \left(c_{\mathrm{A}}q^*_{\mathrm{A}}L_{\mathrm{AA}} + c_{\mathrm{B}}q^*_{\mathrm{B}}L_{\mathrm{AB}}\right)\frac{c_{\mathrm{A}}}{T^2}\frac{\partial T}{\partial x} - L_{\mathrm{AA}}\frac{c^2_{\mathrm{A}}}{T}\frac{\partial \mu_{\mathrm{A},T}}{\partial x} \\
&- L_{\mathrm{AB}}\frac{c_{\mathrm{A}}c_{\mathrm{B}}}{T}\frac{\partial \mu_{\mathrm{B},T}}{\partial x} \\
J_{\mathrm{B,solv}} = &- \left(c_{\mathrm{A}}q^*_{\mathrm{A}}L_{\mathrm{BA}} + c_{\mathrm{B}}q^*_{\mathrm{B}}L_{\mathrm{BB}}\right)\frac{c_{\mathrm{B}}}{T^2}\frac{\partial T}{\partial x} - L_{\mathrm{BA}}\frac{c_{\mathrm{B}}c_{\mathrm{A}}}{T}\frac{\partial \mu_{\mathrm{A},T}}{\partial x} \\
&- L_{\mathrm{BB}}\frac{c^2_{\mathrm{B}}}{T}\frac{\partial \mu_{\mathrm{B},T}}{\partial x}
\end{aligned} \tag{12.34}$$

Converting the chemical potential gradients to concentration gradients this becomes, using ideal solution conditions,

$$\begin{aligned}
J'_q &= -\lambda_\mu\frac{\partial T}{\partial x} - RT^2D''_{\mathrm{AT,solv}}\frac{\partial c_{\mathrm{A}}}{\partial x} - RT^2D''_{\mathrm{BT,solv}}\frac{\partial c_{\mathrm{B}}}{\partial x} \\
J_{\mathrm{A,solv}} &= -c_{\mathrm{A}}D'_{\mathrm{AT,solv}}\frac{\partial T}{\partial x} - D_{\mathrm{AA,solv}}\frac{\partial c_{\mathrm{A}}}{\partial x} - D_{\mathrm{AB,solv}}\frac{\partial c_{\mathrm{B}}}{\partial x} \\
J_{\mathrm{B,solv}} &= -c_{\mathrm{B}}D'_{\mathrm{BT,solv}}\frac{\partial T}{\partial x} - D_{\mathrm{BA,solv}}\frac{\partial c_{\mathrm{A}}}{\partial x} - D_{\mathrm{BB,solv}}\frac{\partial c_{\mathrm{B}}}{\partial x}
\end{aligned} \tag{12.35}$$

where the transport coefficients are given by

$$\lambda_\mu = \lambda + L_{\rm AA}\left(\frac{c_{\rm A}q^*_{\rm A}}{T}\right)^2 + 2L_{\rm AB}\frac{c_{\rm A}q^*_{\rm A}c_{\rm B}q^*_{\rm B}}{T^2} + L_{\rm BB}\left(\frac{c_{\rm B}q^*_{\rm B}}{T}\right)^2$$

$$D''_{\rm AT,solv} = \frac{c_{\rm A}q^*_{\rm A}L_{\rm AA} + c_{\rm B}q^*_{\rm B}L_{\rm BA}}{T^2}, \quad D''_{\rm BT,solv} = \frac{c_{\rm A}q^*_{\rm A}L_{\rm AB} + c_{\rm B}q^*_{\rm B}L_{\rm BB}}{T^2}$$

$$D'_{\rm AT,solv} = \frac{c_{\rm A}q^*_{\rm A}L_{\rm AA} + c_{\rm B}q^*_{\rm B}L_{\rm AB}}{T^2}, \quad D'_{\rm BT,solv} = \frac{c_{\rm A}q^*_{\rm A}L_{\rm BA} + c_{\rm B}q^*_{\rm B}L_{\rm BB}}{T^2}$$

$$D_{\rm AA,solv} = L_{\rm AA}c_{\rm A}R, \quad D_{\rm AB,solv} = L_{\rm AB}c_{\rm A}R$$

$$D_{\rm BA,solv} = L_{\rm BA}c_{\rm B}R, \quad D_{\rm BB,solv} = L_{\rm BB}c_{\rm B}R \tag{12.36}$$

Here λ_μ is the thermal conductivity in a system without concentration gradients. Using Onsager symmetry, it follows that the Dufour coefficients, $D''_{\rm AT,solv}$ and $D''_{\rm BT,solv}$, are equal to the thermal diffusion coefficients, $D'_{\rm AT,solv}$ and $D'_{\rm BT,solv}$. The matrix of diffusion coefficients in the solvent frame of reference, given in the bottom two lines, is *not* symmetric. Once one has measured the diffusion coefficients one can calculate $L_{\rm AA}$, $L_{\rm AB} = L_{\rm BA}$ and $L_{\rm BB}$. By using Eq. (12.33), we then have the three independent resistivities, R_{ij} for $i, j =$ A or B. Together with Eq. (12.8) and the values of λ, $q^*_{\rm A}$, $q^*_{\rm B}$ one can then obtain r_{ij} for $i, j = q$, A or B. The rest of the resistivities then follows using Eqs. (12.5) and (12.6). From the relations (12.9)–(12.11) between the resistivities, in the four by four matrix, we can further obtain the complete matrix. This makes it possible to compare these values with values obtained in any other frame of reference.

12.4.3 *Other frames of reference*

Most of the reference velocities given in Sec. 4.4 are averages of velocities of the components and can be written as

$$\mathrm{v}_{\rm ref} \equiv a_{\rm A}\mathrm{v}_{\rm A} + a_{\rm B}\mathrm{v}_{\rm B} + a_{\rm C}\mathrm{v}_{\rm C} \quad \text{with} \quad a_{\rm A} + a_{\rm B} + a_{\rm C} = 1 \tag{12.37}$$

Exceptions are the laboratory or the wall frame of reference, where $v_{\rm ref} = 0$, and the surface frame of reference, which uses the velocity of the surface as a reference velocity. Using Eq. (12.37), it follows that the diffusion fluxes satisfy

Table 12.1 Coefficients for transformations between frames of reference.

	a_A	a_B	a_C
solvent	0	0	1
average molar	x_A	x_B	x_C
average volume	$c_\mathrm{A}V_\mathrm{A}$	$c_\mathrm{B}V_\mathrm{B}$	$c_\mathrm{C}V_\mathrm{C}$
barycentric	ρ_A/ρ	ρ_B/ρ	ρ_C/ρ

$$\frac{a_\mathrm{A}}{c_\mathrm{A}}J_{\mathrm{A,ref}} + \frac{a_\mathrm{B}}{c_\mathrm{B}}J_{\mathrm{B,ref}} + \frac{a_\mathrm{C}}{c_\mathrm{C}}J_{\mathrm{C,ref}} = 0 \tag{12.38}$$

The fluxes are therefore dependent in these frames of reference. The particular values of the averaging coefficients are given in the Table 12.1 for all frames of reference that were discussed in Sec. 4.4.

For each choice of reference velocity, it is sufficient to use only three of the equations in Eq. (12.7). By using Eq. (12.38), these three equations can be written as

$$\begin{aligned}
\frac{\partial T}{\partial x} &= -\frac{1}{\lambda}\left[J'_q - \left(q^*_\mathrm{A} - \frac{a_\mathrm{A}c_\mathrm{C}}{c_\mathrm{A}a_\mathrm{C}}q^*_\mathrm{C}\right)J_{\mathrm{A,ref}} - \left(q^*_\mathrm{B} - \frac{a_\mathrm{B}c_\mathrm{C}}{c_\mathrm{B}a_\mathrm{C}}q^*_\mathrm{C}\right)J_{\mathrm{B,ref}}\right] \\
\frac{c_\mathrm{A}}{T}\frac{\partial \mu_{\mathrm{A},T}}{\partial x} &= -\frac{c_\mathrm{A}q^*_\mathrm{A}}{T^2}\frac{\partial T}{\partial x} - \frac{1}{c_\mathrm{A}}\left(R_\mathrm{AA} - \frac{a_\mathrm{A}}{a_\mathrm{C}}R_\mathrm{AC}\right)J_{\mathrm{A,ref}} \\
&\quad - \frac{1}{c_\mathrm{B}}\left(R_\mathrm{AB} - \frac{a_\mathrm{B}}{a_\mathrm{C}}R_\mathrm{AC}\right)J_{\mathrm{B,ref}} \\
\frac{c_\mathrm{B}}{T}\frac{\partial \mu_{\mathrm{B},T}}{\partial x} &= -\frac{c_\mathrm{B}q^*_\mathrm{B}}{T^2}\frac{\partial T}{\partial x} - \frac{1}{c_\mathrm{A}}\left(R_\mathrm{BA} - \frac{a_\mathrm{A}}{a_\mathrm{C}}R_\mathrm{BC}\right)J_{\mathrm{A,ref}} \\
&\quad - \frac{1}{c_\mathrm{B}}\left(R_\mathrm{BB} - \frac{a_\mathrm{B}}{a_\mathrm{C}}R_\mathrm{BC}\right)J_{\mathrm{B,ref}}
\end{aligned} \tag{12.39}$$

Defining new resistivities in the chosen frame of reference by

$$\begin{aligned}
R_{\mathrm{AA,ref}} &\equiv R_\mathrm{AA} - \frac{a_\mathrm{A}}{a_\mathrm{C}}R_\mathrm{AC}, \quad R_{\mathrm{AB,ref}} \equiv R_\mathrm{AB} - \frac{a_\mathrm{B}}{a_\mathrm{C}}R_\mathrm{AC} \\
R_{\mathrm{BA,ref}} &\equiv R_\mathrm{BA} - \frac{a_\mathrm{A}}{a_\mathrm{C}}R_\mathrm{BC}, \quad R_{\mathrm{BB,ref}} \equiv R_\mathrm{BB} - \frac{a_\mathrm{B}}{a_\mathrm{C}}R_\mathrm{BC}
\end{aligned} \tag{12.40}$$

Eqs. (12.39b, c) can be written as

$$\begin{aligned}
\frac{c_\mathrm{A}}{T}\frac{\partial \mu_{\mathrm{A},T}}{\partial x} &= -\frac{c_\mathrm{A} q^*_\mathrm{A}}{T^2}\frac{\partial T}{\partial x} - \frac{1}{c_\mathrm{A}} R_{\mathrm{AA,ref}} J_{\mathrm{A,ref}} \\
&\quad - \frac{1}{c_\mathrm{B}} R_{\mathrm{AB,ref}} J_{\mathrm{B,ref}} \\
\frac{c_\mathrm{B}}{T}\frac{\partial \mu_{\mathrm{B},T}}{\partial x} &= -\frac{c_\mathrm{B} q^*_\mathrm{B}}{T^2}\frac{\partial T}{\partial x} - \frac{1}{c_\mathrm{A}} R_{\mathrm{BA,ref}} J_{\mathrm{A,ref}} \\
&\quad - \frac{1}{c_\mathrm{B}} R_{\mathrm{BB,ref}} J_{\mathrm{B,ref}}
\end{aligned} \tag{12.41}$$

The 2×2 matrix $R_{ij,\mathrm{ref}}$ is not symmetric, but the description can be directly related to the experimental situation. By inverting the equations, we obtain for the component fluxes

$$\begin{aligned}
J_{\mathrm{A,ref}} &= -L_{\mathrm{AA,ref}} \frac{c_\mathrm{A}^2}{T}\left(\frac{\partial \mu_{\mathrm{A},T}}{\partial x} + \frac{q^*_\mathrm{A}}{T}\frac{\partial T}{\partial x}\right) \\
&\quad - L_{\mathrm{AB,ref}} \frac{c_\mathrm{A} c_\mathrm{B}}{T}\left(\frac{\partial \mu_{\mathrm{B},T}}{\partial x} + \frac{q^*_\mathrm{B}}{T}\frac{\partial T}{\partial x}\right) \\
J_{\mathrm{B,ref}} &= -L_{\mathrm{BA,ref}} \frac{c_\mathrm{A} c_\mathrm{B}}{T}\left(\frac{\partial \mu_{\mathrm{A},T}}{\partial x} + \frac{q^*_\mathrm{A}}{T}\frac{\partial T}{\partial x}\right) \\
&\quad - L_{\mathrm{BB,ref}} \frac{c_\mathrm{B}^2}{T}\left(\frac{\partial \mu_{\mathrm{B},T}}{\partial x} + \frac{q^*_\mathrm{B}}{T}\frac{\partial T}{\partial x}\right)
\end{aligned} \tag{12.42}$$

where

$$\begin{aligned}
L_{\mathrm{AA,ref}} &= \frac{R_{\mathrm{BB,ref}}}{R_{\mathrm{AA,ref}}R_{\mathrm{BB,ref}} - R_{\mathrm{BA,ref}}R_{\mathrm{AB,ref}}} \\
L_{\mathrm{AB,ref}} &= \frac{-R_{\mathrm{BA,ref}}}{R_{\mathrm{AA,ref}}R_{\mathrm{BB,ref}} - R_{\mathrm{BA,ref}}R_{\mathrm{AB,ref}}} \\
L_{\mathrm{BA,ref}} &= \frac{-R_{\mathrm{AB,ref}}}{R_{\mathrm{AA,ref}}R_{\mathrm{BB,ref}} - R_{\mathrm{BA,ref}}R_{\mathrm{AB,ref}}} \\
L_{\mathrm{BB,ref}} &= \frac{R_{\mathrm{AA,ref}}}{R_{\mathrm{AA,ref}}R_{\mathrm{BB,ref}} - R_{\mathrm{BA,ref}}R_{\mathrm{AB,ref}}}
\end{aligned} \tag{12.43}$$

and vice versa

$$
\begin{aligned}
R_{\mathrm{AA,ref}} &= \frac{L_{\mathrm{BB,ref}}}{L_{\mathrm{AA,ref}}L_{\mathrm{BB,ref}} - L_{\mathrm{BA,ref}}L_{\mathrm{AB,ref}}} \\
R_{\mathrm{AB,ref}} &= \frac{-L_{\mathrm{BA,ref}}}{L_{\mathrm{AA,ref}}L_{\mathrm{BB,ref}} - L_{\mathrm{BA,ref}}L_{\mathrm{AB,ref}}} \\
R_{\mathrm{BA,ref}} &= \frac{-L_{\mathrm{AB,ref}}}{L_{\mathrm{AA,ref}}L_{\mathrm{BB,ref}} - L_{\mathrm{BA,ref}}L_{\mathrm{AB,ref}}} \\
R_{\mathrm{BB,ref}} &= \frac{L_{\mathrm{AA,ref}}}{L_{\mathrm{AA,ref}}L_{\mathrm{BB,ref}} - L_{\mathrm{BA,ref}}L_{\mathrm{AB,ref}}}
\end{aligned}
\tag{12.44}
$$

The 2×2 conductivity and the resistivity matrices are both asymmetric. By expressing the heat flux and the component fluxes in terms of the temperature and chemical potential gradients, we find

$$
\begin{aligned}
J'_q = &- \left[\lambda + \frac{1}{T^2}\left(c_{\mathrm{A}}q^*_{\mathrm{A}} - \frac{a_{\mathrm{A}}}{a_{\mathrm{C}}}c_{\mathrm{C}}q^*_{\mathrm{C}}\right)\left(c_{\mathrm{A}}q^*_{\mathrm{A}}L_{\mathrm{AA,ref}} + c_{\mathrm{B}}q^*_{\mathrm{B}}L_{\mathrm{AB,ref}}\right)\right. \\
&\left. + \frac{1}{T^2}\left(c_{\mathrm{B}}q^*_{\mathrm{B}} - \frac{a_{\mathrm{B}}}{a_{\mathrm{C}}}c_{\mathrm{C}}q^*_{\mathrm{C}}\right)\left(c_{\mathrm{A}}q^*_{\mathrm{A}}L_{\mathrm{BA,ref}} + c_{\mathrm{B}}q^*_{\mathrm{B}}L_{\mathrm{BB,ref}}\right)\right]\frac{\partial T}{\partial x} \\
&- \left[\left(c_{\mathrm{A}}q^*_{\mathrm{A}} - \frac{a_{\mathrm{A}}}{a_{\mathrm{C}}}c_{\mathrm{C}}q^*_{\mathrm{C}}\right)L_{\mathrm{AA,ref}} + \left(c_{\mathrm{B}}q^*_{\mathrm{B}} - \frac{a_{\mathrm{B}}}{a_{\mathrm{C}}}c_{\mathrm{C}}q^*_{\mathrm{C}}\right)L_{\mathrm{BA,ref}}\right]\frac{c_{\mathrm{A}}}{T}\frac{\partial \mu_{\mathrm{A},T}}{\partial x} \\
&- \left[\left(c_{\mathrm{A}}q^*_{\mathrm{A}} - \frac{a_{\mathrm{A}}}{a_{\mathrm{C}}}c_{\mathrm{C}}q^*_{\mathrm{C}}\right)L_{\mathrm{AB,ref}} + \left(c_{\mathrm{B}}q^*_{\mathrm{B}} - \frac{a_{\mathrm{B}}}{a_{\mathrm{C}}}c_{\mathrm{C}}q^*_{\mathrm{C}}\right)L_{\mathrm{BB,ref}}\right]\frac{c_{\mathrm{B}}}{T}\frac{\partial \mu_{\mathrm{B},T}}{\partial x} \\
J_{\mathrm{A,ref}} = &- \frac{c_{\mathrm{A}}}{T^2}\left(c_{\mathrm{A}}q^*_{\mathrm{A}}L_{\mathrm{AA,ref}} + c_{\mathrm{B}}q^*_{\mathrm{B}}L_{\mathrm{AB,ref}}\right)\frac{\partial T}{\partial x} - L_{\mathrm{AA,ref}}\frac{c^2_{\mathrm{A}}}{T}\frac{\partial \mu_{\mathrm{A},T}}{\partial x} \\
&- L_{\mathrm{AB,ref}}\frac{c_{\mathrm{A}}c_{\mathrm{B}}}{T}\frac{\partial \mu_{\mathrm{B},T}}{\partial x} \\
J_{\mathrm{B,ref}} = &- \frac{c_{\mathrm{B}}}{T}\left(c_{\mathrm{A}}q^*_{\mathrm{A}}L_{\mathrm{BA,ref}} + c_{\mathrm{B}}q^*_{\mathrm{B}}L_{\mathrm{BB,ref}}\right)\frac{\partial T}{\partial x} - L_{\mathrm{BA,ref}}\frac{c_{\mathrm{A}}c_{\mathrm{B}}}{T}\frac{\partial \mu_{\mathrm{A},T}}{\partial x} \\
&- L_{\mathrm{BB,ref}}\frac{c^2_{\mathrm{B}}}{T}\frac{\partial \mu_{\mathrm{B},T}}{\partial x}
\end{aligned}
\tag{12.45}
$$

We express the chemical potential gradients in terms of gradients of the concentration. We restrict ourselves to ideal solution of components A and B. By introducing the transport coefficients in the chosen frame of reference,

we find

$$\begin{aligned}
\lambda_\mu &= \lambda + \frac{1}{T^2}\left(c_{\rm A}q^*_{\rm A} - \frac{a_{\rm A}}{a_{\rm C}}c_{\rm C}q^*_{\rm C}\right)\left(c_{\rm A}q^*_{\rm A}L_{\rm AA,ref} + c_{\rm B}q^*_{\rm B}L_{\rm AB,ref}\right) \\
&\quad + \frac{1}{T^2}\left(c_{\rm B}q^*_{\rm B} - \frac{a_{\rm B}}{a_{\rm C}}c_{\rm C}q^*_{\rm C}\right)\left(c_{\rm A}q^*_{\rm A}L_{\rm BA,ref} + c_{\rm B}q^*_{\rm B}L_{\rm BB,ref}\right) \\
D''_{\rm AT,ref} &= \frac{1}{T^2}\left[\left(c_{\rm A}q^*_{\rm A} - \frac{a_{\rm A}}{a_{\rm C}}c_{\rm C}q^*_{\rm C}\right)L_{\rm AA,ref} + \left(c_{\rm B}q^*_{\rm B} - \frac{a_{\rm B}}{a_{\rm C}}c_{\rm C}q^*_{\rm C}\right)L_{\rm BA,ref}\right] \\
D''_{\rm BT,ref} &= \frac{1}{T^2}\left[\left(c_{\rm A}q^*_{\rm A} - \frac{a_{\rm A}}{a_{\rm C}}c_{\rm C}q^*_{\rm C}\right)L_{\rm AB,ref} + \left(c_{\rm B}q^*_{\rm B} - \frac{a_{\rm B}}{a_{\rm C}}c_{\rm C}q^*_{\rm C}\right)L_{\rm BB,ref}\right] \\
D'_{\rm AT,ref} &= \frac{1}{T^2}\left(c_{\rm A}q^*_{\rm A}L_{\rm AA,ref} + c_{\rm B}q^*_{\rm B}L_{\rm AB,ref}\right) \\
D'_{\rm BT,ref} &= \frac{1}{T^2}\left(c_{\rm A}q^*_{\rm A}L_{\rm BA,ref} + c_{\rm B}q^*_{\rm B}L_{\rm BB,ref}\right) \\
D_{\rm AA,ref} &= L_{\rm AA,ref}c_{\rm A}R, \quad D_{\rm AB,ref} = L_{\rm AB,ref}c_{\rm A}R \\
D_{\rm BA,ref} &= L_{\rm BA,ref}c_{\rm B}R, \quad D_{\rm BB,ref} = L_{\rm BB,ref}c_{\rm B}R
\end{aligned} \tag{12.46}$$

we can write Eq. (12.45) in the usual form

$$\begin{aligned}
J'_q &= -\lambda_\mu\frac{\partial T}{\partial x} - RT^2D''_{\rm AT,ref}\frac{\partial c_{\rm A}}{\partial x} - RT^2D''_{\rm BT,ref}\frac{\partial c_{\rm B}}{\partial x} \\
J_{\rm A,ref} &= -c_{\rm A}D'_{\rm AT,ref}\frac{\partial T}{\partial x} - D_{\rm AA,ref}\frac{\partial c_{\rm A}}{\partial x} - D_{\rm AB,ref}\frac{\partial c_{\rm B}}{\partial x} \\
J_{\rm B,ref} &= -c_{\rm B}D'_{\rm BT,ref}\frac{\partial T}{\partial x} - D_{\rm BA,ref}\frac{\partial c_{\rm A}}{\partial x} - D_{\rm BB,ref}\frac{\partial c_{\rm B}}{\partial x}
\end{aligned} \tag{12.47}$$

Given the experimental values of the transport coefficients used in Eq. (12.47), one can calculate $L_{\rm AA,ref}$, $L_{\rm AB,ref}$, $L_{\rm BA,ref}$, $L_{\rm BB,ref}$, $q^*_{\rm A}$, $q^*_{\rm B}$ and λ using Eq. (12.46). The two by two resistivity matrix, $R_{\rm AA,ref}$, $R_{\rm AB,ref}$, $R_{\rm BA,ref}$, $R_{\rm BB,ref}$, then follows using Eq. (12.44). The two by two resistivity matrix, $R_{\rm AA}$, $R_{\rm AB}$, $R_{\rm BA}$, $R_{\rm BB}$, then follows using Eq. (12.40). The coefficients $R_{\rm AC} = R_{\rm CA}$, $R_{\rm BC} = R_{\rm CB}$, $R_{\rm CC}$ and $q^*_{\rm C}$ can then be found using Eqs. (12.9)-(12.11). In order to find the four by four matrix of resistivities r_{jk} one finally uses Eq. (12.8). Using the four by four matrix of resistivities, one can then go to all other frames of reference and also calculate the Maxwell–Stefan diffusion coefficients.

Exercise 12.4.1. *Fick's law in the solvent frame of reference can be written* $J_{A,solv} = -D_{AA,solv}\partial c_A/\partial x$. *With the average volume frame of reference, we write* $J_{A,vol} = -D_{AA,vol}\partial c_A/\partial x$. *For what condition is* $D_{AA,vol} \simeq D_{AA,solv}$?

- **Solution:** When $D_{\mathrm{AA,vol}} \simeq D_{\mathrm{AA,solv}}$, using Fick's law, it follows that $J_{\mathrm{A,solv}} \simeq J_{\mathrm{A,vol}}$. For the solvent and average volume frames of reference, we write

$$J_{\mathrm{A,solv}} = c_{\mathrm{A}}\left(\mathrm{v_A} - \mathrm{v_{solv}}\right)$$
$$J_{\mathrm{A,vol}} = c_{\mathrm{A}}\left(\mathrm{v_A} - \mathrm{v_{vol}}\right)$$

The fluxes and the diffusion constants are therefore approximately the same when

$$\mathrm{v_{solv}} \simeq \mathrm{v_{vol}}$$

Consider a two-component mixture where component 2 is the solvent. We then have

$$\mathrm{v_{solv}} = \mathrm{v_2}$$
$$\mathrm{v_{vol}} = c_1 V_1 \mathrm{v_1} + c_2 V_2 \mathrm{v_2} = \mathrm{v_2} + c_1 V_1\left(\mathrm{v_1} - \mathrm{v_2}\right)$$

We see that $\mathrm{v_{solv}} \simeq \mathrm{v_{vol}}$, when $c_1 V_1 \ll c_2 V_2 \simeq 1$. This is true for an ideal solution of component 1 in component 2.

12.4.4 *An example: Kinetic demixing of oxides*

Consider an oxygen ion conductor of thickness l and composition (A,B)O where A and B hold the same lattice position and charge +2. Examples of such crystals are (Co, Mg)O and (Fe,Cr)O. A chemical potential difference of oxygen is applied across the crystal in order to measure oxygen ion diffusion in the lattice. This is accomplished by using different oxygen pressures on the two sides [179–182].

$$\Delta\mu_{\mathrm{O_2}} = RT \ln \frac{p_{\mathrm{O_2}}(2)}{p_{\mathrm{O_2}}(1)} \tag{12.48}$$

The oxides have oxygen deficiencies, so oxygen transfer by vacancy jumping is likely. Such jumping will be promoted in the presence of a chemical potential difference. Diffusion is then measured with respect to the crystal walls, for various oxygen pressure ratios. In terms of the resistivity to diffusion, the rate equation is

$$-\frac{c_{\mathrm{O_2}}}{T}\frac{\Delta\mu_{\mathrm{O_2}}}{l} = R_{OO}\mathrm{v_{ref}} \tag{12.49}$$

where

$$R_{OO} = \frac{R}{D_{OO} c_{\mathrm{O}_2}} \tag{12.50}$$

With a pressure ratio of 100, a temperature of 1000 K and a sample thickness $l = 2 \times 10^{-5}$ m, the gradient in the chemical potential of oxygen across the crystal is 1.44×10^9J/mol m. A typical oxygen vacancy concentration is 0.50 mol/m^3. In the experiment, one determines v_{ref} in Eq. (12.49), and calculates R_{OO} or the diffusion coefficient from Eq. (12.50). A typical value is D_{OO}=10^{-11} m^2/s.

The positions of A and B will change with respect to the oxygen as the vacancies are moving, and demixing can occur. The equations above can describe this. We take as frame of reference the (moving) oxygen lattice $\mathrm{v}_{\mathrm{ref}}$. At constant temperature, the force-flux relations are from Eq. (12.29)

$$\begin{aligned} -\frac{c_A}{T}\frac{\partial \mu_{A,T}}{\partial x} &= R_{AA}\mathrm{v}_{\mathrm{A,ref}} + R_{AB}\mathrm{v}_{\mathrm{B,ref}} \\ -\frac{c_B}{T}\frac{\partial \mu_{B,T}}{\partial x} &= R_{BA}\mathrm{v}_{\mathrm{A,ref}} + R_{BB}\mathrm{v}_{\mathrm{B,ref}} \end{aligned} \tag{12.51}$$

We use Gibbs–Duhem's equation $\sum c_i d\mu_i = 0$ for the ions to expand the description (12.49). By adding the two equations above, we then obtain;

$$\frac{c_O}{T}\frac{\partial \mu_{O,T}}{\partial x} = (R_{AA} + R_{BA})\mathrm{v}_{\mathrm{A,ref}} + (R_{AB} + R_{BB})\mathrm{v}_{\mathrm{B,ref}} \tag{12.52}$$

At steady state, the velocity of A must be equal and opposite to that of B in order to maintain charge neutrality, $\mathrm{v}_{\mathrm{A,ref}} = -\mathrm{v}_{\mathrm{B,ref}} = -\mathrm{v}_{ss}$. This gives

$$\begin{aligned} \frac{\partial \mu_{A,T}}{\partial x} &= \frac{T}{c_A}(R_{AA} + R_{BA})v_{ss} \\ \frac{\partial \mu_{B,T}}{\partial x} &= \frac{T}{c_B}(R_{BA} + R_{BB})v_{ss} \\ \frac{\partial \mu_{O,T}}{\partial x} &= -\frac{T}{c_O}(R_{AA} + 2R_{BA} + R_{BB})v_{ss} \end{aligned} \tag{12.53}$$

The coupling coefficients are mostly unknown. When $R_{BB} = 2R_{AA}$ and the coupling coefficient is zero, a difference in chemical potentials of A and B of 2 is maintained [179, 183]. A positive coupling coefficient makes the difference in chemical potentials smaller, a negative will make it larger. The process leads to demixing, and with time this may destabilize the material.

12.5 A relation between the heats of transfer and the enthalpy

A useful concept in the description of heat transport is the heat of transfer, defined in Eq. (12.8). As we discussed in Sec. 8.3, the heats of transfer play an important role for transport through a surface. In order to clarify how the heat of transfer for the surface is related to the heat of transfer in the homogeneous phase in Sec. 12.3, we first discuss them for the homogeneous phase in some more detail.

The total heat flux is given by

$$J_q = J'_q + H_{\mathrm{A}} J_{\mathrm{A}} + H_{\mathrm{B}} J_{\mathrm{B}} + H_{\mathrm{C}} J_{\mathrm{C}} \tag{12.54}$$

The total heats of transfer are therefore given by

$$Q^*_m \equiv \left[\frac{J_q}{J_m}\right]_{\partial T/\partial x=0, J_n=0} = q^*_m + H_m \quad \text{for } m = \text{ A, B or C} \tag{12.55}$$

(Compare Sec. 8.4). With the total heat flux as a variable instead of the measurable heat flux, the entropy production becomes

$$\sigma = J_q \frac{\partial}{\partial x}\left(\frac{1}{T}\right) + \sum_{m=\text{ A, B, C}} J_m \left(-\frac{\partial}{\partial x}\frac{\mu_m}{T}\right) \tag{12.56}$$

For the steady state conditions we are considering, J_q, J_{A}, J_{B} and J_{C} are independent of the position. This makes it possible to integrate the entropy production from a to b in order to obtain the total entropy production of the film between a and b per unit of surface area:

$$\sigma_{ab} \equiv \int_a^b \sigma dx = J_q \left(\frac{1}{T(b)} - \frac{1}{T(a)}\right) - \sum_{m=\text{A, B, C}} J_m \left(\frac{\mu_m(b)}{T(b)} - \frac{\mu_m(a)}{T(a)}\right) \tag{12.57}$$

We note that this relation is also true when a and b are in different homogeneous phases separated by an interface. Using the relation between the total heat flux and the measurable heat flux, and a thermodynamic identity for the temperature dependence of the chemical potentials, both in point a

and b, this entropy production can be written as

$$\begin{aligned}\sigma_{ab} \equiv \int_a^b \sigma dx &= J'_q(a)\left(\frac{1}{T(b)} - \frac{1}{T(a)}\right) \\ &\quad - \sum_{m=\text{A, B, C}} J_m \left(\frac{\mu_m(b) - \mu_m(a; T(b))}{T(b)}\right) \\ &= J'_q(b)\left(\frac{1}{T(b)} - \frac{1}{T(a)}\right) - \sum_{m=\text{ A, B, C}} J_m \left(\frac{\mu_m(b; T(a)) - \mu_m(a)}{T(a)}\right)\end{aligned} \tag{12.58}$$

where $\mu_m(a; T(b))$ means that the chemical potential is calculated at the local concentrations of all components in a at the temperature $T(b)$. Similar definitions are used for the other terms. The resulting force-flux relations for the film, when we use the measurable heat flux on the left hand side, are

$$\begin{aligned}\frac{1}{T(b)} - \frac{1}{T(a)} &= R^{ab}_{qq}(a) J'_q(a) + \sum_{m=\text{ A, B, C}} R^{ab}_{qm}(a) J_m \\ -\frac{\mu_n(b) - \mu_n(a; T(b))}{T(b)} &= R^{ab}_{nq}(a) J'_q(a) + \sum_{m=\text{ A, B, C}} R^{ab}_{nm}(a) J_m\end{aligned} \tag{12.59}$$

where $n =$ A, B or C. When we use the measurable heat flux on the right hand side, we obtain

$$\begin{aligned}\frac{1}{T(b)} - \frac{1}{T(a)} &= R^{ab}_{qq}(b) J'_q(b) + \sum_{m=\text{ A, B, C}} R^{ab}_{qm}(b) J_m \\ -\frac{\mu_n(b; T(a)) - \mu_n(a)}{T(a)} &= R^{ab}_{nq}(b) J'_q(b) + \sum_{m=\text{ A, B, C}} R^{ab}_{nm}(b) J_m\end{aligned} \tag{12.60}$$

Both resistivity matrices are symmetric.

We may again calculate the heats of transfer in both a and b and find

$$\begin{aligned}q^{*ab}_m(a) &\equiv \left[\frac{J'_q(a)}{J_m}\right]_{\Delta T=0, J_n=0} = -\frac{R^{ab}_{qm}(a)}{R^{ab}_{qq}(a)} \\ &= -\frac{R^{ab}_{mq}(a)}{R^{ab}_{qq}(a)} \quad \text{for } m = \text{ A, B or C} \\ q^{*ab}_m(b) &\equiv \left[\frac{J'_q(b)}{J_m}\right]_{\Delta T=0, J_n=0} = -\frac{R^{ab}_{qm}(b)}{R^{ab}_{qq}(b)} \\ &= -\frac{R^{ab}_{mq}(b)}{R^{ab}_{qq}(b)} \quad \text{for } m = \text{ A, B or C}\end{aligned} \tag{12.61}$$

where $\Delta T = T(b) - T(a)$. Integrating Gibbs–Duhem's equation (12.2) to linear order in the differences across the film one obtains in a:

$$\sum_{m=\text{ A, B, C}} c_m(a) \frac{\mu_m(b) - \mu_m(a; T(b))}{T(b)} = 0 \tag{12.62}$$

and the analogous relation in b. Using this in Eq. (12.59) in a and b one obtains for the measurable heats of transfer:

$$\sum_{m=\text{ A, B, C}} c_m(a) q_m^{*ab}(a) = \sum_{m=\text{ A, B, C}} c_m(b) q_m^{*ab}(b) = 0 \tag{12.63}$$

The total heats of transfer are defined using the total heat fluxes. The total heat flux is independent of the position, so the total heats of transfer also have this property. Using the relation between the measurable heats of transfer, it then follows that

$$q_m^{*ab}(b) - q_m^{*ab}(a) = -[H_m(b) - H_m(a)] \quad \text{for } m = \text{ A, B or C} \tag{12.64}$$

In a homogeneous phase, the difference in the enthalpy between position b and a is usually small, so the heat of transfer does not change much across a film. We saw in Secs. 8.3 and 11.2 that the exact same relation is valid for the heats of transfer on the two sides of a surface. In that case, however, the enthalpy difference is often large. This leads to large heat effects at surfaces. The relation of the heat of transfer to an enthalpy means that the quantity is mostly related to interaction energies, cf. Eq. (8.12). We saw in Ch.11 how this explained the sign of the heat of transfer of the surface.

As we mentioned in Sec. 8.3, an interesting consequence of these relations, for a surface as well as for a film, is that they can be combined. We can obtain the same relation for a heterogeneous layer between two arbitrary planes, i.e. a sequence of homogeneous films with surfaces in between.

Chapter 13

A Nonisothermal Concentration Cell

We give equations that govern energy conversion in a concentration cell in contact with two thermal reservoirs. A procedure for determination of the electric potential from the temperature difference between the electrodes is developed. We cast flux equations in a form that is convenient for integration across the heterogeneous cell.

We have seen that electric energy can be obtained from a difference in temperature (Chapter 9) or chemical potential (Chapter 10). In this chapter, electric energy is derived from thermal as well as chemical sources. We want to find the electric potential profile across a concentration cell that is exposed to a gradient in temperature when a direct current is passing. The temperature is controlled at the beginning and at the end of the cell. For the rest, the system is thermally isolated.

The purpose of the chapter is to develop a procedure for analysis of energy conversion. We shall introduce terminology and examine a simple cell. The procedure [184] is extended in Chapter 15 to a formation cell.

The cell of interest is a concentration cell:

$$T^{\mathrm{a,o}},\ \mathrm{Na\ (Hg)}\ |\beta\text{"-alumina}\ |\ \mathrm{Na\ (Hg)},\ T^{\mathrm{c,o}} \tag{13.1}$$

The cell conditions are illustrated in Fig. 13.1. The electrodes consists of liquid mixtures of sodium in mercury (amalgam solutions). They are kept at different temperatures by means of heat baths. The electrolyte, the contact between the liquid pools, consists of $Na_2O{\cdot}Al_2O_3$ (β"-alumina). This solid state material has constant composition and conducts charge by sodium ions only. The system is only an example, but the electrodes of this cell are relevant for high temperature batteries like the Na-S [185] and Na-$NiCl_2$-battery [186]. When a positive electric current is passing the cell, there is consumption of sodium on the left hand side and production

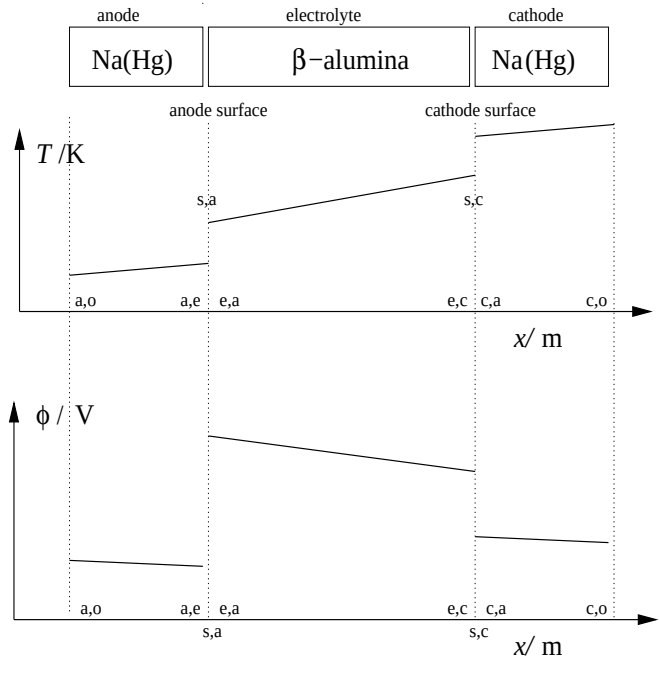

Figure 13.1 The temperature and electric potential profiles across the electrode concentration cell.

of sodium on the right hand side. The electric current leads to heating of one electrode, and as we shall see, cooling of the other electrode. Such reversible electrode heat effects have been studied in several systems that are similar to the present cell [187]. Ito *et al.* [188] studied conditions during water electrolysis in hydroxide melts, Flem *et al.* [78,80] studied aluminium electrodes in contact with a fluoride mixture.

For pedagogical reasons, we start with the most general description. Relations between the variables will then appear (see Sec. 13.1.3).

The terminology used for electrochemical cells throughout the book is clarified in Figs. 13.1 and 13.2. At positions a,o and c,o in Fig. 13.1, the temperatures are $T^{\mathrm{a,o}}$ and $T^{\mathrm{c,o}}$ and the electric potentials are $\phi^{\mathrm{c,o}}$ and $\phi^{\mathrm{a,o}}$. A location is indicated by a superscript of two letters with a comma between; the first letter refers to the phase, the second refers to the neighboring phase. The total cell potential, $\Delta_{\mathrm{tot}}\phi$, between the end points is:

$$\Delta_{\mathrm{tot}}\phi = \phi^{\mathrm{c,o}} - \phi^{\mathrm{a,o}} = \Delta_{\mathrm{a}}\phi + \Delta_{\mathrm{a,e}}\phi + \Delta_{\mathrm{e}}\phi + \Delta_{\mathrm{e,c}}\phi + \Delta_{\mathrm{c}}\phi \qquad (13.2)$$

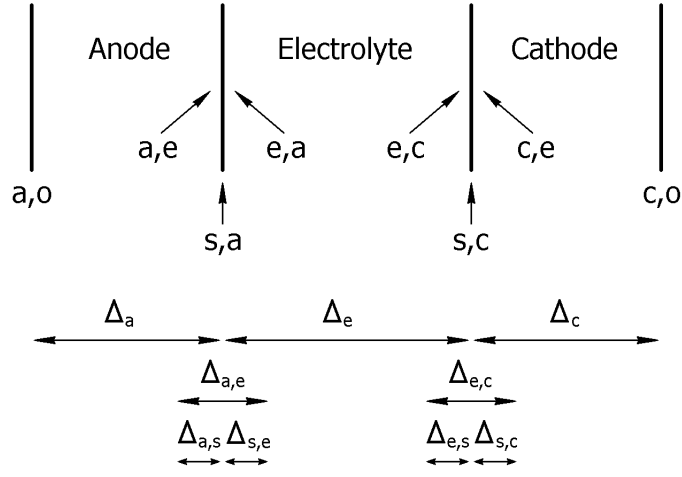

Figure 13.2 Notation used for transport in electrochemical cells. The first symbol of a location (a superscript) refers to the phase, and the second to the neighbouring phase. A Δ with one subscript, x, denotes the difference across phase x. A Δ with two subscripts, x, y, denotes the value in y minus the value in x.

The terminology in this equation is clarified in Fig. 13.2. The present cell has five subsystems. From left to right we have: the anode, the anode surface, the electrolyte, the cathode surface and the cathode. There are three homogeneous phases and two surfaces. When the electrodes are in contact with different thermal reservoirs, the total potential is a thermoelectric potential.

13.1 The homogeneous phases

We need expressions for $T(x)$, $\mu_{\mathrm{Na},T}(x)$ and $\phi(x)$ between positions a,o and c,o in the presence of a current density, j, in order to find the thermoelectric potential. One solution is illustrated in Fig. 13.1. We start the analysis with the homogeneous phases, taking the anode as the detailed example.

13.1.1 *Entropy production and flux equations for the anode*

The anode amalgam extends from position (a,o) to (a,e). Charge is conducted by electrons in the metal solution. A temperature gradient causes sodium to move, leading in the stationary state to a Soret equilibrium

for Na in Hg. Sodium must also be transported through the amalgam to supply the reaction at a,e. Heat is transported by conduction as well as by charge and mass transport. The entropy production is therefore, cf. Eq. (4.15),

$$\sigma^{\mathrm{a}} = J_q'^{\mathrm{a}} \left(\frac{\partial}{\partial x} \frac{1}{T} \right) + J_{\mathrm{Na}}^{\mathrm{a}} \left(-\frac{1}{T} \frac{\partial \mu_{\mathrm{Na},T}^{\mathrm{a}}}{\partial x} \right) + j \left(-\frac{1}{T} \frac{\partial \phi}{\partial x} \right) \tag{13.3}$$

where $J_q'^{\mathrm{a}}$ is the measurable heat flux, $J_{\mathrm{Na}}^{\mathrm{a}}$ the sodium flux and $\mu_{\mathrm{Na}}^{\mathrm{a}}$ the chemical potential of Na. The subscript T indicates that $\mu_{\mathrm{Na}}^{\mathrm{a}}$ is differentiated at constant temperature. The equations of transport are:

$$\begin{aligned} \frac{\partial}{\partial x} \frac{1}{T} &= R_{qq}^{\mathrm{a}} J_q'^{\mathrm{a}} + R_{q\mu}^{\mathrm{a}} J_{\mathrm{Na}}^{\mathrm{a}} + R_{q\phi}^{\mathrm{a}} j \\ -\frac{1}{T} \frac{\partial \mu_{\mathrm{Na},T}^{\mathrm{a}}}{\partial x} &= R_{\mu q}^{\mathrm{a}} J_q'^{\mathrm{a}} + R_{\mu\mu}^{\mathrm{a}} J_{\mathrm{Na}}^{\mathrm{a}} + R_{\mu\phi}^{\mathrm{a}} j \\ -\frac{1}{T} \frac{\partial \phi}{\partial x} &= R_{\phi q}^{\mathrm{a}} J_q'^{\mathrm{a}} + R_{\phi\mu}^{\mathrm{a}} J_{\mathrm{Na}}^{\mathrm{a}} + R_{\phi\phi}^{\mathrm{a}} j \end{aligned} \tag{13.4}$$

It will also be convenient to express the fluxes in the forces

$$\begin{aligned} J_q'^{\mathrm{a}} &= L_{qq}^{\mathrm{a}} \frac{\partial}{\partial x} \frac{1}{T} + L_{q\mu}^{\mathrm{a}} \left(-\frac{1}{T} \frac{\partial \mu_{\mathrm{Na},T}^{\mathrm{a}}}{\partial x} \right) + L_{q\phi}^{\mathrm{a}} \left(-\frac{1}{T} \frac{\partial \phi}{\partial x} \right) \\ J_{\mathrm{Na}}^{\mathrm{a}} &= L_{\mu q}^{\mathrm{a}} \frac{\partial}{\partial x} \frac{1}{T} + L_{\mu\mu}^{\mathrm{a}} \left(-\frac{1}{T} \frac{\partial \mu_{\mathrm{Na},T}^{\mathrm{a}}}{\partial x} \right) + L_{\mu\phi}^{\mathrm{a}} \left(-\frac{1}{T} \frac{\partial \phi}{\partial x} \right) \\ j &= L_{\phi q}^{\mathrm{a}} \frac{\partial}{\partial x} \frac{1}{T} + L_{\phi\mu}^{\mathrm{a}} \left(-\frac{1}{T} \frac{\partial \mu_{\mathrm{Na},T}^{\mathrm{a}}}{\partial x} \right) + L_{\phi\phi}^{\mathrm{a}} \left(-\frac{1}{T} \frac{\partial \phi}{\partial x} \right) \end{aligned} \tag{13.5}$$

The conductivity matrix is the inverse of the resistivity matrix and can be found using Kramers' rule, see Sec. 7.4. Resistivities as well as conductivities satisfy the Onsager relations.

We are looking for expressions where $T(x)$, $\mu_{\mathrm{Na},T}(x)$ and $\phi(x)$ are given in terms of measured transport properties, and continue to rewrite the linear relations between the fluxes and forces. We solve for $\partial\phi/\partial x$ from Eq. (13.5c) and eliminate this gradient in Eq. (13.5a, b). The result is

$$\begin{aligned} J_q'^{\mathrm{a}} &= l_{qq}^{\mathrm{a}} \frac{\partial}{\partial x} \frac{1}{T} + l_{q\mu}^{\mathrm{a}} \left(-\frac{1}{T} \frac{\partial \mu_{\mathrm{Na},T}^{\mathrm{a}}}{\partial x} \right) + \frac{\pi^{\mathrm{a}}}{F} j \\ J_{\mathrm{Na}}^{\mathrm{a}} &= l_{\mu q}^{\mathrm{a}} \frac{\partial}{\partial x} \frac{1}{T} + l_{\mu\mu}^{\mathrm{a}} \left(-\frac{1}{T} \frac{\partial \mu_{\mathrm{Na},T}^{\mathrm{a}}}{\partial x} \right) + \frac{t_{\mathrm{Na}}^{\mathrm{a}}}{F} j \\ \frac{\partial \phi}{\partial x} &= -\frac{\pi^{\mathrm{a}}}{TF} \frac{\partial T}{\partial x} - \frac{t_{\mathrm{Na}}^{\mathrm{a}}}{F} \frac{\partial \mu_{\mathrm{Na},T}^{\mathrm{a}}}{\partial x} - r^{\mathrm{a}} j \end{aligned} \tag{13.6}$$

where the Peltier heat, π^{a}, the transference coefficient, $t^{\mathrm{a}}_{\mathrm{Na}}$, and the ohmic resistivity, r^{a}, are defined by (see Eqs. (10.9) and (9.15)):

$$\begin{aligned}
\pi^{\mathrm{a}} &= \left(\frac{J'^{\mathrm{a}}_q}{j/F}\right)_{dT=0,\ d\mu^{\mathrm{a}}_{\mathrm{Na},T}=0} = -F\left(T\frac{\partial\phi/\partial x}{\partial T/\partial x}\right)_{j=0,\ d\mu^{\mathrm{a}}_{\mathrm{Na},T}=0} = F\frac{L^{\mathrm{a}}_{q\phi}}{L^{\mathrm{a}}_{\phi\phi}} \\
t^{\mathrm{a}}_{\mathrm{Na}} &= \left(\frac{J^{\mathrm{a}}_{\mathrm{Na}}}{j/F}\right)_{dT=0,\ d\mu^{\mathrm{a}}_{\mathrm{Na},T}=0} = -F\left(\frac{\partial\phi/\partial x}{\partial\mu^{\mathrm{a}}_{\mathrm{Na},T}/\partial x}\right)_{j=0,\ dT=0} = F\frac{L^{\mathrm{a}}_{\mu\phi}}{L^{\mathrm{a}}_{\phi\phi}} \\
r^{\mathrm{a}} &= -\left(\frac{\partial\phi/\partial x}{j}\right)_{dT=0,\ d\mu^{\mathrm{a}}_{\mathrm{Na},T}=0} = \frac{T}{L^{\mathrm{a}}_{\phi\phi}}
\end{aligned} \tag{13.7}$$

where we used the Onsager relations. Measured values of π^{a}, $t^{\mathrm{a}}_{\mathrm{Na}}$ and r^{a} give, using these expressions, the conductivities $L^{\mathrm{a}}_{\phi\phi}$, $L^{\mathrm{a}}_{q\phi} = L^{\mathrm{a}}_{\phi q}$ and $L^{\mathrm{a}}_{\mu\phi} = L^{\mathrm{a}}_{\phi\mu}$. The conductivities with a small l are given by

$$\begin{aligned}
l^{\mathrm{a}}_{qq} &= L^{\mathrm{a}}_{qq} - \frac{L^{\mathrm{a}}_{q\phi}L^{\mathrm{a}}_{\phi q}}{L^{\mathrm{a}}_{\phi\phi}} \\
l^{\mathrm{a}}_{q\mu} &= l^{\mathrm{a}}_{\mu q} = L^{\mathrm{a}}_{q\mu} - \frac{L^{\mathrm{a}}_{q\phi}L^{\mathrm{a}}_{\phi\mu}}{L^{\mathrm{a}}_{\phi\phi}} \\
l^{\mathrm{a}}_{\mu\mu} &= L^{\mathrm{a}}_{\mu\mu} - \frac{L^{\mathrm{a}}_{\mu\phi}L^{\mathrm{a}}_{\phi\mu}}{L^{\mathrm{a}}_{\phi\phi}}
\end{aligned} \tag{13.8}$$

Values of l^{a}_{qq}, $l^{\mathrm{a}}_{q\mu} = l^{\mathrm{a}}_{\mu q}$ and $l^{\mathrm{a}}_{\mu\mu}$ together with the conductivities $L^{\mathrm{a}}_{\phi\phi}$, $L^{\mathrm{a}}_{q\phi} = L^{\mathrm{a}}_{\phi q}$ and $L^{\mathrm{a}}_{\mu\phi} = L^{\mathrm{a}}_{\phi\mu}$, obtained from π^{a}, $t^{\mathrm{a}}_{\mathrm{Na}}$ and r^{a}, make it possible to calculate the conductivities L^{a}_{qq}, $L^{\mathrm{a}}_{q\mu} = L^{\mathrm{a}}_{\mu q}$ and $L^{\mathrm{a}}_{\mu\mu}$. The conductivity $l^{\mathrm{a}}_{\mu\mu}$ can be found, using Eq. (13.6b), by measuring the diffusion coefficient for Na in Hg:

$$D^{\mathrm{a}}_{\mathrm{Na}} = -\left(\frac{J^{\mathrm{a}}_{\mathrm{Na}}}{\partial c^{\mathrm{a}}_{\mathrm{Na}}/\partial x}\right)_{j=0,dT=0} = \frac{l^{\mathrm{a}}_{\mu\mu}}{T}\left(\frac{\partial\mu^{\mathrm{a}}_{\mathrm{Na}}}{\partial c^{\mathrm{a}}_{\mathrm{Na}}}\right) \tag{13.9}$$

where $c^{\mathrm{a}}_{\mathrm{Na}}$ is the sodium concentration. The remaining coefficients $l^{\mathrm{a}}_{q\mu} = l^{\mathrm{a}}_{\mu q}$ and l^{a}_{qq} are determined from the stationary state thermal conductivity, λ^{a}, and the heat of transfer $q^{*,\mathrm{a}}_{\mathrm{Na}}$ (defined in Eq. (8.4)),

$$\begin{aligned}
q^{*,\mathrm{a}}_{\mathrm{Na}} &= -\left(T\frac{\partial\mu^{\mathrm{a}}_{\mathrm{Na},T}/\partial x}{\partial T/\partial x}\right)_{j=0,J^{\mathrm{a}}_{\mathrm{Na}}=0} = \left(\frac{J'^{\mathrm{a}}_q}{J^{\mathrm{a}}_{\mathrm{Na}}}\right)_{dT=0,\ j=0} = \frac{l^{\mathrm{a}}_{q\mu}}{l^{\mathrm{a}}_{\mu\mu}} \\
\lambda^{\mathrm{a}} &= -\left(\frac{J'^{\mathrm{a}}_q}{\partial T/\partial x}\right)_{j=0,J^{\mathrm{a}}_{\mathrm{Na}}=0} = \frac{1}{T^2}\left(l^{\mathrm{a}}_{qq} - \frac{l^{\mathrm{a}}_{q\mu}l^{\mathrm{a}}_{\mu q}}{l^{\mathrm{a}}_{\mu\mu}}\right) = \frac{1}{T^2R^{\mathrm{a}}_{qq}}
\end{aligned} \tag{13.10}$$

This gives a practical form of the linear force-flux relations:

$$\begin{aligned}
\frac{\partial T}{\partial x} &= -\frac{1}{\lambda^{\mathrm{a}}}\left[J_q'^{\mathrm{a}} - q^{*,\mathrm{a}}_{\mathrm{Na}}\left(J^{\mathrm{a}}_{\mathrm{Na}} - \frac{t^{\mathrm{a}}_{\mathrm{Na}}}{F}j\right) - \frac{\pi^{\mathrm{a}}}{F}j\right] \\
\frac{\partial \mu^{\mathrm{a}}_{\mathrm{Na},T}}{\partial x} &= -\frac{q^{*,\mathrm{a}}_{\mathrm{Na}}}{T}\frac{\partial T}{\partial x} - \frac{T}{l^{\mathrm{a}}_{\mu\mu}}\left(J^{\mathrm{a}}_{\mathrm{Na}} - \frac{t^{\mathrm{a}}_{\mathrm{Na}}}{F}j\right) \\
\frac{\partial \phi}{\partial x} &= -\frac{\pi^{\mathrm{a}}}{TF}\frac{\partial T}{\partial x} - \frac{t^{\mathrm{a}}_{\mathrm{Na}}}{F}\frac{\partial \mu^{\mathrm{a}}_{\mathrm{Na},T}}{\partial x} - r^{\mathrm{a}}j
\end{aligned} \tag{13.11}$$

The profiles we are seeking are expressed in terms of measurable transport properties. The expressions above defined the measurements to find the coupling coefficients π^{a}, $t^{\mathrm{a}}_{\mathrm{Na}}$ and $q^{*,\mathrm{a}}_{\mathrm{Na}}$, and the diagonal coefficients r^{a}, $D^{\mathrm{a}}_{\mathrm{Na}}$ and λ^{a}. Knowledge of these coefficients makes it possible to solve the expressions above.

13.1.2 *Position dependent transport coefficients*

We shall see that the boundary conditions for the sodium flux leads to a position dependent transference coefficient of Na in amalgam.

The transference coefficient is defined as the flow of sodium to the site of the electrode reaction, caused by the constant electric current, for a position independent temperature, chemical potential, or concentration of sodium; i.e. $c^{\mathrm{a}}_{\mathrm{Na}}(x,t) = c^{\mathrm{a}}_{\mathrm{Na}}(t)$. The ratio of the two fluxes varies from position 0 at the iron contact to position d_{a} at the electrode surface, because the sodium flux varies across the electrode at these conditions. This can be found from the mass balance for sodium:

$$\frac{\partial c^{\mathrm{a}}_{\mathrm{Na}}(x,t)}{\partial t} = -\frac{\partial J^{\mathrm{a}}_{\mathrm{Na}}(x,t)}{\partial x} \tag{13.12}$$

The flux of Na that is leaving the electrode, is given by the integral:

$$\frac{\partial}{\partial t}\int_0^{d^{\mathrm{a}}} c^{\mathrm{a}}_{\mathrm{Na}}dx = -J^{\mathrm{a}}_{\mathrm{Na}}(d^{\mathrm{a}},t) + J^{\mathrm{a}}_{\mathrm{Na}}(0,t) = -J^{\mathrm{a}}_{\mathrm{Na}}(d^{\mathrm{a}},t) = -\frac{j}{F} \tag{13.13}$$

The sodium flux is zero at position 0, and equal to j/F at position d^{a}. The electric current is independent of the position and the time. We now use the definition of the transference coefficient, Eq. (13.7b). When the gradients of the concentration and temperature are zero, $J^{\mathrm{a}}_{\mathrm{Na}}(x,t) = t^{\mathrm{a}}_{\mathrm{Na}}(x,t)j/F$, and we have

$$\frac{\partial c^{\mathrm{a}}_{\mathrm{Na}}(t)}{\partial t} = -\frac{\partial J^{\mathrm{a}}_{\mathrm{Na}}(x,t)}{\partial x} = -\frac{j}{F}\frac{\partial t^{\mathrm{a}}_{\mathrm{Na}}(x,t)}{\partial x} = -\frac{j}{d^{\mathrm{a}}F} \tag{13.14}$$

The solutions for $J^{\mathrm{a}}_{\mathrm{Na}}(x,t)$and $t_{\mathrm{Na}}(x,t)$ are therefore

$$J^{\mathrm{a}}_{\mathrm{Na}}(x,t) = \frac{xj}{d^{\mathrm{a}}F} \rightarrow t^{\mathrm{a}}_{\mathrm{Na}}(x,t) = \frac{x}{d^{\mathrm{a}}} \tag{13.15}$$

Both solutions are time independent. The concentration of sodium is slowly decreasing, however. The solution is in that sense only quasi-stationary. But the transference coefficient has been found to be time independent, and to increase linearly from 0 at the metal contact to 1 at the electrode surface.

The Peltier coefficient is also position dependent. This dependency can be derived using the expression for the measurable heat flux, $J'^{\mathrm{a}}_q = T\left(J_s - J_{\mathrm{Na}}S^{\mathrm{a}}_{\mathrm{Na}}\right)$, cf. Eq. (4.12). By introducing this into Eq. (13.7a) we have

$$\begin{aligned}\pi^{\mathrm{a}}(x) &= \left(\frac{J'^{\mathrm{a}}_q}{j/F}\right)_{dT=0,\, d\mu^{\mathrm{a}}_{\mathrm{Na},T}=0} = T\left(\frac{J_s - J_{\mathrm{Na}}S^{\mathrm{a}}_{\mathrm{Na}}}{j/F}\right)_{dT=0,\, d\mu^{\mathrm{a}}_{\mathrm{Na},T}=0} \\ &= -T\left[S^*_{\mathrm{e}^-} + t^{\mathrm{a}}_{\mathrm{Na}}(x)S^{\mathrm{a}}_{\mathrm{Na}}\right]\end{aligned} \tag{13.16}$$

where $S^*_{\mathrm{e}^-}$ is by definition the transported entropy of the electrons (cf. Chapter 9).

Remark 13.1. *As the position dependence of t^a_{Na} and π^a shows, these quantities are not just material properties. They also depend on the boundary conditions, see also Ref. [189].*

Remark 13.2. *The entropy and the transported entropy are functions of the temperature and other intensive variables that characterize the local thermodynamic state. We have neglected such dependencies here.*

13.1.3 *The profiles of the homogeneous anode*

We can now obtain some relations between the variables. The heat of transfer can be determined from the expression for the electric potential gradient in Eq. (13.11), when J_{Na} and j are zero. This gives

$$\frac{\partial\phi}{\partial x} = \frac{1}{F}\left[S^*_{\mathrm{e}^-} + t^{\mathrm{a}}_{\mathrm{Na}}(x)\left(S^{\mathrm{a}}_{\mathrm{Na}} + \frac{q^{*,\mathrm{a}}_{\mathrm{Na}}}{T}\right)\right]\frac{\partial T}{\partial x} \tag{13.17}$$

The electric potential gradient cannot depend on the position dependent transference number. It follows that the transported heat is:

$$q^{*,\mathrm{a}}_{\mathrm{Na}} = -TS^{\mathrm{a}}_{\mathrm{Na}} \tag{13.18}$$

For small fluxes, we can expect that the sodium flux is a linear function of the position. The boundary conditions then give $J^{\mathrm{a}}_{\mathrm{Na}}(x) = t^{\mathrm{a}}_{\mathrm{Na}}(x) j/F = xj/d^{\mathrm{a}}F$. This further simplifies Eq. (13.11) considerably. After some algebra, we obtain

$$\begin{aligned}
\frac{\partial T}{\partial x} &= -\frac{1}{\lambda^{\mathrm{a}}}\left[J'^{\mathrm{a}}_q - \pi^{\mathrm{a}}\frac{j}{F}\right] = -\frac{1}{\lambda^{\mathrm{a}}}\left[J'^{\mathrm{a}}_q + T\left(S^*_{\mathrm{e}^-} + \frac{x}{d^{\mathrm{a}}}S^{\mathrm{a}}_{\mathrm{Na}}\right)\frac{j}{F}\right] \\
\frac{\partial \mu^{\mathrm{a}}_{\mathrm{Na},T}}{\partial x} &= S^{\mathrm{a}}_{\mathrm{Na}}\frac{\partial T}{\partial x} \rightarrow \frac{\partial \mu^{\mathrm{a}}_{\mathrm{Na}}}{\partial x} = 0 \\
\frac{\partial \phi}{\partial x} &= \frac{S^*_{\mathrm{e}^-}}{F}\frac{\partial T}{\partial x} - r^{\mathrm{a}} j
\end{aligned} \tag{13.19}$$

The equations say that true equilibrium is established for Na across the electrode, as $\partial\mu^{\mathrm{a}}_{\mathrm{Na}}/\partial x = 0$. The electric potential drop consists of an ohmic potential drop, plus a contribution from the temperature difference. The heat transport has, likewise, also two contributions. The derivation in Sec. 13.1.1 may seem cumbersome, but it is important to take all terms along to find the condition of chemical equilibrium Eq. (13.19b). In a simpler analysis, one could introduce in the entropy production, $J^{\mathrm{a}}_{\mathrm{Na}}(x) = xj/d^{\mathrm{a}}F$, to give two forces and fluxes directly. While this appears to be simpler, it may hide the relation $q^{*,\mathrm{a}}_{\mathrm{Na}} = -TS^{\mathrm{a}}_{\mathrm{Na}}$ and the condition for a constant chemical potential of the sodium.

13.1.4 *Contributions from the cathode*

The formulae are the same for the cathode and the anode, but the boundary conditions differ. The sodium flux is j/F at position $d^{\mathrm{a}} + d^{\mathrm{e}}$ (the cathode surface) and 0 at the position of the metal contact, $d^{\mathrm{a}} + d^{\mathrm{e}} + d^{\mathrm{c}}$. The transference coefficient is therefore

$$t^{\mathrm{c}}_{\mathrm{Na}}(x) = 1 - \frac{x - d^{\mathrm{a}} - d^{\mathrm{e}}}{d^{\mathrm{c}}} \tag{13.20}$$

The Peltier coefficient and the heat of transport are, cf. Eqs. (13.16) and (13.18),

$$\pi^{\mathrm{c}} = -T\left[S^*_{\mathrm{e}^-} + t^{\mathrm{c}}_{\mathrm{Na}}(x) S^{\mathrm{c}}_{\mathrm{Na}}\right] \quad \text{and} \quad q^{*,\mathrm{c}}_{\mathrm{Na}} = -TS^{\mathrm{c}}_{\mathrm{Na}} \tag{13.21}$$

The rest of the equations are similar to the ones written for the anode. Analogous to Eq. (13.19) we find

$$\frac{\partial T}{\partial x} = -\frac{1}{\lambda^{\mathrm{c}}}\left\{J_q'^{\mathrm{c}} + T\left[S^*_{\mathrm{e}^-} + \left(1 - \frac{x - d^{\mathrm{a}} - d^{\mathrm{e}}}{d^{\mathrm{c}}}\right) S^{\mathrm{c}}_{\mathrm{Na}}\right]\frac{j}{F}\right\}$$

$$\frac{\partial \mu^{\mathrm{c}}_{\mathrm{Na},T}}{\partial x} = S^{\mathrm{c}}_{\mathrm{Na}}\frac{\partial T}{\partial x} \rightarrow \frac{\partial \mu^{\mathrm{c}}_{\mathrm{Na}}}{\partial x} = 0 \tag{13.22}$$

$$\frac{\partial \phi}{\partial x} = \frac{S^*_{\mathrm{e}^-}}{F}\frac{\partial T}{\partial x} - r^{\mathrm{c}} j$$

Integration is now easy. In Fig. 13.1, $\Delta_{\mathrm{c}}\phi$ is negative. This corresponds to $T^{\mathrm{c,e}} > T^{\mathrm{c,o}}$.

13.1.5 *The electrolyte contribution*

The entropy production in the non-isothermal electrolyte of β"-alumina is

$$\sigma^{\mathrm{e}} = J_q'^{\mathrm{e}}\frac{\partial}{\partial x}\left(\frac{1}{T}\right) + j\left[-\frac{1}{T}\frac{\partial \phi}{\partial x}\right] \tag{13.23}$$

The flux equations are

$$\begin{aligned}\frac{\partial}{\partial x}\left(\frac{1}{T}\right) &= R^{\mathrm{e}}_{qq}J_q'^{\mathrm{e}} + R^{\mathrm{e}}_{q\phi}j\\ -\frac{1}{T}\frac{\partial \phi}{\partial x} &= R^{\mathrm{e}}_{\phi q}J_q'^{\mathrm{e}} + R^{\mathrm{e}}_{\phi\phi}j\end{aligned} \tag{13.24}$$

or alternatively,

$$\begin{aligned}J_q'^{\mathrm{e}} &= L^{\mathrm{e}}_{qq}\tfrac{\partial}{\partial x}\left(\frac{1}{T}\right) + L^{\mathrm{e}}_{q\phi}\left(-\frac{1}{T}\frac{\partial \phi}{\partial x}\right)\\ j &= L^{\mathrm{e}}_{\phi q}\frac{\partial}{\partial x}\left(\frac{1}{T}\right) + L^{\mathrm{e}}_{\phi\phi}\left(-\frac{1}{T}\frac{\partial \phi}{\partial x}\right)\end{aligned} \tag{13.25}$$

The Peltier coefficient for the electrolyte is:

$$\pi^{\mathrm{e}} = \left(\frac{J_q'^{\mathrm{e}}}{j/F}\right)_{dT=0} = -F\frac{R^{\mathrm{e}}_{q\phi}}{R^{\mathrm{e}}_{qq}} = F\frac{L^{\mathrm{e}}_{q\phi}}{L^{\mathrm{e}}_{\phi\phi}} = TS^*_{\mathrm{Na}^+} \tag{13.26}$$

The stationary state thermal conductivity and the ohmic resistivity are given by:

$$\lambda^{\mathrm{e}} = \frac{1}{T^2 R^{\mathrm{e}}_{qq}} \quad \text{and} \quad r^{\mathrm{e}} = \frac{T}{L^{\mathrm{e}}_{\phi\phi}} \tag{13.27}$$

The flux equations can then be written

$$\begin{aligned}\frac{\partial T}{\partial x} &= -\frac{1}{\lambda^{\mathrm{e}}}\left(J_q'^{\mathrm{e}} - \pi^{\mathrm{e}}\frac{j}{F}\right) = -\frac{1}{\lambda^{\mathrm{e}}}\left(J_q'^{\mathrm{e}} - TS^*_{\mathrm{Na}^+}\frac{j}{F}\right)\\ \frac{\partial \phi}{\partial x} &= -\frac{\pi^{\mathrm{e}}}{TF}\frac{\partial T}{\partial x} - r^{\mathrm{e}}j = -\frac{1}{F}S^*_{\mathrm{Na}^+}\frac{\partial T}{\partial x} - r^{\mathrm{e}}j\end{aligned} \tag{13.28}$$

where the Onsager relation has been used. The electric potential difference across the electrolyte is linear in the temperature difference. The sign of $\Delta_{\mathrm{e}}\phi$ is negative in Fig. 13.1. This corresponds to a temperature increase across the electrolyte from the anode to the cathode and an ohmic potential drop.

13.2 Surface contributions

13.2.1 *The anode surface*

This surface has the position (s,a) in Figs. 13.1 and 13.2. After sodium arrives at the anode surface, the reaction is:

$$\mathrm{Na(a)} \rightarrow \mathrm{Na^+(e)} + \mathrm{e^-(a)} \tag{13.29}$$

The electron is subsequently transferred to the conduction band in the metal, and the sodium ion is transferred to the β''-alumina. The contribution from the sodium to the reaction Gibbs energy is

$$\Delta_n G^{\mathrm{s,a}} = -\mu^{\mathrm{s,a}}_{\mathrm{Na}} = -\mu^{\mathrm{s,a}}_{\mathrm{Na}}\left(T^{\mathrm{s,a}}\right) \tag{13.30}$$

The entropy production in the non-isothermal anode surface becomes, cf. Eq. (5.15):

$$\begin{aligned}\sigma^{\mathrm{s,a}} = {} & J_q'^{\mathrm{a,e}}\left(\Delta_{\mathrm{a,s}}\frac{1}{T}\right) + J_q'^{\mathrm{e,a}}\left(\Delta_{\mathrm{s,e}}\frac{1}{T}\right) - J^{\mathrm{a,e}}_{\mathrm{Na}}\frac{\Delta_{\mathrm{a,s}}\mu_{\mathrm{Na},T}\left(T^{\mathrm{s,a}}\right)}{T^{\mathrm{s,a}}}\\ & - j\frac{\Delta_{\mathrm{a,e}}\phi}{T^{\mathrm{s,a}}} - r\frac{\Delta_n G^{\mathrm{s,a}}}{T^{\mathrm{s,a}}}\end{aligned} \tag{13.31}$$

For stationary state conditions the sodium flux is equal to the reaction rate, which is equal to j/F. This gives

$$-J^{\mathrm{a,e}}_{\mathrm{Na}}\frac{\Delta_{\mathrm{a,s}}\mu_{\mathrm{Na},T}\left(T^{\mathrm{s,a}}\right)}{T^{\mathrm{s,a}}} - r\frac{\Delta_n G^{\mathrm{s,a}}}{T^{\mathrm{s,a}}} = \frac{j}{F}\frac{\mu^{\mathrm{a,e}}_{\mathrm{Na}}\left(T^{\mathrm{s,a}}\right)}{T^{\mathrm{s,a}}} \tag{13.32}$$

We introduce this expression in Eq. (13.31) and obtain

$$\sigma^{\mathrm{s,a}} = J_q'^{\mathrm{a,e}}\left(\Delta_{\mathrm{a,s}}\frac{1}{T}\right) + J_q'^{\mathrm{e,a}}\left(\Delta_{\mathrm{s,e}}\frac{1}{T}\right) - j\left(\frac{\Delta_{\mathrm{a,e}}\phi - \mu^{\mathrm{a,e}}_{\mathrm{Na}}\left(T^{\mathrm{s,a}}\right)/F}{T^{\mathrm{s,a}}}\right) \tag{13.33}$$

By taking along all fluxes, like we did in the bulk anode, we find that the chemical potential at the surface, $\mu_{\mathrm{Na}}^{\mathrm{s,a}}$, is equal to the constant chemical potential in the anode, $\mu_{\mathrm{Na}}^{\mathrm{a}}$.

We next assume, as explained in Chapter 8, that the inverse temperature differences from one side of the surface do not couple to the measurable heat fluxes on the other side, see also Sec. 9.2. This gives

$$\begin{aligned}
\Delta_{\mathrm{a,s}}\left(\frac{1}{T}\right) &= R_{qq}^{\mathrm{s,a}} J_q'^{\mathrm{a,e}} + R_{q\phi}^{\mathrm{s,a}} j \\
\Delta_{\mathrm{s,e}}\left(\frac{1}{T}\right) &= R_{qq}^{\mathrm{s,e}} J_q'^{\mathrm{e,a}} + R_{q\phi}^{\mathrm{s,e}} j \\
-\frac{1}{T^{\mathrm{s,a}}}\left(\Delta_{\mathrm{a,e}}\phi - \frac{\mu_{\mathrm{Na}}^{\mathrm{a,e}}\left(T^{\mathrm{s,a}}\right)}{F}\right) &= R_{\phi q}^{\mathrm{s,a}} J_q'^{\mathrm{a,e}} + R_{\phi q}^{\mathrm{s,e}} J_q'^{\mathrm{e,a}} + R_{\phi\phi}^{\mathrm{s,a}} j
\end{aligned} \tag{13.34}$$

The resistivities satisfy the Onsager relations. The relations for both sides of the surface may be written in a form similar to Eq. (13.11)

$$\begin{aligned}
\Delta_{\mathrm{a,s}} T &= -\frac{1}{\lambda^{\mathrm{s,a}}}\left(J_q'^{\mathrm{a,e}} - \pi^{\mathrm{a,e}}\frac{j}{F}\right) \\
\Delta_{\mathrm{s,e}} T &= -\frac{1}{\lambda^{\mathrm{s,e}}}\left(J_q'^{\mathrm{e,a}} - \pi^{\mathrm{e,a}}\frac{j}{F}\right) \\
\Delta_{\mathrm{a,e}}\phi - \frac{1}{F}\mu_{\mathrm{Na}}^{\mathrm{a,e}}\left(T^{\mathrm{s,a}}\right) &= -\frac{\pi^{\mathrm{a,e}}}{T^{\mathrm{a,e}}F}\Delta_{\mathrm{a,s}} T - \frac{\pi^{\mathrm{e,a}}}{T^{\mathrm{e,a}}F}\Delta_{\mathrm{s,e}} T - r^{\mathrm{s,a}} j
\end{aligned} \tag{13.35}$$

where the coefficients are now given by

$$\begin{aligned}
\pi^{\mathrm{a,e}} &= \left(\frac{J_q'^{\mathrm{a,e}}}{j/F}\right)_{\Delta_{\mathrm{a,s}} T=0} = -F\frac{R_{q\phi}^{\mathrm{s,a}}}{R_{qq}^{\mathrm{s,a}}} \\
\pi^{\mathrm{e,a}} &= \left(\frac{J_q'^{\mathrm{e,a}}}{j/F}\right)_{\Delta_{\mathrm{s,e}} T=0} = -F\frac{R_{q\phi}^{\mathrm{s,e}}}{R_{qq}^{\mathrm{s,e}}} \\
\lambda^{\mathrm{s,a}} &= \frac{1}{R_{qq}^{\mathrm{s,a}} T^{\mathrm{s,a}} T^{\mathrm{a,e}}} \quad \text{and} \quad \lambda^{\mathrm{s,e}} = \frac{1}{R_{qq}^{\mathrm{s,e}} T^{\mathrm{s,a}} T^{\mathrm{e,a}}} \\
r^{\mathrm{s,a}} &= T^{\mathrm{s,a}}\left(R_{\phi\phi}^{\mathrm{s,a}} - \frac{R_{q\phi}^{\mathrm{s,a}} R_{\phi q}^{\mathrm{s,a}}}{R_{qq}^{\mathrm{s,a}}} - \frac{R_{q\phi}^{\mathrm{s,e}} R_{\phi q}^{\mathrm{s,e}}}{R_{qq}^{\mathrm{s,e}}}\right)
\end{aligned} \tag{13.36}$$

The transport properties $\pi^{\mathrm{a,e}}$ and $\pi^{\mathrm{e,a}}$ are ratios of fluxes in homogeneous phases, and are therefore equal for the surface and the adjacent homogeneous phase. The coefficient π^{e}, defined in the previous section, expresses

that the charge transport by sodium ion leads to heat transport away from the anode surface. Using Eqs. (13.16) and the analogous relation in the electrolyte, we have

$$\pi^{\mathrm{a,e}} = -T^{\mathrm{a,e}}\left(S^*_{\mathrm{e}^-} + S^{\mathrm{a,e}}_{\mathrm{Na}}\right) \quad \text{and} \quad \pi^{\mathrm{e,a}} = -T^{\mathrm{e,a}} S^*_{\mathrm{Na}^+} \tag{13.37}$$

where $S^*_{\mathrm{Na}^+}$ is the transported entropy of the sodium ion in the β''-alumina. Substituting these relations in Eq. (13.35) gives

$$\Delta_{\mathrm{a,s}} T = -\frac{1}{\lambda^{\mathrm{s,a}}}\left(J'^{\mathrm{a,e}}_q + T^{\mathrm{a,e}}\left(S^*_{\mathrm{e}^-} + S^{\mathrm{a,e}}_{\mathrm{Na}}\right)\frac{j}{F}\right)$$

$$\Delta_{\mathrm{s,e}} T = -\frac{1}{\lambda^{\mathrm{s,e}}}\left(J'^{\mathrm{e,a}}_q + T^{\mathrm{e,a}} S^*_{\mathrm{Na}^+}\frac{j}{F}\right)$$

$$\Delta_{\mathrm{a,e}}\phi - \frac{1}{F}\mu^{\mathrm{a,e}}_{\mathrm{Na}}\left(T^{\mathrm{s,a}}\right) = \frac{1}{F}\left(S^*_{\mathrm{e}^-} + S^{\mathrm{a,e}}_{\mathrm{Na}}\right)\Delta_{\mathrm{a,s}} T + \frac{1}{F} S^*_{\mathrm{Na}^+}\Delta_{\mathrm{s,e}} T - r^{\mathrm{s,a}} j \tag{13.38}$$

Using $\mu^{\mathrm{a,e}}_{\mathrm{Na}}\left(T^{\mathrm{s,a}}\right) = \mu^{\mathrm{a}}_{\mathrm{Na}} - S^{\mathrm{a,e}}_{\mathrm{Na}}\Delta_{\mathrm{a,s}} T = \mu^{\mathrm{s,a}}_{\mathrm{Na}} - S^{\mathrm{a,e}}_{\mathrm{Na}}\Delta_{\mathrm{a,s}} T$ the relation for the electric potential reduces to

$$\Delta_{\mathrm{a,e}}\phi - \frac{1}{F}\mu^{\mathrm{s,a}}_{\mathrm{Na}} = \frac{1}{F} S^*_{\mathrm{e}^-}\Delta_{\mathrm{a,s}} T + \frac{1}{F} S^*_{\mathrm{Na}^+}\Delta_{\mathrm{s,e}} T - r^{\mathrm{s,a}} j \tag{13.39}$$

In Fig. 13.1, $\Delta_{\mathrm{a,e}}\phi$ is positive. This is consistent with the negative reaction Gibbs energy (a tendency for Na to react) and a decrease in temperature across the surface.

The above results now show that the expressions for the surface are natural prolongations of the expressions for the homogeneous phases. They are simplified because there is no sodium adsorption at the surface. The similarity in the description of the homogeneous regions and the surface makes it simple to integrate across the heterogeneous system. The Peltier heats on both sides of the surface were equal to their values in the homogeneous phases. Only three new coefficients are needed to describe the surface, $\lambda^{\mathrm{s,a}}$, $\lambda^{\mathrm{s,e}}$ and $r^{\mathrm{s,a}}$.

Remark 13.3. *The Nernst equation for the surface in its two equivalent formulations is*

$$\begin{aligned}\Delta_{a,e}\phi + \frac{1}{F}\Delta_n G^{s,a} &= \Delta_{a,e}\phi - \frac{1}{F}\mu^{s,a}_{Na} = \Delta_{a,e}\psi + \frac{1}{F}\left(\mu^{a,e}_{e^-} + \mu^{e,a}_{Na^+} - \mu^{s,a}_{Na}\right)\\ &\equiv \Delta_{a,e}\psi + \frac{1}{F}\Delta_r G^{s,a} = 0\end{aligned} \tag{13.40}$$

and the total cell potential is

$$\Delta_{tot}\phi = \Delta_a\psi + \Delta_{a,e}\psi + \Delta_e\psi + \Delta_{e,c}\psi + \Delta_c\psi + \frac{1}{F}\left(\Delta_r G^{s,a} + \Delta_r G^{s,c}\right) - \frac{1}{F}\left(\mu_{Na}^{a,e} - \mu_{Na}^{c,e}\right) \tag{13.41}$$

13.2.2 *The cathode surface*

We can now write, by direct analogy, the equations of interest for the cathode surface. The surface has the position (s,c) in Figs. 13.1 and 13.2. The sodium ion and the electron are transported to the anode surface and react according to:

$$\mathrm{Na^+(e) + e^-(c) \rightarrow Na(c)} \tag{13.42}$$

The contribution from the sodium to the reaction Gibbs energy is

$$\Delta_n G^{\mathrm{s,c}} = \mu_{\mathrm{Na}}^{\mathrm{s,c}} = \mu_{\mathrm{Na}}^{\mathrm{s,c}}\left(T^{\mathrm{s,c}}\right) \tag{13.43}$$

where the reaction rate is equal to j/F. The entropy production rate and the flux equations follow in a similar manner as for the anode. The equations to be solved are analogous to Eq. (13.35).

$$\begin{aligned}
\Delta_{\mathrm{e,s}}T &= -\frac{1}{\lambda^{\mathrm{s,e}}}\left[J_q'^{\mathrm{e,c}} - \pi^{\mathrm{e,c}}\frac{j}{F}\right] \\
\Delta_{\mathrm{s,c}}T &= -\frac{1}{\lambda^{\mathrm{s,c}}}\left[J_q'^{\mathrm{c,e}} - \pi^{\mathrm{c,e}}\frac{j}{F}\right] \\
\Delta_{\mathrm{e,c}}\phi + \frac{1}{F}\mu_{\mathrm{Na}}^{\mathrm{c,e}}\left(T^{\mathrm{s,c}}\right) &= -\frac{\pi^{\mathrm{e,c}}}{T^{\mathrm{e,c}}F}\Delta_{\mathrm{e,s}}T - \frac{\pi^{\mathrm{c,e}}}{T^{\mathrm{c,e}}F}\Delta_{\mathrm{s,c}}T - r^{\mathrm{s,c}}j
\end{aligned} \tag{13.44}$$

where we added the electric potential differences. Using Eqs. (13.16), (13.26) and (13.43), for the cathode surface gives

$$\begin{aligned}
\Delta_{\mathrm{e,s}}T &= -\frac{1}{\lambda^{\mathrm{s,e}}}\left(J_q'^{\mathrm{e,c}} + T^{\mathrm{e,c}}S^*_{\mathrm{Na^+}}\frac{j}{F}\right) \\
\Delta_{\mathrm{s,c}}T &= -\frac{1}{\lambda^{\mathrm{s,c}}}\left(J_q'^{\mathrm{c,e}} + T^{\mathrm{c,e}}\left(S^*_{\mathrm{e^-}} + S^{\mathrm{c,e}}_{\mathrm{Na}}\right)\frac{j}{F}\right) \\
\Delta_{\mathrm{e,c}}\phi + \frac{1}{F}\mu_{\mathrm{Na}}^{\mathrm{s,c}} &= \frac{1}{F}S^*_{\mathrm{Na^+}}\Delta_{\mathrm{e,s}}T + \frac{1}{F}S^*_{\mathrm{e^-}}\Delta_{\mathrm{s,c}}T - r^{\mathrm{s,c}}j
\end{aligned} \tag{13.45}$$

which is the analogue of Eq. (13.38). The chemical potential of sodium in the cathode is constant and equal to the chemical potential at the cathode surface. This is similar to in the anode.

13.3 The thermoelectric potential

When thermal reservoirs of temperatures $T^{\mathrm{a,o}}$ and $T^{\mathrm{c,o}}$ are available, and the chemical potential difference between the electrodes is known, we can now find the resulting total electric potential from Eq. (13.2). For the anode, we neglect the dependence of the various coefficients on the temperature and the chemical potential of the sodium and integrate Eq. (13.19). This gives

$$\begin{aligned} \Delta_{\mathrm{a}} T &= -\frac{d^{\mathrm{a}}}{\lambda^{\mathrm{a}}}\left[J_q'^{\mathrm{a}} - \pi^{\mathrm{a}}\left(d^{\mathrm{a}}/2\right)\frac{j}{F}\right] \\ \Delta_{\mathrm{a}}\mu^{\mathrm{a}}_{\mathrm{Na}} &= 0 \\ \Delta_{\mathrm{a}}\phi &= \frac{S^*_{\mathrm{e}^-}}{F}\Delta_{\mathrm{a}} T - r^{\mathrm{a}} d^{\mathrm{a}} j \end{aligned} \tag{13.46}$$

For the cathode, we integrate Eq. (13.22) and find similarly

$$\begin{aligned} \Delta_{\mathrm{c}} T &= -\frac{d^{\mathrm{c}}}{\lambda^{\mathrm{c}}}\left\{J_q'^{\mathrm{c}} - \pi^{\mathrm{c}}\left(d^{\mathrm{a}} + d^{\mathrm{e}} + d^{\mathrm{c}}/2\right)\frac{j}{F}\right\} \\ \Delta_{\mathrm{c}}\mu^{\mathrm{c}}_{\mathrm{Na}} &= 0 \\ \Delta_{\mathrm{c}}\phi &= \frac{S^*_{\mathrm{e}^-}}{F}\Delta_{\mathrm{c}} T - r^{\mathrm{c}} d^{\mathrm{c}} j \end{aligned} \tag{13.47}$$

For the electrolyte, we integrate Eq. (13.28) and find

$$\begin{aligned} \Delta_{\mathrm{e}} T &= -\frac{d^{\mathrm{e}}}{\lambda^{\mathrm{e}}}\left(J_q'^{\mathrm{e}} - \pi^{\mathrm{e}}\frac{j}{F}\right) \\ \Delta_{\mathrm{e}}\phi &= -\frac{1}{F}S^*_{\mathrm{Na}^+}\Delta_{\mathrm{e}} T - r^{\mathrm{e}} d^{\mathrm{e}} j \end{aligned} \tag{13.48}$$

Furthermore, using Eqs. (13.39) and (13.45) for the anode and cathode surfaces as well as $\mu^{\mathrm{s,a}}_{\mathrm{Na}} = \mu^{\mathrm{a}}_{\mathrm{Na}}$ and $\mu^{\mathrm{s,c}}_{\mathrm{Na}} = \mu^{\mathrm{c}}_{\mathrm{Na}}$ we have

$$\begin{aligned} \Delta_{\mathrm{tot}}\phi = \phi^{\mathrm{c,o}} - \phi^{\mathrm{a,o}} &= \Delta_{\mathrm{a}}\phi + \Delta_{\mathrm{a,e}}\phi + \Delta_{\mathrm{e}}\phi + \Delta_{\mathrm{e,c}}\phi + \Delta_{\mathrm{c}}\phi \\ &= \frac{1}{F}\left(\mu^{\mathrm{a}}_{\mathrm{Na}} - \mu^{\mathrm{c}}_{\mathrm{Na}}\right) + \frac{S^*_{\mathrm{e}^-}}{F}\left(T^{\mathrm{s,a}} - T^{\mathrm{a,o}} + T^{\mathrm{c,o}} - T^{\mathrm{s,c}}\right) \\ &\quad - \frac{S^*_{\mathrm{Na}^+}}{F}\left(T^{\mathrm{s,c}} - T^{\mathrm{s,a}}\right) \\ &\quad - \left(r^{\mathrm{a}} d^{\mathrm{a}} + r^{\mathrm{s,a}} + r^{\mathrm{e}} d^{\mathrm{e}} + r^{\mathrm{s,c}} + r^{\mathrm{c}} d^{\mathrm{c}}\right) j \end{aligned} \tag{13.49}$$

The expressions for all the temperature differences (13.46), (13.47), and (13.48), and the electrode potentials, Eqs. (13.38) and (13.45), give the conversion between thermal, chemical and electric energy in the cell. Kjelstrup and Bedeaux [130] calculated the corresponding profiles of temperature and electric potential in the solid oxide fuel cell. Kjelstrup *et al.* calculated the present cell [184].

This page intentionally left blank

Chapter 14

The Transported Entropy

We describe how the transported entropy can be determined by measuring the Seebeck coefficient of an electrochemical cell. Selected values of the transported entropies are presented. The transported entropies obey certain transformation properties, because potential differences and the electric current density are independent of the frame of reference.

We saw in Chapters 8 and 13, that the conversion from thermal to electric energy, or vice versa, depended on the magnitude of the transported entropies in conductors of the system. For electronic conductors, this quantity is normally not large, typically a few J/K mol [153,190]. This seriously limits the efficiency of thermal energy conversion. By using ions as charge carriers instead of electrons, attempts have been made to find cells with larger thermoelectric powers. Large Peltier coefficients have been found in cells with complex formations [78,191] and with gas electrodes [192].

Systematic knowledge about transported entropies has been gathered by Agar [148,193]. The purpose of this chapter is to describe how transported entropies can be determined, which relations they must obey, and what their properties are. We describe how transported entropies can be obtained from measurements in three example cells:

$$T^{\mathrm{l}},\ \mathrm{Mo(s)|Pb(l)|PbCl_2(l),\ MCl(l)|Pb(l)|Mo(s)},\ T^{\mathrm{r}} \qquad \text{(a)}$$

$$T^{\mathrm{a}},\ \mathrm{M(Hg)|}\beta''\text{-alumina|M(Hg)},\ T^{\mathrm{c}} \qquad \text{(b)}$$

$$T^{\mathrm{l}},\ \mathrm{Ag(s)|AgCl(s)|MCl(aq)|AgCl\ (s)|Ag(s)},\ T^{\mathrm{r}} \qquad \text{(c)}$$

Cell a has electrodes of liquid lead, and an electrolyte mixture of two molten salts. The liquid lead pools are connected to the potentiometer via molybdenum wires [194]. Cell b was described in Chapter 13 with M = Na [195]. Cell c has an aqueous electrolyte [196], and shall be further discussed in

Chapter 15. The metal contacts to the cells a and c are thermostatted at temperatures T^{l} and T^{r}. In cell b, they are thermostatted to T^{a} and T^{c} respectively.

14.1 The Seebeck coefficient of cell a

Cell a has five homogeneous phases and four interfaces. The homogeneous phases are denoted l, a, e, c and r, respectively. The surfaces between them are denoted (s,l), (s,a), (s,c) and (s,r).

The chemical reaction on the electrodes takes half a mole of lead from the anode surface

$$\frac{1}{2}\mathrm{Pb} \;\rightarrow\; \frac{1}{2}\mathrm{Pb}^{2+} + \mathrm{e}^{-} \tag{14.1}$$

and adds the same amount to the cathode surface when a faraday of charge is passed through the cell. For a positive electric current density j both the (s,a) and the (s,c) surface move to the left relative to the (s,l) and the (s,r) surfaces, with a small velocity proportional to j. The ions of the two salts move in the electrolyte. Chemical potential gradients of the salts develop in a temperature gradient after a few hours. We are interested in the state when the chemical potential gradient of $PbCl_2$ produced by the non-zero electric current density is balanced by the thermal force, that is, in the Soret equilibrium. In this state, there is no transport of $PbCl_2$ or MCl relative to the (s,a) and the (s,c) surfaces. We will show that one can then find the transported entropy of lead ions in a simple way.

The entropy production in the metal phases is

$$\sigma = J'_q \left(\frac{\partial}{\partial x} \frac{1}{T} \right) + j \left(-\frac{1}{T} \frac{\partial \phi}{\partial x} \right) \tag{14.2}$$

The equations for the temperature gradient and the electric potential gradient are the same as derived in Sec. 9.1

$$\begin{aligned} \frac{\partial T}{\partial x} &= -\frac{1}{\lambda} \left(J'_q - \pi \frac{j}{F} \right) \\ \frac{\partial \phi}{\partial x} &= -\frac{\pi}{TF} \frac{\partial T}{\partial x} - rj \end{aligned} \tag{14.3}$$

The Peltier coefficients for the solid Mo phases and for the lead pools are:

$$\pi^{\mathrm{l}} = \pi^{\mathrm{r}} = T S^*_{\mathrm{e}^-,\mathrm{Mo}} \quad \text{and} \quad \pi^{\mathrm{a}} = \pi^{\mathrm{c}} = T S^*_{\mathrm{e}^-,\mathrm{Pb}} \tag{14.4}$$

Neglecting the variation of the coefficients λ, r, π, $S^*_{\mathrm{e}^-,\mathrm{Mo}}$, $S^*_{\mathrm{e}^-,\mathrm{Pb}}$ with the temperature, the equations give for the molybdenum phases:

$$\begin{aligned}
\Delta_{\mathrm{l}}T &= -\frac{d^{\mathrm{l}}}{\lambda^{\mathrm{l}}}\left(J_q'^{\mathrm{l}} - \pi^{\mathrm{l}}\frac{j}{F}\right) \quad \text{and} \quad \Delta_{\mathrm{l}}\phi = -\frac{1}{F}S^*_{\mathrm{e}^-,\mathrm{Mo}}\Delta_{\mathrm{l}}T - r^{\mathrm{l}}d^{\mathrm{l}}j \\
\Delta_{\mathrm{r}}T &= -\frac{d^{\mathrm{r}}}{\lambda^{\mathrm{r}}}\left(J_q'^{\mathrm{r}} - \pi^{\mathrm{r}}\frac{j}{F}\right) \quad \text{and} \quad \Delta_{\mathrm{r}}\phi = -\frac{1}{F}S^*_{\mathrm{e}^-,\mathrm{Mo}}\Delta_{\mathrm{r}}T - r^{\mathrm{r}}d^{\mathrm{r}}j
\end{aligned} \tag{14.5}$$

and for the lead phases:

$$\begin{aligned}
\Delta_{\mathrm{a}}T &= -\frac{d^{\mathrm{a}}}{\lambda^{\mathrm{a}}}\left(J_q'^{\mathrm{a}} - \pi^{\mathrm{a}}\frac{j}{F}\right) \quad \text{and} \quad \Delta_{\mathrm{a}}\phi = -\frac{1}{F}S^*_{\mathrm{e}^-,\mathrm{Pb}}\Delta_{\mathrm{a}}T - r^{\mathrm{a}}d^{\mathrm{a}}j \\
\Delta_{\mathrm{c}}T &= -\frac{d^{\mathrm{c}}}{\lambda^{\mathrm{c}}}\left(J_q'^{\mathrm{c}} - \pi^{\mathrm{c}}\frac{j}{F}\right) \quad \text{and} \quad \Delta_{\mathrm{c}}\phi = -\frac{1}{F}S^*_{\mathrm{e}^-,\mathrm{Pb}}\Delta_{\mathrm{c}}T - r^{\mathrm{c}}d^{\mathrm{c}}j
\end{aligned} \tag{14.6}$$

The molybdenum-lead interfaces were described in Sec. 9.2. The potential drops across these interfaces were, cf. Eq. (9.18):

$$\begin{aligned}
\Delta_{\mathrm{l,a}}\phi &= -\frac{1}{F}S^*_{\mathrm{e}^-,\mathrm{Mo}}\left(T^{\mathrm{s,l}} - T^{\mathrm{l,a}}\right) - \frac{1}{F}S^*_{\mathrm{e}^-,\mathrm{Pb}}\left(T^{\mathrm{a,l}} - T^{\mathrm{s,l}}\right) - r^{\mathrm{s,l}}j \\
\Delta_{\mathrm{c,r}}\phi &= -\frac{1}{F}S^*_{\mathrm{e}^-,\mathrm{Pb}}\left(T^{\mathrm{s,r}} - T^{\mathrm{c,r}}\right) - \frac{1}{F}S^*_{\mathrm{e}^-,\mathrm{Mo}}\left(T^{\mathrm{r,c}} - T^{\mathrm{s,r}}\right) - r^{\mathrm{s,r}}j
\end{aligned} \tag{14.7}$$

The entropy production of the interface has a similar structure as in Sec. 13.2. For the lead-electrolyte interface, we have in a frame of reference that moves along with the surface

$$\sigma^{\mathrm{s,a}} = J_q'^{\mathrm{a}}\left(\Delta_{\mathrm{a,s}}\frac{1}{T}\right) + J_q'^{\mathrm{e}}\left(\Delta_{\mathrm{s,e}}\frac{1}{T}\right) + j\left[-\frac{1}{T^{\mathrm{s,a}}}\left(\Delta_{\mathrm{a,e}}\phi + \frac{\Delta_n G^{\mathrm{s,a}}}{F}\right)\right] \tag{14.8}$$

The reaction rate is proportional to the electric current density, $r^{\mathrm{s}} = j/F$, and so is the transport of Pb into the surface, $J^{\mathrm{a}}_{\mathrm{Pb}} = j/2F$. The contribution to the reaction Gibbs energy from the neutral components is $\Delta_n G^{\mathrm{s,a}} = -\mu^{\mathrm{a,e}}_{\mathrm{Pb}}\left(T^{\mathrm{s,a}}\right)/2$. As the quantities of interest do not depend on the chosen frame of reference, we may use a different frame of reference than the one used above. The linear relations are, using the same approximations as in

Sec. 9.2,

$$\Delta_{\mathrm{a,s}}T = -\frac{1}{\lambda^{\mathrm{s,a}}_{aa}}\left(J'^{\mathrm{a}}_q - \pi^{\mathrm{a}}\frac{j}{F}\right)$$

$$\Delta_{\mathrm{s,e}}T = -\frac{1}{\lambda^{\mathrm{s,a}}_{ee}}\left(J'^{\mathrm{e}}_q - \pi^{\mathrm{e}}\frac{j}{F}\right) \tag{14.9}$$

$$\Delta_{\mathrm{a,e}}\phi - \frac{1}{2F}\mu^{\mathrm{a,e}}_{\mathrm{Pb}} = -\frac{1}{F}S^{*}_{\mathrm{e^-,Pb}}\Delta_{\mathrm{a,s}}T - \frac{1}{2F}S^{*,\mathrm{e}}_{\mathrm{Pb^{2+}}}\Delta_{\mathrm{s,e}}T - r^{\mathrm{s,a}}j$$

where $r^{\mathrm{s,a}}$ is the ohmic resistivity of the surface. The Peltier coefficients on the anode and cathode sides were given in Eq. (14.4). The Peltier coefficient in the electrolyte

$$\pi^{\mathrm{e}} = \frac{1}{2}T^{\mathrm{e}}S^{*,\mathrm{e}}_{\mathrm{Pb^{2+}}} \tag{14.10}$$

expresses that the stationary state charge transport by lead ions gives heat transport away from the surface corresponding to one equivalent of lead ion.

For the electrolyte-lead surface we find similarly

$$\Delta_{\mathrm{e,s}}T = -\frac{1}{\lambda^{\mathrm{s,c}}_{ee}}\left(J'^{\mathrm{e}}_q - \pi^{\mathrm{e}}\frac{j}{F}\right)$$

$$\Delta_{\mathrm{s,c}}T = -\frac{1}{\lambda^{\mathrm{s,c}}_{ee}}\left(J'^{\mathrm{c}}_q - \pi^{\mathrm{c}}\frac{j}{F}\right) \tag{14.11}$$

$$\Delta_{\mathrm{e,c}}\phi + \frac{1}{2F}\mu^{\mathrm{c,e}}_{\mathrm{Pb}} = -\frac{1}{2F}S^{*,\mathrm{e}}_{\mathrm{Pb^{2+}}}\Delta_{\mathrm{e,s}}T - \frac{1}{F}S^{*}_{\mathrm{e^-,Pb}}\Delta_{\mathrm{s,c}}T - r^{\mathrm{s,c}}j$$

The entropy production of the electrolyte has four terms

$$\sigma = J'_q\left(\frac{\partial}{\partial x}\frac{1}{T}\right) + J_{\mathrm{PbCl_2}}\left(-\frac{1}{T}\frac{\partial \mu_{\mathrm{PbCl_2},T}}{\partial x}\right)$$
$$+ J_{\mathrm{MCl}}\left(-\frac{1}{T}\frac{\partial \mu_{\mathrm{MCl},T}}{\partial x}\right) + j\left(-\frac{1}{T}\frac{\partial \phi}{\partial x}\right) \tag{14.12}$$

We will again use the frame of reference in which the electrode-electrolyte surfaces are not moving. We are interested in the stationary state when J_{MCl} and $J_{\mathrm{PbCl_2}}$ are zero. Only two terms then remain in the entropy production, and we obtain the same transport equations as those found for the molybdenum wires and the lead pools:

$$\begin{aligned}\Delta_{\mathrm{e}}T &= -\frac{d^{\mathrm{e}}}{\lambda^{\mathrm{e}}}\left(J'^{\mathrm{e}}_q - \pi^{\mathrm{e}}\frac{j}{F}\right)\\ \Delta_{\mathrm{e}}\phi &= -\frac{1}{2F}S^{*,\mathrm{e}}_{\mathrm{Pb^{2+}}}\Delta_{\mathrm{e}}T - r^{\mathrm{e}}d^{\mathrm{e}}j\end{aligned} \tag{14.13}$$

All coefficients refer to the stationary state in question. This means that the resistivity, for instance, is the resistivity of a mixture with salt and gradients, which was assumed to be constant in Eq. (14.13). The stationary state Peltier coefficient for the electrolyte is given in Eq. (14.10).

The total cell potential is now obtained by adding all contributions

$$\begin{aligned}
F\Delta_{\mathrm{tot}}\phi &= F\left(\Delta_{\mathrm{l}}\phi + \Delta_{\mathrm{l,a}}\phi + \Delta_{\mathrm{a}}\phi + \Delta_{\mathrm{a,e}}\phi + \Delta_{\mathrm{e}}\phi + \Delta_{\mathrm{e,c}}\phi\right.\\
&\quad \left. + \Delta_{\mathrm{c}}\phi + \Delta_{\mathrm{c,r}}\phi + \Delta_{\mathrm{r}}\phi\right)\\
&= -\frac{1}{2}\left[\mu^{\mathrm{c,e}}_{\mathrm{Pb}}\left(T^{\mathrm{s,c}}\right) - \mu^{\mathrm{a,e}}_{\mathrm{Pb}}\left(T^{\mathrm{s,a}}\right)\right] + \left(S^{*}_{\mathrm{e^-,Mo}} - S^{*}_{\mathrm{e^-,Pb}}\right)\left(T^{\mathrm{s,r}} - T^{\mathrm{s,l}}\right)\\
&\quad + \left(S^{*}_{\mathrm{e^-,Pb}} - \frac{1}{2}S^{*,\mathrm{e}}_{\mathrm{Pb^{2+}}}\right)\left(T^{\mathrm{s,c}} - T^{\mathrm{s,a}}\right)\\
&\quad - \left(r^{\mathrm{l}}d^{\mathrm{l}} + r^{\mathrm{s,l}} + r^{\mathrm{a}}d^{\mathrm{a}} + r^{\mathrm{s,a}} + r^{\mathrm{e}}d^{\mathrm{e}} + r^{\mathrm{s,c}} + r^{\mathrm{c}}d^{\mathrm{c}} + r^{\mathrm{s,r}} + r^{\mathrm{r}}d^{\mathrm{r}}\right)jF\\
&= -\frac{1}{2}\left[H^{\mathrm{c,e}}_{\mathrm{Pb}}\left(T^{\mathrm{s,c}}\right) - H^{\mathrm{a,e}}_{\mathrm{Pb}}\left(T^{\mathrm{s,a}}\right)\right] + \left(S^{*}_{\mathrm{e^-,Mo}} - S^{*}_{\mathrm{e^-,Pb}}\right)\left(T^{\mathrm{s,r}} - T^{\mathrm{s,l}}\right)\\
&\quad + \left(S^{*}_{\mathrm{e^-,Pb}} - \frac{1}{2}\left(S^{*,\mathrm{e}}_{\mathrm{Pb^{2+}}} - S_{\mathrm{Pb}}\right)\right)\left(T^{\mathrm{s,c}} - T^{\mathrm{s,a}}\right)\\
&\quad - \left(r^{\mathrm{l}}d^{\mathrm{l}} + r^{\mathrm{s,l}} + r^{\mathrm{a}}d^{\mathrm{a}} + r^{\mathrm{s,a}} + r^{\mathrm{e}}d^{\mathrm{e}} + r^{\mathrm{s,c}} + r^{\mathrm{c}}d^{\mathrm{c}} + r^{\mathrm{s,r}} + r^{\mathrm{r}}d^{\mathrm{r}}\right)jF
\end{aligned} \tag{14.14}$$

where we used the assumption that the temperatures on both sides of the potentiometer are equal, i.e. $T^{\mathrm{l,o}} = T^{\mathrm{r,o}}$. Contributions due to the temperature dependence of the entropies and the ohmic resistivities have been neglected.

When the two electrode pools are thermostatted at $T^{\mathrm{s,l}} = T^{\mathrm{a,l}} = T^{\mathrm{a,e}} = T^{\mathrm{s,a}} \equiv T^{\mathrm{a}}$ and $T^{\mathrm{s,c}} = T^{\mathrm{c,e}} = T^{\mathrm{c,r}} = T^{\mathrm{s,r}} \equiv T^{\mathrm{c}}$, the electric current is zero, and if one neglects the temperature dependence of the enthalpy, the expression reduces to

$$F\Delta_{\mathrm{tot}}\phi = \left[S^{*}_{\mathrm{e^-,Mo}} - \frac{1}{2}\left(S^{*,\mathrm{e}}_{\mathrm{Pb^{2+}}} - S_{\mathrm{Pb}}\right)\right]\left(T^{\mathrm{c}} - T^{\mathrm{a}}\right) \tag{14.15}$$

The Seebeck coefficient can thus be defined as

$$\eta_{\mathrm{S}} = \left(\frac{\Delta_{\mathrm{tot}}\phi}{\Delta T}\right)_{j=0} = \frac{1}{F}\left[S^{*}_{\mathrm{e^-,Mo}} - \frac{1}{2}\left(S^{*,\mathrm{e}}_{\mathrm{Pb^{2+}}} - S_{\mathrm{Pb}}\right)\right] \tag{14.16}$$

Table 14.1 The transported entropy of Pb^{2+} at 798 K [194].

MCl	x_{PbCl_2}	$\eta_{S,1}$ / μV K^{-1}	$S^*_{Pb^{2+}}$ / J mol^{-1} K^{-1}
LiCl	0.7	4.8	103
	0.5	8.9	106
NaCl	0.8	15.2	101
	0.57	8.1	102
KCl	0.68	23.8	100
	0.54	21.0	100
RbCl	0.8	23.4	100
	0.5	32.4	102
CsCl	0.6	23.9	99
–	1	−10.1	102

The electric potential difference can be measured with good accuracy, and so can the temperature difference. The ratio gives a possibility for an accurate determination of $S^{*,e}_{Pb^{2+}}$ [194]. The alternative, to determine the transported entropy from the Peltier heat, is less accurate.

The cell in this section was described under stationary state conditions, when the salt fluxes are zero. The more general case was described for different systems by Grimstvedt *et al.* [197] and Flem *et al.* [80].

14.2 The transported entropy of Pb^{2+} in cell a

The Seebeck coefficient of cell a is according to the above derivations:

$$\eta_{S,1} = \frac{1}{F}\left(S^*_{e^-,Mo} - \frac{1}{2}S^{*,e}_{Pb^{2+}} + \frac{1}{2}S_{Pb}\right) \tag{14.17}$$

The corresponding expression for the cell of Sec. 9.1 was

$$\eta_{S,2} = \frac{1}{F}\left(S^*_{e^-,Mo} - S^*_{e^-,Pb}\right) \tag{14.18}$$

Their difference was used to find the properties of lead ion

$$\eta_{S,1} - \eta_{S,2} = \frac{1}{F}\left(S^*_{e^-,Pb} - \frac{1}{2}S^*_{Pb^{2+}} + \frac{1}{2}S_{Pb}\right) \tag{14.19}$$

The Seebeck coefficient for Mo(s)|Pb(l)| Mo(s) is $\eta_{S,2} = 20.6\ \mu$V/K. The coefficient for main cell is, $\eta_{S,1}$, with pure $PbCl_2$ is $-10.1\ \mu$V/K at 798 K. We use the transported entropy of electrons in lead as a reference, i.e. $S^*_{e^-,Pb} \equiv 0$. The transported entropy $S^{*,e}_{Pb^{2+}}$ in pure $PbCl_2$ is then found to be 102 J/mol K. Some selected values for electrolyte mixtures are given in Table 14.1 [194]. Surprisingly, the transported entropy of lead varies only very little, from 99 to 106, as the cation M^+ is exchanged or as the composition changes.

14.3 The transported entropy of the cation in cell b

We saw in Chapter 13 that the total cell potential of cell b (with M = Na) was:

$$\begin{aligned}\Delta_{tot}\phi - \frac{1}{F}\left(\mu^{a,e}_{Na} - \mu^{c,e}_{Na}\right) &= \Delta_a\phi + \Delta_{a,e}\phi + \Delta_e\phi + \Delta_{e,c}\phi + \Delta_c\phi \\ &\quad - \frac{1}{F}\left(\mu^{a,e}_{Na} - \mu^{c,e}_{Na}\right) \\ &= \frac{S^*_{e^-}}{F}\left(T^{a,e} - T^{c,e}\right) - \frac{S^*_{Na^+}}{F}\left(T^{e,c} - T^{e,a}\right) \\ &\quad - \left(r^a d^a + r^{s,a} + r^{s,e} + r^e d^e + r^{s,e} + r^{s,c} + r^c d^c\right) j\end{aligned} \tag{14.20}$$

The electrodes, including their surfaces, are thermostatted at temperatures T^a and T^c [198]. This means that $T^{a,e} = T^{s,a} = T^{e,a} = T^a$ and $T^{e,c} = T^{s,c} = T^{c,e} = T^c$. The potentiometer is at temperature $T^{a,o} = T^{c,o} \equiv T^o$. The potential difference becomes:

$$\left(\Delta_{tot}\phi\right)_{j\to 0} = \frac{1}{F}\left(S_{Na} + S^*_{e^-} - S^*_{Na^+}\right)\left(T^c - T^a\right) \tag{14.21}$$

The Seebeck coefficient for a cell with a metal M is therefore

$$\eta_S = \frac{1}{F}\left(S_M - S^*_{M^+} + S^*_{e^-}\right) \tag{14.22}$$

Only the combination of the transported entropy of the M^+-ions in the β''-alumina and of the electrons in the iron can be obtained from the Seebeck-coefficient. In order to allocate a value to a single charge carrier, a reference must be chosen. It is customary to use the transported entropy in lead (Pb) as a zero reference [27]. The transported entropy of electrons in Fe then, is small and positive, 1 J/K mol.

Table 14.2 The transported entropy of cations in selected materials [198].

Material	Conducting	Transported entropy
	ion	/ J K^{-1} mol^{-1}
Na-β''-alumina	Na^+	60 ± 5
K-β''-alumina	K^+	60 ± 3
Ag-β''-alumina	Ag^+	57 ± 5
NaF	Na^+	81 ± 8
Na_3AlF_6	Na^+	140 ± 7

Results for Na^+, obtained from such measurements, are listed in Table 14.2 together with results for some other ions.

14.4 The transported entropy of the ions cell c

The total cell potential of cell c, when operated at stationary state conditions, can be found by adding all contributions of the separate parts, as will be described in more detail in Chapter 15:

$$\begin{aligned}\Delta\phi &= \Delta_{\mathrm{l,a}}\phi + \Delta_{\mathrm{a}}\phi + \Delta_{\mathrm{a,e}}\phi + \Delta_{\mathrm{e}}\phi + \Delta_{\mathrm{e,c}}\phi + \Delta_{\mathrm{c}}\phi + \Delta_{\mathrm{c,r}}\phi \\ &= -\frac{1}{F}\left(\mu^{\mathrm{r,c}}_{\mathrm{Ag}} - \mu^{\mathrm{l,a}}_{\mathrm{Ag}}\right) + \frac{1}{F}\left(\mu^{\mathrm{c,e}}_{\mathrm{AgCl}} - \mu^{\mathrm{a,e}}_{\mathrm{AgCl}}\right) \\ &\quad + \frac{1}{F}\left(S^*_{\mathrm{e^-}} - S_{\mathrm{Ag}}\right)\left(\Delta_{\mathrm{l,s}}T + \Delta_{\mathrm{s,r}}T\right) \\ &\quad - \frac{1}{F}S^*_{\mathrm{Ag^+}}\left(T^{\mathrm{s,r}} - T^{\mathrm{s,c}} + T^{\mathrm{s,a}} - T^{\mathrm{s,l}}\right) \\ &\quad + \frac{1}{F}S_{\mathrm{AgCl}}\left(\Delta_{\mathrm{a,s}}T + \Delta_{\mathrm{s,c}}T\right) + \frac{1}{F}S^*_{\mathrm{Cl^-}}\left(T^{\mathrm{s,c}} - T^{\mathrm{s,a}}\right) \\ &\quad - \left(r^{\mathrm{s,l}} + r^{\mathrm{a}}d^{\mathrm{a}} + r^{\mathrm{s,a}} + r^{\mathrm{e}}d^{\mathrm{e}} + r^{\mathrm{s,c}} + r^{\mathrm{c}}d^{\mathrm{c}} + r^{\mathrm{s,r}}\right) j \qquad (14.23)\end{aligned}$$

Again, we took all thermodynamic properties and all transported entropies independent of the temperature. By introducing the expression for the chemical potentials and neglecting the temperature dependence of the

enthalpies, we obtain

$$\begin{aligned}\Delta\phi = {} & \frac{1}{F}\left(T^{\mathrm{s,r}} - T^{\mathrm{s,l}}\right) S_{\mathrm{Ag}} - \frac{1}{F} S^*_{\mathrm{Ag^+}} \left(T^{\mathrm{s,r}} - T^{\mathrm{s,c}} + T^{\mathrm{s,a}} - T^{\mathrm{s,l}}\right) \\ & - \frac{1}{F} S^*_{\mathrm{e^-}} \left(\Delta_{\mathrm{l,s}} T + \Delta_{\mathrm{s,r}} T\right) - \frac{1}{F} S_{\mathrm{AgCl}} \left(T^{\mathrm{s,c}} - T^{\mathrm{s,a}}\right) \\ & + \frac{1}{F} S^*_{\mathrm{Cl^-}} \left(T^{\mathrm{s,c}} - T^{\mathrm{s,a}}\right) \\ & - \left(r^{\mathrm{s,l}} + r^{\mathrm{a}} d^{\mathrm{a}} + r^{\mathrm{s,a}} + r^{\mathrm{e}} d^{\mathrm{e}} + r^{\mathrm{s,c}} + r^{\mathrm{c}} d^{\mathrm{c}} + r^{\mathrm{s,r}}\right) j \end{aligned} \tag{14.24}$$

In the thermostatted cell the surfaces of the electrodes, where the electrochemical reactions take place, are thermostatted. Consider therefore the case that all solid state parts of the electrode, including the adjacent electrolyte layer, are thermostatted. The temperature is T^{a} on the anode side and T^{c} on the cathode side. Using Eq. (14.24) for zero electric current one obtains:

$$\Delta\phi = \frac{1}{F}\left(S_{\mathrm{Ag}} - S_{\mathrm{AgCl}} + S^*_{\mathrm{e^-}} + S^*_{\mathrm{Cl^-}}\right)\left(T^{\mathrm{c}} - T^{\mathrm{a}}\right) \tag{14.25}$$

The Seebeck coefficient for the cell in stationary state is

$$\eta_{\mathrm{S}} = \left(\frac{\Delta\phi}{T^{\mathrm{c}} - T^{\mathrm{a}}}\right) = \frac{1}{F}\left[S_{\mathrm{Ag}} - S_{\mathrm{AgCl}} + S^*_{\mathrm{e^-}} + S^*_{\mathrm{Cl^-}}\right] \tag{14.26}$$

A determination of the slope of the plot of the experimental $\Delta\phi$ versus $(T^{\mathrm{c}} - T^{\mathrm{a}})$ allows us to determine $S^*_{\mathrm{Cl^-}} + S^*_{\mathrm{e^-}}$ when thermodynamic entropies of Ag and AgCl are known. At 298 K, $S_{\mathrm{Ag}} = 42.7$ J/K mol and $S_{\mathrm{AgCl}} = 96.2$ J/K mol. These values were used, and the results for $S^*_{\mathrm{Cl^-}}$ are given in Table 14.3 [196]. The transported entropy of electrons was neglected. The transported entropy for chloride ions is relatively constant as a function of composition (apart from that in HCl(aq)). This is similar to the result found for Pb^{2+} in Sec. 14.2.

By taking along also MCl as a component, and defining the heat of transfer for transport of MCl in the aqueous solution, we can find an equivalent formulation for the Seebeck coefficient [27]

$$\begin{aligned}\eta_{\mathrm{S}} & \equiv \left(\frac{\Delta\phi}{T^{\mathrm{c}} - T^{\mathrm{a}}}\right) \\ & = \frac{1}{F}\left[S_{\mathrm{Ag}} - S_{\mathrm{AgCl}} + S^*_{\mathrm{e^-}} - \left(t_{\mathrm{M^+}} S^*_{\mathrm{M^+}} - t_{\mathrm{Cl^-}} S^*_{\mathrm{Cl^-}} - t_{\mathrm{M^+}} \frac{q^*_{\mathrm{MCl}}}{T} - t_{\mathrm{M^+}} S_{\mathrm{MCl}}\right)\right] \end{aligned} \tag{14.27}$$

Table 14.3 Thermoelectric properties of cell c. The temperature is 298 K and c_{MCl} is 10 mol/m^3 [196].

MCl	$\Delta\phi/\Delta_{\mathrm{e}}T$ mV/K	$S^{\mathrm{e}}_{\mathrm{MCl}}$ J/mol K	$S^{*,\mathrm{e}}_{\mathrm{M^+}}$ J/mol K	$S^{*,\mathrm{e}}_{\mathrm{Cl^-}}$ J/mol K	q^*_{MCl} kJ/mol
HCl	0.30	135	60	118	12.70
LiCl	0.68	148	29	120	0.01
NaCl	0.63	194	86	118	2.90
KCl	0.69	236	121	124	2.00
CsCl	0.61	266	162	120	3.75

Using the relation

$$S^*_{\mathrm{M^+}} + S^*_{\mathrm{Cl^-}} = \frac{q^*_{\mathrm{MCl}}}{T} + S_{\mathrm{MCl}} \tag{14.28}$$

Eq. (14.27) reduces to Eq. (14.26). Equation (14.28) is an example of a transformation property, which will be further discussed in the next section.

Before the gradient in chemical potential is established in the temperature gradient, at time $t = 0$, one may show [27] that the Seebeck coefficient is given by:

$$\eta_{\mathrm{S},t=0} = \frac{1}{F}\left[S_{\mathrm{Ag}} - S_{\mathrm{AgCl}} + S^*_{\mathrm{e^-}} + S^*_{\mathrm{Cl^-}} + t_{\mathrm{M^+}}\frac{q^*_{\mathrm{MCl}}}{T}\right] \tag{14.29}$$

This expression was used to find q^*_{MCl} from the knowledge of $t_{\mathrm{M^+}}$ and $S^*_{\mathrm{Cl^-}}$. The remaining unknown, $S^*_{\mathrm{M^+}}$, was finally found from Eq. (14.28). All results are given in Table 14.3.

Table 14.3 also gives typical order of magnitude results for thermoelectric potentials. Few systems have Seebeck coefficients larger than 1 mV/K [191]. The heat of transfer increases with the mass of the cation (HCl is an exception).

14.5 Transformation properties

Using the invariance of various properties, for instance, the measurable heat flux and the temperature gradient, for the choice of the frame of reference, one can derive transformation properties. Examples of such transformation properties were given in Eqs. (14.28) and (13.18). We shall now derive more of these properties, to clarify how they are obtained.

In Eqs. (14.2) through (14.6) we used a frame of reference in which both the molybdenum and the lead phases were not moving. In any other frame of reference the metal ions and the metal have a finite velocity. The

corresponding electron, ion and metal fluxes are then different, and instead of Eq. (14.3a) one should then use in the molybdenum phase

$$\frac{\partial T}{\partial x} = -\frac{1}{\lambda}\left(J'_q + \pi^{\mathrm{Mo}}_{\mathrm{e}^-} J_{\mathrm{e}^-} + \pi^{\mathrm{Mo}}_{\mathrm{Mo}^{2+}}\ J_{\mathrm{Mo}^{2+}} + q^*_{\mathrm{Mo}} J_{\mathrm{Mo}}\right) \tag{14.30}$$

In the original frame of reference $J_{\mathrm{Mo}^{2+}} = J_{\mathrm{Mo}} = 0$ and $J_{\mathrm{e}^-} = -j/F$, so that Eq. (14.30) reduces to Eq. (14.3a). In a frame of reference where the molybdenum has a velocity v one has $J_{\mathrm{Mo}^{2+}} = \mathrm{v}c_{\mathrm{Mo}^{2+}}$, $J_{\mathrm{Mo}} = \mathrm{v}c_{\mathrm{Mo}}$ and $J_{\mathrm{e}^-} = -j/F + \mathrm{v}c_{\mathrm{e}^-}$. As neither the temperature gradient nor the measurable heat flux depend on the frame of reference, it follows that all contributions proportional to v must cancel. With $c_{\mathrm{Mo}^{2+}} = c_{\mathrm{Mo}} = 0.5\ c_{\mathrm{e}^-}$, it follows that

$$\pi^{\mathrm{Mo}}_{\mathrm{e}^-} + \frac{1}{2}\pi^{\mathrm{Mo}}_{\mathrm{Mo}^{2+}} + \frac{1}{2}q^*_{\mathrm{Mo}} = 0 \tag{14.31}$$

The transported entropies defined by

$$\pi^{\mathrm{Mo}}_{\mathrm{e}^-} = T S^*_{\mathrm{e}^-,\mathrm{Mo}} \quad \text{and} \quad \pi^{\mathrm{Mo}}_{\mathrm{Mo}^{2+}} = T S^*_{\mathrm{Mo}^{2+},\mathrm{Mo}} \tag{14.32}$$

and the heat of transfer

$$q^*_{\mathrm{Mo}} = -T S_{\mathrm{Mo}} \tag{14.33}$$

give

$$S^*_{\mathrm{e}^-,\mathrm{Mo}} + \frac{1}{2} S^*_{\mathrm{Mo}^{2+},\mathrm{Mo}} = \frac{1}{2} S_{\mathrm{Mo}} \tag{14.34}$$

For the lead phases, we find Eqs. (14.30) through (14.34), with Mo replaced by Pb.

For a one-component electrolyte, AX, we have that [27]

$$S^*_{\mathrm{A}^+} + S^*_{\mathrm{X}^-} = S_{\mathrm{AX}} \tag{14.35}$$

With two components, AX in water, or AX and BX, the corresponding relation is [27]

$$S^*_{\mathrm{A}^+} + S^*_{\mathrm{X}^-} = \frac{q^*_{\mathrm{AX}}}{T} + S_{\mathrm{AX}} \tag{14.36}$$

The transported entropies are large; they sum to a value equal to or near the thermodynamic entropy of the electrolyte they derive from.

In the preceeding sections, we saw that the transported entropy of the ion that enters the reversible electrode reaction is remarkably unaffected by the composition of the electrolyte. Similar results have been reported in the literature. Grimstvedt *et al.* [197] found that the transported entropy of silver ion was constant for a wide range of compositions in a cell with silver electrodes and an electrolyte mixture of Ag_2SO_4 and Li_2SO_4. The values did not depend on the state of the electrolyte, whether it was liquid

or solid (hexagonal or cubic), as long as the Li^+-concentration was not too high. Richter *et al.* [199,200] reported similar results for silver nitrate melts, and Ratkje and Tomii [201] found that $S^*_{O^{2-}}$ was the same in a cell with oxygen electrodes and tetragonal or cubic structures of yttria stabilized zirconia. Why is the transported entropy for the ion that is involved in the electrode reaction so constant? Is the transported entropy a property of the electrode surface, rather than of the electrolyte? The relations that arise from the invariance of the heat flux to the frame of reference indicate that the transported entropy is determined largely by the discontinuity in the charge carrier at the electrode interface [80, 197].

Remark 14.1. *The entropies of the components are thermodynamic quantities which depend on the temperature and composition only. The transported entropies depend also on the heats of transfer and on the electrodes that are used in the cell.*

The heat of transfer in a one-component system is zero, but in a two-component system like Na in Hg, we had

$$q^*_{Na} = -TS_{Na} \tag{14.37}$$

The same relation was obtained for the heat of transfer of water in Nafion 117 (the fuel cell model in Chapter 19):

$$q^*_w = -TS_w \tag{14.38}$$

These relations, which apply to the homogeneous phase, allocate rather large values to the heats of transfer.

14.6 Concluding comments

The transported entropy of an ion is large [189, 202, 203]; the same order of magnitude as the entropy of the compound it derives from. The single electrode Peltier heat is seldom of a comparable magnitude [197,204,205], as the single electrode Peltier heat contains differences of transported entropies and thermodynamic entropies. Single electrode heat effects were estimated by Xu *et al.* [204].

The Peltier heats of two electrodes combine for isothermal conditions to the reaction entropy of a cell [27]. Transported entropies cancel in such a combination, as required from a thermodynamic analysis of the whole cell. Cells with identical electrodes are not efficient as thermoelectric generators for this reason. When two identical electrodes are used to make an electrochemical cell, the cell entropy change is small, and the Seebeck effect is small.

This may change in a formation cell, which has different electrodes. The reaction entropy can be large in a formation cell. When the reaction entropy is negative, as in a fuel cell that runs on hydrogen and oxygen, heat is released in the surroundings during operation. When the reaction entropy is positive, the cell can convert heat into electric energy and be used as a thermoelectric convertor. This is the case for certain fuel cells operating on carbon [206]. The aluminium electrolysis cell is another example where electrolyte excess heat is beneficial for the energy conversion [28, 80, 207, 208]. Under (hypothetical) reversible conditions, the conversion from heat to electric energy is 100% [209] in cells with a positive entropy of reaction. This gives an argument for linking such electrochemical processes to sources of waste heat.

This page intentionally left blank

Chapter 15

Adiabatic Electrode Reactions

We describe energy conversion during synthesis or removal of solid AgCl on a silver electrode in an adiabatic cell. Equations describing the temperature and electric potential profiles across the heterogeneous system are given. These make it possible to calculate, for instance, the surface temperature at the site of the electrode reaction.

We have seen in earlier chapters that non-equilibrium thermodynamics gives detailed information about the origin and magnitude of all contributions to the electric potential of a cell. The aim of this chapter is to find the temperature and electric potential profiles across a cell when the reaction rate or the current density is sizeable. The temperature and electric potential profiles were determined in Chapter 13 without active use of the energy balances. In this chapter, we shall include these balances in the solutions. To illustrate the procedure, we give the solutions for a well-known system. The results can be used to answer questions like: How can we find the potential profile that arises from the formation of a compound at the surface between two homogeneous phases? What is the surface temperature during transport of charge? Such questions may be of interest in electrochemical synthesis, where the conditions for synthesis of new compounds are important [210, 211]. As usual, we consider only stationary state conditions.

The example chosen to illustrate the solution procedure uses silver-silver chloride electrodes. The electrodes have adjacent layers of solid Ag and AgCl, with AgCl in contact with an aqueous solution of MCl. Here M is either an alkali metal or hydrogen:

$$T^{\mathrm{l}},\ \mathrm{Ag(s)} \mid \mathrm{AgCl(s)} \mid \mathrm{MCl(aq)} \mid \mathrm{AgCl(s)} \mid \mathrm{Ag(s)}, T^{\mathrm{r}} \tag{15.1}$$

The electrolyte MCl is completely dissociated. A concentration gradient of MCl arises in the temperature gradient. There are five homogeneous regions

in the cell. They are denoted (l), (a), (e), (c) and (r), respectively. The four interfaces are denoted (s,l), (s,a), (s,c) and (s,r). Silver is connected to an external circuit. The temperatures of the silver are T^{l} (on the left hand side) and T^{r} (on the right hand side). The heterogeneous conductor is otherwise adiabatic.

Electrons conduct charge in the metal phases, and experiments have shown that Ag^+ conducts charge in AgCl. The splitting of atomic silver to the ion and electron (or the reverse reaction) takes place at the interfaces (s,l) and (s,r), between Ag and AgCl. Formation (or removal) of AgCl from Ag^+ and Cl^- takes place at the interfaces (s,a) and (s,c) near the electrolyte. This event is the focus of interest.

All surfaces move with a velocity proportional to the electric current with respect to the wall. The surfaces (s,l) and (s,r) move to the left, while the surfaces (s,a) and (s,c) move to the right when the electric current is positive. The silver does not move with respect to the wall. We shall not need these velocities, and avoid having to deal with the volume change of the reaction by describing all phenomena in the surface frame of reference, as discussed in Chapter 5.

15.1 The homogeneous phases

15.1.1 *The silver phases*

We have already set the temperature in the silver phases constant. The only product in the entropy production is then the electric force times the flux. The electric potential difference across the silver is

$$\frac{\partial \phi}{\partial x} = -rj \tag{15.2}$$

15.1.2 *The silver chloride phases*

The entropy production of the silver chloride phases has two terms;

$$\sigma = J'_q \frac{\partial}{\partial x}\left(\frac{1}{T}\right) + j\left(-\frac{1}{T}\frac{\partial \phi}{\partial x}\right) \tag{15.3}$$

The flux equations to be solved in this phase are therefore:

$$\begin{aligned} J'_q &= -\lambda \frac{\partial T}{\partial x} + \pi \frac{j}{F} \\ \frac{\partial \phi}{\partial x} &= -\frac{\pi}{FT}\frac{\partial T}{\partial x} - rj \end{aligned} \tag{15.4}$$

The Peltier coefficient in silver chloride is given by the transported entropy of the silver ions:

$$\pi^{\mathrm{a}} = \pi^{\mathrm{c}} = T S^*_{\mathrm{Ag}^+} \tag{15.5}$$

15.1.3 *The electrolyte*

The electrolyte can transport heat, mass and charge. The entropy production is

$$\sigma = J'_q \frac{\partial}{\partial x}\left(\frac{1}{T}\right) + J_{\mathrm{MCl}}\left(-\frac{1}{T}\frac{\partial \mu_{\mathrm{MCl},T}}{\partial x}\right) + j\left(-\frac{1}{T}\frac{\partial \phi}{\partial x}\right) \tag{15.6}$$

In the stationary state, $J_{\mathrm{MCl}} = 0$. The entropy production and the flux equations then take the form given in Eqs. (15.3) and (15.4). Only chloride ions carry charge, so that the Peltier coefficient of the electrolyte is given by

$$\pi^{\mathrm{e}} = -T S^*_{\mathrm{Cl}^-} \tag{15.7}$$

15.2 The interfaces

15.2.1 *The silver-silver chloride interfaces*

On the anode side, silver reacts to give silver ion and electron between the pure phases of silver and silver chloride:

$$\mathrm{Ag} \;\rightarrow \mathrm{Ag}^+ + \mathrm{e}^- \tag{15.8}$$

The opposite reaction takes place on the cathode side. The contribution to the reaction Gibbs energy due to the neutral component silver is

$$\Delta_n G^{\mathrm{s,l}} = -\mu^{\mathrm{l,a}}_{\mathrm{Ag}}\left(T^{\mathrm{s,l}}\right) = -\mu^{\mathrm{l,a}}_{\mathrm{Ag}}\left(T^{\mathrm{l}}\right) + S^{\mathrm{l,a}}_{\mathrm{Ag}}\Delta_{\mathrm{l,s}}T \tag{15.9}$$

The reaction rate is proportional to the current density, $r^{\mathrm{s,l}} = j/F$. The entropy production for the surface between the silver and silver chloride layers is

$$\sigma^{\mathrm{s,l}} = J'^{\mathrm{l,a}}_q \Delta_{\mathrm{l,s}}\left(\frac{1}{T}\right) + J'^{\mathrm{a,l}}_q \Delta_{\mathrm{s,a}}\left(\frac{1}{T}\right) - j\frac{1}{T^{\mathrm{s,l}}}\left[\Delta_{\mathrm{l,a}}\phi + \frac{1}{F}\Delta_n G^{\mathrm{s,l}}\right] \tag{15.10}$$

These fluxes are all independent of the frame of reference. The temperature of the silver close to the silver chloride is $T^{\mathrm{l,a}}$. On the surface it is $T^{\mathrm{s,l}}$, and on the other side of the surface in the silver chloride it is $T^{\mathrm{a,l}}$. Similar to the procedure in Sec. 13.2 we decouple the heat fluxes on both sides of the

surface. The heat fluxes and the potential difference can then be written as

$$
\begin{aligned}
J_q'^{\mathrm{l,a}} &= -\lambda_{\mathrm{l}}^{\mathrm{s,l}} \Delta_{\mathrm{l,s}} T + \pi^{\mathrm{l,a}} \frac{j}{F} \\
J_q'^{\mathrm{a,l}} &= -\lambda_{\mathrm{a}}^{\mathrm{s,l}} \Delta_{\mathrm{s,a}} T + \pi^{\mathrm{a,l}} \frac{j}{F} \\
\Delta_{\mathrm{l,a}}\phi + \frac{1}{F}\Delta_n G^{\mathrm{s,l}} &= -\frac{\pi^{\mathrm{l,a}}}{FT^{\mathrm{l}}} \Delta_{\mathrm{l,s}} T - \frac{\pi^{\mathrm{a,l}}}{FT^{\mathrm{a,l}}} \Delta_{\mathrm{s,a}} T - r^{\mathrm{s,l}} j
\end{aligned}
\tag{15.11}
$$

Solving for the temperature differences and introducing Eq. (15.9) into Eq. (15.11) we find

$$
\begin{aligned}
\Delta_{\mathrm{l,s}} T &= -\frac{1}{\lambda_{\mathrm{l}}^{\mathrm{s,l}}} \left(J_q'^{\mathrm{l,a}} - \pi^{\mathrm{l,a}} \frac{j}{F} \right) \\
\Delta_{\mathrm{s,a}} T &= -\frac{1}{\lambda_{\mathrm{a}}^{\mathrm{s,l}}} \left(J_q'^{\mathrm{a,l}} - \pi^{\mathrm{a,l}} \frac{j}{F} \right) \\
\Delta_{\mathrm{l,a}}\phi - \frac{1}{F}\mu_{\mathrm{Ag}}^{\mathrm{l,a}} &= \frac{1}{F}\left(S_{\mathrm{e^-}}^* - S_{\mathrm{Ag}}^{\mathrm{l,a}} \right) \Delta_{\mathrm{l,s}} T - \frac{1}{F} S_{\mathrm{Ag^+}}^* \Delta_{\mathrm{s,a}} T - r^{\mathrm{s,l}} j
\end{aligned}
\tag{15.12}
$$

where the Peltier coefficients are

$$
\begin{aligned}
\pi^{\mathrm{l,a}} &\equiv F \left(\frac{J_q'^{\mathrm{l,a}}}{j} \right)_{\Delta_{\mathrm{l,s}} T = 0} = -T^{\mathrm{l}} S_{\mathrm{e^-}}^* \\
\pi^{\mathrm{a,l}} &\equiv F \left(\frac{J_q'^{\mathrm{a,l}}}{j} \right)_{\Delta_{\mathrm{s,a}} T = 0} = T^{\mathrm{a,l}} S_{\mathrm{Ag^+}}^*
\end{aligned}
\tag{15.13}
$$

Here $S_{\mathrm{e^-}}^*$ and $S_{\mathrm{Ag^+}}^*$ are the transported entropies in the silver and the silver chloride. These coefficients are the same as in the homogeneous phases.

The equations for the silver chloride-silver interface on the cathode side are, analogously,

$$
\begin{aligned}
\Delta_{\mathrm{c,s}} T &= -\frac{1}{\lambda_{\mathrm{c}}^{\mathrm{s,r}}} \left(J_q'^{\mathrm{c,r}} - \pi^{\mathrm{c,r}} \frac{j}{F} \right) \\
\Delta_{\mathrm{s,r}} T &= -\frac{1}{\lambda_{\mathrm{r}}^{\mathrm{s,r}}} \left(J_q'^{\mathrm{r,c}} - \pi^{\mathrm{r,c}} \frac{j}{F} \right) \\
\Delta_{\mathrm{c,r}}\phi + \frac{1}{F}\mu_{\mathrm{Ag}}^{\mathrm{r,c}} &= -\frac{1}{F} S_{\mathrm{Ag^+}}^* \Delta_{\mathrm{c,s}} T + \frac{1}{F}\left(S_{\mathrm{e^-}}^* - S_{\mathrm{Ag}}^{\mathrm{r,c}} \right) \Delta_{\mathrm{s,r}} T - r^{\mathrm{s,r}} j
\end{aligned}
\tag{15.14}
$$

with the Peltier coefficients

$$\begin{aligned}\pi^{\mathrm{c,r}} &\equiv F\left(\frac{J_q'^{\mathrm{c,r}}}{j}\right)_{\Delta_{\mathrm{c,s}}T=0} = T^{\mathrm{c,r}}S^*_{\mathrm{Ag^+}}\\ \pi^{\mathrm{r,c}} &\equiv F\left(\frac{J_q'^{\mathrm{r,c}}}{j}\right)_{\Delta_{\mathrm{s,a}}T=0} = -T^{\mathrm{r}}S^*_{\mathrm{e^-}}\end{aligned} \tag{15.15}$$

These coefficients are the same as those given by Eq. (15.13) when the temperatures are the same.

15.2.2 *The silver chloride-electrolyte interfaces*

The reaction, which takes place in the interface between silver chloride and the electrolyte on the anode side, is

$$\mathrm{Ag^+ + Cl^-} \rightarrow \mathrm{AgCl} \tag{15.16}$$

The opposite reaction takes place on the cathode side. The contribution to the reaction Gibbs energy due to the neutral component AgCl, is

$$\Delta_n G^{\mathrm{s,a}} = \mu^{\mathrm{a,e}}_{\mathrm{AgCl}}\left(T^{\mathrm{s,a}}\right) = \mu^{\mathrm{a,e}}_{\mathrm{AgCl}}\left(T^{\mathrm{a,e}}\right) - S^{\mathrm{a,e}}_{\mathrm{AgCl}}\Delta_{\mathrm{a,s}}T \tag{15.17}$$

The reaction rate is proportional to the current density, $r^{\mathrm{s,a}} = j/F$. The entropy production of the surface is

$$\sigma^{\mathrm{s,a}} = J_q'^{\mathrm{a,e}}\Delta_{\mathrm{a,s}}\left(\frac{1}{T}\right) + J_q'^{\mathrm{e,a}}\Delta_{\mathrm{s,e}}\left(\frac{1}{T}\right) - j\frac{1}{T^{\mathrm{s,a}}}\left[\Delta_{\mathrm{a,e}}\phi + \frac{1}{F}\Delta_n G^{\mathrm{s,a}}\right] \tag{15.18}$$

The flux equations are

$$\begin{aligned}J_q'^{\mathrm{a,e}} &= -\lambda^{\mathrm{s,a}}_{\mathrm{a}}\Delta_{\mathrm{a,s}}T + \pi^{\mathrm{a,e}}\frac{j}{F}\\ J_q'^{\mathrm{e,a}} &= -\lambda^{\mathrm{s,a}}_{\mathrm{e}}\Delta_{\mathrm{s,e}}T + \pi^{\mathrm{e,a}}\frac{j}{F}\\ \Delta_{\mathrm{a,e}}\phi + \frac{1}{F}\Delta_n G^{\mathrm{s,a}} &= -\frac{\pi^{\mathrm{a,e}}}{FT^{\mathrm{a,e}}}\Delta_{\mathrm{a,s}}T - \frac{\pi^{\mathrm{e,a}}}{FT^{\mathrm{e,a}}}\Delta_{\mathrm{s,e}}T - r^{\mathrm{s,a}}j\end{aligned} \tag{15.19}$$

The Peltier coefficients are (see also below)

$$\begin{aligned}\pi^{\mathrm{a,e}} &\equiv F\left(\frac{J'^{\mathrm{a,e}}_q}{j}\right)_{\Delta_{\mathrm{a,s}}T=0} = T^{\mathrm{a,e}}S^*_{\mathrm{Ag^+}}\\ \pi^{\mathrm{e,a}} &\equiv F\left(\frac{J'^{\mathrm{e,a}}_q}{j}\right)_{\Delta_{\mathrm{s,e}}T=0} = -T^{\mathrm{e,a}}S^*_{\mathrm{Cl^-}}\end{aligned} \tag{15.20}$$

Using Eqs. (15.17) and (15.20) one may write Eq. (15.19) as

$$\begin{aligned}\Delta_{\mathrm{a,s}}T &= -\frac{1}{\lambda^{\mathrm{s,a}}_{\mathrm{a}}}\left(J'^{\mathrm{a,e}}_q - \pi^{\mathrm{a,e}}\frac{j}{F}\right)\\ \Delta_{\mathrm{s,e}}T &= -\frac{1}{\lambda^{\mathrm{s,a}}_{\mathrm{e}}}\left(J'^{\mathrm{e,a}}_q - \pi^{\mathrm{e,a}}\frac{j}{F}\right)\end{aligned} \tag{15.21}$$

$$\Delta_{\mathrm{a,e}}\phi + \frac{1}{F}\mu^{\mathrm{a,e}}_{\mathrm{AgCl}} = -\frac{1}{F}\left(S^*_{\mathrm{Ag^+}} - S^{\mathrm{a,e}}_{\mathrm{AgCl}}\right)\Delta_{\mathrm{a,s}}T + \frac{1}{F}S^*_{\mathrm{Cl^-}}\Delta_{\mathrm{s,e}}T - r^{\mathrm{s,a}}j$$

For the surface between the aqueous electrolyte, and the silver chloride on the cathode side, we obtain similarly

$$\begin{aligned}\Delta_{\mathrm{e,s}}T &= -\frac{1}{\lambda^{\mathrm{s,c}}_{\mathrm{e}}}\left(J'^{\mathrm{e,c}}_q - \pi^{\mathrm{e,c}}\frac{j}{F}\right)\\ \Delta_{\mathrm{s,c}}T &= -\frac{1}{\lambda^{\mathrm{s,c}}_{\mathrm{c}}}\left(J'^{\mathrm{c,e}}_q - \pi^{\mathrm{c,e}}\frac{j}{F}\right)\end{aligned} \tag{15.22}$$

$$\Delta_{\mathrm{e,c}}\phi - \frac{1}{F}\mu^{\mathrm{c,e}}_{\mathrm{AgCl}} = \frac{1}{F}S^*_{\mathrm{Cl^-}}\Delta_{\mathrm{e,s}}T - \frac{1}{F}\left(S^*_{\mathrm{Ag^+}} - S^{\mathrm{c,e}}_{\mathrm{AgCl}}\right)\Delta_{\mathrm{s,c}}T - r^{\mathrm{s,c}}j$$

where the Peltier coefficients are given by

$$\begin{aligned}\pi^{\mathrm{e,c}} &\equiv F\left(\frac{J'^{\mathrm{e,c}}_q}{j}\right)_{\Delta_{\mathrm{e,s}}T=0} = -T^{\mathrm{e,c}}S^*_{\mathrm{Cl^-}}\\ \pi^{\mathrm{c,e}} &\equiv F\left(\frac{J'^{\mathrm{c,e}}_q}{j}\right)_{\Delta_{\mathrm{s,c}}T=0} = T^{\mathrm{c,e}}S^*_{\mathrm{Ag^+}}\end{aligned} \tag{15.23}$$

15.3 Temperature and electric potential profiles

Consider now the total cell. The silver phases have temperatures T^{l} and T^{r}. Between these phases the system is adiabatic. We pass a finite

electric current through the cell, and shall find a solution for the temperature and electric potential profiles. We assume that the system is close to global equilibrium at the temperature T_{eq}. This makes it possible to find an analytic solution. It implies that we can use values of enthalpies, entropies, transported entropies, Peltier coefficients, thermal conductivities and resistivities at this temperature in the various equations. We neglect contributions higher than linear order in their deviation from global equilibrium. Farther away from equilibrium the equations must usually be solved numerically.

Integrating Eq. (15.2) in the anode and cathode silver layers, one obtains

$$\Delta_{\mathrm{l}}\phi = -r^{\mathrm{l}} d^{\mathrm{l}} j \quad \text{and} \quad \Delta_{\mathrm{r}}\phi = -r^{\mathrm{r}} d^{\mathrm{r}} j \tag{15.24}$$

where d^{l} and d^{r} are the silver layer thicknesses. These thicknesses depend on the time and in that sense the solution is only quasi-stationary. For the stationary conditions considered $d^{\mathrm{l}}+d^{\mathrm{r}}$ is independent of the time, however. The resistivities have their equilibrium value, so that $r^{\mathrm{l}} = r^{\mathrm{r}}$. The total potential difference across the silver layers is therefore independent of the time if the system is close to global equilibrium.

In the stationary state, the energy flux J_u (cf. Eq. (4.16)) is everywhere constant. The energy flux on the left side of a surface is therefore equal to the energy flux on the right side. The energy flux is the sum of the measurable heat flux, the comoving enthalpy and the electric potential energy carried along by the electric current. The energy flux depends on the frame of reference. We choose the surface as the frame of reference. For the silver-silver chloride surface on the anode side this gives

$$J_u = J_q'^{\mathrm{l,a}} + H_{\mathrm{Ag}} J^{\mathrm{l}}_{\mathrm{Ag}} + \phi^{\mathrm{l,a}} j = J_q'^{\mathrm{a,l}} + \phi^{\mathrm{a,l}} j \tag{15.25}$$

As all the fluxes are of the first order, we may use the zeroth order value of the electric potential difference, $\Delta_{\mathrm{l,a}}\phi = \mu^{\mathrm{l,a}}_{\mathrm{Ag}}(T_{eq})/F$, in this expression, cf. Eq. (15.12). For the enthalpy of the silver we should similarly take the value at the equilibrium temperature. This gives

$$\begin{aligned} J_q'^{\mathrm{l,a}} + H_{\mathrm{Ag}} J^{\mathrm{l}}_{\mathrm{Ag}} &= J_q'^{\mathrm{a,l}} + \mu^{\mathrm{l,a}}_{\mathrm{Ag}}(T_{eq})\,\frac{j}{F} \to J_q'^{\mathrm{l,a}} + T_{eq} S_{\mathrm{Ag}} \frac{j}{F} \\ &= J_q'^{\mathrm{a,l}} \end{aligned} \tag{15.26}$$

where we used $J^{\mathrm{l}}_{\mathrm{Ag}} = j/F$. With Eqs. (15.12) and (15.13) we obtain the

temperature and potential difference across the surface

$$\begin{aligned}
\Delta_{\mathrm{l,a}}T &= -\left(\frac{1}{\lambda_{\mathrm{l}}^{\mathrm{s,l}}}+\frac{1}{\lambda_{\mathrm{a}}^{\mathrm{s,l}}}\right)J_q'^{\mathrm{l,a}} - T_{eq}\left[\frac{S_{\mathrm{e}^-}^*}{\lambda_{\mathrm{l}}^{\mathrm{s,l}}}+\frac{S_{\mathrm{Ag}}-S_{\mathrm{Ag}^+}^*}{\lambda_{\mathrm{a}}^{\mathrm{s,l}}}\right]\frac{j}{F} \\
F\Delta_{\mathrm{l,a}}\phi &= \mu_{\mathrm{Ag}}^{\mathrm{l,a}} + \left[\frac{S_{\mathrm{Ag}}-S_{\mathrm{e}^-}^*}{\lambda_{\mathrm{l}}^{\mathrm{s,l}}}+\frac{S_{\mathrm{Ag}^+}^*}{\lambda_{\mathrm{a}}^{\mathrm{s,l}}}\right]J_q'^{\mathrm{l,a}} \\
&\quad - T_{eq}\left[\frac{S_{\mathrm{e}^-}^*}{\lambda_{\mathrm{l}}^{\mathrm{s,l}}}\left(S_{\mathrm{e}^-}^*-S_{\mathrm{Ag}}\right)-\frac{S_{\mathrm{Ag}^+}^*}{\lambda_{\mathrm{a}}^{\mathrm{s,l}}}\left(S_{\mathrm{Ag}}-S_{\mathrm{Ag}^+}^*\right)\right]\frac{j}{F} - Fr^{\mathrm{s,l}}j
\end{aligned} \tag{15.27}$$

The chemical potential in Eq. (15.27b) does not have the equilibrium value, however. For the conditions used, it follows that the measurable heat fluxes are constant in the homogeneous phases. At the interface, they jump, and so do the temperature and the electric potential. The jumps may be positive or negative depending on the coefficients and on the current density used.

In the silver chloride on the anode side, Eqs. (15.4) and (15.5) give to linear order

$$\begin{aligned}
\Delta_{\mathrm{a}}T &= -\frac{1}{\lambda^{\mathrm{a}}}\left(J_q'^{\mathrm{a}} - T_{eq}S_{\mathrm{Ag}^+}^*\frac{j}{F}\right)d^{\mathrm{a}} \\
\Delta_{\mathrm{a}}\phi &= -\frac{1}{F}S_{\mathrm{Ag}^+}^*\Delta_{\mathrm{a}}T - r^{\mathrm{a}}d^{\mathrm{a}}j
\end{aligned} \tag{15.28}$$

where we used the fact that in a stationary state the heat flux is independent of the position. The thermal conductivity, the electric resistivity and the transported entropy have their equilibrium values. Furthermore, d^{a} is the thickness of the silver chloride layer on the anode silver. This thickness depends on the time and in that sense the solution is only quasi-stationary. Using Eq. (15.26) it follows that

$$\begin{aligned}
\Delta_{\mathrm{a}}T &= -\frac{1}{\lambda^{\mathrm{a}}}\left[J_q'^{\mathrm{l,a}} + T_{eq}\left(S_{\mathrm{Ag}}-S_{\mathrm{Ag}^+}^*\right)\frac{j}{F}\right]d^{\mathrm{a}} \\
F\Delta_{\mathrm{a}}\phi &= \frac{1}{\lambda^{\mathrm{a}}}S_{\mathrm{Ag}^+}^*\left[J_q'^{\mathrm{l,a}} + T_{eq}\left(S_{\mathrm{Ag}}-S_{\mathrm{Ag}^+}^*\right)\frac{j}{F}\right]d^{\mathrm{a}} - Fr^{\mathrm{a}}d^{\mathrm{a}}j
\end{aligned} \tag{15.29}$$

At the surface between the silver chloride and the electrolyte, we have

$$J_q'^{\mathrm{a}} + H_{\mathrm{AgCl}}J_{\mathrm{AgCl}}^{\mathrm{a}} + \phi^{\mathrm{a,e}}j = J_q'^{\mathrm{e}} + \phi^{\mathrm{e,a}}j \tag{15.30}$$

To first order in the deviation from equilibrium, we obtain

$$J_q'^{\mathrm{a}} + H_{\mathrm{AgCl}} J^{\mathrm{a}}_{\mathrm{AgCl}} = J_q'^{\mathrm{e}} - \mu^{\mathrm{a,e}}_{\mathrm{AgCl}} \frac{j}{F} \rightarrow J_q'^{\mathrm{l,a}} + T_{eq} \left(S_{\mathrm{Ag}} - S_{\mathrm{AgCl}} \right) \frac{j}{F} = J_q'^{\mathrm{e}} \tag{15.31}$$

where we used $J^{\mathrm{a}}_{\mathrm{AgCl}} = -j/F$. Together with Eqs. (15.18), (15.20) and (15.21) this gives

$$\begin{aligned}
\Delta_{\mathrm{a,e}} T = & - \left(\frac{1}{\lambda^{\mathrm{s,a}}_{\mathrm{a}}} + \frac{1}{\lambda^{\mathrm{s,a}}_{\mathrm{e}}} \right) J_q'^{\mathrm{l,a}} \\
& - T_{eq} \left[\frac{1}{\lambda^{\mathrm{s,a}}_{\mathrm{a}}} \left(S_{\mathrm{Ag}} - S^*_{\mathrm{Ag^+}} \right) + \frac{1}{\lambda^{\mathrm{s,a}}_{\mathrm{e}}} \left(S_{\mathrm{Ag}} - S_{\mathrm{AgCl}} + S^*_{\mathrm{Cl^-}} \right) \right] \frac{j}{F} \\
F \Delta_{\mathrm{a,e}} \phi = & - \mu^{\mathrm{a,e}}_{\mathrm{AgCl}} + \left[\frac{1}{\lambda^{\mathrm{s,a}}_{\mathrm{a}}} \left(S^*_{\mathrm{Ag^+}} - S_{\mathrm{AgCl}} \right) - \frac{1}{\lambda^{\mathrm{s,a}}_{\mathrm{e}}} S^*_{\mathrm{Cl^-}} \right] J_q'^{\mathrm{l,a}} - F r^{\mathrm{s,a}} j \\
& + T_{eq} \left[\frac{1}{\lambda^{\mathrm{s,a}}_{\mathrm{a}}} \left(S^*_{\mathrm{Ag^+}} - S_{\mathrm{AgCl}} \right) \left(S_{\mathrm{Ag}} - S^*_{\mathrm{Ag^+}} \right) \right. \\
& \left. - \frac{1}{\lambda^{\mathrm{s,a}}_{\mathrm{e}}} S^*_{\mathrm{Cl^-}} \left(S_{\mathrm{Ag}} - S_{\mathrm{AgCl}} + S^*_{\mathrm{Cl^-}} \right) \right] \frac{j}{F}
\end{aligned} \tag{15.32}$$

In the electrolyte, Eq. (15.4) in an analogous way gives

$$\begin{aligned}
\Delta_{\mathrm{e}} T &= - \frac{1}{\lambda^{\mathrm{e}}} \left(J_q'^{\mathrm{e}} + T_{eq} S^*_{\mathrm{Cl^-}} \frac{j}{F} \right) d^{\mathrm{e}} \\
\Delta_{\mathrm{e}} \phi &= \frac{1}{F} S^*_{\mathrm{Cl^-}} \Delta_{\mathrm{e}} T - r^{\mathrm{e}} d^{\mathrm{e}} j
\end{aligned} \tag{15.33}$$

where we used the fact that in a stationary state the heat flux is independent of the position. The thickness of the electrolyte layer d^{e} is independent of the time. Together with Eq. (15.31), this results in

$$\begin{aligned}
\Delta_{\mathrm{e}} T &= - \frac{1}{\lambda^{\mathrm{e}}} \left(J_q'^{\mathrm{l,a}} + T_{eq} \left(S_{\mathrm{Ag}} - S_{\mathrm{AgCl}} + S^*_{\mathrm{Cl^-}} \right) \frac{j}{F} \right) d^{\mathrm{e}} \\
F \Delta_{\mathrm{e}} \phi &= - \frac{1}{\lambda^{\mathrm{e}}} S^*_{\mathrm{Cl^-}} \left(J_q'^{\mathrm{l,a}} + T_{eq} \left(S_{\mathrm{Ag}} - S_{\mathrm{AgCl}} + S^*_{\mathrm{Cl^-}} \right) \frac{j}{F} \right) d^{\mathrm{e}} - F r^{\mathrm{e}} d^{\mathrm{e}} j
\end{aligned} \tag{15.34}$$

At the surface between the electrolyte and the silver chloride, we have

$$J_q'^{\mathrm{e}} + \phi^{\mathrm{e,c}} j = J_q'^{\mathrm{c}} + H_{\mathrm{AgCl}} J^{\mathrm{c}}_{\mathrm{AgCl}} + \phi^{\mathrm{c,e}} j \tag{15.35}$$

To first order in the electric current, we may use the zeroth order value of the electric potential difference in this expression. This gives

$$J_q'^{\mathrm{e}} = J_q'^{\mathrm{c}} + H_{\mathrm{AgCl}} J^{\mathrm{c}}_{\mathrm{AgCl}} + \mu^{\mathrm{a,e}}_{\mathrm{AgCl}} \frac{j}{F} \to J_q'^{\mathrm{l,a}} + T_{eq} S_{\mathrm{Ag}} \frac{j}{F} = J_q'^{\mathrm{c}} \qquad (15.36)$$

where we used $J^{\mathrm{c}}_{\mathrm{AgCl}} = -j/F$. Together with Eqs. (15.23) and (15.23), this gives

$$\begin{aligned}
\Delta_{\mathrm{e,c}} T &= -\left(\frac{1}{\lambda^{\mathrm{s,c}}_{\mathrm{e}}} + \frac{1}{\lambda^{\mathrm{s,c}}_{\mathrm{c}}} \right) J_q'^{\mathrm{l,a}} \\
&\quad - T_{eq} \left[\frac{1}{\lambda^{\mathrm{s,c}}_{\mathrm{e}}} \left(S_{\mathrm{Ag}} - S_{\mathrm{AgCl}} + S^*_{\mathrm{Cl^-}} \right) + \frac{1}{\lambda^{\mathrm{s,c}}_{\mathrm{c}}} \left(S_{\mathrm{Ag}} - S^*_{\mathrm{Ag^+}} \right) \right] \frac{j}{F} \\
F \Delta_{\mathrm{e,c}} \phi &= \mu^{\mathrm{c,e}}_{\mathrm{AgCl}} - \left(\frac{S^*_{\mathrm{Cl^-}}}{\lambda^{\mathrm{s,c}}_{\mathrm{e}}} - \frac{S^*_{\mathrm{Ag^+}} - S_{\mathrm{AgCl}}}{\lambda^{\mathrm{s,c}}_{\mathrm{c}}} \right) J_q'^{\mathrm{l,a}} - F r^{\mathrm{s,c}} j \\
&\quad - T_{eq} \left[\frac{S^*_{\mathrm{Cl^-}}}{\lambda^{\mathrm{s,c}}_{\mathrm{e}}} \left(S_{\mathrm{Ag}} - S_{\mathrm{AgCl}} + S^*_{\mathrm{Cl^-}} \right) \right. \\
&\quad \left. - \frac{S^*_{\mathrm{Ag^+}} - S_{\mathrm{AgCl}}}{\lambda^{\mathrm{s,c}}_{\mathrm{c}}} \left(S_{\mathrm{Ag}} - S^*_{\mathrm{Ag^+}} \right) \right] \frac{j}{F}
\end{aligned} \qquad (15.37)$$

In the silver chloride layer on the cathode side, Eqs. (15.4) and (15.5) give

$$\begin{aligned}
\Delta_{\mathrm{c}} T &= -\frac{1}{\lambda^{\mathrm{c}}} \left(J_q'^{\mathrm{c}} - T_{eq} S^*_{\mathrm{Ag^+}} \frac{j}{F} \right) d^{\mathrm{c}} \\
\Delta_{\mathrm{c}} \phi &= -\frac{1}{F} S^*_{\mathrm{Ag^+}} \Delta_{\mathrm{c}} T - r^{\mathrm{c}} d^{\mathrm{c}} j
\end{aligned} \qquad (15.38)$$

The heat flux in the silver chloride is constant. Furthermore, d^{c} is the thickness of the silver chloride layer on the anode silver. This thickness depends on the time and in that sense the solution is only quasi-stationary. The total thickness of the silver chloride layers, $d^{\mathrm{a}} + d^{\mathrm{c}}$, is however independent of the time. The resistivities have their equilibrium value, so that $r^{\mathrm{a}} = r^{\mathrm{c}}$. The total potential difference due to the resistivity across the silver chloride layers is therefore independent of the time, if the system is close to global equilibrium. Using Eq. (15.36), it follows that

$$\begin{aligned}
\Delta_{\mathrm{c}} T &= -\frac{1}{\lambda^{\mathrm{c}}} \left(J_q'^{\mathrm{l,a}} + T_{eq} \left(S_{\mathrm{Ag}} - S^*_{\mathrm{Ag^+}} \right) \frac{j}{F} \right) d^{\mathrm{c}} \\
F \Delta_{\mathrm{c}} \phi &= \frac{1}{\lambda^{\mathrm{c}}} S^*_{\mathrm{Ag^+}} \left(J_q'^{\mathrm{l,a}} + T_{eq} \left(S_{\mathrm{Ag}} - S^*_{\mathrm{Ag^+}} \right) \frac{j}{F} \right) d^{\mathrm{c}} - F r^{\mathrm{c}} d^{\mathrm{c}} j
\end{aligned} \qquad (15.39)$$

For the silver-silver chloride surface on the cathode side, we have

$$J_q'^{\mathrm{c}} + \phi^{\mathrm{c,r}} j = J_q'^{\mathrm{r,c}} + H_{\mathrm{Ag}} J^{\mathrm{r}}_{\mathrm{Ag}} + \phi^{\mathrm{r,c}} j \tag{15.40}$$

To first order in the electric current, we may use the zeroth order value of the electric potential difference in this expression. This gives

$$J_q'^{\mathrm{c}} = J_q'^{\mathrm{r,c}} + H_{\mathrm{Ag}} J^{\mathrm{r}}_{\mathrm{Ag}} - \mu^{\mathrm{r,c}}_{\mathrm{Ag}} \frac{j}{F} \rightarrow J_q'^{\mathrm{l,a}} = J_q'^{\mathrm{r,c}} \tag{15.41}$$

where we used $J^{\mathrm{r}}_{\mathrm{Ag}} = j/F$. Together with Eqs. (15.14) and (15.15) one obtains, for the temperature and potential difference across the surface,

$$\begin{aligned}
\Delta_{\mathrm{c,r}} T &= -\left(\frac{1}{\lambda^{\mathrm{s,r}}_{\mathrm{c}}} + \frac{1}{\lambda^{\mathrm{s,r}}_{\mathrm{r}}}\right) J_q'^{\mathrm{l,a}} - T_{eq}\left(\frac{S_{\mathrm{Ag}} - S^*_{\mathrm{Ag^+}}}{\lambda^{\mathrm{s,r}}_{\mathrm{c}}} + \frac{S^*_{\mathrm{e^-}}}{\lambda^{\mathrm{s,r}}_{\mathrm{r}}}\right)\frac{j}{F} \\
F\Delta_{\mathrm{c,r}}\phi &= -\mu^{\mathrm{r,c}}_{\mathrm{Ag}} + \left(\frac{S^*_{\mathrm{Ag^+}}}{\lambda^{\mathrm{s,r}}_{\mathrm{c}}} - \frac{S^*_{\mathrm{e^-}} - S_{\mathrm{Ag}}}{\lambda^{\mathrm{s,r}}_{\mathrm{r}}}\right) J_q'^{\mathrm{l,a}} \\
&\quad + T_{eq}\left(\frac{S_{\mathrm{Ag}} - S^*_{\mathrm{Ag^+}}}{\lambda^{\mathrm{s,r}}_{\mathrm{c}}} S^*_{\mathrm{Ag^+}} - \frac{S^*_{\mathrm{e^-}} - S_{\mathrm{Ag}}}{\lambda^{\mathrm{s,r}}_{\mathrm{r}}} S^*_{\mathrm{e^-}}\right)\frac{j}{F} - F r^{\mathrm{s,r}} j
\end{aligned} \tag{15.42}$$

The total temperature difference across the cell is

$$\begin{aligned}
T^{\mathrm{r}} - T^{\mathrm{l}} &= \Delta_{\mathrm{l,a}} T + \Delta_{\mathrm{a}} T + \Delta_{\mathrm{a,e}} T + \Delta_{\mathrm{e}} T + \Delta_{\mathrm{e,c}} T + \Delta_{\mathrm{c}} T + \Delta_{\mathrm{c,r}} T \\
&= -\Bigg(\frac{1}{\lambda^{\mathrm{s,l}}_{\mathrm{l}}} + \frac{1}{\lambda^{\mathrm{s,l}}_{\mathrm{a}}} + \frac{d^{\mathrm{a}}}{\lambda^{\mathrm{a}}} + \frac{1}{\lambda^{\mathrm{s,a}}_{\mathrm{a}}} + \frac{1}{\lambda^{\mathrm{s,a}}_{\mathrm{e}}} + \frac{d^{\mathrm{e}}}{\lambda^{\mathrm{e}}} \\
&\quad + \frac{1}{\lambda^{\mathrm{s,c}}_{\mathrm{e}}} + \frac{1}{\lambda^{\mathrm{s,c}}_{\mathrm{c}}} + \frac{d^{\mathrm{c}}}{\lambda^{\mathrm{c}}} + \frac{1}{\lambda^{\mathrm{s,r}}_{\mathrm{c}}} + \frac{1}{\lambda^{\mathrm{s,r}}_{\mathrm{r}}}\Bigg) J_q'^{\mathrm{l,a}} \\
&\quad - T_{eq}\Bigg[\left(\frac{1}{\lambda^{\mathrm{s,l}}_{\mathrm{a}}} + \frac{1}{\lambda^{\mathrm{s,a}}_{\mathrm{a}}} + \frac{1}{\lambda^{\mathrm{s,c}}_{\mathrm{c}}} + \frac{1}{\lambda^{\mathrm{s,r}}_{\mathrm{c}}}\right)\left(S_{\mathrm{Ag}} - S^*_{\mathrm{Ag^+}}\right) \\
&\quad + \left(\frac{d^{\mathrm{a}}}{\lambda^{\mathrm{a}}} + \frac{d^{\mathrm{c}}}{\lambda^{\mathrm{c}}}\right)\left(S_{\mathrm{Ag}} - S^*_{\mathrm{Ag^+}}\right) + \left(\frac{1}{\lambda^{\mathrm{s,l}}_{\mathrm{l}}} + \frac{1}{\lambda^{\mathrm{s,r}}_{\mathrm{r}}}\right) S^*_{\mathrm{e^-}} + \frac{d^{\mathrm{e}}}{\lambda^{\mathrm{e}}} S^*_{\mathrm{Cl^-}} \\
&\quad + \left(\frac{1}{\lambda^{\mathrm{s,a}}_{\mathrm{e}}} + \frac{1}{\lambda^{\mathrm{s,c}}_{\mathrm{e}}}\right)\left(S_{\mathrm{Ag}} - S_{\mathrm{AgCl}} + S^*_{\mathrm{Cl^-}}\right)\Bigg]\frac{j}{F}
\end{aligned} \tag{15.43}$$

From this equation, we find the heat flux $J_q'^{\mathrm{l,a}}$ in terms of the temperature difference $T^{\mathrm{r}} - T^{\mathrm{l}}$ and the electric current.

The total cell potential can then be found from

$$
\begin{aligned}
F\Delta\phi &= F\left(\Delta_{\mathrm{l}}\phi + \Delta_{\mathrm{l,a}}\phi + \Delta_{\mathrm{a}}\phi + \Delta_{\mathrm{a,e}}\phi + \Delta_{\mathrm{e}}\phi + \Delta_{\mathrm{e,c}}\phi + \Delta_{\mathrm{c}}\phi + \Delta_{\mathrm{c,r}}\phi + \Delta_{\mathrm{r}}\phi\right) \\
&= \mu^{\mathrm{l,a}}_{\mathrm{Ag}} - \mu^{\mathrm{r,c}}_{\mathrm{Ag}} - \mu^{\mathrm{a,e}}_{\mathrm{AgCl}} + \mu^{\mathrm{c,e}}_{\mathrm{AgCl}} + \left[\left(\frac{1}{\lambda^{\mathrm{s,l}}_{\mathrm{l}}} + \frac{1}{\lambda^{\mathrm{s,r}}_{\mathrm{r}}}\right)\left(S_{\mathrm{Ag}} - S^*_{\mathrm{e^-}}\right)\right. \\
&\quad - \left(\frac{1}{\lambda^{\mathrm{s,a}}_{\mathrm{a}}} + \frac{1}{\lambda^{\mathrm{s,c}}_{\mathrm{c}}}\right) S_{\mathrm{AgCl}} + \left(\frac{1}{\lambda^{\mathrm{s,l}}_{\mathrm{a}}} + \frac{d^{\mathrm{a}}}{\lambda^{\mathrm{a}}} + \frac{1}{\lambda^{\mathrm{s,a}}_{\mathrm{a}}} + \frac{1}{\lambda^{\mathrm{s,c}}_{\mathrm{c}}} + \frac{d^{\mathrm{c}}}{\lambda^{\mathrm{c}}} + \frac{1}{\lambda^{\mathrm{s,r}}_{\mathrm{c}}}\right) S^*_{\mathrm{Ag^+}} \\
&\quad \left. - \left(\frac{1}{\lambda^{\mathrm{s,a}}_{\mathrm{e}}} + \frac{d^{\mathrm{e}}}{\lambda^{\mathrm{e}}} + \frac{1}{\lambda^{\mathrm{s,c}}_{\mathrm{e}}}\right) S^*_{\mathrm{Cl^-}}\right] J'^{\mathrm{l,a}}_q - T_{eq}\left[\left(\frac{1}{\lambda^{\mathrm{s,l}}_{\mathrm{l}}} + \frac{1}{\lambda^{\mathrm{s,r}}_{\mathrm{r}}}\right) S^*_{\mathrm{e^-}}\left(S^*_{\mathrm{e^-}} - S_{\mathrm{Ag}}\right)\right. \\
&\quad + \left(\frac{1}{\lambda^{\mathrm{s,a}}_{\mathrm{a}}} + \frac{1}{\lambda^{\mathrm{s,c}}_{\mathrm{c}}}\right)\left(S_{\mathrm{AgCl}} - S^*_{\mathrm{Ag^+}}\right)\left(S_{\mathrm{Ag}} - S^*_{\mathrm{Ag^+}}\right) \\
&\quad - \left(\frac{1}{\lambda^{\mathrm{s,l}}_{\mathrm{a}}} + \frac{d^{\mathrm{a}}}{\lambda^{\mathrm{a}}} + \frac{d^{\mathrm{c}}}{\lambda^{\mathrm{c}}} + \frac{1}{\lambda^{\mathrm{s,r}}_{\mathrm{c}}}\right) S^*_{\mathrm{Ag^+}}\left(S_{\mathrm{Ag}} - S^*_{\mathrm{Ag^+}}\right) \\
&\quad \left. + \left(\frac{1}{\lambda^{\mathrm{s,a}}_{\mathrm{e}}} + \frac{d^{\mathrm{e}}}{\lambda^{\mathrm{e}}} + \frac{1}{\lambda^{\mathrm{s,c}}_{\mathrm{e}}}\right) S^*_{\mathrm{Cl^-}}\left(S_{\mathrm{Ag}} - S_{\mathrm{AgCl}} + S^*_{\mathrm{Cl^-}}\right)\right] \frac{j}{F} \\
&\quad - F\left(r^{\mathrm{l}}d^{\mathrm{l}} + r^{\mathrm{s,l}} + r^{\mathrm{a}}d^{\mathrm{a}} + r^{\mathrm{s,a}} + r^{\mathrm{e}}d^{\mathrm{e}} + r^{\mathrm{s,c}} + r^{\mathrm{c}}d^{\mathrm{c}} + r^{\mathrm{s,r}} + r^{\mathrm{r}}d^{\mathrm{r}}\right) j
\end{aligned}
\tag{15.44}
$$

Using the assumed constant nature of the enthalpies and the entropies this expression can be written as

$$
\begin{aligned}
F\Delta\phi &= (T^{\mathrm{r}} - T^{\mathrm{l}})S_{\mathrm{Ag}} - \left(T^{\mathrm{c,e}} - T^{\mathrm{a,e}}\right) S_{\mathrm{AgCl}} + \left[\left(\frac{1}{\lambda^{\mathrm{s,l}}_{\mathrm{l}}} + \frac{1}{\lambda^{\mathrm{s,r}}_{\mathrm{r}}}\right)\left(S_{\mathrm{Ag}} - S^*_{\mathrm{e^-}}\right)\right. \\
&\quad - \left(\frac{1}{\lambda^{\mathrm{s,a}}_{\mathrm{a}}} + \frac{1}{\lambda^{\mathrm{s,c}}_{\mathrm{c}}}\right) S_{\mathrm{AgCl}} + \left(\frac{1}{\lambda^{\mathrm{s,l}}_{\mathrm{a}}} + \frac{d^{\mathrm{a}}}{\lambda^{\mathrm{a}}} + \frac{1}{\lambda^{\mathrm{s,a}}_{\mathrm{a}}} + \frac{1}{\lambda^{\mathrm{s,c}}_{\mathrm{c}}} + \frac{d^{\mathrm{c}}}{\lambda^{\mathrm{c}}} + \frac{1}{\lambda^{\mathrm{s,r}}_{\mathrm{c}}}\right) S^*_{\mathrm{Ag^+}} \\
&\quad \left. - \left(\frac{1}{\lambda^{\mathrm{s,a}}_{\mathrm{e}}} + \frac{d^{\mathrm{e}}}{\lambda^{\mathrm{e}}} + \frac{1}{\lambda^{\mathrm{s,c}}_{\mathrm{e}}}\right) S^*_{\mathrm{Cl^-}}\right] J'^{\mathrm{l,a}}_q - T_{eq}\left[\left(\frac{1}{\lambda^{\mathrm{s,l}}_{\mathrm{l}}} + \frac{1}{\lambda^{\mathrm{s,r}}_{\mathrm{r}}}\right) S^*_{\mathrm{e^-}}\left(S^*_{\mathrm{e^-}} - S_{\mathrm{Ag}}\right)\right. \\
&\quad + \left(\frac{1}{\lambda^{\mathrm{s,a}}_{\mathrm{a}}} + \frac{1}{\lambda^{\mathrm{s,c}}_{\mathrm{c}}}\right)\left(S_{\mathrm{AgCl}} - S^*_{\mathrm{Ag^+}}\right)\left(S_{\mathrm{Ag}} - S^*_{\mathrm{Ag^+}}\right) \\
&\quad - \left(\frac{1}{\lambda^{\mathrm{s,l}}_{\mathrm{a}}} + \frac{d^{\mathrm{a}}}{\lambda^{\mathrm{a}}} + \frac{d^{\mathrm{c}}}{\lambda^{\mathrm{c}}} + \frac{1}{\lambda^{\mathrm{s,r}}_{\mathrm{c}}}\right) S^*_{\mathrm{Ag^+}}\left(S_{\mathrm{Ag}} - S^*_{\mathrm{Ag^+}}\right) \\
&\quad \left. + \left(\frac{1}{\lambda^{\mathrm{s,a}}_{\mathrm{e}}} + \frac{d^{\mathrm{e}}}{\lambda^{\mathrm{e}}} + \frac{1}{\lambda^{\mathrm{s,c}}_{\mathrm{e}}}\right) S^*_{\mathrm{Cl^-}}\left(S_{\mathrm{Ag}} - S_{\mathrm{AgCl}} - S^*_{\mathrm{Cl^-}}\right)\right] \frac{j}{F} \\
&\quad - F\left(r^{\mathrm{l}}d^{\mathrm{l}} + r^{\mathrm{s,l}} + r^{\mathrm{a}}d^{\mathrm{a}} + r^{\mathrm{s,a}} + r^{\mathrm{e}}d^{\mathrm{e}} + r^{\mathrm{s,c}} + r^{\mathrm{c}}d^{\mathrm{c}} + r^{\mathrm{s,r}} + r^{\mathrm{r}}d^{\mathrm{r}}\right) j
\end{aligned}
\tag{15.45}
$$

For the temperature difference $T^{\mathrm{c,e}} - T^{\mathrm{a,e}}$, we have

$$\begin{aligned} T^{\mathrm{c,e}} - T^{\mathrm{a,e}} &= \Delta_{\mathrm{a,e}}T + \Delta_{\mathrm{e}}T + \Delta_{\mathrm{e,c}}T \\ &= -\left(\frac{1}{\lambda_{\mathrm{a}}^{\mathrm{s,a}}} + \frac{1}{\lambda_{\mathrm{e}}^{\mathrm{s,a}}} + \frac{d^{\mathrm{e}}}{\lambda^{\mathrm{e}}} + \frac{1}{\lambda_{\mathrm{e}}^{\mathrm{s,c}}} + \frac{1}{\lambda_{\mathrm{c}}^{\mathrm{s,c}}}\right) J_q'^{\mathrm{l,a}} \\ &\quad - T_{eq}\left[\left(\frac{1}{\lambda_{\mathrm{a}}^{\mathrm{s,a}}} + \frac{1}{\lambda_{\mathrm{c}}^{\mathrm{s,c}}}\right)\left(S_{\mathrm{Ag}} - S^*_{\mathrm{Ag^+}}\right) + \frac{d^{\mathrm{e}}}{\lambda^{\mathrm{e}}} S^*_{\mathrm{Cl^-}}\right. \\ &\quad \left. + \left(\frac{1}{\lambda_{\mathrm{e}}^{\mathrm{s,a}}} + \frac{1}{\lambda_{\mathrm{e}}^{\mathrm{s,c}}}\right)\left(S_{\mathrm{Ag}} - S_{\mathrm{AgCl}} + S^*_{\mathrm{Cl^-}}\right)\right] \frac{j}{F} \end{aligned} \tag{15.46}$$

With fixed end point temperatures, we see that the heat flux out of the cell is proportional to the electric current passing the cell. Substitution of Eqs. (15.43) and (15.46) into Eq. (15.45), gives

$$\begin{aligned} F\Delta\phi = &-\left[\left(\frac{1}{\lambda_{\mathrm{a}}^{\mathrm{s,l}}} + \frac{d^{\mathrm{a}}}{\lambda^{\mathrm{a}}} + \frac{1}{\lambda_{\mathrm{a}}^{\mathrm{s,a}}} + \frac{1}{\lambda_{\mathrm{c}}^{\mathrm{s,c}}} + \frac{d^{\mathrm{c}}}{\lambda^{\mathrm{c}}} + \frac{1}{\lambda_{\mathrm{c}}^{\mathrm{s,r}}}\right)\left(S_{\mathrm{Ag}} - S^*_{\mathrm{Ag^+}}\right)\right. \\ &+ \left(\frac{1}{\lambda_{\mathrm{l}}^{\mathrm{s,l}}} + \frac{1}{\lambda_{\mathrm{r}}^{\mathrm{s,r}}}\right) S^*_{\mathrm{e^-}} + \left(\frac{1}{\lambda_{\mathrm{e}}^{\mathrm{s,a}}} + \frac{d^{\mathrm{e}}}{\lambda^{\mathrm{e}}} + \frac{1}{\lambda_{\mathrm{e}}^{\mathrm{s,c}}}\right)\left(S_{\mathrm{Ag}} - S_{\mathrm{AgCl}} + S^*_{\mathrm{Cl^-}}\right)\Big] J_q'^{\mathrm{l,a}} \\ &- T_{eq}\left[\left(\frac{1}{\lambda_{\mathrm{a}}^{\mathrm{s,l}}} + \frac{d^{\mathrm{a}}}{\lambda^{\mathrm{a}}} + \frac{1}{\lambda_{\mathrm{a}}^{\mathrm{s,a}}} + \frac{1}{\lambda_{\mathrm{c}}^{\mathrm{s,c}}} + \frac{d^{\mathrm{c}}}{\lambda^{\mathrm{c}}} + \frac{1}{\lambda_{\mathrm{c}}^{\mathrm{s,r}}}\right)\left(S_{\mathrm{Ag}} - S^*_{\mathrm{Ag^+}}\right)^2\right. \\ &+ \left(\frac{1}{\lambda_{\mathrm{l}}^{\mathrm{s,l}}} + \frac{1}{\lambda_{\mathrm{r}}^{\mathrm{s,r}}}\right) S^*_{\mathrm{e^-}} S^*_{\mathrm{e^-}} + \left(\frac{1}{\lambda_{\mathrm{e}}^{\mathrm{s,a}}} + \frac{1}{\lambda_{\mathrm{e}}^{\mathrm{s,c}}}\right)\left(S_{\mathrm{Ag}} - S_{\mathrm{AgCl}} + S^*_{\mathrm{Cl^-}}\right)^2 \\ &\left. + \frac{d^{\mathrm{e}}}{\lambda^{\mathrm{e}}} S^*_{\mathrm{Cl^-}} S^*_{\mathrm{Cl^-}}\right] \frac{j}{F} \\ &- F\left(r^{\mathrm{l}}d^{\mathrm{l}} + r^{\mathrm{s,l}} + r^{\mathrm{a}}d^{\mathrm{a}} + r^{\mathrm{s,a}} + r^{\mathrm{e}}d^{\mathrm{e}} + r^{\mathrm{s,c}} + r^{\mathrm{c}}d^{\mathrm{c}} + r^{\mathrm{s,r}} + r^{\mathrm{r}}d^{\mathrm{r}}\right) j \end{aligned} \tag{15.47}$$

With the heat flux from Eq. (15.43), this equation gives the potential of the adiabatic cell.

The solution given in this section is for a system close to global equilibrium at a temperature T_{eq}. It uses values of enthalpies, entropies, transported entropies, Peltier coefficients, thermal conductivities and resistivities at this temperature. The solution quantifies what happens when a current is passing the cell. The local temperature and potential may rise or fall depending on the relative value of the coefficients. It provides insight in the possible behavior of the system. Further away from equilibrium, the equations should be solved numerically.

This page intentionally left blank

Chapter 16

The Liquid Junction Potential

We describe a concentration cell with two aqueous electrolytes at constant temperature. The magnitude and origin of the liquid junction potential is determined.

A precise description of liquid junctions in electrochemical cells is important in analytical chemistry [27, 212–216]. Liquid junctions, or salt bridges, are used to separate electrolyte solutions. They are also used in reference electrodes. The exact relationship between the unknown concentration of a species in a test solution and the cell potential is of interest. The test solution contains the salt MX, and the cell has a X^--reversible electrode and a reference electrode. Assume that two measurements are taken of the cell potential, $\Delta\phi_1$ and $\Delta\phi_2$. The Nernst equation has been used to link the concentrations of two test solutions, giving:

$$(\Delta\phi_1)_{j=0} - (\Delta\phi_2)_{j=0} = \frac{RT}{F} \ln \frac{c_{M^+(1)}}{c_{M^+(2)}} \tag{16.1}$$

In this chapter, we shall find the cell potentials $\Delta\phi_1$ and $\Delta\phi_2$ for a typical cell, (16.2), so that we can test this relation. We shall calculate all the contributions to the cell potential for a cell with a liquid junction and compare the results with experimental values, see [214–216].

The most common reference electrode in analytical chemistry is the Ag(s)| AgCl(s) electrode. It is often used in combination with a liquid junction or a salt bridge. The concentration of salt, normally KCl, in the junction is high, usually 4 kmol m^{-3}. The salt KCl is used because the mobilities of the cation and the anion are almost the same. The salt bridge or the liquid junction is therefore assumed to give a negligible contribution to the cell potential. This contribution cancels when two potential values are subtracted, as in Eq. (16.1). We shall quantify this statement, using

HCl in the test solution. Since the mobility of protons is higher than the mobilities of other ions, a junction between HCl and KCl solutions is suited for an analysis of how and when the liquid junction contributes to the cell potential. The experimental cell is thus

$$\mathrm{Ag(s)|\ AgCl(s)|HCl(aq,\ } c_{\mathrm{HCl}}\mathrm{)||KCl(aq,\ } c_{\mathrm{KCl}}\mathrm{)|AgCl(s)|Ag(s)} \tag{16.2}$$

The right hand side of the cell, $|\mathrm{KCl(aq,\ } c_{\mathrm{KCl}}\mathrm{)|AgCl(s)|Ag(s)}$, is the reference electrode mentioned above. To simplify matters, we have chosen the Ag(s)|AgCl(s) electrode also on the left hand side. The solution compartments contain solutions of uniform composition of HCl and KCl, respectively. Inside the junction, denoted ||, the concentration of HCl decreases from the value in the left reservoir, $c^{(1)}_{\mathrm{HCl}}$, to zero in the right reservoir, $c^{(2)}_{\mathrm{HCl}} = 0$, while the concentration of the KCl increases from zero in the left reservoir, $c^{(1)}_{\mathrm{KCl}} = 0$, to the value in the right reservoir, $c^{(2)}_{\mathrm{KCl}}$. We consider the situation when the cell compartments next to the junction have a large volume compared to the junction, and are well stirred, so that all concentration gradients are located to the liquid junction. This is called *restricted diffusion*. In practice, the liquid junction is a capillary with a porous plug that prevents convection in the high density KCl solution.

The problem of the liquid junction is old, dating back to Planck [217,218] and Henderson [219,220]. Extensive discussions of liquid junctions and their use in salt bridges were given by Kotyk and Janacek [212] and Førland *et al.* [27]. We shall derive the contribution to the potential difference following the systematic procedure of the preceding sections, and update earlier results [27] by more recent ones [215].

The cell temperature is constant. The disappearance of silver (silver chloride) on one side is therefore balanced by the appearance of silver (silver chloride) on the other side. The remaining salt contributions from the electrode can be integrated with the electrolyte contribution to the total cell potential, giving:

$$(\Delta\phi)_{j=0} = (\Delta_{\mathrm{e}}\phi)_{j=0} \tag{16.3}$$

We shall find the cell potential by calculating the right hand side of this equation. The agreement between calculated and experimental results of this type can be very good, within ±0.2 mV [215].

16.1 The flux equations for the electrolyte

Contributions to $\Delta\phi$ arise from changes in chemical potentials. When the electrode compartments are stirred, they have no chemical potential gradients, and need not be considered. The liquid junction contributes by $\Delta_{\mathrm{e}}\phi$,

the liquid junction potential. The liquid junction potential can be derived from its entropy production. The entropy production in the junction has contributions from the fluxes of both KCl and HCl as well as from the electric current

$$\sigma^{\mathrm{e}} = -J^{\mathrm{e}}_{\mathrm{KCl}} \frac{1}{T} \frac{\partial}{\partial x} \mu^{\mathrm{e}}_{\mathrm{KCl}} - J^{\mathrm{e}}_{\mathrm{HCl}} \frac{1}{T} \frac{\partial}{\partial x} \mu^{\mathrm{e}}_{\mathrm{HCl}} - j \frac{1}{T} \frac{\partial \phi^{\mathrm{e}}}{\partial x} \tag{16.4}$$

The frame of reference for the fluxes is water. The flux-force relations are, accordingly:

$$\begin{aligned} J^{\mathrm{e}}_{\mathrm{KCl}} &= -L^{\mathrm{e}}_{11} \frac{1}{T} \frac{\partial}{\partial x} \mu^{\mathrm{e}}_{\mathrm{KCl}} - L^{\mathrm{e}}_{12} \frac{1}{T} \frac{\partial}{\partial x} \mu^{\mathrm{e}}_{\mathrm{HCl}} - L^{\mathrm{e}}_{1\phi} \frac{1}{T} \frac{\partial \phi^{\mathrm{e}}}{\partial x} \\ J^{\mathrm{e}}_{\mathrm{HCl}} &= -L^{\mathrm{e}}_{12} \frac{1}{T} \frac{\partial}{\partial x} \mu^{\mathrm{e}}_{\mathrm{KCl}} - L^{\mathrm{e}}_{22} \frac{1}{T} \frac{\partial}{\partial x} \mu^{\mathrm{e}}_{\mathrm{HCl}} - L^{\mathrm{e}}_{2\phi} \frac{1}{T} \frac{\partial \phi^{\mathrm{e}}}{\partial x} \\ j &= -L^{\mathrm{e}}_{\phi 1} \frac{1}{T} \frac{\partial}{\partial x} \mu^{\mathrm{e}}_{\mathrm{KCl}} - L^{\mathrm{e}}_{\phi 2} \frac{1}{T} \frac{\partial}{\partial x} \mu^{\mathrm{e}}_{\mathrm{HCl}} - L^{\mathrm{e}}_{\phi\phi} \frac{1}{T} \frac{\partial \phi^{\mathrm{e}}}{\partial x} \end{aligned} \tag{16.5}$$

The transference coefficients are defined as

$$\begin{aligned} t^{\mathrm{e}}_{\mathrm{KCl}} &\equiv F \left(\frac{J^{\mathrm{e}}_{\mathrm{KCl}}}{j} \right)_{\mu_{\mathrm{KCl}}, \mu_{\mathrm{HCl}}} = F \frac{L^{\mathrm{e}}_{1\phi}}{L^{\mathrm{e}}_{\phi\phi}} \\ t^{\mathrm{e}}_{\mathrm{HCl}} &\equiv F \left(\frac{J^{\mathrm{e}}_{\mathrm{HCl}}}{j} \right)_{\mu_{\mathrm{KCl}}, \mu_{\mathrm{HCl}}} = F \frac{L^{\mathrm{e}}_{2\phi}}{L^{\mathrm{e}}_{\phi\phi}} \end{aligned} \tag{16.6}$$

Using the Onsager's relations, integration of Eq. (16.5c) together with Eq. (16.6) gives the potential difference due to the liquid junction:

$$(\Delta_{\mathrm{e}} \phi)_{j=0} = \int_1^2 d\phi^{\mathrm{e}} = -\frac{1}{F} \int_1^2 (t^{\mathrm{e}}_{\mathrm{KCl}} d\mu^{\mathrm{e}}_{\mathrm{KCl}} + t^{\mathrm{e}}_{\mathrm{HCl}} d\mu^{\mathrm{e}}_{\mathrm{HCl}}) \tag{16.7}$$

This is the formula for the liquid junction potential*. For zero electric current, the mass fluxes become

$$\begin{aligned} (J^{\mathrm{e}}_{\mathrm{KCl}})_{j=0} &= -l^{\mathrm{e}}_{11} \frac{1}{T} \frac{\partial}{\partial x} \mu^{\mathrm{e}}_{\mathrm{KCl}} - l^{\mathrm{e}}_{12} \frac{1}{T} \frac{\partial}{\partial x} \mu^{\mathrm{e}}_{\mathrm{HCl}} \\ (J^{\mathrm{e}}_{\mathrm{HCl}})_{j=0} &= -l^{\mathrm{e}}_{12} \frac{1}{T} \frac{\partial}{\partial x} \mu^{\mathrm{e}}_{\mathrm{KCl}} - l^{\mathrm{e}}_{22} \frac{1}{T} \frac{\partial}{\partial x} \mu^{\mathrm{e}}_{\mathrm{HCl}} \end{aligned} \tag{16.8}$$

*This definition of the liquid junction potential differs from what is normally used in the literature, see e.g. [221], where only a part of $\Delta\phi$ (namely $\Delta\phi_2$, see below) is taken as due to the liquid junction.

The diffusional coefficients l^{e}_{ij} are related to coefficients for mass and charge transfer by

$$l^{\mathrm{e}}_{ij} = L^{\mathrm{e}}_{ij} - \frac{L^{\mathrm{e}}_{i\phi} L^{\mathrm{e}}_{\phi j}}{L^{\mathrm{e}}_{\phi\phi}} \tag{16.9}$$

The concentration of the components KCl and HCl are everywhere defined by the concentration of their cations. The transference coefficients of KCl and HCl are therefore identical to the transference numbers of K^+ and H^+, respectively. Following the analysis in Sec. 10.3, these can be expressed in terms of the mobilities, $u^{\mathrm{e}}_{\mathrm{K}^+}$, $u^{\mathrm{e}}_{\mathrm{H}^+}$ and $u^{\mathrm{e}}_{\mathrm{Cl}^-}$, and concentrations, $c^{\mathrm{e}}_{\mathrm{K}^+}$, $c^{\mathrm{e}}_{\mathrm{H}^+}$ and $c^{\mathrm{e}}_{\mathrm{Cl}^-}$, of the ions. This results in, cf. Eq. (10.51),

$$\begin{aligned} t^{\mathrm{e}}_{\mathrm{KCl}} = t^{\mathrm{e}}_{\mathrm{K}^+} &= \frac{u^{\mathrm{e}}_{\mathrm{K}^+} c^{\mathrm{e}}_{\mathrm{K}^+}}{u^{\mathrm{e}}_{\mathrm{K}^+} c^{\mathrm{e}}_{\mathrm{K}^+} + u^{\mathrm{e}}_{\mathrm{H}^+} c^{\mathrm{e}}_{\mathrm{H}^+} + u^{\mathrm{e}}_{\mathrm{Cl}^-} c^{\mathrm{e}}_{\mathrm{Cl}^-}} \\ t^{\mathrm{e}}_{\mathrm{HCl}} = t^{\mathrm{e}}_{\mathrm{H}^+} &= \frac{u^{\mathrm{e}}_{\mathrm{H}^+} c^{\mathrm{e}}_{\mathrm{H}^+}}{u^{\mathrm{e}}_{\mathrm{K}^+} c^{\mathrm{e}}_{\mathrm{K}^+} + u^{\mathrm{e}}_{\mathrm{H}^+} c^{\mathrm{e}}_{\mathrm{H}^+} + u^{\mathrm{e}}_{\mathrm{Cl}^-} c^{\mathrm{e}}_{\mathrm{Cl}^-}} \end{aligned} \tag{16.10}$$

The concentrations of the ions are related to the KCl and HCl concentrations by

$$c^{\mathrm{e}}_{\mathrm{K}^+} = c^{\mathrm{e}}_{\mathrm{KCl}} \quad , \quad c^{\mathrm{e}}_{\mathrm{H}^+} = c^{\mathrm{e}}_{\mathrm{HCl}} \quad \text{and} \quad c^{\mathrm{e}}_{\mathrm{Cl}^-} = c^{\mathrm{e}}_{\mathrm{KCl}} + c^{\mathrm{e}}_{\mathrm{HCl}} \tag{16.11}$$

The electric conductivity of the solution is, cf. Eq. (10.36),

$$\kappa^{\mathrm{e}} = \frac{L^{\mathrm{e}}_{\phi\phi}}{T} = \left(u^{\mathrm{e}}_{\mathrm{K}^+} c^{\mathrm{e}}_{\mathrm{K}^+} + u^{\mathrm{e}}_{\mathrm{H}^+} c^{\mathrm{e}}_{\mathrm{H}^+} + u^{\mathrm{e}}_{\mathrm{Cl}^-} c^{\mathrm{e}}_{\mathrm{Cl}^-} \right) F \tag{16.12}$$

For the other coefficients, we use Nernst–Einstein's assumption, see Sec. 10.6,

$$L^{\mathrm{e}}_{12} = 0, \quad L^{\mathrm{e}}_{11} = \frac{L^{\mathrm{e}}_{1\phi}}{F} \quad \text{and} \quad L^{\mathrm{e}}_{22} = \frac{L^{\mathrm{e}}_{2\phi}}{F} \tag{16.13}$$

By introducing these relations into the mass flux equations, we obtain the *Nernst–Planck flux equations*

$$\begin{aligned} J^{\mathrm{e}}_{\mathrm{KCl}} &= -\frac{\kappa^{\mathrm{e}}}{F} t^{\mathrm{e}}_{\mathrm{K}^+} \frac{\partial}{\partial x} \left(\mu^{\mathrm{e}}_{\mathrm{KCl}} + F\phi^{\mathrm{e}} \right) \\ J^{\mathrm{e}}_{\mathrm{HCl}} &= -\frac{\kappa^{\mathrm{e}}}{F} t^{\mathrm{e}}_{\mathrm{H}^+} \frac{\partial}{\partial x} \left(\mu^{\mathrm{e}}_{\mathrm{HCl}} + F\phi^{\mathrm{e}} \right) \end{aligned} \tag{16.14}$$

By introducing the electric potential gradient, using Eqs. (16.5c) and (16.6), we obtain

$$\begin{aligned} \left(J^{\mathrm{e}}_{\mathrm{KCl}} \right)_{j=0} &= -\frac{\kappa^{\mathrm{e}}}{F} t^{\mathrm{e}}_{\mathrm{K}^+} \left[t^{\mathrm{e}}_{\mathrm{H}^+} \frac{\partial}{\partial x} \left(\mu^{\mathrm{e}}_{\mathrm{KCl}} - \mu^{\mathrm{e}}_{\mathrm{HCl}} \right) + t^{\mathrm{e}}_{\mathrm{Cl}^-} \frac{\partial}{\partial x} \mu^{\mathrm{e}}_{\mathrm{KCl}} \right] \\ \left(J^{\mathrm{e}}_{\mathrm{HCl}} \right)_{j=0} &= -\frac{\kappa^{\mathrm{e}}}{F} t^{\mathrm{e}}_{\mathrm{H}^+} \left[t^{\mathrm{e}}_{\mathrm{K}^+} \frac{\partial}{\partial x} \left(\mu^{\mathrm{e}}_{\mathrm{HCl}} - \mu^{\mathrm{e}}_{\mathrm{KCl}} \right) + t^{\mathrm{e}}_{\mathrm{Cl}^-} \frac{\partial}{\partial x} \mu^{\mathrm{e}}_{\mathrm{HCl}} \right] \end{aligned} \tag{16.15}$$

where we used $t^{\mathrm{e}}_{\mathrm{K}^+} + t^{\mathrm{e}}_{\mathrm{H}^+} + t^{\mathrm{e}}_{\mathrm{Cl}^-} = 1$. The equations express that there are two types of diffusion superimposed on each other, interdiffusion of two cations (the first term to the right), and diffusion of cation-anion pairs (the last term to the right).

16.2 The liquid junction potential

The equations above determine the liquid junction potential. The chemical potentials are

$$\begin{aligned}\mu^{\mathrm{e}}_{\mathrm{KCl}} &= \mu^0_{\mathrm{KCl}} + RT\ln a^{\mathrm{e}}_{\mathrm{KCl}} = \mu^0_{\mathrm{KCl}} + RT\ln\left(c^{\mathrm{e}}_{\mathrm{Cl}^-} c^{\mathrm{e}}_{\mathrm{K}^+} y^{\mathrm{e}}_{\mathrm{KCl}}\right)\\ \mu^{\mathrm{e}}_{\mathrm{HCl}} &= \mu^0_{\mathrm{HCl}} + RT\ln a^{\mathrm{e}}_{\mathrm{HCl}} = \mu^0_{\mathrm{HCl}} + RT\ln\left(c^{\mathrm{e}}_{\mathrm{Cl}^-} c^{\mathrm{e}}_{\mathrm{H}^+} y^{\mathrm{e}}_{\mathrm{HCl}}\right)\end{aligned} \tag{16.16}$$

By introducing these chemical potentials and Eqs. (16.10) and (16.11) into Eq. (16.7), the liquid junction potential becomes:

$$\begin{aligned}&(\Delta_{\mathrm{e}}\phi)_{j=0}\\ &\quad= -\frac{1}{F}\int_1^2 \left(\frac{u^{\mathrm{e}}_{\mathrm{K}^+} c^{\mathrm{e}}_{\mathrm{K}^+} d\mu^{\mathrm{e}}_{\mathrm{KCl}} + u^{\mathrm{e}}_{\mathrm{H}^+} c^{\mathrm{e}}_{\mathrm{H}^+} d\mu^{\mathrm{e}}_{\mathrm{HCl}}}{u^{\mathrm{e}}_{\mathrm{K}^+} c^{\mathrm{e}}_{\mathrm{K}^+} + u^{\mathrm{e}}_{\mathrm{H}^+} c^{\mathrm{e}}_{\mathrm{H}^+} + u^{\mathrm{e}}_{\mathrm{Cl}^-} c^{\mathrm{e}}_{\mathrm{Cl}^-}}\right)\\ &\quad= -\frac{RT}{F}\int_1^2 \left[d\ln c^{\mathrm{e}}_{\mathrm{Cl}^-} + \frac{\left(u^{\mathrm{e}}_{\mathrm{K}^+} - u^{\mathrm{e}}_{\mathrm{Cl}^-}\right) dc^{\mathrm{e}}_{\mathrm{K}^+} + \left(u^{\mathrm{e}}_{\mathrm{H}^+} - u^{\mathrm{e}}_{\mathrm{Cl}^-}\right) dc^{\mathrm{e}}_{\mathrm{H}^+}}{u^{\mathrm{e}}_{\mathrm{K}^+} c^{\mathrm{e}}_{\mathrm{K}^+} + u^{\mathrm{e}}_{\mathrm{H}^+} c^{\mathrm{e}}_{\mathrm{H}^+} + u^{\mathrm{e}}_{\mathrm{Cl}^-} c^{\mathrm{e}}_{\mathrm{Cl}^-}}\right]\\ &\qquad - \frac{RT}{F}\int_1^2 \left(\frac{u^{\mathrm{e}}_{\mathrm{K}^+} c^{\mathrm{e}}_{\mathrm{K}^+} d\ln y^{\mathrm{e}}_{\mathrm{KCl}} + u^{\mathrm{e}}_{\mathrm{H}^+} c^{\mathrm{e}}_{\mathrm{H}^+} d\ln y^{\mathrm{e}}_{\mathrm{HCl}}}{u^{\mathrm{e}}_{\mathrm{K}^+} c^{\mathrm{e}}_{\mathrm{K}^+} + u^{\mathrm{e}}_{\mathrm{H}^+} c^{\mathrm{e}}_{\mathrm{H}^+} + u^{\mathrm{e}}_{\mathrm{Cl}^-} c^{\mathrm{e}}_{\mathrm{Cl}^-}}\right)\end{aligned} \tag{16.17}$$

In order to compare with expressions in the literature, we split the integral into three terms:

$$(\Delta_{\mathrm{e}}\phi)_{j=0} = \Delta_{\mathrm{e}}\phi_1 + \Delta_{\mathrm{e}}\phi_2 + \Delta_{\mathrm{e}}\phi_3 \tag{16.18}$$

The first term is due to a difference in salt concentration between the reservoirs at the ends of the junction:

$$\Delta_{\mathrm{e}}\phi_1 = -\frac{RT}{F}\int_1^2 d\ln c^{\mathrm{e}}_{\mathrm{Cl}^-} = -\frac{RT}{F}\ln\frac{c^{(2)}_{\mathrm{Cl}^-}}{c^{(1)}_{\mathrm{Cl}^-}} = -\frac{RT}{F}\ln\frac{c^{(2)}_{\mathrm{KCl}}}{c^{(1)}_{\mathrm{HCl}}} \tag{16.19}$$

This contribution is the Nernst potential, see e.g. [221]. The contribution is zero when the concentrations are the same, $c^{(2)}_{\mathrm{KCl}} = c^{(1)}_{\mathrm{HCl}}$ (the Lewis–Sargent cell). It leads to an expression of the type Eq. (16.1) when values

for two HCl solutions are subtracted from one another. The remaining contributions therefore give correction terms.

The second term is due to differences in the ionic mobilities

$$\Delta_{\mathrm{e}}\phi_2 = -\frac{RT}{F}\int_1^2 \frac{\left(u^{\mathrm{e}}_{\mathrm{H^+}} - u^{\mathrm{e}}_{\mathrm{Cl^-}}\right) dc^{\mathrm{e}}_{\mathrm{H^+}}}{u^{\mathrm{e}}_{\mathrm{K^+}}c^{\mathrm{e}}_{\mathrm{K^+}} + u^{\mathrm{e}}_{\mathrm{H^+}}c^{\mathrm{e}}_{\mathrm{H^+}} + u^{\mathrm{e}}_{\mathrm{Cl^-}}c^{\mathrm{e}}_{\mathrm{Cl^-}}} - \frac{RT}{F}\int_1^2 \frac{\left(u^{\mathrm{e}}_{\mathrm{K^+}} - u^{\mathrm{e}}_{\mathrm{Cl^-}}\right) dc^{\mathrm{e}}_{\mathrm{K^+}}}{u^{\mathrm{e}}_{\mathrm{K^+}}c^{\mathrm{e}}_{\mathrm{K^+}} + u^{\mathrm{e}}_{\mathrm{H^+}}c^{\mathrm{e}}_{\mathrm{H^+}} + u^{\mathrm{e}}_{\mathrm{Cl^-}}c^{\mathrm{e}}_{\mathrm{Cl^-}}} \tag{16.20}$$

The term is the leading term of the Lewis–Sargent cell. We see also that KCl does not contribute much, as the mobilities of the K^+ and the Cl^- ions are almost equal, see [97]. Equation (16.20) applies to a cell with two electrolytes. The name liquid junction potential has frequently been associated with this term alone.

The third contribution stems from variations in the activity coefficients

$$\Delta_{\mathrm{e}}\phi_3 = -\frac{RT}{F}\int_1^2 \left(\frac{u^{\mathrm{e}}_{\mathrm{K^+}}c^{\mathrm{e}}_{\mathrm{K^+}}\, d\ln y^{\mathrm{e}}_{\mathrm{KCl}} + u^{\mathrm{e}}_{\mathrm{H^+}}c^{\mathrm{e}}_{\mathrm{H^+}}\, d\ln y^{\mathrm{e}}_{\mathrm{HCl}}}{u^{\mathrm{e}}_{\mathrm{K^+}}c^{\mathrm{e}}_{\mathrm{K^+}} + u^{\mathrm{e}}_{\mathrm{H^+}}c^{\mathrm{e}}_{\mathrm{H^+}} + u^{\mathrm{e}}_{\mathrm{Cl^-}}c^{\mathrm{e}}_{\mathrm{Cl^-}}}\right) \tag{16.21}$$

This contribution is frequently neglected. Values around 10 mV are typical (see the next section).

In order to integrate Eqs. (16.20) and (16.21), we must know the mobilities and activity coefficients as functions of the concentrations across the junction. Equation (16.21) can only be integrated numerically. Henderson [219, 220] had already integrated Eq. (16.20) in 1907, assuming linear profiles for the concentrations. Take as the origin the start of the liquid junction. Linear concentration profiles are given by

$$\begin{gathered} c^{\mathrm{e}}_{\mathrm{H^+}}(x) = c^{(1)}_{\mathrm{HCl}}\frac{d_{\mathrm{lj}} - x}{d_{\mathrm{lj}}}, \\ c^{\mathrm{e}}_{\mathrm{K^+}}(x) = c^{(2)}_{\mathrm{KCl}}\frac{x}{d_{\mathrm{lj}}} \quad \text{and} \quad c^{\mathrm{e}}_{\mathrm{Cl^-}}(x) = c^{(1)}_{\mathrm{HCl}}\frac{d_{\mathrm{lj}} - x}{d_{\mathrm{lj}}} + c^{(2)}_{\mathrm{KCl}}\frac{x}{d_{\mathrm{lj}}} \end{gathered} \tag{16.22}$$

where d_{lj} is the thickness of the liquid junction. By introducing these concentration profiles into Eq. (16.20), we obtain:

$$\Delta_{\mathrm{e}}\phi_2 = -\int_0^{d_{\mathrm{lj}}} \frac{(RT/F)\left[\left(u^{\mathrm{e}}_{\mathrm{K^+}} - u^{\mathrm{e}}_{\mathrm{Cl^-}}\right)c^{(2)}_{\mathrm{KCl}} - \left(u^{\mathrm{e}}_{\mathrm{H^+}} - u^{\mathrm{e}}_{\mathrm{Cl^-}}\right)c^{(1)}_{\mathrm{HCl}}\right] d\left(x/d_{\mathrm{lj}}\right)}{\left(u^{\mathrm{e}}_{\mathrm{H^+}} + u^{\mathrm{e}}_{\mathrm{Cl^-}}\right)c^{(1)}_{\mathrm{HCl}} + \left[\left(u^{\mathrm{e}}_{\mathrm{K^+}} + u^{\mathrm{e}}_{\mathrm{Cl^-}}\right)c^{(2)}_{\mathrm{KCl}} - \left(u^{\mathrm{e}}_{\mathrm{H^+}} + u^{\mathrm{e}}_{\mathrm{Cl^-}}\right)c^{(1)}_{\mathrm{HCl}}\right]\left(x/d_{\mathrm{lj}}\right)} \tag{16.23}$$

By integrating this expression, we have

$$\Delta_{\mathrm{e}}\phi_2 = -\frac{RT}{F}\left[\frac{\left(u^{\mathrm{e}}_{\mathrm{K}^+} - u^{\mathrm{e}}_{\mathrm{Cl}^-}\right)c^{(2)}_{\mathrm{KCl}} - \left(u^{\mathrm{e}}_{\mathrm{H}^+} - u^{\mathrm{e}}_{\mathrm{Cl}^-}\right)c^{(1)}_{\mathrm{HCl}}}{\left(u^{\mathrm{e}}_{\mathrm{K}^+} + u^{\mathrm{e}}_{\mathrm{Cl}^-}\right)c^{(2)}_{\mathrm{KCl}} - \left(u^{\mathrm{e}}_{\mathrm{H}^+} + u^{\mathrm{e}}_{\mathrm{Cl}^-}\right)c^{(1)}_{\mathrm{HCl}}}\right] \times \ln\left[\frac{\left(u^{\mathrm{e}}_{\mathrm{K}^+} + u^{\mathrm{e}}_{\mathrm{Cl}^-}\right)c^{(2)}_{\mathrm{KCl}}}{\left(u^{\mathrm{e}}_{\mathrm{H}^+} + u^{\mathrm{e}}_{\mathrm{Cl}^-}\right)c^{(1)}_{\mathrm{HCl}}}\right] \tag{16.24}$$

This is Henderson's equation.

16.3 Liquid junction potential calculations compared

We shall compare calculated solutions of Eqs. (16.20) and (16.21) for three cases.

1. Concentration profiles from Eqs. (16.8) with diffusional coefficients from Miller [72,73], and transference coefficients from Lindeberg [222]. These calculations are the most precise ones. They predict the measured potential across a known concentration gradient within ±0.2mV [215].

2. Concentration profiles from Eqs. (16.15), with assumption (16.13) for diffusion coefficients and accurate transference coefficients from Lindeberg [222].

3. Concentration profiles from Eqs. (16.15), with assumption (16.13) for diffusion coefficients and transference coefficients from ionic mobilities at infinite electrolyte dilution (see Table 10.1).

The data was taken from various sources. Miller [73] estimated the concentration dependence of diffusional mobilities in solutions of HCl and KCl from solutions with one electrolyte. The diffusional mobilities in his LNI approximation, λ_{ij}, are related to our coefficients by

$$l_{ij} = \frac{T\sum_{k=1}^{3}\sum_{l=1}^{3} z_k z_l \left(\lambda_{ij}\lambda_{kl} - \lambda_{il}\lambda_{kj}\right)}{\sum_{k=1}^{3}\sum_{l=1}^{3} z_k \lambda_{kl} z_l} \tag{16.25}$$

where z_i is the ionic charge. The λ_{ij}-coefficients are tabulated in Ref. [73]. The ionic mobility, u_{i}, for all ions i, has dimension $\mathrm{ms}^{-1}/\mathrm{Vm}^{-1}$ in the

following formulae according to Lindeberg [222]:

$$\begin{aligned} Fu_{\mathrm{H^+}} &= 34.983 - 11.7953\sqrt{c_{\mathrm{H^+}}}/\left(1 + 2.175\sqrt{c_{\mathrm{H^+}}}\right) - 2.376c_{\mathrm{H^+}} \\ &\quad - 3.856\sqrt{c_{\mathrm{K^+}}}/\left(1 + 0.468\sqrt{c_{\mathrm{K^+}}}\right) + 3.114c_{\mathrm{K^+}} \\ Fu_{\mathrm{K^+}} &= 7.353 - 5.915\sqrt{I}/\left(1 + 2.501\sqrt{I}\right) - 0.204I \\ Fu_{\mathrm{Cl^-}} &= 7.633 - 5.915\sqrt{I}/\left(1 + 2.501\sqrt{I}\right) - 0.204I \end{aligned} \tag{16.26}$$

where I is the (dimensionless) ionic strength of the solution, $I = \frac{1}{2}\sum_i^n c_i z_i^2$. The concentrations in the formulae have dimensions of kmol m^{-3}, and F is Faraday's constant.

Activity coefficients for the electrolytes in their mixtures were taken from MacInnes [223]. A quadratic term in c_{KCl} was added to fit newer experimental data [224].

$$\begin{aligned} \ln y_{\mathrm{HCl}} &= -2.3284\sqrt{I}/\left[1 + 1.30\sqrt{I}\right] + 0.4472c_{\mathrm{HCl}} + 0.3050c_{\mathrm{KCl}} + 0.03c_{\mathrm{KCl}}^2 \\ \ln y_{\mathrm{KCl}} &= -2.3444\sqrt{I}/\left[1 + 1.294\sqrt{I}\right] + 0.04738I + 0.01985I^2 \end{aligned} \tag{16.27}$$

The three calculated concentration profiles are shown in Fig. 16.1 for a junction of unit thickness (i.e. the actual thickness was used as the unit). The stippled lines were calculated for case 1 above, while the solid lines represent cases 2 and 3 (inseparable). A linear variation in concentration is also shown.

The concentrations of KCl and HCl in this figure were $c_{\mathrm{KCl}}(2) = 4$ kmol m^{-3} and $c_{\mathrm{HCl}}(1) = 0.1$ kmol m^{-3}, respectively. All profiles show that the concentration of HCl in the junction is always smaller than that given by a linear variation. The situation for KCl depends on the method of calculation. However, the deviation from a linear profile is smaller than 10%. We explain the deficit of HCl in the junction compared to that given by a linear profile by the high mobility of $\mathrm{H^+}$.

The next step was to calculate the cell potential for the different concentration profiles. Cases 2 and 3, naturally, did not give results that were significantly different from one another. Cases 1 and 2 deviated in their prediction of the measured stationary state cell potential by ±1 mV. When these results were compared to a potential integrated for linear concentration profiles (Henderson's approximation, see Eq. (16.24)), $\Delta\phi_2$ and $\Delta\phi_3$ were underestimated by 0.1 mV. We conclude that even if the concentration profiles seem different, they do not have an important impact on the

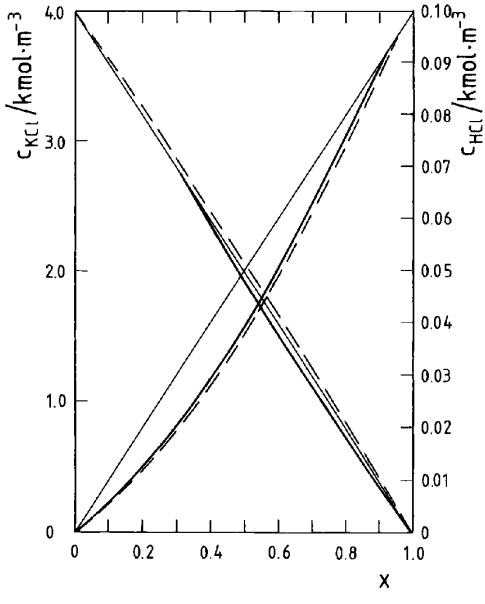

Figure 16.1 The three calculated concentration profiles for a junction of unit thickness. The dashed lines were calculated for case 1 above, while the solid lines represent cases 2 and 3 (inseparable). A linear variation in concentration is also shown. Reproduced from Zeitschr. Phys. Chemie 174 (1991) 179–198 with permission from Oldenburg Wissenschaftsverlag [215].

cell potential. An explanation may be that the sequence of thermodynamic states that make up the path of integration is more important than its actual location in space. The difference between the states that are traversed in Cases 1 and 2 is small.

All contributions to the cell potential vary with the concentrations in the reservoirs, see Table 16.1 and Figs. 16.1 and 16.2. The table shows the calculated contributions to the measured cell potential for selected reservoir concentrations of Case 2. The figures give further information on $\Delta\phi_2$ and $\Delta\phi_3$, respectively.

The term $\Delta\phi_1$ gives the major contribution to the cell potential. When $c_{\mathrm{KCl}} = 4$ kmol m^{-3} and c_{HCl} decrease from 0.1 to 0.001 kmol m^{-3}, this term varied from 95 to 213 mV. The Nernst term predicted the total potential within 10% for the concentration combinations given in Table 16.1. If a better accuracy is needed in the analysis, the other terms must be taken into account.

Table 16.1 Contributions to the liquid junction potential at 298 K in cell d, Ag(s)|AgCl(s)|HCl(aq, c_{KCl})‖KCl(aq, c_{HCl})| AgCl(s)|Ag(s). The contributions are calculated with Nernst–Einstein's assumption (16.13)

c_{HCl}	$\Delta\phi_1$	$\Delta\phi_2$	$\Delta\phi_3$	Total cell	c_{KCl}
/kmol m^{-3}	Nernst-term / mV	Mobility-term / mV	Activity-term / mV	potential /mV	/kmol m^{-3}
0.1	94.8	−4.3	−2.6	88.0	4
0.01	153.9	−3.6	−8.6	141.8	–
0.001	213.1	−4.5	−10.0	198.7	–
0.1	41.4	−14.8	−4.5	22.2	0.5
0.01	100.5	−4.8	−9.2	86.6	–
0.001	159.7	−3.3	−10.4	146.0	–

The variation in $\Delta\phi_2$ gives the main deviation between the Nernst equation and the total cell potential in most cases (see Table 16.1). The term is the most important at low concentrations of the two electrolytes. In asymmetrical cells like the ones given in the table, the contribution is of the order of 5 mV. The term can to good approximation be determined using constant ionic mobilities in Eqs. (16.20) and (16.21): The contribution from mobility differences *changed* less than 1 mV by replacing the concentration dependent mobilities with mobilities at infinitely dilution, see Breer *et al.* [215].

The variation in $\Delta\phi_3$ (see Fig. 16.2) increases in importance from 2 to 10% as c_{HCl} decreases from 0.1 to 0.001 kmol m^{-3}. The variation seems to approach an upper limit as $c_{\mathrm{HCl}} \to 0$ (see the upper curve in Fig. 16.2). This term can be neglected when HCl and KCl are both dilute. The liquid junction potential, as defined here, included the Nernst contribution, $\Delta\phi_1$. The Nernst contribution alone most often does not give sufficient accuracy in concentration determinations. An accurate method for the calculation of the correction term is then needed.

16.4 Concluding comments

We have seen, i.e. from Table 16.1, that the Nernst equation (16.1) is not sufficient for accurate calculations of solution concentrations of ions from measurements of cell potentials in cells with liquid junctions. The cell potential of isothermal concentration cells can, however, be obtained with reasonable accuracy by integrating across the liquid junction using constant ionic mobilities, and by using Nernst–Einstein's or Henderson's assumptions to find the concentration gradients.

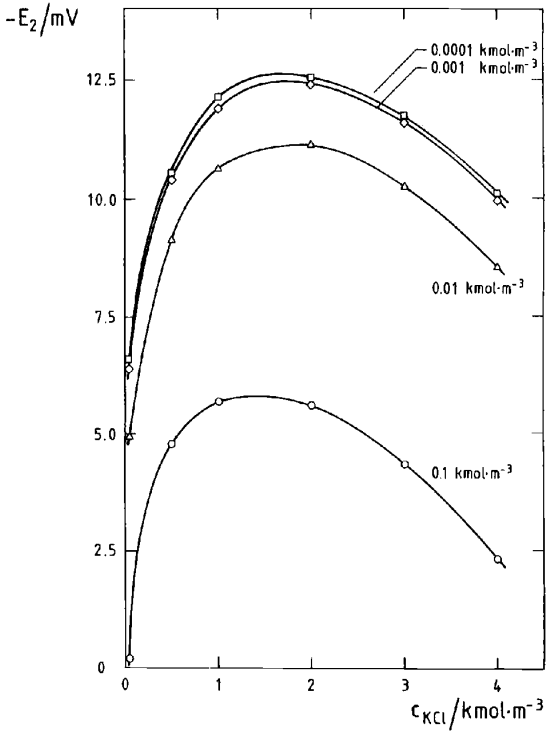

Figure 16.2 The contribution to the cell potential from the activity coefficient, here called E_2 (corresponding to $\Delta\phi_3$ in the text), as a function of KCl concentration for different HCl concentrations. Reproduced from Zeitschr. Phys. Chemie 174 (1991) 179–198 with permission from Oldenburg Wissenschaftsverlag [215].

In order to increase the accuracy of the calculation further, activity coefficients must be used. Such information is frequently not known. This gives one the motivation for efforts to find a replacement of the liquid junction. A solid state reference electrode [225] does not have the disadvantages of the calomel electrode.

We have shown how the theoretical method is well suited for the evaluation of experimental results. The possibility to test assumptions that are made in the theory is important for further developments.

This page intentionally left blank

Chapter 17

The Formation Cell

We describe conversion of chemical energy into electrical energy in formation cells. We find the electric potential profile across the cell from the corresponding variations in chemical potential and/or temperature at zero electric current density.

Electrochemical energy conversion was the main topic of Chapters 13–16. It will be continued here for the most important electrochemical cell, the formation cell. Such cells have different electrodes. Common examples are batteries, fuel cells and electrolysis cells. The literature on these systems is enormous. The aim of this chapter is to see how non-equilibrium thermodynamics can be used to describe the profiles in intensive variables of a formation cell taking advantage of the lessons learned in Chapters 13–16.

A systematic description of the coupled transports of heat, mass and charge in formation cells is obtained from the entropy production of the various phases of the cell [129, 226]. Only the electrolyte phase was studied earlier [189, 227, 228]. The flux equations relate thermoelectric effects, concentration cell effects and the chemical reactions in the formation cell. Thermoelectric effects and concentration cells were described in Chapters 13–16. The *position dependent transference coefficient* and the *position dependent Peltier coefficient* (see Chapter 13) are needed here in order to integrate across the cell.

In order to take advantage of the results in Chapters 13 and 15, we use the electrodes that were described in these chapters. The formation cell example becomes:

$$\mathrm{Fe(s)|Na(Hg)|NaCl(aq)|AgCl(s)|Ag(s)} \tag{17.1}$$

The cell has an amalgam electrode to the left, and is connected to the potentiometer by an iron lead. The amalgam electrode on the left hand side

was described in Sec. 13.1. The right hand side electrode, is the Ag|AgCl electrode, which was described in Secs. 15.1–3. The silver is connected to the other side of the potentiometer directly. The left hand side electrode reaction is:

$$\mathrm{Na\,(Hg)} \rightarrow \mathrm{Na^+(aq)} + \mathrm{e^-} \tag{17.2}$$

One mole of Na disappears from the amalgam into the electrolyte per mole of electrons passing the external circuit from left to right. At the surface of the chloride layer that faces the electrolyte we have:

$$\mathrm{AgCl\,(s)} \rightarrow \mathrm{Cl^-(aq)} + \mathrm{Ag^+} \tag{17.3}$$

One mole of $\mathrm{Cl^-}$ is produced in the electrolyte, while one mole of silver ions is produced in the chloride, close to this surface. The silver ions are transported to the surface between the chloride layer and the metal. The right hand side electrode reaction

$$\mathrm{Ag^+} + \mathrm{e^-} \rightarrow \mathrm{Ag(s)} \tag{17.4}$$

takes place at the surface between the metal and the chloride. The total cell reaction is:

$$\mathrm{Na(Hg)} + \mathrm{AgCl(s)} \rightarrow \mathrm{Na^+(aq)} + \mathrm{Cl^-(aq)} + \mathrm{Ag(s)} \tag{17.5}$$

One mole of Ag(s) and of NaCl(aq) are produced and one mole of Na(Hg) and AgCl(s) are consumed per faraday passing the cell.

In the electrolyte the total amount of dissolved NaCl goes up with one mole per faraday passing the cell. Because of the electroneutral nature of the electrolyte, the concentrations of the sodium and the chloride ions are the same at every position in the electrolyte. When the sodium ion enters the electrolyte from the amalgam surface, it is therefore quickly accompanied by a chloride ion coming into the electrolyte from the AgCl surface. The integrated divergence of the NaCl flux is equal to one mole per faraday passing the cell.

The method of analysis uses, just as in Chapters 13–16, neutral components as thermodynamic variables. Since the use of ionic components is more common, we shall also show how the transition between these formulations can be made. We shall refer extensively to Chapters 13–16 and apply formulae that were derived for the electrodes in these chapters. In this manner, the present chapter can focus on the boundary conditions that are special for the formation cell. We use the terminology given in Chapters 9 and 13, see Figs. 9.1 and 13.2. The isothermal cell is considered first as a reference, before we deal with the non-isothermal cell.

17.1 The isothermal cell

17.1.1 *The electromotive force*

When the cell is isothermal, there is no contribution to the cell's electromotive force, emf, from the uniform phases. The only contributions are from the chemical reactions at the electrode surfaces. For the Na-amalgam electrode, we obtain in the limit of a vanishing electric current (see Sec. 10.2):

$$\Delta_{\mathrm{a,e}}\phi = -\frac{1}{F}\Delta_n G^{\mathrm{s,a}} = \frac{1}{F}\left(\mu^{\mathrm{a,e}}_{\mathrm{Na}} - t^{\mathrm{e}}_{\mathrm{Na^+}}\mu^{\mathrm{e,a}}_{\mathrm{NaCl}}\right) \tag{17.6}$$

For the surface between the electrolyte and the AgCl, we similarly have

$$\Delta_{\mathrm{e,c}}\phi = -\frac{1}{F}\Delta_n G^{\mathrm{s,c}} = \frac{1}{F}\left[\mu^{\mathrm{c,e}}_{\mathrm{AgCl}} - t^{\mathrm{e}}_{\mathrm{Cl^-}}\mu^{\mathrm{e,c}}_{\mathrm{NaCl}}\right] \tag{17.7}$$

Compared to the case considered in Sec. 10.2 the terms due to the salt are new. These are needed to describe the increase of the salt content of the electrolyte. It is important that $t_{\mathrm{Na^+}} + t_{\mathrm{Cl^-}} = 1$. *We will discuss the origin in more detail below using a description in terms of ions.* For the surface between the AgCl and the Ag, the expression is

$$\Delta_{\mathrm{c,r}}\phi = -\frac{1}{F}\Delta_n G^{\mathrm{s,r}} = -\frac{1}{F}\mu^{\mathrm{c,r}}_{\mathrm{Ag}} \tag{17.8}$$

For a zero electric current and zero temperature difference, the chemical potential of the salt is constant, $\mu^{\mathrm{e,a}}_{\mathrm{NaCl}} = \mu^{\mathrm{e,c}}_{\mathrm{NaCl}} = \mu^{\mathrm{e}}_{\mathrm{NaCl}}$. This is the reason that the potential contribution to the cell from the electrolyte is zero. The total potential difference across the electrode surfaces and the electrolyte is then

$$\Delta\phi = \Delta_{\mathrm{a,e}}\phi + \Delta_{\mathrm{e,c}}\phi + \Delta_{\mathrm{c,r}}\phi = \frac{1}{F}\left[\mu^{\mathrm{a,e}}_{\mathrm{Na}} - \mu^{\mathrm{c,r}}_{\mathrm{Ag}} + \mu^{\mathrm{c,e}}_{\mathrm{AgCl}} - \mu^{\mathrm{e}}_{\mathrm{NaCl}}\right] \tag{17.9}$$

where we used that $t_{\mathrm{Na^+}} + t_{\mathrm{Cl^-}} = 1$. This is the Nernst equation for the total cell, alternatively written as

$$\Delta\phi = -\frac{1}{F}\left[\Delta_n G^{\mathrm{s,a}} + \Delta_n G^{\mathrm{s,c}} + \Delta_n G^{\mathrm{s,r}}\right] = -\frac{\Delta_n G}{F} \tag{17.10}$$

17.1.2 *The transference coefficient of the salt in the electrolyte*

The transference coefficient of the salt in an electrolyte is defined by:

$$t^{\mathrm{e}}_{\mathrm{NaCl}}(x,t) \equiv F\left(\frac{J^{\mathrm{e}}_{\mathrm{NaCl}}(x,t)}{j}\right)_{\partial\mu^{\mathrm{e}}_{\mathrm{NaCl}}/\partial x = \partial T/\partial x = 0} \tag{17.11}$$

Depending on the boundary conditions, the transference coefficient may be position-, and possibly also time-dependent. When the chemical potential and the temperature are constant, the salt concentration is independent of the position in the electrolyte, $c^{\mathrm{e}}_{\mathrm{NaCl}}(t)$. The time-dependence of the salt concentration satisfies

$$\frac{\partial}{\partial t} c^{\mathrm{e}}_{\mathrm{NaCl}}(t) = -\frac{\partial}{\partial x} J^{\mathrm{e}}_{\mathrm{NaCl}}(x,t) \tag{17.12}$$

where $J^{\mathrm{e}}_{\mathrm{NaCl}}$ is the salt flux. By integrating this equation from $x = 0$ to $x = d_e$, we obtain

$$\frac{\partial}{\partial t} \int_0^{d_e} c^{\mathrm{e}}_{\mathrm{NaCl}}(t)\, dx = -J^{\mathrm{e}}_{\mathrm{NaCl}}(d_e,t) + J^{\mathrm{e}}_{\mathrm{NaCl}}(0,t) = J^{\mathrm{e,a}}_{\mathrm{NaCl}}(t) - J^{\mathrm{e,c}}_{\mathrm{NaCl}}(t) \tag{17.13}$$

The accumulation of salt in the electrolyte per unit of cross-sectional area is the difference in the salt flux at the two electrodes. The integrated salt content in the electrolyte increases with j/F moles of NaCl per unit of time and per unit of cross sectional area. The increase in the salt content in the electrolyte is therefore given by:

$$\frac{\partial}{\partial t} c^{\mathrm{e}}_{\mathrm{NaCl}}(t) = \frac{j}{d_e F} \tag{17.14}$$

Equation (17.13) together with Eq. (17.14) imply that the salt flux is independent of time. For the gradient of the transference coefficient, we therefore find

$$\frac{\partial}{\partial x} t^{\mathrm{e}}_{\mathrm{NaCl}}(x,t) = \frac{F}{j}\frac{\partial}{\partial x} J^{\mathrm{e}}_{\mathrm{NaCl}}(x,t) = -\frac{F}{j}\frac{\partial}{\partial t} c^{\mathrm{e}}_{\mathrm{NaCl}}(t) = -\frac{1}{d_e} \tag{17.15}$$

It follows that the transference coefficient is independent of time and given by

$$t^{\mathrm{e}}_{\mathrm{NaCl}}(x) = t^{\mathrm{e}}_{\mathrm{Na^+}} - \frac{x}{d_e} = t^{\mathrm{e}}_{\mathrm{Na^+}}\left(1 - \frac{x}{d_e}\right) - t^{\mathrm{e}}_{\mathrm{Cl^-}}\frac{x}{d_e} \tag{17.16}$$

The integration constant has been chosen such that the average of the transference coefficient over the electrolyte is equal to $0.5\left(t^{\mathrm{e}}_{\mathrm{Na^+}} - t^{\mathrm{e}}_{\mathrm{Cl^-}}\right)$. An alternative derivation of the potential difference across the electrolyte, using a description in terms ionic fluxes and forces (see below), shows that this is the correct choice of the integration constant.

The transference coefficient of the salt is equal to the transference number of the sodium ion, $t^{\mathrm{e}}_{\mathrm{Na^+}}$, at the anode surface and equal to minus the transference number of the chloride ion, $-t^{\mathrm{e}}_{\mathrm{Cl^-}} = -(1 - t^{\mathrm{e}}_{\mathrm{Na^+}})$, at the cathode surface (the interface between the electrolyte and AgCl). The ionic transfer numbers are weak functions of concentrations and will be taken constant.

Remark 17.1. *The relation between the ion fluxes, the salt flux and the electric current depends on the electrode surface reactions. As a consequence the transference coefficient of a salt also depends on the electrode surface reactions [227]. In the formation cell, where the electrodes are different, this leads to position dependent transference coefficients for salts.*

17.1.3 *An electrolyte with a salt concentration gradient*

The electrolyte has one independent component, the salt NaCl. The entropy production is

$$\sigma^{\mathrm{e}} = -J^{\mathrm{e}}_{\mathrm{NaCl}} \frac{1}{T} \frac{\partial}{\partial x} \mu^{\mathrm{e}}_{\mathrm{NaCl}} - j \frac{1}{T} \frac{\partial \phi}{\partial x} \tag{17.17}$$

The frame of reference for the salt flux is water. The flux equations are

$$\begin{aligned} J^{\mathrm{e}}_{\mathrm{NaCl}} &= -L^{\mathrm{e}}_{\mu\mu} \frac{1}{T} \frac{\partial}{\partial x} \mu^{\mathrm{e}}_{\mathrm{NaCl}} - L^{\mathrm{e}}_{\mu\phi} \frac{1}{T} \frac{\partial \phi}{\partial x} \\ j &= -L^{\mathrm{e}}_{\phi\mu} \frac{1}{T} \frac{\partial}{\partial x} \mu^{\mathrm{e}}_{\mathrm{NaCl}} - L^{\mathrm{e}}_{\phi\phi} \frac{1}{T} \frac{\partial \phi}{\partial x} \end{aligned} \tag{17.18}$$

The transference coefficient was defined in Eq. (17.11) and satisfies:

$$t^{\mathrm{e}}_{\mathrm{NaCl}}(x) \equiv F \left(\frac{J^{\mathrm{e}}_{\mathrm{NaCl}}(x)}{j} \right)_{\partial \mu^{\mathrm{e}}_{\mathrm{NaCl}}/\partial x = \partial T/\partial x = 0} = F \frac{L^{\mathrm{e}}_{\mu\phi}}{L^{\mathrm{e}}_{\phi\phi}} \tag{17.19}$$

In the limit of a vanishing electric current, we find, using Onsager relations, the reversible contribution to the potential gradient

$$\left(\frac{\partial \phi}{\partial x} \right)_{j \to 0} = -\frac{t^{\mathrm{e}}_{\mathrm{NaCl}}}{F} \frac{\partial}{\partial x} \mu^{\mathrm{e}}_{\mathrm{NaCl}} \tag{17.20}$$

The corresponding potential difference is thus

$$\Delta_{\mathrm{e}} \phi = \int_{\mathrm{e,a}}^{\mathrm{e,c}} d\phi = -\int_{\mathrm{e,a}}^{\mathrm{e,c}} \frac{t^{\mathrm{e}}_{\mathrm{NaCl}}}{F} d\mu^{\mathrm{e}}_{\mathrm{NaCl}} \tag{17.21}$$

We now assume that the variation of the chemical potential across the electrolyte is linear in x. Furthermore, using Eq. (17.16) this results in

$$\Delta_{\mathrm{e}} \phi = -\frac{1}{2F} \left(t^{\mathrm{e}}_{\mathrm{Na^+}} - t^{\mathrm{e}}_{\mathrm{Cl^-}} \right) \left(\mu^{\mathrm{e,c}}_{\mathrm{NaCl}} - \mu^{\mathrm{e,a}}_{\mathrm{NaCl}} \right) = -\frac{1}{2F} \left(t^{\mathrm{e}}_{\mathrm{Na^+}} - t^{\mathrm{e}}_{\mathrm{Cl^-}} \right) \Delta_{\mathrm{e}} \mu^{\mathrm{e}}_{\mathrm{NaCl}} \tag{17.22}$$

For dilute solutions, we can use the ideal expression for the chemical potentials and obtain:

$$\Delta_{\mathrm{e}}\phi = -\frac{RT}{F}\left(t^{\mathrm{e}}_{\mathrm{Na^+}} - t^{\mathrm{e}}_{\mathrm{Cl^-}}\right)\ln\left(\frac{c^{\mathrm{e,c}}_{\mathrm{NaCl}}}{c^{\mathrm{e,a}}_{\mathrm{NaCl}}}\right) = -\frac{RT}{F}\frac{u^{\mathrm{e}}_{\mathrm{Na^+}} - u^{\mathrm{e}}_{\mathrm{Cl^-}}}{u^{\mathrm{e}}_{\mathrm{Na^+}} + u^{\mathrm{e}}_{\mathrm{Cl^-}}}\ln\left(\frac{c^{\mathrm{e,c}}_{\mathrm{NaCl}}}{c^{\mathrm{e,a}}_{\mathrm{NaCl}}}\right) \tag{17.23}$$

We derived the formula using neutral components and fluxes. The ionic transference numbers were expressed in terms of mobilities in the final equality using Eq. (10.51), which gives:

$$t^{\mathrm{e}}_{\mathrm{Na^+}} = \frac{u^{\mathrm{e}}_{\mathrm{Na^+}}}{u^{\mathrm{e}}_{\mathrm{Na^+}} + u^{\mathrm{e}}_{\mathrm{Cl^-}}} \quad \text{and} \quad t^{\mathrm{e}}_{\mathrm{Cl^-}} = \frac{u^{\mathrm{e}}_{\mathrm{Cl^-}}}{u^{\mathrm{e}}_{\mathrm{Na^+}} + u^{\mathrm{e}}_{\mathrm{Cl^-}}} \tag{17.24}$$

The same expression was obtained already by Planck [217, 218] using the electroneutrality condition $J_{\mathrm{Na^+}} = J_{\mathrm{Cl^-}}$ and Nernst–Planck flux equations. It is called the Planck potential. The transference number of $\mathrm{Na^+}$ is 0.396, while the transference number of $\mathrm{Cl^-}$ is 0.604, both at infinite dilution of the electrolyte in water. With a tenfold change in concentration across the cell, the electrolyte contribution becomes 11.8 mV. This value is normally negligible compared to the contribution from the electrodes. It is required, however, in order to find the potential profile across the cell.

The effect of the different boundary conditions in a cell with two identical electrodes and the formation cell can now be compared. When both electrodes are reversible to the $\mathrm{Na^+}$-ion, the corresponding expression was

$$\Delta_{\mathrm{e}}\phi = \frac{2RT}{F}t^{\mathrm{e}}_{\mathrm{Cl^-}}\ln\left(\frac{c^{\mathrm{e,c}}_{\mathrm{NaCl}}}{c^{\mathrm{e,a}}_{\mathrm{NaCl}}}\right) \tag{17.25}$$

This expression can be obtained from Eq. (10.56) for $j = 0$ by replacing $\mathrm{AgNO_3}$ by NaCl. The magnitude of the contribution is in both cases some mV.

The total potential difference across electrode surfaces and electrolyte is, finally,

$$\begin{aligned}\Delta\phi &= \Delta_{\mathrm{a,e}}\phi + \Delta_{\mathrm{e}}\phi + \Delta_{\mathrm{e,c}}\phi + \Delta_{\mathrm{c,r}}\phi \\ &= \frac{1}{F}\Bigg[\mu^{\mathrm{a,e}}_{\mathrm{Na}} - \mu^{\mathrm{c,r}}_{\mathrm{Ag}} + \mu^{\mathrm{c,e}}_{\mathrm{AgCl}} - t_{\mathrm{Na^+}}\mu^{\mathrm{e,a}}_{\mathrm{NaCl}} - t_{\mathrm{Cl^-}}\mu^{\mathrm{e,c}}_{\mathrm{NaCl}} \\ &\quad - \frac{1}{2}\left(t^{\mathrm{e}}_{\mathrm{Na^+}} - t^{\mathrm{e}}_{\mathrm{Cl^-}}\right)\Delta_{\mathrm{e}}\mu^{\mathrm{e}}_{\mathrm{NaCl}}\Bigg] \\ &= \frac{1}{F}\left[\mu^{\mathrm{a,e}}_{\mathrm{Na}} - \mu^{\mathrm{c,r}}_{\mathrm{Ag}} + \mu^{\mathrm{c,e}}_{\mathrm{AgCl}} - \frac{1}{2}\left(\mu^{\mathrm{e,a}}_{\mathrm{NaCl}} + \mu^{\mathrm{e,c}}_{\mathrm{NaCl}}\right)\right]\end{aligned} \tag{17.26}$$

where we used Eq. (17.6) for $\Delta_{\mathrm{a,e}}\phi$, Eq. (17.7) for $\Delta_{\mathrm{e,c}}\phi$ and Eq. (17.8) for $\Delta_{\mathrm{c,r}}\phi$. For a constant concentration of the salt, the above expression reduces to the one, Eq. (17.9), given in the previous subsection. The difference between Eq. (17.26) and Eq. (17.9) is that Eq. (17.26) contains the average chemical potential of the salt.

17.1.4 *The Planck potential derived from ionic fluxes and forces*

Planck [217,218] derived the expression for his potential from a description that uses ions as components. In the ionic formulation (see Sec. 10.6) one writes the entropy production in the electrolyte as:

$$\sigma^{\mathrm{e}} = J^{\mathrm{e}}_{\mathrm{Na^+}}\left[-\frac{1}{T}\frac{\partial}{\partial x}\left(\mu^{\mathrm{e}}_{\mathrm{Na^+}} + F\psi^{\mathrm{e}}\right)\right] + J^{\mathrm{e}}_{\mathrm{Cl^-}}\left[-\frac{1}{T}\frac{\partial}{\partial x}\left(\mu^{\mathrm{e}}_{\mathrm{Cl^-}} - F\psi^{\mathrm{e}}\right)\right] \tag{17.27}$$

where ψ^{e} is the electrostatic potential (Maxwell potential), and the combinations of the chemical and the electrostatic potentials are the electrochemical potentials. Because the anode surface reaction is reversible to $\mathrm{Na^+}$ and not to $\mathrm{Cl^-}$, while the cathode surface reaction is reversible to $\mathrm{Cl^-}$ and not to $\mathrm{Na^+}$, the relations between the fluxes is:

$$J^{\mathrm{e}}_{\mathrm{Na^+}} = \frac{j}{2F} + J^{\mathrm{e}}_{\mathrm{NaCl}} \quad \text{and} \quad J^{\mathrm{e}}_{\mathrm{Cl^-}} = -\frac{j}{2F} + J^{\mathrm{e}}_{\mathrm{NaCl}} \tag{17.28}$$

or equivalently,

$$\frac{j}{F} = J^{\mathrm{e}}_{\mathrm{Na^+}} - J^{\mathrm{e}}_{\mathrm{Cl^-}} \quad \text{and} \quad J^{\mathrm{e}}_{\mathrm{NaCl}} = \frac{1}{2}\left(J^{\mathrm{e}}_{\mathrm{Na^+}} + J^{\mathrm{e}}_{\mathrm{Cl^-}}\right) \tag{17.29}$$

Eliminating the ionic fluxes from Eq. (17.27) using Eq. (17.28), the entropy production becomes

$$\sigma^{\mathrm{e}} = -J^{\mathrm{e}}_{\mathrm{NaCl}}\frac{1}{T}\frac{\partial}{\partial x}\mu^{\mathrm{e}}_{\mathrm{NaCl}} - j\frac{1}{T}\frac{\partial}{\partial x}\left(\psi + \frac{\mu^{\mathrm{e}}_{\mathrm{Na^+}}}{2F} - \frac{\mu^{\mathrm{e}}_{\mathrm{Cl^-}}}{2F}\right) \tag{17.30}$$

Comparing this relation with Eq. (17.17), we identify

$$\phi = \psi + \frac{\mu^{\mathrm{e}}_{\mathrm{Na^+}}}{2F} - \frac{\mu^{\mathrm{e}}_{\mathrm{Cl^-}}}{2F} \tag{17.31}$$

The linear flux-force relations that follow from the entropy production given in Eq. (17.27) are:

$$\begin{aligned} J^{\mathrm{e}}_{\mathrm{Na^+}} &= -L^{++}\frac{1}{T}\frac{\partial}{\partial x}\left(\mu^{\mathrm{e}}_{\mathrm{Na^+}} + F\psi\right) - L^{+-}\frac{1}{T}\frac{\partial}{\partial x}\left(\mu^{\mathrm{e}}_{\mathrm{Cl^-}} - F\psi\right) \\ J^{\mathrm{e}}_{\mathrm{Cl^-}} &= -L^{-+}\frac{1}{T}\frac{\partial}{\partial x}\left(\mu^{\mathrm{e}}_{\mathrm{Na^+}} + F\psi\right) - L^{--}\frac{1}{T}\frac{\partial}{\partial x}\left(\mu^{\mathrm{e}}_{\mathrm{Cl^-}} - F\psi\right) \end{aligned} \tag{17.32}$$

Following the explanation about the ionic fluxes in Sec. 10.6, we use that to linear order in the salt concentration, the ionic conductivities are

$$L^{++} = Tc^{\mathrm{e}}_{\mathrm{NaCl}}u_{\mathrm{Na^+}}, \quad L^{-+} = L^{+-} = 0, \quad L^{--} = Tc^{\mathrm{e}}_{\mathrm{NaCl}}u_{\mathrm{Cl^-}} \tag{17.33}$$

where we used $c^{\mathrm{e}}_{\mathrm{Na^+}} = c^{\mathrm{e}}_{\mathrm{Cl^-}} = c^{\mathrm{e}}_{\mathrm{NaCl}}$. This gives the Nernst–Planck flux equations for $\mathrm{Na^+}$ and $\mathrm{Cl^-}$:

$$\begin{aligned} J^{\mathrm{e}}_{\mathrm{Na^+}} &= -c^{\mathrm{e}}_{\mathrm{NaCl}}u_{\mathrm{Na^+}}\frac{\partial}{\partial x}\left(\mu^{\mathrm{e}}_{\mathrm{Na^+}} + F\psi\right) \\ J^{\mathrm{e}}_{\mathrm{Cl^-}} &= -c^{\mathrm{e}}_{\mathrm{NaCl}}u_{\mathrm{Cl^-}}\frac{\partial}{\partial x}\left(\mu^{\mathrm{e}}_{\mathrm{Cl^-}} - F\psi\right) \end{aligned} \tag{17.34}$$

At zero electric current, $J^{\mathrm{e}}_{\mathrm{Na^+}} = J^{\mathrm{e}}_{\mathrm{Cl^-}}$, so that the electrostatic potential gradient becomes

$$\frac{\partial}{\partial x}\psi = -\frac{1}{F\left(u_{\mathrm{Na^+}} + u_{\mathrm{Cl^-}}\right)}\left(u_{\mathrm{Na^+}}\frac{\partial}{\partial x}\mu^{\mathrm{e}}_{\mathrm{Na^+}} - u_{\mathrm{Cl^-}}\frac{\partial}{\partial x}\mu^{\mathrm{e}}_{\mathrm{Cl^-}}\right) \tag{17.35}$$

In the neutral electrolyte one has

$$\frac{\partial}{\partial x}\mu^{\mathrm{e}}_{\mathrm{Na^+}} = \frac{\partial}{\partial x}\mu^{\mathrm{e}}_{\mathrm{Cl^-}} = \frac{1}{2}\frac{\partial}{\partial x}\mu^{\mathrm{e}}_{\mathrm{NaCl}} \tag{17.36}$$

This, together with Eqs. (17.31) and (17.35), results in

$$\frac{\partial}{\partial x}\phi = \frac{\partial}{\partial x}\psi = -\frac{\left(u_{\mathrm{Na^+}} - u_{\mathrm{Cl^-}}\right)}{2F\left(u_{\mathrm{Na^+}} + u_{\mathrm{Cl^-}}\right)}\frac{\partial}{\partial x}\mu^{\mathrm{e}}_{\mathrm{NaCl}} \tag{17.37}$$

By integrating across the electrolyte, we have again the Planck potential of Eq. (17.23)

$$\Delta_{\mathrm{e}}\phi = -\frac{\left(u_{\mathrm{Na^+}} - u_{\mathrm{Cl^-}}\right)}{2F\left(u_{\mathrm{Na^+}} + u_{\mathrm{Cl^-}}\right)}\Delta_{\mathrm{e}}\mu^{\mathrm{e}}_{\mathrm{NaCl}} = -\frac{RT\left(u_{\mathrm{Na^+}} - u_{\mathrm{Cl^-}}\right)}{F\left(u_{\mathrm{Na^+}} + u_{\mathrm{Cl^-}}\right)}\ln\frac{c^{\mathrm{e,c}}_{\mathrm{NaCl}}}{c^{\mathrm{e,a}}_{\mathrm{NaCl}}} \tag{17.38}$$

The chemical potential of an ideal solution was introduced in the last identity. The ionic and the component description are therefore found to be equivalent, as they should be. This also verifies that the choice of the integration constant in the expression for the transference number of the salt given in Eq. (17.16) was correct.

17.2 A non-isothermal cell with a non-uniform electrolyte

In the most general case, the phases of a heterogeneous system are neither uniform nor isothermal. In order to give the most general description,

we shall need to refer a property under evaluation to a temperature. For instance, the chemical potential at the surface, $\mu^{\mathrm{s,a}}_{\mathrm{Na}}$, is normally, but not always, evaluated at the surface temperature, $T^{\mathrm{s,a}}$. If the quantity is evaluated at a different temperature this will be explicitly indicated. Thus the chemical potential of the sodium in the bulk anode close to the surface, $\mu^{\mathrm{a,e}}_{\mathrm{Na}}(T^{\mathrm{s,a}})$, is evaluated at the temperature of the surface. Again we limit ourselves to stationary states, defined here as states for which all fluxes are independent of the time. When integrating across the homogeneous regions, we neglect as before the temperature variation of entropies and transported entropies in order to be able to give an analytical result. These results can be extended using numerical integration.

17.2.1 *The homogeneous anode phase*

The entropy production in the amalgam electrode is given by

$$\sigma^{\mathrm{a}} = -J'^{\mathrm{a}}_q \frac{1}{T^2}\frac{\partial T}{\partial x} - J^{\mathrm{a}}_{\mathrm{Na}}\frac{1}{T}\frac{\partial}{\partial x}\mu^{\mathrm{a}}_{\mathrm{Na},T} - j\frac{1}{T}\frac{\partial \phi}{\partial x} \tag{17.39}$$

The resulting linear flux-force relations are

$$\begin{aligned}
J'^{\mathrm{a}}_q &= -L^{\mathrm{a}}_{qq}\frac{1}{T^2}\frac{\partial T}{\partial x} - L^{\mathrm{a}}_{q\mu}\frac{1}{T}\frac{\partial}{\partial x}\mu^{\mathrm{a}}_{\mathrm{Na},T} - L^{\mathrm{a}}_{q\phi}\frac{1}{T}\frac{\partial \phi}{\partial x}\\
J^{\mathrm{a}}_{\mathrm{Na}} &= -L^{\mathrm{a}}_{\mu q}\frac{1}{T^2}\frac{\partial T}{\partial x} - L^{\mathrm{a}}_{\mu\mu}\frac{1}{T}\frac{\partial}{\partial x}\mu^{\mathrm{a}}_{\mathrm{Na},T} - L^{\mathrm{a}}_{\mu\phi}\frac{1}{T}\frac{\partial \phi}{\partial x}\\
j &= -L^{\mathrm{a}}_{\phi q}\frac{1}{T^2}\frac{\partial T}{\partial x} - L^{\mathrm{a}}_{\phi\mu}\frac{1}{T}\frac{\partial}{\partial x}\mu^{\mathrm{a}}_{\mathrm{Na},T} - L^{\mathrm{a}}_{\phi\phi}\frac{1}{T}\frac{\partial \phi}{\partial x}
\end{aligned} \tag{17.40}$$

The position dependent transference coefficient for NaCl was discussed in Sec. 17.1 (see Eq. (17.16)). In the present case, the flux of sodium is zero in $x = -d_a$ and equal to j/F in $x = 0$. The transference coefficient in this case is given by

$$t^{\mathrm{a}}_{\mathrm{Na}}(x) \equiv F\left(\frac{J^{\mathrm{a}}_{\mathrm{Na}}(x)}{j}\right)_{\partial T/\partial x = \partial \mu^{\mathrm{a}}_{\mathrm{Na}}/\partial x = 0} = F\frac{L^{\mathrm{a}}_{\mu\phi}(x)}{L^{\mathrm{a}}_{\phi\phi}} = 1 + \frac{x}{d_a} \tag{17.41}$$

The *position dependent Peltier coefficient* is defined analogously, from an analysis of the divergence of the heat flux and the resulting heat production:

$$\begin{aligned}
\pi^{\mathrm{a}}(x) &\equiv F\left(\frac{J'^{\mathrm{a}}_q(x)}{j}\right)_{\partial T/\partial x = \partial \mu^{\mathrm{a}}_{\mathrm{Na}}/\partial x = 0} = F\frac{L^{\mathrm{a}}_{q\phi}(x)}{L^{\mathrm{a}}_{\phi\phi}}\\
&= -T(x)\left[t^{\mathrm{a}}_{\mathrm{Na}}(x)S^{\mathrm{a}}_{\mathrm{Na}} + S^{*,\mathrm{a}}_{\mathrm{e}^-}\right]
\end{aligned} \tag{17.42}$$

The position dependent Peltier coefficient is given by the entropy of Na and the transported entropy of the electrons. The derivation is analogous to the one in the electrolyte. Note that $\pi^{\mathrm{a},0} = \pi^{\mathrm{a}}(-d_a)$ and $\pi^{\mathrm{a,e}} = \pi^{\mathrm{a}}(0)$.

Using Onsager's relations and the definitions of the transference number of Na and the Peltier coefficient, we find for the zero current electric potential gradient:

$$\begin{aligned}\left(\frac{\partial\phi}{\partial x}\right)_{j\to 0} &= -\frac{1}{F}\left[t^{\mathrm{a}}_{\mathrm{Na}}(x)\frac{\partial}{\partial x}\mu^{\mathrm{a}}_{\mathrm{Na},T} + \frac{\pi^{\mathrm{a}}(x)}{T(x)}\frac{\partial T}{\partial x}\right] \\ &= -\frac{1}{F}\left[t^{\mathrm{a}}_{\mathrm{Na}}(x)\left(\frac{\partial}{\partial x}\mu^{\mathrm{a}}_{\mathrm{Na}} + S^{\mathrm{a}}_{\mathrm{Na}}\frac{\partial T}{\partial x}\right) + \frac{\pi^{\mathrm{a}}(x)}{T(x)}\frac{\partial T}{\partial x}\right] \\ &= -\frac{1}{F}\left[\left(1+\frac{x}{d_a}\right)\frac{\partial}{\partial x}\mu^{\mathrm{a}}_{\mathrm{Na}} - S^{*,\mathrm{a}}_{\mathrm{e}^-}\frac{\partial T}{\partial x}\right] \end{aligned} \tag{17.43}$$

By integrating across the electrode, taking the chemical potential and the temperature profiles linear, we obtain for the zero current potential difference:

$$\Delta_{\mathrm{a}}\phi = -\frac{1}{2F}\Delta_{\mathrm{a}}\mu^{\mathrm{a}}_{\mathrm{Na}} + \frac{1}{F}S^{*,\mathrm{a}}_{\mathrm{e}^-}\Delta_{\mathrm{a}}T \tag{17.44}$$

where we note that $\Delta_{\mathrm{a}}\mu^{\mathrm{a}}_{\mathrm{Na}} = \mu^{\mathrm{a,e}}_{\mathrm{Na}}(T^{\mathrm{a,e}}) - \mu^{\mathrm{a,o}}_{\mathrm{Na}}(T^{\mathrm{a,o}})$. Using the ideal expression for the chemical potential gives

$$\Delta_{\mathrm{a}}\phi = -\frac{RT}{2F}\ln\frac{c^{\mathrm{a,e}}_{\mathrm{Na}}}{c^{\mathrm{a,o}}_{\mathrm{Na}}} + \frac{1}{F}S^{*,\mathrm{a}}_{\mathrm{e}^-}\Delta_{\mathrm{a}}T \tag{17.45}$$

Under conditions when $c^{\mathrm{a,o}}_{\mathrm{Na}} > c^{\mathrm{a,e}}_{\mathrm{Na}}$, the first contribution will be positive. For stirred amalgam $\Delta_{\mathrm{a}}\mu^{\mathrm{a}}_{\mathrm{Na}} = 0$, in which case this term does not contribute. When we add the first term in Eq. (17.44) to Eq. (17.9), and in Eq. (17.26), the contribution $\mu^{\mathrm{a,e}}_{\mathrm{Na}}$ changes to the average $0.5(\mu^{\mathrm{a,e}}_{\mathrm{Na}} + \mu^{\mathrm{a,o}}_{\mathrm{Na}})$ in both equations.

17.2.2 *The electrolyte*

By including the contribution due to the temperature gradient in Eq. (17.17), the entropy production in the electrolyte is given by

$$\sigma^{\mathrm{e}} = -J'^{\mathrm{e}}_q\frac{1}{T^2}\frac{\partial T}{\partial x} - J^{\mathrm{e}}_{\mathrm{NaCl}}\frac{1}{T}\frac{\partial}{\partial x}\mu^{\mathrm{e}}_{\mathrm{NaCl},T} - j\frac{1}{T}\frac{\partial\phi}{\partial x} \tag{17.46}$$

The resulting linear flux-force relations are

$$\begin{aligned} J_q'^{\mathrm{e}} &= -L^{\mathrm{e}}_{qq}\frac{1}{T^2}\frac{\partial T}{\partial x} - L^{\mathrm{e}}_{q\mu}\frac{1}{T}\frac{\partial}{\partial x}\mu^{\mathrm{e}}_{\mathrm{NaCl},T} - L^{\mathrm{e}}_{q\phi}\frac{1}{T}\frac{\partial \phi}{\partial x} \\ J^{\mathrm{e}}_{\mathrm{NaCl}} &= -L^{\mathrm{e}}_{\mu q}\frac{1}{T^2}\frac{\partial T}{\partial x} - L^{\mathrm{e}}_{\mu\mu}\frac{1}{T}\frac{\partial}{\partial x}\mu^{\mathrm{e}}_{\mathrm{NaCl},T} - L^{\mathrm{e}}_{\mu\phi}\frac{1}{T}\frac{\partial \phi}{\partial x} \\ j &= -L^{\mathrm{e}}_{\phi q}\frac{1}{T^2}\frac{\partial T}{\partial x} - L^{\mathrm{e}}_{\phi\mu}\frac{1}{T}\frac{\partial}{\partial x}\mu^{\mathrm{e}}_{\mathrm{NaCl},T} - L^{\mathrm{e}}_{\phi\phi}\frac{1}{T}\frac{\partial \phi}{\partial x} \end{aligned} \tag{17.47}$$

The position dependent transference coefficient, $t^{\mathrm{e}}_{\mathrm{NaCl}}(x)$, was discussed in Sec. 17.1, see Eq. (17.16). The *position dependent Peltier coefficient* is defined analogously, from an analysis of the divergence of the heat flux and the resulting heat production:

$$\begin{aligned} \pi^{\mathrm{e}}(x) &\equiv F\left(\frac{J_q'^{\mathrm{e}}(x)}{j}\right)_{\partial T/\partial x=\partial\mu^{\mathrm{e}}_{\mathrm{NaCl}}/\partial x=0} = F\frac{L^{\mathrm{e}}_{q\phi}(x)}{L^{\mathrm{e}}_{\phi\phi}} \\ &= T(x)\left[-t^{\mathrm{e}}_{\mathrm{NaCl}}(x)S^{\mathrm{e}}_{\mathrm{NaCl}} + \left(1-\frac{x}{d_e}\right)t^{\mathrm{e}}_{\mathrm{Na^+}}S^{*,\mathrm{e}}_{\mathrm{Na^+}} - \frac{x}{d_e}t^{\mathrm{e}}_{\mathrm{Cl^-}}S^{*,\mathrm{e}}_{\mathrm{Cl^-}}\right] \end{aligned} \tag{17.48}$$

The position dependent Peltier coefficient is given by the entropy of NaCl and transported entropies of its ions. The transported entropies enter the analysis as integration constants at the surfaces, just as the transference numbers did in the expression for the transference coefficient. Note that $\pi^{\mathrm{e,a}} = \pi^{\mathrm{e}}(0)$ and $\pi^{\mathrm{e,c}} = \pi^{\mathrm{e}}(d_e)$.

Using Onsager's relations and the definitions of the transference number of NaCl and the Peltier coefficient in Eq. (17.47c), we find for the currentless electric potential gradient:

$$\begin{aligned} \left(\frac{\partial\phi}{\partial x}\right)_{j\to 0} &= -\frac{1}{F}\left[t^{\mathrm{e}}_{\mathrm{NaCl}}(x)\frac{\partial}{\partial x}\mu^{\mathrm{e}}_{\mathrm{NaCl},T} + \frac{\pi^{\mathrm{e}}(x)}{T(x)}\frac{\partial T}{\partial x}\right] \\ &= -\frac{1}{F}\left[t^{\mathrm{e}}_{\mathrm{NaCl}}(x)\left(\frac{\partial}{\partial x}\mu^{\mathrm{e}}_{\mathrm{NaCl}} + S^{\mathrm{e}}_{\mathrm{NaCl}}\frac{\partial T}{\partial x}\right) + \frac{\pi^{\mathrm{e}}(x)}{T(x)}\frac{\partial T}{\partial x}\right] \\ &= -\frac{1}{F}\Bigg[\left(t^{\mathrm{e}}_{\mathrm{Na^+}} - \frac{x}{d_e}\right)\frac{\partial}{\partial x}\mu^{\mathrm{e}}_{\mathrm{NaCl}} + \left(\left(1-\frac{x}{d_e}\right)t^{\mathrm{e}}_{\mathrm{Na^+}}S^{*,\mathrm{e}}_{\mathrm{Na^+}} \\ &\qquad - \frac{x}{d_e}t^{\mathrm{e}}_{\mathrm{Cl^-}}S^{*,\mathrm{e}}_{\mathrm{Cl^-}}\right)\frac{\partial T}{\partial x}\Bigg] \end{aligned} \tag{17.49}$$

By integrating across the electrolyte, taking the chemical potential and the temperature profiles to be linear, we obtain for the zero current potential difference:

$$\Delta_{\rm e}\phi = -\frac{1}{2F}\left(t^{\rm e}_{\rm Na^+} - t^{\rm e}_{\rm Cl^-}\right)\Delta_{\rm e}\mu^{\rm e}_{\rm NaCl} - \frac{1}{2F}\left(t^{\rm e}_{\rm Na^+}S^{*,{\rm e}}_{\rm Na^+} - t^{\rm e}_{\rm Cl^-}S^{*,{\rm e}}_{\rm Cl^-}\right)\Delta_{\rm e}T \tag{17.50}$$

where we note that $\Delta_{\rm e}\mu^{\rm e}_{\rm NaCl} = \mu^{\rm e,c}_{\rm NaCl}\left(T^{\rm e,c}\right) - \mu^{\rm e,a}_{\rm NaCl}\left(T^{\rm e,a}\right)$. We have assumed that the transported entropies were constant in the integration. The first contribution is probably larger than the second. We did not introduce a Soret equilibrium in the electrolyte.

17.2.3 *The surface of the anode*

The electrode reaction at the interface between Na(Hg) and NaCl(aq) is given in Eq. (17.2). The contribution to the reaction Gibbs energy due to the neutral components is, cf. Eq. (17.6):

$$\Delta_n G^{\rm s,a} = -\mu^{\rm a,e}_{\rm Na}(T^{\rm s,a}) + t^{\rm e}_{\rm Na^+}\mu^{\rm e,a}_{\rm NaCl}(T^{\rm s,a}) \tag{17.51}$$

for the non-isothermal case. The entropy production in the non-isothermal anode surface is:

$$\sigma^{\rm s,a} = J'^{\rm a,e}_q\left(\frac{1}{T^{\rm s,a}} - \frac{1}{T^{\rm a,e}}\right) + J'^{\rm e,a}_q\left(\frac{1}{T^{\rm e,a}} - \frac{1}{T^{\rm s,a}}\right) - r^{\rm s,a}\frac{\Delta_n G^{\rm s,a}}{T^{\rm s,a}} - j\frac{\Delta_{\rm a,e}\phi}{T^{\rm s,a}} \tag{17.52}$$

The reaction rate is given in terms of the electric current, $r^{\rm s,a} = j/F$. This results in

$$\sigma^{\rm s,a} = J'^{\rm a,e}_q\Delta_{\rm a,s}\left(\frac{1}{T}\right) + J'^{\rm e,a}_q\Delta_{\rm s,e}\left(\frac{1}{T}\right) - j\frac{1}{T^{\rm s,a}}\left[\Delta_{\rm a,e}\phi + \frac{\Delta_n G^{\rm s,a}}{F}\right] \tag{17.53}$$

The flux equations are accordingly

$$\begin{aligned}
J'^{\rm a,e}_q &= L^{\rm s,a}_{aa}\Delta_{\rm a,s}\left(\frac{1}{T}\right) + L^{\rm s,a}_{ae}\Delta_{\rm s,e}\left(\frac{1}{T}\right) - L^{\rm s,a}_{a\phi}\frac{1}{T^{\rm s,a}}\left[\Delta_{\rm a,e}\phi + \frac{\Delta_n G^{\rm s,a}}{F}\right] \\
J'^{\rm e,a}_q &= L^{\rm s,a}_{ea}\Delta_{\rm a,s}\left(\frac{1}{T}\right) + L^{\rm s,a}_{ee}\Delta_{\rm s,e}\left(\frac{1}{T}\right) - L^{\rm s,a}_{e\phi}\frac{1}{T^{\rm s,a}}\left[\Delta_{\rm a,e}\phi + \frac{\Delta_n G^{\rm s,a}}{F}\right] \\
j &= L^{\rm s,a}_{\phi a}\Delta_{\rm a,s}\left(\frac{1}{T}\right) + L^{\rm s,a}_{\phi e}\Delta_{\rm s,e}\left(\frac{1}{T}\right) - L^{\rm s,a}_{\phi\phi}\frac{1}{T^{\rm s,a}}\left[\Delta_{\rm a,e}\phi + \frac{\Delta_n G^{\rm s,a}}{F}\right]
\end{aligned} \tag{17.54}$$

The Peltier coefficients for the bulk phases at the anode surface are:

$$\pi^{\mathrm{a,e}} \equiv F\left(\frac{J_q'^{\mathrm{a,e}}}{j}\right)_{\Delta_{\mathrm{a,s}}T=\Delta_{\mathrm{s,e}}T=\Delta_{\mathrm{s,e}}\mu_{\mathrm{NaCl}}=0} = F\frac{L^{\mathrm{s,a}}_{a\phi}}{L^{\mathrm{s,a}}_{\phi\phi}} = -T^{\mathrm{a,e}}\left(S^{\mathrm{a,e}}_{\mathrm{Na}} + S^{*,\mathrm{a,e}}_{\mathrm{e}^-}\right)$$

$$\pi^{\mathrm{e,a}} \equiv F\left(\frac{J_q'^{\mathrm{e,a}}}{j}\right)_{\Delta_{\mathrm{a,s}}T=\Delta_{\mathrm{s,e}}T=\Delta_{\mathrm{s,e}}\mu_{\mathrm{NaCl}}=0} = F\frac{L^{\mathrm{s,a}}_{e\phi}}{L^{\mathrm{s,a}}_{\phi\phi}} = T^{\mathrm{e,a}}t^{\mathrm{e}}_{\mathrm{Na}^+}\left(S^{*,\mathrm{e,a}}_{\mathrm{Na}^+} - S^{\mathrm{e,a}}_{\mathrm{NaCl}}\right) \tag{17.55}$$

We see that $\pi^{\mathrm{a,e}} = \pi^{\mathrm{a}}(0)$ and $\pi^{\mathrm{e,a}} = \pi^{\mathrm{e}}(0)$, cf. Eqs. (17.42) and (17.48). The Peltier coefficient can be regarded as a transference coefficient of heat. It depends on the location in the same manner.

By using Onsager's relations, the potential difference across the anode surface becomes

$$\begin{aligned}\Delta_{\mathrm{a,e}}\phi &= -\frac{1}{F}\left[\Delta_n G^{\mathrm{s,a}} + \pi^{\mathrm{a,e}}\left(\frac{T^{\mathrm{s,a}} - T^{\mathrm{a,e}}}{T^{\mathrm{a,e}}}\right) + \pi^{\mathrm{e,a}}\left(\frac{T^{\mathrm{e,a}} - T^{\mathrm{s,a}}}{T^{\mathrm{e,a}}}\right)\right] \\ &= -\frac{1}{F}\left[-\mu^{\mathrm{a,e}}_{\mathrm{Na}} + t^{\mathrm{e}}_{\mathrm{Na}^+}\mu^{\mathrm{e,a}}_{\mathrm{NaCl}} - S^{*,\mathrm{a,e}}_{\mathrm{e}^-}\left(T^{\mathrm{s,a}} - T^{\mathrm{a,e}}\right) + t^{\mathrm{e}}_{\mathrm{Na}^+}S^{*,\mathrm{e,a}}_{\mathrm{Na}^+}\left(T^{\mathrm{e,a}} - T^{\mathrm{s,a}}\right)\right]\end{aligned} \tag{17.56}$$

The main contribution to the surface potential drop is given by the reaction Gibbs energy. For constant temperature at the surface, this expression reduces to the one given in Eq. (17.6).

17.2.4 *The homogeneous phases and the surface of the cathode*

The chemical reaction that produces Cl^- in the electrolyte and Ag^+ to conduct charge in AgCl is given by Eq. (17.3). The contribution to the reaction Gibbs energy due to the neutral components is:

$$\Delta_n G^{\mathrm{s,c}} = t^{\mathrm{e}}_{\mathrm{Cl}^-}\mu^{\mathrm{e,c}}_{\mathrm{NaCl}}\left(T^{\mathrm{s,c}}\right) - \mu^{\mathrm{c,e}}_{\mathrm{AgCl}}\left(T^{\mathrm{s,c}}\right) \tag{17.57}$$

The entropy production of the electrolyte-AgCl surface is:

$$\sigma^{\mathrm{s,c}} = J_q'^{\mathrm{e,c}}\Delta_{\mathrm{e,s}}\left(\frac{1}{T}\right) + J_q'^{\mathrm{c,e}}\Delta_{\mathrm{s,c}}\left(\frac{1}{T}\right) - j\frac{1}{T^{\mathrm{s,c}}}\left[\Delta_{\mathrm{c,e}}\phi + \frac{1}{F}\Delta_n G^{\mathrm{s,c}}\right] \tag{17.58}$$

The Peltier coefficients are then

$$\pi^{\mathrm{e,c}} \equiv F\left(\frac{J_q'^{\mathrm{e,c}}}{j}\right)_{\Delta_{\mathrm{e,s}}T=\Delta_{\mathrm{s,c}}T=\Delta_{\mathrm{e,s}}\mu^{\mathrm{e}}_{\mathrm{NaCl}}=0} = F\frac{L^{\mathrm{s,c}}_{e\phi}}{L^{\mathrm{s,c}}_{\phi\phi}} = T^{\mathrm{e,c}}t^{\mathrm{e}}_{\mathrm{Cl}^-}\left(S^{\mathrm{e,c}}_{\mathrm{NaCl}} - S^{*,\mathrm{e,c}}_{\mathrm{Cl}^-}\right)$$

$$\pi^{\mathrm{c,e}} \equiv F\left(\frac{J_q'^{\mathrm{c,e}}}{j}\right)_{\Delta_{\mathrm{e,s}}T=\Delta_{\mathrm{s,c}}T=\Delta_{\mathrm{e,s}}\mu^{\mathrm{e}}_{\mathrm{NaCl}}=0} = F\frac{L^{\mathrm{s,c}}_{c\phi}}{L^{\mathrm{s,c}}_{\phi\phi}} = T^{\mathrm{c,e}}\left(S^{*,\mathrm{c,e}}_{\mathrm{Ag}^+} + S^{\mathrm{c,e}}_{\mathrm{AgCl}}\right) \tag{17.59}$$

The zero current potential difference is accordingly:

$$\begin{aligned}\Delta_{\mathrm{e,c}}\phi &= -\frac{1}{F}\left[\Delta_n G^{\mathrm{s,c}} + \frac{\pi^{\mathrm{e,c}}}{T^{\mathrm{e,c}}}\Delta_{\mathrm{e,s}}T + \frac{\pi^{\mathrm{c,e}}}{T^{\mathrm{c,e}}}\Delta_{\mathrm{s,c}}T\right] \\ &= -\frac{1}{F}\left[t^{\mathrm{e}}_{\mathrm{Cl^-}}\mu^{\mathrm{e,c}}_{\mathrm{NaCl}} - \mu^{\mathrm{c,e}}_{\mathrm{AgCl}} - t^{\mathrm{e}}_{\mathrm{Cl^-}}S^{*,\mathrm{e}}_{\mathrm{Cl^-}}\Delta_{\mathrm{e,s}}T + S^{*,\mathrm{c}}_{\mathrm{Ag^+}}\Delta_{\mathrm{s,c}}T\right] \quad (17.60)\end{aligned}$$

Entropies and transported entropies were taken constant in the integration, as usual.

The electric potential drop across the bulk phase of AgCl is given by Eq. (15.14) for zero current:

$$\Delta_{\mathrm{c}}\phi = -\frac{1}{F}S^{*,\mathrm{c}}_{\mathrm{Ag^+}}\Delta_{\mathrm{c}}T \quad (17.61)$$

The electrochemical reaction taking place between the pure phases of silver and silver chloride is given by Eq. (17.4). The contribution to the reaction Gibbs energy $\Delta_n G^{\mathrm{s,r}}$ due to the neutral components is:

$$\Delta_n G^{\mathrm{s,r}} = \mu^{\mathrm{r,c}}_{\mathrm{Ag}}\left(T^{\mathrm{s,r}}\right) \quad (17.62)$$

Analogous to the derivation of Eq. (17.60), we obtain, for the currentless potential difference

$$\begin{aligned}\Delta_{\mathrm{c,r}}\phi &= -\frac{1}{F}\left[\Delta_n G^{\mathrm{s,r}} + \frac{\pi^{\mathrm{c,r}}}{T^{\mathrm{c,r}}}\Delta_{\mathrm{c,s}}T + \frac{\pi^{\mathrm{r,c}}}{T^{\mathrm{r,c}}}\Delta_{\mathrm{s,r}}T\right] \\ &= -\frac{1}{F}\left[\mu^{\mathrm{r,c}}_{\mathrm{Ag}} + S^{*,\mathrm{c}}_{\mathrm{Ag^+}}\Delta_{\mathrm{c,s}}T - S^{*,\mathrm{r}}_{\mathrm{e^-}}\Delta_{\mathrm{s,r}}T\right] \quad (17.63)\end{aligned}$$

where the Peltier coefficients are given by

$$\pi^{\mathrm{c,r}} = T^{\mathrm{c,r}}S^{*,\mathrm{c}}_{\mathrm{Ag^+}} \quad \text{and} \quad \pi^{\mathrm{r,c}} = -T^{\mathrm{r,c}}\left(S^{\mathrm{r}}_{\mathrm{Ag}} + S^{*,\mathrm{r}}_{\mathrm{e^-}}\right) \quad (17.64)$$

The potential difference across the silver cathode for $j = 0$ is:

$$\Delta_{\mathrm{r}}\phi = \int_{\mathrm{r,c}}^{\mathrm{r.o}} d\phi = \frac{1}{F}S^{*,\mathrm{r}}_{\mathrm{e}}\Delta_{\mathrm{r}}T \quad (17.65)$$

17.2.5 *The cell potential*

By adding all contributions to the cell potential, we have the electromotive force:

$$\begin{aligned}\Delta\phi &= \Delta_{\mathrm{a}}\phi + \Delta_{\mathrm{a,e}}\phi + \Delta_{\mathrm{e}}\phi + \Delta_{\mathrm{e,c}}\phi + \Delta_{\mathrm{c}}\phi + \Delta_{\mathrm{c,r}}\phi + \Delta_{\mathrm{r}}\phi \\ &= -\frac{1}{F}\left[-\frac{1}{2}\left(\mu^{\mathrm{a,o}}_{\mathrm{Na}} + \mu^{\mathrm{a,e}}_{\mathrm{Na}}\right) + \frac{1}{2}\left(\mu^{\mathrm{e,a}}_{\mathrm{NaCl}} + \mu^{\mathrm{e,c}}_{\mathrm{NaCl}}\right) - \mu^{\mathrm{c,e}}_{\mathrm{AgCl}} + \mu^{\mathrm{r,c}}_{\mathrm{Ag}}\right] \\ &\quad - S^{*,\mathrm{a}}_{\mathrm{e^-}}\left(T^{\mathrm{s,a}} - T^{\mathrm{a,o}}\right) + S^{*,\mathrm{c}}_{\mathrm{Ag^+}}\left(T^{\mathrm{s,r}} - T^{\mathrm{s,r}}\right) - S^{*,\mathrm{r}}_{\mathrm{e^-}}\left(T^{\mathrm{r,o}} - T^{\mathrm{s,r}}\right) \\ &\quad + t^{\mathrm{e}}_{\mathrm{Na^+}} S^{*,\mathrm{e}}_{\mathrm{Na^+}}\left(\Delta_{\mathrm{s,e}}T - \frac{1}{2}\Delta_{\mathrm{e}}T\right) + t^{\mathrm{e}}_{\mathrm{Cl^-}} S^{*,\mathrm{e}}_{\mathrm{Cl^-}}\left(\frac{1}{2}\Delta_{\mathrm{e}}T - \Delta_{\mathrm{e,s}}T\right)\end{aligned} \tag{17.66}$$

In the absence of temperature differences the expression reduces to

$$\Delta\phi = -\frac{1}{F}\left[-\frac{1}{2}\left(\mu^{\mathrm{a,o}}_{\mathrm{Na}} + \mu^{\mathrm{a,e}}_{\mathrm{Na}}\right) + \frac{1}{2}\left(\mu^{\mathrm{e,a}}_{\mathrm{NaCl}} + \mu^{\mathrm{e,c}}_{\mathrm{NaCl}}\right) - \mu^{\mathrm{c,e}}_{\mathrm{AgCl}} + \mu^{\mathrm{r,c}}_{\mathrm{Ag}}\right] \tag{17.67}$$

If the amalgam is stirred it reduces to Eq. (17.26) and if the electrolyte is also stirred it reduces to Eq. (17.9).

17.3 Concluding comments

We have shown above, using one example of a formation cell, how the cell potential can be derived using non-equilibrium thermodynamics. Depending on experimental conditions, or the application in question, one can introduce various levels of precision in the formulation. These possibilities are not contained in the classical description that uses equilibrium thermodynamics.

The position dependent transference coefficient for mass transport, and the position dependent Peltier coefficient for heat transport in the electrolyte and the amalgam, were needed to arrive at the description of the cell's electromotive force. The expressions were determined by the reactions at the electrode surfaces. Therefore, they depend not only on the electrolyte, but also on the electrodes used.

We found the electric potential profile in the cell, and the cell potential in the limit of zero electric current. Temperature and concentration profiles are also attainable, but are not discussed here. The simultaneous solution of such profiles for the polymer fuel cell shall be given in Chapter 19. More complicated systems can be similarly dealt with.

This page intentionally left blank

Chapter 18

Power from Regular and Thermal Osmosis

We describe transport of heat and mass across membranes in regular osmosis and thermal osmosis. The equations are, for instance, relevant for salt power plants. It is discussed how concentration and temperature differences can be used to produce power.

Fluxes across membranes have often large coupling coefficients. We saw in Chapters 7–10 that the energy conversion efficiency of a process can be linked to the coupling between the fluxes. The larger the coupling coefficient is, the more work can be done, or the smaller is the entropy production during energy conversion. This makes membranes important for energy conversion purposes.

We consider here the coupled heat and mass transport across a membrane. Only water and heat transport are considered. This is relevant for the production of mechanical power from renewable energy sources like geothermal sources, or energy sources that have different chemical potentials of water. It is a challenge to make practical use of such opportunities, and membrane technology is one such possibility [23, 229–232]. We examine first the potential power of the energy available by mixing sea water and fresh water. We continue discussing the membrane transport processes that are needed to perform the mixing. A thermal source can also be used to give membrane transport and work. The analysis is restricted to stationary states. The possibility to use charge transport across membranes to give work is considered in Chapters 10 and 19.

18.1 The potential work of a salt power plant

Salt power plants exploit the negative Gibbs energy of mixing sea water and fresh water. At the core of the plant is a membrane separating sea

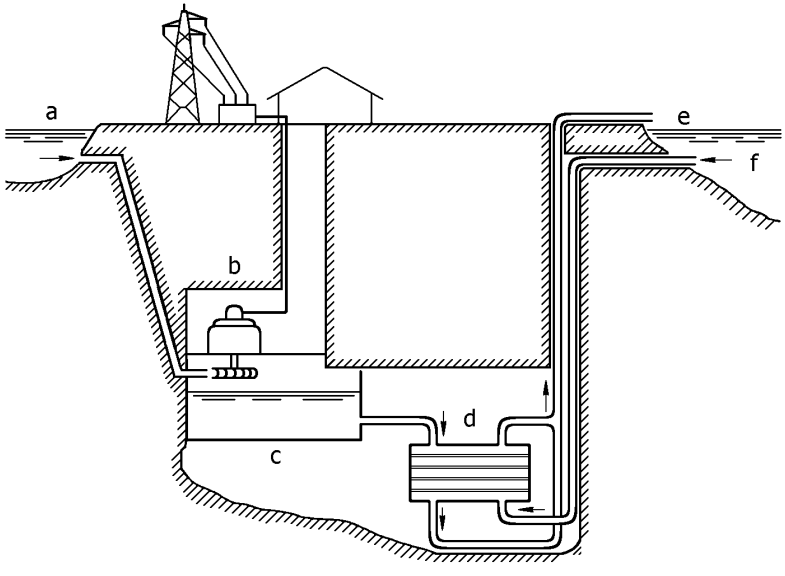

Figure 18.1 An osmotic power plant with fresh water reservior at the sea level, a, turbines, b, and fresh water reservoir at the ground level, c. The membrane module is d, e is outlet of brakish water, and f is inlet of sea water.

water and fresh water. The spontaneous tendency for the two solutions to mix leads to water transport across the membrane from the dilute to the concentrated salt solution. A hydrostatic pressure difference arises. The process can be utilized for power production [231–234]. The plant can be submersed 120 to 150 m into the ground, see Fig. 18.1. Fresh water is taken from the reservoir at a, and led through pipes to turbines at b. This is where the power is produced. The fresh water is next fed to a membrane module, d. Several membranes are framed in one modular unit, and the plant can have many of these. Sea water is led to the other side of the membrane from the sea at f. The fresh water will go through the membrane, thanks to osmosis, against a pressure difference, and reach the surface at e. The pressure on the sea water side is high, but not so high that it prevents water from moving.

Let us examine first the maximum energy that is available for power production. The Gibbs energy of mixing gives the maximum work obtainable from the process at constant temperature and pressure (see Sec. 2.4)

$$-W_{\text{ideal}} = \Delta_{\text{mix}} G \tag{18.1}$$

In the present case, the mixing process is primarily driven by the entropy of mixing, $\Delta_{\text{mix}}S$, because $\Delta_{\text{mix}}H \approx 0$. We want to estimate the order of magnitude of $T\Delta_{\text{mix}}S$. Consider therefore the mixing of one mole of pure water into an excess of salt solution (with n_{w} moles of water and n_{s} moles of salt). The pure water has molar entropy S^0_{w}. We assume that the partial molar entropy of salt, S_{s}, and water, S_{w}, remain constant during mixing. This gives

$$\begin{aligned}\Delta_{\text{mix}}S &= [(n_{\text{w}}+1)S_{\text{w}} + n_{\text{s}}S_{\text{s}}] - \left[(n_{\text{w}}S_{\text{w}} + n_{\text{s}}S_{\text{s}}) + S^0_{\text{w}}\right] = S_{\text{w}} - S^0_{\text{w}} \\ &= -R\ln\ x_{\text{w}} \end{aligned} \tag{18.2}$$

where x_w is the mole fraction of water in the saline solution, and S^0_{w} is the standard state entropy of water for $x_{\text{w}} = 1$. The water concentration in sea water is 54.9 kmol/m^3, while it is 55.6 kmol/m^3 in fresh water (when $x_{\text{w}} = 1$). This gives for sea water $x_{\text{w}} = 54.9/55.6 = 0.987$. At a temperature of 10 °C, this gives

$$\Delta_{\text{mix}}G = -T\Delta_{\text{mix}}S = RT\ln\ x_{\text{w}} = -30.1 \text{ J/mol} \quad \text{or -1.60 kJ/ kg water} \tag{18.3}$$

This means that a saline power plant can deliver maximum 1.60 kJ work per kg of water transported between the two energy levels. Or when 1 m^3/s of river water is mixed with 1 m^3/s of sea water, the maximum power attainable is 1.6 MW. The available energy corresponds to the potential energy change of lifting one m^3 of water to a height of 163 m [234]. The calculated height is the maximum depth for the position of the membrane module in Fig. 18.1. When work is extracted from the power plant, the mixture will lose some internal energy. This cooling is of the order of 0.1 °C, and is thus not significant.

In reality, not all but a fraction of the potential energy is recovered. The membrane module is not placed as low as 163 m below the fresh water intake. The plant efficiency depends on the entropy production in the various parts. The entropy production in the membrane plays an important role here.

18.2 The membrane as a barrier to transport of heat and mass

In the central part of our power producing system, the membrane is surrounded by two homogeneous phases. Membrane transport originates from concentration and/or temperature differences between these phases. As a component moves from a homogeneous phase across the interface and into the membrane, its surroundings change considerably. The equilibrium

between electrolyte solutions and ion-exchange membranes was described by Ratkje and coworkers [235–237]. An ion-exchange membrane has a high density of ionic groups, corresponding to a salt solution of 1 to 3 kmol m^{-3}, so the ion distribution within a membrane compares well to that of an ionic melt [235–237]. Ion-exchange membranes dissolve therefore a lot of water. They are mostly hydrophilic, but the Nafion membrane that is used in fuel cells has teflon containing parts (hydrophobic) in addition to ionic groups (hydrophilic).

When there is equilibrium between the membrane and both adjacent solutions, the chemical potentials of components that can be transported are constant, and so are the temperatures. Using as example, water and electrolyte NaCl, we have

$$\mu_{\mathrm{w}}^{\mathrm{l}} = \mu_{\mathrm{w}}^{\mathrm{m}} = \mu_{\mathrm{w}}^{\mathrm{r}}$$

$$\mu_{\mathrm{NaCl}}^{\mathrm{l}} = \mu_{\mathrm{NaCl}}^{\mathrm{m}} = \mu_{\mathrm{NaCl}}^{\mathrm{r}} \tag{18.4}$$

$$T^{\mathrm{l}} = T^{\mathrm{m}} = T^{\mathrm{r}} \tag{18.5}$$

The homogeneous phases next to the membrane are indicated by superscripts l and r (left and right). The membrane phase is indicated by superscript m. Take a cation-exchange membrane as example. The membrane has water and cations, say Na^+, and membrane anionic sites, denoted by M^-. Sulphonic acid groups are common for such sites. The membrane is electroneutral and Na^+ and M^- together form the compound NaM. A membrane-solution equilibrium is established after hours or days.

During transport, there is only *local* equilibrium everywhere. The equilibrium that can be established *at the membrane-solution interface*, is called the *Donnan equilibrium*. This equilibrium for the left hand side of the membrane means that

$$\mu_{\mathrm{w}}^{\mathrm{l}} = \mu_{\mathrm{w}}^{\mathrm{m,1}} \quad \text{and} \quad \mu_{\mathrm{NaCl}}^{\mathrm{l}} = \mu_{\mathrm{NaCl}}^{\mathrm{m,l}}$$
$$T^{\mathrm{l}} = T^{\mathrm{m,l}} \tag{18.6}$$

Donnan equilibria can exist on both sides. This simplifies the transport problem, as we do not need to consider the membrane surfaces as extra thermodynamic systems. We can still have $\mu_{\mathrm{i}}^{\mathrm{m,1}} \neq \mu_{\mathrm{i}}^{\mathrm{m,r}}$. When the transport of heat and mass are so rapid that there is not sufficient time to re-establish equilibrium across the interface during transport, heat or mass may accumulate near the surface. This may happen if the enthalpy of absorption of water is large. With fast water transport, and slow heat conduction, a temperature difference may arise across the surface, or across the membrane. We shall include the surface as a thermodynamic system in

our description, to prepare for such a possibility. Equation (18.6) is then not fulfilled.

Following Scatchard [238], we assume that any local state in the membrane can be characterized by an external solution in equilibrium with the membrane at that location. This means that a membrane state for NaM shall be given by $\mu^{\mathrm{m}}_{\mathrm{NaCl}}$, which is the chemical potential of NaCl in an external solution in equilibrium with the membrane. As we cannot measure $\mu^{\mathrm{m}}_{\mathrm{Na^+}}$, $\mu^{\mathrm{m}}_{\mathrm{M^-}}$ or $\mu^{\mathrm{m}}_{\mathrm{NaM}} = \mu^{\mathrm{m}}_{\mathrm{Na^+}} + \mu^{\mathrm{m}}_{\mathrm{M^-}}$, we can measure differences in $\mu^{\mathrm{m}}_{\mathrm{NaCl}}$ and this is the most adequate way to find the state of the membrane. A continuous path of integration across the membrane, equivalent to the membrane path, is therefore a sequence of *external solutions states*, in equilibrium with the real membrane. This path can be determined experimentally (see Chapter 20), and may be easier to use than the actual path for some purposes. Also in Chapter 11, we used a state in equilibrium with the actual state, rather than the actual state itself, following Førland *et al.* [27]. In the description of evaporation, we used the vapor pressure of a liquid to define the chemical potential of the liquid.

18.3 Membrane transport of heat and mass

Let us first consider the transport of heat and solvent water in more detail. There is probably a heat effect due to enthalpy difference, when water passes from the external solution to the membrane, and from the membrane to the solution again. In the stationary state, the total heat flux, J_q (but not the measurable heat flux), and the water flux, J_{w}, are constant. The total heat flux is the measurable heat fluxes plus the comoving enthalpy:

$$J_q = J'^{\mathrm{l}}_q + H^{\mathrm{l}}_{\mathrm{w}} J_{\mathrm{w}} = J'^{\mathrm{m}}_q + H^{\mathrm{m}}_{\mathrm{w}} J_{\mathrm{w}} = J'^{\mathrm{r}}_q + H^{\mathrm{r}}_{\mathrm{w}} J_{\mathrm{w}} \tag{18.7}$$

The adsorption enthalpies at the surfaces are

$$\Delta^{\mathrm{l}}_{\mathrm{ads}} H = H^{\mathrm{m,l}} - H^{\mathrm{l,m}} \text{ and } \Delta^{\mathrm{r}}_{\mathrm{ads}} H = H^{\mathrm{m,r}} - H^{\mathrm{r,m}} \tag{18.8}$$

These determine the heat effects at both surfaces. There is entropy production at the two surfaces and in the membrane. We examine the flux equations that arise from the entropy production below.

The entropy production in the membrane phase is:

$$\sigma = J'_q \frac{d}{dx}\left(\frac{1}{T}\right) + J_{\mathrm{w}}\left(-\frac{1}{T}\frac{d\mu_{\mathrm{w},T}}{dx}\right) \tag{18.9}$$

Following Chapter 8, the gradients in temperature and chemical potential can be written as:

$$\begin{aligned} \frac{dT}{dx} &= -\frac{1}{\lambda^{\mathrm{m}}}\left[J_q + q^{*,\mathrm{m}} J_{\mathrm{w}}\right] \\ \frac{d\mu_{\mathrm{w},T}}{dx} &= \frac{q^{*,\mathrm{m}}}{T}\frac{dT}{dx} - r^{\mathrm{m}} J_{\mathrm{w}} \end{aligned} \tag{18.10}$$

where $q^{*,\mathrm{m}}$ is the heat of transfer in the membrane, λ^{m} is its thermal conductivity at $J_{\mathrm{w}} = 0$, and r^{m} is the resistance to mass transport.

The differential of the chemical potential at constant temperature is $d\mu_{\mathrm{w,T}} = d\mu_{\mathrm{w}} - S_{\mathrm{w}} dT = d\mu_{\mathrm{w}}^{\mathrm{c}} + V_{\mathrm{w}} dp$ (see Appendix 3.A). When a salt dissociates into ν ions, $d\mu_{\mathrm{w}}^{\mathrm{c}} = -\nu g R T dc_{\mathrm{s}}/c_{\mathrm{w}}$, where the factor g takes care of the non-ideality of the solution, $g = 1 + d\ln\gamma_{\mathrm{s}}/d\ln c_{\mathrm{s}}$, and γ_{s} is the mean activity coefficient of the solute. This gives

$$d\mu_{\mathrm{w,T}} = -\nu g R T dc_{\mathrm{s}}/c_{\mathrm{w}} + V_{\mathrm{w}} dp \tag{18.11}$$

The first term expresses that there is an osmotic pressure difference between the solutions, the last term that there is a hydrostatic pressure difference. With identical compositions on the two sides, this reduces to $d\mu_{\mathrm{w},T} = V_{\mathrm{w}} dp$. In the absence of a pressure difference, and with ideal solutions, $d\mu_{\mathrm{w,T}} = -2RT dc_{\mathrm{s}}/c_{\mathrm{w}}$.

Following Sec. 11.1, we write the entropy production in the left hand side membrane surface:

$$\begin{aligned} \sigma^{\mathrm{s}} &= J_q'^{\mathrm{l,m}}\left(\frac{1}{T^{\mathrm{m,l}}} - \frac{1}{T^{\mathrm{l,m}}}\right) - J_{\mathrm{w}}\frac{1}{T^{\mathrm{m,l}}}\left(\mu_{\mathrm{w,T}}^{\mathrm{m,l}}\left(T^{\mathrm{m,l}}\right) - \mu_{\mathrm{w,T}}^{\mathrm{l,m}}\left(T^{\mathrm{m,l}}\right)\right) \\ &= J_q'^{\mathrm{l,m}}\Delta_{\mathrm{l,m}}\left(\frac{1}{T}\right) + J_{\mathrm{w}}\left[-\frac{1}{T^{\mathrm{m,l}}}\Delta_{\mathrm{l,m}}\mu_{\mathrm{w,T}}\left(T^{\mathrm{m,l}}\right)\right] \end{aligned} \tag{18.12}$$

The expression is analogous to Eq. (11.8). The usual terminology is used. The equimolar surface of the membrane is the frame of reference. The flux equations for the surface are similar to Eqs. (8.17)

$$\begin{aligned} \Delta_{\mathrm{l,m}} T &= -\frac{1}{\lambda^{\mathrm{s,l}}}\left(J_q'^{\mathrm{l,m}} - q^{*\mathrm{s,l}} J_{\mathrm{w}}\right) \\ \Delta_{\mathrm{l,m}}\mu_{\mathrm{w,T}}\left(T^{\mathrm{m,l}}\right) &= -\frac{q^{*\mathrm{s,l}}}{T^{\mathrm{l,m}}}\Delta_{\mathrm{l,m}} T - r^{\mathrm{s,l}} J_{\mathrm{w}} \end{aligned} \tag{18.13}$$

where the thermal conductivity for zero mass flux and the resistivity for mass flux are given by

$$\begin{aligned} \lambda^{\mathrm{s,l}} &= \frac{1}{T^{\mathrm{l,m}} T^{\mathrm{m,l}}} \left(l^{\mathrm{s,l}}_{\mathrm{mm}} - \frac{l^{\mathrm{s,l}}_{\mathrm{mw}} l^{\mathrm{s,l}}_{\mathrm{wm}}}{l^{\mathrm{s,l}}_{\mathrm{ww}}} \right) \\ r^{\mathrm{s,l}} &= \frac{T^{\mathrm{m,l}}}{l^{\mathrm{s,l}}_{\mathrm{ww}}} \end{aligned} \tag{18.14}$$

and the measurable transported heat of the left surface by

$$q^{*\mathrm{s,l}} = \left(\frac{J^{\prime \mathrm{l,m}}_q}{J_{\mathrm{w}}} \right)_{\Delta_{\mathrm{l,m}} T = 0} = \frac{l^{\mathrm{s,l}}_{\mathrm{mw}}}{l^{\mathrm{s,l}}_{\mathrm{ww}}} \tag{18.15}$$

The equations for the right hand side of the membrane surface are similar. These shall now be used to describe osmosis and thermal osmosis.

18.4 Osmosis

When the thermal conductivity of the system is high, and the solutions have the same temperature, one may expect isothermal conditions. The water flux becomes:

$$\begin{aligned} \Delta_{\mathrm{l,m}} \mu_{\mathrm{w}} &= -r^{\mathrm{s,l}} J_{\mathrm{w}} \\ \frac{d\mu_{\mathrm{w}}}{dx} &= -r^{\mathrm{m}} J_{\mathrm{w}} \\ \Delta_{\mathrm{m,r}} \mu_{\mathrm{w}} &= -r^{\mathrm{s,r}} J_{\mathrm{w}} \end{aligned} \tag{18.16}$$

We obtain a jump in chemical potential at the surfaces and a gradual change across the membrane. When r^{m} is constant, the chemical potential of water is a linear function of position across the membrane. The chemical potential of water on the left side is $\mu^{\mathrm{l,m}}_{\mathrm{w}}$, and on the right side, $\mu^{\mathrm{r,m}}_{\mathrm{w}}$. When the water flux is constant, the difference is:

$$\mu^{\mathrm{r,m}}_{\mathrm{w}} - \mu^{\mathrm{l,m}}_{\mathrm{w}} = -\left(r^{\mathrm{s,l}} + r^{\mathrm{m}} d_{\mathrm{m}} + r^{\mathrm{s,r}} \right) J_{\mathrm{w}} = \overline{r^{\mathrm{m}}} d_{\mathrm{m}} J_{\mathrm{w}} \tag{18.17}$$

where d_{m} is the thickness and $\overline{r^{\mathrm{m}}} = \left(r^{\mathrm{s,l}} + r^{\mathrm{m}} d_{\mathrm{m}} + r^{\mathrm{s,r}} \right)$ is the average resistivity of membrane plus surfaces. A symmetric membrane has $r^{\mathrm{s,l}} = r^{\mathrm{s,r}}$. When these coefficients are small, the surfaces pose no barrier to transport. Some filter-membranes are asymmetric and have $r^{\mathrm{s,l}} >> r^{\mathrm{m}} d_{\mathrm{m}}$. Accordingly, there can be a jump in μ_{w} at this surface. Equilibrium means that $J_{\mathrm{w}} = 0$.

The osmotic pressure, Π, of a solution is the *excess* pressure which must be placed on the solution in order to prevent any diffusion of solvent through

the membrane. The chemical potential obeys $d\mu_{\rm w}^{\rm c} + V_{\rm w} dp = 0$, giving

$$\Pi_{J_{\rm w}=0} \equiv \left(p^{\rm c} - p^{\rm a}\right)_{J_{\rm w}=0} = \frac{\nu g R T}{V_{\rm w} c_{\rm w}} \left(c_{\rm s}^{r} - c_{\rm s}^{1}\right) \tag{18.18}$$

This equation was integrated with constant $c_{\rm w}$. A concentration difference $\Delta c_{\rm s} = c_{\rm s}^{r} - c_{\rm s}^{1} = (100-1)\text{mol/m}^3$ HCl, gives an osmotic pressure of 8.8 N/m^2 at 300 K. More precise integrations for membranes with more components were presented by Holt *et al.* [239].

The osmotic pressure of a solution is the pressure at which the solution would be in equilibrium with the pure solvent. It must *not* be confused with the hydrostatic pressure exerted by the solution. The difference between the osmotic pressure and the hydrostatic pressure drives solvent through the membrane [23].

The average resistivity to diffusion, $\overline{r^{\rm m}}$, can be found from an experiment with $dp/dx = 0$. The water flux is:

$$J_{\rm w} = \left(\frac{J_V}{V_{\rm w}}\right)_{dp=0} = -\frac{\Delta \mu_{\rm w}^{\rm c}}{\overline{r^{\rm m}} d_{\rm m}} = -\frac{\nu g R T}{\overline{r^{\rm m}} c_{\rm w}} \frac{\Delta c_{\rm s}}{d_{\rm m}} \tag{18.19}$$

J_V is measured, and $\overline{r^{\rm m}}$ is calculated for given concentrations, $V_{\rm w}$, and membrane thickness $d_{\rm m}$. The resistivity to water diffusion in an ion-exchange membrane depends on the ions that occupy the ionic sites. For the cation exchange membrane Aciplex K-181, Nummedal [240] calculated $\overline{r^{\rm m}} = 4.2 \times 10^7$, 9.1×10^7, 7.7×10^7 and 7.1^7 Wm mol^{-2} for the hydrogen, lithium, sodium and potassium forms of the membrane, respectively [241]. The membrane was 9.4×10^{-5} m thick.

Exercise 18.4.1. *In reverse osmosis, water is forced through the membrane to the dilute side by applying a pressure difference that is larger than the osmotic pressure to the salt solution. Calculate the pressure needed to produce fresh water from salt water (NaCl) at 300 K. A volume flux of $J_V = 1.8 \times 10^{-7}$ $m^3/\ m^2 s$ should be produced to meet the needs of the local community. The molar volume of water is 18×10^{-6} m^3/mol. The salt concentration difference for NaCl is $\Delta c_s = -0.05$ mol/m^3, $c_w = 55.6$ $kmol/m^3$, the membrane thickness is 10^{-4} m, and $\overline{r^m} = 7.7 \times 10^7$ $Ws\ mol^{-2}$.*

- **Solution:** The pressure difference is from Eq. (18.18):

$$\Delta p = p^{\rm r} - p^{\rm l} = -\frac{2RT}{c_{\rm w} V_{\rm w}} \Delta c_{\rm s} + \frac{J_{\rm w}}{V_{\rm w}} \overline{r^{\rm m}} d_{\rm m}$$

  We have used $g = 1, \nu = 2$ in the expression for the chemical potential. By introducing appropriate numbers, $\Delta p = 2.4 \times 10^6$ Pa $= 24$ bar. The last term dominates.

18.5 Thermal osmosis

The coupling between the mass flux and the heat flux means that a mass flux may lead to a temperature difference across the membrane, or vice versa, a temperature difference may lead to a mass flux.

The equations to be solved for the chemical potential profile, for mass transport due to temperature differences across the ion-exchange membrane, is:

$$\begin{aligned}\Delta_{\mathrm{a,m}}\mu_{\mathrm{w}} &= -r^{\mathrm{s,a}}J_{\mathrm{w}} + q^{*,\mathrm{s,a}}\frac{\Delta_{\mathrm{a,m}}T}{T^{\mathrm{m,1}}}\\ \frac{d\mu_{\mathrm{w}}}{dx} &= -r^{\mathrm{m}}J_{\mathrm{w}} + q^{*,\mathrm{s,m}}\frac{1}{T}\frac{dT}{dx}\\ \Delta_{\mathrm{m,c}}\mu_{\mathrm{w}} &= -r^{\mathrm{s,c}}J_{\mathrm{w}} + q^{*,\mathrm{s,c}}\frac{\Delta_{\mathrm{m,c}}T}{T^{\mathrm{m,c}}}\end{aligned} \tag{18.20}$$

Because of the symmetry of the problem, the heats of transfer are equal in magnitude, $q^{*,\mathrm{s,a}} = q^{*,\mathrm{s,c}} = q^{*,\mathrm{s}}$. According to the development in Chapter 11 on evaporation and condensation, this coefficient is sizable, a fraction of the enthalpy of the phase transition.

$$q^{*,\mathrm{s}} = -k\Delta_{\mathrm{ads}}H \tag{18.21}$$

In the stationary state, J_{w} is constant, and the chemical potential difference across the membrane is

$$\mu_{\mathrm{w}}^{\mathrm{c}} - \mu_{\mathrm{w}}^{\mathrm{a}} = -\overline{r_{\mathrm{w}}}J_{\mathrm{w}} + q^{*,\mathrm{s}}\left(\frac{\Delta_{\mathrm{a,m}}T}{T^{\mathrm{m,1}}} + \frac{\Delta_{\mathrm{m,c}}T}{T^{\mathrm{m,2}}}\right) + q^{*,\mathrm{m}}\int_{T^{\mathrm{m,a}}}^{T^{\mathrm{m,c}}}\frac{dT}{T} \tag{18.22}$$

A volume flux can arise from the temperature difference between the two sides, even if the concentrations on the two sides are the same, in contrast to the situation described by Eq. (18.17). This is *thermal osmosis*, see Katchalsky and Curran [23]. The thermal osmotic pressure of the solution on the right hand side relative to the pressure on the left hand side, is the excess pressure that must be placed on this side to obtain a balance of forces characterized by $J_{\mathrm{w}} = 0$:

$$\Pi_{J_{\mathrm{w}}=0} \equiv \left(p^{\mathrm{r}} - p^{1}\right)_{J_{\mathrm{w}}=0} = \frac{q^{*,\mathrm{s}}}{V_{\mathrm{w}}}\left(\frac{\Delta_{\mathrm{a,m}}T}{T^{\mathrm{m,a}}} + \frac{\Delta_{\mathrm{m,c}}T}{T^{\mathrm{c,m}}}\right) + \frac{q^{*,\mathrm{m}}}{V_{\mathrm{w}}}\int_{T^{\mathrm{m,a}}}^{T^{\mathrm{sm,c}}}\frac{dT}{T} \tag{18.23}$$

Observations of increased pressure have been made in nature when the temperature on the surface falls below 0°C. In arctic regions that have a sustained temperature gradient in a porous ground, one has observed transport of undercooled water [27, 242]. This phenomenon, which is called frost

heave, can lead to a considerable pressure difference, up to 11 bar/K [27]. The coupling of mass transport to a thermal driving force may also explain the swelling of a porous electrode in the aluminium electrolysis caused by salt transport into the electrode, which is exposed to a temperature gradient [243,244]. Katchalsky and Curran [23] speculated on the importance of small ΔT and Π in biological systems.

We see from Eq. (18.23) that the sign and magnitude of the thermal osmotic pressure is determined by the sign and magnitude of the heats of transfer. Consider the situation where the membrane conducts well, and the surfaces conduct badly. The last term can then be neglected. The other extreme possibility is that the surface temperature drops are negligible. The last term will then dominate. While the normal osmotic pressure is an equilibrium property, the pressure that arise during thermal osmosis depends on the value of the coupling coefficients. The balance of forces is called Soret equilibrium.

The profile in temperature and chemical potential across the membrane was calculated for the Aciplex cation-exchange membrane K-181 in its KM form [241], using different values of $r_{qq}^{\mathrm{s,a}} = r_{qq}^{\mathrm{s,c}} = r_{qq}^{\mathrm{m}}/k$ and $q^{*,\mathrm{m}}$, and assuming $q^{*,\mathrm{s}} = 0$ [240]. The results of the calculation are shown in Figs. 18.2 and 18.3. The temperature profile was calculated from:

$$\begin{aligned} T^{\mathrm{m,l}} - T^{\mathrm{l,m}} &= -r_{qq}^{\mathrm{s,l}} \left(J_q'^{\mathrm{m,l}} - q^{*,\mathrm{s}} J_{\mathrm{w}} \right) \\ dT/dx &= -r_{qq}^{\mathrm{m}} \left(J_q'^{\mathrm{m}} - q^{*,\mathrm{m}} J_{\mathrm{w}} \right) \\ T^{\mathrm{r,m}} - T^{\mathrm{m,r}} &= -r_{qq}^{\mathrm{s,r}} \left(J_q'^{\mathrm{m,r}} - q^{*,\mathrm{s}} J_{\mathrm{w}} \right) \end{aligned} \tag{18.24}$$

The thermal conductivity λ^{m} was estimated as a weighted combination of the matrix conductivity (0.2 W/m K) and the conductivity of the water phase (0.6 W/m K) and

$$r_{qq}^{\mathrm{m}} = 1/\lambda^{\mathrm{m}} \tag{18.25}$$

A few percent variation in λ^{m} can be expected when K^+ is replaced by another cation. The surface resistivity was the membrane resistivity scaled by a factor k, where $k = 1$ means that there is no excess resistance in the surface over that in a comparable length of the membrane [240]. The results for the membrane in the K^+-form are shown (see Figs. 18.2 and 18.3)

We see a linear variation in the chemical potential of water (Fig. 18.3) as well as in the temperature across the membrane (Fig. 18.2). As soon as the surface thermal resistance becomes significant compared to the bulk resistance, there are jumps in the intensive variables at the surface. A large percentage of the total temperature drop may occur here if the thermal conductivity becomes very low, cf. Eqs. (18.24) The jumps in $\mu_{w,T}$ are according to Eqs. (18.22).

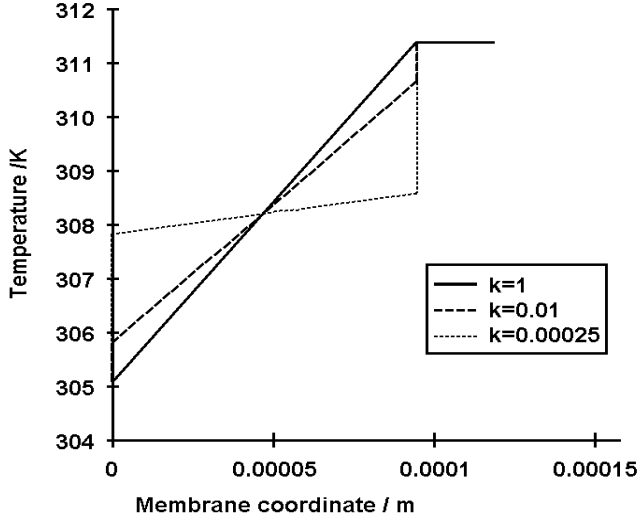

Figure 18.2 The variation in temperature across a symmetric cation exchange membrane during thermal osmosis [240]. For boundary conditions, see the text.

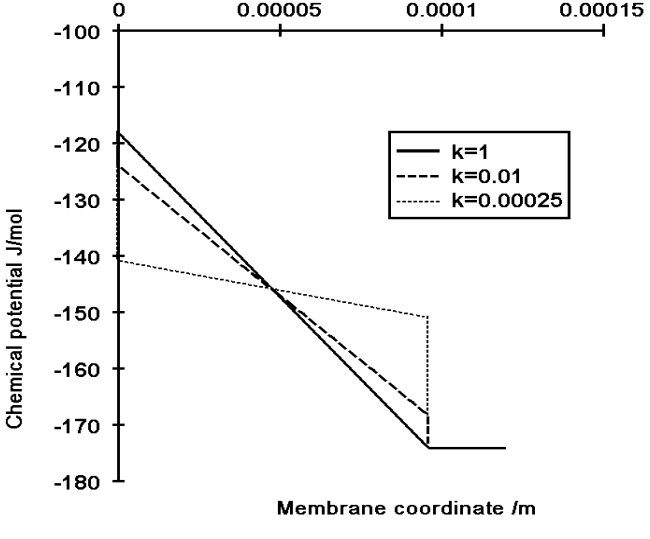

Figure 18.3 The variation in chemical potential across a symmetric cation exchange membrane corresponding to the figure above [240].

Exercise 18.5.1. *A 9 mm stack of cation exchange membranes has solutions of HCl on both sides. There is a temperature difference of 6.5 K at 300 K across the stack. Calculate the thermo-osmotic pressure, when the heat of transfer for the membrane is $q^{*,m} = -2$ kJ/mol. Assume equilibrium across the surfaces.*

- **Solution:** With equilibrium at the membrane surfaces, and $J_{\rm w} = 0$, $dT/dx = \Delta T/d_{\rm m}$, the pressure difference is, accordingly,

$$\Pi_{J_{\rm w}=0} \equiv \left(p^{\rm r} - p^{\rm l}\right)_{J_{\rm w}=0} = \frac{q^{*,{\rm m}}}{V_{\rm w}} \int_{T^{\rm s,l}}^{T^{\rm s,r}} \frac{dT}{T} \simeq \frac{q^{*,{\rm m}}}{V_{\rm w}} \frac{\Delta T}{\overline{T}}$$

$$= -\frac{2000 \text{ Nm}}{18\ 10^{-6}\text{m}^3} \frac{6.5}{300}$$

$$= -2.4 \times 10^6 \text{ Pa} = -24.1 \text{ bar}$$

The positive temperature difference leads to water accumulation on the left hand side. We see that even a modest heat of transfer can give a substantial pressure rise.

Chapter 19

Modeling the Polymer Electrolyte Fuel Cell

The heterogeneous polymer electrolyte fuel cell is described by sets of equations for its five subsystems. The transport equations are solved for a one-dimensional cell at stationary state. Information is obtained about the concentration profiles, temperature profiles and electric potential profiles across the cell. The local entropy production as well as total entropy production is described. Peltier coefficients and heats of transfer are essential for a consistent description.

The polymer membrane fuel cell converts hydrogen and oxygen to water and electric work. The anode surface reaction is

$$\frac{1}{2}\mathrm{H_2(g)} \rightarrow \mathrm{H^+} + e^- \tag{19.1}$$

while the cathode surface reaction is

$$\frac{1}{4}\mathrm{O_2(g)} + \mathrm{H^+} + e^- \rightarrow \frac{1}{2}\mathrm{H_2O(l)} \tag{19.2}$$

The gases are humid, and t_w^m moles of water is transferred through the membrane per mole of protons transferred. The overall cell reaction becomes

$$\frac{1}{2}\mathrm{H_2(g)} + \frac{1}{4}\mathrm{O_2(g)} + \mathrm{t_w^m H_2O(l)} \rightarrow \left(\mathrm{t_w^m} + \frac{1}{2}\right)\mathrm{H_2O(l)} \tag{19.3}$$

A fuel cell is also a heat producer. This makes them interesting to be used in households where both work and heat are needed. We shall now calculate the electric potential profile of the cell and the corresponding heat effects during stationary cell operation, see also [25, 245–247].

19.1 The potential work of a fuel cell

An overall perspective on the cell performance gives the distribution of heat and work. The maximum work done by a process from the reactants' state to the products' state is, according to Sec. 2.4 equal to:

$$-W_{\text{ideal}} = \Delta_r U + p_0 \Delta_r V - T_0 \Delta_r S \tag{19.4}$$

where the pressure and temperature of the surroundings are $p_0 = 1$ bar and $T_0 = 298$ K. Subscript r refers to the cell reaction, and U, V and S have their usual meanings. At one bar, $-W_{\text{ideal}} = \Delta_r H - T_0 \Delta_r S$. We can calculate the maximum work from the reaction for 1 bar and 340 K with the data in Table 19.1. The enthalpy of formation of a component

Table 19.1 Standard thermodynamic data for fuel cell components at 298 K [248].

Component	$\Delta_f H^0$/ kJ/mol	S^0/ J/K mol	c_P^0/ J/K mol
H_2	0	131	29
O_2	0	205	29
H_2O(l)	−285	70	75
H_2O(g)	−242	189	34

i is $H_i = H_i^0 + c_{P,i}(T - T_0)$, where H_i is the partial molar enthalpy of i, and H_i^0 is the standard enthalpy. The partial molar entropy is $S_i = S_i^0 + c_{P,i} \ln T/T_0$, where S_i^0 is the standard entropy. This gives for the reaction at 340 K: $\Delta_r H = \frac{1}{2}(-284 - 1) - \frac{1}{4} \cdot 1 = -142$ kJ/mol and $\Delta_r S = \frac{1}{2}(74 - 135) - \frac{1}{4}210 = -82.5$ J/K mol. The maximum work from the system becomes $-W_{\text{ideal}}(p_0, 340K) = 117.4$ kJ/mol. The maximum work decreases as the temperature increases, because $\Delta c_{P,i}(T - T_0) > \Delta c_{P,i} T_0 \ln T/T_0$. The open circuit potential, E, (the emf) is the limit of E when $j \to 0$, where j is the electric current density. The emf is given by Nernst equation, $(EF)_{j \to 0} = -\Delta_r G = -\Delta_r H + T \Delta_r S$ when T is constant.

The cell dissipates much of the potential work as heat when a current is drawn from the cell. The lost work is the entropy production times T_0:

$$\frac{dW_{lost}}{dt} = T_0 \frac{dS_{irr}}{dt} = T_0 \frac{d}{dt}(\Delta S_0 + \Delta_r S) \tag{19.5}$$

Here, ΔS_0 is the entropy change in the surroundings during operation. The lost work is zero when $\Delta S_0 + \Delta_r S = 0$, and the process is reversible.

Because $\Delta_r S < 0$ and $\Delta S_0 > 0$, there is a positive heat effect in the surroundings during reversible operation. The lost work, or the dissipation of energy as heat, varies with the electric current that is drawn from the cell. Already at moderate current densities, the cell's potential is halved, its power is reduced accordingly, and the heat production in the environment is significant.

We shall use the method developed in the previous chapters to find the fluxes of heat and mass through the system that accompany a particular constant electric current density. We shall calculate concentration profiles, temperature profiles and electric potential profiles across the cell, as well as the local and total entropy production for three choices of j, as was done in [245].

19.2 The cell and its five subsystems

It is well known that most of the dissipation of energy in a fuel cell takes place at the electrode surfaces. The reactions at these surfaces are also the origin of the electric potential of the cell. It is thus natural to divide the heterogeneous cell into five subsystems; where these two surfaces are central. They are sandwiched between three bulk phases.

The series of five subsystems is illustrated in Fig. 19.1. The central section (labeled 1) is a proton-conducting, water-containing membrane. The membrane has an anode surface to the left, and a cathode surface to the right (labeled 2). The close-up of one electrode surface shows how the catalyst particles cluster in a carbon and polymer-containing matrix. The outer sections, labeled 3, are porous carbon matrices for transport of heat, electrons and gas. The gas arrives at the surfaces along the pore walls, see Chapter 21), while the charge transport takes place in the solid part of the matrix.

We shall solve equations for a unit of cross-sectional area of these layers, using experimental data for a polymer electrolyte fuel cell with a Nafion 115 membrane [245,247,249] and electric current densities of 500, 2500 and 5000 A/m^2. The set of equations can be solved using an initial guess of a constant water flux. The thicknesses of the backing, surface and membrane were 180, 10 and 127 μm, respectively. Thermodynamic data are given in Table 19.1. Transport data for all five subsystems are summarized in Table 19.2. The graphite resistivities were $r^a = r^c = 10^{-4}$ ohm m [249]. The thermal conductivities, $\lambda^a = \lambda^c = 1$ W/K m, were estimated from the thermal conductivity of porous graphite. The effective binary diffusion coefficients, D_{wH} and D_{ON}, were set to 5×10^{-5} m^2 s^{-1}.

In the stationary state, the mass fluxes are given by the electric current density j:

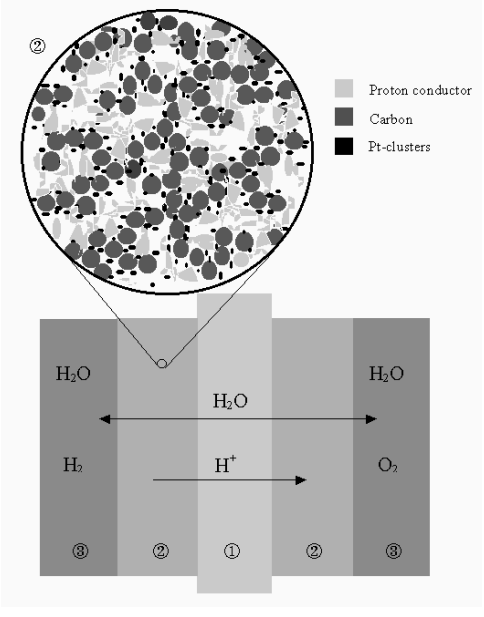

Figure 19.1 A schematic picture of the polymer electrolyte fuel cell. The water-filled membrane (1), the electrode surfaces (2) and the porous carbon matrix that constitute the electrode backings (3) are shown. The agglomerate structure of the electrode surface is illustrated by the close-up. Courtesy of S. Møller-Holst.

Table 19.2 Transport properties used in the calculations

Transport property	Dimension	Value
$r^a = r^c$	ohm m	10^{-4}
$r^{s,a} = r^{s,c}$	ohm m^2	7.2×10^{-6}
λ^m	W/Km	0.2
$\lambda^a = \lambda^c$	W/Km	1
$\lambda^{s,a} = \lambda^{s,c}$	W/Km^2	10^3
$D_{wH} = D_{ON}$	m^2/s	5×10^{-5}
D_m	m^2/s	1.5×10^{-10}
j_0	A/m^2	2.5×10^{-3}
t_w^m		1.2
$q^{*,i}$	J/mol	$-TS^i$

$$J_{\mathrm{H}_2} = \frac{j}{2F}$$
$$J_{\mathrm{O}_2} = -\frac{j}{4F} \tag{19.6}$$

where F is Faraday's constant. There is a constant flux of water J_w^a across the anode backing and anode surface that keeps the membrane from drying out. The fluxes refer to the whole membrane area, even if the actual transport takes place across a smaller area, the cross-sectional area of all the pores. Positive direction of transport is from the anode to the cathode. We limit ourselves to transports in one direction across the cell in the calculation. The water balance for the cell gives:

$$J_w^{\mathrm{c}} = J_w^{\mathrm{a}} + \frac{j}{2F} \tag{19.7}$$

We proceed to give the entropy production for three bulk subsystems, the two surfaces and the corresponding flux equations. The gas pressure is everywhere constant.

19.3 The electrode backing and the membrane

19.3.1 *The entropy production in the homogeneous phases*

Consider first the three bulk phases, Secs. 3 and 1 in Fig. 19.1, in the stationary state. The anode has two component fluxes; hydrogen and water. The entropy production rate in the anode backing is

$$\sigma^a = J_q' \frac{d}{dx}\left(\frac{1}{T}\right) - J_D^a \frac{1}{T}\frac{d\mu_{w,T}}{dx} - j\frac{1}{T}\frac{d\phi}{dx} \tag{19.8}$$

with the interdiffusion flux of water and hydrogen

$$J_D^a = \left(\frac{J_w}{x_w} - \frac{J_{H_2}}{x_{H_2}}\right) x_w \tag{19.9}$$

Here, we have used $x_w d\mu_{w,T} + x_{\mathrm{H}_2} d\mu_{\mathrm{H}_2,\mathrm{T}} = 0$.

For the membrane we have:

$$\sigma^m = J_q'^m \frac{d}{dx}\left(\frac{1}{T}\right) - J_w^m \frac{1}{T}\frac{d\mu_{w,T}}{dx} - j\frac{1}{T}\frac{d\phi}{dx} \tag{19.10}$$

The only component flux in the membrane is the water flux. Superscript m stands for membrane, and a and c for anode and cathode, respectively.

The cathode backing has three component fluxes; oxygen, water and nitrogen. The entropy production is:

$$\sigma^c = J'_q \frac{d}{dx}\left(\frac{1}{T}\right) - J^c_w \frac{1}{T}\frac{d\mu_{w,T}}{dx} - J_{O_2}\frac{1}{T}\frac{d\mu_{O_2,T}}{dx} - J_{N_2}\frac{1}{T}\frac{d\mu_{N_2,T}}{dx} - j\frac{1}{T}\frac{d\phi}{dx} \tag{19.11}$$

The flux of nitrogen in the cathode backing is zero. It is common to assume that the chemical potential gradient of water is zero. For our purpose, the entropy production in the cathode backing may then be written as:

$$\sigma^c = J'_q \frac{d}{dx}\left(\frac{1}{T}\right) - J^c_{O_2}\frac{1}{T}\frac{d\mu_{O_2,T}}{dx} - j\frac{1}{T}\frac{d\phi}{dx} \tag{19.12}$$

The linear flux-force relations that follow from Eqs. (19.8), (19.10) and (19.12) are

$$\begin{aligned} J'_q &= L_{qq}\frac{d}{dx}\left(\frac{1}{T}\right) - L_{q\mu}\frac{1}{T}\frac{d\mu_T}{dx} - L_{q\phi}\frac{1}{T}\frac{d\phi}{dx} \\ J &= L_{\mu q}\frac{d}{dx}\left(\frac{1}{T}\right) - L_{\mu\mu}\frac{1}{T}\frac{d\mu_T}{dx} - L_{\mu\phi}\frac{1}{T}\frac{d\phi}{dx} \\ j &= L_{\phi q}\frac{d}{dx}\left(\frac{1}{T}\right) - L_{\phi\mu}\frac{1}{T}\frac{d\mu_T}{dx} - L_{\phi\phi}\frac{1}{T}\frac{d\phi}{dx} \end{aligned} \tag{19.13}$$

where J is $J^c_{O_2}$, J^a_D, or J^m_w and μ_T is $\mu_{O_2,T}$ or $\mu_{w,T}$. Furthermore, L_{ij} are phenomenological coefficients. We rewrite the set of equations, by eliminating the electric potential gradient in the heat and mass fluxes. This gives:

$$\begin{aligned} J'_q &= l_{qq}\frac{d}{dx}\left(\frac{1}{T}\right) - l_{q\mu}\frac{1}{T}\frac{d\mu_T}{dx} + \frac{L_{q\phi}}{L_{\phi\phi}}j \\ J &= l_{\mu q}\frac{d}{dx}\left(\frac{1}{T}\right) - l_{\mu\mu}\frac{1}{T}\frac{d\mu_T}{dx} + \frac{L_{\mu\phi}}{L_{\phi\phi}}j \\ j &= L_{\phi q}\frac{d}{dx}\left(\frac{1}{T}\right) - L_{\phi\mu}\frac{1}{T}\frac{d\mu_T}{dx} - L_{\phi\phi}\frac{1}{T}\frac{d\phi}{dx} \end{aligned} \tag{19.14}$$

The coefficients are related by

$$l_{ij} = L_{ij} - \frac{L_{\phi i}L_{j\phi}}{L_{\phi\phi}} \tag{19.15}$$

The appropriate transference coefficient is

$$t = \left(\frac{J}{j/F}\right)_{d\mu_T=0, dT=0} = F\frac{L_{\mu\phi}}{L_{\phi\phi}} \tag{19.16}$$

The Peltier coefficient is

$$\pi = \left(\frac{J'_q}{j/F}\right)_{d\mu_T=0, dT=0} = F\frac{L_{q\phi}}{L_{\phi\phi}} \tag{19.17}$$

and the measurable heat of transfer

$$q^* = \left(\frac{J'_q}{J}\right)_{j=0, dT=0} = \frac{l_{q\mu}}{l_{\mu\mu}} \tag{19.18}$$

We introduce these definitions into the last set of flux equations, solve the expression for the gradient in chemical potential, and introduce the expression for $d\mu_T/dx$ into the heat flux. Equation 19.14 becomes

$$\begin{aligned}
\frac{dT}{dx} &= -\frac{1}{\lambda}\left[J'_q - q^*\left(J - t\frac{j}{F}\right) - \pi\frac{j}{F}\right] \\
\frac{d\mu_T}{dx} &= -\frac{q^*}{T}\frac{dT}{dx} - \frac{1}{l_{\mu\mu}}\left(J - t\frac{j}{F}\right) \\
\frac{d\phi}{dx} &= -\frac{\pi}{TF}\frac{dT}{dx} - \frac{t}{F}\frac{d\mu_T}{dx} - rj
\end{aligned} \tag{19.19}$$

where the stationary state thermal conductivity, λ, the mass transfer coefficient $l_{\mu\mu}$ (on a mole fraction basis) and the resistivity r are:

$$\begin{aligned}
\lambda &= \frac{l_{qq}}{T^2} - (q^*)^2\frac{l_{\mu\mu}}{T^2} \\
l_{\mu\mu} &= \frac{Dx}{RT} \\
r &= T/L_{\phi\phi}
\end{aligned} \tag{19.20}$$

Here, D is the appropriate diffusion coefficient and r is the electric resistivity. The variables have their specific meaning in the various subsystems of the cell, and this shall be specified below.

19.3.2 *The anode backing*

The anode backing has transport of heat, hydrogen, water and charge. Hydrogen and water are transported in the pores of the backing at constant pressure, p. The transport of charge and heat takes place in the solid materials of the backing. We introduce the expression for the chemical

potential of water $\mu = \mu^0 + RT \ln x_w / x_w^*$, where x_w^* is the mole fraction at saturation. The result is

$$\begin{aligned}
\frac{dT}{dx} &= -\frac{1}{\lambda^a}\left[J_q'^a + q^{*,a}\left(J_D^a - t_D^a \frac{j}{F}\right) + \pi^a \frac{j}{F}\right] \\
\frac{dx_w}{dx} &= -\frac{q^{*,a} x_w}{RT^2}\frac{dT}{dx} - \frac{1}{D_{wH}}\left(J_D^a - t_D^a \frac{j}{F}\right) \\
\frac{d\phi}{dx} &= -\frac{\pi^a}{TF}\frac{dT}{dx} - \frac{t_D^a RT}{F x_w}\frac{dx_w}{dx} - r^a j
\end{aligned} \tag{19.21}$$

Equation (19.21a) has three contributions to the temperature gradient. When the current density is large, the last contribution is significant compared to the Fourier type contribution and the contribution from the water flux. Likewise, there is a contribution to the gradient in the mole fraction of water from the temperature gradient, but this contribution is not significant in magnitude. The electric potential gradient does not only have an ohmic contribution, $-r^a j$. The other two contributions here are small, but they are needed to satisfy the second law.

The mole fraction of water is calculated from the partial pressure of water and the total pressure, $x_w = p_w/p^0$. At the left side boundary, the mole fraction is $x_w^0 = p_w^{*,a}/p^0$, given by the saturation pressure at the temperature of this location, $p^*(T^a)$. The three main coefficients and the three coupling coefficients characterize the transport of heat, mass and charge through the backing. The Peltier heat of the anode is:

$$\frac{\pi^a}{T} = -\frac{1}{2}S_{\mathrm{H_2}} - S_{e^-}^* \tag{19.22}$$

where the transported entropy of electrons in carbon, $S_{e^-}^*$, is -2 J/K [190]. In Sec. 19.5, we show that a possible choice for the heat of transfer of water is:

$$q^{*,a} = -T S_w^a \tag{19.23}$$

The six transport coefficients for the anode backing were used to solve Eqs. (19.21) and the energy balance:

$$\frac{d}{dx}J_u = \frac{d}{dx}J_q'^a + j\frac{d\phi}{dx} + J_{\mathrm{H_2}}\frac{dH_{\mathrm{H_2}}}{dx} + J_w^a \frac{dH_w}{dx} = 0 \tag{19.24}$$

Here, J_u is the constant energy flux through the backing, and $dH_i/dx = C_{p,i}\,(dT/dx)$. The equations were solved with boundary pressures for hydrogen and oxygen of $p = 1,013 \times 10^5$ Pa and $0.21p$, respectively. Temperatures at the boundaries were 340 K. The outcome of the calculation for all five subsystems is illustrated in Figs. 19.2, 19.3 and 19.4.

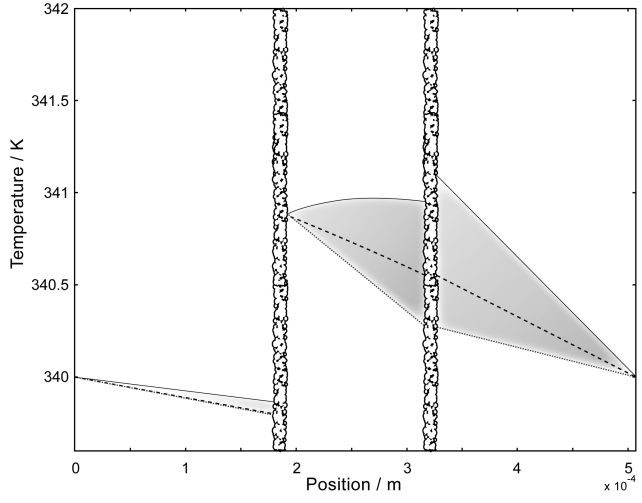

Figure 19.2 The temperature profile across the cell as a function of current densities 500, 2500 and 5000 A/m^2. The highest current density gives the highest curves.

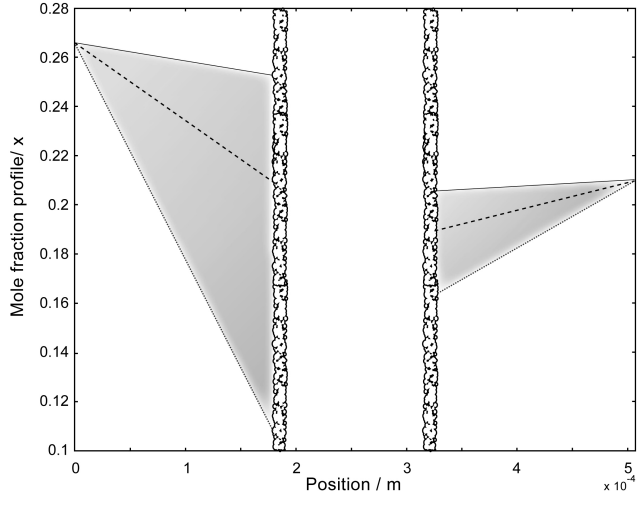

Figure 19.3 The mole fraction profile of water (left) and oxygen (right) as a function of current densities 500, 2500 and 5000 A/m^2. The highest current density gives the lowest curve.

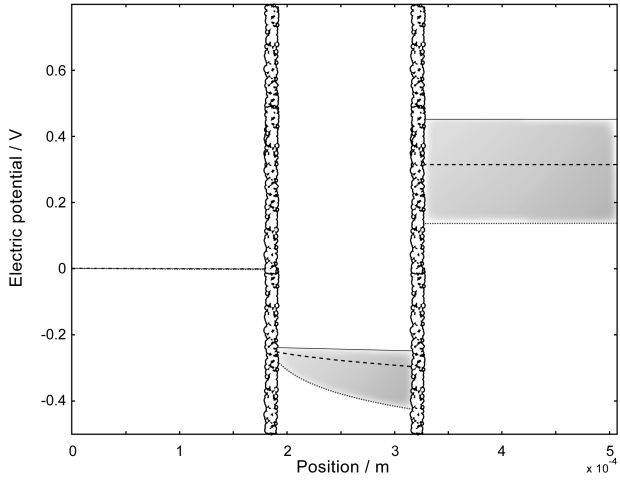

Figure 19.4 The electric potential profile across the cell as a function of current densities 500, 2500 and 5000 A/m^2. The highest current density gives the lowest curve.

The temperature profile in the anode backing has a negative slope in Fig. 19.2, meaning that the coupling terms dominate since the heat flux is negative. The mole fraction profiles show a sinking concentration of water on the left hand side in Fig. 19.3. The higher the current density, the bigger is the slope of this profile. There is a negligible change in the electric potential in the backing in Fig. 19.4, corresponding to a small resistivity, small temperature differences and a relatively small variation in chemical potential of hydrogen. We return to the figures when we describe the other sections of the cell.

19.3.3 *The membrane*

The transport equations (19.19) for the membrane are:

$$\begin{aligned}
\frac{dT}{dx} &= -\frac{1}{\lambda^m}\left[J_q'^{,m} - q^{*,m}(J_w^m - t_w^m\frac{j}{F}) - \pi^m\frac{j}{F}\right] \\
\frac{d\mu_{w,T}}{dx} &= -\frac{q^{*,m}}{T}\frac{dT}{dx} - \frac{1}{l_{\mu\mu}^m}\left(J_w^m - t_w^m\frac{j}{F}\right) \\
\frac{d\phi}{dx} &= -\frac{\pi^m}{TF}\frac{dT}{dx} - \frac{t_w^m}{F}\frac{d\mu_{w,T}}{dx} - r^m j
\end{aligned} \tag{19.25}$$

with the stationary state thermal conductivity λ^m, the electric resistivity r^m, the water transference number t_w^m, and the diffusion coefficient of water in the membrane (on a concentration basis):

$$l_{\mu\mu}^m = D_w^m \frac{c_w}{RT}$$

See Table 19.2 for coefficient values. The water activity in the membrane is calculated from its definition, $a_w = p_w/p_w^*$. We have assumed that there is equilibrium for water at the electrode/membrane interface, and that there are no significant pressure gradients within the membrane [250]. The water in the membrane is not in an ideal solution. The experimental relation between the water activity and the membrane water content is [251]:

$$\begin{aligned} \lambda(a_w < 1) &= 0.043 + 17.81a_w - 39.85a_w^2 + 36.0a_w^3 \\ \lambda(1 < a_w < 3) &= 14 + 1.4a_w \\ \lambda(a_w > 3) &= 16.8 \end{aligned} \tag{19.26}$$

where the water content λ is the mole water per mole membrane ionic site:

$$\lambda = c_w M/\rho \tag{19.27}$$

Here, M is the molar mass of the polymer in the membrane, and ρ is the membrane dry density. At the cathode side of the membrane, we use $a_w^c = 1$. The mass flux becomes:

$$J_w^m = -\frac{q^{*,m} D_w^m \lambda \rho}{RMT^2}\frac{dT}{dx} - \frac{D_w^m \rho}{M}\frac{d\lambda_w}{dx} + t_w^m j/F \tag{19.28}$$

We replace $d\lambda/dx$ by $(d\lambda/da_w)(da_w/dx)$ and solve for da_w/dx, and using $d\lambda/da_w$ from Eq. (19.26), the differential equations become:

$$\begin{aligned} \frac{dT}{dx} &= -\frac{J_q'^m}{\lambda^m} + \frac{q^{*,m}}{\lambda^m}\left(J_w^m - t_w^m \frac{j}{F}\right) + \frac{\pi^m j}{\lambda^m F} \\ \frac{da_w}{dx} &= -\frac{q^{*,m}\lambda}{(d\lambda/da_w)RT^2}\frac{dT}{dx} - \frac{(J_w^m - t_w^m j/F)M}{(d\lambda/da_w)\rho D_w^m} \\ \frac{d\phi}{dx} &= -\frac{\pi^m}{TF}\frac{dT}{dx} - \frac{t_w^m RT}{Fa_w}\frac{da_w}{dx} - r^m j \end{aligned} \tag{19.29}$$

The Peltier coefficient for the membrane is:

$$\frac{\pi^m}{T} = S_{H^+}^* - t_w^m S_w^m \tag{19.30}$$

We take an expression for the heat of transfer $q^{*,m}$ similar to that in the anode:

$$q^{*,m} = -TS_w^m \tag{19.31}$$

The electric resistivity, r^m was given by Springer *et al.* [251]:

$$(r^m)^{-1} = \exp\left(1268\left(\frac{1}{303} - \frac{1}{T}\right)\right)(0.5139\lambda - 0.326) \tag{19.32}$$

The membrane diffusion coefficient $D^m = 1.5 \times 10^{-10}$ m^{2}s was also given by Springer *et al.* [251]. For the thermal conductivity of the membrane, we used an estimate for a water filled polymer, $\lambda^m = 0.2$ W/K m [246]. The membrane density and molar mass were 1.64 kg/m^3 and 1.1 kg/mol, respectively. The water transference coefficient of water in Nafion 115 in equilibrium with vapor was 1.2 [157]. The $\pi^m/T^{m,c}$ was taken from the literature [252].

Energy conservation in the membrane means that, cf. Eq. (4.16),

$$\frac{d}{dx}J_u = \frac{d}{dx}(J_q'^m + j\phi^m + J_w^m H_w^m) = 0 \tag{19.33}$$

The equations were solved to give the gradient in electric potential, the temperature and concentration profiles across the membrane, see Figs. 19.2 through 19.4.

The non-linear electric potential profile in the membrane, shown in Fig. 19.4, can be understood from these properties. As the membrane water content goes down at the anode surface, the resistance increases, and so does the potential drop. This is the biggest contribution to the electric potential gradient across the membrane. The contribution from the water chemical potential is not big, since we assume equilibrium for water at both electrode surfaces. The temperature may rise or fall, depending on j. A changing value of $j\phi^m$, leads indeed to a change in $J_q'^m$, see Fig. 19.5 below.

19.3.4 *The cathode backing*

The flux equations (19.19) for the cathode backing are

$$\begin{aligned}
\frac{dT}{dx} &= -\frac{1}{\lambda^c}\left[J_q'^c + \pi^c\frac{j}{F}\right] \\
\frac{dx_{O_2}}{dx} &= \frac{j}{4FD_{ON}} \\
\frac{d\phi}{dx} &= -\frac{\pi^c}{F}\frac{dT}{dx} - \frac{RT}{4Fx_{O_2}}\frac{dx_{O_2}}{dx} - r^c j
\end{aligned} \tag{19.34}$$

where we introduced $t_{O_2} = 1/4$ and neglected coupling between the oxygen and other gas fluxes. The stationary state thermal conductivity is λ^c, and the electric resistivity is r^c. The oxygen concentration gradient is determined by the interdiffusion coefficient of oxygen in nitrogen, by D_{ON}. The Peltier coefficient for the cathode backing is:

$$\frac{\pi^c}{T} = \frac{1}{4}S_{O_2} - S_e^* - t_w^c S_w^c = \frac{1}{4}S_{O_2} - S_e^* - \left(\frac{J_w^a}{j} + \frac{1}{2}\right) S_w^c \tag{19.35}$$

The Peltier coefficient includes an extra contribution from water. Energy conservation in the cathode backing means that

$$\frac{d}{dx}J_u = \frac{d}{dx}(J_q'^c + j\phi^c + J_w^c H_w^c + J_{N_2}H_{N_2} + J_{O_2}H_{O_2}) = 0 \tag{19.36}$$

where $dH_i/dx = C_{P,i}dT/dx$. These equations were solved for the profiles of T, x_w and ϕ in the cathode. The equations were solved with a mole fraction of oxygen at the right side boundary equal to $x_{O_2}^0 = p_{O_2}/p = 0.21$, see Figs. 19.2, 19.3 and 19.4. The consumption of oxygen is proportional to j. The diffusion coefficient D_{ON} therefore determined the mole fraction profile of oxygen in the cathode backing. The temperature profile indicates a large heat flux out of the cell. In fact, most of the heat produced in the cell comes out of the cathode. Again, the electric potential gradient was negligible.

19.4 The electrode surfaces

The entropy production of the electrode surfaces between the i-phase and the o-phase is:

$$\sigma^s = J_q'^i \Delta_{i,s}\left(\frac{1}{T}\right) + J_q'^o \Delta_{s,o}\left(\frac{1}{T}\right) - J_w^i \frac{1}{T^s}\Delta_{i,s}\mu_{w,T} - J_w^o \frac{1}{T^s}\Delta_{s,m}\mu_{w,T}$$
$$- j\frac{1}{T^s}\left(\Delta_{i,o}\phi + \frac{\Delta_n G^s}{F} + \frac{\Delta\mu_{g,T}}{v_g F}\right) \tag{19.37}$$

The first superscript indicates the phase, and the second the position in the phase. Superscript i means into (the left hand side of) the surface, while o means out (the right hand side) of the surface. For terminology, see Secs. 9.1 and 13.1. (The excess entropy production in the anode and cathode surfaces, in J/s K m^2, are $\sigma^{s,a}$ and $\sigma^{s,c}$.) There is a discontinuity in the heat flux at the surface; we distinguish between the flux into the surface, $J_q'^i$, and out of the surface, $J_q'^o$. This can be seen in Fig. 19.5

below. The last term comes from transport of the reacting gas into the surface. The force-flux relations are:

$$\begin{aligned}
\Delta_{i,s}\left(\frac{1}{T}\right) &= r^s_{ii}J'^i_q + r^s_{i\mu}J^i_w + r^s_{io}J'^o_q + r^s_{im}J^o_w + r^s_{i\phi}j \\
-\frac{1}{T^s}\Delta_{i,s}\mu_{w,T} &= r^s_{\mu i}J'^i_q + r^s_{\mu\mu}J^i_w + r^s_{\mu o}J'^o_q + r^s_{\mu m}J^o_w + r^s_{\mu\phi}j \\
\Delta_{s,o}\left(\frac{1}{T}\right) &= r^s_{oi}J'^i_q + r^s_{o\mu}J^i_w + r^s_{oo}J'^o_q + r^s_{om}J^o_w + r^s_{o\phi}j \\
-\frac{1}{T^s}\Delta_{s,o}\mu_{w,T} &= r^s_{mi}J'^i_q + r^s_{m\mu}J^i_w + r^s_{mo}J'^o_q + r^s_{mm}J^o_w + r^s_{m\phi}j \\
-\frac{1}{T^s}\left(\Delta\phi + \frac{\Delta_n G^s}{F} + \frac{\Delta\mu_{g,T}}{v_g F}\right) &= r^s_{\phi i}J'^i_q + r^s_{\phi\mu}J^i_w + r^s_{\phi o}J'^o_q + r^s_{\phi m}J^o_w + r^s_{\phi\phi}j
\end{aligned} \tag{19.38}$$

We assume that $r^s_{io} = r^s_{oi} = 0$, and $r^s_{im} = r^s_{mi} = 0$. It follows that:

$$\begin{aligned}
J'^i_q &= \frac{r^s_{\mu\mu}}{D^{i\mu}}\Delta_{i,s}\left(\frac{1}{T}\right) - \frac{r^s_{i\mu}}{D^{i\mu}}\left(-\frac{1}{T^s}\Delta_{i,s}\mu_{w,T}\right) + \pi^i\frac{j}{F} \\
J^i_w &= -\frac{r^s_{\mu i}}{D^{i\mu}}\Delta_{i,s}\left(\frac{1}{T}\right) + \frac{r^s_{ii}}{D^{i\mu}}\left(-\frac{1}{T^s}\Delta_{i,s}\mu_{w,T}\right) + t^i\frac{j}{F} \\
J'^o_q &= \frac{r^s_{mm}}{D^{om}}\Delta_{s,o}\left(\frac{1}{T}\right) - \frac{r^s_{om}}{D^{om}}\left(-\frac{1}{T^s}\Delta_{s,o}\mu_{w,T}\right) + \pi^o\frac{j}{F} \\
J^o_w &= -\frac{r^s_{mo}}{D^{om}}\Delta_{s,o}\left(\frac{1}{T}\right) + \frac{r^s_{oo}}{D^{om}}\left(-\frac{1}{T^s}\Delta_{s,o}\mu_{w,T}\right) + t^o\frac{j}{F}
\end{aligned} \tag{19.39}$$

where the denominators are

$$\begin{aligned}
D^{i\mu} &= r^s_{ii}r^s_{\mu\mu} - r^s_{i\mu}r^s_{\mu i} \\
D^{om} &= r^s_{oo}r^s_{mm} - r^s_{om}r^s_{mo}
\end{aligned} \tag{19.40}$$

and the transference numbers and Peltier coefficients are

$$\begin{aligned}
t^i_w &= F\left(\frac{J^i_w}{j}\right)_{dT=0,d\mu=0} = F\frac{r^s_{i\phi}r^s_{\mu i} - r^s_{ii}r^s_{\mu\phi}}{D^{i\mu}} \\
t^o_w &= F\left(\frac{J^o_w}{j}\right)_{dT=0,d\mu=0} = F\frac{r^s_{o\phi}r^s_{mo} - r^s_{oo}r^s_{m\phi}}{D^{om}}
\end{aligned} \tag{19.41}$$

$$\begin{aligned}\pi^i &= F\left(\frac{J_q'^i}{j}\right)_{dT=0,d\mu=0} = F\frac{r^s_{\mu\phi}r^s_{\mu i} - r^s_{\mu\mu}r^s_{i\phi}}{D^{i\mu}} \\ \pi^o &= F\left(\frac{J_q'^o}{j}\right)_{dT=0,d\mu=0} = F\frac{r^s_{m\phi}r^s_{mo} - r^s_{mm}r^s_{o\phi}}{D^{om}}\end{aligned} \tag{19.42}$$

These coefficients are equal to the coefficients that were defined for the bulk phases. The heats of transfer from the linear relations are:

$$\begin{aligned}q^{*,i} &= -\frac{r^s_{i\mu}}{r^s_{ii}} \\ q^{*,o} &= -\frac{r^s_{om}}{r^s_{oo}}\end{aligned} \tag{19.43}$$

By introducing these ratios, we obtain expressions for the jump in temperature and in chemical potential at the surface:

$$\begin{aligned}\Delta_{i,s}T &= -\frac{1}{\lambda^s_i}\left[J_q'^i - q^{*,i}\left(J^i_w - t^i_w\frac{j}{F}\right) - \pi^i\frac{j}{F}\right] \\ \Delta_{i,s}\mu_{w,T} &= -\frac{q^{*,i}}{T^{i,o}}\Delta_{i,s}T - \frac{T^s}{l^i_{\mu\mu}}(J^i_w - t^i_w j/F) \\ \Delta_{s,o}T &= -\frac{1}{\lambda^s_o}\left[J_q'^o - q^{*,o}\left(J^o_w - t^o_w\frac{j}{F}\right) - \pi^o\frac{j}{F}\right] \\ \Delta_{s,o}\mu_{w,T} &= -\frac{q^{*,o}}{T^{o,i}}\Delta_{s,o}T - \frac{T^s}{l^o_{\mu\mu}}\left(J^o_w - t^o_w\frac{j}{F}\right)\end{aligned} \tag{19.44}$$

Here, λ^s_i and λ^s_o are stationary state thermal conductivities of the i and o side of the surface, respectively, and $l^i_{\mu\mu}$ and $l^o_{\mu\mu}$ are corresponding stationary state mass conductivities. The heat fluxes have a Fourier-type contribution as well as a contribution from the Peltier heat and the heat of transfer.

The effective electric force becomes:

$$\begin{aligned}\Delta_{i,o}\phi_{\text{eff}} &= \Delta_{i,o}\phi + \frac{\Delta_n G^s}{F} + \frac{\Delta\mu_{g,T}}{v_g F} \\ &= -\frac{\pi^i}{T^{i,o}F}\Delta_{i,s}T - \frac{\pi^o}{T^{o,i}F}\Delta_{s,o}T - \frac{t^i_w}{F}\Delta_{i,s}\mu_{w,T} - \frac{t^o_w}{F}\Delta_{s,o}\mu_{w,T} - r^s j\end{aligned} \tag{19.45}$$

where r^s is the ohmic surface resistivity. The electric potential drop at the surface has contributions from the Peltier coefficients, the chemical

potential difference, the reaction Gibbs energy, and the resistance drop across the surface.

These equations capture the most important phenomena at the electrode surfaces. They are further detailed below. It is remarkable that the fluxes are analogous to their bulk counterparts.

19.4.1 *The anode catalyst surface*

At the anode catalyst surface, the enthalpy of hydrogen is converted into electric energy and heat. There is a change in the enthalpy as water goes from the vapor state to the condensed state in the membrane. This releases heat. Conservation of energy across the phase boundary means that

$$J_u = J_q'^a + j\phi^a + J_{\mathrm{H}_2} H_{\mathrm{H}_2} + J_w^a H_w^a = J_q'^m + j\phi^m + J_w^m H_w^m \tag{19.46}$$

The flux of hydrogen stops at the surface, while the electric current density and the water flux are continuous through the surface:

$$J_w^a = J_w^m. \tag{19.47}$$

The difference in the electric potential between the two sides of the surface $\phi^m - \phi^a = \Delta_{a,m}\phi$ is generated by the heat and enthalpy changes. The heat fluxes in and out of the anode surface are illustrated in detail in Fig. 19.5 for the same current densities and conditions as before.

We see a discontinuity in the heat flux at both electrode surfaces, and a varying heat flux in the membrane, for reasons we explained above. Nernst equation is obeyed when the entropy production is zero in an isothermal surface, $\Delta_{a,m}\phi = -\Delta_n G^{s,a}/F$, see Sec. 5.4.1.

The electrochemical reaction takes place at the surface, and the reaction rate at stationary state is equal to j/F. We assume that there is equilibrium for adsorption of hydrogen at the surface. This means that the reaction Gibbs energy in the surface can be expressed by thermodynamic properties of the gas:

$$\begin{aligned}
\Delta_{a,m}\phi_{\mathrm{eff}} &= \Delta_{a,m}\phi + \frac{\Delta_n G^{s,a}}{F} + \frac{\Delta\mu_{H_2,T}(T^{s,a})}{2F} \\
&= \Delta_{a,m}\phi - \frac{1}{2F}\left(\mu_{H_2}^s - \Delta_{a,s}\mu_{H_2,T}(T^{s,a})\right) \\
&= \Delta_{a,m}\phi - \frac{1}{2F}(H_{H_2} - T^{s,a}S_{H_2})
\end{aligned} \tag{19.48}$$

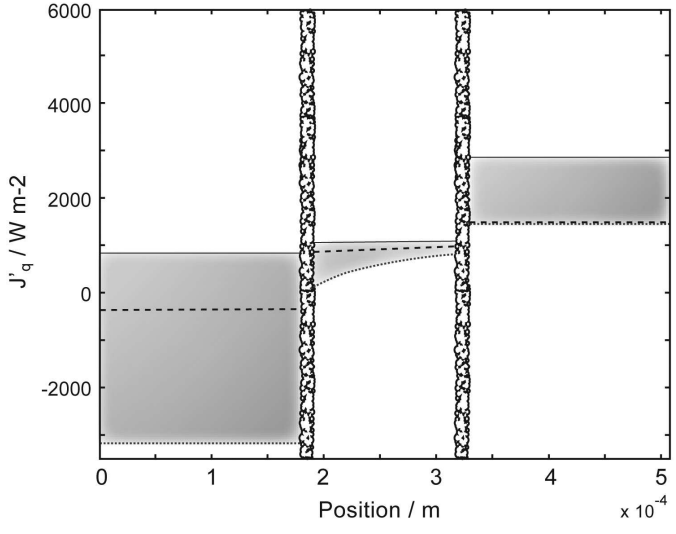

Figure 19.5 The heat fluxes in the cell as a function of current densities 500 (unbroken line), 2500 (dotted curve) and 5000 (dashed curve) A/m^2.

The equations of transport that derive from $\sigma^{s,a}$ are:

$$\begin{aligned}
\Delta_{a,s}T &= -\frac{J_q'^a}{\lambda_a^s} + \frac{q^{*,a}}{\lambda_a^s}(J_w - t_w j/F) + \pi^a j/\lambda_a^s F \\
\Delta_{a,s}\mu_{w,T} &= -\frac{q^{*,a}}{T^{a,m}}\Delta_{a,s}T - \frac{(J_w - t_w j/F)}{l_{\mu\mu}^s} \\
\Delta_{s,m}T &= -\frac{J_q'^m}{\lambda_m^s} + \frac{q^{*,m}}{\lambda_m^s}(J_w - t_w j/F) + \pi^m j/\lambda_m^s F \\
\Delta_{s,m}\mu_{w,T} &= -\frac{q^{*,m}}{T^{m,a}}\Delta_{s,m}T - \frac{(J_w - t_w j/F)}{l_{\mu\mu}^s} \\
\Delta\phi_{\text{eff}} &= -\frac{\pi^a}{T^{a,m}F}\Delta_{a,s}T - \frac{\pi^m}{T^{m,a}F}\Delta_{s,m}T - \frac{t_w}{F}\Delta_{a,m}\mu_{w,T} - r^s j
\end{aligned} \tag{19.49}$$

The conditions at the surface are not known in detail. In order to simplify matter enough to make possible a calculation of the profiles of T, x_w and ϕ across the cell, we assume that there is equilibrium for water across the surface.

$$\Delta\mu_w = (H_w^a - T^a S_w^a) - (H_w^m - T^m S_w^m) = 0 \tag{19.50}$$

This relation may be used to find the temperature of the membrane, consistent with T^a and the thermodynamic properties. The chemical potential difference at constant temperature, is then equal to

$$\begin{aligned} \Delta_{a,s}\mu_{w,T}(T^{s,a}) &= T^{s,a}(S_w^s - S_w^a) \\ \Delta_{s,m}\mu_{w,T}(T^{s,a}) &= T^{s,a}(S_w^m - S_w^s) \end{aligned} \tag{19.51}$$

These equations, together with the energy balance and Eq. (19.50) were solved for the temperature jumps and the electric potential drop at the surface. The Peltier coefficients are known, while the thermal and mass conductivities are not. Condition Eq. (19.50) is a useful replacement for the flux equations for $\Delta_{a,s}\mu_{w,T}$ and $\Delta_{s,m}\mu_{w,T}$. Necessary coefficient estimates were given in Table 19.2. For the anode surface resistivity, we used $r^s = 7.2\ 10^{-6}$ ohm m^2. Vie [246] determined the thermal conductivity of the catalyst surfaces from experiments, $\lambda^s = 1000$ W/Km^2 from a model similar to this one, but without coupling terms.

Figure 19.4 gives a relatively large jump in the electric potential at the anode surface, while Fig. 19.2 shows a small jump in the temperature. Both jumps are connected to the entropy change of the electrode reaction, Eq. (19.48).

19.4.2 *The cathode catalyst surface*

Energy conservation at the cathode surface gives

$$\begin{aligned} J_u &= J_q'^m + j\phi^m + J_w^m H_w^m \\ &= J_q'^c + j\phi^c + (J_w^a + j/2F)H_w^c + J_{O_2} H_{O_2} \end{aligned} \tag{19.52}$$

The effective electric force becomes:

$$\begin{aligned} \Delta_{m,c}\phi_{\text{eff}} &= \Delta_{m,c}\phi + \frac{\Delta_n G^{s,c}}{F} - \frac{\Delta\mu_{O_2,T}}{4F} \\ &= \Delta_{m,c}\phi + \frac{1}{2F}(H_w^c - T^{s,c}S_w^c) - \frac{1}{4F}(H_{\mathrm{O}_2} - T^{s,c}H_{\mathrm{O}_2}) \end{aligned} \tag{19.53}$$

The potential jump across the surface is $\Delta_{m,c}\phi = \phi^c - \phi^m$. The equations to be solved for the profiles are:

$$\begin{aligned}
\Delta_{m,s}T &= -\frac{1}{\lambda_m^s}\left[J_q'^m - q^{*,m}\left(J_w^m - t_w^m\frac{j}{F}\right) - \pi^m\frac{j}{F}\right] \\
\Delta_{m,s}\mu_{w,T} &= -\frac{q^{*,m}}{T^{m,c}}\Delta_{m,s}T - \frac{1}{L_{\mu\mu}^m}\left(J_w^m - t_w^m\frac{j}{F}\right) \\
\Delta_{s,c}T &= -\frac{1}{\lambda_c^s}\left[J_q'^c - q^{*,c}\left(J_w^c - t_w^c\frac{j}{F}\right) - \pi^c\frac{j}{F}\right] \\
\Delta_{s,c}\mu_{w,T} &= -\frac{q^{*,c}}{T^{c,m}}\Delta_{s,c}T - \frac{1}{l_{\mu\mu}^c}\left(J_w^c - t_w^c\frac{j}{F}\right)
\end{aligned} \tag{19.54}$$

We assume again equilibrium for water across the surface, cf. Eq. (19.50), as well as equilibrium for oxygen adsorption at the surface. The Peltier heats are the ones given before. The electric potential of the cell is generated at the cathode. It can be calculated from

$$\begin{aligned}
F(\Delta_{m,c}\phi_{\text{eff}} + \eta^c) = &-\frac{\pi^m}{T^{m,c}}\Delta_{m,s}T - \frac{\pi^c}{T^{c,m}}\Delta_{s,c}T \\
&- t_w^m\Delta_{m,s}\mu_{w,T} - t_w^c\Delta_{s,c}\mu_{w,T} - r^s j
\end{aligned} \tag{19.55}$$

The overpotential of the oxygen electrode, η^c, or the resistance of the activated electrochemical reaction, is not yet accounted for. It can be shown, using mesoscopic non-equilibrium thermodynamics, that the overpotential must be subtracted from the right-hand side of Eq. (19.53) [51]. The value of the cathode overpotential was determined by Vie and Kjelstrup [247]:

$$\eta^c = \frac{2RT}{F}\ln\frac{j}{j_0} \tag{19.56}$$

with the exchange current density for oxygen in air of $j_0 = 2.5\ 10^{-3}$ A/m^2. The resulting jump in electric potential is shown in Fig. 19.4.

19.5 A model in agreement with the second law

The entropy production for a unit cross-sectional area ($\Omega = 1\text{m}^2$) of the cell is the integral over contributions from all five subsystems:

$$\frac{dS_{irr}}{dt} = \Omega\left[\int_{0\text{a}}^{\text{a,m}}\sigma^{\text{a}}dx + \sigma^{\text{s,a}} + \int_{\text{a,m}}^{\text{c,m}}\sigma^{\text{m}}dx + \sigma^{\text{s,c}} + \int_{\text{c,m}}^{0,\text{c}}\sigma^{\text{c}}dx\right] \geq 0 \tag{19.57}$$

where dS_{irr}/dt has dimension W/K. The second law gives $dS_{irr}/dt > 0$.

The entropy balance for the whole cell is:

$$\frac{dS_{irr}}{dt} = \left[J_s^{\mathrm{c}} - J_s^{\mathrm{a}}\right]\Omega \tag{19.58}$$

The entropy flux was defined in Sec. 4.2, $J_s = J_q'/T + \Sigma_i J_i S_i$. Here, J_q' is the measurable heat flux, J_i is the mass flux of component i, S_i is the partial molar entropy of i, and T is the temperature. These fluxes give

$$\begin{aligned}\frac{1}{W}\frac{dS_{irr}}{dt} &= \left(\frac{J_q'^{\mathrm{c}}}{T^{\mathrm{c}}} + J_w^{\mathrm{c}} S_w^{\mathrm{c}} + J_{\mathrm{O_2}} S_{\mathrm{O_2}}\right) - \left(\frac{J_q'^{\mathrm{a}}}{T^{\mathrm{a}}} + J_w^{\mathrm{a}} S_w^{\mathrm{a}} + J_{\mathrm{H_2}} S_{\mathrm{S_2}}\right) \\ &= \frac{J_q'^{\mathrm{c}}}{T^{\mathrm{c}}} - \frac{J_q'^{\mathrm{a}}}{T^{\mathrm{c}}} + \frac{j}{F}\left[\frac{1}{2}(S_w^{\mathrm{c}} - S_{H_2}) - \frac{1}{4}S_{O_2}\right] + J_w^{\mathrm{a}}\left[S_w^{\mathrm{c}} - S_w^{\mathrm{a}}\right]\end{aligned} \tag{19.59}$$

The measurable heat fluxes have, as we have seen, several terms, not only Fourier type terms. All terms are important in the development of a consistent thermodynamic model. In such a model, we must find the same value for the entropy production from Eq. (19.57) as from (19.59).

The entropy production was therefore determined by integrating across the sections of the cell. The accumulated entropy production for the cell in Figs. 19.1–19.4 is shown in Fig. 19.6 for three current densities. We see, as expected, that most of the entropy is produced at the cathode. The entropy production increases with the current density in the cell. The integrated value agreed within numerical accuracy with the value calculated from Eq. (19.59).

The cell was leaking heat to both sides, more to the cathode side, than to the anode side, see Fig. 19.5. A reduction in the overpotential in the cathode surface had a substantial effect on $\sigma^{s,c}$ and the heat fluxes. The thermal conductivities of the backing and surface were significant for the temperature rise in the system, but not for the entropy production. The value of the diffusion coefficient for water in the membrane has a large effect on the possibility to find a solution. The membrane resistivity gave significant contributions to the entropy production.

In order to see the importance of coupling terms in the heat fluxes, we introduce the heat fluxes from the subsections above. This gives

$$\begin{aligned}\frac{1}{W}\frac{dS_{irr}}{dt} = &-\frac{\lambda^c}{T^0}\left(\frac{dT}{dx}\right)^c + \frac{\pi^c}{T}\frac{j}{F} \\ &+ \frac{\lambda^a}{T^0}\left(\frac{dT}{dx}\right)^a - \frac{q^{*,a}}{T}\left(J_D^a - t_D^a\frac{j}{F}\right) - \frac{\pi^a}{T}\frac{j}{F} \\ &+ \frac{j}{F}\left[\frac{1}{2}(S_w^c - S_{H_2}) - \frac{1}{4}S_{O_2}\right] + J_w^a\left(S_w^c - S_w^a\right)\end{aligned} \tag{19.60}$$

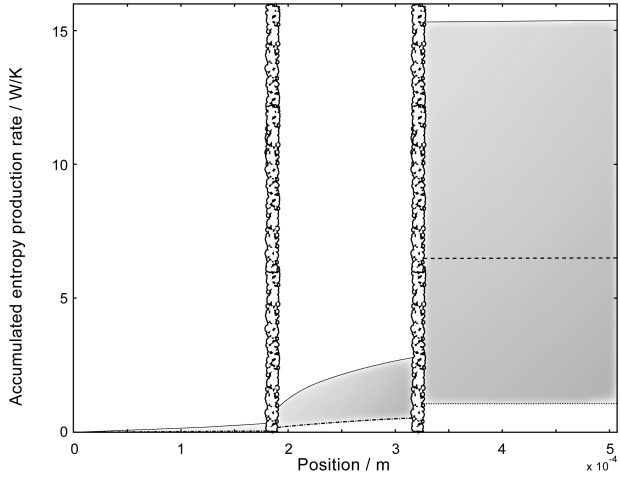

Figure 19.6 The accumulated entropy production in the polymer electrolyte fuel cell, obtained by integration from the anode to the cathode backing, for current densities 500 (lower curves), 2500 (central curves) and 5000 (upper curves) A/m^2.

The next step is to introduce the expressions for the Peltier coefficients (19.22) and (19.35), and the relation for the anode $J_D^a - t_D^a j/F = J_w^a$. Part of the difference of the Peltier coefficients then cancel with the entropy of the reaction. This is so because the heat effect connected with conversion of reactants to products, does not contribute to the entropy production, but to the electric work. The terms containing the heats of transfer are reversible, and must not give any net entropy production. This is achieved when

$$q^{*,a} = -TS_w^a \tag{19.61}$$

and

$$\frac{q^{*,c}}{T} - \frac{q^{*,a}}{T} = -S_w^c + S_w^a \tag{19.62}$$

With these relations, we also have

$$\frac{1}{W}\frac{dS_{irr}}{dt} = -\frac{\lambda^c}{T^0}\left(\frac{dT}{dx}\right)^c + \frac{\lambda^a}{T^0}\left(\frac{dT}{dx}\right)^a \tag{19.63}$$

The total entropy production in the cell ends up as heat conducted to the surroundings in this model.

19.6 Concluding comments

We have demonstrated how non-equilibrium thermodynamics can be used to characterize energy conversion in a polymer fuel cell. The method can be used for any heterogeneous electrochemical cell. We have presented a set of simultaneous solutions for mole fractions, electric potentials and temperature profiles across a single polymer electrolyte fuel cell using data for a Nafion 117 membrane. From the solutions, we have calculated the local entropy production in each subsystem of the cell in two ways. We found that heat may escape the cell in an asymmetric manner, largely dependent on the thermal conductivity of the surfaces. The calculations were done for a one-dimensional cell.

Knowledge of entropy production, lost work and local heat fluxes is important for auxiliary equipment design and for further research planning. The largest reduction in entropy production, or increase in power output, can be obtained by reducing the overpotential of the cathode, but it is worthwhile paying more attention also to the membrane as a dissipating part of the cell.

Chapter 20

Measuring Membrane Transport Properties

Non-equilibrium thermodynamics can be used to design experiments. We present methods and experimental results that have been obtained with cation-exchange membranes.

Membranes are widely used to separate mixtures of all kinds. A membrane can be generally seen as a barrier to transport. Biological membranes separate the interior of a cell from its exterior, or organelles from the cell inside. Inorganic and organic membranes selectively conduct ions, for instance, in ion-selective electrodes, and can be used as sensors. Clay and sand can be used to filter impurities from drinking water, and can also be thought of as membranes in a wide sense.

Non-equilibrium thermodynamics has since long been used to describe transport in membranes [23, 24, 227, 230, 250, 253–255]. The theory needs input values for transport coefficients, in order to be used for modeling. When such coefficients are not known, experiments can be designed to measure them, using the same theory.

This chapter describes experimental methods which can be used to find transport properties for ion-exchange membranes [27, 77, 157, 239, 256–258]. The methods, which are designed from the theoretical framework, may also be used for other membranes. We shall illustrate them with data for ion-exchange membranes. We saw that ion-exchange membranes were used for energy conversion in fuel cells (Chapter 19) and in osmotic power plants (Chapter 18). They are also used to separate salt solutions and to produce clean water [229].

The cells reported are of the type

$$\mathrm{Ag(s)|AgCl(s)|NCl,\ ACl\ (aq)|^{mem}|\ NCl,\ ACl\ (aq)|AgCl(s)|Ag(s)} \quad (20.1)$$

The aqueous solution contained up to two chlorides, NCl and ACl. The membranes were cation exchange membranes, the CR membrane was from Ionics and the Nafion 117 membrane, from Dupont. The electrodes were reversible to the ion in solution, Ag(s)| AgCl(s) or (Pt)|H_2(g).

20.1 The membrane in equilibrium with electrolyte solutions

Equilibrium constants for membrane-electrolyte equilibria can be calculated from measurements of membrane compositions and their corresponding electrolyte compositions. This was done for some selected electrolyte mixtures in equilibrium with the CR membrane from Ionics [235, 236]:

$$\begin{aligned} \mathrm{HCl} + \mathrm{NaM} &\rightleftharpoons \mathrm{HM} + \mathrm{NaCl} \qquad K_{\mathrm{eq},1} = \frac{a_{\mathrm{HM}} a_{\mathrm{NaCl}}}{a_{\mathrm{HCl}} a_{\mathrm{NaM}}} = 0.72 \\ \mathrm{NaCl} + \mathrm{KM} &\rightleftharpoons \mathrm{NaM} + \mathrm{KCl} \qquad K_{\mathrm{eq},2} = \frac{a_{\mathrm{NaM}} a_{\mathrm{KCl}}}{a_{\mathrm{NaCl}} a_{\mathrm{KM}}} = 0.54 \\ \mathrm{SrCl_2} + \mathrm{KM} &\rightleftharpoons \mathrm{SrM_2} + \mathrm{KCl} \qquad K_{\mathrm{eq},3} = \frac{a_{\mathrm{KCl}} a_{\mathrm{SrM_2}}}{a_{\mathrm{KM}} a_{\mathrm{SrCl_2}}} = 5.6 \end{aligned} \tag{20.2}$$

Here, M^- denotes a cation site in the membrane. The ion exchange capacity of the CR 386 membrane is 1.6 kmol m^{-3} and the membrane is 1.2 μm thick. The equilibrium constants show that the membrane has a small preference for HM over NaM, a very small preference for NaM over KM, and a high preference for SrM_2 over KM. When the equilibrium constant is close to unity, the cations are nearly statistically distributed over the cation sites in the membrane. The higher value for the mixture of SrM_2 and KM indicates that the divalent ion binds to more than one site.

The path of transport through a membrane is everywhere at local equilibrium. The path can thus be defined also by means of solutions that are in equilibrium with the membrane at any given location between the two sides. This is convenient when one needs to integrate across a membrane.

20.2 The membrane resistivity

Ion-exchange membranes are normally good conductors. It is therefore difficult to separate the membrane resistance from the resistance of adjacent layers. The membrane resistivity can therefore best be found by measuring a stack of several membranes [157, 259]. The single membrane pieces are first equilibrated in the electrolyte. The membranes are pressed together between two electrodes. A constant pressure is applied. For an isothermal

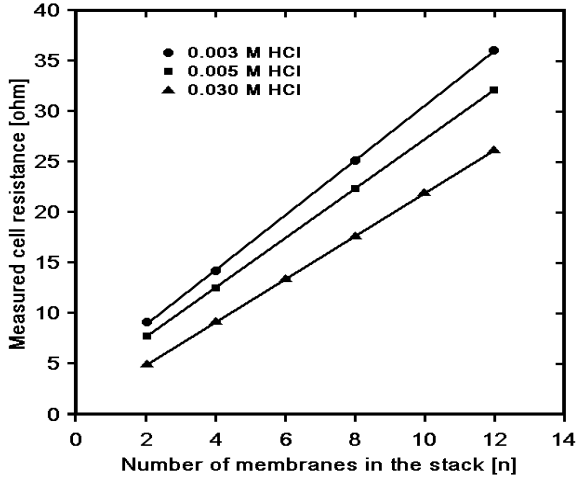

Figure 20.1 The resistance of a stack of CR Ionics membranes, $R(n)$, as a function of the number of membranes in the stack, n [157]. The membranes were equilibrated in various solutions of HCl.

stack of uniform composition, the ohmic resistance is

$$R = -\left(\frac{\Delta\phi}{I}\right)_{dT=0,d\mu_i=0} \tag{20.3}$$

The total cell potential, $\Delta\phi$, is measured at a high frequency, in order to avoid frequency dependent phenomena (see Chapter 21). The cell resistance, $R(n)$, is then

$$R(n) = R_o + nR_{\rm ms} \tag{20.4}$$

where R_o is the resistance of the wires and the liquid layers at the electrodes, n is the number of membranes and $R_{\rm ms}$ is the resistance of one membrane, $R_{\rm m}$, and a surface layer, $R_{\rm s}$:

$$R_{\rm ms} = R_{\rm m} + R_{\rm s} \tag{20.5}$$

A plot of $R(n)$ versus n gives a straight line, see Fig. 20.1 which shows data for HCl in Nafion 117. The slope of the line gives $R_{\rm ms}$.

The membrane resistance and the surface resistance can be separated, assuming that $R_{\rm s}$ depends on the electrolyte concentration, while $R_{\rm m}$ does not. When the surface resistance is proportional to the specific resistivity of the solution, ρ, we can find $R_{\rm m}$ by plotting $R_{\rm ms}$ versus ρ. This plot is

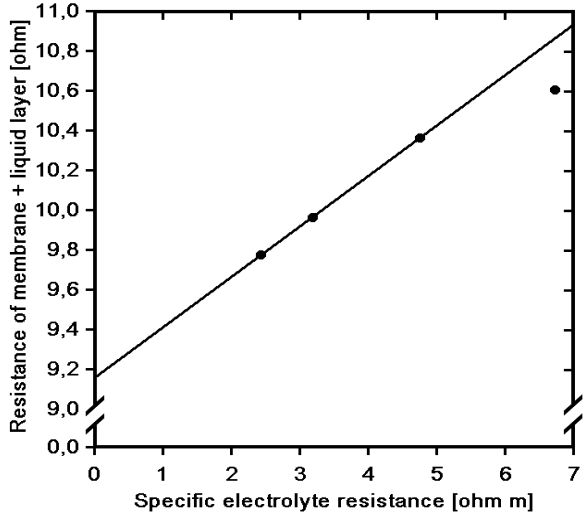

Figure 20.2 The resistance of a single CR Ionics membrane with interface layer, R_{ms}, as a function of the resistivity, ρ, of the KCl solution in equilibrium with the membrane [157].

shown in Fig. 20.2. The surface resistance R_{s} is more than 10% of R_{m} for HCl in equilibrium with CR 386 from Ionics [157, 259].

The deviation from the straight line at high concentrations in Fig. 20.2 was explained by membrane swelling [157, 259]. The membrane specific resistivity can now be found from R_{m}, the membrane area, Ω_{m}, and the membrane thickness, d_{m}:

$$r_{\mathrm{m}} = R_{\mathrm{m}} \left(\frac{\Omega_{\mathrm{m}}}{d_{\mathrm{m}}} \right) \tag{20.6}$$

Results for the membranes were $\kappa_{\mathrm{m}} = 1/r_{\mathrm{m}} = 0.420 \pm 0.04$ (CR 386) and 2.03 ± 0.04 S/m (Nafion 117). The technique was used to find specific conductivities for mixtures of monovalent cations, and mixtures of mono- and divalent cations.

The conductivity can be modeled with a formula similar to the one given in Sec. 16.1

$$\kappa^{\mathrm{m}} = -\left[\frac{\Delta\phi}{j} \right]_{dT=0,\ d\mu_{i,T}=0} = F^2 c \left(u_{\mathrm{N}^+} x_{\mathrm{NM}} + u_{\mathrm{A}^+} x_{\mathrm{AM}} \right) \tag{20.7}$$

Table 20.1 Cation mobilities in Nafion and Ionics CR. The mobility has dimension 10^8 m^2/Vs and refers to 298 K.

Cation	$\left(u_+^o\right)_\infty$	Nafion 117	Ionics CR386
H^+	36.3	14.8	2.30
Na^+	5.19	2.7	0.30
K^+	7.61	–	0.38
Ca^{2+}	6.16	2.5	–
Sr^{2+}	–	–	0.09

where c is the concentration of cation sites in the membrane, and x_i is the equivalent fraction of ion i in the membrane. Some ion mobilities are given in Table 20.1 for one cation in Nafion 117 and Ionics CR386. Mobilities in Nafion 117 are approximately half the values in infinitely dilute aqueous solutions, $\left(u_+^o\right)_\infty$. With $x_{\mathrm{AM}+}\, x_{\mathrm{NM}} = 1$, we eliminate x_{NM} in Eq. (20.7), and obtain

$$\kappa^{\mathrm{m}} = F^2 c \left[\left(u_{\mathrm{A}^+} - u_{\mathrm{N}^+}\right) x_{\mathrm{AM}} + u_{\mathrm{N}^+}\right] \tag{20.8}$$

Mobilities of ions in dilute aqueous solutions are essentially constant. Equation (20.6) predicts that κ is a linear function of x_{M^+}, if the membrane mobilities are constant. This was not observed, and the following model was proposed:

$$\begin{aligned} u_{\mathrm{A}^+} &= u^o_{\mathrm{A}^+}(1 - k x_{\mathrm{NM}}) \\ u_{\mathrm{N}^+} &= u^o_{\mathrm{N}^+}(1 - k x_{\mathrm{AM}}) \end{aligned} \tag{20.9}$$

Here, $u^o_{\mathrm{A}^+}$ and $u^o_{\mathrm{N}^+}$ are the mobilities of AM and NM respectively, and k is an empirical constant describing the interaction of ions. The constant expresses how likely it is that the movement of one ion is obstructed by movement of the other. Conductivity data from several investigators [157, 235, 260, 261] were fitted to this model. Results are given in Table 20.2. A zero interaction constant was found in the presence of protons. It seems likely, considering the amount of water present in the membranes (40-50w%), that the transport mechanism of protons is different from that of other ions. The mobility ratio is smaller in the membrane than in a dilute solution. The membrane serves to retard the fast ion, and to accelerate the slow ion. This seems likely for a membrane, where exchange of ions between the sites is important. The ionic mobilities can be

Table 20.2 Mobility ratios and interaction constants for cations. The membrane is CR 386 from Ionics. Results are compared to infinitely dilute aqueous solutions.

Cation pair	$\left(u^o_{A^+}/u^o_{N^+}\right)_{M^-}$	k	$\left(u^o_{A^+}/u^o_{N^+}\right)_\infty$	Reference
H^+/Na^+	4.2 ± 0.2	0	7.0	[157]
H^+/K^+	4.9 ± 0.1	0	4.8	[157]
Na^+/K^+	0.97 ± 0.03	0.16 ± 0.06	0.68	[260, 261]
K^+/Sr^{2+}	4.2	0.28	–	[235]

used to estimate ionic transport numbers from

$$\begin{aligned} t_{A^+} &= \left(\frac{J_{ACl}}{j}\right)_{dT=0,d\mu_i=0} = \frac{u^o_{A^+}(1-kx_{NM})}{\kappa/cF^2} \\ t_{A^+} &= \left[1 + \frac{u^o_{N^+}(1-kx_{AM})}{u^o_{A^+}(1-kx_{NM})}\frac{x_{NM}}{x_{AM}}\right]^{-1} \end{aligned} \tag{20.10}$$

and $t_{N^+} = 1 - t_{A^+}$. These transport numbers were confirmed by independent measurements for membranes with protons [27], see Sec. 20.3. For alkali-metal mixtures the following approximation was good [260, 261]

$$t_{A^+} \approx x_{AM} \tag{20.11}$$

The last situation is compatible with $u^o_{A^+}(1-kx_{NM}) \approx u^o_{N^+}(1-kx_{AM})$. The membrane transport number can thus, in the simplest case, be determined from knowledge of membrane composition alone.

20.3 Ionic transport numbers

Ottøy *et al.* [257] developed a technique to determine the transport number in a two-component mixture as continuous function of composition. A stack of membranes was used. The stack had so many membranes (usually 8 to 10) that the boundary solutions were not changed during the experiment (by diffusion). Half of the stacks were equilibrated in a *reference* solution, the other half in the *test* solution. In this manner, he was able to find the concentration dependent transport number.

Consider again the membrane in equilibrium with KCl and HCl in cell (20.1). Experiments were performed at constant pressure, constant temperature and constant chemical potential of water, that is, the electrolyte solutions had the same ionic strength. The reference solution was put on

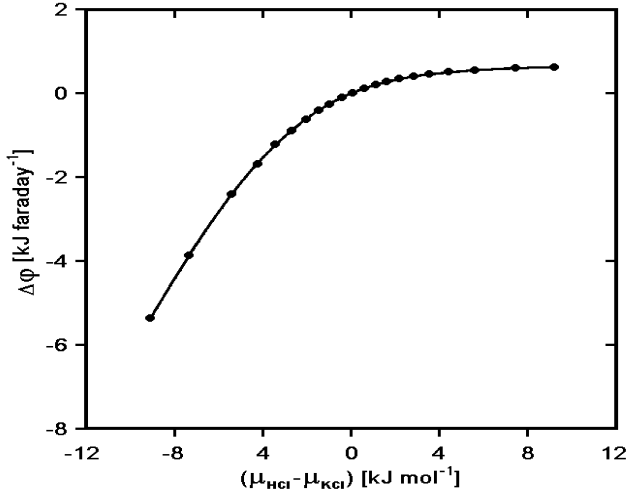

Figure 20.3 The electric potential difference in cell 20.1 as a function of $[\mu^{c}_{HCl} - \mu^{c}_{KCl}]$. Reproduced from J. Membr. Sci. 74 (1992) 1–8 with permission from Elsevier.

the left hand side, and the test solution was put on the right hand side. The gradient in the electric potential became

$$\left(\frac{d\phi}{dx}\right)_{j=0,dT=0,d\mu_w=0} = -t_{HM}\frac{d\mu^{c}_{HCl}}{dx} - t_{KM}\frac{d\mu^{c}_{KCl}}{dx} \tag{20.12}$$

The transport of KCl across the membrane, is everywhere defined by the transport of K^+. The transference number of KCl is therefore equal to the transport number of K^+, $t_{KM} = t_{K^+}$, with the membrane as the frame of reference. In evaluating the transport of HCl, the electrode reactions must be accounted for. In the *absence* of KCl, there is no net mass transport by charge transport alone, and $t_{HM} = 0$. In the *presence* of KCl, as it is here, mass balances give a net transfer of HCl, opposite in sign, but equal in magnitude to the flux of KCl. The transference coefficient of HCl is therefore $t_{HM} = -t_{K^+}$. This gives

$$t_{K^+} = \frac{d\phi}{d\left[\mu^{c}_{HCl} - \mu^{c}_{KCl}\right]} \tag{20.13}$$

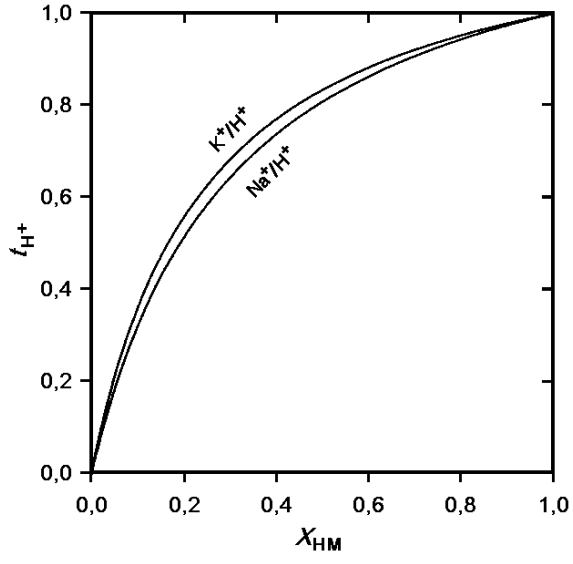

Figure 20.4 The transference number of H^+ as a function of membrane composition x_{HM} for the systems KM-HM and NaM-HM. Reproduced from J. Membr. Sci. 74 (1992) 1–8 with permission from Elsevier.

The differentials of the variables can be related to differentials of differences, since we keep the reference solution constant:

$$t_{\mathrm{K}^+} = \frac{d\Delta\phi}{d\Delta\left[\mu^{\mathrm{c}}_{\mathrm{HCl}} - \mu^{\mathrm{c}}_{\mathrm{KCl}}\right]} \tag{20.14}$$

The composition on the left hand side of the stack is varied in the experiment. By plotting the potential difference as a function of $\Delta\left[\mu_{\mathrm{HCl}} - \mu_{\mathrm{KCl}}\right]$, we can find the transference number from the tangent to the curve in any point (any composition) on the curve. An example of such a curve is shown in Fig. 20.3. Results for two systems are presented in Fig. 20.4.

The measured transport number was compared to the results calculated from the mobility model above, Eq. (20.8). Agreement was found within the experimental uncertainty (3% for HM-KM and HM-NaM). Cell potentials can be measured with high precision when $j = 0$. Such emf measurements can be used to give accurate transport numbers, better that numbers obtained from the Hittorf method. The problem, which is to find the concentration dependence of the transport number, can also be solved.

20.4 The transference number of water and the water permeability

The water transference number, t_{w}, gives the number of water molecules transported with the electric current in the membrane. According to the definition;

$$t_{\mathrm{w}} = \left(\frac{J_{\mathrm{w}}}{j/F} \right)_{dT=0, d\mu_i=0} \tag{20.15}$$

The transference number of water can be found in several ways. For a cation membrane in a proton form, some authors use the potential difference of the following isothermal cell [157, 262]:

$$(\mathrm{Pt})\mathrm{H}_2(g)|\mathrm{H}_2\mathrm{O}(\mathrm{g},\, a_{\mathrm{w}}^{\mathrm{l}})\ |\mathrm{mem}|\mathrm{H}_2\mathrm{O}\ (\mathrm{g},\, a_{\mathrm{w}}^{\mathrm{r}})|\mathrm{H}_2(g)(\mathrm{Pt}) \tag{20.16}$$

The membrane was equilibrated prior to the experiment in HCl. The membrane was then put in contact with saturated vapor only; the activity of water in the vapor was controlled by the temperature and by the amount of LiCl in a water solution that was in equilibrium with the vapor. The potential difference across the membrane is:

$$(\Delta\phi)_{j=0} = -t_{\mathrm{w}} RT \ln \frac{a_{\mathrm{w}}^{\mathrm{r}}}{a_{\mathrm{w}}^{l}} \tag{20.17}$$

The difference in chemical potential of water across the membrane was applied, keeping $a_{\mathrm{w}}^{\mathrm{l}}$ constant. By plotting $\Delta\phi$ versus $\ln a_{\mathrm{w}}^{\mathrm{r}}/a_{\mathrm{w}}^{l}$, a linear relation was found, see Fig. 20.5. The transference number is therefore constant. The value 1.2 was obtained for Nafion 117 at 298 K. When the membrane is equilibrated with electrolyte solutions, the equilibrium is shifted towards higher water contents, and the water transference number rises to 2.6 [263].

The water transference number for a membrane in contact with liquid solutions, can also be accurately determined from the streaming potential [258]. An additional advantage with this measurement is that the water permeability can also be obtained. The streaming potential experiments are done with constant temperature and concentration in the cell. A pressure difference is applied across the membrane. It is assumed that the pressure gradient is linear in the membrane, with $dp/dx = \Delta p/d_{\mathrm{m}}$.

The streaming potential of Cell (20.1) is

$$\left[\frac{\Delta\phi}{\Delta p} \right]_{dT=0, d\mu_i^{\mathrm{c}}=0} = -t_{\mathrm{ACl}} V_{\mathrm{ACl}} - t_{\mathrm{NCl}} V_{\mathrm{NCl}} - t_{\mathrm{w}} V_{\mathrm{w}} - \Delta V_{\mathrm{el}} \tag{20.18}$$

When the transference numbers of the electrolytes have been determined (see Sec. 20.3), and the volume difference of the electrode reactions is corrected for $\Delta V_{\mathrm{el}} = V_{\mathrm{Ag}} - V_{\mathrm{AgCl}}$, the unknown t_{w} can be found.

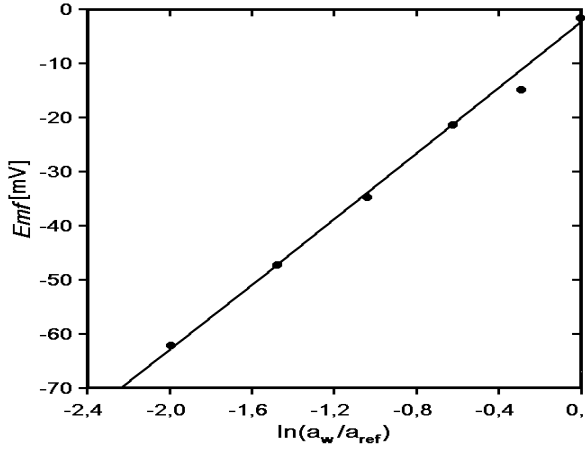

Figure 20.5 The emf of cell 20.1 as a function of $\ln a_{\mathrm{w}}^{\mathrm{r}}/a_{\mathrm{w}}^{l}$ at 298 K [157].

Several systems have been investigated for t_{w} [260,264]. For monovalent cation mixtures, a model for t_{w} is

$$t_{\mathrm{w}} = r_{\mathrm{A}^+} t_{\mathrm{A}^+} + r_{\mathrm{N}^+} t_{\mathrm{N}^+} = (r_{\mathrm{A}^+} - r_{\mathrm{N}^+})\, t_{\mathrm{A}^+} + r_{\mathrm{N}^+} \tag{20.19}$$

with constant coefficients r_{A^+} and r_{N^+}. A linear variation in t_{w} with t_{A^+} may mean that a constant number of water molecules is carried with each ion. For membrane mixtures of divalent and mono-valent cations, the model fails. The number of water molecules carried with each ion may then vary with the composition. The water transference number is largely reduced, and may even become negative, if the membrane becomes permeable to anions. The presence of an anion will add a negative term to Eq. (20.19). This straightforward interpretation of the water transference number as the sum of water molecules carried with each type of ion, is probably oversimplified. It is known that the dynamics of water in the pore varies largely with the ionic sites and the counter-ions that are present. The values of r_{A^+} and r_{N^+} are not equal to the waters of hydration [259]. Membrane hydrophobicity will increase t_{w}.

Typical results from a streaming potential measurements are shown in Fig. 20.6. The curves are extrapolated to zero time, $t = 0$, to determine the streaming potential. We see that the potential difference across the cell, for a given pressure difference, is a linear function of $\sqrt{t}$ on a scale of seconds. This behavior can be predicted. The pressure difference leads to a volume flux, which is superimposed on the electro-osmotic flux. The volume flux

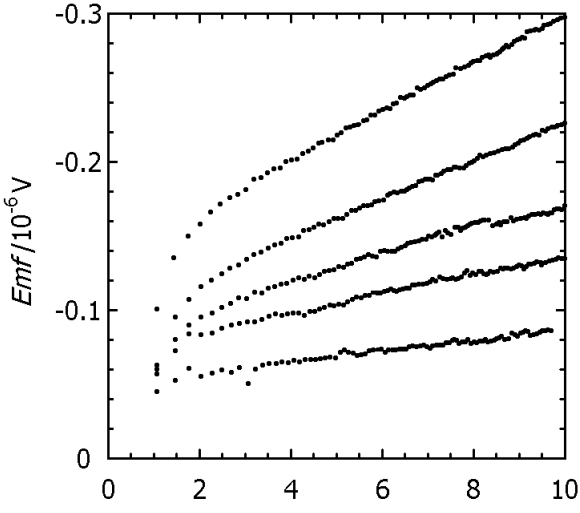

Figure 20.6 The variation in the emf due to a pressure difference, as a function of $\sqrt{t}$. (Courtesy of T. Okada).

leads to a dilution of the solution on the receiving side, and a concentration of the solution on the donating side. The presence of concentration gradients on both sides of the membrane adds to the potential difference (20.18) as time goes on. When the solution contains only one electrolyte, the addition is [258]

$$\Delta\phi_{\rm pol} = -L_p \frac{8RT\sqrt{t}}{\sqrt{\pi D_1}} \Delta p \tag{20.20}$$

where D_1 is Fick's diffusion constant for diffusion of electrolyte in water, L_p is the membrane hydraulic permeability

$$L_p = -\left(\frac{J_V}{\Delta p}\right)_{dT=0, d\mu_i^c=0} \tag{20.21}$$

and J_V is the volume flux. For cells with one electrolyte, $J_V = J_1 V_1 + J_w V_w + j\Delta V_{\rm el}$. By plotting the observed potential $(\Delta\phi + \Delta\phi_{\rm pol})$ versus $\sqrt{t}$, the streaming potential is obtained by extrapolation to $t = 0$, and L_p is obtained from the slope of the curve.

The water permeability was found in this manner for NaM and SrM_2 in the Ionics membrane. It was 2.4 and 0.9×10^{-14} m^2/kgs respectively. The water permeability in Nafion membranes were larger by a factor 50. The value did *not* compare well with the diffusion coefficient for water obtained for uniform pressure. This indicates that the pressure difference

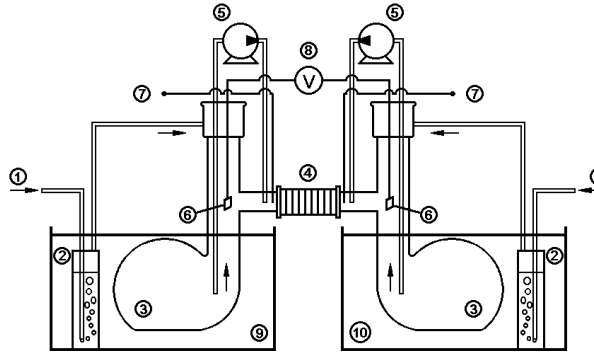

Figure 20.7 Schematic drawing of the thermocell apparatus. Numbers define 1) the N_2 gas supply and 2) bubble flasks, 3) electrode compartments, 4) Nafion membrane stack, 5) multispeed pumps, 6) Ag|AgCl-electrodes, 7) thermocouples, 8) potentiometer and 9,10) water baths. Reproduced from J. Membr. Sci. 107 (1995) 219–228 with permission from Elsevier.

may lead to viscous transport phenomena in nanometer (nm) small pores. Convective behavior has been observed in molecular dynamics simulations for pore diameters as small as a few molecular diameters [265].

20.5 The Seebeck coefficient

By measuring the thermoelectric potential, one can find the Peltier heat of the membrane. An apparatus for this measurement is shown in Fig. 20.7. Again, a membrane stack can be used. In this case, the temperature gradient is controlled by the stack. The variation in the thermoelectric potential is shown in Fig. 20.8.

The potential variation follows the recording of the thermistor in the solution with the high temperature. Eventually a stationary state is reached. The ratio of the two quantities gives the Seebeck-coefficient. For a cell with HCl, the measurements gave [263]

$$\left(\frac{\Delta\phi}{F\Delta T}\right)_{j=0,\Delta p=0} \equiv -t_{\mathrm{w}}S_{\mathrm{w}} + S^{*}_{\mathrm{H^+}} = 13 \quad \mathrm{J/Kmol} \tag{20.22}$$

By introducing $t_{\mathrm{w}} = 2.6$ and $S_{\mathrm{w}} = 69.9$ J/K mol into this equation, we find $S^{*}_{\mathrm{H^+}} = 195 \pm 14$ J/K mol. High values for transported entropies of protons are known from other systems [205]. From measurements of the Seebeck coefficient, one can calculate the Peltier heat.

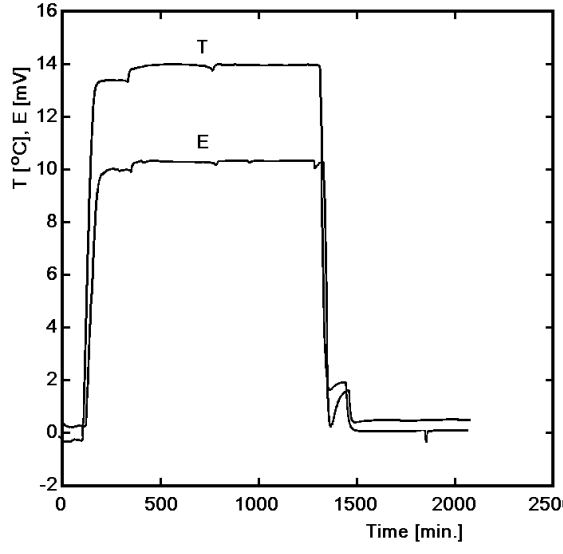

Figure 20.8 The emf of the thermocell as a function of time, when a temperature difference ΔT is applied to the cell. Reproduced from J. Membr. Sci. 107 (1995) 219–228 with permission from Elsevier.

20.6 Interdiffusion coefficients

Diffusion experiments were done in the cell [27, 256]

$$\mathrm{NaCl}(x_{\mathrm{NaCl,I}}, aq),\ \mathrm{HCl}(x_{\mathrm{HCl,I}}, aq)|^{\mathrm{mem}}|\mathrm{HCl}(x_{\mathrm{HCl,II}}, aq) \tag{20.23}$$

There are no electrodes in this cell, so $\Delta\phi = 0, j = 0$. NaCl is component 1, HCl is component 2, and water is component 3. With isothermal solutions of constant ionic strength, $\Delta\mu_3 = 0$ and $\Delta T = 0$, the flux equations can be rewritten as

$$\begin{aligned} J_1 &= -l_{11}\frac{d\mu_1}{dx} - l_{12}\frac{d\mu_2}{dx} \\ J_2 &= -l_{21}\frac{d\mu_1}{dx} - l_{22}\frac{d\mu_2}{dx} \end{aligned} \tag{20.24}$$

Because the solutions are electroneutral, the salt transports must obey $J_1 + J_2 = 0$, when $j = 0$. Since the chemical potential gradients are independent of each other, it follows that

$$l_{11} + l_{12} = 0 \qquad l_{21} + l_{22} = 0 \tag{20.25}$$

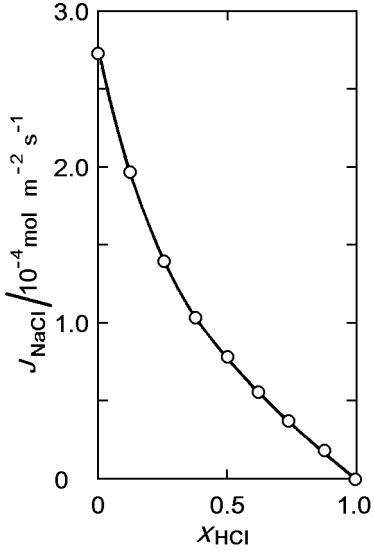

Figure 20.9 The flux of NaCl across an Ionics CR membrane during stationary state interdiffusion of Na^+ and H^+ [256]. The right hand side of the membrane has pure HCl, while the left hand side as a mixture of NaCl and HCl given by the mole fraction $x_{HCl,I}$.

so that the problem reduces to determination of *one* coefficient, l_{11}

$$J_1 = -l_{11}\frac{d}{dx}(\mu_1 - \mu_2) \tag{20.26}$$

The flux of NaCl to the right was measured as a function of $x_{\mathrm{HCl},I}$ in the left hand side solution, see Fig. 20.9, where x_{HCl} is the mole fraction of HCl in the solution. The stationary flux is the same everywhere in the membrane. The sum of the cation mole fractions of Na^+ and H^+ is unity in the membrane as well as in the solutions. The membrane thickness d_{m}, was measured from the left where $x = 0$ to the right where $x = d_{\mathrm{m}}$.

In order to relate l_{11} to the appropriate composition, consider first the case that has $c_{\mathrm{HCl},I} = 0$. The flux J_1 is the maximum one in Fig. 20.9. There is a concentration profile of NaM in the membrane, starting from pure NaM on the left hand side, going to 0 on the right hand side, see Fig. 20.10.

The concentration of HCl is next increased to $x'_{\mathrm{HCl},I}$, and the flux is lower, J'_1. The value of the force at the inlet of the membrane is the same as in the first case, not at $x = 0$, but at a position x' from the

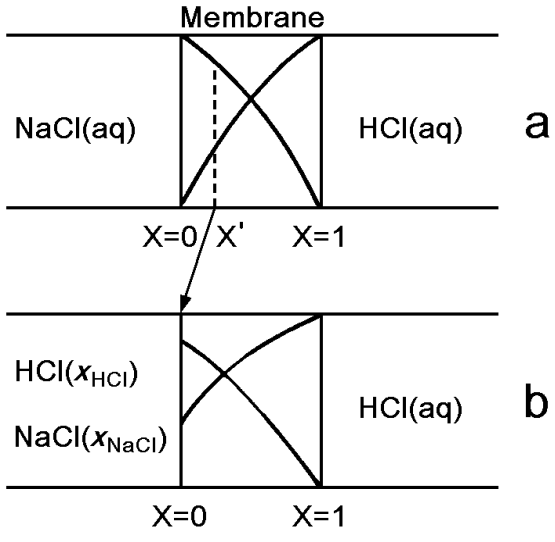

Figure 20.10 Expected concentration profiles across the membrane in the case that $x_{\mathrm{HCl},I} = 0$ (upper part of figure) and when it has changed to $x'_{\mathrm{HCl},I}$ (lower part of figure).

surface. Similarly, in the next measurement, the flux J_1'' can be related to the position x'' in the first experiment where the value of the driving force is the same. Now, if the membrane was thinner in the second and consecutive experiments, that is if it was $d_\mathrm{m} - x'$ in the second, $d_\mathrm{m} - x''$ in the third and so on numbered experiment, the values of the fluxes would have been the same. Since the membranes all have the same thickness, the positions with the same force must be related by

$$\frac{J_1'}{J_1} = \frac{d_\mathrm{m} - x'}{d_\mathrm{m}}$$

This relation makes possible a determination of x'. But then we know the composition of the solution in equilibrium with the membrane at this position. From the series of experiments we can then draw the concentration profile between 0 and d_m. We can also draw a profile of chemical potentials for the two components through the membrane. This allows us to find their gradients, the gradient difference, and finally the driving force for interdiffusion. The calculation of l_{11} follows. The composition of the solutions in equilibrium with the membrane can finally be related to the membrane compositions, through the equilibrium constant, and we have achieved the task of finding $l_{11}(x_\mathrm{HM})$.

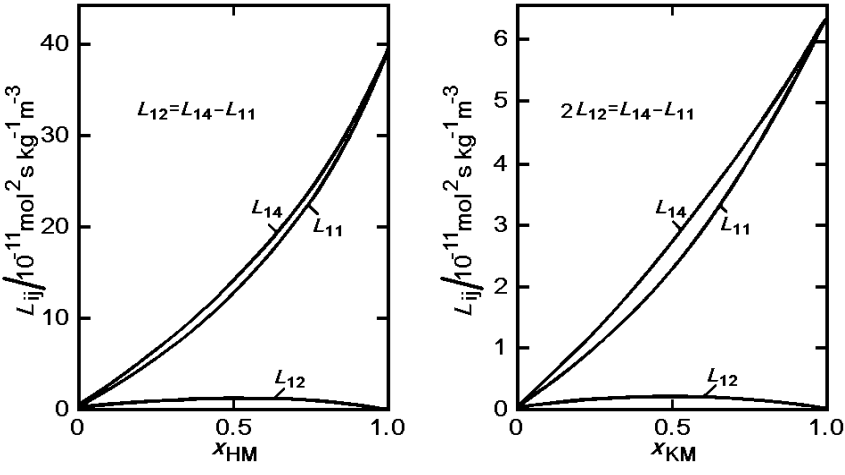

Figure 20.11 Membrane transport coefficients for transport of mass and charge in the isothermal system NaM-HM. Reproduced from Ber. Bunsenges. Physik. Chem. 92 (1988) 825–832 with permission from Royal Society of Chemistry.

Determination of $l_{11}(x_{\mathrm{HM}}), L_{14,}$ and L_{44} gives L_{11}. Values that were found in this manner are shown in Fig. 20.11. Independent determinations of L_{11} and L_{14} make possible a control of the Nernst–Einstein assumption. This was done for some systems, and it was found that L_{12} was small compared to the other coefficients [27, 250], see Fig. 20.11. The Nernst–Einstein assumption of equal diffusional and electric mobilities may thus be reasonably good in simple cation exchange membranes.

Chapter 21

The Impedance of an Electrode Surface

We derive the impedance of an electrode surface. The surface is part of a heterogeneous system, the polymer electrolyte fuel cell. We introduce the chemical potential of the surface dipole, in order to be able to describe storage, depletion and redistribution of charges in the surface. An equivalent circuit is predicted and compared with experimental results.

The impedance of an electrochemical cell is defined as minus the ratio of the applied oscillating potential difference, $\Delta\phi$, and the resulting electric current density, $j_{\rm tot}$, that is produced in the outer circuit [266]:

$$Z^{\rm cell} \equiv -\frac{\Delta\phi(\omega)}{j_{\rm tot}(\omega)} \tag{21.1}$$

Measurements of $\Delta\phi$ and $j_{\rm tot}$ can be done with high precision as a function of frequency ω, see e.g. Macdonald [267]. With two identical electrodes available, we measure the impedance of the path of charge transfer in two electrode materials ($Z^{\rm a}$), two electrode surfaces ($Z^{\rm s}$) and in the electrolyte ($Z^{\rm e}$) between these:

$$Z^{\rm cell} = 2Z^{\rm a} + 2Z^{\rm s} + Z^{\rm e} \tag{21.2}$$

Frequently, $Z^{\rm a}$ is negligible. The variation in $Z^{\rm s}$ with ω can be used to investigate rate limiting processes at the electrode surface. Spectra are normally illustrated as Nyquist plots of $Z^{\rm cell}$ according to

$$Z^{\rm cell} = \mathrm{Re}\, Z^{\rm cell} + \mathrm{i}\, \mathrm{Im}\, Z^{\rm cell} \tag{21.3}$$

where the imaginary part of the impedance is plotted as a function of the real part. One example of such plots are shown in Fig. 21.1. The electrolyte

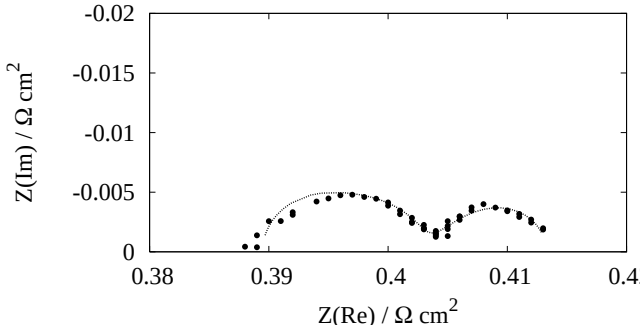

Figure 21.1 The Nyquist plot of the impedance of two hydrogen electrodes at 1 bar and 50°C in an unpolarized cell with a Nation membrane.

impedance is normally ohmic, and can be found from this figure by taking the limit of Z^{cell} for $\omega \to \infty$. This enables us to find Z^{s} as $(Z^{\text{cell}} - Z^{\text{e}})/2$.

The aim of this chapter is to demonstrate how the surface impedance, Z^{s}, can be determined using non-equilibrium thermodynamics. We shall use as an example the hydrogen electrode of the polymer fuel cell [81]. Other cases have also been investigated [268–271]. The experimental cell has as catalyst 0.5 mg Pt/cm^2 sprayed on to a standard E-TEK electrode backing material. The electrolyte is a Nafion®117 membrane. The electrode surface is part of a heterogeneous system, as shown in the close-up of Fig. 19.1. The experimental results at 50°C give two semicircles, at zero applied potential. Two semi-circles indicate that there are two rate-limiting steps involved, see Fig. 21.1. The problem is thus to find a model that can explain two such steps.

21.1 The hydrogen electrode. Mass balances

Consider the heterogeneous structure in Fig. 19.1 more detail. There is a porous carbon matrix layer located before the electrode surface, where adsorption and diffusion takes place. Charge transfer takes place at the platinum surface (the catalyst). There is a region (called s) with an excess of catalyst material of thickness in the order of 0.01 mm. This constitutes our thermodynamic surface. The thicknesses of the carbon matrix and the water-filled membrane that conducts protons on the other side of the surface are larger, in the order of 0.2 mm.

It is reasonable that one of the rate-limiting steps is the charge transfer step. But what is the other one? We shall assume that it is related to the processes in the porous carbon matrix [81, 268]. The reason is as follows.

Only a small fraction of the platinum metal has an interface with the gas in the pores. This means that only a few active sites are accessible directly from the gas. In order to reach most of the active sites on the Pt surface, hydrogen molecules must first adsorb to one of the surfaces involved (the gas-carbon, the gas-membrane or the gas-Pt surface), and then move to the rest of the Pt surface by diffusion along the mentioned surfaces. They arrive at the active sites after passing some three phase contact lines (cf. Chapter 6). Hydrogen molecules *cannot go directly* to the contact line from the gas phase. This would lead to an infinite velocity of the gas close to the contact line, which is impossible, see Remark 6.2. Early adsorption on a surface is therefore crucial for the hydrogen to reach most of the active sites on the Pt. Therefore, as the area of the Pt surface that is accessible to the gas is only a fraction of the porous carbon surface, we assume that the absorption/desorption on the walls of the pores is rate-limiting. We have (per mole of electrons produced)

$$\frac{1}{2}\mathrm{H_2(g)} \rightarrow \frac{1}{2}\mathrm{H_2(a)} \tag{21.4}$$

The gas diffuses along the pore surface to the platinum catalyst in the x-direction. During diffusion some molecules desorb to form hydrogen in the gas phase again, so the adsorption has first order reaction kinetics in both directions:

$$r(x,t) = \frac{1}{2}k^{\mathrm{a}}_{\mathrm{H_2}}c^{\mathrm{g}}_{\mathrm{H_2}} - \frac{1}{2}k^{\mathrm{d}}_{\mathrm{H_2}}c^{\mathrm{a}}_{\mathrm{H_2}}\,(x,t) \tag{21.5}$$

We use a course-grained description, in which all concentrations are given in $\mathrm{mol/m^3}$. The concentration $c^{\mathrm{g}}_{\mathrm{H_2}}$ is then the gas concentration in the pores times the porosity of the carbon layer. The course-grained concentration $c^{\mathrm{a}}_{\mathrm{H_2}}$, is the surface excess concentration in $\mathrm{mol/m^2}$ times the surface area of the pores per unit of volume in $\mathrm{m^{-1}}$, and $k^{\mathrm{a}}_{\mathrm{H_2}}$ and $k^{\mathrm{d}}_{\mathrm{H_2}}$ are rate constants.

The reaction

$$\frac{1}{2}\mathrm{H_2(a)} \rightarrow \mathrm{H(s)} \tag{21.6}$$

takes place at the platinum surface. The charge transfer step follows. The hydrogen atom dissociates on active sites of the platinum into protons in the membrane and electrons in the electronically conducting carbon matrix:

$$\mathrm{H(s)} \rightarrow \mathrm{H^+(m)} + \mathrm{e^-(a)} \tag{21.7}$$

Water is present in the carbon matrix and the membrane, but we neglect any role of water for this reaction here.

Each excess proton near the metal surface forms a dipole with an excess electron in the metal surface. The surface thus has a dipole layer. The

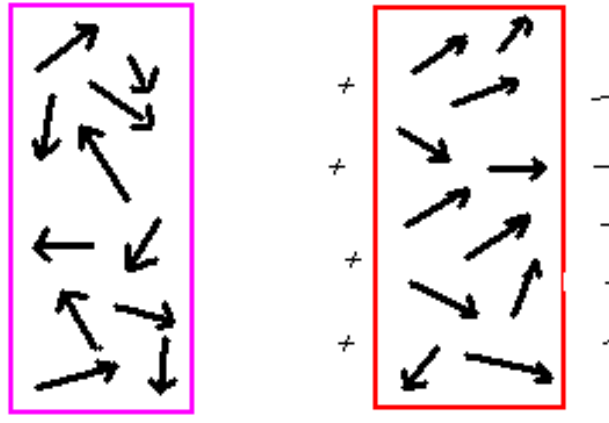

Figure 21.2 Dipoles at an unpolarized and a polarized surface. One dipole is made up by an ion and its image charge(s). This defines the surface polarization P^s or the surface double layer. The dipoles have a preferred direction in an electric field.

surface thickness is such that the excess adsorptions (in $\mathrm{mol/m^2}$) of protons, $\Gamma_{\mathrm{H^+}}$, and of electrons, $\Gamma_{\mathrm{e^-}}$ are equal. The dipole adsorption is

$$\Gamma_{\mathrm{p}}(t) \equiv \Gamma_{\mathrm{H^+}}(t) \tag{21.8}$$

A schematic illustration of the dipoles in the surface is given in Fig. 21.2. In an unpolarized surface, the dipoles have a random direction. In an electric field, the dipoles will orient themselves preferably in the direction of the field. The amount of dipoles in the surface depends probably on the surface polarization, i.e. the applied electric potential or the electric current density.

The charge transfer reaction increases the number of dipoles in the surface while the electric current j decreases it, giving

$$\frac{d}{dt}\Gamma_{\mathrm{p}} = r^{\mathrm{s}}_{\mathrm{ct}} - \frac{j}{F} \tag{21.9}$$

where $r^{\mathrm{s}}_{\mathrm{ct}}$ refers to the rate of the charge transfer reaction, and F is Faraday's constant. The surface polarization in the direction normal to the surface is equal to the dipole concentration times Faraday's constant, times the average distance, d_{s}, between the charges

$$P^{\mathrm{s}} = d_{\mathrm{s}} F \Gamma_{\mathrm{p}} \tag{21.10}$$

With constant d_s, it follows that the surface polarization and the adsorption of dipoles depend on each other. By eliminating Γ_p from Eq. (21.9), we obtain

$$r_{ct}^s = \frac{1}{F}\left(j + \frac{1}{d_s}\frac{dP^s}{dt}\right) \tag{21.11}$$

The surface polarization divided by the surface thickness gives the surface potential difference times the capacitance of the dipole layer, c_p,

$$\frac{P^s}{d_s} = F\Gamma_p = c_p^s \Delta_s \phi \tag{21.12}$$

The polarization P^s of Eqs. (21.10) and (21.12), is the polarization of the double layer and c_p^s in Eq. (21.12) is the capacitance of the double layer.

21.2 The oscillating field

Consider the potential difference between the anode and the centre of the membrane (i.e. half the cell potential) in the oscillating field in the presence of a direct current. The contributions from the dc and ac currents are superimposed:

$$\Delta\phi = \Delta\phi_{dc} + \Delta\phi_{ac}\exp(i\omega t) \tag{21.13}$$

The contribution to the emf of the two hydrogen electrodes are equal and opposite, and in the total cell potential they cancel each other. Each contribution is then the sum of the potential difference across one surface and half the membrane:

$$\Delta\phi_{dc} = \Delta_s\phi_{dc} + \frac{1}{2}\Delta_m\phi_{dc} \quad \text{and} \quad \Delta\phi_{ac} = \Delta_s\phi_{ac} + \frac{1}{2}\Delta_m\phi_{ac} \tag{21.14}$$

The electric current similarly has direct (dc) and alternating (ac) current contributions

$$j = j_{dc} + j_{ac}\exp(i\omega t) \tag{21.15}$$

In the membrane, which conducts by protons, one has

$$\Delta_m\phi_{dc} = r_m j_{dc} \quad \text{and} \quad \Delta_m\phi_{ac} = r_m j_{ac} \tag{21.16}$$

We want to find the potential differences across the surface.

The surface polarization can also be written as the sum of a stationary and an oscillating contribution

$$P^s = P_{dc}^s + P_{ac}^s\exp(i\omega t) \tag{21.17}$$

For the dc and the ac contributions to r_{ct}^s this gives, using Eq. (21.11),

$$r_{ct,dc}^s = \frac{1}{F}j_{dc} \quad \text{and} \quad r_{ct,ac}^s = \frac{1}{F}\left(j_{ac} + \frac{i\omega P_{ac}^s}{d_s}\right) \tag{21.18}$$

21.3 Reaction Gibbs energies

The reaction Gibbs energy of the adsorption is:

$$\Delta_r G^{\mathrm{s}}_{\mathrm{ad}}(x,t) = \frac{1}{2}\left(\mu^{\mathrm{a}}_{\mathrm{H_2}}(x,t) - \mu^{\mathrm{g}}_{\mathrm{H_2}}\right) \tag{21.19}$$

We assume equilibrium between the chemical potential of adsorbed hydrogen just before the surface and of atoms in the platinum surface, giving $2\mu^{\mathrm{s}}_{\mathrm{H}} = \mu^{\mathrm{a}}_{\mathrm{H_2}}(x=0)$, where $x=0$ is the position of the surface. The hydrogen gas in the experiment has a constant (position and time independent) pressure, leading to a constant $\mu^{\mathrm{g}}_{\mathrm{H_2}}$. The anode is located at $x<0$ and the membrane at $x>0$. In the coarse-grained description, transport takes place along a coordinate normal to the surface of the membrane. All variables are then independent of coordinates parallel to the surface.

The change in Gibbs energy at the surface due to the neutral species is:

$$\Delta_n G^{\mathrm{s}}_{\mathrm{ct}}(t) \equiv -\frac{1}{2}\mu^{\mathrm{a}}_{\mathrm{H_2}}(x=0,t) \tag{21.20}$$

For the total electrode reaction, we obtain

$$\Delta_n G^{\mathrm{s}} = \Delta_r G^{\mathrm{s}}_{\mathrm{ad}}(x=0,t) + \Delta_n G^{\mathrm{s}}_{\mathrm{ct}}(t) = -\frac{1}{2}\mu^{\mathrm{g}}_{\mathrm{H_2}} \tag{21.21}$$

21.4 The electrode surface impedance

We describe the consecutive steps. We consider the electrode backing to be continuous along the x-axis, while the electrode interfaces are described as a Gibbs surface starting at position 0. Processes in the membrane are neglected.

21.4.1 *The adsorption-diffusion layer in front of the catalyst*

The time-dependence of the concentration of hydrogen at position x in the anode is given by

$$\frac{\partial c^{\mathrm{a}}_{\mathrm{H_2}}(x,t)}{\partial t} = -\frac{\partial J^{\mathrm{a}}_{\mathrm{H_2}}(x,t)}{\partial x} + \frac{1}{2}k^{\mathrm{a}}_{\mathrm{H_2}}c^{\mathrm{g}}_{\mathrm{H_2}} - \frac{1}{2}k^{\mathrm{d}}_{\mathrm{H_2}}c^{\mathrm{a}}_{\mathrm{H_2}}(x,t) \tag{21.22}$$

where

$$J^{\mathrm{a}}_{\mathrm{H_2}}(x,t) = -D^{\mathrm{a}}_{\mathrm{H_2}}\frac{\partial c^{\mathrm{a}}_{\mathrm{H_2}}(x,t)}{\partial x} \tag{21.23}$$

is the coarse-grained diffusion flux (in $\mathrm{mol/m^2 s}$) of molecular hydrogen along the surface of the pores in the carbon matrix to the catalyst surface

at $x = 0$ and $D^{\mathrm{a}}_{\mathrm{H}_2}$ is the diffusion constant (in m^2/s). Equilibrium in the adsorption reaction gives the equilibrium concentration of adsorbed hydrogen, from Eq. (21.5)

$$c^{\mathrm{a}}_{\mathrm{H}_2,eq} = c^{\mathrm{g}}_{\mathrm{H}_2} \frac{k^{\mathrm{a}}_{\mathrm{H}_2}}{k^{\mathrm{d}}_{\mathrm{H}_2}} \tag{21.24}$$

The rate coefficients may depend on the state of the material, whether it is polarized or not, and on the pressure. A constant hydrogen pressure in the pore gives a constant gas concentration, $c^{\mathrm{a}}_{\mathrm{H}_2}$, and therefore also a constant value for $c^{\mathrm{a}}_{\mathrm{H}_2,eq}$.

We shall use a linear approximation to the kinetics of the adsorption/desorption reaction. This is appropriate for low hydrogen coverage. We introduce the deviation from the equilibrium concentration

$$c^{\mathrm{a}}_{\mathrm{H}_2}(x,t) \equiv c^{\mathrm{a}}_{\mathrm{H}_2,eq} + \delta c^{\mathrm{a}}_{\mathrm{H}_2}(x,t) \tag{21.25}$$

Equation (21.22) then becomes, for $\delta c^{\mathrm{a}}_{\mathrm{H}_2}$

$$\frac{\partial \delta c^{\mathrm{a}}_{\mathrm{H}_2}(x,t)}{\partial t} = D^{\mathrm{a}}_{\mathrm{H}_2} \frac{\partial^2 \delta c^{\mathrm{a}}_{\mathrm{H}_2}(x)}{\partial x^2} - \frac{1}{2} k^{\mathrm{d}}_{\mathrm{H}_2} \delta c^{\mathrm{a}}_{\mathrm{H}_2}(x,t) \tag{21.26}$$

For a dc electric current Eq. (21.26) reduces to

$$0 = D^{\mathrm{a}}_{\mathrm{H}_2} \frac{\partial^2 \delta c^{\mathrm{a}}_{\mathrm{H}_2,\mathrm{dc}}(x)}{\partial x^2} - \frac{1}{2} k^{\mathrm{d}}_{\mathrm{H}_2} \delta c^{\mathrm{a}}_{\mathrm{H}_2,\mathrm{dc}}(x) \tag{21.27}$$

The solution is given by

$$\delta c^{\mathrm{a}}_{\mathrm{H}_2,\mathrm{dc}}(x) = -\frac{j_{\mathrm{dc}}}{F\sqrt{2D^{\mathrm{a}}_{\mathrm{H}_2} k^{\mathrm{d}}_{\mathrm{H}_2}}} \exp\left(x\sqrt{\frac{k^{\mathrm{d}}_{\mathrm{H}_2}}{2D^{\mathrm{a}}_{\mathrm{H}_2}}}\right) \tag{21.28}$$

where we used

$$2J^{\mathrm{a}}_{\mathrm{H}_2}(x=0) = r^{\mathrm{s}}_{\mathrm{ct,dc}} = r^{\mathrm{s}}_{\mathrm{ad,dc}} = j_{\mathrm{dc}}/F \tag{21.29}$$

We see from Eq. (21.28) that $\delta c^{\mathrm{a}}_{\mathrm{H}_2,dc}$ is negative when $j_{\mathrm{dc}} > 0$ and positive when $j_{\mathrm{dc}} < 0$. When the thickness d of the carbon layer is smaller than $\sqrt{2D^{\mathrm{a}}_{\mathrm{H}_2}/k^{\mathrm{d}}_{\mathrm{H}_2}}$ one must use a diffusion flux in $x = -d$ equal to zero. One must then replace $\exp\left[x\sqrt{k^{\mathrm{d}}_{\mathrm{H}_2}/2D^{\mathrm{a}}_{\mathrm{H}_2}}\right]$ by $\cosh\left[(x+d)\sqrt{k^{\mathrm{d}}_{\mathrm{H}_2}/2D^{\mathrm{a}}_{\mathrm{H}_2}}\right] / \cosh\left[d\sqrt{k^{\mathrm{d}}_{\mathrm{H}_2}/2D^{\mathrm{a}}_{\mathrm{H}_2}}\right]$ in Eqs. (21.28) and (21.32) and make a similar replacement in Eqs. (21.35) and (21.37). This implies that the mass transport at low frequencies will be reduced compared to the expressions given.

We use

$$\mu^{\mathrm{a}}_{\mathrm{H}_2}(x,t) = \mu^{\mathrm{a},0}_{\mathrm{H}_2} + RT\ln\left(\frac{c^{\mathrm{a}}_{\mathrm{H}_2}(x,t)}{c^{\mathrm{a},0}_{\mathrm{H}_2}}\right)$$
$$= \mu^{\mathrm{a},0}_{\mathrm{H}_2} + RT\ln\left(\frac{c^{\mathrm{a}}_{\mathrm{H}_2,eq}}{c^{\mathrm{a},0}_{\mathrm{H}_2}}\right) + RT\ln\left(\frac{c^{\mathrm{a}}_{\mathrm{H}_2}(x,t)}{c^{\mathrm{a}}_{\mathrm{H}_2,eq}}\right)$$
$$= \mu^{\mathrm{a}}_{\mathrm{H}_2,eq} + RT\ln\left(\frac{c^{\mathrm{a}}_{\mathrm{H}_2}(x,t)}{c^{\mathrm{a}}_{\mathrm{H}_2,eq}}\right) \tag{21.30}$$

for the chemical potential of hydrogen, where $\mu^{\mathrm{a},0}_{\mathrm{H}_2}$ and $c^{\mathrm{a},0}_{\mathrm{H}_2}$ are standard values. To linear order in $\delta c^{\mathrm{a}}_{\mathrm{H}}$, this gives

$$\mu^{\mathrm{a}}_{\mathrm{H}_2}(x,t) = \mu^{\mathrm{a}}_{\mathrm{H}_2,eq} + RT\ln\left(1+\frac{\delta c^{\mathrm{a}}_{\mathrm{H}_2}(x,t)}{c^{\mathrm{a}}_{\mathrm{H}_2,eq}}\right) = \mu^{\mathrm{a}}_{\mathrm{H}_2,eq} + RT\frac{\delta c^{\mathrm{a}}_{\mathrm{H}_2}(x,t)}{c^{\mathrm{a}}_{\mathrm{H}_2,eq}} \tag{21.31}$$

By introducing Eq. (21.28), we obtain

$$\mu^{\mathrm{a}}_{\mathrm{H}_2,dc}(x) = \mu^{\mathrm{a}}_{\mathrm{H}_2,eq} - \frac{j_{\mathrm{dc}}RT}{Fc^{\mathrm{a}}_{\mathrm{H}_2,eq}\sqrt{2D^{\mathrm{a}}_{\mathrm{H}_2}k^{\mathrm{d}}_{\mathrm{H}_2}}}\exp\left(x\sqrt{\frac{k^{\mathrm{d}}_{\mathrm{H}_2}}{2D^{\mathrm{a}}_{\mathrm{H}_2}}}\right) \tag{21.32}$$

The Gibbs energy change over the whole layer becomes

$$\Delta_r G_{\mathrm{ad,dc}} = \mu^{\mathrm{s}}_{\mathrm{H,dc}} - \frac{1}{2}\mu^{\mathrm{g}}_{\mathrm{H}_2} = \frac{1}{2}\left[\mu^{\mathrm{a}}_{\mathrm{H}_2,dc}(x=0) - \mu^{\mathrm{a}}_{\mathrm{H}_2,dc}(x=-\infty)\right]$$
$$= -\frac{j_{\mathrm{dc}}RT}{2Fc^{\mathrm{a}}_{\mathrm{H}_2,eq}\sqrt{2D^{\mathrm{a}}_{\mathrm{H}_2}k^{\mathrm{d}}_{\mathrm{H}_2}}} \tag{21.33}$$

$\Delta_r G_{\mathrm{ad,dc}}$ gives a contribution to the surface potential drop via $\delta\mu^{\mathrm{a}}_{\mathrm{H}_2,\mathrm{dc}}(x=0)$.

The ac contribution to $c^{\mathrm{a}}_{\mathrm{H}_2}(x,t)$ is also small. Equation (21.26) together with Eq. (21.23) therefore reduce to

$$i\omega\delta c^{\mathrm{a}}_{\mathrm{H}_2,\mathrm{ac}}(x) = D^{\mathrm{a}}_{\mathrm{H}_2}\frac{\partial^2\delta c^{\mathrm{a}}_{\mathrm{H}_2,\mathrm{ac}}(x)}{\partial x^2} - \frac{1}{2}k^{\mathrm{d}}_{\mathrm{H}_2}\delta c^{\mathrm{a}}_{\mathrm{H}_2,\mathrm{ac}}(x) \tag{21.34}$$

The solution to Eq. (21.34) becomes

$$\delta c^{\mathrm{a}}_{\mathrm{H}_2,ac}(x) = -A\exp\left[x\sqrt{\frac{k^{\mathrm{d}}_{\mathrm{H}_2}}{2D^{\mathrm{a}}_{\mathrm{H}_2}}(1+i\omega\tau_{\mathrm{ad}})}\right] \tag{21.35}$$

where the relaxation time of the adsorption is

$$\tau_{\rm ad} = \frac{2}{k^{\rm d}_{\rm H_2}} = \frac{2c^{\rm a}_{\rm H_2,\mathit{eq}}}{k^{\rm a}_{\rm H_2} c^{\rm g}_{\rm H_2}} \tag{21.36}$$

We used Eq. (21.24) in the last equality. The constant A in Eq. (21.35) must be determined from the boundary condition in $x = 0$. The resulting contribution to the chemical potential, cf. Eq. (21.31), due to the ac current is

$$\begin{aligned}\mu^{\rm a}_{\rm H_2,\mathit{ac}}(x) &= RT\delta c^{\rm a}_{\rm H_2,\mathit{ac}}(x)/c^{\rm a}_{\rm H_2,\mathit{eq}} \\ &= -\frac{ART}{c^{\rm a}_{\rm H_2,\mathit{eq}}} \exp\left[x\sqrt{\frac{k^{\rm d}_{\rm H_2}}{2D^{\rm a}_{\rm H_2}}(1+i\omega\tau_{\rm ad})}\right]\end{aligned} \tag{21.37}$$

The contribution due to a small dc current has already been given as the second term on the right hand side of Eq. (21.32).

The total amount of adsorbed hydrogen molecules on the pore surface due to the ac current, is

$$n^{\rm a}_{\rm H_2,\mathit{ac}} = \int_{-\infty}^{0} \delta c^{\rm a}_{\rm H_2,\mathit{ac}}(x)\,dx = -A\sqrt{\frac{2D^{\rm a}_{\rm H_2}}{k^{\rm d}_{\rm H_2}(1+i\omega\tau_{\rm ad})}} \tag{21.38}$$

The ac contribution to the reaction rate for the adsorption reaction is then given by

$$r^{\rm s}_{\rm ad,ac} = -k^{\rm d}_{\rm H_2}\int_{-\infty}^{0} \delta c^{\rm a}_{\rm H_2,\mathit{ac}}(x)\,dx = -k^{\rm d}_{\rm H_2} n^{\rm a}_{\rm H_2,\mathit{ac}} = A\sqrt{\frac{2D^{\rm a}_{\rm H_2}k^{\rm d}_{\rm H_2}}{1+i\omega\tau_{\rm ad}}} \tag{21.39}$$

The corresponding reaction rate for the charge transfer reaction is given by

$$r^{\rm s}_{\rm ct,ac} = 2J^{\rm a}_{\rm H_2}(x=0) = A\sqrt{2D^{\rm a}_{\rm H_2}k^{\rm d}_{\rm H_2}(1+i\omega\tau_{\rm ad})} = (1+i\omega\tau_{\rm ad})r^{\rm s,a}_{\rm ad,ac} \tag{21.40}$$

The ac contribution to the reaction Gibbs energy of the adsorption is

$$\Delta_r G_{\rm ad,ac} = \frac{1}{2}(\mu^{\rm a}_{\rm H_2,ac}(x=0) - \mu^{\rm g}_{\rm H_2,ac}) = \frac{1}{2}\mu^{\rm a}_{\rm H_2,ac}(x=0) = -\frac{ART}{2c^{\rm a}_{\rm H_2,\mathit{eq}}} \tag{21.41}$$

where we used Eq. (21.37). By eliminating A in Eq. (21.41) using Eq. (21.40) we find,

$$\Delta_r G_{\rm ad,ac} = -Z_{\rm ad}F^2 r^{\rm s}_{\rm ct,ac} \tag{21.42}$$

where

$$Z_{\rm ad} = \frac{RT}{2F^2 c^{\rm a}_{{\rm H}_2,eq}\sqrt{2D^{\rm a}_{{\rm H}_2}k^{\rm d}_{{\rm H}_2}\,(1+i\omega\tau_{\rm ad})}} \tag{21.43}$$

This is the impedance of a so-called Gerischer element. The second semicircle of the impedance diagram Fig. 21.1 for the hydrogen electrode of the fuel cell fits well to such an element [81]. Other elements can only be fitted with larger inaccuracies. The expression predicts that the impedance becomes smaller as the equilibrium adsorption of the hydrogen to the pore surface in the carbon matrix becomes larger.

21.4.2 *The charge transfer reaction*

Consider next the surface between the membrane and the adsorption-diffusion layer in the electrode. The excess entropy production of this surface, $\sigma^{\rm s}_{\rm ct}$, of an isothermal surface is according to Chapter 5, see also [270]:

$$T\sigma^{\rm s}_{\rm ct,ac} = -j_{\rm ac}\Delta_{\rm s}\phi_{\rm ac} + i\omega P^{\rm s}_{\rm ct,ac}\left(\frac{D-D^{\rm s}_{eq}}{\varepsilon_0}\right)_{\rm ac} - r^{\rm s}_{\rm ct,ac}\Delta_n G^{\rm s}_{\rm ct,ac} \tag{21.44}$$

The D in this equation is the displacement field and ε_0 is the dielectric constant of vacuum. The equilibrium displacement field is zero for free charges, $D^{\rm s}_{eq} = 0$. The displacement field is given by $D = -\varepsilon_0\Delta_{\rm s}\phi_{\rm ac}/d_{\rm s}$. Using Eq. (21.18) for the ac contribution we obtain

$$T\sigma^{\rm s}_{\rm ct,ac} = -r^{\rm s}_{\rm ct,ac}\left(\Delta_n G^{\rm s}_{\rm ct,ac} + F\Delta_{\rm s}\phi_{\rm ac}\right) \tag{21.45}$$

The force and the flux are related by

$$\Delta_{\rm s}\phi_{\rm ac} + \frac{\Delta_n G^{\rm s}_{\rm ct,ac}}{F} = -\rho^{\rm s}_{\rm ct}Fr^{\rm s}_{\rm ct,ac} \tag{21.46}$$

where $\rho^{\rm s}_{\rm ct}$ is the resistivity of the charge transfer reaction. The electrochemical reaction rate is normally not related to its driving force by a linear relation. In this experiment, the alternating contribution to the forces are small (± 5 mV), however, so that we can use a linear theory. The adsorption-diffusion layer has an impact on $\Delta_s\phi_{\rm ac}$, through the chemical potential of hydrogen atoms at position $x = 0$. The resistivity is independent of the driving force, but can depend on the temperature and the polarization induced by the dc-field.

The dc contribution to the excess entropy production is found using $\omega = 0$ and $j_{\rm dc} = Fr^{\rm s}_{\rm ct,dc}$. This gives

$$T\sigma^{\rm s}_{\rm ct,dc} = -j_{\rm dc}\left(\Delta_{\rm s}\phi_{\rm dc} + \frac{\Delta_n G^{\rm s}_{\rm ct,dc}}{F}\right) \tag{21.47}$$

For small dc-currents the linear law is thus:

$$\Delta_{\rm s}\phi_{\rm dc} + \frac{\Delta_n G^{\rm s}_{\rm ct,dc}}{F} = -\rho^{\rm s}_{\rm ct} F r^{\rm s}_{\rm ct,dc} = -\rho^{\rm s}_{\rm ct} j_{\rm dc} \tag{21.48}$$

which is exactly the same relation as for the ac current, Eq. (21.46).

21.4.3 *The impedance spectrum*

The impedance spectrum in Fig. 21.1 is the sum of contributions from each layer, cf. Eq. (21.2). The surface impedance can be defined as

$$Z^{\rm s} \equiv -\frac{\Delta_{\rm s}\phi_{\rm ac}}{j_{\rm ac}} \tag{21.49}$$

We can now find the surface impedance by adding Eqs. (21.42) and (21.46). This gives

$$\Delta_{\rm s}\phi_{\rm ac} + \frac{\Delta_n G^{\rm s}_{\rm ac}}{F} = \Delta_{\rm s}\phi_{\rm ac} = -\left(\rho^{\rm s}_{\rm ct} + Z_{\rm ad}\right) F r^{\rm s}_{\rm ct,ac} \tag{21.50}$$

using a constant chemical potential of the hydrogen gas, cf. Eq. (21.21). Furthermore, it follows from Eqs. (21.11) and (21.12) that

$$F r^{\rm s}_{\rm ct,ac} = j_{\rm ac} + i\omega c^{\rm s}_{\rm p} \Delta_{\rm s}\phi_{\rm ac} \tag{21.51}$$

By combining Eqs. (21.49)–(21.51), we obtain the surface impedance

$$Z^{\rm s} = \frac{\rho^{\rm s}_{\rm ct} + Z_{\rm ad}}{1 + i\omega c^{\rm s}_{\rm p}\left(\rho^{\rm s}_{\rm ct} + Z_{\rm ad}\right)} \tag{21.52}$$

When $\omega \to \infty$, we see that

$$Z^{\rm s}_{\omega\to\infty} = 0 \tag{21.53}$$

In this case, the measurement gives the ohmic resistance of the cell.

The limiting behavior $\omega \to 0$ gives

$$Z^{\rm s}_{\omega\to 0} = Z_{\omega\to 0,\rm ad} + \rho^{\rm s}_{\rm ct} \tag{21.54}$$

The expression for $Z_{\rm ad}$ can be abbreviated by:

$$Z_{\rm ad} = \frac{1}{Y_0\sqrt{\tau^{-1}_{\rm ad} + i\omega}} \tag{21.55}$$

with the relaxation time, $\tau_{\rm ad} = 2/k^{\rm d}_{\rm H_2}$, see Eq. (21.36), and the admittance:

$$Y_0 = \frac{4F^2}{RT} c^{\rm a}_{{\rm H}_2,eq}\sqrt{D^{\rm a}_{\rm H_2}} \tag{21.56}$$

The relaxation time is constant, while the admittance is proportional to the concentration of hydrogen in the gas phase.

In practice there may be non-ideal contributions to the impedance of the surface. A constant phase element (CPE) has been used, rather than a capacitance in parallel with the resistance, to compensate for surface heterogeneities. The CPE is defined by:

$$\mathrm{Z_{CPE}} = \frac{1}{\mathrm{T_{ct}}(i\omega)^{\alpha_{\mathrm{ct}}}} \tag{21.57}$$

The phase angle of the CPE is constant and independent of the frequency. When α_{ct}=1, $\mathrm{T_{ct}}$= $c_{\mathrm{p}}^{\mathrm{s}}$. The more depressed the semi-circle is, the lower is the value of α. The corresponding relaxation time is:

$$\tau_{\mathrm{ct}} = (\mathrm{T_{ct}}\rho_{\mathrm{ct}})^{1/\alpha_{\mathrm{ct}}} \tag{21.58}$$

The experimental results below support, with the modification Eq. (21.58), the theoretical model.

21.5 A test of the model

The theoretical expression (21.56) predicted a pressure variation in the admittance, Y_0. The impedance of the cell was therefore measured at five pressures between 1 and 4 bar, and at constant temperature (50°C). The applied dc potential was also varied. The impedance was found sweeping over a frequency range from 10 kHz to 10 mHz. An amplitude of 5 mV was used. Figure 21.1 gives results for zero applied potentials at 1 bar.

The high frequency intercept with the real axis in Fig. 21.1 was constant in all spectra recorded, it was 0.39 ± 0.01 Ω cm^2. This value, which is the resistance of the Nafion®117 membrane in the cell, is in good agreement with results reported in the literature for this temperature [268].

The high frequency regime of the impedance diagram, is according to the previous section, Eqs. (21.52) and (21.57), related to the charge transfer step. The peak is not a perfect semicircle, which is possibly caused by the heterogeneity of the electrode surface. The relaxation time of this phenomenon depends on the applied potential (not shown), which is likely for a charge transfer step. The relaxation times for the two steps are given in Table 21.1 as a function of hydrogen pressure, for an unpolarized electrode.

The low frequency semicircle was fitted to the Gerischer phase element. The relaxation time τ_{ad} did not vary with the applied dc potential, as predicted from Eq. (21.36). The admittance varied linearly with $c^{\mathrm{a}}_{\mathrm{H_2},eq}$, as predicted from Eq. (21.56) and shown in Fig. 21.3. The slope of Fig. 21.3

Table 21.1 Relaxation times as a function of hydrogen pressure.

p_{H_2}/bar	τ_{ct}/s	τ_{ad}/s
1	2.9	6
2.26	5.5	6
3.06	6.5	6
4.00	6.9	6

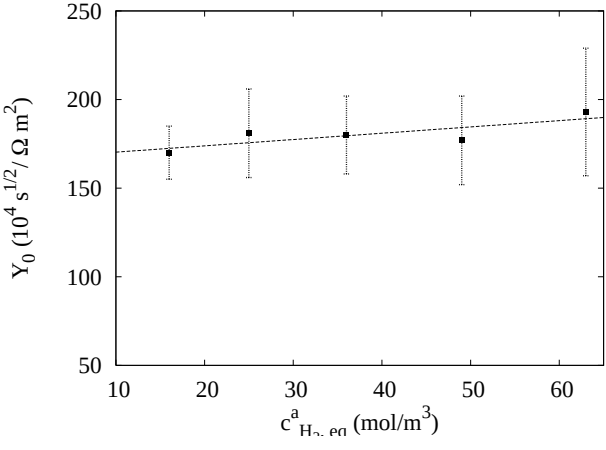

Figure 21.3 The admittance Y_0 of the hydrogen electrode of the polymer electrolyte fuel cell plotted as a function of hydrogen pressure. Reproduced from J. Membr. Sci. 282 (2006) 96–108 with permission of Elsevier.

was used to find a diffusion coefficient, $D^{a}_{H_2} = 1\times10^{-7}$ m^2/s [268], assuming $k^{a}_{H_2} = k^{d}_{H_2}$.

Lower temperatures have revealed a shoulder in the impedance diagram. This means that the model described above is not complete, but must be refined, probably by including a rate-limiting role for the hydration of protons, see [268, 272–274].

21.6 The reaction overpotential

When impedance experiments are done in the presence of a constant applied potential, the total potential is a sum of a constant part and an oscillating part:

$$\Delta\phi_{tot}(t) = \Delta\phi_{dc} + \Delta\phi(\omega) \tag{21.59}$$

We can deal with the two parts separately. The constant part of the potential produces a constant (dc) current that determines the state of surface polarization. This state can be regarded as stationary. The balance equation for dipoles then gives $j/F = r^{\mathrm{s}} = j_{\mathrm{dc}}/F$, and the entropy production reduces to

$$T\sigma^{\mathrm{s}} = -j_{\mathrm{dc}} \left(\Delta\phi + \frac{\Delta_n G^{\mathrm{s}}}{F} \right) \tag{21.60}$$

The parenthesis is the effective driving force for the chemical reaction. The electrochemical reaction is frequently an activated process and the net driving force can be substantial at the cathode of the fuel cell (cf. Chapter 19). The current density is a linear function of the driving force, only when the force is small. When the driving force is large, the relationship becomes nonlinear, see e.g. [97].

The overpotential of a polarizable electrode is measured under steady state conditions with the help of three electrodes. A net current is passed between the working electrode (the electrode of interest) and an auxiliary electrode. The electric potential drop across the surface for the given current density is $\Delta\phi(j_{\mathrm{dc}})$. The open circuit potential between the working electrode and a reference electrode is $\Delta\phi_{j\to 0}$. The overpotential is found as the difference between $\Delta\phi(j_{\mathrm{dc}})$ and $\Delta\phi_{j\to 0}$:

$$\eta = \Delta\phi(j_{\mathrm{dc}}) - \Delta\phi_{j\to 0} \tag{21.61}$$

The measurement gives the overpotential as a function of current density. The non-linear relation is the so-called Butler–Volmer relation. The relation between η and j_{dc} is complicated because the dipole adsorption depends on the state of the electrode, here represented by P^{s}. Rubi and Kjelstrup showed how this relation can be derived using non-equilibrium thermodynamics on the mesoscopic level [51].

Chapter 22

Non-Equilibrium Molecular Dynamics Simulations

We describe a computer simulation technique that is designed to study transport processes. The name of the method is non-equilibrium molecular dynamics simulations (NEMD). We shall describe how we can find transport coefficients in one-phase fluids and heterogeneous systems from NEMD. Molecular explanations of the coefficients values are of interest. In a system that transports heat and mass, we can use NEMD to verify the assumption of local equilibrium and of Onsager reciprocal relations. We examine also the linear nature of the flux-force relations.

Non-equilibrium molecular dynamics simulations (NEMD) is a computer technique that is designed to investigate particle behavior in systems with gradients in intensive variables. The system behavior follows from the interaction between the particles. Such interactions can for instance be described by a pair potential like the Lennard-Jones potential [275, 276].

Algorithms that characterize NEMD were developed by Hafskjold and coworkers [277]. Gradients are applied to the system by perturbation of its boundaries, in so-called *boundary driven* NEMD. Alternatively, one can set up a flux via the boundaries, and study resulting gradients. The method simulates therefore experiments in its determination of transport properties. We present the useful technique here, drawing especially on the work of Hafskjold and coworkers [65, 66, 149, 277–283] and others [284–288]. In addition to presenting the technique, we present some results [39, 40, 65, 67, 112, 289] that confirm the basic assumptions in classical non-equilibrium thermodynamics. We will not discuss the use of the Kubo relations (see Fig. 1.2) to determine transport coefficients using equilibrium molecular dynamics simulations from integrals over equilibrium flux-flux correlation functions.

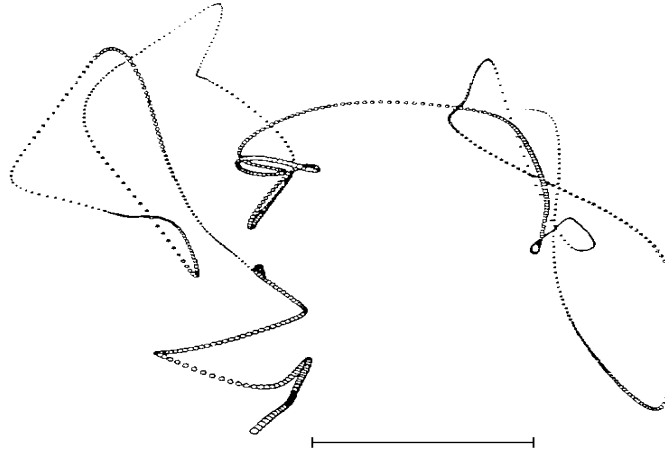

Figure 22.1 A typical trajectory for one particle in a gas (only one particle is shown). The particle moves according to Newton's laws and interacts with a Lennard-Jones potential. The distance between the points is one time-step in the calculation. The length of the mean free path is shown by the bar. (Courtesy of B. Hafskjold)

In NEMD, the computer is used to solve Newton's equations of motion for the particles in the system. On a microscopic level, the particle motion appears chaotic, even if Newton's laws are reversible in time. A typical trajectory for one particle in a system in equilibrium is given in Fig. 22.1. Many particles are moved around in the box, but only one trajectory is shown. Whenever this trajectory changes, a collision takes place. The particles collide with each other and with the walls. All thermodynamic and transport properties of the system are derived from the mechanical properties of the set of colliding particles in NEMD.

After 4000 time steps of calculation, the particles in each layer already have a molecular velocity distribution equal to a Maxwell distribution. It has also been verified that the temperature, as calculated from the equipartition principle, is the same in all three directions in space, in a homogeneous system as well as a heterogeneous one. Figure 22.2 shows the temperature in a volume element in the center of a system with two types of particles. We see the fluctuations in the dimensionless temperature, $T^* = k_B T/\varepsilon$, where ε is the potential depth of the Lennard-Jones type potential of the heavy particles and k_B is Boltzmann's constant. The technique uses dimensionless variables, which are further explained in Table 22.1. The fluctuations in Fig. 22.2 obeyed $\delta T/T < 0.03$ [65].

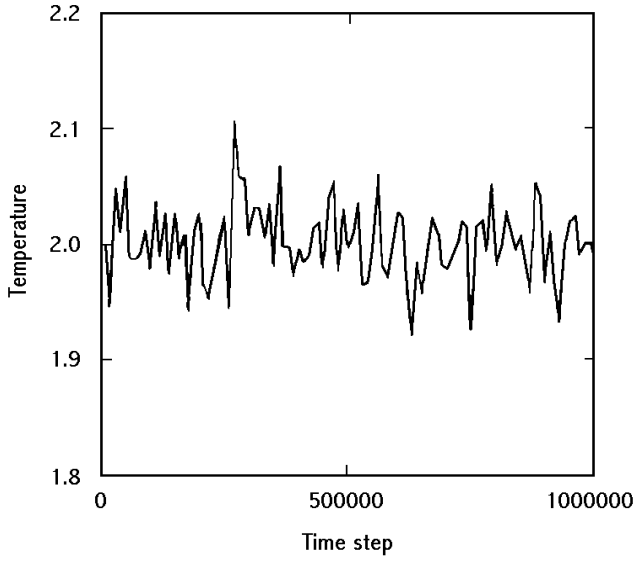

Figure 22.2 Fluctuations in dimensionless temperature at some position in the box during stationary state heat conductance in a two-component mixture. The system is the same as in Fig. 22.6 (Courtesy of B. Hafskjold).

NEMD and other computer techniques utilize periodic boundary conditions, in order to obtain a larger and more representative system in a computer-efficient manner. Instead of finding the average over one large system, one finds the average over many small identical systems. A particle leaving one box enters the next in a way that makes the system periodic, and introduces a plane of symmetry in the center of each box. NEMD simulations are often run until a stationary state is obtained. An average over a layer with only a few particles, but over long time intervals, can then replace an average over many particles (the ergodic hypothesis). The average behavior of all particles is taken as the collective behavior of the ensemble in a layer.

NEMD simulations can be used to study properties of ensembles of particles, in both global equilibrium and out of global equilibrium. In global equilibrium, all boundaries are set with the same conditions; out of global equilibrium they are not. In order to determine transport properties, one often requires also the equilibrium properties of the system. It is therefore of interest to use NEMD to find both types of data. Variations of variables like the particle density, the temperature and the pressure, in the homogeneous

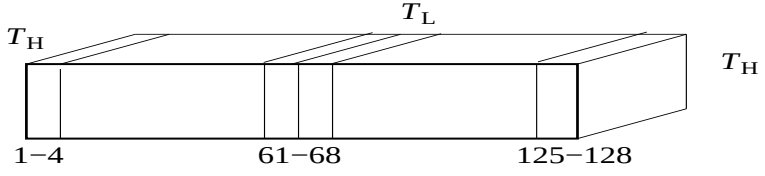

Figure 22.3 The box in a NEMD simulation is divided into a number of equal layers (128 in this case). Boundary conditions, indicated here by the temperatures T_L and T_H, are symmetric around the center of the box.

phases, and across the interface between a liquid and its vapor, are of interest. One can use this information to first find the equation of state (in equilibrium systems), and then the transport properties (in non-equilibrium systems).

Simulations cannot be expected to give values found by experiments, even if much progress has been made in this direction the last few years [290]. The expression for the interaction potential is a *guess* for a real system. The advantage of NEMD is that *trends and variations* in properties can be traced back to part(s) of the interaction potential that causes the variation. This property means that NEMD gives molecular insight in system behavior. It becomes possible to distinguish between important and minor effects. This is important when it is necessary to introduce assumptions. This is the usefulness of NEMD: it acts as a tool to help understand experimental results, and it can be used to test assumptions made in the theory. Since it is difficult to do experiments in heterogeneous systems, the technique is very valuable.

We continue to describe details of the NEMD technique before we present results that confirm the hypothesis of local equilibrium and of the Onsager relations, in a one-phase system, and at a surface.

22.1 The system

The NEMD simulation starts with construction of a rectangular box with dimensions L_x, L_y and L_z. Here x is the direction along the box, y is the vertical direction and z is the depth direction, see Fig. 22.3. The box contains N particles. The density is changed by varying the box size, using:

$$\rho = V\frac{N_{\mathrm{A}}}{N} = L_x L_y L_z \frac{N_{\mathrm{A}}}{N} \tag{22.1}$$

where N_{A} is Avogadro's number and ρ is the overall molar density of particles. We are interested in transports in the $x-$direction. In this direction,

the box is divided into equal layers for monitoring of local properties. The cell used is usually not cubic $L_x > L_y = L_z$. The temperature, density, pressure, composition, enthalpy, fluxes, and other properties of interest can be computed in each layer. The box in Fig. 22.3 has, say, a temperature gradient between the ends and the center of the box. All the stationary state simulations were done such that profiles (fluxes) are symmetric (anti-symmetric) with respect to the center of the box in the x-direction. Periodic boundary conditions are used. When a particle crosses one of the boundary planes it is reinserted with the same velocity on the opposite side of the box.

Irreversibilities are introduced by controlling some variables in layers in the middle or near the ends of the box (in the x-direction). The walls of the box can either be directly interacting walls, like in a porous system [288], or regions where the temperature, chemical potential, or momentum is set by a local perturbation of the system [284]. A gradient in chemical potential or a concentration gradient can be introduced by manipulating the particle types and molecular properties in the end and center regions, for instance, by particle swapping [291–293].

In the simulations of a homogeneous mixture we used $N = 512$ with equal numbers of each component and $L_x = 2L_y = 2L_z$ [65]. The box was divided into 32 layers in the x-direction. In order to give the system a certain temperature profile, layers 1 and 32 at the end of the box were thermostatted to a high temperature T_H and layers 16 and 17 in the center of the box were thermostatted to a low temperature T_L. The amounts of energy added and removed are equal, so that total energy is conserved and the energy flux is constant. A diffusion flux was simulated by swapping particles of different types between the layers in the center and the layers at the end of the cell. The velocities of these particles were scaled so that no kinetic energy was exchanged and total momentum was conserved.

In the simulations of a one component two-phase system, $N = 4096$ was used with $L_x = 16L_y = 16L_z$ [39, 40]. The box was divided into 128 layers in the x-direction. Layers 1–4 and 125–128 were thermostatted to a high temperature while layers 61–64 and 65–68 were thermostatted to a low temperature, see Fig. 22.4. A mass flux from the vapor to the liquid (condensation) was simulated by removing particles from the low temperature layers in the center, layers 61–68, moving them to one of the high temperature layers at the ends of the cell. In this process, the particle maintains its y- and z-coordinates, while its x-coordinate is changed by $\pm L_x/2$.

When a non-equilibrium system is in a stationary state, the fluxes of energy and mass are constant. A liquid and a vapor phase may coexist in this case, when the boundary conditions are appropriate. The liquid

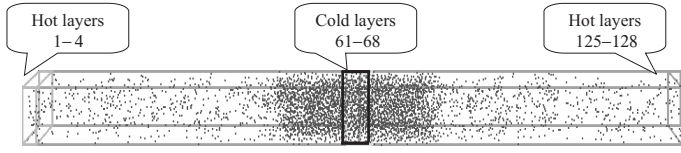

Figure 22.4 Lennard-Jones spline particles distributed in a temperature gradient that leads to phase separation. The cell is symmetric, with hot ends and a cold center.

phase appears in the middle of the box, since energy is removed there. On each high-temperature side, a vapor phase is formed. Two surfaces are then formed between the vapor and liquid without disturbances from the boundaries of the box. The situation is thus ideal for studies of the surface. A snapshot of the situation is illustrated in Fig. 22.4.

22.1.1 *The interaction potential*

Between every pair of particles, a potential exists, so that particles close to each other repel and particles farther away from each other attract each other. A common pair potential for particle interaction in fluids is the Lennard-Jones pair potential, or simply the Lennard-Jones potential:

$$u_{ij} = 4\epsilon_{ij}\left[\left(\frac{\sigma_{ij}}{r_{ij}}\right)^{12} - \left(\frac{\sigma_{ij}}{r_{ij}}\right)^{6}\right] \tag{22.2}$$

Here, u_{ij} is the potential between particle i and j, ϵ_{ij} is the minimum of the potential between particle i and j, $\mathbf{r}_i$ and $\mathbf{r}_j$ are the positions of particle i and j, $r_{ij} \equiv |\mathbf{r}_i - \mathbf{r}_j|$ is the distance between particle i and j, and σ_{ij} is the distance between particles when the potential is equal to zero. In a one component system, there is only one such distance σ and one minimum potential ϵ. In a two component mixture, there are three different σ's and three different minimum potentials.

In the computations one usually uses a cut-off Lennard-Jones potential, which is taken to be equal to zero for distances beyond a cut-off distance, $r > r_c$. One also uses a shifted cut-off Lennard-Jones potential, which is taken to be equal to the cut-off Lennard-Jones potential minus its value in $r = r_c$. The cut-off Lennard-Jones potential is often used in molecular dynamics simulations. This potential accelerates the particles when they move across r_c and changes the system's energy. In order to avoid this contribution and obtain a consistent description of equilibrium as well as non-equilibrium properties, it is necessary to shift the cut-off Lennard-Jones

potential. The Lennard-Jones spline potential, with the spline distance $r_s = (26/7)^{1/6}\,\sigma_{ij}$, is given by:

$$
\begin{aligned}
u_{ij} &= 4\epsilon_{ij}\left[\left(\frac{\sigma_{ij}}{r_{ij}}\right)^{12} - \left(\frac{\sigma_{ij}}{r_{ij}}\right)^{6}\right] \quad r \le r_s \\
u_{ij} &= \alpha_{ij}\left(r_{ij} - r_c\right)^3 + \beta_{ij}\left(r_{ij} - r_c\right)^2 \quad r_s \le r \le r_c \\
r_c &= \frac{67}{48} r_s \simeq 1.737\sigma_{ij} \\
\alpha_{ij} &= -\frac{387072}{61009}\frac{\epsilon_{ij}}{r_s^3} \\
\beta_{ij} &= -\frac{24192}{3211}\frac{\epsilon_{ij}}{r_s^2}
\end{aligned}
\tag{22.3}
$$

The potential obtained in this manner is a modified version of the Lennard-Jones potential. The two potentials are the same until the distance is r_s. After that the spline potential continues until the cut-off distance, r_c, by Eq. (22.3b)–(22.3e), while the Lennard-Jones potential continues by Eq. (22.2). The spline potential is less long-ranged than the Lennard-Jones potential. Plots of the two potentials are given in Fig. 22.5. The spline potential was used to generate the picture in Fig. 22.4.

Lennard-Jones potentials do not deal with charged particles. In order to deal with ionic or polarized systems, one normally adds a Coulomb type potential or a Yukawa potential to the expressions above [66]. Charged systems are much less studied than electroneutral systems.

The NEMD program uses *reduced variables* instead of real variables. Examples of reduced variables are given in Table 22.1. Variables are made dimensionless by division by σ_{ij}, mass, minimum interaction potential for component 1. In this table, k_B is the Boltzmann constant. The advantage of using reduced variables in NEMD is that they can be converted to any fluid of interest. For instance, for argon-like particles $\epsilon/k_{\mathrm{B}} = 124$ K, $m = 6.64 \times 10^{-26}$ kg, and $\sigma = 3.42 \times 10^{-10}$ m. When Lennard-Jones potentials are used to model a mixture, each molecule is approximated by a sphere of a given diameter σ and with a given interaction parameter ϵ.

22.2 Calculation techniques

In NEMD, all molecular properties are calculated from the mechanical properties of the system. Some of these calculations are explained below for a box divided into 128 layers. The expressions for 32 layers can be obtained by replacing 128 and 64 by 32 and 16 in the formulae below. The results are

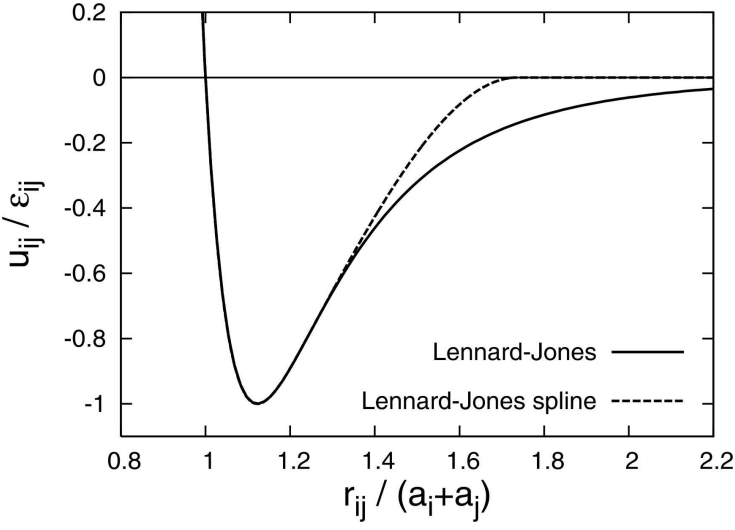

Figure 22.5 The Lennard-Jones potential (solid line) and the Lennard-Jones spline potential (stipled line) as a function of the dimensionless inverse distance between particles. The symbols a_i and a_j correspond to σ_{ij} in the text.

mostly reported in reduced units, see Table 22.1, so that conversion into real variables can be done as one prefers. Consider again the box in Fig. 22.3. For stationary states, the fluxes can be found using time averages in all 128 layers. Likewise, we can calculate the average kinetic energies, potential energies and the number of particles in each layer. Using the symmetry of the system around the center of the box, the mean of the properties in each half is calculated. In this way, the statistics become even better. The result then stems from a system with only 64 layers, where each layer is the mean of the corresponding two layers in the original system. The volume of such a pair of layers is $V/64$, where $V = L_x L_y L_z$ is the volume of the box. The particle density of component k in a layer is the number of particles of that component, $N_{k,\nu}$, in each pair of layers divided by the volume of the pair of layers:

$$\rho_{k,\nu} \equiv N_{k,\nu} \frac{64}{V} \tag{22.4}$$

The molar flux, $\mathbf{J}_{k,\nu}$, and the average velocity, $\mathbf{v}_{k,\nu}$, of component k in each pair of layers ν, with $\nu = 1, \ldots, 64$, is found from:

$$\mathbf{J}_{k,\nu} \equiv \frac{\rho_{k,\nu}\mathbf{v}_{k,\nu}}{N_{\mathrm{A}}} \equiv \frac{64}{VN_{\mathrm{A}}} \sum_{i \in k, i \in layers} \mathbf{v}_i \tag{22.5}$$

Table 22.1 Examples of reduced variables in molecular dynamics simulations.

Variable	Reduction formula
Energy	$U^* = U/\varepsilon_{11}$
Velocity	$\mathrm{v}^* = v\,(m_1/\varepsilon_{11})^{1/2}$
Distance	$r^* = r/\sigma_{11}$
Mass	$m^* = m/m_1$
Temperature	$T^* = k_\mathrm{B}T/\varepsilon_{11}$
Density	$\rho^* = \rho\sigma_{11}^3$
Time	$t^* = (t/\sigma_{11})\,(\varepsilon_{11}/m_1)^{1/2}$
Pressure	$p^* = p\sigma_{11}^3/\varepsilon_{11}$
Surface tension	$\gamma^* = \gamma\ \sigma_{11}^2/\ \varepsilon_{11}$

where $\mathbf{v}_i$ is the velocity of particle i. The sum is over particles of component k in layers ν and $129-\nu$. The x-component of the velocities in layer $129-\nu$ are inverted before adding them in Eq. (22.5). The frame of reference for the velocities and thus for the flux is the wall of the box. In the stationary states considered the mass flux is in the x-direction. The temperature, T_ν, in each pair of layers ν, is given from the average kinetic energy according to the equipartition principle:

$$\frac{3}{2}kT_\nu N_\nu = \frac{3}{2}kT_\nu \sum_{i\in k} N_{k,\nu} = \frac{1}{2}\sum_{i\in layers} m_i|\mathbf{v}_i - \mathbf{v}_\nu|^2 \qquad (22.6)$$

where m_i is the mass of particle i.

The pressure tensor is found by time averaging the microscopic pressure tensor.

$$p_{\nu,\alpha\beta} = \frac{64}{V}\sum_{i\in layers}\left(m_i \mathrm{v}_{i,\alpha}\mathrm{v}_{i,\beta} + \sum_{j\neq i} F_{ij,\alpha}r_{ij,\beta}\right) \qquad (22.7)$$

where $\mathrm{v}_{i,\alpha}$, is the velocity of particle i in the direction α, $F_{ij,\alpha}$ is the force exerted on particle i by particle j in the direction α, and $r_{ij,\beta} = r_{i,\beta} - r_{j,\beta}$ is the component of the vector from particle j to particle i in the direction β. The x-component of the velocities in layer $129-\nu$ are inverted before adding them in Eqs. (22.6) and (22.7). For a one-dimensional transport problem, like the one illustrated in Fig. 22.3, there is no change in the densities in the direction parallel to the surface, but there is a large change in density in the direction normal to the surface (the direction of transport). This causes the pressure in the directions parallel, $p_\parallel = p_{yy} = p_{zz}$, and normal,

$p_\perp = p_{xx}$, to the surface to be different in the interfacial region. The off-diagonal elements of the pressure tensor are found to be zero. The surface tension is due to the difference between the parallel and the normal pressure and is calculated from

$$\gamma = \frac{L_x}{128} \sum_{\nu=1}^{64} \left(p_\parallel - p_\perp \right) \tag{22.8}$$

Todd *et al.* [294] developed an alternative algorithm for pressure calculation in heterogeneous systems; the method-of-planes. This gives the pressure tensor for planar surfaces [112].

The measurable heat flux in each layer, $\mathbf{J}'_{q,\nu}$, cannot be computed directly, because it is not a mechanical property. It is, however, related to the total heat flux (the energy flux), $\mathbf{J}_{q,\nu}$, by

$$\mathbf{J}'_{q,\nu} = \mathbf{J}_{q,\nu} - \sum_{i \in k} H_k \mathbf{J}_{k,\nu} \tag{22.9}$$

where H_k is the partial molar enthalpy of component k. In order to determine the partial molar enthalpy, we need the enthalpy as a function of composition, which in principle requires a series of simulations [280, 282]. The total heat flux can be expressed in terms of mechanical quantities as follows [276, 295]:

$$\mathbf{J}_{q,\nu} = \frac{64}{V} \sum_{i \in layers} \left(\left[\frac{1}{2} m_i \mathrm{v}_i^2 + \phi_i \right] \mathbf{v}_i + \frac{1}{2} \sum_{j \neq i} \left[\mathbf{v}_i \cdot \mathbf{F}_{ij} \right] \mathbf{r}_{ij} \right) \tag{22.10}$$

where ϕ_i is the potential energy of particle i in the field of all the other particles, $\mathbf{F}_{ij}$ is the force acting on i due to j, and $\mathbf{r}_{ij} = \mathbf{r}_i - \mathbf{r}_j$ is the vector from the position of j to the position of i. The measurable heat flux can then be determined from Eq. (22.9). Three important cases avoid the non-trivial task of determining H_k; (1) binary isotope mixtures with $H_1 = H_2$, giving $\mathbf{J}'_{q,\nu} = \mathbf{J}_{q,\nu}$ in the mean molar reference frame, for which $\mathbf{J}_1 = -\mathbf{J}_2$, and (2) binary mixtures for which $\mathbf{J}_1 = \mathbf{J}_2 = 0$, again with $\mathbf{J}'_q = \mathbf{J}_q$ as the result, and (3) ideal mixtures with H_k equal to the molar enthalpy of component k. The energy flux is computed for each layer with Eq. (22.10), except that the first summation includes only those particles i that are in the given layer. The energy flux is then computed from the amount of energy added and withdrawn. When the system is not uniform, care must be taken in the computation of the measurable heat flux.

Transport coefficients can also be calculated from equilibrium systems, using the Kubo relations [296].

22.3 Verifying the assumption of local equilibrium

NEMD simulations were used by Hafskjold and coworkers [39, 65, 66, 111, 112] to confirm the assumption of local equilibrium in systems where heat and mass were transported. A binary homogeneous mixture and a pure two-phase system were studied. Both systems were subject to enormous temperature gradients, of the order of magnitude 10^8 K/m. This temperature gradient, as well as the magnitude of the mass flows considered, are mostly beyond realization in a laboratory.

22.3.1 *Local equilibrium in a homogeneous binary mixture*

An equimolar binary isotope gas mixture of $N = 512$ particles in a rectangular, closed box was studied in a temperature gradient [65, 149]. The enthalpy, H, and the pressure, p, were calculated for each layer in the presence and absence of the temperature gradient. For the same state

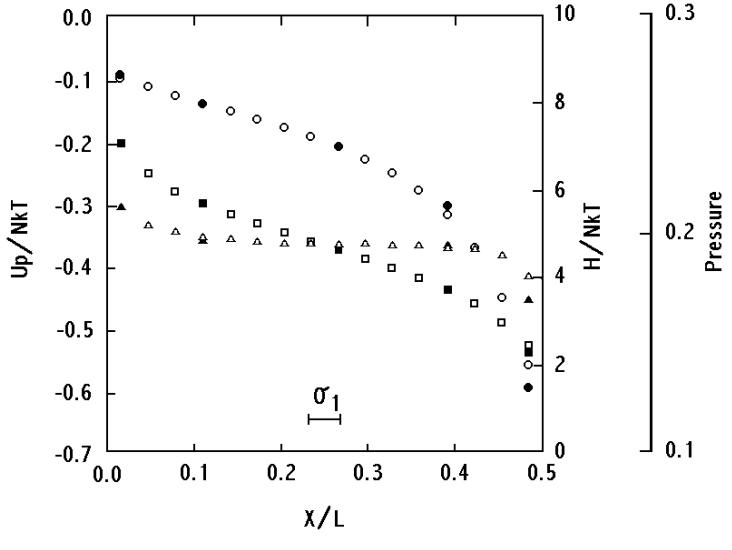

Figure 22.6 The enthalpy (circles), the potential energy (squares) and the pressure (triangles) in a two-component mixture in a temperature gradient (open symbols) and in mixtures that are in global equilibrium with the same state variables (filled symbols). The particles interact with a Lennard-Jones spline potential. They have the same diameter, the same potential depth, and a mass ratio of $m_1/m_2 = 10$. Reproduced from Stat. Phys. 78 (1995) 463–494 with permission of Springer.

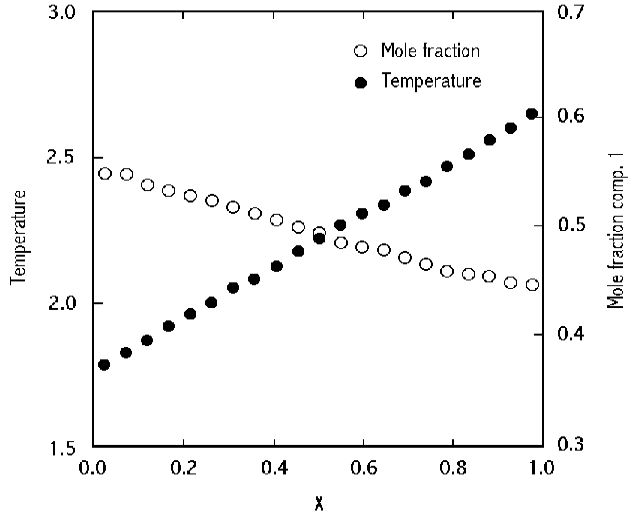

Figure 22.7 The dimensionless temperature gradient and the corresponding gradient in mole fraction for the system described in Fig. 22.6. (Courtesy of B. Hafskjold)

variables, identical local values for H (circle symbols), p (triangular symbols) and potential energy U (square symbols) were obtained in the two cases [65]. The results are shown with open symbols in Fig. 22.6. Selected results for equilibrium calculations for the same state variables are shown with filled symbols in the same figure. The results are the same, so it was concluded that thermodynamic relations are valid locally in the temperature gradient. The extreme gradient across the volume element thus did *not* lead to a violation of the assumption of local equilibrium. Hafskjold and coworkers [282] reported that the assumption of local equilibrium was also true with a mass flux across the system. A surprisingly low number of particles was enough to give a statistical basis for calculation of thermodynamic properties. This can be explained by the use of averages over a sufficiently long time interval. On the average there were N_ν =16 particles in a volume element, and the fluctuation in N_ν was $\delta N_\nu/N_\nu \approx 0.3$. This fluctuation in particle number is the cause of the temperature fluctuation seen in Fig. 22.2, but $\delta T/T$ was only ≈ 0.03. A system in local equilibrium and a system in global equilibrium differ in the way they fluctuate [109]. It was also found that heavy particles concentrated in the cold parts of the box while the light particles concentrated in the warm parts, see Fig. 22.7 [149]. This is discussed further below.

22.3.2 *Local equilibrium in a gas-liquid interface*

We also studied the two-phase systems in a temperature gradient [39]. The phase diagram of the system was first determined. It is given in reduced units in Fig. 22.8. The relations between the pressure, temperature and the density were determined for the homogeneous phases; the vapor as well as in the liquid. For the surface, the relation between the surface tension and the temperature was determined. The NEMD cell contained 4096 particles in this case. This number ensures that there are enough particles in the vapor phase to obtain meaningful averages. In order to address the question of whether one is in the vapor or in the surface it is important to choose the overall molar density such that the vapor region is much thicker than the mean free path of the particles in this region. The cell was non-cubic, with ratios $L_x/L_y = L_x/L_z = 16$, where L_i is the length of the cell in the i-th direction. By choosing the proper overall particle density and temperatures, and using the phase diagram in Fig. 22.8, a temperature gradient was used to generate a liquid region in the center of the cell with vapor on both sides. The box was subdivided into 128 layers, with a thickness $\sqrt[3]{1/2\rho}$ in meters, where $\rho = N/L_xL_yL_z$ is the overall density in the box. The mean free path (cf. Fig. 22.1) was calculated from the formula, $\ell = 1/(\sigma^2\rho_\nu\pi\sqrt{2})$, from kinetic gas theory, where σ is the diameter of the particles and ν is one of the vapor layers. In the simulations the mean free path had values up to about 10 layer thicknesses close to the triple point.

A particle flux from the vapor to the liquid (condensation) was simulated, using the algorithm that removed a particle from the low temperature layers in the center and inserted it into one of the high temperature layers at the end of the cell. The particle maintained its y- and z-coordinates while its x-coordinate was changed by $\pm L_x/2$. In order to avoid large perturbations of the energy of the system, the particle insertion was done with a probability given by the Boltzmann factor. NEMD simulations were done for a number of cases along the phase line where two phases coexist, with a heat flux present, and with or without a particle flux. A snapshot of the density profiles in the half of the cell is shown for two cases in Fig. 22.9.

Gibbs [62] defined the surface as a transition region with a finite thickness bounded by planes of similarly chosen points, cf. Sec. 3.3. The simulation results illustrated in Fig. 22.9 show that we can identify two such planes, for instance, planes where on one side the equation of state for the fluid is still valid, while on the other side this is no longer the case. The region where the equation of state for the liquid or for the vapor are not valid, is then the surface. By such choices, the surface was found to have a thickness of about 10 layers, which is about 5 nm in real units, for densities away from the critical point. Ten layers is about the mean free path in the

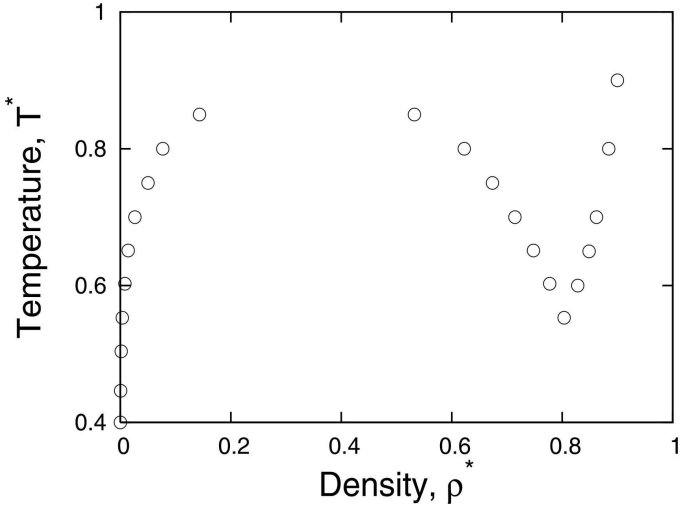

Figure 22.8 Phase diagram for the Lennard-Jones spline fluid. Reproduced from J. Colloid Interface Sci. 232 (2000) 178–185 with permission of Elsevier.

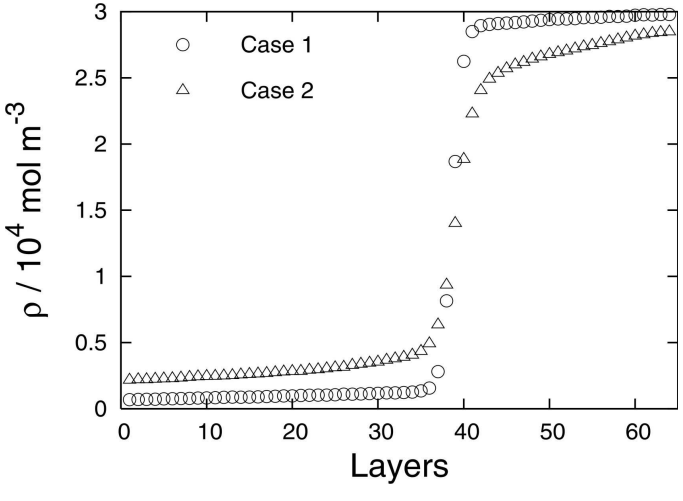

Figure 22.9 Density profiles from two NEMD simulations of heat and mass transfer through a surface. Case 1 is far from and Case 2 is close to the critical point. Data are taken from Røsjorde *et al.* [39].

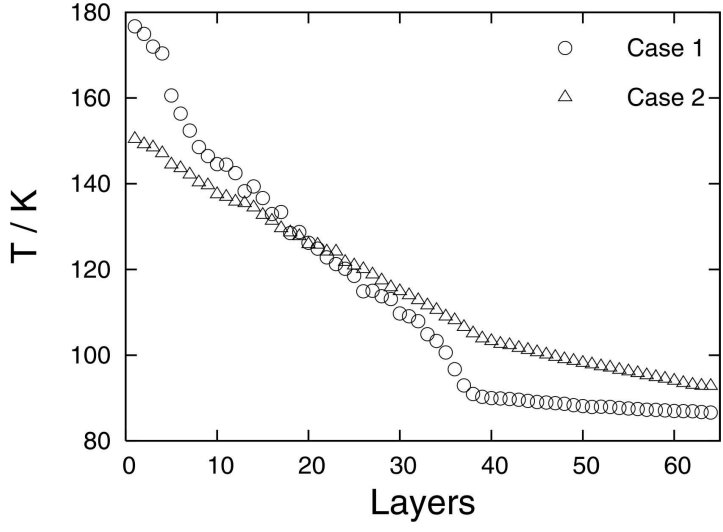

Figure 22.10 Temperature profiles from two NEMD simulations of heat and mass transfer through a surface, see also Fig. 22.9. Case 1 is far from and Case 2 is close to the critical point. Data are taken from Røsjorde *et al.* [39]

vapor close to the triple point. The thickness increased to about 25 layers close to the critical point. The thickness, in particular, close to the triple point, is more than one would expect on the basis of a visual inspection of the curves. Such a visual inspection can therefore not be used to determine the surface position. The deviation from the equation of state for the homogeneous phase already occurs before it shows up in the graph.

The temperature of the surface was calculated from the kinetic energies of the particles within these boundaries. It was found to be in good approximation equal to the temperature of the first liquid layer outside the closed surface. The temperatures of all layers are plotted for the same cases of Fig. 22.9 in Fig. 22.10. For each layer, and for the closed surface, the temperatures computed from velocity components along or normal to the surface were the same. This serves as a first confirmation of the validity of the assumption of local equilibrium.

Finally, the surface tension from the NEMD simulations was plotted as a function of the temperature of the surface, see Fig. 22.11. For comparison, the results of simulations for the equilibrium surface were also given. The figure shows that the surface is in local equilibrium in the presence of temperature gradients of up to 3×10^8 K/m between the cold and the hot layers.

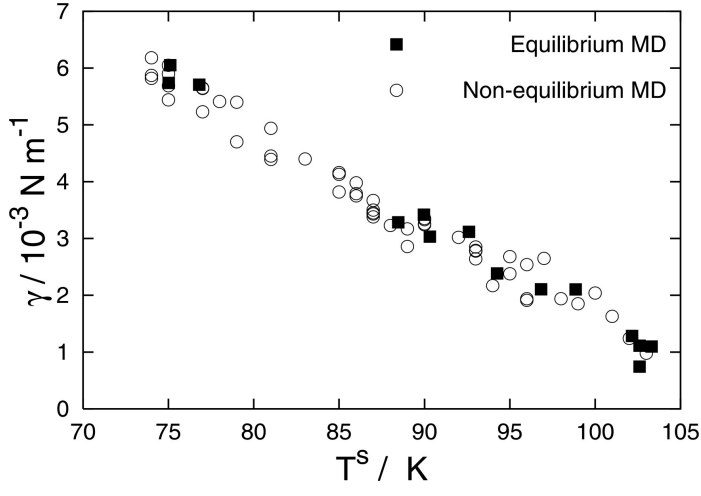

Figure 22.11 The surface tension as a function of the temperature of the surface. The points in the curve derive from equilibrium (filled squares) and non-equilibrium molecular dynamics simulations (open circles). Reproduced from J. Colloid Interface Sci. 299 (2006) 452–463 with permission of Elsevier.

Simon and coworkers [112] considered heat transfer in a box with 2000 molecules of n-octane. The molecules interacted with a truncated Lennard-Jones potential, and had vibrational and rotational degrees of freedom. The equimolar surface was determined as mentioned above. Also, for these simulations, the surface tension for the stationary states was found to be the same function of the surface temperature as in equilibrium. This again verified local equilibrium.

The value of the surface tension depends strongly on the cut-off of the potential. If one wants to compare the predictions with experimental values, one should add tail corrections [297].

22.4 Verifications of the Onsager relations

Transport coefficients can be determined from NEMD simulations to test for instance the Onsager relations. The coefficients are calculated, once the forces and their corresponding fluxes are computed.

22.4.1 *A homogeneous binary mixture*

Consider the binary mixture of isotopes that was studied by Hafskjold and Kjelstrup Ratkje [65]. The barycentric frame of reference, see Sec. 4.4.1,

was used, with $J_1 = -J_2$, and the following flux-force relations:

$$\begin{aligned} J'_q &= l_{qq}\left(\frac{d}{dx}\frac{1}{T}\right) + l_{q\mu}\left[-\frac{1}{T}\frac{d(\mu_{T,1}-\mu_{T,2})}{dx}\right] \\ J_1 &= l_{\mu q}\left(\frac{d}{dx}\frac{1}{T}\right) + l_{\mu\mu}\left[-\frac{1}{T}\frac{d(\mu_{T,1}-\mu_{T,2})}{dx}\right] \end{aligned} \tag{22.11}$$

By calculating $l_{q\mu}$ independent from $l_{\mu q}$, Onsager relations can be tested. With a known heat flux and temperature difference across a (sub-)system, the stationary state thermal conductivity is given by:

$$\lambda = -\left(\frac{J'_q}{dT/dx}\right)_{J_1=0} = \left(l_{qq} - \frac{l_{q\mu}l_{\mu q}}{l_{\mu\mu}}\right)\frac{1}{T^2} \tag{22.12}$$

The heat of transfer is

$$q^* = \left(\frac{J'_q}{J_1}\right)_{dT=0} = \frac{l_{q\mu}}{l_{\mu\mu}} \tag{22.13}$$

Using Gibbs–Duhem's equation, $w_1 d\mu_1 + w_2 d\mu_2 = 0$, the differential of the difference of the chemical potentials at constant temperature and pressure can be expressed by the weight fraction of the components, w_i:

$$\frac{d\left(\mu_{T,1}-\mu_{T,2}\right)}{dx} = \frac{1}{w_2}\frac{\partial\mu_1}{\partial w_1}\frac{\partial w_1}{\partial x} \tag{22.14}$$

where we used $w_1 + w_2 = 1$. The thermal diffusion factor α can be defined as (see also Sec. 8.2):

$$\alpha_T = -\left(\frac{\partial \ln(w_1/w_2)/\partial x}{\partial \ln T/\partial x}\right)_{J_1=0} = -\frac{T}{w_1 w_2}\left(\frac{\partial w_1/\partial x}{\partial T/\partial x}\right)_{J_1=0} = \frac{l_{\mu q}}{l_{\mu\mu}}\frac{\partial \ln w_1}{\partial \mu_1} \tag{22.15}$$

The component flux can be expressed as

$$J_1 = -\rho w_1 D\left(w_2\alpha_T\frac{d\ln T}{dx} + \frac{d}{dx}\ln w_1\right) \tag{22.16}$$

with the diffusion coefficient

$$D = \frac{l_{\mu\mu}}{\rho w_2 T}\frac{\partial\mu_1}{\partial w_1} \tag{22.17}$$

When the thermal conductivity, thermal diffusion factor, heat of transfer, and diffusion coefficient can be computed from NEMD results, Eqs. (22.12),

Table 22.2 Transport coefficients for heat and mass in the Lennard-Jones/spline isotope mixture, given in reduced Lennard-Jones units for various reduced number densities ρ^*.

ρ^*	$l^*_{\mu\mu}$	$l^*_{q\mu}$	$l^*_{\mu q}$	l^*_{qq}
0.100	4.1	0.015	0.017	4.66
0.153	3.0	0.008	0.008	2.10
0.200	4.3	0.025	0.029	6.68
0.400	3.8	0.052	0.049	11.23

(22.13), (22.15) and (22.17) can be solved for the Onsager coefficients, see e.g. [65, 277, 279].

The four coefficients were determined for a series of temperature and number densities [65]. Results are given in Table 22.2 for $T^* = 2.0$ with $\rho^* = 0.1$, 0.2 and 0.4, and for $T^* = 1.35$ with $\rho^* = 0.153$. The magnitude of the coupling coefficient depends largely on the relative mass, and the relative size of the particles, while the relative magnitude of the potential minima in the Lennard-Jones potential has a marked influence on the sign of the coefficient [144, 277]. The dimensionless interdiffusion coefficient $l^*_{\mu\mu}$ is relatively constant over the range of densities that were studied, while the others varied. The coupling coefficient is small. The uncertainties in the coefficients are about one standard deviation (not explicitly given). We can conclude within these uncertainties, that the Onsager relations

$$l_{q\mu} = l_{\mu q} \tag{22.18}$$

are valid.

22.4.2 *A gas-liquid interface*

The Onsager relations were also investigated for surface transport [67]. A one-component gas-liquid interface was used, see Sec. 11.1. From Eq. (11.14) and Eq. (11.12) we have

$$\begin{aligned} \Delta_{\mathrm{l,g}}\left(\frac{1}{T}\right) &= \frac{1}{T^{\mathrm{g}}} - \frac{1}{T^{\mathrm{l}}} = r^{\mathrm{s,g}}_{qq} J'^{\mathrm{g}}_q + r^{\mathrm{s,g}}_{q\mu} J \\ -\frac{\Delta_{\mathrm{l,g}}\mu(T^{\mathrm{l}})}{T^{\mathrm{l}}} &= -\frac{\mu^{\mathrm{g}}(T^{\mathrm{l}}) - \mu^{\mathrm{l}}(T^{\mathrm{l}})}{T^{\mathrm{l}}} = r^{\mathrm{s,g}}_{\mu q} J'^{\mathrm{g}}_q + r^{\mathrm{s,g}}_{\mu\mu} J \end{aligned} \tag{22.19}$$

Using Eq. (11.4) it follows that $J'^{\mathrm{g}}_q = J'^{\mathrm{l}}_q - \Delta_{\mathrm{l,g}} H J$. Eliminating J'^{g}_q from Eq. (22.19) in favor of J'^{l}_q and using Eq. (11.6), it follows after some algebra

that

$$\begin{aligned}\Delta_{\mathrm{l,g}}\left(\frac{1}{T}\right) &= \frac{1}{T^{\mathrm{g}}} - \frac{1}{T^{\mathrm{l}}} = r_{qq}^{\mathrm{s,l}} J_q'^{\mathrm{l}} + r_{q\mu}^{\mathrm{s,l}} J \\ -\frac{\Delta_{\mathrm{l,g}}\mu(T^{\mathrm{g}})}{T^{\mathrm{g}}} &= -\frac{\mu^{\mathrm{g}}(T^{\mathrm{g}}) - \mu^{\mathrm{l}}(T^{\mathrm{g}})}{T^{\mathrm{g}}} = r_{\mu q}^{\mathrm{s,l}} J_q'^{\mathrm{l}} + r_{\mu\mu}^{\mathrm{s,l}} J\end{aligned} \tag{22.20}$$

In the calculations, it was documented that the Onsager relation

$$r_{q\mu}^{\mathrm{s,g}} = r_{\mu q}^{\mathrm{s,g}} \tag{22.21}$$

was valid. The coefficients for the liquid side are given by

$$\begin{aligned} r_{qq}^{\mathrm{s,l}} &= r_{qq}^{\mathrm{s,g}} = r_{qq}^{\mathrm{s}} \\ r_{q\mu}^{\mathrm{s,l}} &= r_{\mu q}^{\mathrm{s,l}} = r_{\mu q}^{\mathrm{s,g}} - r_{qq}^{\mathrm{s,g}} \Delta_{\mathrm{l,g}} H \\ r_{\mu\mu}^{\mathrm{s,l}} &= r_{\mu\mu}^{\mathrm{s,g}} - 2 r_{\mu q}^{\mathrm{s,g}} \Delta_{\mathrm{l,g}} H + r_{qq}^{\mathrm{s,g}} \left(\Delta_{\mathrm{l,g}} H\right)^2 \end{aligned} \tag{22.22}$$

The results for the coupling coefficients are shown in Fig. 22.12. The Onsager relations, $r_{q\mu}^{\mathrm{s,g}} = r_{\mu q}^{\mathrm{s,g}}$ and $r_{q\mu}^{\mathrm{s,l}} = r_{\mu q}^{\mathrm{s,l}}$, were valid within the numerical accuracy of the calculation for gradients up to 10^9 K/m [67].

22.5 Linearity of the flux-force relations

One of the basic postulates of non-equilibrium thermodynamics is that fluxes are linear combinations of all conjugate forces, see Eq. (7.12). This postulate can also be tested by NEMD [67]. The surface transfer coefficients, described in the previous subsection, were calculated using the linear relations in Eqs. (22.19) and (22.20). There was no need to invoke non-linear terms in these calculations. The coefficients depended on the state of the surface, here on the state variable γ, or equivalently, on the surface temperature. The coefficients were thus not functions of the forces or of the fluxes for temperature gradients investigated (up to 10^9 K/m). This is in accordance with the assumptions used in Sec. 7.2. Paolini *et al.* [298] found linear response for gradients up to 5.8 x 10^{10} K/m in a Lennard-Jones fluid near the triple point. We do not consider systems with a shear gradient in this book. For large shear gradients, non-linear contributions to the heat flux were important [299, 300].

22.6 Molecular mechanisms

NEMD offer insight in the transport mechanism. Simon and coworkers [112] determined the resistivity of the surface to heat transfer in a box with 2000

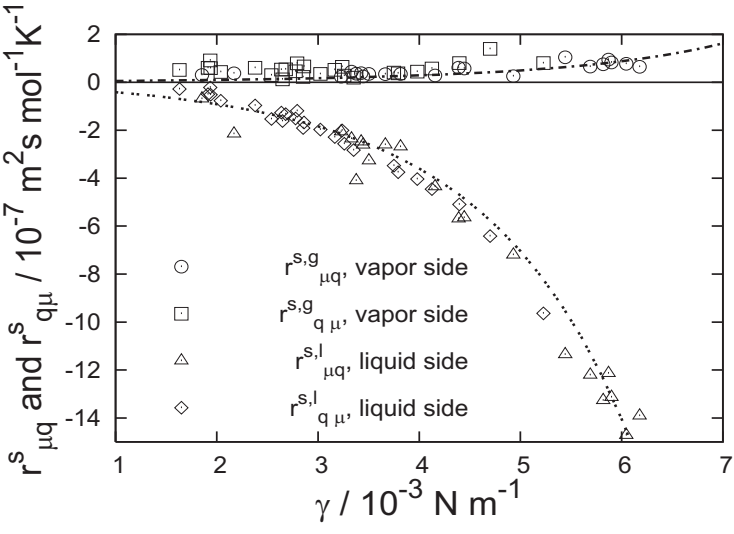

Figure 22.12 The coupling coefficient for evaporation and condensation of one component, on the vapor side (top) and the liquid side (bottom). Coefficients were obtained from NEMD simulations (points), and from kinetic theory (stipled lines). Reproduced from J. Colloid Interface Sci. 299 (2006) 452–463 with permission of Elsevier.

molecules of n-octane. The molecules interacted with a truncated Lennard-Jones potential, and had vibrational and rotational degrees of freedom. The equimolar surface was determined as mentioned above. The temperatures on each side of the surface were found. In the simulations there was no particle flux, i.e. $J = 0$ so that $J'^{\mathrm{g}}_q = J'^{\mathrm{l}}_q$. In this case Eq. (22.19) reduced to

$$\frac{1}{T^{\mathrm{g}}} - \frac{1}{T^{\mathrm{l}}} = r^{\mathrm{s}}_{qq} J'^{\mathrm{g}}_q \quad \text{and} \quad -\frac{\mu^{\mathrm{g}}(T^{\mathrm{l}}) - \mu^{\mathrm{l}}(T^{\mathrm{l}})}{T^{\mathrm{l}}} = r^{\mathrm{s}}_{\mu q} J'^{\mathrm{g}}_q \tag{22.23}$$

The thermal resistivity r^{s}_{qq} and one of the coupling coefficients $r^{\mathrm{s}}_{\mu q}$ were then calculated from these relations. The results for r^{s}_{qq} were about five times, and for $r^{\mathrm{s}}_{\mu q}$ about two times smaller than those predicted by kinetic theory. This result may be explained by the molecular degrees of freedom of n-octane. Heat transfer at the surface is more efficient for such a molecule than for a hard sphere. The form of the Lennard-Jones potential is probably also important. The longer-range cut-off Lennard-Jones potential gave larger coefficients than the Lennard-Jones spline-potential [167, 170].

Chapter 23

The Non-Equilibrium Two-Phase van der Waals Model

We use a non-equilibrium version of the van der Waals square gradient model to obtain the surface excess densities following Gibbs, and show that these obey the condition of local equilibrium. The surface temperature can thus be well defined. The surface as described by excess densities is therefore autonomous, i.e. behaves like a separate thermodynamic system. This result is remarkable, given that the continuous description of the interfacial region is not autonomous. The continuous, as well as the integrated, van der Waals square gradient model can be used to describe condensation and evaporation.

The van der Waals square gradient model for the liquid-vapor interface in a one-component fluid gives a continuous description of all thermodynamic variables through the interfacial region. The model which is well understood for equilibrium conditions [93], has now been solved for non-equilibrium conditions [106–108]. This makes it possible to investigate the basic postulate of Chapter 3.5, that the surface is a thermodynamic system by itself, with its own variables of state. This postulate, about the so-called autonomous nature of the surface, has been questioned in the literature [93–96]. Some evidence from non-equilibrium molecular dynamics that support the idea of an autonomous surface was given in Chapter 22, see also [39,67,112]. We shall see here that the solution of the non-equilibrium van der Waals square gradient model also supports the postulate.

According to Gibbs, the variables of the surface are the excess extensive thermodynamic variables, see Chapter 3. They were obtained by integrating their continuous variation (on the molecular scale) across the surface, subtracting the extrapolated bulk phase-values into the surface, see Fig. 3.3. The procedure is well established for systems in equilibrium. It was

extended to non-equilibrium systems in Chapter 3.5. The assumption of local equilibrium in the surface, for excess properties obtained in this manner, was the basis for the derivations in all chapters.

The continuous thermodynamic functions through the surface, found by solving the non-equilibrium van der Waals square gradient model, shall be used here for an examination of the thermodynamic properties of the surface. Most importantly, we wish to establish methods for calculation of surface properties. Various questions can be investigated, for instance the impact of the choice of the position of the dividing surface.

Van der Waals gave his equation of state for the continuous transition between the liquid and the vapor in his thesis in 1882. He introduced a square gradient contribution to the Helmholtz energy density in 1893 [104], which made it possible to calculate the density profile through the interface between the coexisting vapor and liquid phases, and to obtain the surface tension. The van der Waals square gradient model, and its extensions [105], played an important role in the understanding of phase transitions, especially the behavior near the critical point [93]. We shall see in this chapter that the application of the systematic procedures of non-equilibrium thermodynamics to the square gradient model, will enable us to obtain an autonomous description of the surface in terms of excess densities. We can also describe heat and mass transport into and through the interface using this model. The work described in this chapter is based on three papers by Bedeaux *et al.* [106–108].

We start by presenting the thermodynamic densities which follow from the common van der Waals equation of state [301]. We use these properties to describe the homogeneous parts of our system. Section 23.2 explains the gradient term that is added to obtain the van der Waals square gradient model, the model we need for the interfacial region. The normal and the parallel pressure in the interfacial region affect the thermodynamic relations in different ways in this region. Section 23.3 presents the conservation laws for matter, momentum and energy in the form needed for calculation of the local entropy flux. The local entropy production is derived.

The flux equations and the conservation laws in Sec. 23.4 are used to solve the non-equilibrium behavior of the liquid-vapor interface. The numerical solution procedure is given in Sec. 23.5. In Sec. 23.6 we show ways to extrapolate the various densities from the vapor and the liquid phases back to the surface. On this basis, we present the excess densities [62] in Sec. 23.7, and show that the surface is autonomous using four equivalent definitions of the surface temperature. This strongly supports the idea of an autonomous liquid-vapor surface [39, 112]. The model therefore adds knowledge on how to find surface properties. For the systematic procedure on how to obtain the description in terms of excess densities from a

continuous description, we refer to [36]. We shall restrict ourselves to flat surfaces. The van der Waals square gradient model may also be used for curved surfaces [101].

23.1 Van der Waals equation of states

On our way to find a full description of the heterogeneous two-phase fluid, we consider first the homogeneous fluids. The pressure of a real liquid in coexistence with its vapor was described for the first time by van der Waals:

$$p_W = \frac{cRT}{1-Bc} - Ac^2 = \frac{RT}{V-B} - \frac{A}{V^2} \tag{23.1}$$

Here c is the number of moles per unit volume and $V = 1/c$, the molar volume. The constant B is the smallest volume to which one can compress one mole of a fluid and is roughly equal to 2 times the "hard sphere" volume of a mole of particles. The constant A describes the attraction between pairs of molecules. For low densities the expression reduces to the ideal gas law, $p_W = cRT$. Figure 23.1 shows p_W as a function of V for $T > T_c$, $T = T_c$ and $T < T_c$, where T_c is the critical temperature. For temperatures above the critical temperature the first term on the right hand side dominates, so that the pressure is a monotonically decreasing function of the molar volume. For temperatures below the critical temperature, the second term also becomes important and the pressure as a function of the molar volume goes through a minimum and then through a maximum, before it decreases to zero. For these temperatures a liquid and a vapor phase coexist. By setting the first two derivatives of p_W equal to zero at the critical temperature, we find $T_c = 8A/27RB$ (see e.g. [97]). The corresponding critical molar volume and pressure are $V_c = 3B$ and $p_c = A/27B^2$.

For water, which is plotted in Fig. 23.1, the constants in Eq. (23.1) are $A = 0.339$ Jm^3/mol^2 and $B = 1.87 \times 10^{-5}$ m^3/mol. This gives $T_c = 647$ K, $V_c = 5.6 \times 10^{-5}$ m^3/mol and $p_c = 3.6 \times 10^7$ Pa $= 360$ bar. The experimental values are $T_c = 647$ K, $V_c = 5.6 \times 10^{-5}$ m^3/mol and $p_c = 220$ bar. This reflects that A and B have been determined from the critical temperature and the molar volume. The critical pressure predicted by van der Waals is then too high and as such it is an indication of how accurate the van der Waals description is. The van der Waals equation of state has a reliable qualitative and semi-quantitative predictive power.

Exercise 23.1.1. *When the temperature is below the critical temperature, Fig. 23.1 gives two stable molar volumes for any pressure. The smaller*

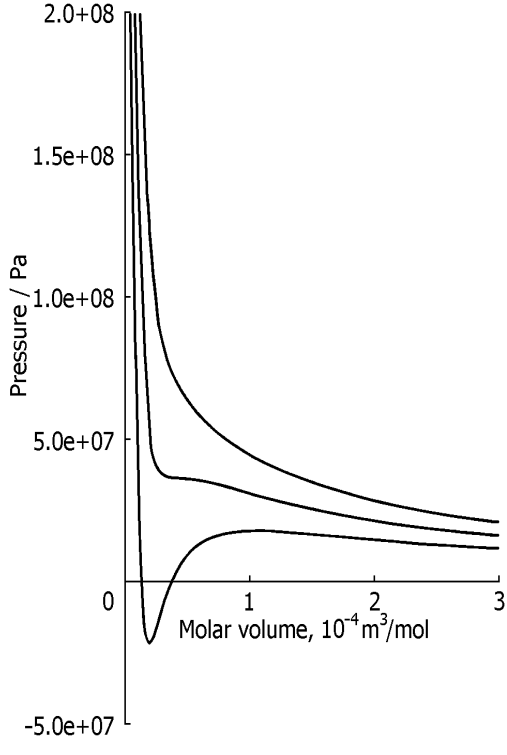

Figure 23.1 The pressure of water in Pascals according to the van der Waals equation. Three isotherms are given for $T < T_c$, $T = T_c$ and $T < T_c$.

one represents the liquid molar volume and the larger one, the vapor molar volume. Use Gibbs–Duhem's equation

$$\int_{p^l}^{p^g} V_W \, dp = 0$$

where V_W is the volume calculated from the van der Waals equation of state, to derive the constant pressure-line that has equal areas with the curve under and above the line. Derive expressions for the pressure, p_{EA}, and the coexisting densities of liquid and vapor as a function of temperature (Maxwell's equal area rule).

- **Solution:** It is convenient to change variables in the expression above and integrate over the volume, because v_W is a multiple valued func-

tion. The equal area pressure p_{EA} must obey:

$$\int_{v^{\mathrm{l}}}^{v^{\mathrm{g}}} d(Vp) - \int_{v^{\mathrm{l}}}^{v^{\mathrm{g}}} p_W \, dV$$

$$= p_{EA}(V^{\mathrm{g}} - V^{\mathrm{l}}) + RT \ln\left(\frac{V^{\mathrm{l}} - B}{V^{\mathrm{g}} - B}\right) + A\left(\frac{1}{V^{\mathrm{l}}} - \frac{1}{V^{\mathrm{g}}}\right) = 0$$

The points connected by this pressure have $\mu^{\mathrm{g}} - \mu^{\mathrm{l}} = 0$. The pressure in the liquid and the vapor are also the same

$$p_{EA} = \frac{RT}{V^{\mathrm{l}} - B} - \frac{A}{(V^{\mathrm{l}})^2} = \frac{RT}{V^{\mathrm{g}} - B} - \frac{A}{(V^{\mathrm{g}})^2}$$

Given the temperature, these are two equations for the unknown molar volumes. The solution gives these molar volumes and shows that they are a function of the temperature alone. Further substitution into van der Waals equation of state gives the pressure as a function of the temperature.

We want to find the remaining thermodynamic functions as a function of V or c and T. The Gibbs relation for the molar Helmholtz energy is

$$dF_W = -S_W dT - p_W dV \tag{23.2}$$

where S_W is the molar entropy. This expression makes it possible to integrate the pressure over the volume to get the molar Helmholtz energy. Using an integration constant such that the expression reduces to the ideal gas value for large V, we obtain, [301] page 234,

$$F_W = -RT \ln\left[\frac{e\,(V - B)}{\Lambda^3 N_A}\right] - \frac{A}{V} = -RT \ln\left[\frac{e\,(1 - Bc)}{c\Lambda^3 N_A}\right] - Ac \tag{23.3}$$

Here $\Lambda \equiv N_A h/\sqrt{2\pi MRT}$ is the mean thermal de Broglie wavelength, where N_A is Avogrado's number, h is Planck's constant and M the molar mass in kg/mol. By differentiating with respect to the temperature, we obtain the molar entropy

$$S_W = R \ln\left[\frac{e\,(V - B)}{\Lambda^3 N_A}\right] + \frac{3}{2}R = R \ln\left[\frac{e\,(1 - Bc)}{c\Lambda^3 N_A}\right] + \frac{3}{2}R \tag{23.4}$$

where we assumed A and B to be independent of the temperature. The molar Helmholtz energy F_W and the molar enthalpy H_W satisfy

$$F_W = U_W - TS_W = \mu_W - p_W V \quad \text{and} \quad H_W = U_W + p_W V = \mu_W + TS_W \tag{23.5}$$

where U_W is the molar internal energy and μ_W the chemical potential. We find

$$\begin{aligned}
\mu_W &= -RT \ln\left[\frac{e\,(V-B)}{\Lambda^3 N_A}\right] + \frac{RTV}{V-B} - 2\frac{A}{V} \\
&= -RT \ln\left[\frac{e\,(1-Bc)}{c\Lambda^3 N_A}\right] + \frac{RT}{1-Bc} - 2Ac \\
H_W &= \frac{3}{2}RT - 2\frac{A}{V} + \frac{VRT}{V-B} = \frac{3}{2}RT - 2Ac + \frac{RT}{1-Bc} \\
U_W &= \frac{3}{2}RT - \frac{A}{V} = \frac{3}{2}RT - Ac
\end{aligned} \tag{23.6}$$

The thermodynamic relations (23.2) and (23.5) lead to the explicit form of F_W, S_W, μ_W, U_W and H_W. These quantities satisfy all the usual thermodynamic relations. In particular, they satisfy the Gibbs relation

$$dU_W = TdS_W - p_W dV \tag{23.7}$$

and the Gibbs–Duhem equation

$$d\mu_W = -S_W dT + V dp_W \tag{23.8}$$

23.2 Van der Waals square gradient model for the interfacial region

Consider next the two-phase region where the density varies from the pure vapor to the pure liquid density, see Fig. 23.2. Van der Waals gave the molar Helmholtz energy, F, as a function of position, x, when the system was in equilibrium. We extend the van der Waals description and add the time, t, as a variable. This gives

$$F(x,t) = F_W\left(c(x,t), T(x,t)\right) + \frac{m}{2c(x,t)}\left(\frac{dc(x,t)}{dx}\right)^2 \tag{23.9}$$

The first term on the right hand side describes the homogeneous fluids. The last term, with the square of the gradient of $c(x,t)$, describes the interfacial region and gives the name to the model. The density $c(x,t)$ and the temperature $T(x,t)$ are both functions of x and t. The equilibrium density profile for a pressure of 200 bar and a temperature of 561.65 K is shown in Fig. 23.2. The material coefficient m was independent of density and temperature in the original model. For the chemical potential we use

$$\mu(x,t) \equiv \mu_W\left(c(x,t), T(x,t)\right) - m\frac{d^2c(x,t)}{dx^2} \tag{23.10}$$

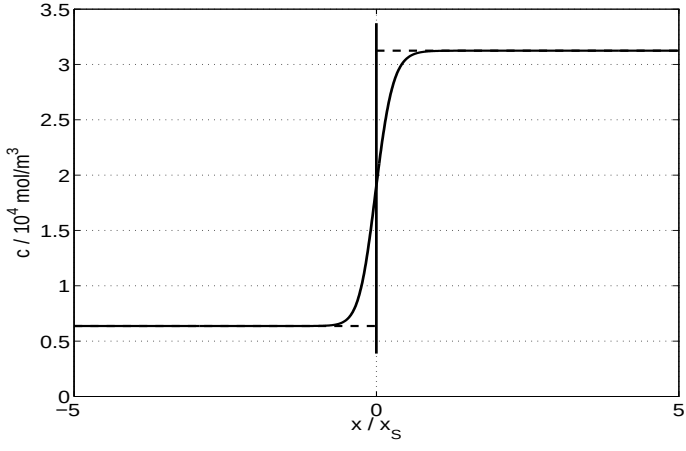

Figure 23.2 The equilibrium density profile of water for a pressure of 200 bar and a temperature of 561.65 K. The length scale is given as fractions of the scaling length, see Sec. 23.6.

We identify the normal pressure by

$$p_\perp(x,t) = p_W\left(c(x,t), T(x,t)\right) + \frac{m}{2}\left(\frac{dc(x,t)}{dx}\right)^2 - mc(x,t)\frac{d^2c(x,t)}{dx^2} \tag{23.11}$$

In equilibrium, the temperature is constant, and μ and $p_\perp$ become constant (independent of x) [93]. From μ, $p_\perp$ and the formulae of the previous section, we find the density profile, $c_{eq}(x)$ at equilibrium. This is used as input in the numerical solution (see Sec. 23.6) used to find the profile in Fig. 23.2.

We define the pressure parallel to the surface by

$$\begin{aligned} p_\parallel(x,t) &\equiv c(x,t)\left[\mu(x,t) - f(x,t)\right] \\ &= p_W\left(c(x,t), T(x,t)\right) - \frac{m}{2}\left(\frac{dc(x,t)}{dx}\right)^2 - mc(x,t)\frac{d^2c(x,t)}{dx^2} \end{aligned} \tag{23.12}$$

The surface tension $\gamma(t)$ is equal to minus the excess of the parallel pressure. A precise definition of excess quantities follows. Using an equilibrium surface tension of 61×10^{-3} J/m^2 for water at room temperature, we obtain $m = 3\times10^{-20}$ Jm^5/mol. The molar entropy is defined by

$$S(x,t) \equiv \left(\frac{\partial F}{\partial T}\right)_v = \left(\frac{\partial F_W}{\partial T}\right)_v = S_W\left(c(x,t), T(x,t)\right) \tag{23.13}$$

where we used that m is independent of the temperature. Furthermore, we define the molar internal energy as

$$\begin{aligned} U(x,t) &\equiv F(x,t) + T(x,t)\, S(x,t) \\ &= T(x,t)\, S(x,t) - p_{\parallel}(x,t)\, V(x,t) + \mu(x,t) \\ &= U_W\left(c(x,t), T(x,t)\right) + \frac{m}{2c(x,t)} \left(\frac{dc(x,t)}{dx}\right)^2 \end{aligned} \tag{23.14}$$

and finally the molar enthalpy by

$$\begin{aligned} H(x,t) &\equiv U(x,t) + p_{\parallel}(x,t)\, V(x,t) = T(x,t) S(x,t) + \mu(x,t) \\ &= H_W\left(c(x,t), T(x,t)\right) - m \frac{d^2 c(x,t)}{dx^2} \end{aligned} \tag{23.15}$$

Equations (23.12) through (23.15) relate U, S, H, $p_{\parallel}$ and μ. The equation of state values for U_W, S_W, H_W, p_W and μ_W satisfy the same thermodynamic relations. Other thermodynamic relations for U, S, H, $p_{\parallel}$ and μ are true only when they can be derived from the above definitions. The parallel pressure, but not the normal pressure, satisfies the above thermodynamic relations. Away from the surface, the parallel and the normal pressure become equal. Van der Waals was able to show that the surface tension was equal to

$$\gamma_{eq} = -\int \left[p_{\parallel,eq}(x) - p_{\perp,eq}(x)\right] dx \tag{23.16}$$

Furthermore, van der Waals was able to show that the surface tension was equal to

$$\gamma_{eq} = m \int \left(\frac{dc_{eq}(x)}{dx}\right)^2 dx \tag{23.17}$$

Do these formulae also hold when the heterogeneous system is far from equilibrium? We return to this point in Sec. 23.8.

Exercise 23.2.1. *The value of m for water is about 3×10^{-20} J/mol^2. Give an estimate of the surface tension, using a surface thickness of 1 nm and known densities of water liquid and water vapor to estimate the derivative.*

- **Solution:** The density of water is about 5×10^4 mol/m^3. The density of the vapor is on a comparative scale negligible. This gives, as an estimate of the density gradient, 5×10^{13} mol/m^4. We apply Eq. (23.16) and find $\gamma = 75\times10^{-3}$ N/m for the water-vapor interface. The result is close to what is found experimentally (72×10^{-3} J/m^2). From the gradient in the molar density profile at room temperature, we obtain for comparison $\gamma = 61\times10^{-3}$ N/m for the water-vapor interface.

It is interesting to calculate how much the parallel pressure in the interfacial region deviates from the normal pressure at equilibrium. The normal pressure is the pressure in the homogeneous phases at room temperature, approximately 1 bar. Using the values for the thickness and the surface tension (61×10^{-3} J/m^2) in the exercise above, one finds that $p_{\parallel} = -750$ bar. This large negative pressure is one of the reasons why a microscopically thin region has a macroscopic importance.

23.3 Balance equations

We aim to construct the entropy production for the van der Waals square gradient model. Following the systematic procedure of Chapter 4, we need to combine the Gibbs equation with the conservation laws for mass, energy (the first law) and momentum.

Conservation of matter gives

$$\frac{\partial c\left(x,t\right)}{\partial t} = -\frac{\partial J\left(x,t\right)}{\partial x} \tag{23.18}$$

where J is the molar flux. The velocity of the fluid is

$$\mathrm{v}\left(x,t\right) \equiv \frac{J\left(x,t\right)}{c\left(x,t\right)} \tag{23.19}$$

The barycentric time derivative is useful for an observer that moves along with the fluid

$$\frac{d}{dt} \equiv \frac{\partial}{\partial t} + \mathrm{v}\left(x,t\right)\frac{\partial}{\partial x} \tag{23.20}$$

By multiplying this relation with the molar density, we have

$$c\left(x,t\right)\frac{d}{dt} = c\left(x,t\right)\frac{\partial}{\partial t} + J\left(x,t\right)\frac{\partial}{\partial x} \tag{23.21}$$

It follows from Eq. (23.18) that the molar volume satisfies

$$c\left(x,t\right)\frac{dV\left(x,t\right)}{dt} = \frac{\partial \mathrm{v}\left(x,t\right)}{\partial x} \tag{23.22}$$

A useful identity, true for an arbitrary local property $a\left(x,t\right)$, which follows from Eq. (23.18), is

$$\begin{aligned} c\left(x,t\right)\frac{da\left(x,t\right)}{dt} &= \frac{\partial c\left(x,t\right)a\left(x,t\right)}{\partial t} + \frac{\partial c\left(x,t\right)\mathrm{v}\left(x,t\right)a\left(x,t\right)}{\partial x} \\ &= \frac{\partial c\left(x,t\right)a\left(x,t\right)}{\partial t} + \frac{\partial J\left(x,t\right)a\left(x,t\right)}{\partial x} \end{aligned} \tag{23.23}$$

For a system without gravitational forces or viscous friction, acceleration is caused only by the normal pressure. The equation of motion is

$$Mc\left(x,t\right)\frac{d\mathrm{v}\left(x,t\right)}{dt}=M\left[\frac{\partial J\left(x,t\right)}{\partial t}+\frac{\partial J\left(x,t\right)\mathrm{v}\left(x,t\right)}{\partial x}\right]=-\frac{\partial p_{\perp}\left(x,t\right)}{\partial x} \tag{23.24}$$

where M is the molar mass.

The total molar energy is the sum of internal and kinetic energies per mole:

$$E\left(x,t\right)=U\left(x,t\right)+\frac{1}{2}M\mathrm{v}^{2}\left(x,t\right) \tag{23.25}$$

The total energy is conserved so that

$$\frac{\partial c\left(x,t\right)E\left(x,t\right)}{\partial t}=-\frac{\partial J_{e}\left(x,t\right)}{\partial x} \tag{23.26}$$

where J_e is the total energy flux. We define the measurable heat flux, J_q', by

$$J_{e}\left(x,t\right)\equiv J\left(x,t\right)E\left(x,t\right)+p_{\parallel}\left(x,t\right)\mathrm{v}\left(x,t\right)+J_{q}'\left(x,t\right) \tag{23.27}$$

and substitute this definition into Eq. (23.26). We then obtain, using Eq. (23.18),

$$c\left(x,t\right)\frac{dE\left(x,t\right)}{dt}=-\frac{\partial}{\partial x}\left[p_{\parallel}\left(x,t\right)\mathrm{v}\left(x,t\right)+J_{q}'\left(x,t\right)\right] \tag{23.28}$$

For the kinetic energy, we find using Eq. (23.24)

$$c\left(x,t\right)\frac{d}{dt}\left(\frac{1}{2}M\mathrm{v}^{2}\left(x,t\right)\right)=-\mathrm{v}\left(x,t\right)\frac{\partial}{\partial x}p_{\perp}\left(x,t\right) \tag{23.29}$$

The change in kinetic energy is caused by the gradient in the normal pressure. By subtracting Eq. (23.29) from Eq. (23.28), we obtain, for the internal energy per mole

$$\begin{aligned}\frac{\partial c\left(x,t\right)U\left(x,t\right)}{\partial t}+\frac{\partial}{\partial x}\left[J\left(x,t\right)H\left(x,t\right)-p_{\perp}\left(x,t\right)\mathrm{v}\left(x,t\right)\right]\\=-\frac{\partial J_{q}'\left(x,t\right)}{\partial x}-p_{\perp}\left(x,t\right)\frac{\partial\mathrm{v}\left(x,t\right)}{\partial x}\end{aligned} \tag{23.30}$$

or alternatively,

$$\frac{\partial c\left(x,t\right)U\left(x,t\right)}{\partial t}+\frac{\partial\left[J_{q}'\left(x,t\right)+J\left(x,t\right)H\left(x,t\right)\right]}{\partial x}=\mathrm{v}\left(x,t\right)\frac{\partial p_{\perp}\left(x,t\right)}{\partial x} \tag{23.31}$$

The above expressions apply inside the interfacial region. Outside the interfacial region, $p_\perp$ approaches $p_\parallel$ so that the term between the square brackets in Eq. (23.30) reduces to $J(x,t)\,U(x,t)$. The left hand side of this equation can then be written as $c(x,t)\,dU(x,t)/dt$.

23.4 The entropy production

In agreement with Eq. (4.1) in Chapter 4, we write the entropy balance of a volume element as:

$$c(x,t)\frac{dS(x,t)}{dt} = \frac{\partial c(x,t)\,S(x,t)}{\partial t} + \frac{\partial J(x,t)\,S(x,t)}{\partial x}$$
$$= -\frac{\partial J_s(x,t)}{\partial x} + \sigma(x,t) \tag{23.32}$$

where $J_s(x,t)$ is the entropy flux and $\sigma(x,t)$ the local entropy production. The following Gibbs equation applies in the interfacial region as well as in the homogeneous phases:

$$T(x,t)\frac{dS(x,t)}{dt}$$
$$= V(x,t)\left\{\frac{\partial c(x,t)\,U(x,t)}{\partial t} + \frac{\partial}{\partial x}\left[J(x,t)\left(H(x,t) - p_\perp(x,t)\,V(x,t)\right)\right]\right\}$$
$$+ p_\perp(x,t)\frac{dV(x,t)}{dt} \tag{23.33}$$

In the interface, the work term contains $p_\perp$ rather than $p_\parallel$. The second term between the curly brackets reduces to the usual one, $c(x,t)\,dU(x,t)/dt$, outside the interface. In the homogeneous phases, $p_\perp = p_\parallel$, and the Gibbs equation obtains its normal form.

In order to obtain expressions for $J_s(x,t)$ and $\sigma(x,t)$, we combine Eq. (23.33) with Eq. (23.22) and (23.30) into

$$c(x,t)\frac{dS(x,t)}{dt} = -\frac{1}{T(x,t)}\frac{\partial J'_q(x,t)}{\partial x}$$
$$= -\frac{\partial}{\partial x}\left[\frac{J'_q(x,t)}{T(x,t)}\right] + J'_q(x,t)\frac{\partial}{\partial x}\left[\frac{1}{T(x,t)}\right] \tag{23.34}$$

The entropy flux is then given in terms of the measurable heat flux by

$$J_s(x,t) = \frac{J'_q(x,t)}{T(x,t)} \tag{23.35}$$

while the entropy production is given by

$$\sigma = J'_q(x,t)\,\frac{\partial}{\partial x}\left[\frac{1}{T(x,t)}\right] = -\frac{J'_q(x,t)}{T^2(x,t)}\frac{\partial T(x,t)}{\partial x} \tag{23.36}$$

23.5 Flux equations

The entropy production (23.36) gives the following linear force-flux relation:

$$\frac{\partial T(x,t)}{\partial x} = -r(x,t)\,J'_q(x,t) \tag{23.37}$$

or alternatively Fourier's law

$$J'_q(x,t) = -\frac{1}{r(x,t)}\frac{\partial T(x,t)}{\partial x} = -\lambda(x,t)\,\frac{\partial T(x,t)}{\partial x} \tag{23.38}$$

As usual the thermal conductivity, λ, or alternatively the thermal resistivity, r, may depend on both the local temperature and density.

In a system that is out of local equilibrium, these quantities may also depend on the density in adjacent locations, or on the derivatives of the density. This gives for the thermal resistivity:

$$r(x,t) = r\left(T(x,t), c(x,t), \frac{dc(x,t)}{dx}, \frac{d^2c(x,t)}{dx^2}, \ldots.\right) \tag{23.39}$$

Bedeaux *et al.* [106] gave a proposal for $r(x,t)$ in which the term due to the gradient is positive:

$$\begin{aligned} r(x,t) &= r^{\mathrm{g}}_{coex}(T(x,t)) \\ &\quad + \left(r^{\mathrm{l}}_{coex}(T(x,t)) - r^{\mathrm{g}}_{coex}(T(x,t))\right)\left(\frac{c(x,t) - c^{\mathrm{g}}_{coex}(T(x,t))}{c^{\mathrm{l}}_{coex}(T(x,t)) - c^{\mathrm{g}}_{coex}(T(x,t))}\right) \\ &\quad + \alpha\left(T(x,t), c(x,t)\right) m\left(\frac{dc(x,t)}{dx}\right)^2 \end{aligned} \tag{23.40}$$

Here, r^{g}_{coex} and r^{l}_{coex} are the thermal resistivities of the homogeneous vapor and liquid phases at coexistence, respectively. The first two terms give a smooth transition from the value of the resistivity in the vapor to the value in the liquid. The third term gives a peak in the resistivity around the surface. This term can give rise to significant temperature differences across the interface, which are expected to increase with the surface tension. The first two terms will also contribute to the temperature difference across the surface. All temperature effects disappear when one approaches the critical point, as is to be expected.

We shall use $\alpha = 5 \times 10^{-4}$. This constant value distributes the contribution to the resistivity in the interfacial region symmetrically. Non-equilibrium molecular dynamic simulations found most of the resistivity on the vapor side of the surface [40, 112]. In Sec. 23.13, we therefore use

$$\alpha\left(T(x), c(x)\right) = \alpha\left(\frac{c^{\mathrm{l}}_{coex}(T_{eq})}{c(x)}\right)^2 \tag{23.41}$$

for the dependence on the concentration.

The equations describing the non-equilibrium behavior of the system cannot be solved analytically. One has to use numerical methods. A numerical solution method was developed for stationary heat and molar fluxes [106]. We will therefore first discuss how stationarity simplifies the equations. It follows from Eqs. (23.18) and (23.19), that the molar flux satisfies

$$\frac{dc(x)\mathrm{v}(x)}{dx} \equiv \frac{dJ(x)}{dx} = 0 \tag{23.42}$$

In a stationary state the velocity of the surface is zero:

$$\mathrm{v}^{\mathrm{s}} = \frac{dx^{\mathrm{s}}}{dt} = 0 \tag{23.43}$$

Furthermore, it follows from the equation of motion (23.24) that

$$\frac{dp_{\perp}(x)}{dx} = -M\frac{dJ(x)\,\mathrm{v}(x)}{dx} = M\left[\frac{J(x)}{c(x)}\right]^2\frac{dc(x)}{dx} \tag{23.44}$$

From Eq. (23.31), it follows that

$$\frac{dJ_q(x)}{dx} = \mathrm{v}(x)\frac{dp_{\perp}(x)}{dx} = M\left[\frac{J(x)}{c(x)}\right]^3\frac{dc(x)}{dx} \tag{23.45}$$

where the total heat flux is as usual related to the measurable heat flux by $J_q(x) \equiv J'_q(x) + JH(x)$.

When one integrates the equations for the molar flux, the pressure and the total heat flux, it follows that $J(x)$, $p_{\perp}(x) + MJ\mathrm{v}(x)$ and $J_q(x) + \frac{1}{2}MJ\mathrm{v}^2(x)$ are position independent constants.

23.6 A numerical solution method

In order to obtain the concentration and temperature profiles of the non-equilibrium van der Waals square gradient model, one must solve a number of ordinary differential equations which follow from the analysis above. The

fluid is enclosed in a container with walls at x_{in} and x_{out}, where $x_{in} < x_{out}$. Boundary conditions are given at both ends of the box, x_{in} and x_{out}. This gives a so-called two-point boundary-value problem.

A popular method [302] to solve a two-point boundary value problem is to consider a related initial value problem, in which one guesses some initial values, calculates the values at the other end and then adjusts the guesses until the boundary conditions at the other end are fulfilled. Such procedures go under the name of shooting methods. The difficulty with the application of shooting methods for the non-equilibrium two-phase system under consideration is that the integration of the initial value problem is unstable. Very small differences in the guesses of the initial values were found to result in solutions of a very different solution class, upon integration through the interface. The standard solution [302] to this problem is to use one of the many finite difference methods, whereby one generally chooses a finite grid and converts the equations in finite difference equations. These can then be solved by matrix inversion. We present results from such solutions in the sections to follow. For more details on the differential equations and their boundary conditions, see [106].

In the solution procedure it is necessary to scale the variables, so that their typical sizes do not differ too much in the calculations. In the scaling factors, we use the distance over which fluctuations in the molar density are correlated in the liquid, see [93];

$$\begin{aligned}\xi^{\mathrm{l}}(p_{eq}) &= c^{\mathrm{l}}_{eq}(p_{eq})\sqrt{m\kappa^{\mathrm{l}}_{eq}(p_{eq})} \\ &= c^{\mathrm{l}}_{eq}(p_{eq})\sqrt{m}\left[\frac{c^{\mathrm{l}}_{eq}(p_{eq})RT_{eq}(p_{eq})}{\left(1-Bc^{\mathrm{l}}_{eq}(p_{eq})\right)^2} - 2A\left(c^{\mathrm{l}}_{eq}(p_{eq})\right)^2\right]^{-1/2}\end{aligned} \tag{23.46}$$

Here, $T_{eq}(p_{eq})$, $c^{\mathrm{l}}_{eq}(p_{eq})$ and $\kappa^{\mathrm{l}}_{eq}(p_{eq})$ are the temperature, the density and the compressibility of the coexisting liquid at the pressure p_{eq}, respectively. All these quantities are obtained using the equation of state, Eq. (23.1). The correlation length is larger in the liquid than in the vapor. A scaling length of 7 times the correlation length was suitable:

$$x_S \equiv 7\xi^{\mathrm{l}}_W(p_{eq}) \tag{23.47}$$

At a distance x_S from the surface, the gradient contributions to the thermodynamic variables were of the order of 10^{-8} and therefore negligible. The temperature, pressure and molar density were scaled with

$$T_S \equiv T_{eq}(p_{eq}), \quad p_S \equiv p_{eq} \quad \text{and} \quad c_S \equiv c^{\mathrm{l}}_{eq}(p_{eq}) \tag{23.48}$$

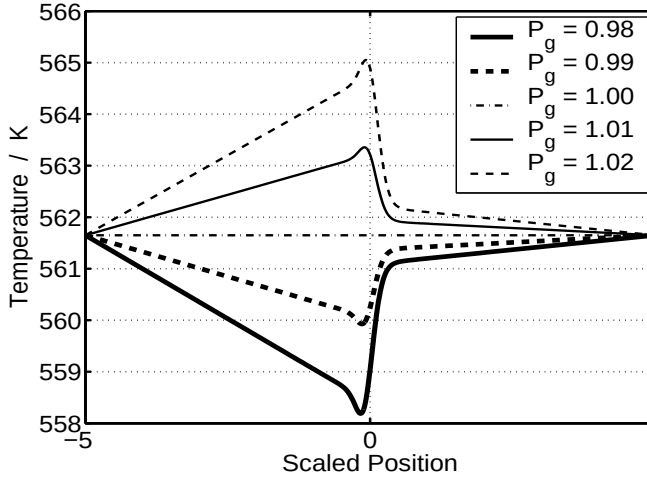

Figure 23.3 The temperature profiles for five values of pressure. Reproduced from Physica A 330 (2003) 329–353 with permission of Elsevier.

When $p_{eq} = 200$ bar, the scaling parameters are

$$x_S = 2.8062 \text{ nm}, \quad T_S = 561.65 \text{ K}, \quad p_S = 200 \text{ bar}, \quad c_S = 3.1243 \times 10^4 \text{ mol/m}^3 \tag{23.49}$$

The size of the box was $10x_S = 28.062$ nm. Scaled quantities are indicated by a curly bar above the symbol, like $\widetilde{x} = x/x_S$.

Calculations were done for non-equilibrium stationary states of water. In the first set of cases, the pressure at the vapor end of the box was changed to 0.98, 0.99, 1.01 or 1.02 times $p_S = p_{eq} = 200$ bar, while the temperatures at the ends were kept equal to $T_S = T_{eq}(p_{eq})$. In the second set of cases, the temperature at the liquid end was set to 0.98, 0.99, 1.01 or 1.02 times $T_S = 561.65$ K, while the pressure and the temperature at the other end were kept equal to $p_S = p_{eq} = 200$ bar and $T_S = T_{eq}(p_{eq})$. The four first cases were named PG98, PG99, PG101, PG102, and the four last were named TL98, TL99, TL101, and TL102 respectively.

The temperature profiles for the changes in the pressure are shown in Fig. 23.3, and for the changes in the liquid temperature in Fig. 23.4. In both cases $\alpha = 5 \times 10^{-4}$ was used. This value leads to a dip or a peak in the temperature profile in the interfacial region in Fig. 23.3. For smaller values of α the temperature difference across the surface decreases and for bigger values it increases. The figures give a temperature gradient in the liquid and the vapor up to 10^8 K/m. The density profiles were all found to be rather similar to the equilibrium density profile, see Ref. [106].

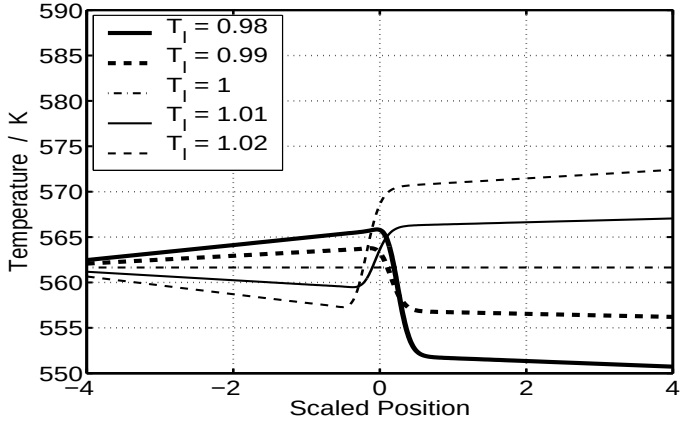

Figure 23.4 The temperature profiles for five values of the liquid temperature. Reproduced from Physica A 330 (2003) 329–353 with permission of Elsevier.

23.7 Procedure for extrapolation of bulk densities and fluxes

A surface is defined by its excess thermodynamic variables. An excess variable is found in Chapter 3, by subtracting from the actual value the extrapolated value in the homogeneous phases up to the dividing surface. The extrapolation procedure was tested using the non-equilibrium van der Waals square gradient model [106]. The following auxiliary variables are used: On the x-coordinate axis, the left hand side of the vapor phase starts at position x_{in}. The liquid phase ends at position x_{out}. The dividing surface has position x^{s}, and x_S is the system's scaling length (a characteristic molecular length).

The systematic procedure consists then of the following steps:

1. Choose an arbitrary, time-independent position x^{s} in the interfacial region as the dividing surface.

2. Introduce a distance d, which is the distance from the dividing surface beyond which the gradient contributions become very small.

3. Define an nth-order polynomial fit of the density in the vapor phase by dividing the segment between $x_{in} + x_S$ and $x^{\mathrm{s}} - d$ into n equal pieces and draw an nth-order polynomial through these points.

4. In the liquid phase, do the same by dividing the segment between $x^{\mathrm{s}} + d$ and $x_{out} - x_S$ into n pieces.

The values of both d and n were found by trying a range of values. The procedure is illustrated for the Helmholtz energy density in Fig. 23.5. The figure shows the extrapolated energy density as stippled lines. In their calculations, Bedeaux and coworkers [106–108] used $x_{out} = -x_{in} = 5x_S$. By using $x_{in} + x_S$ and $x_{out} - x_S$ rather than x_{in} and x_{out}, one reduces an already small dependence on the finite size of the box. The curve fit in 3 gives n- and d-dependent extrapolations of the bulk densities to the dividing surface. For ease of notation, we suppress the explicit dependence of the extrapolated densities on n and d. The extrapolated densities cannot inherently be precisely defined, but their variance can be made as small as a few parts in 10^5. Values shown in this chapter refer to $n = 2$, $\widetilde{d} = 2.5$ and a box with a length $10x_S$.

The extrapolated enthalpy, entropy, Helmholtz energy and Gibbs energy density in the vapor and the liquid phase as a function of n and d can all be defined in this manner. In his definition of these excess variables, Gibbs used quantities per unit of volume [62]. The extrapolated parallel pressure is defined in the same way as the extrapolated densities. The extrapolated normal pressure is defined below. The temperature is an intensive variable and has as such no excess. We shall still use extrapolations of the temperature into the surface.

Extrapolated fluxes are defined using the constant nature of $J(x)$, $p_\perp(x) + MJ\mathrm{v}(x)$ and $J'_q(x) + JH(x) + \frac{1}{2}MJ\mathrm{v}^2(x)$ in the stationary state, see Sec. 23.5. The proper extrapolation of a constant is the constant itself, so that:

$$J(x_{in}) \equiv J^{\mathrm{g}}(x) \equiv J^{\mathrm{l}}(x) \equiv J(x_{out}) \equiv J$$

$$\begin{aligned} p_\perp(x_{in}) + MJ\mathrm{v}(x_{in}) &\equiv p^{\mathrm{g}}(x) + MJ\mathrm{v}^{\mathrm{g}}(x) \equiv p^{\mathrm{l}}(x) + MJ\mathrm{v}^{\mathrm{l}}(x) \\ &\equiv p_\perp(x_{out}) + MJ\mathrm{v}(x_{out}) \end{aligned}$$

$$\begin{aligned} J'_q(x_{in}) + JH(x_{in}) + \frac{1}{2}MJ\mathrm{v}^2(x_{in}) &\equiv J'^{\mathrm{g}}_q(x) + JH^{\mathrm{g}}(x) + \frac{1}{2}MJ\left[\mathrm{v}^{\mathrm{g}}(x)\right]^2 \\ &\equiv J'^{\mathrm{l}}_q(x) + JH^{\mathrm{l}}(x) + \frac{1}{2}MJ\left[\mathrm{v}^{\mathrm{l}}(x)\right]^2 \\ &\equiv J'_q(x_{out}) + JH(x_{out}) + \frac{1}{2}MJ\mathrm{v}^2(x_{out}) \end{aligned} \tag{23.50}$$

When d is sufficiently large compared to the thickness of the surface (x_S), the extrapolated parallel and normal pressures were found to be the same (in five significant decimals):

$$p^{\mathrm{g}}_\parallel(x) = p^{\mathrm{g}}_\perp(x) \equiv p^{\mathrm{g}}(x) = p^{\mathrm{l}}_\parallel(x) = p^{\mathrm{l}}_\perp(x) \equiv p^{\mathrm{l}}(x) \tag{23.51}$$

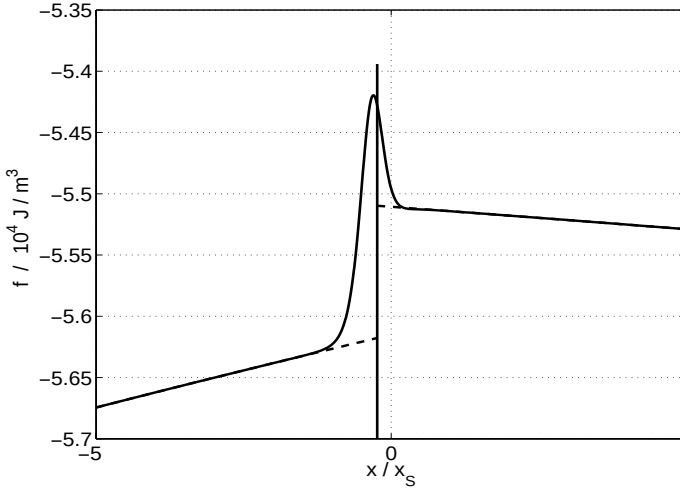

Figure 23.5 The Helmholtz energy density for the case TL102.

In the present case, when we wanted to verify the autonomous nature of the surface, it was important to take all terms in Eq. (23.50) along.

23.8 Defining excess densities

From the extrapolated bulk densities we can now define the n- and d-dependent excess thermodynamic densities of the surface. The excess density in moles per unit of surface area* is, for instance:

$$c^{\mathrm{exc}} \equiv \int \left[c\left(x\right) - c^{\mathrm{l}}\left(x\right)\theta\left(x - x^{\mathrm{s}}\right) - c^{\mathrm{g}}\left(x\right)\theta\left(x^{\mathrm{s}} - x\right)\right]dx \tag{23.52}$$

where the integral is over the length of the box, and θ is the Heaviside function (see Sec. 3.3). Excess densities are given per unit of area of the dividing surface. As the equimolar excess density is zero, it is not convenient to give these quantities per mole.

We define the surface tension by

$$\gamma^{\mathrm{exc}} \equiv -\int \left[p_{\parallel}(x) - p_{\parallel}^{\mathrm{l}}\left(x\right)\theta\left(x - x^{\mathrm{s}}\right) - p_{\parallel}^{\mathrm{g}}\left(x\right)\theta\left(x^{\mathrm{s}} - x\right)\right]dx \tag{23.53}$$

*In this chapter we use the symbol c to denote mole per surface area, following Bedeaux *et al.* [106–108]. The symbol Γ was used for this property in Chapter 3.

In equilibrium $p_{\parallel}^{\mathrm{l}}(x) = p_{\parallel}^{\mathrm{g}}(x) = p_{\perp}(x)$, and the expression reduces to Eq. (23.16) for the surface tension. The excess internal energy density (in J/ m^2) is

$$u^{\mathrm{exc}} \equiv \int [c(x)\, U(x) - c^{\mathrm{l}}(x)\, U^{\mathrm{l}}(x)\, \theta(x - x^{\mathrm{s}}) - c^{\mathrm{g}}(x)\, U^{\mathrm{g}}(x)\, \theta(x^{\mathrm{s}} - x)] dx \tag{23.54}$$

For the excess Helmholtz energy, f^{exc}, the excess entropy, s^{exc}, and the excess enthalpy, h^{exc}, of the surface we use similar definitions. The Helmholtz energy density for the case TL102 was plotted in Fig. 23.5. The figure gives the excess Helmholtz energy as the difference between the solid and stippled lines. All excess densities are per unit of surface area. One can define the excess Gibbs energy by

$$g^{\mathrm{exc}} \equiv \int [c(x)\, \mu(x) - c^{\mathrm{l}}(x)\, \mu^{\mathrm{l}}(x)\, \theta(x - x^{\mathrm{s}}) - c^{\mathrm{g}}(x)\, \mu^{\mathrm{g}}(x)\, \theta(x^{\mathrm{s}} - x)] dx \tag{23.55}$$

In the following section, we shall discuss how to define the equimolar surface and the surface of tension.

23.9 Thermodynamic properties of Gibbs' surface

In order to determine the excess functions, we need the thermodynamic relations for the liquid-vapor interface as given by Gibbs [62]. These relations were already given in Chapter 3.4. In order to notify global equilibrium, we introduce the subscript eq. The chemical potential at T_{eq} is thus denoted $\mu_{eq}(T_{eq})$. For an arbitrary choice of the dividing surface, we have

$$\begin{aligned}
\gamma_{eq}^{\mathrm{s}} &= f_{eq}^{\mathrm{s}} - \mu_{eq}^{\mathrm{s}}(T_{eq}^{\mathrm{s}}) c_{eq}^{\mathrm{s}} \\
u_{eq}^{\mathrm{s}} &= f_{eq}^{\mathrm{s}} + T_{eq} s_{eq}^{\mathrm{s}} = T_{eq} s_{eq}^{\mathrm{s}} + \gamma_{eq}^{\mathrm{s}} + \mu_{eq}(T_{eq}) c_{eq}^{\mathrm{s}} \\
h_{eq}^{\mathrm{s}} &= u_{eq}^{\mathrm{s}} - \gamma_{eq}^{\mathrm{s}} = T_{eq} s_{eq}^{\mathrm{s}} + \mu_{eq}(T_{eq}) c_{eq}^{\mathrm{s}} \\
g_{eq}^{\mathrm{s}} &= h_{eq}^{\mathrm{s}} - T_{eq} s_{eq}^{\mathrm{s}} = \mu_{eq}(T_{eq}) c_{eq}^{\mathrm{s}}
\end{aligned} \tag{23.56}$$

These excess densities depend only on the temperature and the choice of the dividing surface. Superscript s is now used to indicate a property of the surface, which depends on the choice of the dividing surface.

For a heterogeneous system that is no longer in global equilibrium, we deduce the following relations for an arbitrary dividing surface:

$$\begin{aligned}
\gamma^{\mathrm{exc}} &= f^{\mathrm{exc}} - g^{\mathrm{exc}} \\
u^{\mathrm{exc}} &= f^{\mathrm{exc}} + (Ts)^{\mathrm{exc}} = (Ts)^{\mathrm{exc}} + \gamma^{\mathrm{exc}} + g^{\mathrm{exc}} \\
h^{\mathrm{exc}} &= u^{\mathrm{exc}} - \gamma^{\mathrm{exc}} = (Ts)^{\mathrm{exc}} + g^{\mathrm{exc}} \\
g^{\mathrm{exc}} &= h^{\mathrm{exc}} - (Ts)^{\mathrm{exc}}
\end{aligned} \tag{23.57}$$

The expressions are obtained from the excesses of Eqs. (23.12), (23.14), (23.15) and $g(x,t)$, but now for the non-equilibrium system. Here, $(Ts)^{\mathrm{exc}}$ is defined similarly to the other excess densities. By using the assumption of local equilibrium, we can convert these expressions into Gibbs' relations for the surface. The condition for local equilibrium is that all excess densities of the system have the equilibrium value at the temperature T^{s}. The temperature and the chemical potential of the surface are then:

$$\begin{aligned}
T^{\mathrm{s}} &\equiv \frac{h^{\mathrm{exc}} - \mu_{eq}(T^{\mathrm{s}})c^{\mathrm{exc}}}{s^{\mathrm{exc}}} = \frac{(Ts)^{\mathrm{exc}} + g^{\mathrm{exc}} - \mu_{eq}(T^{\mathrm{s}})c^{\mathrm{exc}}}{s^{\mathrm{exc}}} \\
\mu^{\mathrm{s}} &\equiv \mu_{eq}(T^{\mathrm{s}})
\end{aligned} \tag{23.58}$$

By defining

$$\begin{gathered}
\gamma^{\mathrm{s}} \equiv \gamma^{\mathrm{exc}}, \quad c^{\mathrm{s}} \equiv c^{\mathrm{exc}}, \quad u^{\mathrm{s}} \equiv u^{\mathrm{exc}}, \quad h^{\mathrm{s}} \equiv h^{\mathrm{exc}} \\
s^{\mathrm{s}} \equiv s^{\mathrm{exc}}, \quad g^{\mathrm{s}} \equiv \mu_{eq}(T^{\mathrm{s}})c^{\mathrm{exc}}, \quad f^{\mathrm{s}} \equiv f^{\mathrm{exc}} - g^{\mathrm{exc}} + \mu_{eq}(T^{\mathrm{s}})c^{\mathrm{exc}}
\end{gathered} \tag{23.59}$$

and substituting Eqs. (23.58) and (23.59) into Eq. (23.57), we obtain the relations given by Gibbs, cf. Eq. (23.56)

$$\begin{aligned}
\gamma^{\mathrm{s}} &= f^{\mathrm{s}} - \mu_{eq}(T^{\mathrm{s}})c^{\mathrm{s}} = f^{\mathrm{s}} - \mu^{\mathrm{s}}c^{\mathrm{s}} \\
u^{\mathrm{s}} &= f^{\mathrm{s}} + T^{\mathrm{s}}s^{\mathrm{s}} = T^{\mathrm{s}}s^{\mathrm{s}} + \gamma^{\mathrm{s}} + \mu_{eq}(T^{\mathrm{s}})c^{\mathrm{s}} = T^{\mathrm{s}}s^{\mathrm{s}} + \gamma^{\mathrm{s}} + \mu^{\mathrm{s}}c^{\mathrm{s}} \\
h^{\mathrm{s}} &= u^{\mathrm{s}} - \gamma^{\mathrm{s}} = T^{\mathrm{s}}s^{\mathrm{s}} + \mu_{eq}(T^{\mathrm{s}})c^{\mathrm{s}} = T^{\mathrm{s}}s^{\mathrm{s}} + \mu^{\mathrm{s}}c^{\mathrm{s}} \\
g^{\mathrm{s}} &= h^{\mathrm{s}} - T^{\mathrm{s}}s^{\mathrm{s}} = \mu_{eq}(T^{\mathrm{s}})c^{\mathrm{s}} = \mu^{\mathrm{s}}c^{\mathrm{s}}
\end{aligned} \tag{23.60}$$

While Gibbs only gave these relations for a surface in an equilibrium two-phase system, we have now derived them, assuming the validity of local equilibrium, for the non-equilibrium system.

23.10 An autonomous surface

The assumption of local equilibrium, which was first discussed in Chapter 3, is basic to non-equilibrium thermodynamics. It was used above

to identify the excess densities for the surface in a non-equilibrium system. It is therefore important to know how good this assumption is. We show in this section that it can be expected to hold for thermodynamic forces that are typical for the fluid phases as well as for the interfacial region. This means that the surface as described by excess densities can be regarded as being autonomous.

In the fluid phases, the assumption of local equilibrium means that the van der Waals equation of state applies everywhere. This was true when the rate of evaporation or condensation was smaller than the Mach number, and when the distance to the surface was larger than 2 in scaled units. In that case $(p_\perp - p_W)/p_W < 10^{-5}$. This difference cannot be measured and it is therefore fair to say that the liquid and the vapor phases are in local equilibrium.

For the interface, local equilibrium requires that the surface densities have their equilibrium values at the temperature of the surface $T^{\rm s}$:

$$\begin{gathered}\gamma \equiv \gamma_{eq}(T^{\rm s}), \quad c^{\rm s} \equiv c^{\rm s}_{eq}(T^{\rm s}), \quad u^{\rm s} \equiv u^{\rm s}_{eq}(T^{\rm s}), \quad h^{\rm s} \equiv h^{\rm s}_{eq}(T^{\rm s}) \\ s^{\rm s} \equiv s^{\rm s}_{eq}(T^{\rm s}), \quad f^{\rm s} - g^{\rm s} \equiv f^{\rm s}_{eq}(T^{\rm s}) - g^{\rm s}_{eq}(T^{\rm s})\end{gathered} \tag{23.61}$$

This must apply for any choice of the dividing surface, and we will show that this is true in the next section.

We proceed now with four different calculations of the surface temperature to check the assumption of local equilibrium under very harsh conditions. Evaporation or condensation velocities are between 0.27 and 1.6 meters per second in the vapor phase, and extremely large temperature gradients, for example 10^8 K/m, were used. A constant $\alpha = 5 \times 10^{-4}$ (cf. Sec. 23.5) was used. To distinguish between calculations, the temperatures are given symbols as follow:

1. $T^{\rm es}$: The surface temperature from Eq. (23.58) for the equimolar surface.

2. $T^{\rm st}$: The surface temperature from Eq. (23.58) for the surface of tension.

3. $T^{\rm s}_\gamma$: The surface temperature found by comparing γ from Eq. (23.53) to the listed equilibrium values, see Table 13 in Ref. [107], and choosing $\gamma = \gamma(T^{\rm s}_\gamma)$. Any surface property in Eq. (23.61) can be used for this calculation. We have chosen the surface tension because it is independent of the choice of the dividing surface.

4. $T^{\rm s}_{\gamma,eq}$: The surface temperature obtained from the daring proposition

$$\gamma\left(T^{\rm s}_{\gamma,eq}\right) = m\int\left[\left(\frac{dc\,(x)}{dx}\right)^2 - \left(\frac{dc^{\rm l}\,(x)}{dx}\right)^2\theta\,(x-x^{\rm s}) - \left(\frac{dc^{\rm g}\,(x)}{dx}\right)^2\theta\,(x^{\rm s}-x)\right]dx \tag{23.62}$$

Van der Waals showed that the surface tension is equal to m times the integral of the square gradient of the molar density in global equilibrium. The proposition assumes that the molar density profile has the same structure as the corresponding equilibrium profile at the temperature of the surface. As this proposition concerns the whole shape of the density distribution, it is a rather strong criterion for the validity of local equilibrium. In equilibrium, this expression reduces to the one given by van der Waals, Eq. (23.16), in the limit that $d \to \infty$. Also, this definition uses values for the surface tension in equilibrium [107].

In very good approximation, all surface temperatures turn out to be the same, see the five first columns in Table 23.1. The values $T^{\rm s}_{\gamma}$, $T^{\rm s}_{\gamma,eq}$, $T^{\rm es}$ and $T^{\rm st}$ are equal for PG98, PG99, PG101 and PG102 within one part in 10^7. For TL98, TL99, TL101 and TL102, $T^{\rm s}_{\gamma}$ and $T^{\rm s}_{\gamma,eq}$ are equal within

Table 23.1 The surface temperatures (in K) for $n = 2$ and $\widetilde{d} = 2.5$ [107]. The six different methods of calculation are explained in the text.

	$T^{\rm s}_{\gamma}$	$T^{\rm s}_{\gamma,eq}$	$T^{\rm es}$	$T^{\rm st}$	$T^{\rm g}(x^{\rm es})$	$T^{\rm l}(x^{\rm es})$
PG98	560.6651	560.6650	560.6651	560.6651	558.4364	561.0823
PG99	561.1563	561.1563	561.1563	561.1563	560.0528	561.3672
PG101	562.1447	562.1447	562.1447	562.1447	563.2270	561.9293
PG102	562.6421	562.6420	562.6421	562.6421	564.7860	562.2065
TL98	553.1456	553.1451	553.0787	553.0804	565.9413	551.9061
TL99	557.3527	557.3525	557.3364	557.3369	563.8449	556.8704
TL101	566.0117	566.0114	565.9966	565.9977	559.3648	566.1843
TL102	570.4054	570.4043	570.3482	570.3541	557.0069	570.4118

two parts in 10^6. The values of $T^{\rm es}$ and $T^{\rm st}$ are equal within two parts in 10^5 and they differ less than one part in 10^4 from $T^{\rm s}_\gamma$ and $T^{\rm s}_{\gamma,eq}$. With less extreme conditions, the differences between the definitions of the surface temperature become significantly smaller.

We can thus safely conclude that $T^{\rm s}_\gamma$, $T^{\rm s}_{\gamma,eq}$, $T^{\rm es}$ and $T^{\rm st}$ all give the same value for the surface temperature $T^{\rm s}$. All these surface temperatures were defined using the assumption that the surface is in local equilibrium, in other words, that the surface is autonomous. That all these definitions result in the same surface temperature is remarkable. The equilibrium as well as the non-equilibrium van der Waals square gradient model are not autonomous in their continuous description of the interfacial region. The Gibbs surface defined for the excess densities on the basis of the non-equilibrium continuous model is autonomous, however. The conclusion does not depend on the choice of the dividing surface. The property of local equilibrium is therefore true for an arbitrary dividing surface with reasonable driving forces. The fact that $T^{\rm s}_{\gamma,eq}$ is not different from the other temperatures indicates that we have a surface with a structure that is not easily perturbed.

The extrapolated temperatures of the liquid and the vapor at the equimolar surface are also given in Table 23.1. We see that a change in the pressure of the vapor up 2%, gives a temperature difference of not more than 2.65 K across the surface. The extrapolated temperature of the liquid differs by not more than 0.44 K from the temperature of the surface. If one changes the temperature of the liquid, the temperature difference across the surface goes up to 14.04 K. The extrapolated temperature of the liquid now differs by not more than 1.24 K from the temperature of the surface. Given that the surface thickness is in the order of a few nanometers, the temperature difference across the surface is still substantial. The surface temperature is closer to the extrapolated temperature of the liquid than to the extrapolated temperature of the vapor. The difference between the extrapolated temperature of the liquid and the surface temperature is about 17% of the total difference for PG98 and about 9% for TL98. *The accuracy in the determination of the surface temperature is such that one can conclude that it is not correct to take the surface temperature equal to the extrapolated liquid temperature.*

In the NEMD studies of the surface [39, 40, 112], it was not possible to obtain temperature profiles with an accuracy comparable to those using the van der Waals model. Given the accuracy of these calculations the temperature difference between the liquid and the surface appeared to be negligible; i.e. they were of the same order of magnitude as the accuracy. The van der Waals model is more sensitive and therefore a more appropriate tool to study such aspects.

23.11 Excess densities depend on the choice of dividing surface

We saw above that the assumption of local equilibrium did not depend on the choice of the dividing surface. The property of local equilibrium becomes even more remarkable when we see that the excess densities depend significantly on the dividing surface. This dependence shall be illustrated here. Before we give the actual values for the equimolar surface and the surface of tension, we discuss the relation between the different surfaces.

23.11.1 *Properties of dividing surfaces*

The equimolar surface and the surface of tension, used above, are the two most common choices of the dividing surface for a one-component liquid-vapor interface. We define the position, x^{es}, of the equimolar surface by taking this position such that the excess density is zero in Eq. (23.52). This gives

$$0 = \int [c(x) - c^{\mathrm{l}}(x)\,\theta(x - x^{\mathrm{es}}) - c^{\mathrm{g}}(x)\,\theta(x^{\mathrm{es}} - x)]dx \tag{23.63}$$

where the integral is over the whole box. The position, x^{st}, of the surface of tension is similarly defined by setting the first moment of the excess parallel pressure equal to zero

$$0 = \int \left(x - x^{\mathrm{st}}\right)[p_{\parallel}(x) - p_{\parallel}^{\mathrm{l}}(x)\,\theta\left(x - x^{\mathrm{st}}\right) - p_{\parallel}^{\mathrm{g}}(x)\,\theta\left(x^{\mathrm{st}} - x\right)]dx \tag{23.64}$$

When one uses the surface of tension, the excess of the molar density is unequal to zero. When one, on the other hand, uses the equimolar surface, the first moment of the excess parallel pressure is not equal to zero. Other choices are possible, however. The definition of the thermodynamic densities for the surface in Sec. 23.9 apply to an arbitrary choice. One can, for instance, set one's excess energy density equal to zero, and use the equation to determine the corresponding position x^{s} of the dividing surface. We shall use the superscript s to indicate such an alternative choice.

Distances between the alternative choices of the dividing surface are properties of the surface [62]. The Tolman length is the distance between the surface of tension and the equimolar surface.

$$\delta^{\mathrm{st}} \equiv x^{\mathrm{st}} - x^{\mathrm{es}} \tag{23.65}$$

The sign in this definition is appropriate when the liquid is on the right hand side of the surface. If the liquid is on the left hand side, this expression gives $-\delta^{\mathrm{st}}$. The Tolman length plays a role in the dependence of γ^{es} on

Table 23.2 The position of the equimolar surface, the surface of tension and the Tolman length (all in nm). The surface is in equilibrium at a pressure of 200 bar, or in the non-equilibrium state, PG98 at a pressure of 196 bar.

State	x^{es}	x^{st}	$\delta^{\mathrm{st}} = x^{\mathrm{st}} - x^{\mathrm{es}}$
Equilibrium	0.0000	−0.0258	−0.0258
Case PG98	−0.1203	−0.1499	−0.0296

the curvature of the surface. In general case, the distance to the equimolar surface is

$$\delta^{\mathrm{s}} \equiv x^{\mathrm{s}} - x^{\mathrm{es}} \tag{23.66}$$

In equilibrium, all these lengths are a function of temperature alone [62]. We chose $x^{\mathrm{es}} = 0$ in equilibrium. Table 23.2 gives x^{es}, x^{st} and δ^{st} (using $\widetilde{d} = 2.5$ and $n = 2$) for the equilibrium interface of water at a coexistence pressure of 200 bar, and for the non-equilibrium surface at a vapor pressure of 196 bar.

The Tolman length is negative for the van der Waals square gradient model. The surface of tension is thus on the vapor side of the equimolar surface, a typical result for square gradient models [303]. Molecular dynamics simulations find a positive δ^{st} of the same order of magnitude [304].

23.11.2 *Surface excess densities for two dividing surfaces*

Stable values were obtained for the excess densities using $n = 2$ and $\widetilde{d} = 2.5$ in the extrapolation procedure. We denote the values by γ^{es}, u^{es}, f^{es}, s^{es}, h^{es} and g^{es} for the equimolar surface and c^{st}, γ^{st}, u^{st}, f^{st}, s^{st}, h^{st} and g^{st} for the surface of tension. The results are listed in Tables 23.3 and 23.4, along with the surface position. The results show that the two sets of excess variables, apart from the surface tension, are significantly different.

One set of densities can be calculated from the other. Using their definition in Sec. 23.8 and Eq. (23.59), we find

$$\begin{aligned} u^{\mathrm{s}} &= u^{\mathrm{es}} + \int_{x^{\mathrm{es}}}^{x^{\mathrm{s}}} \left(c^{\mathrm{l}}(x)\, u^{\mathrm{l}}(x) - c^{\mathrm{g}}(x)\, u^{\mathrm{g}}(x) \right) dx \\ &= u^{\mathrm{es}} + \delta^{\mathrm{s}} \left(c^{\mathrm{l}}(x^{\mathrm{es}})\, u^{\mathrm{l}}(x^{\mathrm{es}}) - c^{\mathrm{g}}(x^{\mathrm{es}})\, u^{\mathrm{g}}(x^{\mathrm{es}}) \right) \\ &\quad + \frac{1}{2} (\delta^{\mathrm{s}})^2 \frac{d}{dx} \left(c^{\mathrm{l}}(x)\, u^{\mathrm{l}}(x) - c^{\mathrm{g}}(x)\, u^{\mathrm{g}}(x) \right) \Big|_{x = x^{\mathrm{es}}} + \cdots . \end{aligned} \tag{23.67}$$

Table 23.3 The position and the excess densities of the equimolar surface.

	$x^{\rm es}$	$\gamma^{\rm es}$	$u^{\rm es}$	$f^{\rm es}$	$s^{\rm es}$	$h^{\rm es}$	$g^{\rm es}$
	nm	mJ/m^2	mJ/m^2	mJ/m^2	μJ/K m^2	mJ/m^2	mJ/m^2
EQ	0.0000	7.89510	85.5004	7.8951	138.17	77.605	0.0000
PG98	−0.1203	8.03148	85.2016	12.117	137.64	77.170	4.0852
PG99	−0.0607	7.96333	85.3480	10.012	137.90	77.385	2.0492
PG101	0.0620	7.82677	85.6583	5.7635	138.45	77.832	−2.0633
Pg102	0.1253	7.75832	85.8213	3.6167	138.74	78.063	−4.1416
TL98	0.5237	9.09685	90.9243	−7.1863	147.95	81.827	−16.283
TL99	0.2744	8.49571	88.1952	0.4412	143.00	79.699	−8.0545
TL101	−0.3042	7.29962	82.8788	15.091	133.53	75.579	7.7916
TL102	−0.6447	6.71485	80.3785	21.933	129.16	73.664	15.218

and similar expressions for the other excess densities. Since $\delta^{\rm s}$ is very small, it is usually sufficient to only use the linear term of this expansion. This then results in

$$
\begin{aligned}
c^{\rm s} &= \delta^{\rm s}\left(c^{\rm l}-c^{\rm g}\right), \quad u^{\rm s} = u^{\rm es} + \delta^{\rm s}\left(c^{\rm l}u^{\rm l} - c^{\rm g}u^{\rm g}\right), \\
h^{\rm s} &= h^{\rm es} + \delta^{\rm s}\left(c^{\rm l}h^{\rm l} - c^{\rm g}h^{\rm g}\right) \quad s^{\rm s} = s^{\rm es} + \delta^{\rm s}\left(c^{\rm l}s^{\rm l} - c^{\rm g}s^{\rm g}\right), \\
f^{\rm s} - g^{\rm s} &= f^{\rm es} - g^{\rm es} + \delta^{\rm s}\left(c^{\rm l}f^{\rm l} - c^{\rm g}f^{\rm g}\right) - \delta^{\rm s}\left(c^{\rm l}\mu^{\rm l} - c^{\rm g}\mu^{\rm g}\right)
\end{aligned}
\tag{23.68}
$$

For ease of notation we have suppressed the fact that the differences of the extrapolated densities should be evaluated in $x^{\rm es}$. The reason that one should only give this relation for $f^{\rm s} - g^{\rm s}$ and not for $f^{\rm s}$ and $g^{\rm s}$ separately follows from their definition in Eq. (23.59). All relations in Eq. (23.68) were found to apply in very good approximation.

23.11.3 *The surface temperature from excess density differences*

From the autonomous nature of the surface, it follows that all linear expansion coefficients in Eq. (23.68) should have their equilibrium value at the temperature of the surface. All excess densities for the equilibrium surface are functions of the temperature alone. The state of the surface is therefore given in terms of the temperature alone. By applying Eq. (23.68) to the

Table 23.4 The position and the excess densities of the surface of tension.

	x^{st}	c^{st}	γ^{st}	u^{st}	f^{st}	s^{st}	h^{st}	g^{st}
	nm	μmol/m^2	mJ/m^2	mJ/m^2	mJ/m^2	μ J/m^{2}K	mJ/m^2	mJ/m^2
EQ	−0.0258	−0.64280	7.89510	89.1927	42.350	83.402	81.298	34.455
PG98	−0.1499	−0.73912	8.03148	89.4138	51.752	74.602	81.382	43.721
PG99	−0.0885	−0.69133	7.96333	89.3034	47.077	78.967	81.340	39.114
PG101	0.0381	−0.59349	7.82677	89.0811	37.568	87.909	81.254	29.741
PG102	0.1033	−0.54344	7.75832	88.9682	32.731	92.484	81.210	24.973
TL98	0.5082	−0.40248	9.09685	93.4151	13.906	113.98	84.318	4.8086
TL99	0.2541	−0.51614	8.49571	91.2750	27.799	99.227	82.779	19.304
TL101	−0.3365	−0.78624	7.29962	87.2205	57.694	66.230	79.921	50.395
TL102	−0.6852	−0.95145	6.71486	85.4247	74.029	47.345	78.710	67.314

equilibrium surface, we find

$$
\begin{aligned}
c^{\mathrm{s}}_{eq}(T_{eq}) &= \delta^{\mathrm{s}}_{eq}(T_{eq})[c^{\mathrm{l}}_{eq}(T_{eq}) - c^{\mathrm{g}}_{eq}(T_{eq})] \\
u^{\mathrm{s}}_{eq}(T_{eq}) &= u^{\mathrm{es}}_{eq}(T_{eq}) + \delta^{\mathrm{s}}_{eq}(T_{eq})[c^{\mathrm{l}}_{eq}(T_{eq})u^{\mathrm{l}}_{eq}(T_{eq}) - c^{\mathrm{g}}_{eq}(T_{eq})u^{\mathrm{g}}_{eq}(T_{eq})] \\
&= u^{\mathrm{es}}_{eq}(T_{eq}) + c^{\mathrm{s}}_{eq}(T_{eq}) \left[\frac{c^{\mathrm{l}}_{eq}(T_{eq})u^{\mathrm{l}}_{eq}(T_{eq}) - c^{\mathrm{g}}_{eq}(T_{eq})u^{\mathrm{g}}_{eq}(T_{eq})}{c^{\mathrm{l}}_{eq}(T_{eq}) - c^{\mathrm{g}}_{eq}(T_{eq})} \right]
\end{aligned}
\tag{23.69}
$$

and similar expressions for $h^{\mathrm{s}}, s^{\mathrm{s}}$ and $f^{\mathrm{s}} - g^{\mathrm{s}}$. When the system is not in equilibrium, the property of local equilibrium implies that the relations in Eq. (23.69) remain valid, but now at the temperature of the surface. This means that for a surface in local equilibrium, the extrapolated bulk densities must satisfy

$$
\begin{aligned}
c^{\mathrm{l}} - c^{\mathrm{g}} &= c^{\mathrm{l}}_{eq}(T^{\mathrm{s}}) - c^{\mathrm{g}}(T^{\mathrm{s}}) \\
c^{\mathrm{l}}u^{\mathrm{l}} - c^{\mathrm{g}}u^{\mathrm{g}} &= c^{\mathrm{l}}_{eq}(T^{\mathrm{s}})u^{\mathrm{l}}_{eq}(T^{\mathrm{s}}) - c^{\mathrm{g}}_{eq}(T^{\mathrm{s}})u^{\mathrm{g}}_{eq}(T^{\mathrm{s}})
\end{aligned}
\tag{23.70}
$$

and similar expressions for h^{s}, s^{s} and $f^{\mathrm{s}} - g^{\mathrm{s}}$. *From knowledge of the molar density difference in the non-equilibrium situation, one can find the surface temperature that gives the corresponding density difference at equilibrium.* This is equivalent to the statement that the linear coefficients in the

expansion in Eq. (23.67) have their equilibrium value. Furthermore, it follows that

$$\begin{aligned} c^{\mathrm{s}}(T^{\mathrm{s}}) &= \delta^{\mathrm{s}}(T^{\mathrm{s}})[c^{\mathrm{l}}_{eq}(T^{\mathrm{s}}) - c^{\mathrm{g}}_{eq}(T^{\mathrm{s}})] \\ u^{\mathrm{s}}(T^{\mathrm{s}}, c^{\mathrm{s}}(T^{\mathrm{s}})) &= u^{\mathrm{es}}(T^{\mathrm{s}}) + \delta^{\mathrm{s}}(T^{\mathrm{s}}) \left[c^{\mathrm{l}}_{eq}(T^{\mathrm{s}})u^{\mathrm{l}}_{eq}(T^{\mathrm{s}}) - c^{\mathrm{g}}_{eq}(T^{\mathrm{s}})u^{\mathrm{g}}_{eq}(T^{\mathrm{s}})\right] \\ &= u^{\mathrm{es}}(T^{\mathrm{s}}) + c^{\mathrm{s}}(T^{\mathrm{s}}) \left[\frac{c^{\mathrm{l}}_{eq}(T^{\mathrm{s}})u^{\mathrm{l}}_{eq}(T^{\mathrm{s}}) - c^{\mathrm{g}}_{eq}(T^{\mathrm{s}})u^{\mathrm{g}}_{eq}(T^{\mathrm{s}})}{c^{\mathrm{l}}_{eq}(T^{\mathrm{s}}) - c^{\mathrm{g}}_{eq}(T^{\mathrm{s}})}\right] \end{aligned} \tag{23.71}$$

and similar expressions for h^{s}, s^{s} and $f^{\mathrm{s}} - g^{\mathrm{s}}$. Also this is a good approximation for all variables concerned. A better agreement can of course be found by taking the nonlinear contributions in Eq. (23.67) along. For all practical purposes, Eq. (23.70) gives a simple and therefore very useful formula for the surface temperature during evaporation or condensation.

23.12 The entropy balance and the excess entropy production

We continue to verify the consistency of the integrated van der Waals square gradient model, with the framework of non-equilibrium thermodynamics for surfaces. The entropy balance of the surface in a stationary state is [305]:

$$Js^{\mathrm{l}}(x^{\mathrm{s}}) + \frac{J'^{\mathrm{l}}_q(x^{\mathrm{s}})}{T^{\mathrm{l}}(x^{\mathrm{s}})} - Js^{\mathrm{g}}(x^{\mathrm{s}}) - \frac{J'^{\mathrm{g}}_q(x^{\mathrm{s}})}{T^{\mathrm{g}}(x^{\mathrm{s}})} = \sigma^{\mathrm{s}} \tag{23.72}$$

where the excess entropy production σ^{s} is given by:

$$\begin{aligned} \sigma^{\mathrm{s}} = \int_{x_{in}}^{x_{out}} dx \Bigg\{ & J'_q(x) \frac{d}{dx}\left[\frac{1}{T(x)}\right] - J'^{\mathrm{g}}_q(x) \frac{d}{dx}\left[\frac{1}{T^{\mathrm{g}}(x)}\right] \theta(x^{\mathrm{s}} - x) \\ & - J'^{\mathrm{l}}_q(x) \frac{d}{dx}\left[\frac{1}{T^{\mathrm{l}}(x)}\right] \theta(x - x^{\mathrm{s}}) \Bigg\} \end{aligned} \tag{23.73}$$

It was shown that σ^{s} is the proper excess of $\sigma(x)$ [108].

The problem left is to show that the excess entropy production can be written in the form given in Chapter 5. We use $J'_q(x) = J_q - H(x)J$, Eq. (23.50c) and neglect the small kinetic energy. The total heat flux J_q

and the mass flux J are independent of x, and we can write

$$\begin{aligned}\sigma^{\mathrm{s}} &= J_q \int_{x_{in}}^{x_{out}} dx \left\{ \frac{d}{dx}\left[\frac{1}{T(x)}\right] - \frac{d}{dx}\left[\frac{1}{T^{\mathrm{g}}(x)}\right]\theta(x^{\mathrm{s}}-x) \right. \\ &\left. -\frac{d}{dx}\left[\frac{1}{T^{\mathrm{l}}(x)}\right]\Theta(x-x^{\mathrm{s}})\right\} - J\int_{x_{in}}^{x_{out}} dx \left\{ H(x)\frac{d}{dx}\left[\frac{1}{T(x)}\right] \right. \\ &\left. -H^{\mathrm{g}}(x)\frac{d}{dx}\left[\frac{1}{T^{\mathrm{g}}(x)}\right]\Theta(x^{\mathrm{s}}-x) - H^{\mathrm{l}}(x)\frac{d}{dx}\left[\frac{1}{T^{\mathrm{l}}(x)}\right]\theta(x-x^{\mathrm{s}})\right\} \\ &= J_e\left[\frac{1}{T^{\mathrm{l}}(x^{\mathrm{s}})} - \frac{1}{T^{\mathrm{g}}(x^{\mathrm{s}})}\right] - J\int_{x_{in}}^{x_{out}} dx \left\{ H(x)\frac{d}{dx}\left[\frac{1}{T(x)}\right] \right. \\ &\left. -H^{\mathrm{g}}(x)\frac{d}{dx}\left[\frac{1}{T^{\mathrm{g}}(x)}\right]\Theta(x^{\mathrm{s}}-x) - H^{\mathrm{l}}(x)\frac{d}{dx}\left[\frac{1}{T^{\mathrm{l}}(x)}\right]\theta(x-x^{\mathrm{s}})\right\}\end{aligned} \tag{23.74}$$

In the second identity, we used the temperature and the extrapolated temperatures that are equal at the ends ($x = x_{in}$ or x_{out}) of the box.

The Gibbs–Helmholtz equation for a constant normal pressure is:

$$H(x)\frac{d}{dx}\left(\frac{1}{T(x)}\right) = \frac{d}{dx}\left(\frac{\mu(x)}{T(x)}\right) \tag{23.75}$$

By substituting Eq. (23.75) into Eq. (23.74), and using μ/T equal to $\mu^{\mathrm{g}}/T^{\mathrm{g}}$ or equal to $\mu^{\mathrm{l}}/T^{\mathrm{l}}$ at the ends of the box, one finds

$$\begin{aligned}\sigma^{\mathrm{s}} &= J_q\left[\frac{1}{T^{\mathrm{l}}(x^{\mathrm{s}})} - \frac{1}{T^{\mathrm{g}}(x^{\mathrm{s}})}\right] - J\int_{x_{in}}^{x_{out}} dx \left\{ \frac{d}{dx}\left(\frac{\mu(x)}{T(x)}\right) \right. \\ &\left. -\frac{d}{dx}\left(\frac{\mu^{\mathrm{g}}(x)}{T^{\mathrm{g}}(x)}\right)\Theta(x^{\mathrm{s}}-x) - \frac{d}{dx}\left(\frac{\mu^{\mathrm{l}}(x)}{T^{\mathrm{l}}(x)}\right)\Theta(x-x^{\mathrm{s}})\right\} \\ &= J_q\left[\frac{1}{T^{\mathrm{l}}(x^{\mathrm{s}})} - \frac{1}{T^{\mathrm{g}}(x^{\mathrm{s}})}\right] - J\left[\frac{\mu^{\mathrm{l}}(x^{\mathrm{s}})}{T^{\mathrm{l}}(x^{\mathrm{s}})} - \frac{\mu^{\mathrm{g}}(x^{\mathrm{s}})}{T^{\mathrm{g}}(x^{\mathrm{s}})}\right]\end{aligned} \tag{23.76}$$

which is the usual expression found using non-equilibrium thermodynamics for the excess entropy production, see Chapters 5 and 11 [4, 36, 38–40].

By eliminating the total heat flux in terms of the measurable heat flux in the gas, we obtain

$$\sigma^{\mathrm{s}} = J_q'^{\mathrm{g}}(x^{\mathrm{s}})\left[\frac{1}{T^{\mathrm{l}}(x^{\mathrm{s}})} - \frac{1}{T^{\mathrm{g}}(x^{\mathrm{s}})}\right] - J\left[\frac{\mu^{\mathrm{l}}(T^{\mathrm{l}}(x^{\mathrm{s}})) - \mu^{\mathrm{g}}(T^{\mathrm{l}}(x^{\mathrm{s}}))}{T^{\mathrm{l}}(x^{\mathrm{s}})}\right] \tag{23.77}$$

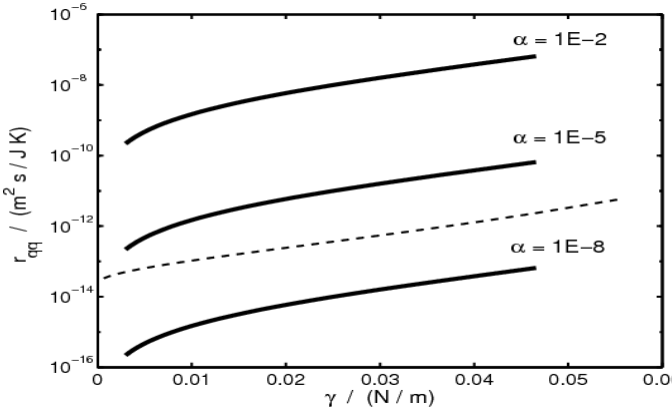

Figure 23.6 The heat transfer coefficients, r^{s}_{qq} (solid lines) for three values of α, and the kinetic theory value $r^{\mathrm{s,kin}}_{qq}$ (dashed line), as a function of the surface tension.

which is Eq. (11.8) used in Chapter 11 to describe evaporation and condensation. The expression containing the pressure and the vapor pressure of the liquid given in Eq. (11.13) follows from this expression. In deriving Eq. (23.77) we used Eq. (23.75) for the vapor

$$H^{\mathrm{g}} = \frac{d\left(\mu^{\mathrm{g}}/T\right)}{d\left(1/T\right)} \tag{23.78}$$

In the derivation of Eq. (23.77) from Eq. (23.76), a term of the second order in the thermodynamic forces is neglected.

23.13 Resistivities to heat and mass transfer

We have so far confirmed that the surface can be regarded as an autonomous system. Using the entropy production given in Eq. (23.77), we are now in a position to give the linear force-flux relations from the non-equilibrium van der Waals square gradient model. We write them on the resistance form, as it was done also in Chapter 11:

$$\begin{aligned} \frac{1}{T^{\mathrm{l}}\left(x^{\mathrm{s}}\right)} - \frac{1}{T^{\mathrm{g}}\left(x^{\mathrm{s}}\right)} &= r^{\mathrm{s}}_{qq} J'^{\mathrm{g}}_{q}\left(x^{\mathrm{s}}\right) + r^{\mathrm{s}}_{q\mu} J \\ -\frac{\mu^{\mathrm{l}}(T^{\mathrm{l}}\left(x^{\mathrm{s}}\right)) - \mu^{\mathrm{g}}(T^{\mathrm{l}}\left(x^{\mathrm{s}}\right))}{T^{\mathrm{l}}\left(x^{\mathrm{s}}\right)} &= r^{\mathrm{s}}_{\mu q} J'^{\mathrm{g}}_{q}\left(x^{\mathrm{s}}\right) + r^{\mathrm{s}}_{\mu\mu} J \end{aligned} \tag{23.79}$$

The resistivities are of interest.†

†A common factor $T^{\mathrm{l}}\left(x^{\mathrm{s}}\right)$ was absorbed in the resistivities in Refs. [36–40].

Section 23.5 used the parameter α in Eq. (23.40) to determine the resistance to heat flow. In the numerical results quoted above, a constant value was used. The temperature profiles were sensitive to the choice of this constant. We shall now address the problem of how to choose α such that it reproduces the magnitude of the temperature difference across the surface from kinetic theory [36] and non-equilibrium molecular dynamics. Non-equilibrium molecular dynamics simulations gave most of the resistivity on the vapor side of the surface [40, 112]. In this section, we therefore use

$$\alpha\left(T(x), c(x)\right) = \alpha\left(\frac{c^{\mathrm{l}}_{coex}(T_{eq})}{c(x)}\right)^2 \tag{23.80}$$

for the dependence of α on the concentration. The coefficient α on the right hand side is now kept constant in the numerical calculations. The resistivities for heat and mass transfer were calculated for various conditions as a function of this α [108]. Figure 23.6 illustrates various results for r^{s}_{qq}. Close to the critical point ($\gamma = 0$) all resistivities should approach zero. The values obtained numerically support this. Away from the critical point, the resistivities increased roughly proportional to α. The dashed curve in Fig. 23.6 is obtained from kinetic theory, using Eq. (11.23), and has been put in for comparison. Kinetic theory is only valid far from the critical point.

Few experimental results near the triple point are available [160, 162] to fit r^{s}_{qq} and $r^{\mathrm{s}}_{\mu\mu}$. It was shown that these results could be described using non-equilibrium thermodynamics [38]. The experimental results for the transfer resistivities are about a factor of thirty larger than the corresponding kinetic theory-values. Part of the reason may be that convection due to the Marangoni effect plays a role [306], see also [166] for a discussion. Recent molecular dynamics simulations done in our group for a long-range Lennard-Jones potential give larger coupling coefficients, but certainly not large enough to explain the difference. The reason for the discrepancy between kinetic theory and experiments is therefore as yet unclear.

The coupling coefficients $r^{\mathrm{s}}_{q\mu} = r^{\mathrm{s}}_{\mu q}$ found from the van der Waals square gradient model, when we use $\alpha = 5 \times 10^{-4}$, are much larger than the values given by kinetic theory. The heat of transfer $q^{*,\mathrm{s}} = -r^{\mathrm{s}}_{q\mu}/r^{\mathrm{s}}_{qq}$ is about -7400 J/mol in the van der Waals model close to the triple point. The corresponding values found using NEMD simulations for the cutoff Lennard-Jones interaction give -9400 J/mol [167], the Lennard-Jones spline potential gives -320 J/mol [40] and the cutoff Lennard-Jones interaction for octane gives -1200 J/mol [112]. The value from kinetic theory is -363 J/mol [167]. It is surprising that the values differ so much in magnitude.

23.14 Concluding comments

The non-equilibrium van der Waals square gradient model has been found to give a simple and robust method to describe the liquid-vapor interface. The model gives continuous profiles for all thermodynamic variables through the interface region. *While the model itself is not autonomous, it leads to an autonomous description of the surface in terms of the excess densities.* A number of definitions of the surface temperature was given and it was verified that they all gave the same value of this temperature. The autonomous description treats the surface as a separate thermodynamic system [62, 93–95] and is simpler than the description suggested by Defay and coworkers [96]. The model opens up possibilities to calculate and analyze the surface resistivities to heat and mass transfer.

References

[1] L. Waldmann. Non-equilibrium thermodynamics of boundary conditions. *Z. Naturforschung*, 22a:1269–1280, 1967.

[2] D. Bedeaux, A.M. Albano and P. Mazur. Boundary conditions and nonequilibrium thermodynamics. *Physica A*, 82:438–462, 1976.

[3] A.M. Albano and D. Bedeaux. Non-equilibrium electrothermodynamics of polarizable multicomponent fluids with an interface. *Physica A*, 147:407–435, 1987.

[4] D. Bedeaux. Nonequilibrium thermodynamics and statistical physics of surfaces. *Adv. Chem. Phys.*, 64:47–109, 1986.

[5] D. Bedeaux and J. Vlieger. *Optical Properties of Surfaces*. Imperial College University Press, London, 1st edition, 2002.

[6] D. Bedeaux and J. Vlieger. *Optical Properties of Surfaces*. Imperial College University Press, London, 2nd revised edition, 2004.

[7] W. Thomson (Lord Kelvin). *Mathematical and Physical Papers. Collected from different Scientific Periodicals from May, 1841, to the Present Time*, Vol. II. Cambridge University Press, London, 1884.

[8] L. Onsager. Reciprocal relations in irreversible processes. I. *Phys. Rev.*, 37:405–426, 1931.

[9] L. Onsager. Reciprocal relations in irreversible processes. II. *Phys. Rev.*, 38:2265–2279, 1931.

[10] H. Hemmer, H. Holden and S. Kjelstrup Ratkje, editors. *The Collected Works of Lars Onsager*. World Scientific, Singapore, 1996.

[11] J. Meixner. Zur Thermodynamik der Thermodiffusion. *Ann. Physik 5. Folge*, 39:333–356, 1941.

[12] J. Meixner. Reversible Bewegungen von Flüssigkeiten und Gasen. *Ann. Physik 5. Folge*, 41:409–425, 1942.

[13] J. Meixner. Zur Thermodynamik der irreversibelen Prozesse in Gasen mit chemisch reagirenden, dissozierenden und anregbaren Komponenten. *Ann. Physik 5. Folge*, 43:244–270, 1943.

[14] J. Meixner. Zur Thermodynamik der irreversibelen Prozesse. *Zeitschr. Phys. Chem. B*, 53:235–263, 1943.

[15] I. Prigogine. *Etude Thermodynamique des Phenomenes Irreversibles*. Desoer, Liege, 1947.

[16] P. Mitchell. Coupling of phosphorylation to electron and hydrogen transfer by a chemi-osmotic type of mechanism. *Nature (London)*, 191:144–148, 1961.

[17] K.G. Denbigh. *The Thermodynamics of the Steady State*. Methuen, London, 1951.

[18] I. Prigogine. *Thermodynamics of Irreversible Processes*. Charles C. Thomas, Springfield, 1st edition, 1955.

[19] S.R. de Groot and P. Mazur. *Non-Equilibrium Thermodynamics*. North-Holland, Amsterdam, 1962.

[20] S.R. de Groot and P. Mazur. *Non-Equilibrium Thermodynamics*. Dover, London, 1984.

[21] R. Haase. *Thermodynamics of Irreversible Processes*. Addison-Wesley, Reading, MA, 1969.

[22] R. Haase. *Thermodynamics of Irreversible Processes*. Dover, London, 1990.

[23] A. Katchalsky and P. Curran. *Nonequilibrium Thermodynamics in Biophysics*. Harvard University Press, Cambridge, Massachusetts, 1975.

[24] S.R. Caplan and A. Essig. *Bioenergetics and Linear Non-Equilibrium Thermodynamics — The Steady State*. Harvard University Press, Cambridge, Massachusetts, USA, 1983.

[25] H.V. Westerhoff and K. van Dam. *Thermodynamics and Control of Biological Free-Energy Transduction*. Elsevier, Amsterdam, 1987.

[26] K. S. Førland, T. Førland and S. Kjelstrup Ratkje. *Irreversible Thermodynamics. Theory and Application*. Wiley, Chichester, 1st edition, 1988.

[27] K. S. Førland, T. Førland, and S. Kjelstrup. *Irreversible Thermodynamics. Theory and Application*. Tapir, Trondheim, Norway, 3rd edition, 2001.

[28] S. Kjelstrup and D. Bedeaux. *Elements of Irreversible Thermodynamics for Engineers*. Int. Centre of Applied Thermodynamics, Instanbul, Turkey, 1st edition, 2001.

[29] S. Kjelstrup, D. Bedeaux and E. Johannessen. *Elements of Irreversible Thermodynamics for Engineers*. Tapir Akademiske Forlag, Trondheim, Norway, 2nd revised edition, 2006.

[30] D.D. Fitts. *Nonequilibrium Thermodynamics*. McGraw-Hill, New York, 1962.

[31] G.D.C. Kuiken. *Thermodynamics for Irreversible Processes*. Wiley, Chichester, 1994.

[32] Y.P. Pao. Application of kinetic theory to problem of evaporation and condensation. *Phys. Fluids*, 14:306–312, 1971.

[33] Y.P. Pao. Temperature and density jumps in kinetic theory of gases and vapors. *Phys. Fluids*, 14:1340–1346, 1971.

[34] J.W. Cipolla Jr., H. Lang and S.K. Loyalka. Kinetic theory of condensation and evaporation. II. *J. Chem. Phys.*, 61:69–77, 1974.

[35] C. Cercignani. Strong evaporation of a polyatomic gas. In S. Fisher, editor, *Rarified Gas Dynamics*, Vol. 74, pages 305–320, New York, 1981. Progr. Astronaut. Aeronaut. AIAA.

[36] D. Bedeaux, L.F.J. Hermans and T. Ytrehus. Slow evaporation and condensation. *Physica A*, 169:263–280, 1990.

[37] D. Bedeaux, J.A.M. Smit, L.F.J. Hermans and T. Ytrehus. Slow evaporation and condensation. 2. A dilute mixture. *Physica A*, 182:388–418, 1992.

[38] D. Bedeaux and S. Kjelstrup. Transfer coefficients for evaporation. *Physica A*, 270:413–426, 1999.

[39] A. Røsjorde, D.W. Fossmo, D. Bedeaux, S. Kjelstrup and B. Hafskjold. Non-equilibrium molecular dynamics simulations of steady-state heat and mass transport in condensation I: Local equilibrium. *J. Colloid Interface Sci.*, 232:178–185, 2000.

[40] A. Røsjorde, D. Bedeaux, S. Kjelstrup and B. Hafskjold. Non-equilibrium molecular dynamics simulations of steady-state heat and mass transport in condensation II: Transfer coefficients. *J. Colloid Interface Sci.*, 240:355–364, 2001.

[41] V.I. Roldughin and V.M. Zhdanov. Non-equilibrium thermodynamics and kinetic theory of gas mixtures in the presence of interfaces. *Advances in Colloid and Interface Science*, 98:121–215, 2002.

[42] R. Krishna and J.A. Wesselingh. The Maxwell–Stefan approach to mass transfer. *Chem. Eng. Sci.*, 52:861–911, 1997.

[43] D. Bedeaux and P. Mazur. Mesoscopic non-equilibrium thermodynamics for quantum systems. *Physica A*, 298:81–100, 2001.

[44] W. Muschik, C. Papenfuss and H. Ehrentraut. A sketch of continuum thermodynamics. *J. Non-Newtonian Fluid Mech.*, 96:255–290, 2001.

[45] I. Pagonabarraga and J.M. Rubi. Derivation of the Langmuir adsorption equation from non-equilibrium thermodynamics. *Physica A*, 188:553–567, 1992.

[46] I. Pagonabarraga, A. Perez-Madrid and J.M. Rubi. Fluctuating hydrodynamics approach to chemical reactions. *Physica A*, 237:205–219, 1997.

[47] D. Reguera and J.M. Rubi. Kinetic equations for diffusion in the presence of entropic barriers. *Phys. Rev. E*, 64:061106 (1–8), 2001.

[48] D. Reguera and J.M. Rubi. Nonequilibrium translational-rotational effects in nucleation. *J. Chem. Phys.*, 115:7100–7106, 2001.

[49] T. Tsuruta and G. Nagayama. DSMC analysis of interface mass transfer in evaporation/condensation based on molecular dynamics study. *Thermal Science & Engineering*, 10:9–15, 2002.

[50] D. Bedeaux, S. Kjelstrup and J.M. Rubi. Nonequilibrium translational effects in evaporation and condensation. *J. Chem. Phys.*, 119:9163–9170, 2003.

[51] J.M. Rubi and S. Kjelstrup. Mesoscopic nonequilibrium thermodynamics gives the same thermodynamic basis to Butler–Volmer and Nernst equations. *J. Phys. Chem. B*, 107:13471–13477, 2003.

[52] S. Kjelstrup, J.M. Rubi and D. Bedeaux. Energy dissipation in slipping biological pumps. *Phys. Chem. Chem. Phys.*, 7:4009–4018, 2005.

[53] S. Kjelstrup, J.M. Rubi and D. Bedeaux. Active transport: Kinetic description on thermodynamic grounds. *J. Theoretical Biology*, 234:7–12, 2005.

[54] J.M. Rubi, D. Bedeaux and S. Kjelstrup. Thermodynamics for small molecule stretching experiments. *J. Phys. Chem. B*, 110:12733–12737, 2006.

[55] V.P. Carey. *Statistical Thermodynamics and Microscale Thermophysics*. Cambridge University Press, Cambridge, UK, 1999.

[56] D. Kondepudi and I. Prigogine. *Modern Thermodynamics. From Heat Engines to Dissipative Structures*. Wiley, Chichester, 1998.

[57] H.C. Öttinger. *Beyond Equilibrium Thermodynamics*. Wiley-Interscience, Hoboken, 2005.

[58] E.M. Hansen and S. Kjelstrup. Application of nonequilibrium thermodynamics to the electrode surfaces of aluminium electrolysis cells. *J. Electrochem. Soc.*, 143:3440–3447, 1996.

[59] G. Bertrand and R. Prud'homme. Possibilitiess of Surface reaction Coupling with Transport Phenomena. *Int. J. Quantum Chemistry*, 7:159–168, 1977.

[60] G. Bertrand. Active Transport by Membranes: An Example of a General Property of Reactive Surfaces. *J. Non-Equilib. Thermodyn.*, 6:165–172, 1981.

[61] D. Bedeaux and S. Kjelstrup. Heat, mass and charge transport and chemical reactions at surfaces. *Int. J. of Thermodynamics*, 8:25–41, 2005.

[62] J.W. Gibbs. *The Scientific Papers of J.W. Gibbs*. Dover, New York, 1961.

[63] E.A. Guggenheim. The conceptions of electrical potential difference between two phases and the individual activities of ions. *J. Phys. Chem.*, 33:842–849, 1928.

[64] D. Jou, J. Casas-Vázquez and G. Lebon. *Extended Irreversible Thermodynamics*. Springer-Verlag, Berlin, 2nd edition, 1996.

[65] B. Hafskjold and S. Kjelstrup Ratkje. Criteria for local equilibrium in a system with transport of heat and mass. *J. Stat. Phys.*, 78:463–494, 1995.

[66] F. Bresme, B. Hafskjold and I. Wold. Nonequilibrium molecular dynamics study of heat conduction in ionic systems. *J. Phys. Chem.*, 100:1879–1888, 1996.

[67] J. Xu, S. Kjelstrup, D. Bedeaux, A. Røsjorde and L. Rekvig. Verification of Onsager's reciprocal relations for evaporation and condensation using non-equilibrium molecular dynamics simulations. *J. Colloid Interface Sci.*, 299:452–463, 2006.

[68] J. Xu, S. Kjelstrup and D. Bedeaux. Molecular dynamics simulations of a chemical reaction; conditions for local equilibrium in a temperature gradient. *Phys. Chem. Chem. Phys.*, 8:2017–2027, 2006.

[69] R. Taylor and R. Krishna. *Multicomponent Mass Transfer*. Wiley, New York, 1993.

[70] E.L. Cussler. *Diffusion, Mass Transfer in Fluid Systems*. Cambridge, 2nd edition, 1997.

[71] D.G. Miller. Thermodynamics of irreversible processes. The experimental verification of the Onsager reciprocal relations. *Chem. Revs.*, 60:15–37, 1960.

[72] D.G. Miller. Application of irreversible thermodynamics to electrolyte solutions. I. Determination of ionic transport coefficients l_{ij} for isothermal vector transport processes in binary electrolyte systems. *J. Phys. Chem.*, 70:2639–2659, 1966.

[73] D.G. Miller. Application of irreversible thermodynamics to electrolyte solutions. II. Ionic coefficients l_{ij} for isothermal vector transport processes in ternary systems. *J. Phys. Chem.*, 71:616–632, 1967.

[74] D.G. Miller and M.J. Pikal. A test of the Onsager reciprocal relations and a discussion of the ionic isothermal vector transport coefficient l_{ij} for aqueous $AgNO_3$ at 25^oC. *J. Solution Chem.*, 1:111–130, 1972.

[75] M. Spallek, H.G. Hertz, S. Kashammer, H. Weingärtner. Ternary diffusion and onsager reciprocity relations in aqueous $ZnCl_2$+KCl and $CdCl_2$+KCl revisited. *Ber. Bunsenges. Phys. Chem.*, 96:764–769, 1995.

[76] O. Annunziata, L. Paduano, A.J. Pearlstein, D.G. Miller and J.G. Albright. Extraction of thermodynamic data from ternary diffusion coefficients. Use of precision diffusion measurements for aqueous lysozyme chloride-NaCl at 25^o to determine the change in lysozyme chloride chemical potential with increasing NaCl concentration well into the supersaturation region. *J. Am. Chem. Soc.*, 122:5916–5928, 2000.

[77] T.S. Brun and D. Vaula. Correlation of measurements of electroosmosis and streaming potentials in ion exchange membranes. *Ber. Bunsenges. Physik. Chem.*, 71:824–829, 1967.

[78] B. Flem, S. Kjelstrup and Å. Sterten. Peltier heats in cryolite melts with alumina. *Light Metals*, pp. 203–209, 1996.

[79] B. Flem. *Peltier Heats in Cryolite Melts with Alumina*. PhD thesis, Department of Physical Chemistry, Norwegian Institute of Technology, Trondheim, 1996.

[80] B. Flem, Q. Xu, S. Kjelstrup and Å. Sterten. Thermoelectric powers of cells with NaF-AlF_3-Al_2O_3 melts. *J. Non-Equilib. Thermodyn.*, 26:125–151, 2001.

[81] A.K. Meland, D. Bedeaux and S. Kjelstrup. A Gerischer phase element in the impedance diagram of the polymer electrolyte fuel cell anode. *J. Phys. Chem. B*, 109:21380–21388, 2005.

[82] J. Szargut, D.R. Morris and F.R. Steward. *Exergy Analysis of Thermal, Chemical and Metallurgical Processes*. Hemisphere, New York, 1988.

[83] K.G. Denbigh. The second-law efficiency of chemical processes. *Chem. Engng. Sci.*, 6:1–9, 1956.

[84] A. Bejan. *Entropy Generation Through Heat and Fluid Flow*. Wiley, New York, 1982.

[85] A. Bejan. Entropy generation minimization: The new thermodynamics of finite-size devices and finite-time processes. *J. Appl. Phys.*, 79:1191–1218, 1996.

[86] S. Kjelstrup Ratkje and J. de Swaan Arons. Denbigh revisited: Reducing lost work in chemical processes. *Chem. Eng. Sci.*, 50:1551–1560, 1995.

[87] G.M. de Koeijer, E. Johannessen and S. Kjelstrup. The second law optimal path of a four-bed SO_2 converter with five heat exchangers. *Energy*, 29:525–546, 2004.

[88] E. Johannessen and S. Kjelstrup. Minimum entropy production rate in plug flow reactors: An optimal control problem solved for SO_2 oxidation. *Energy*, 29:2403–2423, 2004.

[89] L. Nummedal, A. Røsjorde, E. Johannessen and S. Kjelstrup. Second law optimization of a tubular steam reformer. *Chem. Eng. Proc.*, 44:429–440, 2005.

[90] A. Røsjorde and S. Kjelstrup. The second law optimal state of a diabatic binary tray distillation column. *Chem. Eng. Sci.*, 60:1199–1210, 2005.

[91] E. Johannessen and S. Kjelstrup. A highway in state space for reactors with minimum entropy production. *Chem. Eng. Sci*, 60:3347–3361, 2006.

[92] A. Zvolinschi, E. Johannessen and S. Kjelstrup. The second law optimal operation of a paper drying machine. *Chem. Eng. Sci.*, 61:3653–3662, 2006.

[93] J.S. Rowlinson and B. Widom. *Molecular Theory of Capillarity*. Oxford University Press, Oxford, 1982.

[94] G. Bakker. Kapillarität und Oberflachespannung. In W. Wien, F. Harms and H. Lenz, editors, *Handbuch der Experimentalphysik*, Vol. 6, Chapter 10. Akad. Verlag, Leipzig, Germany, 1928.

[95] E.A. Guggenheim. *Thermodynamics*. North-Holland, Amsterdam, 7th edition, 1985.

[96] R. Defay and I. Prigogine. *Surface Tension and Absorption*. Longmans and Green, London, 1966.

[97] P.W. Atkins. *Physical Chemistry*. Oxford University Press, Oxford, 6th edition, 1998.

[98] E.M. Blokhuis and D. Bedeaux. Microscopic expressions for the rigidity constants of a simple liquid-vapour interface. *J. Chem. Phys.*, 95:6986–6988, 1991.

[99] E.M. Blokhuis and D. Bedeaux. Derivation of microscopic expressions for the rigidity constants of a simple liquid-vapour interface. *Physica A*, 184:42–70, 1992.

[100] E.M. Blokhuis and D. Bedeaux. The pressure tensor of a spherical interface. *J. Chem. Phys.*, 97:3576–3586, 1992.

[101] E.M. Blokhuis and D. Bedeaux. Van der Waals theory of curves surfaces. *Mol. Phys.*, 80:705–720, 1993.

[102] E.M. Blokhuis and D. Bedeaux. Microscopic theories of curves liquid surfaces. *Heterogeneous Chemistry Reviews*, 1:55–68, 1994.

[103] J. Groenewold and D. Bedeaux. Microscopic integral relations for the curvature dependent surface tension in a two-phase multi-component system. *Physica A*, 214:356–378, 1995.

[104] J.D. van der Waals. The thermodynamic theory of capillarity under the hypothesis of a continuous variation of density (in Dutch). *Verhandel. Konink. Akad. Weten. Amsterdam*, 1:56, 1893.

[105] J.W. Cahn and J.E. Hillard. Free energy of nonuniform systems. I. Interfacial free energy. *J. Chem. Phys.*, 28:258–267, 1958.

[106] D. Bedeaux, E. Johannessen and A. Røsjorde. The non-equilibrium van der Waals square gradient model. I. The model and its numerical solution. *Physica A*, 330:329–353, 2003.

[107] E. Johannessen and D. Bedeaux. The non-equilibrium van der Waals square gradient model. II. Local equilibrium and the Gibbs surface. *Physica A*, 330:354–372, 2003.

[108] E. Johannessen and D. Bedeaux. The non-equilibrium van der Waals

square gradient model. III. Heat and mass transfer coefficients. *Physica A*, 336:252–270, 2004.

[109] J.M. Ortiz de Zárate and J.V. Sengers. *Hydrodynamic Fluctuations in Fluids and Fluid Mixtures*. Elsevier, Amsterdam, 2006.

[110] I. Prigogine. Le domain de validité de la thermodynamique des phenomenes irreversibles. *Physica*, 15:272–283, 1949.

[111] F. Bresme. Equilibrium and nonequilibrium molecular simulations of the central force model of water. *J. Chem. Phys.*, 115:7564–7574, 2001.

[112] J.-M. Simon, S. Kjelstrup, D. Bedeaux and B. Hafskjold. Thermal flux through a surface of n-octane. A non-equilibrium molecular dynamics study. *J. Phys. Chem. B*, 108:7186–7195, 2004.

[113] B.J.A. Zielinska and D. Bedeaux. A hydrodynamic theory for fluctuations around equilibrium of a liquid-vapour interface. *Physica A*, 112:265–286, 1982.

[114] R.H. Perry and D.W. Green. *Perry's Chemical Engineers Handbook*. McGraw-Hill, New York, 7th edition, 1997.

[115] J. Ross and P. Mazur. Some deductions from a statistical mechanical theory of chemical kinetics. *J. Chem. Phys.*, 35:19–28, 1961.

[116] Y. Demirel. *Non-equilibrium Thermodynamics. Transport and Rate Processes in Physical and Biological Systems*. Elsevier, Amsterdam, 2002.

[117] I. Prigogine. *Thermodynamics of Irreversible Processes*. Interscience, New York, 2nd edition, 1961.

[118] R. S. Schechter. *The Variational Method in Engineering*. McGraw-Hill, New York, 1967.

[119] S. Kjelstrup Ratkje, E. Sauar, E.M. Hansen, K. Lien and B. Hafskjold. Analysis of entropy production rates for design of distillation columns. *Ind. Eng. Chem. Res.*, 34:3001–3007, 1995.

[120] B. Andresen, P. Salamon and R. S. Berry. Thermodynamics in finite time. *Physics Today*, September:62–70, 1984.

[121] J.R. Welty, C.E. Wicks and R.E. Wilson. *Fundamentals of Momentum, Heat and Mass Transfer*. Wiley, Chichester, UK, 3rd edition, 1984.

[122] M. J. Moran and H. N. Shapiro. *Fundamentals of Engineering Thermodynamics*. Wiley, New York, 2nd edition, 1993.

[123] D. Bedeaux and S. Kjelstrup. Non-equilibrium thermodynamics for surfaces. Lecture notes of NorFA Summer School, Chalmers University of Technology, Gøteborg, Sweden, September 2002.

[124] D. Bedeaux and S. Kjelstrup. Irreversible thermodynamics — a tool to describe phase transitions far from global equilibrium. *Chem. Eng. Sci.*, 59:109–118, 2004.

[125] D. Bedeaux, S. Kjelstrup, L. Zhu and G.J.M. Koper. Non-equilibrium thermodynamics. A tool to describe heterogeneous catalysis. *Phys. Chem. Chem. Phys.*, 8:5421–5427, 2006.

[126] A.M. Albano, D. Bedeaux and J. Vlieger. On the description of interfacial electromagnetic properties using singular fields, charge density and currents at a dividing surface. *Physica A*, 102:105–119, 1980.

[127] D. Ronis, D. Bedeaux and I. Oppenheim. On the derivation of dynamical equations for a system with an interface. I. General theory. *Physica A*, 90:487–506, 1978.

[128] D. Ronis and I. Oppenheim. On the derivation of dynamical equations for a system with an interface. II. The gas-liquid interface. *Physica A*, 90:487–506, 1983.

[129] D. Bedeaux and S. Kjelstrup Ratkje. The dissipated energy of electrode surfaces. Temperature jumps from coupled transport processes. *J. Electrochem. Soc.*, 136:767–779, 1996.

[130] S. Kjelstrup and D. Bedeaux. Jumps in electric potential and in temperature at the electrode surfaces of the solid oxide fuel cell. *Physica A*, 244:213–226, 1997.

[131] Y.D. Shikhmurzaev. The moving contact line on a smooth solid surface. *Int. J. Multiphase Flow*, 19:589–610, 1993.

[132] D. Bedeaux. Nonequilibrium thermodynamic description of the three-phase contact line. *J. Chem. Phys.*, 120:3744–3748, 2004.

[133] Y.D. Shikhmurzaev. Moving contact lines in liquid/liquid/solid systems. *J. Fluid Mech.*, 334:211–249, 1997.

[134] B.D. Coleman and C. Truesdell. On the reciprocal relations of Onsager. *J. Chem. Phys.*, 53:28–31, 1960.

[135] J. Wei. Irreversible thermodynamics in engineering. *Ind. Eng. Chem.*, 58:55–60, 1974.

[136] I. Prigogine. *From being to becoming. Time and complexity in the physical sciences.* W.H. Freeman, San Francisco, 1980.

[137] P. Curie. Oeuvres. *(Paris)*, p. 118, 1908.

[138] R. B. Bird, W. E. Stewart and E. N. Lightfoot. *Transport Phenomena.* Wiley, Chichester, UK, 1960.

[139] H.J.V. Tyrell and K.R. Harris. *Diffusion in Liquids. A theoretical and experimental study.* Butterworths, London, 1984.

[140] S. Killie, B. Hafskjold, O. Borgen, S. Kjelstrup Ratkje and E. Hovde. High pressure diffusion measurements by Mach-Zender interferometry. *AIChE J.*, 37:142–146, 1991.

[141] C.A. Angell. Supercooled Water. In F. Franks, editor, *Water a comprehensive treatise; Water and aqueous solutions at subzero temperatures*, Vol. 7. Plenum Press, New York, USA, 1982.

[142] W.H. Furry, R.C. Jones and L. Onsager. On the theory of isotope separation by thermal diffusion. *Phys. Rev.*, 55:1083–1095, 1939.

[143] A. Lunden. In *A. Lodding and T. Lagerwall, editors, Atomic Transport in Solids and Liquids*, Thermomigration of chemical components and isotopes in solid and molten salts, pp. 302–308. Verlag der Zeitschrift für Naturforschung, Tübingen, 1971.

[144] B. Rousseau, C. Niete-Draghi and J. Bonet Avalos. The role of the molecular association in the change of the sign of the soret coefficient in aquous mixtures. *Europhysics Letters*, 67:976–982, 2004.

[145] L.J.T.M. Kempers. A comprehensive thermodynamic theory of the soret effect in a multicomponent gas, liquid or solid. *J. Chem. Phys.*, 115:6330–6341, 2001.

[146] A.G. Guy. Prediction of thermal diffusion in binary mixtures of nonelectrolyte liquids by the use of nonequilibrium thermodynamics. *Int. J. Thermophys.*, 7:563–572, 1986.

[147] T. Holt, E. Lindeberg and S. Kjelstrup Ratkje. The effect of gravity and temperature gradients on methane distribution in oil reservoirs. *SPE-paper no. 1176*, 1983.

[148] J.N. Agar. In *P. Delahay, editor, Advances in Electrochemistry and Electrochemical Engineering*, Vol. 3, Thermogalvanic cells. Interscience, New York, 1963.

[149] J.M. Kincaid, X. Li and B. Hafskjold. Nonequilibrium molecular dynamics calculation of the thermal diffusion factor. *Fluid Phase Equil.*, 76:113–121, 1992.

[150] L. Zhu and G. Frens. Indications for a surface temperature excess in heterogeneous catalysis. *J. Phys. Chem. B*, 110:18307–18312, 2006.

[151] L. Zhu, G.J.M. Koper and D. Bedeaux. Heats of transfer in the diffusion layer before the surface and the surface temperature for a catalytic hydrogen oxidation ($H_2 + \frac{1}{2}\ O_2 \rightarrow H_2O$) reaction. *J. Phys. Chem. A*, 110:4080–4088, 2006.

[152] E.M. Hansen. *Modeling of Aluminium Electrolysis Cells Using Non-Equilibrium Thermodynamics*. PhD thesis, University of Leiden, Leiden, The Netherlands, 1997.

[153] T.C. Harman and J.M. Honig. *Thermoelectric and Thermomagnetic Effects and Applications*. McGraw-Hill, New York, 1967.

[154] V.E. Zinoviev. *Thermophysical Properties of Metals at High Temperatures*. Metallurgiya, Moscov, 1989.

[155] R.W. Cahn, editor. *Physical Metallurgy*. North-Holland, Amsterdam, 1965.

[156] J.O'M. Bockris and D.M. Drazic. *Electro-chemical Science*. Taylor & Francis, London, 1972.

[157] Magnar Ottøy. *Mass and Heat Transfer in Ion-Exchange Membranes*.

PhD thesis, Norwegian University of Science and Technology, Department of Physical Chemistry, Trondheim, Norway, 1996. ISBN 82-7119-933-1, ISSN 0802-3271.

[158] J.L. Jackson. Charge neutrality in electrolyte solutions and the liquid junction potential. *J. Phys. Chem.*, 78:2060–2064, 1974.

[159] H.S. Harned and B.B. Owen. *Physical Chemistry of Electrolytic Solutions*. Reinhold, New York, 3rd edition, 1958.

[160] G. Fang and C.A. Ward. Temperature measured close to the interface of an evaporating liquid. *Phys. Rev. E*, 59:417–428, 1999.

[161] G. Fang and C.A. Ward. Examination of the statistical rate theory expression for liquid evaporation rates. *Phys. Rev. E*, 59:441–453, 1999.

[162] G. Fang. *Rate of liquid evaporation: Statistical rate theory approach.* PhD thesis. Graduate Department Mechanical and Industrial Engineering, University of Toronto, Canada, 1999.

[163] C.T. Mills and L.F. Phillips. Onsager heat of transport at the anilinevapour interface. *Chem. Phys. Letters*, 366:279–283, 2002.

[164] R.A. James and L.F. Phillips. Onsager heat of transport for water vapour at the surface of glycerol-water mixtures. *Chem. Phys. Letters*, 425:49–52, 2006.

[165] F. Graner, R.M. Bowley and P. Nozieres. The growth-kinetics of He-3 crystals. *J. Low Temperature Physics*, 80:113–133, 1990.

[166] M. Bond and H. Struchtrup. Mean evaporation and condensation coefficients based on energy dependent condensation probability. *Phys. Rev. E*, 70:061605 (21 pages), 2004.

[167] S. Kjelstrup, T. Tsuruta and D. Bedeaux. The inverted temperature profile across a vapour/liquid surface analyzed by molecular computer simulations. *J. Colloid Interface Sci.*, 256:451–461, 2002.

[168] J.W. Cipolla Jr., H. Lang and S.K. Loyalka. Temperature and Partial Pressure Jumps During Evaporation and Condensation of a Multicomponent Mixture. In Beeker and Fiebig, editors, *Rarified Gas Dynamics*, Vol. II, pages F.4–1 to F.4–10. DFVLR-Press, Portz-Wahn, Germany, 1974.

[169] T. Ytrehus. Molecular-flow effects in evaporation and condensation at interfaces. *Multiphase Science and Technology*, 9:205–327, 1997.

[170] J. Ge, S. Kjelstrup, D. Bedeaux, J.M. Simon and B. Rousseau. Coefficients for evaporation of a system with a Lennard-Jones long range spline potential. *Phys. Rev. E*, in press, 2007.

[171] M.-L. Olivier, J.-D. Rollier and S. Kjelstrup. Equilibrium properties and surface transfer coefficients from molecular dynamics simulations of two-component fluids. *Colloids and Surfaces A: Physicochem. Eng. Aspects*, 210:199–222, 2002.

[172] T. Tsuruta and G. Nagayama. Interphase mass transfer rate between liquid and vapor based on molecular dynamics study. In G.J. Hwang, editor, *Proceed. 11th Int. Symp. on Transport Phenomena*, pp. 527–532, Hsinchu, Taiwan, 1998. Tsing Hua University.

[173] L.F. Phillips. Onsager heat of transport as a consequence of detailed balance at the gas-liquid interface. *Chem. Phys. Letters*, 396:350–352, 2004.

[174] D.R. Lide. *CRC Handbook of Chemistry and Physics*. CRC Press, New York, 78th edition, 1997.

[175] S. Kjelstrup and G. de Koeijer. Transport equations for distillation of ethanol and water from the entropy production rate. *Chem. Eng. Science*, 58:1147–1161, 2003.

[176] P.N. Shankar and M.D. Despande. On the temperature distibution in a liquid-vapour phase change between plane liquid surfaces. *Phys. Fluids A*, 2:1030–1038, 1990.

[177] J.A. Wesselingh and R. Krishna. *Mass Transfer in Multicomponent Mixtures*. Delft University Press, Delft, 2000.

[178] L.J.T.M. Kempers. A thermodynamic theory of the Soret effect in a multicomponent liquid. *J. Phys. Chem.*, 90:6541–6548, 1989.

[179] M. Martin. Materials in thermodynamic potential gradients. *Pure Appl. Chem.*, 75:889–903, 2003.

[180] I.V. Belova, M.J. Brown and G.E. Murch. Analysis of kinetic demixing in a mixed oxide (A,B)O in an oxygen potential gradient. *Acta Materialia*, 51:1821–1826, 2003.

[181] I.V. Belova, M.J. Brown and G.E. Murch. Analysis of kinetic demixing of (A,B)O oxides in an electric field and an oxygen potential gradient. *Solid State Ionics*, 167:175–182, 2004.

[182] M.J. Brown, I.V. Belova and G.E. Murch. Prediction of a kinetic demixing in a quarternary mixed oxide (A,B,C)O in an oxygen potential gradient. *Phil. Mag.*, 86:1855–1865, 2003.

[183] M. Palcut. Kinetic demixing in oxygen conducting oxide exposed to chemical potential gradient. Technical report, Norwegian University of Science and Technology, 2005.

[184] S. Kjelstrup, D. Bedeaux and E.M. Hansen. Surface contributions to emf and half cell potentials of non-isothermal cells. *Periodica Polytechnica Ser. Chem. Eng.*, 41:11–27, 1997.

[185] V. Sharivker, S. Kjelstrup Ratkje and B. Cleaver. Determination of the entropy of molten polysulfides. *Electrochim. Acta*, 41:2381–2384, 1996.

[186] B. Cleaver and V.S. Sharivker. Asymmetric thermal effects in high-temperature cells with solid electrolytes. *J. Electrochem. Soc. 1995*, 142:3409–3413, 1995.

[187] Q. Xu and S. Kjelstrup. Reversible heat effects in the aluminium electrolysis. *Light Metals*, pages 539–546, 1998.

[188] Y. Ito, H. Kaiya, S. Yoshizawa, S. Kjelstrup Ratkje and T. Førland. Electrode heat balances of electrochemical cells: Application to water electrolysis. *J. Electrochem. Soc.*, 131:2504–2509, 1984.

[189] S. Kjelstrup Ratkje, H. Rajabu and T. Førland. Transference coefficients and transference numbers in molten salt mixtures relevant for the aluminium electrolysis. *Electrochim. Acta*, 38:415–423, 1993.

[190] E. M. Hansen, E. Egner and S. Kjelstrup. Peltier effects in electrode carbon. *Metall. and Mater. Trans. B*, 29:69–76, 1998.

[191] T. Ikeshoji and S. Kjelstrup Ratkje. Thermoelectric power of a cell with complex formation. *J. Electrochem. Soc.*, 133:1107–1113, 1986.

[192] S. Kjelstrup, E. Olsen and J. Qian. The peltier heating of aluminium, oxygen and carbon — carbon dioxide electrodes in an electrolyte of sodium and aluminium fluorides saturated with alumina. *Electrochim. Acta*, 46:1141–1150, 2001.

[193] J.N. Agar and W.G. Breck. Thermal diffusion in non-isothermal cells. 1. Theoretical relations and experiments of solutions of thallous salts. *Trans. Faraday Soc.*, 53:167–178, 1956.

[194] V. Blinov, S. Kjelstrup, D. Bedeaux and V.S. Sharivker. The role of the transported entropy of lead in partially thermostatted and adiabatic cells. *J. Electrochem. Soc.*, 148:364–371, 2001.

[195] S. Kjelstrup Ratkje, V.S. Sharivker and B. Cleaver. Reversible heat effects in high temperature batteries: Transported entropy and Thomson coefficients in cells with β-alumina. *Electrochim. Acta*, 39:2659–2664, 1994.

[196] S. Kjelstrup Ratkje, T. Ikeshoji and K. Syverud. Heat and internal energy changes at electrodes and junctions in thermocells. *J. Electrochem. Soc.*, 137:542–560, 1990.

[197] A. Grimstvedt, S. Kjelstrup Ratkje and T. Førland. Theory of thermocells. Transported entropies and heat of transfer in sulfate mixtures. *J. Electrochem. Soc.*, 141:1236–1241, 1994.

[198] V. Sharivker and S. Kjelstrup Ratkje. The transported entropies of ions in solid state fluorides and beta-alumina. *Light Metals*, pp. 197–202, 1996.

[199] J. Richter, A. Heller and W. Vreuls. Investigations of nonisothermal molten salts-initial values of thermoelectric-power for systems $AgNO_3$, $LiNO_3$+$AgNO_3$, and $NaNO_3$+$AgNO_3$ as a function of temperature and composition. *Ber. Bunsenges. Phys. Chem.*, 81:375–380, 1977.

[200] J. Richter and U. Prüser. Untersuchungen des stationären Zustandes

der Thermodiffusion in Thermoketten mit Nitratschmelzen. *Ber. Bunsenges. Phys. Chem.*, 81:508–514, 1977.

[201] S. Kjelstrup Ratkje and S. Møller-Holst. Exergy efficiency and local heat production in solid oxide fuel cells. *Electrochim. Acta*, 38:447–453, 1993.

[202] S. Kjelstrup Ratkje and K.S. Førland. The transported entropy of oxygen ion in yttria stabilized zirconia. *J. Electrochem. Soc.*, 138:2374–2376, 1991.

[203] S. Kjelstrup Ratkje and Y. Tomii. The transported entropy of oxygen ion in zirconia with 3-12 mole percent yttria. *J. Electrochem. Soc.*, 140:59–66, 1993.

[204] Q. Xu, S. Kjelstrup and B. Hafskjold. Estimation of single electrode heats. *Electrochim. Acta*, pp. 2597–2603, 1998.

[205] K. Amezawa, S. Kjelstrup, T. Norby and Y. Ito. Protonic and native conduction in Sr-substituted $LaPO_4$ studied by thermoelectric power measurements. *J. Electrochem. Soc.*, 145:3313–3319, 1998.

[206] W.H.A. Peelen, M. Olivry, S.F. Au, J.D. Fehribach, K. Hemmes. Electrochemical oxidation of carbon in a 62/38 mol Li/K carbonate melt. *J. Appl. Electrochemistry*, 30:1389–1395, 2000.

[207] S. Kjelstrup Ratkje. Local heat during aluminium electrolysis. *Electrochim. Acta*, 36:661–665, 1991.

[208] S. Kjelstrup, J. Qian and G. M. Haarberg. The Peltier heating of the aluminium cathode in contact with cryolite-alumina melts. *Electrochim. Acta*, 45:2707–2717, 2000.

[209] K. Hemmes, G.P.J. Dijkema and H. van der Kooi. From chemical processes to electrochemical processes: The key to minimal entropy production. *Russian J. Electrochemistry*, 40:1100–1104, 2004.

[210] K. Yasuda, T. Nohira, Y.H. Ogata, and Y. Ito. Direct electrolytic reduction of solid silicon dioxide in molten $CaCl_2$ and acceleration of reduction by Si addition to the pellet. *J. Electrochem. Soc.*, 152:D232–D237, 2005.

[211] T. Nohira, D. Miura, Y. Ito. Novel electrochemical method of SiH_4 synthesis in molten LiCl-KCl systems, Part I: Reaction mechanism and an approach to a continuous SiH_4 evolution. *Electrochemistry*, pp. 692–699, 2005.

[212] A. Kotyk and K. Janacek. *Biomembranes*. Plenum Press, New York, 1977.

[213] T. Førland and S. Østvold. The Donnan potential. I. *Acta Chem. Scand. A*, 28:607–611, 1974.

[214] E.E. Johnsen, S. Kjelstrup Ratkje, T. Førland and K.S. Førland. The liquid junction contribution to emf. *Zeitschr. Phys. Chem. Neue Folge*, 168:101–114, 1990.

[215] J. Breer, S. Kjelstrup Ratkje and G.F. Olsen. Control of liquid junctions: The system HCl-KCl. *Zeitschr. Phys. Chemie*, 174:179–198, 1991.

[216] K. Syverud and S.Kjelstrup Ratkje. An operationally defined method for ion selective electrode studies: Potassium selectivity of polyvinyl chloride membranes. *Zeitschr. Phys. Chem.*, 185:245–261, 1994.

[217] M. Planck. Über die Erregung von Electricitä t und Wä rme in Electrolyten. *Ann. Physik u. Chemie. Neue Folge*, 39:161–186, 1890.

[218] M. Planck. Über die Potentialdifferenz zwischen zwei verdünnten Lösungen binärer Electrolyte. *Ann. Physik und Chemie. Neue Folge*, 40:561–576, 1890.

[219] P. Henderson. Zur Thermodynamik der Flüssigkeitsketten. *Z. f. Physik. Chemie*, 59:118–128, 1907.

[220] P. Henderson. Zur Thermodynamik der Flüssigkeitsketten. *Z. f. Physik. Chemie*, 63:325–345, 1908.

[221] A. J. Bard and L. R. Faulkner. *Electrochemical Methods*. Wiley, New York, 1980.

[222] E. Lindeberg. *Elektromotorisk spenning som funksjon av konsentrasjonsprofilene i væskekonstaktene mellom vanige elektrolytter*. PhD thesis, Division of Physical Chemistry, University of Trondheim, NTH, Norway, 1981.

[223] D.A. MacInnes. *The Principles of Electrochemistry*. Reinhold, New York, 1939.

[224] C.Y. Chan and K.H. Khoo. Re-determination of mean ionic activity coefficients for the system HCl+KCl+water at 298.15 K and correlations between Harned and Pitzer equations. *J. Chem. Soc. Faraday*, 6:1371–1379, 1979.

[225] K. Eine, S. Kjelstrup, K. Nagy and K. Syverud. Towards a solid state reference electrode. *Sensors and Actuators B*, 44:381–388, 1997.

[226] D. Bedeaux and S. Kjelstrup. Local properties of a formation cell as described by non-equilibrium thermodynamics. *J. Non-Equilib. Thermodyn.*, 25:161–178, 2000.

[227] T. Førland and S. Kjelstrup Ratkje. Entropy production by heat, mass, charge transfer and specific chemical reactions. *Electrochim. Acta*, 25:157–163, 1980.

[228] K.S. Førland, T. Førland, A. Makange and S. Kjelstrup Ratkje. The coupling between transport of electric charge and chemical reaction. *J. Electrochem. Soc.*, 130:2376–2380, 1983.

[229] F. Helferrich. *Ion-Exchange Membranes*. McGraw-Hill, New York, 1962.

[230] N. Laksminarayanaiah. *Transport Phenomena in Membranes*. Academic Press, New York, 1969.

[231] S. Loeb. Production of energy from concentrated brine by pressure-retarded osmosis. *J. Mem. Sci.*, 1:49–63, 1976.

[232] H.T. Cath, A.E. Childress and M. Elimelech. Forward osmosis: Principles, applications and recent developments. *J. Mem. Sci.*, 281:70–87, 2006.

[233] A. Seppälä and M.J. Lampinen. Thermodynamic optimizing of pressure-retarded osmosis power generation systems. *J. Membrane Sci.*, 161:115–138, 1999.

[234] T. Holt and S. Kjelstrup. *Generell fysikk for universiteter og høgskoler*, Vol. 2. Varmelære og elektromagnetisme, chapter Kraftproduksjon med saltkraftverk, pp. 157–158. Universitetsforlaget, Oslo, Norway, 2001.

[235] T. Holt, S. Kjelstrup Ratkje and T. Førland. Cation exchange membranes as solid solutions. *J. Membrane Sci.*, 25:133–151, 1985.

[236] M. G. Skrede and S. Kjelstrup Ratkje. Cation exchange membranes as solid solutions with Na^+/H^+ and Na^+/K^+. *Zeitschr. Phys. Chem. Neue Folge*, 155:211–222, 1987.

[237] K.S. Førland, T. Okada and S. Kjelstrup Ratkje. Molten Salt Regular Mixture Theory Applied to Ion Exchange Membranes. *J. Electrochem. Soc.*, 140:634–637, 1993.

[238] G. Scatchard. Ion exchange membranes. *J. Am. Chem. Soc.*, 75:2883–2887, 1953.

[239] T. Holt, S. Kjelstrup Ratkje, T. Førland and T. Østvold. Hydrostatic pressure gradients in ion exchange membranes during mass and charge transfer. *J. Membrane Sci.*, 9:69–82, 1981.

[240] L. Nummedal. *Thermal Osmosis in a Cation Exchange Membrane, MSc Thesis no. 49*. University of Trondheim, Norway, 1997.

[241] T. Suzuki, K. Iwano, R. Kiyono and M. Tasaka. Thermoosmosis and transported entropy of water across hydrocarbonsulfonic acid-type cation exchange membranes. *Bull. Chem. Soc. Jpn.*, 68:493–501, 1995.

[242] T. Førland and S. Kjelstrup Ratkje. Irreversible thermodynamic treatment of frost heave. *Engineering Geol.*, 18:225–229, 1981.

[243] I. Nygård and S. Kjelstrup Ratkje. Temperature gradient melt transport and chemical reaction in used carbon cathodes. *Light Metals*, pp. 457–461, 1994.

[244] S. Kjelstrup Ratkje and B. Hafskjold. *Entropy and entropy generation*, chapter Coupled Transport of Heat and Mass. Theory and Appplications, pp. 197–219. Klüver, 1996.

[245] S. Kjelstrup and A. Røsjorde. Local and total entropy production and heat and water fluxes in a one-dimensional polymer electrolyte fuel cell. *J. Phys. Chem. B*, 109:9020–9033, 2005.

[246] P.J.S. Vie. *Characterization and Optimization of the Polymer Elec-*

trolyte Fuel Cell. PhD thesis, Norwegian University of Science and Technology, Department of Chemistry, Trondheim, Norway, 2002. ISBN 82-471-5431-5, ISSN 0809-103X.

[247] P.J.S. Vie and S. Kjelstrup. Thermal conductivities from temperature profiles in the polymer electrolyte fuel cell. *Electrochim. Acta*, 49:1069–1077, 2004.

[248] G. Aylward and T. Findlay. *SI Chemical Data*. Wiley, New York, 3rd edition, 1994.

[249] S. Kjelstrup, P.J.S. Vie and D. Bedeaux. *in T. S. Sørensen, editor, Surface Chemistry and Electrochemistry of Membranes*, chapter Irreversible thermodynamics of membrane surface transport with application to polymer fuel cells, pp. 483–510. Marcel Dekker, New York, 1999.

[250] S. Kjelstrup Ratkje, T. Holt and M.G. Skrede. Cation membrane transport: Evidence for local validity of Nernst-Planck equations. *Ber. Bunsenges. Physik. Chem.*, 92:825–832, 1988.

[251] T.E. Springer, T.A. Zawodzinski Jr. and S. Gottesfeld. Polymer electrolyte fuel cell model. *J. Electrochem. Soc.*, 138:2334–2342, 1991.

[252] S. Kjelstrup Ratkje, M. Ottøy, R. Halseid and M. Strømgård. Thermoelectric power relevant for the solid-polymer-electrolyte fuel cell. *J. Membrane Sci.*, 107:219–228, 1995.

[253] T. Førland, K.S. Førland and S. Kjelstrup Ratkje. The coefficients for isothermal transport. I. Cation exchange membrane and electrodes reversible to a common anion. *Acta Chem. Scand.*, A31:47–55, 1973.

[254] S. Kjelstrup Ratkje. The Coefficients for Isothermal Transport II. Cation Exchange Membrane and Electrodes Reversible to one of the Cations. *Acta Chem. Scand.*, A31:797–798, 1977.

[255] S. Kjelstrup Ratkje. The coefficients for isothermal transport II. Cation exchange membrane and electrodes reversible to one of the cations. *J. Non-Equilib. Thermodyn.*, 4:75–92, 1979.

[256] T. Holt. *Transport and equilibrium properties of a cation exchange membrane*. PhD thesis, Institute of Physical Chemistry, Norwegian Institute of Technology, University of Trondheim, 1983.

[257] M. Ottøy, T. Førland, S. Kjelstrup Ratkje and S. Møller-Holst. Membrane transference numbers from a new emf method. *J. Membrane Sci.*, 74:1–8, 1992.

[258] T. Okada, S. Kjelstrup Ratkje and H. Hanche-Olsen. Water transport in cation-exchange membranes. *J. Membrane Sci.*, 66:179–192, 1992.

[259] S. Kjelstrup, M. Ottøy and T. Okada. In *T. S. Sørensen, editor, Surface Chemistry and Electrochemistry of Membranes*, Water, ion and entropy transport in ion-exchange membranes, pp. 455–481. Marcel Dekker, New York, 1999.

[260] T. Ojala and K. Kontturi. The transport numbers and mobilities of ions in the sodium/lithium and sodium/rubidium systems in a cation-exchange membrane. *Acta Chem. Scand.*, 42:698–701, 1988.

[261] T. Ojala and K. Kontturi. Transport properties of a cation-exchange membrane with sodium and potassium as counterions. *Acta Chem. Scand.*, 43:340–344, 1989.

[262] T.F. Fuller and J. Newman. Experimental determination of the transport number of water in Nafion 117 membrane. *J. Electrochem. Soc.*, 139:1332–1337, 1992.

[263] S. Kjelstrup Ratkje, E. Sauar, E.M. Hansen, K.M. Lien and B. Hafskjold. Analysis of entropy production rates for design of distillation columns. *Ind. Eng. Chem. Res.*, 34:3001–3007, 1995.

[264] T. Okada, S. Kjelstrup Ratkje, S. Møller-Holst, L.O. Jerdal, K. Friestad, G. Xie and R. Holmen. Water and ion transport in the cation-exchange membrane systems NaCl-$SrCl_2$ and KCl-$SrCl_2$. *J. Membrane Sci.*, 111:159–167, 1996.

[265] I. Wold. *Nonequilibrium molecular dynamics simulations of porous media.* PhD thesis, Division of Physical Chemistry, Norwegian University of Science and Technology, Trondheim, Norway, 1997.

[266] M. Sluyters-Rehbach and J.H. Sluyters. In *A.J. Bard, ed., Electroanalytical Chemistry*, Vol. 4, p. 1. Marcel Dekker, New York, 1970.

[267] J.R. Macdonald. *Impedance Spectroscopy. Emphasizing Solid Materials and Systems.* Wiley, New York, 1987.

[268] A.K. Meland, D. Bedeaux and S. Kjelstrup. Rate-limiting proton hydration in the anode of the polymer electrolyte fuel cell. *J. Membrane Sci*, 282:96–108, 2006.

[269] D. Bedeaux and S. Kjelstrup. Impedance spectroscopy of surfaces described by irreversible thermodynamics. *J. Non-Equilib. Thermodyn.*, 24:80–96, 1999.

[270] S. Kjelstrup, P. Pugazhendi and D. Bedeaux. Impedance of the hydrogen polymer fuel cell electrode. Theory and experiments. *Z. Phys. Chemie*, 214:895–916, 2000.

[271] H. Nakajima, T. Nohira, Y. Ito, S. Kjelstrup and D. Bedeaux. The surface adsorption of hydride ions and hydrogen atoms on Zn studied by electrochemical impedance spectroscopy with a non-equilibrium thermodynamic formulation. *J. Non-Equilib. Thermodyn.*, 31:231–255, 2006.

[272] V. Paganin, C. Oliveira, E. Ticianelli, T.E. Springer and E. Gonzalez. Modelistic interpretation of the impedance response of a polymer electrolyte fuel cell. *Electrochim. Acta*, 43:3761–3766, 1998.

[273] T. Freire and E. Gonzalez. Effect of membrane characteristics and

humidification condistions on the impedance response of polymer electrolyte fuel cells. *J. Electroanal. Chem.*, 503:57–68, 2001.

[274] M. Brown, S. Primdahl and M. Mogensen. Structure/performance relations for Ni/yttria-stabilized zirconia anodes for solid oxide fuel cells. *J. Electrochem. Soc.*, 147:475–485, 2000.

[275] D.A. McQuarrie. *Statistical Mechanics*. Harper and Row, New York, 1976.

[276] D.J. Evans and G.P. Morriss. *Statistical Mechanics of Nonequilibrium Liquids*. Academic Press, London, 1990.

[277] B. Hafskjold. *Thermal Nonequilibrium Phenomena in Fluid Mixtures, W. Kohler and S. Wiegand*, editors, Computer Simulations of Thermal Diffusion in Binary Fluid Mixtures. Lecture Notes in Physics. Springer, Berlin, 2002.

[278] B. Hafskjold, T. Ikeshoji and S. Kjelstrup Ratkje. On the molecular mechanism of thermal diffusion in liquids. *Mol. Phys.*, 80:1389–1412, 1993.

[279] T. Ikeshoji and B. Hafskjold. Non-equilibrium molecular dynamics calculation of heat conduction in liquid and through liquid-gas interface. *Mol. Phys.*, 81:251–261, 1994.

[280] B. Hafskjold and T. Ikeshoji. Partial specific quantities computed by nonequilibrium molecular dynamics. *Fluid Phase Equilibria*, 104:173–184, 1995.

[281] S. Kjelstrup and B. Hafskjold. Nonequilibrium molecular dynamics simulations of steady-state heat and mass transport in distillation. *Ind. Eng. Chem. Res.*, 35:4203–4213, 1996.

[282] B. Hafskjold, I. Fujihara and T. Ikeshoji. A comparison of nonequilibrium molecular dynamics and NPT Monte Carlo methods for mixing properties and partial molar quantities. *Mol. Phys.*, 90:999–1006, 1997.

[283] A.H. Fuchs J.-M. Simon, D.K. Dysthe and B. Rousseau. Thermal diffusion in alkane binary mixtures: A molecular dynamics approach. *Fluid Phase Equil.*, 150/151:151–159, 1998.

[284] A. Tenenbaum, G. Ciccotti and R. Gallico. Stationary nonequilibrium states by molecular dynamics. Fourier's law. *Phys. Rev. A*, 25:2778–2787, 1982.

[285] A. Baranyai. Heat flow studies of large temperature gradients by molecular dynamics simulation. *Phys. Rev. E*, 54:6906–6911, 1996.

[286] F. Müller-Plathe and D. Reith. Cause and effect reversed in nonequilibrium molecular dynamics: An easy route to transport coefficients. *Comput. Theor. Polym. Sci.*, pages 203–209, 1999.

[287] D. Reith and F. Müller-Plathe. On the nature of thermal diffusion in binary Lennard-Jones liquids. *J. Chem. Phys.*, 112:2436–2443, 2000.

[288] R.F. Cracknell, D. Nicholson and N. Quirke. A grand canonical Monte Carlo study of Lennard-Jones mixtures in slit pores. 2. Mixtures of two centre ethane with methane. *Mol. Simulation*, 13:161–175, 1994.

[289] J.-M. Simon, S. Kjelstrup, D. Bedeaux, J. Xu and E. Johannessen. Interface film transfer coefficients. Verification of integral relations by nonequilibrium molecular dynamics simulations. *J. Phys. Chem. B*, 110:18528–18536, 2006.

[290] D.K. Dysthe, A.H. Fuchs, B. Rousseau and M. Durandeau. Fluid transport properties by equilibrium molecular dynamics. II. Multicomponent systems. *J. Chem. Phys.*, 110:4060–4067, 1999.

[291] P. Sindzingre, C. Massobrio, G. Ciccotti and D. Frenkel. Calculation of partial enthalpies of an argon-krypton mixture by NPT molecular dynamics. *Chem. Phys.*, 129:213–224, 1989.

[292] A.P. Thompson, D.M. Ford and G.S. Heffelfinger. Molecular simulation of gradient-driven diffusion. *J. Chem. Phys.*, 109:6406–6414, 1998.

[293] A.P. Thompson and G.S. Heffelfinger. Molecular simulation of gradient-driven diffusion of large molecules using constant pressure. *J. Chem. Phys.*, 110:10693–10705, 1999.

[294] B.D. Todd, D.J. Evans and P.J. Daivis. Pressure tensor for inhomogeneous fluid. *Phys. Rev. E*, 52:1627–1638, 1995.

[295] J.H. Irving and J.G. Kirkwood. The statistical mechanical theory of transport processes. IV. The equations of hydrodynamics. *J. Chem. Phys.*, 18:817–829, 1950.

[296] G.V. Paolini and G. Ciccotti. Cross thermotransport in liquid mixtures by nonequilibrium molecular dynamics. *Phys. Rev. A*, 34:1355–1362, 1987.

[297] E.M. Blokhuis, D. Bedeaux, C.D. Holcomb and J.A. Zollweg. Tail corrections to the surface tension of a Lennard-Jones liquid-vapor interface. *Mol. Phys.*, 85:665–669, 1995.

[298] G.V. Paolini, G. Ciccotti and C. Massobrio. Nonlinear thermal response of a Lennard-Jones fluid near the triple point. *Phys. Rev. A*, 34:1355–1362, 1986.

[299] B.D. Todd, P.J. Daivis and D.J. Evans. Heat flux vector in highly inhomogeneous nonequilibrium fluids. *Phys. Rev. E*, 51:4362–4365, 1995.

[300] B.D. Todd and D.J. Evans. Temperature profile for poiseuille flow. *Phys. Rev. E*, 55:2800–2807, 1997.

[301] L.D. Landau and E.M. Lifshitz. *Statistical Physics (Course of Theoretical Physics)*, Vol. 5. Pergamon Press, Oxford, 1980.

[302] H.B. Keller. *Numerical Methods for Two-Point Boundary-value Problems*. Blaisdell Publishing Company, London, 1968.

[303] A.E. van Giessen, E.M. Blokhuis and D.J. Bukman. Mean field curvature corrections to the surface tension. *J. Chem. Phys.*, 108:1148–1156, 1998.

[304] A.E. van Giessen and E.M. Blokhuis. Determination of curvature corrections to the surface tension of a liquid-vapor interface through molecular dynamics simulations. *J. Chem. Phys.*, 116:302–310, 2002.

[305] A.M. Albano, D. Bedeaux and J. Vlieger. On the description of interfacial properties using singular densities and currents at a dividing surface. *Physica A*, 99:293–304, 1979.

[306] C. A. Ward and D. Stanga. Interfacial conditions during evaporation or condensation of water. *Phys. Rev. E*, 64:051509 (9 pp.), 2001.

This page intentionally left blank

Symbol Lists

Table 1. Latin symbols

Symbol	Dimension	Explanation
A_i		extensive variable of a fluctuating system
A, B		empirical constants in van der Waals equation
a		activity
C_p	/J K^{-1}	heat capacity at constant pressure
C_v	/J K^{-1}	heat capacity at constant volume
c	/mol m^{-3}	concentration in homogeneous phases
c^s	/mol m^{-2}	concentration in surfaces
c^c	/mol m^{-3}	concentration in contact lines
D	/Jm^2(s mol)$^{-1}$	Dufour coefficient
D_D	/m^2 s^{-1} K^{-1}	thermal diffusion coefficient
D_T	/m^2 s^{-1} K^{-1}	thermal diffusion coefficient
D	/C m^{-2}	displacement field normal to the surface
D_{eq}	/C m^{-2}	displacement field of system in equilibrium
d	/m	thickness of layer, diameter
E	/V m^{-1}	electric field
E	/J	total energy
e	/C	charge of electron
E_{eq}	/V m^{-1}	electric field of system in equilibrium
F	= 96500 C mol^{-1}	Faraday's constant
F	/N	External force
F	/J	Helmholtz energy
F^s	/J	Helmholtz energy of the surface
F^c	/J	Helmholtz energy of the contact line
F_{ij}	/ N	force exerted on particle i by particle j
f	/J m^{-3}	Helmholtz energy density
f^s	/J m^{-2}	Helmholtz energy density of the surface
f^c	/J m^{-1}	Helmholtz energy density of the contact line
f		Boltzmann's probability density
f	/bar	fugacity
G	/J	Gibbs energy
G^s	/J	Gibbs energy of the surface

Table 1. Latin symbols, continued

Symbol	Dimension	Explanation
G^c	/J	Gibbs energy of the contact line
G_j	/J m^{-3} mol^{-1}	partial molar Gibbs energy of j
g	/J m^{-3}	Gibbs energy density
g^s	/J m^{-2}	Gibbs energy density of the surface
g^c	/J m^{-1}	Gibbs energy density of the contact line
$\Delta_r G$	/J mol^{-1}	reaction Gibbs energy
$\Delta_n G^s$	/J mol^{-1}	reaction Gibbs energy of neutral surface components
g	/ms^{-2}	acceleration of gravity
H	/J	enthalpy
H^s	/J	enthalpy of the surface
H^c	/J	enthalpy of the contact line
H_j	/J mol^{-1}	partial molar enthalpy of j
h	/J m^{-3}	enthalpy density
h^s	/J m^{-2}	enthalpy density of the surface
h^c	/J m^{-1}	enthalpy density of the contact line
h	/= 6.6256 10^{-34}Js	Planck's constant
h	/m	height
h	/W $K^{-1}m^{-2}$	overall heat transfer coefficient
j	/A m^{-2}	electric current density
j_{displ}	/A m^{-2}	displacement current density
J_e	/J m^2 s^{-1}	flux of total energy
J_q	/J m^2 s^{-1}	flux of total heat
J'_q	/J m^2 s^{-1}	flux of measurable heat
J_i	/mol m^2 s^{-1}	general symbol for flux of i
J_s	/J K^{-1} m^2 s^{-1}	flux of entropy
K_2	/ bar $molal^{-1}$	Henry's law's constant
k_B	= 1.381 10^{-23}	Boltzmann's constant
k_μ, k_q		scaling coefficients
L	/m	length of contact line
L_x, L_y, L_z	/m	sides of NEMD box
L_{ij}, l_{ij}		phenomenological coefficient for coupling of fluxes i an k
l	/m	length
l_{ik}		phenomenological coefficient for coupling of diffusional fluxes i and k
M	/J mol^{-2}	constant in van der Waals gradient expression
M_i	/mol kg^{-1}	molar mass of i
m_i	/kg	mass i
m_j	/mol kg^{-1}	molality of j

Table 1. Latin symbols, continued

Symbol	Dimension	Explanation
N		number of particles in NEMD box
N_j	/mol	amount of component j in system i,s,or c
N_A	$6.023{\cdot}10^{23}$	Avogadro's number
n		number of independent components
P	/W	electric power
P	/C m	polarization in the bulk phase
P	/C m^{-2}	polarization density in the bulk phase
P^s	/ C m	polarization of the surface
P^s	/ C m^{-1}	polarization density of the surface
P	/J $s^{-1}m^{-2}$	electric power per unit of area
p	/bar	pressure of system
p^0	/bar	standard pressure (1 bar)
p_0	/bar	pressure of the surroundings
p_W	/bar	pressure of a van der Waals gas
p_i^*	/bar	saturation pressure of pure vapor i
Q	/J	heat delivered to the system
Q_0	/J	heat delivered to the surroundings at T_0
Q^*	/J mol^{-1}	energy of transfer, total heat of transfer
q^*	/J mol^{-1}	heat of transfer
R	= 8.314 J K^{-1} mol^{-1}	gas constant
R	/m	radius
R_{ik}		resistivity coefficient for coupling of fluxes i and k, Maxwell–Stefan resistivities
r_{ik}		resistivity coefficient for coupling of diffusional fluxes i and k, see
r	/mol m^{-3} s^{-1}	rate of chemical reaction in homogeneous phase
r^s	/mol m^{-2} s^{-1}	rate of chemical reaction in surface
r	/ohm m^{-1}	ohmic resistivity
r_1	/m	diameter of particle 1
r_{ij}	/m	distance between particles i and j
S	/J K^{-1}	entropy
S^s	/J K^{-1}	surface excess entropy
S^c	/J K^{-1}	contact line excess entropy
s	/J K^{-1} m^{-3}	entropy per volume
s^s	/J K^{-1} m^{-2}	surface excess entropy per area
s^c	/J K^{-1} m^{-1}	contact line excess entropy per length
s_T	/ K^{-1}	Soret coefficient
S_0	/J K^{-1}	entropy of the surroundings
S_{eq}	/J K^{-1}	entropy at global equilibrium

Table 1. Latin symbols, continued

Symbol	Dimension	Explanation
S^*	/J K^{-1} mol^{-1}	transported entropy (per mol)
S_i	/J K^{-1} mol^{-1}	partial molar entropy
dS_{irr}/dt	/W K^{-1}	total entropy production
T	/K	absolute temperature
T_0	/K	temperature of the surroundings
t	/s	time
t_{ion}		transport number of an ion = the fraction of current carried by the ion
t_j		transference coefficient of component j
U	/J	internal energy
U^s	/J	internal energy of the surface
U^c	/J	internal energy of the contact line
U_j	/J mol^{-1}	partial molar internal energy of j
u	/J m^{-3}	internal energy density
u^s	/J m^{-2}	internal energy density of the surface
u^c	/J m^{-1}	internal energy density of the contact line
u_{ion}	/m^2 s^{-1} V^{-1}	mobility of ion in electric field
u_{ij}		Lennard-Jones pair potential
V	/m^3	volume
V_m	/m^3 mol^{-1}	volume of one mole pure component m
V_j	/m^3 mol^{-1}	partial molar volume of j
v_i	/m s^{-1}	velocity of i
W	/J	work done on the system
W_{ideal}	/J	work done in a reversible process
W_{lost}	/J	work lost compared to a reversible process
W	/kg	weight
W		the system's statistical weight
X_i		general symbol for thermodynamic driving force
x	/m	coordinate for direction of transport
x_i		molar fraction
y_i		activity coefficient for non-electrolyte i
y, z	/m	other coordinates
Z	/ohm m^2	impedance
z	/C m^{-3}	charge density
z		valency of ion

Table 2. Greek symbols

Symbol	Dimension	Explanation
α_i		fluctuation of extensive variable i
α_T		thermal diffusion factor
α_{ij}, β_{ij}		Lennard-Jones parameters
δ	/m	surface or film thickness
η_I		Carnot efficiency
η_S	/V K^{-1}	Seebeck coefficient
ϵ		porosity
ϵ_F		energy of the Fermi level
ϵ_{ij}		minimum potential energy between particles i and j
ε_0	$= 8.854\ 10^{-12}$ J^{-1} C^2 m^{-1}	dielectric constant of vacuum
ε_i	/J^{-1} C^2 m^{-1}	dielectric constant of phase i
ϕ	/J	potential energy of particle in the field of all others
φ		fugacity coefficient
ϕ	/V	electric potential
γ	/N m^{-1}	surface tension
$\gamma_\pm$		mean ionic activity coefficient
η		Carnot efficiency
κ	/S m^{-1}	electrical conductivity
Λ	/m	mean thermal de Broglie wavelength
λ	/W K^{-1} m $^{-1}$	thermal conductivity
Γ	/mol m^{-2}	adsorption or excess surface concentration
Γ^c	/mol m^{-1}	adsorption or excess line concentration
γ	/N m^{-1}	surface tension
γ^c	/N	line tension
μ_j	/J mol^{-1}	chemical potential of j
$\mu_{j,T}$	/J mol^{-1}	chemical potential of j differentiated at constant T
ν_j		stoichiometric coefficient component j
ν		layer number in simulated box
ξ		degree of conversion
Π	/N m^{-2}	viscous pressure tensor
π	/J	Peltier heat, Peltier coefficient
ρ_j	/kg m^{-3}	mass density of component j
ρ	/ohm m	specific resistivity
ρ^s	/ohm m^2	specific surface resistivity

Table 2. Greek symbols, continued

Symbol	Dimension	Explanation
θ		fractional surface coverage
ρ	/kg m^3	density
σ	/J s^{-1} K^{-1} m^{-3}	entropy production in a homogeneous phase
σ^s	/J s^{-1} K^{-1} m^{-2}	surface excess entropy production
σ^c	/J s^{-1} K^{-1} m^{-1}	line excess entropy production
σ_i		condensation coefficient of i
τ	/s	time lag
τ	/J K^{-1} mol^{-1}	Thomson coefficient
τ_j		co-transfer coefficient, for transport of j by i
Ω	/m^2	surface area
Ω_i	/m^2 mol^{-1}	partial molar area of surface component
Ψ	/J s^{-1} m^{-3}	dissipation function
ψ	/V	electrostatic (Maxwell) potential

Table 3. Mathematical symbols, superscripts, subscripts

Symbol	Explanation
d	differential
∂	partial derivative
$\|\|$	parallel component
$\perp$	normal component
δ_{ij}	Kroenecker delta, equal to 1 when i=j, and 0 otherwise
Δ	change in a quantity or variable
$\Delta_{f,t}$	the change is taken from f on the right to t on the left hand side
Σ	sum
$\theta(x)$	Heaviside function, equal to 1 when $x > 0$, and 0 when $x < 0$
ads	subscript meaning adsorbed phase
eq	subscript meaning system in equilibrium
$\bar{e}$	property of electron
a	super- or subscript meaning bulk anode or left side electrode
c	super- or subscript meaning bulk cathode or right side electrode
c	superscript meaning contact line
g	super- or subscript meaning gas phase
l	super- or subscript meaning liquid phase
s	superscript meaning surface
i	super- or subscript meaning phase i
e,a	superscript meaning location a in phase e
crit	subscript indicating critical conditions
<>	average value over an equilibrium distribution
$\equiv$	defined by

This page intentionally left blank

Index

active transport, 109
activity, 42
    of electrolytes, 42
    of ideal mixtures, 42
    coefficients, 42
    of surface components, 44
adiabatic electrochemical cell, 223
adsorption, 25, 177
affinity, 55
Agar, J.N., 115, 222
Albano, A.M., viii, 4, 20, 73, 76, 82, 84, 92, 109, 363, 388
Albright, J.G., 10, 102
Amezawa, K., 232, 322
Andresen, B., 58
Angell, C.A., 114
Annunziata, O., 10, 102
anode surface
    potential drop, 214
Atkins, P.W., viii, 18, 62
Au, S.F., 233
availability, 14

Bakker, G., 17, 35, 362, 392
balance equation
    for entropy, 52
    for entropy in the surface, 80
    for mass, 49
Baranyai, A., 342
Bard, A.J., 254
barycentric time derivative, 369
batteries, 261
Bedeaux, D., viii, 3, 4, 7, 10, 13, 14, 20, 22, 28, 33, 35, 48, 54, 58, 73, 76, 82, 84, 92, 97, 102, 109, 121, 125, 126, 158, 165, 170, 174, 179, 205, 219, 222, 227, 261, 291, 328, 336, 339, 342, 350, 351, 353, 356, 359, 361, 373, 383, 388
Bejan, A., 14, 58, 111
Belova, I., 200
Bernard, G., 84
Berry, R.S., 58
Bertrand, G., 4, 73, 82, 109
biological systems, 109
Bird, R.B., 111, 115
Blinov, V., 222, 227
Blokhuis, E.M., 22, 28, 356, 363, 385
Bockris, J.O'M., 145
Boltzmann distribution, 101
Bond, M., 157, 391
Bonet Avalos, J., 115, 358
Borgen, O., 114
boundary conditions, 11
Bowley, R.M., 157
Breck, W.G., 222
Breer, J., 249, 250, 255
Bresme, F., 6, 35, 342, 347, 351
Brown, M., 339
Brown, M.J., 200
Brun, T.S., 12, 312
Bukman, D.J., 385

Cahn, J.W., 28, 362
Cahn, R.W., 129
capillary pressure, 21
Caplan, S.R., 2, 84, 109, 277, 311
Carey, V.P., 3
Casas-Vázquez, J., 6, 103
Cath, H.T., 277

cathode
potential drop, 212, 217
cell potential, 218, 225
Cercignani, C., 3, 166
Chan, C.Y., 256
chemical potential
definition, 37
of a pure liquid, 161
of electrolyte, 141
of ideal vapor, 161
of non-electrolyte, 112, 176
profiles, 124
chemical potential gradient
in terms of weight fractions, 357
Childress, A.E., 277
Ciccotti, G., 342, 345, 350, 359
Cipolla Jr, J.W., 3, 158, 165, 179
Clausius-Clapeyron's equation, 164
Cleaver, B., 206, 222
co-transfer coefficient, 179
coefficients
coupling, 11
main, 11
Onsager, 11
Coleman, B.D., 103
concentration cell, 140, 205, 249
condensation coefficient, 165
two component system, 179
conductivity
effective, 12
conjugate fluxes and forces, 11, 49, 54
conservation equation
for charge, 50
for charge in the surface, 78
for mass, 49
for mass during electrolysis, 264
for mass in the surface, 77
conservation of energy
during phase transitions, 160
contact angles, 96
contact line, 17
acceleration, 94
coupling of transports, 109
entropy production, 91
motion, 91
convection, 56
coupled transport processes
importance, 9, 14
coupling coefficients, 11, 107
Cracknell, R.F., 342, 345
critical point, 363
Curie principle, 99, 108
Curie, P., 108
Curran, P., 2, 6, 109, 139, 284, 285, 311
currentless potential, 149
Cussler, E.L., 9

Daivis, P.J., 350, 359
de Donder, Th., 55
de Groot, S.R., 2, 7, 35, 48, 54, 56, 67, 101, 103, 108, 109, 112, 185, 192
de Koeijer, G., 14
de Swaan Arons, J., 14
Debije–Hückel theory, 78
Defay, R., 17, 35, 362, 392
Demirel, Y., 55
Denbigh, K.G., 2, 13
Despande, M.D., 182
dielectric constant, 19
diffusion, 250, 253
diffusion coefficient, 113
barycentric frame of reference, 357
of electrolyte, 141
of gases, 115
of ternay mixture, 195
Dijkema, G.P.J., 233
displacement field, 19
dissipation function, 55
distillation, 157
Donnan equilibrium, 280
Drazic, D.M., 145
Dufour effect, 114
Dysthe, D.K., 342, 344

Egner, E., 221, 296

Ehrentraut, H., 3
Eine, K., 259
electric conductivity, 149
  in terms of mobilities, 152
electric fields
  in heterogeneous systems, 19
  in homogeneous systems, 77
  in the surface, 77
electric potential
  profiles, 137
  surface jump, 132
electric resistivity, 128, 141
  of surface, 132
electro-osmosis, 149
electrochemical cell
  energy conversion, 247
  with aqueous electrolyte, 236
  with molten salts, 221
electrochemical potential, 70, 143, 153
electrochemical synthesis, 235, 239
electrode interface
  reversible conditions, 85
electrode surface
  electroneutral character, 330
  reaction, 143
electrolysis cells, 9, 261
electrolyte
  activity, 42
  electric potential, 213
  ideal solution, 152
electromotive force, 153, 205
electroneutrality, 48, 75
  condition, 19, 140
  of electrolyte systems, 150
Elimelech, M., 277
emf, 149
energy balance
  at a liquid-vapor interface, 177
energy of transfer
  in membranes, 283
ensemble average, 343
entropy production, 55
  and Carnot machine efficiency, 62
  basic forms, 54
  coefficient bounds, 106
  due to a chemical reaction, 62
  during evaporation, 159
  during filtering of water, 60
  from Fourier, Fick and Ohm's laws, 61
  from heat transport, 59
  from one mass flux, 58
  in sidewalk pavement, 59
  in terms of Onsager coefficients, 106
  independent variables, 67
  invariance, 54, 84, 150
  lost work, 55
  multicomponent diffusion, 184
  non-isothermal cathode, 208
  non-isothermal electrode surface, 223
  of homogeneous systems, 47
  of surfaces, 73, 76
  reduction by Gibbs-Duhem's equation, 60
  total, 13
entropy production in surface
  from heat transport, 88
  from isothermal evaporation, 88
  from mass transport, 87
  non-isothermal electrode surface, 214
environment, 13
equilibrium
  at a liquid-vapor interface, 157
  global, 17, 22
  local, 6, 17, 33
equimolar surface, 214, 217
equipartition principle, 342
ergodic hypothesis, 343
Essig, A., 2, 84, 109, 311
Euler equation, 103
Evans, D.J., 341, 350, 359
evaporation
  by pressure reduction, 157
  one component, 158

two components, 179
exergy, 14
exergy analysis, 57
external forces, 68, 192

Førland, K.S., 2, 6, 7, 48, 132, 139, 143, 227, 249, 250, 261, 280, 281, 284, 286, 312, 316, 324
Førland, T., 2, 6, 7, 48, 132, 139, 143, 206, 211, 226, 227, 232, 249, 250, 261, 265, 281, 286, 311, 316, 324
Fang, G., 157, 174, 391
Fehribach, J.D., 233
Fermi energy, 129
Fick's law, 8, 141, 200
first law, 51
efficiency, 14
for a polarizable surface, 79
of thermodynamics, 13, 50
first law of thermodynamics, 70
Fitts, D.D., 3, 33, 56, 115
Flem, B., 12, 133, 206, 221, 226, 232
fluctuations
and diffusion, 104
in entropy, 101
long-range, 35
of temperature, 342
short-range, 35
flux-force relations, 99
forces and fluxes
scalar, 54
vectorial, 54
Ford, D.M., 345
formation cells, 140, 261
Fourier's law, 8
frame of reference, 84, 192, 195
average molar, 65, 192
average volume, 65, 192, 200
barycentric, 65, 72, 192, 357
center of mass, 65
component, 208
electrochemical synthesis, 236
equimolar surface of solvent, 177
independence of, 84
laboratory, 49, 64, 72, 84, 214, 217
properties that are invariant of, 84
solvent, 65, 193
surface, 84, 140, 143, 160, 214, 217, 225
wall, 64
Franks, F., 114
free charges
redistribution, 19
Freire, T., 339
Frens, G., 125
friction electricity, 149
Friestad, K., 320
fuel cell, 6, 261
fugacity, 42
Fujihara, I., 352
Fuller, T.F., 319
Furry, W.H., 115

Galilean invariance, 56, 67
Gallico, R., 342
Ge, J., 170
Gibbs energy, 36
Gibbs equation, 20, 36
for polarizable surface, 79
for the surface, 22, 23
local form, 52
Gibbs, J.W., 6, 14, 17, 20, 24, 160, 355, 363, 377, 379, 385, 392
Gibbs–Duhem equation, 22, 23, 29, 162, 184
globally linear systems, 58
Gonzalez, E., 339
Gottesfeld, S., 300
Gouy-Stodola theorem, 14
Graner, F., 157
Green, D.W., 44, 152, 178
Grimstvedt, A., 226, 232
Groenewold, J., 22
Guggenheim, E.A., 6, 17, 35, 71, 87, 139, 150, 362, 392

Haarberg, G., 233
Haase, R., 2, 6, 7, 55, 57, 115, 187
Hafskjold, B., 3, 6, 10, 35, 58, 102, 114, 116, 126, 158, 170, 233, 286, 322, 342, 350, 352, 353, 358, 361, 383, 389, 391
Halseid, R., 300, 319
Hanche-Olsen, H., 312, 319
Hansen, E.M., 4, 58, 205, 219, 221, 296, 322
Harman, T.C., 127, 221
Harned, H.S., 152
Harris, K.R., 114, 186
heat flux
  measurable, 72
  reduced, 72
heat flux, total, 111
heat of transfer, 112, 118, 178, 357
  at interface, 166
heat transport
  reversible, 132
Heaviside function, 25
Heffelfinger, G.S., 345
Helferrich, F., 277, 311
Heller, A., 232
Helmholtz energy, 30
Hemmes, K., 233
Henderson, P., 250, 254
Henry's law, 42
Hermans, L.F.J., 158, 165, 179, 389, 391
Hertz, H.G., 10
heterogeneous systems, 17
  transport, 4
highway hypothesis, 58
Hilliard, J.E., 28, 362
Hittorf experiment, 142
Holcomb, C.D., 356
Holmen, R., 320
Holt, T., 115, 278, 280, 284, 300, 311, 324
Honig, J.M., 127, 221
Hovde, E., 114
hydrodynamic equations, 103

Ikeshoji, T., 221, 222, 229, 230, 342, 350, 352, 358
impedance, 327
impedance spectroscopy, 6
interface, 17, 24
  liquid-vapor, 157
internal degrees of freedom, 3
internal energy
  heterogeneous system, 18
internal variables, 3
Irving, J.H., 350
isotropic systems, 109
Ito, Y., 206, 232, 235, 322, 328
Iwano, K., 284

Jackson, J.L., 150
James, R.A., 157, 174
Jerdal, L.O., 320
Johannessen, E., 7, 14, 28, 35, 55, 58, 174, 361, 373, 388, 391
Johnsen, E.E., 249
Jones, R.C., 115
Jou, D., 6, 103

Kaiya, H., 206
Kashammer, S., 10
Katchalsky, A., 2, 6, 109, 139, 277, 284, 285, 311
Keller, H.B., 374
Kempers, L.J.T.M., 115, 187
Khoo, K.H., 256
Killie, S., 114
Kincaid, J.M., 116, 342, 351, 352
kinetic theory, 157
kinetic theory of gases, 3, 165
  for two-component evaporation, 179
Kirkwood, J.G., 350
Kiyono, R. , 284
Kjelstrup, S., 2–4, 7, 10, 13, 14, 33, 35, 48, 54, 58, 74, 82, 84, 91, 115, 121, 125, 126, 132, 143, 158, 165, 170, 174, 182, 205, 219, 221, 222, 227, 230, 232, 233, 259, 261, 278, 281, 289,

291, 296, 307, 313, 316, 320, 322, 324, 328, 336, 339, 340, 342, 350, 351, 353, 359, 361, 373, 383, 389, 391
Kondepudi, D., 3, 55
Kontturi, K., 316, 320
Koper, G.J.M., 73, 125
Kotyk, A., 250
Kramer's rule, 106
Krishna, R., 3, 7, 9, 184, 186
Kubo relations, 4, 350
Kuiken, G.D.C., 3, 9, 56, 184, 186

Laksminarayanaiah, N., 277, 311
Lampinen, M.J., 277
Landau, L.D., 363
Lang, H., 3, 158, 165, 179
Lebon, G., 6, 103
Lennard-Jones potential, 346
  cut-off, 347
  spline, 347
Lennard-Jones/spline fluid
  phase diagram, 353
Lewis-Sargent cell, 254
Li, X., 116, 342, 351, 352
Lien, K.M., 58, 322
Lifshitz, E.M., 363
Lightfoot, E.N., 111, 115
Lindeberg, E., 115, 255
liquid junction
  potential, 249, 251, 254
local equilibrium, 33, 49, 281
  chemical reaction, 54
  in a contact line, 95
  in a surface, 353
  in binary gas mixture, 351
Loeb, S., 277
lost work, 12
Loyalka, S.K., 3, 158, 165, 179
Lunden, A., 115

Müller-Plathe, F., 342
Møller-Holst, S., 312, 316
Macdonald, J.R., 327
MacInnes, D.A., 256
magnetic field, 67
Makange, A.A., 261
Marangoni effect, 96
Martin, M., 200
mass transfer coefficient
  scaling, 126
Massobrio, C., 345, 359
Maxwell distribution, 165, 342
Maxwell equations, 67
Maxwell potential, 70
Maxwell relations, 36
Maxwell's area rule, 364
Maxwell–Stefan equations, 9, 183, 187
Mazur, P., viii, 2, 4, 7, 35, 48, 54, 56, 67, 73, 75, 82, 92, 101, 103, 108, 109, 112, 185, 192
McQuarrie, D.A., 341
mechanical equilibrium, 51, 56, 72, 96, 192
Meixner, J., 2
Meland, A.K., 13, 91, 328, 336, 339
mesoscopic systems, 3
microscopic reversibility, 100
Miller, D.G., 10, 102, 255
Mills, C.T., 157, 174
minimum entropy production, 58
minimum work, 13
Mitchell, P., 2
Miura, D., 235
mobilities of ions, 152, 252
Mogensen, M., 339
molecular dynamics simulations
  local equilibrium, 351
  non-equilibrium, 6
Moran, M.J., viii, 62
Morris, D.R., 12
Morriss, G.P., 341
multicomponent diffusion, 187
Murch, G.E., 200
Muschik, W., 3

Nagayama, G., 3, 158, 172
Nagy, K., 259

Nakajima, H., 328
Navier-Stokes equations, 65, 103
Nernst equation, 85, 109, 144
Nernst potential, 254
Nernst–Einstein assumption, 151, 252, 326
Nernst–Planck equations, 252, 266, 268
Newman, J., 319
Newton's equations, 341
  time reversibility, 100
Nicholson, D., 342
Niete-Draghi, C., 115, 358
Nohira, T., 235, 328
non-equilibrium statistical mechanics, 4
non-linear equations, 103
Norby, T., 232, 322
Nozieres, P., 157
Nummedal, L., 14, 284
Nygård, I., 286

Ogata, Y.H., 235
Ohm's law, 8, 128
Ojala, T., 316, 320
Okada, T., 280, 312, 313, 319
Oliveira, C., 339
Olivier, M.L., 170, 182
Olivry, M., 233
Olsen, E., 221, 233
Olsen, G.F., 249, 255
Onsager coefficients, 11
  for evaporation and condensation, 157
  from kinetic theory, 179
  scaling of main coefficients, 125
  specification, 111
Onsager relations, 11, 99, 102, 105, 344
Onsager, L., 1, 100, 115
open circuit potential, 149
Oppenheim, I., 74
Ortiz de Zárate, J.M., 33, 35, 352
oscillating potential, 327
osmosis
  thermal, 285
osmotic
  pressure, 284
  thermal pressure, 285
Østvold, T., 284, 311
Öttinger, H.C., 3
Ottøy, M., 300, 312, 313, 316, 319
overpotential, 340
Owen, B.B., 152

Pérez-Madrid, A., 3
Paduano, L., 10, 102
Paganin, V., 339
Pagonabarraga, I., 3, 6
Palcut, M., 200
Pao, Y.P., 3, 158
Paolini, G.V., 350, 359
Papenfuss, C., 3
partial molar properties, 37
Pearlstein, A.J., 10, 102
Peelen, W.H.A., 233
Peltier coefficient, 128, 132, 222
  for electrode, 209, 213, 240
  for surface, 131
  position dependent, 270, 271
Peltier heat, 127, 261
  in coolers, 132
periodic boundary conditions, 343–345
Perry, R.H., 44, 152, 178
phase transition, 176
  with supersaturated vapor, 162
Phillips, L., 157, 174
Pikal, M.J., 10
Planck potential, 266
Planck, M., 250, 266
polarizable systems, 48, 75
polarization
  density, 18
  stationary state, 339
polarized electrodes, 6
potential
  jumps at surfaces, 77
Prüser, U., 232
Prigogine principle, 57

Prigogine's theorem, 67, 72
proof, 192
Prigogine, I., 2, 17, 35, 55, 57, 67, 72, 105, 192, 362, 392
Primdahl, S., 339
Prud'homme, R., 4, 73, 109
Pugazhendi, P., 328, 336

Qian, J., 221, 233
quantum mechanical systems, 3
Quirke, N., 342

Røsjorde, A., 3, 6, 10, 14, 28, 35, 102, 126, 158, 170, 289, 342, 351, 353, 359, 361, 373, 383, 389, 391
Rajabu, H., 261
Raoult's law, 42
Ratkje, S.K., 2, 6, 7, 10, 58, 102, 114, 133, 139, 206, 211, 222, 226, 229, 230, 232, 249, 250, 255, 261, 265, 280, 284, 286, 300, 311, 316, 319, 322, 326, 342, 352, 358
Rayleigh's dissipation function, 55
reciprocal relations, 11
reduced variables
in NEMD, 347
reference component, 28
regression hypothesis, 102
Reguera, D., 3, 6
Reith, D., 342
Rekvig, L., 10, 35, 102, 158, 165, 170, 342, 359, 361
relaxation time, 20
resistivities
main, 187
resistivity matrix, 185, 193
reversible process, 14
Reynolds number, 103
Richter, J., 232
Roldughin, V.I., 3
Rollier, D., 170, 182
Ronis, D., 74
Ross, J., 55
Rousseau, B., 115, 170, 342, 344, 358
Rowlinson, J.S., 17, 28, 126, 362, 375, 392
Rubi, J.M., 3, 6, 13, 84, 158, 307, 340

Sørensen, T.S., 291, 313, 320
Salamon, P., 58
salt power plant, 9
Sauar, E., 58, 322
Saxén relation, 149
scaling coefficient, 125
Scatchard, G.
assumption, 281
Schechter, R.S., 57
second law
efficiency, 14
of thermodynamics, 47, 74, 106, 107
Seebeck coefficient, 133, 230
Seebeck effect, 127
self diffusion coefficient, 115
Sengers, J.V., 33, 35, 352
separation
in temperature gradient, 352
Seppälä, A., 277
Shankar, P.N., 182
Shapiro, H.N., viii, 62
Sharivker, V.S., 206, 222, 227
shear pressure, 56
Shikhmurzaev, Y.D., 92, 97
Simon, J.-M., 35, 170, 342, 350, 351, 356, 361, 373, 383, 391
Sindzingre, P., 345
Skrede, M.G., 280, 300, 311, 326
Sluyters, J.H., 327
Sluyters-Rehbach, M., 327
Smit, J.A.M., 165, 179
Soret coefficient, 114
of electrolytes, 115
of non-electrolytes, 115
sign, 115
of isotopes, 115
Soret effect, 114, 352

space ship, 9
Spallek, M., 10
Springer, T.E., 300, 339
standard state
of electrolyte solutions, 42
of gases, 42
of mixtures, 42
state function, 21
stationary states, 8, 58
Sterten, Å., 12, 133, 221, 226, 232
Steward, F.R., 12
Stewart, W.E., 111, 115
Strømgård, M., 300
streaming potential, 149
Struchtrup, H., 157, 391
subscript
explanations, 83, 130
surface, 17
thickness, 122
autonomous system, 35
chemical potential jumps, 83
closed, 24
concentration, 25
coupling of transport processes, 109
dividing, 25
equimolar, 25, 28, 29
excess density, 28, 76
excess properties, 25
Gibbs, 24
internal energy, 6
of discontinuity, 28
polarization, 20
temperature jumps, 82
thickness, 24, 355
surface potential jump
adiabatic cell, 247
surface tension, 21, 355, 368
two component system, 177
Suzuki, T., 284
systems
electroneutral, 19
multi-component, 18
polarizable, 18, 127, 139
Syverud, K., 222, 229, 249, 259
Szargut, J., 12, 14

Tasaka, M., 284
Taylor, R., 7, 9, 111, 187
tears of wine, 96
temperature jump
surface, 132
temperature jumps
in phase transitions, 157
temperature profiles, 124, 137
Tenenbaum, A., 342, 345
tensorial phenomena, 109
thermal conductivity, 112, 118
of homogeneous materials, 123
scaling, 125
thermal diffusion coefficient, 113
thermal diffusion factor, 357
thermal osmosis, 6
thermoelectric generator, 127
thermoelectric heat pump, 127
thermoelectric potential, 134
Thompson, A.P., 345
Thomson
effect, 129
second relation, 10
Thomson, W., 1, 10, 129
Ticianelli, E., 339
time average, 343
Todd, B.D., 350, 359
Tolman length, 385
Tomii, Y., 232
trajectory of particle, 341
transfer coefficients
from kinetic theory, 165
from molecular dynamics simulations, 170
transference coefficient, 141, 149, 251
of electrolyte, 144
position dependent, 261, 263
postition dependent, 209
transference number, 142
of ion, 152, 252, 264
transport
of heat and mass, 353

transport of heat and charge, 127, 139
  at surfaces, 130
  entropy production, 128
transport of heat and mass, 111
  entropy production, 112
transport of mass and charge, 139
  entropy production, 141
  in electrochemical cells, 140
transport processes
  along the surface, 6
  coupled, 6
transported entropy
  in metals, 128
  of ions, 213, 228
  of ions in water, 230
Truesdell, C., 103
Tsuruta, T., 3, 158, 165, 172
turbulence, 103
Tyrell, H.J.V., 114, 186

van Dam, K., 2, 289
van der Kooi, H., 233
van der Waals, J.D., 28
  equation of state, 362
  model, 28, 362
van Giessen, A.E., 385
Vaula, D., 12, 312
Vie, P.J.S., 289, 291, 300, 306, 307
viscous forces, 192
viscous phenomena, 56
Vlieger, J., viii, 19, 74, 76, 363, 388
Vreuls, W., 232

Ward, C.A., 157, 174, 391
Wei, J., 103
Weingärtner, H., 10
Wesselingh, J.A., 3, 7, 9, 184, 186
Westerhoff, H.V., 2, 289
Widom, B., 17, 28, 126, 362, 375, 392
Wold, I., 322

Xie, G., 320
Xu, J., 6, 10, 35, 54, 102, 158, 165, 170, 342, 359, 361
Xu, Q., 133, 206, 226, 232, 233

Yakawa potential, 347
Yasuda, K., 235
Young's law, 91, 94, 96
Ytrehus, T., 158, 165, 179, 389, 391

Zawodzinski Jr, T.A., 300
Zhadanov, V.M., 3
Zhu, L., 73, 125
Zielinska, B.J.A., 35
Zinoviev, V.E., 129
Zollweg, J.A., 356
Zvolinschi, A., 14, 15

About the Authors

Signe Kjelstrup has been a Professor of Physical Chemistry since 1985 at the Norwegian University of Science and Technology, Trondheim. Since 2005, she has held a part-time Chair on Irreversible Thermodynamics and Sustainable Processes at the Technical University of Delft, The Netherlands. Her works in Non-Equilibrium Thermodynamics concern Electrochemical Cells, Membrane Systems and Entropy Production Minimization in Process Equipments. She is a Honorary Doctor of the University of North East China, and has been a Guest Professor at Kyoto University and at the University of Barcelona. Her book on Irreversible Thermodynamics coauthored with K.S. Førland and T. Førland (Wiley, 1988 and 1994; Tapir, 2001) has been translated into Japanese and Chinese.

Dick Bedeaux was a Professor of Physical Chemistry at the University of Leiden from 1984-2006. Since 2002, he has held a part-time Chair at the Norwegian University of Science and Technology, Trondheim. Bedeaux, together with Albano and Mazur, extended the Theory of Non-Equilibrium Thermodynamics to Surfaces. In the context of Equilibrium Thermodynamics he has worked on Curved Surfaces. Bedeaux is a Fellow of the American Physical Society, and the recipient of the Onsager Medal from the Norwegian University of Science and Technology. Together with Jan Vlieger he wrote the book "Optical Properties of Surfaces" (Imperial College Press, 2002, revised edition, 2004).